ISBN 978-9975-70-913-2

MOLDOVA STATE UNIVERSITY
& INSTITUTE OF POWER ENGINEERING
CENTER FOR EDUCATION AND RESEARCH
IN MATHEMATICS AND COMPUTER SCIENCE

Vladimir PATSIUK

MATHEMATICAL METHODS FOR ELECTRICAL CIRCUITS AND FIELDS CALCULATION

$$\text{rot}\,\vec{E} = -\frac{\partial \vec{B}}{\partial t}$$

$$\text{div}\,\vec{B} = 0$$

$$\text{rot}\,\vec{H} = \vec{j} + \frac{\partial \vec{D}}{\partial t}$$

$$\text{div}\,\vec{D} = \rho$$

Seria
TEXTBOOKS
&
MONOGRAPHS

Chişinău - 2009

ISBN 978-9975-70-913-2

CENTER FOR EDUCATION AND RESEARCH IN MATHEMATICS AND COMPUTER SCIENCE

Textbooks & Monographs, Vol. 8

Vladimir Patsiuk

MATHEMATICAL METHODS FOR ELECTRICAL CIRCUITS AND FIELDS CALCULATION

Center for Education and Research in Mathematics and Computer Sciences (CECMI) of the Moldova State University was established in 2006 due to support of the U. S. Civilian Research & Development Foundation (CRDF) and the Moldovan Research and Development Association (MRDA), grant CERIM-1006-06.

The Center supports the integration of science and education in mathematics and computer science, maintains the young people participation in scientific investigations. The courses on actual directions of theoretical and applied mathematics and computer science are elaborating within the framework of the Center. The Center organizes scientific conferences, summer schools and workshops, publishes manuals and monographs.

Chişinău

2009

MOLDOVA STATE UNIVERSITY
& INSTITUTE OF POWER ENGINEERING
OF THE ACADEMY OF SCIENCES OF MOLDOVA

UDC 621.31+519.6(075.8)
P44

Published by
Center for Education and Research in Mathematics and Computer Science at Moldova State University, grant CERIM-1006-06 award by CRDF/MRDA

The new information technologies and approaches for analysis of transient and steady-state processes in electrical circuits with distributed and lumped parameters are proposed and rigorously founded. The finite volume method for field strength and for capacity of multiply-connected body calculations is developed.

The monograph is directed to the broad circle of specialists in mathematical physics, computational mathematics, electrotechnology and electroenergetics, as well as to persons working for doctor's degree and students.

It is recommended to edition by the Academic Council of the Faculty of Mathematics and Computer Science, Moldova State University and by the Academic Council of the Institute of Power Engineering of the Academy of Sciences of Moldova.

Reviewer: academician of the Academy of Sciences of Moldova Canțer V.

DESCRIEREA CIP A CAMEREI NAȚIONALE A CĂRȚII

Patsiuk, Vladimir

Mathematical methods for electrical circuits and fields calculation : [pentru uzul studenților] / Vladimir Patsiuk ; Centrul de Educație şi Cercetare în Matematică şi Informatică al USM (CECMI). – Ch. : CEP USM, 2009. – 442p. ; 21 cm. – (Serie de monografii şi manuale ; vol.8)

Bibliogr.: p. 435-... (125 tit.). – 150 ex.

ISBN 978-9975-70-913-2

621.31+519.6(075.8)

P44

CONTENTS

INTRODUCTION

Many phenomenon and processes of the ambient medium can be described mathematically as the initial boundary-value problems for partial differential equations. The mathematical models have displayed their great efficiency in technical systems and physical applications. However, in such branches of science as theoretical electrical technology and electroenergetics, the mathematical models development is obviously backward of current requirements and numerous engineering practice demands. This backward slip becomes especially visible if we try to realize some comparative analysis with models, methods and informational technologies applied in the mechanics of continua [77, 78], plasma physics, synergetic and in the other fields of modern natural science, where the numerical integration of the many-dimensional nonlinear evolutionary equations becomes an ordinary event.

Quite a lot of theoretical electrical technology problems have a direct mechanical analogue and they have been solved as far back as the 18th century. The striking example of that is the problem about longitudinal oscillations of elastic bar with added mass. When the mass is equal to zero, we obtain the condition of free end or the condition of short-circuit at the receiving end of the transmission line. And vice versa, when the mass is infinitely large, we obtain the condition of rigid fixing or the condition of idling.

The practical implementation of the electrical power has a shorter history in comparison with mechanical energy, but it is characterized by very rapid development of the whole line: production-transportation-distribution-utilization. The high speed of the electromagnetic wave propagation and relatively moderate distances of the electric power transmission have had an influence upon the approaches of such systems analysis and calculation. The most frequently these systems are represented as the circuits with lumped parameters, but the links parameters between different loads and power supply usually are not taken into consideration. It is characteristic that in electrical circuit calculations the parameter's determination is executed separately at the steady-state regime and at the transient regime. Obviously, it is a consequence of complexity and of laboriousness of the electromagnetic processes study in the integral connection with their natural course in the electrical circuits. As an example one can consider the class of nonstationary boundary-value problems for telegraph equations: the theoretical and practical significance of these problems is more then evident when analyzing the transient and steady-state processes in the electrical circuits in-

cluding the circuits with nonhomogeneous structure. The structural heterogeneity is one of the characteristic futures of the modern electrical power system. It is clear enough that the heterogeneities essentially influence upon the all processes and regimes in the system. It is to mention that the exact solutions are known only for limited number of the boundary-value problems for telegraph equations.

The computer techniques give the possibility to deviate from traditional approaches in the investigation and calculation of the electrical circuits with lumped and distributed parameters.

The basic element of any electrical system is the linear electric circuit consisting of the source (generator), the communication circuit and the load. The limiting regimes for such a circuit are represented by the idling regime (the load resistance value $R_S \to \infty$) and by the short-circuited regime ($R_S = 0$). Seemingly, these simple circuits are investigated with exhaustive completeness (taking into account that these processes are described by well-known telegraph equations – Kirchhoff's laws). It seems to be paradoxically, but more detailed study of these circuits achieves that this is not the case. For example, even for line lengths substantially smaller then the electromagnetic wave length one can discover a number of particular properties that can be easily revealed by solving the concrete initial boundary-value problem of mathematical physics for these circuits.

Another important problem for energetics and computer techniques is accepted to be the problem of creation of so-called "room temperature" superconductors (the energy losses in such superconductors are negligible small or are missing at all). It seems to be paradoxically, but if the whole energetics should be transferred to the superconductors, it will not operate and will collapse.

The efficiency and operational reliability of energetics are the most topical problems. The power losses under the electrical energy transmission and distribution have the direct influence upon the energetic efficiency indices. The losses decrease is possible only on the basis of more exact knowledge about the particular qualities of electroenergetic system operation. As a consequence, the increased requirements upon the theoretical calculation's accuracy become necessary. The engineering accuracy of about 5…10% is not accepted as satisfactory since, for example, if it is necessary to determine the power losses till hundredth part of the percent (it may be hundreds of thousands in a money equivalent), than the voltage and current instantaneous values must be calculated with the accuracy not less then four-five significant digits.

In the countries with developed market economy the customers of the research works usually are the investment funds, large-scale energetic and insurance companies, privately owned firms specialized in energetic auditing. It is obvious that they are interested often in thousandth or even ten thousandth parts of the percent. On implementation of commercial orders connected particularly with the simultaneous increase of the transmission power and of the efficiency, it is often necessary to use the different physico-mathematical models and to carry out the numerous numerical calculations under the widest variety of the initial parameters of the electricity transmission with the purpose of their adjustment to the available experimental or statistical data.

By now one can enumerate not so many nonstationary problems for electrical circuits with distributed and lumped parameters that have been solved and carried to numbers [22, 42, 48, 55, 60, 66, 110, 116, 119]. In the strict sense only the problem about the rectangular potential and current wave motion along the homogeneous semiinfinite line is solved irreproachable [60]. Unfortunately, only this analytical solution can be used as a sample solution for a posteriori accuracy estimation of the approximate methods. We'll consider the accuracy satisfactory if as minimum 2-3 significant digits coincide. In this case the numerical and the analytical solutions represented in graphical form are visually congruent.

The publication's analysis in the field and the personal experience make it clear that it is not still formed the unique and strongly valid approach to the calculation of the wave processes and the power transmission energy datum in the distributed systems with variable (tunable) parameters.

In the cited and in many other works the quite particular cases of the telegraph equation solving under the additional simplifying conditions are considered. For example, quite often when calculating the electrical circuits the only active longitudinal resistance $R > 0$ is taking into account, but the transverse leakance (or shunt conductance) between the direct and the inverse wires is assumed to be equal to zero: $G = 0$ [22, 42, 55, 60, 66, 110, 116]. To the rare exceptions we can relate the paper [48], where the instantaneous connection to the direct voltage of the cable line with nonzero leakage current through the imperfect insulation is investigated.

In spite of this, the traditional approaches and methods for calculations of the loading regimes and commutation transient processes in distributing systems (high-current long extent circuits, communication lines, etc.) are sufficiently intricated and can not pretend to universality. Some more detailed review connected with the analytical or numerical solutions of the long line evolutionary equations one can find in [90, 120, 125].

Reasoning from the requirement of the theoretical electrotechnology development and of the engineering practice the necessity of creation of some thesaurus (based on the latest measuring and computational technologies) containing the numerical models and sample (test) examples for electromagnetic circuits and fields is about to happen. Their following approbation on the physical models must contribute to overcome the existing gap between the theoretical and experimental researches [33, 125] in the problems of electrical power transmission on long distances. The solutions of such model (test) problems should be represented in a maximally simple and convenient form as any specialist (familiar with the theoretical electrotechnology) may use them and may repeat the results varying the initial data at his judgment.

It is well-known that none of the deductive methods of calculation or forecasting "does not like" the heavy gradients (neither by time nor by space). The situation becomes more complicated when it is necessary to calculate the shock wave evolution (strong discontinuities) in the distinctly nonhomogeneous medium with parameters differing in orders. For example, the wave resistances in the backbone power transmission lines and in the distributing networks with cable insertions differ in 8…12 times. If we consider the Franklin's lightning rod or Faraday cage as a piecewise homogeneous long line, then the linear leakance (shunt conductance) at the separate sections changes quite in hundreds of times. Under the emergency situations (such as open-phase fault and drop) the load resistance can suddenly go down from infinitely large values (at the idling regime) till zero (at short-circuited regime).

Nevertheless, the ideas of the method of characteristics and of the first differential approximation turn out to be extremely productive and give a possibility to deduce the uniform computation relations for essentially nonhomogeneous parametrical structures under the connection-disconnection of loads and of other lumped systems [89, 90].

The problem of reactive power determination in the long line as such (with no resorting to its simplified representation in the form of *RCL*-circuits with lumped parameters) can be related to the number of unsolved problems too. In present there exists the problem relating to the financial interrelation between the electrical power supplier and consumer when paying for the reactive power consumption. In case of direct contracts between the large-scale electrical power consumers and the generation source (electric power station) there is no clarity what to pay, because the electric lines can be both the consumers and the generators of the reactive power. This problem becomes more complicated in case when nonsinusoidal effect or

dissymmetry by phases appears under the electrical power supply. In our opinion the idea of instantaneous power decomposition for nonsinusoidal functions on components at the electrical circuit boundaries has no prospects. It is expediently to use the balance equation for reactive powers for the electrical circuit (generator – power transmission line – load) as a whole and then to calculate the reactive power of its elements. There is no clarity in the question about the reactive power under the transient regimes as well (even how to calculate and/or to measure it for registration).

It is to mention the fact that there are a big number of inexactitudes and mistaken theses in the sections related to the power transmission by alternating current on the long distances. This fact has been rightly pointed out still in the paper [109]. Many conclusions and derivations unfortunately are turned not on the base of strict solutions for telegraph equations as such, but on the base of the long line substitution by lumped elements (in many cases namely this substitution serves as a source for incorrect conclusions and derivations).

It is not clear, for example, why it is considered that the maximal efficiency can be reached under the matched load when the power is transmitted in it only by direct wave [15]. The point is that from the steady-state regime equations it is easy to determine that for alternating current line one must distinguish the difference between the regimes under which the maximal efficiency, the maximal values of generated and transmission powers, maximal power factors of the source and of the receiver are reached. In general case under the electrical power transmission along the long line, there are five different load resistances different from complex wave resistance of the line. Sometimes the following recommendation is indicated: the shunt reactors should be disconnected under the natural power regime, because the line under this regime is surely compensated by reactive power. But the solutions of the steady-state regime equations demonstrate [90], that if the powers and the locations of the reactors are chosen in special manner, then the increase of efficiency and of transmission power can be achieved simultaneously (namely in this way the proprietors of the backbone and distributing transmission lines achieve these indexes).

The investigation of the processes in the multiwire electrical lines is accompanied by some difficulties. As a rule, in the reference manuals the distributed parameters values for multiple-phase lines are represented in the averaged form and these averaged values are considered to be equal for all phases of the line. This fact gives the possibility to replace, for example, the three-phase line by single-wire line and to deduce for it corresponding calculations of regimes and processes. In general such a replacement is incor-

rect even for steady-state sinusoidal regime in power transmission line without losses acting on matched load. What is the matched load for single-wire line with arbitrary losses – is clear and physically feasible. In general case it is the complex resistance Z_S, consuming the active and reactive powers from the line.

At the same time the symmetrical matrix of the wave resistances $Z = L^{1/2}C^{-1/2}$ for ideal multiwire electrical lines with nonzero interference between the wires consists of nonzero elements and the boundary conditions $u = Zi$ are to be fulfilled at the receiving end of the line as to ensure the traveling waves regime. Physically this means that nonzero active resistances are to be connected between the phases, but it has been never applied in the practice. Furthermore, one can construct an example of the line with losses when some elements of the matrix Z are real and negative, hence it is necessary to connect some additional EMF sources between the phases to obtain the matched load.

If there is the interference between the wires, then for the single-circuit three-phase line the natural current and the natural power decrease inevitably. For real half-wave line without taking into account the losses the natural power decrease comes to minimum 4…5%, but for the line with losses the efficiency decreases in comparison with the case when the interference between the wires is not taking into account. Hence, the replacement of the three-phase line by the single-wire model represents the sufficiently rough approximation.

As it was mention above, all elements of the electrical power system are characterized by the constructive heterogeneity that influences upon the primary and secondary parameters as well as upon the accuracy of analytical and numerical solutions of the macroscopic electrodynamics problems.

The physical heterogeneity of the electroenergetic objects represents the complicated scientific and technical problem, especially in cases when there are great distinction in dimensions between the zones and sections with different electrical and electrophysical parameters. The Maxwell equations in the differential and integral forms represent the theoretical foundation for this kind of problems. Let's mention that the telegraph equations represent a particular case of the Maxwell equations and this fact reflects the generality of the approach used in the monograph for solution of the topical problems of the electrotechnology and energetics.

The Maxwell equation's utilization for study of the electromagnetic interaction effects in the electrodynamics problems constitutes the sufficiently complicated mathematical problem owing to necessity of taking into con-

sideration the electromagnetic field interaction with the substance in the heterogeneous medium. The complexity of the problem is caused by the following matter. The substance consists of a great number of particles and the motion of the separate particle is impossible to describe. To avoid this difficulty usually some models of continuous medium are used. It is to mention only that the development and the theoretical foundation of such models do not represent a trivial problem especially for heterogeneous mediums.

The subject of present research represents the development of the deductive methods and the mathematical modeling of the electromagnetic wave propagation in the systems and mediums with variable parameters. As a basic implement of the scientific analysis, the tools of mathematical physics and of computational mathematics are applied with reference to electrotechnology and electroenergetics.

When fulfilling this research and redacting the present edition the author has been guided by the following assumptions:

1. The long line is considered as a circuit with distributed parameters and it is not replaced by equivalent recurrent networks with lumped elements even in the cases when it is acceptable.

2. The connection to the line of the facilities represented by the equivalent circuits with lumped parameters is described by the boundary conditions (Kirchhoff's laws) which are valid for arbitrary time moment.

3. The accuracy is considered satisfactory if as minimum 2…3 correct significant digits in obtained numerical solution are ensured.

4. All solutions are to satisfy the law of conservation of electromagnetic energy.

5. Since any steady-state process is next to the transient process, then their calculations must be realized in the same order (as it takes place in reality).

6. The numerical scheme is to be homogeneous and to realize the calculation both in direct time and in inverse time (at least for homogeneous boundary conditions).

7. The primary parameters of the multiwire lines are to be determined on the base of rigorous solutions of the initial boundary-value problems of the electromagnetic field theory.

8. All algorithms and routines must be more efficient and practically feasible then all known now commercial tools based on integration of the long line equations.

The monograph parallel to the original materials contains some reference and general theoretic information. The presented methods and research results for nonstationary phenomenon under the electromagnetic energy

propagation in the nonhomogeneous systems with variable parameters can be successfully used during the courses of theoretical electrical technology, automatic control systems, radio engineering, wave dynamics, mathematical physics, computational methods, etc.

The author would like to thank his colleagues G. Ribacova, D. Zlatanovich, I. P. Stratan, M. V. Chiorsac, A. S. Sidorenco, V. K. Rimskii, V. P. Berzan, A. A. Juravliov, M. L. Shit, Iu. Sainsus, V. I. Cojocaru for productive discussions of the research results and for advices in this edition preparation.

The author would like to express his deepest gratitude to the reviewer, the academician of Moldova Academy of Sciences Canțer V. G., whose remarks and requests turned out to be useful and helpful for improving of present edition.

TABLE OF SYMBOLS AND UNITS

t – time, s;
x – space variable, m;
u – instantaneous voltage value, V;
i – instantaneous current value, A;
P – power, W;
W – energy, J;
η – efficiency;
L – linear inductance, H/m;
C – linear capacity, F/m;
R – linear active resistance, Ω/m;
G – linear leakance (shunt conductance), S/m;
l – line length, m;
λ – wave length, m;
a – speed of electromagnetic wave propagation, m/s;
Δ – time of wave run along the line length, s;
Z_B – wave resistance (impedance) of the long line, Ω;
R_S – active load resistance, Ω;
L_S – load inductance, H;
C_S – load capacity, F;
f – frequency, Hz;
ω – angular (circular) frequency, rad/s;
φ, θ – phase displacement angle, rad;
$\cos \varphi$ – power factor;
τ – time step of finite difference scheme, s;
h – space step of finite difference scheme, m.

CHAPTER I

COMPUTATION OF TRANSIENT AND STEADY-STATE PROCESSES IN LINE CIRCUITS WITH DISTRIBUTED AND LUMPED PARAMETERS

1. Telegraph equations and dimensionless quantities

The electromagnetic power transfer through the long line by means of conduction currents can be described by well known telegraph equations, which represent Kirchhoff's laws for closed circuit generated by subcircuit with the length *dx*:

$$L\frac{\partial i}{\partial t}+\frac{\partial u}{\partial x}+Ri=0;\;\; C\frac{\partial u}{\partial t}+\frac{\partial i}{\partial x}+Gu=0\,. \tag{1.1}$$

The primary parameters in these relations are the followings: L is the inductance of the loop formed by direct and return lines; R is the longitudinal resistance; C, G are the transverse capacity and conductance of the wire insulation leakage.

To mark out the unique solution the system (1.1) must be completed with the boundary and initial conditions. Let at the start time $t = 0$ the line circuit (fig. 1.1) is connected to the external voltage source of the arbitrary form:

$$u=U_0(t)\;\text{ when }\;x=0\,, \tag{1.2}$$

and its receiving end is closed on the impulse-reaction load in the form of the serial RLC – circuit:

$$u=R_s i+L_s\frac{di}{dt}+\frac{1}{C_s}\int_0^t i(\tau)d\tau\;\text{ when }\;x=l\,. \tag{1.3}$$

Obviously, when $R_S = L_S = 0$, $C_S = \infty$ we obtain the short-circuit conditions: $u = 0$, and the condition $R_S = \infty$ corresponds to the idling in the line: $i = 0$ (the load is out off). Such a singular loads (short-circuit or idling) occur relatively rare in practice, however theirs study is of undoubted interest as an initial stage in the transferring to the real (nonsingular) load conditions. Usually the initial conditions for the problem are zero (the electric charge in the circuit is missing before the commutation).

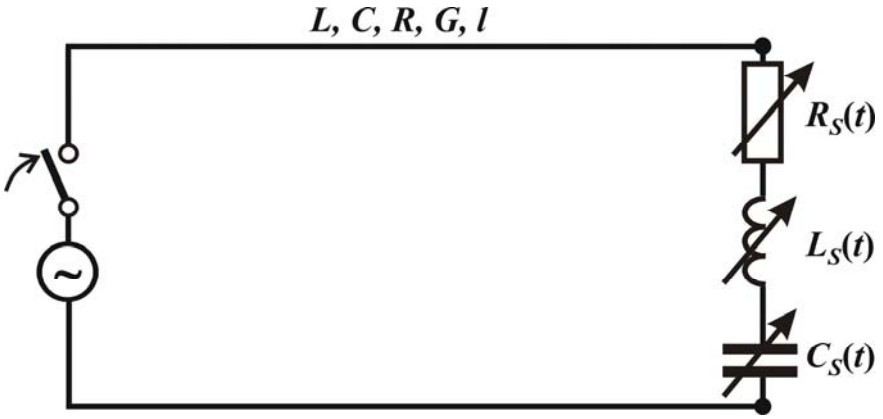

Fig. 1.1. The electric circuit that consists of the voltage source, uniform long line with the lineal parameters *L*, *C*, *R*, *G* and the lumped *RLC* – load at the receiving end.

On power take-off, on switching on the "bucking out" or another kind of systems, the currents and the voltages as a functions of the spatial variable x in the intermediate points of the line $x = x_n$ can possess the discontinuities of the first kind or another jumps. However, the integro-differential relation (1.3) doesn't change its form when substituting $i = i_1 - i_2$ and $u = u_1 - u_2$ (here the subscripts mean the function values at the left and at the right of the point of switching). Let's remark that the impulse-reaction lumped loads can consist of the arbitrary set of serial or parallel connected *RLC* – units. In this case the boundary conditions become more intricate, but it is important only these conditions to remain linear (since then the unique solution exists).

The system of linear differential equations (1.1) is of hyperbolic type [25, 107] that implies evidently the finite velocity of electromagnetic wave propagation determined through parameters of the line by formula $a = 1/\sqrt{LC}$. In the case of multiwire line (when *L*, *C* are the symmetric

square matrixes of self and mutual inductances and capacitances) the wave velocities are congruent with the eigenvalues of matrix

$$A = \begin{Vmatrix} 0 & L^{-1} \\ C^{-1} & 0 \end{Vmatrix}.$$

When solving the initial boundary-value problems (1.1) – (1.3) it is convenient to use the dimensionless (normalized) quantities. Let's introduce into consideration such quantities over the formulas:

$$u = \frac{u^\circ}{U^\circ};\ i = \frac{i^\circ Z_B^\circ}{U^\circ};\ t = \frac{t^\circ}{T^\circ};\ x = \frac{x^\circ}{\lambda^\circ};\ R = \frac{R^\circ \lambda^\circ}{Z_B^\circ}; \tag{1.4}$$

$$G = G^\circ \lambda^\circ Z_B^\circ;\ Z_B^\circ = \sqrt{L^\circ / C^\circ};\ R_S = \frac{R_S^\circ}{Z_B^\circ};\ L_S = \frac{L_S^\circ}{L^\circ \lambda^\circ};\ C_S = \frac{C_S^\circ}{C^\circ \lambda^\circ},$$

here U° is some basic (rated) voltage; Z_B is the impedance in the line; a is the electromagnetic wave velocity; $\lambda = a/f$ is the wave-length on a frequency of the electric power supply; $T = \lambda/a = 1/f$ is the oscillation period; $\Delta = l/a$ is the wave runtime along the line with the length l; the degree sign denotes dimensional quantities. As a unit of length one can use the length of any part of the line, but for sinusoidal voltage line $u = U_0 \sin(2\pi f t)$ the value λ is used usually. In this case, after transferring to dimensionless quantities by formulas (1.4) in the original equations and in the boundary conditions, we obtain that $U_0 = L = C = Z_B = \lambda = a = T = f = 1$.

For secondary parameters in the sinusoidal voltage (current) line and design relations of the complex amplitude method (CAM) we'll use the following notations:

$$Z_0 = \sqrt{\frac{R + j\omega L}{G + j\omega C}};\quad \delta = \alpha + j\beta = \sqrt{(R + j\omega L)(G + j\omega C)};$$

$$Z_S = R_S + j\left(\omega L_S - \frac{1}{\omega C_S}\right);\quad Z_{BX} = Z_0 \frac{Z_S + Z_0 \operatorname{th}(\delta l)}{Z_0 + Z_S \operatorname{th}(\delta l)}; \tag{1.5}$$

$$U_0 = Z_{BX} I_0;\quad U_1 = Z_S I_1;\ U_1 = U_0 \operatorname{ch}(\delta l) - Z_0 I_0 \operatorname{sh}(\delta l);$$

$$S = UI^* = P + jQ = |U||I|\cos\varphi + j|U||I|\sin\varphi .$$

Here $\omega = 2\pi f$ is the circular frequency; Z_0 is complex impedance (characteristic impedance); δ, α, β are propagation, attenuation and phase constants; Z_S is the load resistance; Z_{BX} is the input resistance of the line; U_0, I_0, U_1, I_1 are the complexes of voltages and currents at the sending end and out end of the line with length l; S is the complex power with the active P and reactive Q components.

The relations (1.5) are also referred to by long line formulas or the equations of the steady-state regime.

2. The Fourier series method for calculation of nonsinusoidal regimes in opened and short-circuited circuits with sinusoidal current or voltage sources

Axiomatic structure of the theory of the line electric circuits with distributed and lumped parameters is formed by Ohm's and Kirchhoff's laws. And without controversy the following deductive reasoning arises from these laws. If the concentrated device, consisting from the arbitrary set of *RLC* – units, is connected directly to the supply terminal of the sinusoidal voltage (or current), then, reasoning from the solution of the integro-differential equation

$$u = R_s i + L_s \frac{di}{dt} + \frac{1}{C_s}\int_0^t i(\tau)d\tau ,$$

the current (or voltage) also will change in time by sinusoidal law [59]. The presence in the electric circuit of some elements with distributed parameters as a long line (interconnecting wires) makes such reasoning not so evident even for the steady-state processes. Its examination on the base of strongly valid solutions of the correctly formulated boundary-value problems for telegraph equations leaded to rather unexpected results that require accurate and comprehensive analysis.

Let’s consider the problem of determination of voltage function $u(x,t)$ and current function $i(x,t)$ satisfying the system of hyperbolic equations

$$L\frac{\partial i}{\partial t}+\frac{\partial u}{\partial x}+Ri=0;\ C\frac{\partial u}{\partial t}+\frac{\partial i}{\partial x}+Gu=0 \text{ when } x\in(0,l),\ t>0 \quad (2.1)$$

and the following initial and boundary conditions:

$$u(x,0)=i(x,0)=0,\ x\in[0,l]; \quad (2.2)$$

$$u(0,t)=U_0\sin\omega t,\ u(l,t)=0,\ t\geq 0. \quad (2.3)$$

To simplify the problem solution the condition (2.3) should be written in complex form $u(0,t)=U_0e^{j\omega t},\ u(l,t)=0,\ t\geq 0$.

In case of short circuit at the receive end of the alternating voltage line the boundary conditions are formulated usually only in terms of voltages $u(x,t)$. So in this case the current function $i(x,t)$ can be eliminated from the relations (2.1) – (2.3) and we obtain the problem formulated with respect to voltage function

$$LC\frac{\partial^2 u}{\partial t^2}+(LG+RC)\frac{\partial u}{\partial t}=\frac{\partial^2 u}{\partial x^2}-RGu$$

or

$$\frac{\partial^2 u}{\partial t^2}+(\gamma_R+\gamma_G)\frac{\partial u}{\partial t}=a^2\frac{\partial^2 u}{\partial x^2}-\gamma_R\gamma_G u \text{ when } x\in(0,l),\ t>0; \quad (2.4)$$

$$u(x,0)=\left.\frac{\partial u}{\partial t}\right|_{t=0}=0,\ x\in[0,l]; \quad (2.5)$$

$$u(0,t)=U_0e^{j\omega t},\ u(l,t)=0,\ t\geq 0. \quad (2.6)$$

Here the voltage at the sending end is specified in the complex form using the following notations: $\gamma_R=R/L$, $\gamma_G=G/C$, $a=1/\sqrt{LC}$.

The solution is finding by expansion it in Fourier series [107] that assumes the transfer to the zero boundary data. With this scope let's reformu-

late the problem (2.4) – (2.6) with respect to new function $\widetilde{u}(x,t) = u(x,t) - U_0(1-x/l)e^{j\omega t}$:

$$\frac{\partial^2 \widetilde{u}}{\partial t^2} + (\gamma_R + \gamma_G)\frac{\partial \widetilde{u}}{\partial t} = a^2 \frac{\partial^2 \widetilde{u}}{\partial x^2} - \gamma_R \gamma_G \widetilde{u} + f(x,t) \text{ when } x \in (0,l),\ t > 0; \quad (2.7)$$

$$f(x,t) = U_0(1-x/l)[(\omega^2 - \gamma_R\gamma_G) - j\omega(\gamma_R + \gamma_G)]e^{j\omega t} = U_0(1-x/l)\gamma_\omega e^{j\omega t};$$

$$\gamma_\omega = (\omega^2 - \gamma_R\gamma_G) - j\omega(\gamma_R + \gamma_G);$$

$$\widetilde{u}(x,0) = -U_0\left(1-\frac{x}{l}\right),\ \left.\frac{\partial \widetilde{u}}{\partial t}\right|_{t=0} = -j\omega U_0\left(1-\frac{x}{l}\right),\ x \in [0,l]; \quad (2.8)$$

$$\widetilde{u}(0,t) = \widetilde{u}(l,t) = 0,\ t \geq 0. \quad (2.9)$$

Let's assign $\widetilde{u}(x,t) = \sum_{k=1}^{\infty} c_k(t)\sin\frac{\pi k x}{l}$, $f(x,t) = \sum_{k=1}^{\infty} f_k(t)\sin\frac{\pi k x}{l}$, then substitute them in (2.7). So we obtain the second-degree ordinary differential equation with respect to amplitudes $c_k(t)$

$$\ddot{c}_k(t) + (\gamma_R + \gamma_G)\dot{c}_k(t) + \gamma_k c_k(t) = f_k(t), \quad (2.10)$$

$$\gamma_k = \left(\frac{a\pi k}{l}\right)^2 + \gamma_R\gamma_G,\ f_k(t) = \frac{2U_0\gamma_\omega}{\pi k}e^{j\omega t}.$$

The general solution of this equation in case when $m_1 \neq m_2$ is the following

$$c_k(t) = c_{1k}e^{m_1 t} + c_{2k}e^{m_2 t} + F_k(t);$$

$$F_k(t) = \frac{2U_0\gamma_\omega}{\pi k(j\omega - m_1)}\left(\frac{e^{j\omega t} - e^{m_2 t}}{j\omega - m_2} - \frac{e^{m_1 t} - e^{m_2 t}}{m_1 - m_2}\right),$$

And in the case of multiple roots $m_1 = m_2$ one can obtain

$$c_k(t) = (c_{1k} + c_{2k}t)e^{m_1 t} + F_k(t);$$

$$F_k(t) = \frac{2U_0\gamma_\omega\left[e^{j\omega t} - (1 + t(j\omega - m_1))e^{m_1 t}\right]}{\pi k(j\omega - m_1)^2}.$$

The numbers m_1, m_2 represent the roots of the characteristic equation $m^2 + (\gamma_R + \gamma_G)m + \gamma_k = 0$:

$$m_1 = -\alpha_k + \beta_k,\ m_2 = -\alpha_k - \beta_k,$$

$$\alpha_k = 0.5(\gamma_R + \gamma_G),\ \beta_k = 0.5\sqrt{(\gamma_R - \gamma_G)^2 - \left(\frac{2a\pi k}{l}\right)^2}.$$

The values of the constants c_{1k}, c_{2k} are determined by meeting the initial condition (2.8)

$$c_{1k} = -\frac{2U_0(j\omega - m_2)}{\pi k(m_1 - m_2)},\ c_{2k} = \frac{2U_0(j\omega - m_1)}{\pi k(m_1 - m_2)}.$$

Than the solution of (2.4) – (2.6) takes the following form:

$$u(x,t) = \sum_{k=1}^{\infty}\left[\frac{2U_0}{\pi k(m_1 - m_2)}\left((j\omega - m_1)e^{m_1 t} - (j\omega - m_2)e^{m_2 t}\right) + \right.$$

$$\left. + F_k(t)\right]\sin\frac{\pi k x}{l} + U_0\left(1 - \frac{x}{l}\right)e^{j\omega t}.$$

After some transformation we have

$$u(x,t) = 2U_0\sum_{k=1}^{\infty}\left[\frac{(a\pi k)^2}{l^2(m_1 - m_2)}\left(\frac{e^{m_2 t}}{j\omega - m_2} - \frac{e^{m_1 t}}{j\omega - m_1}\right) + \right.$$

$$+\frac{l^2\gamma_\omega e^{j\omega t}}{(a\pi k)^2-l^2\gamma_\omega}\Bigg]\frac{\sin(\pi kx/l)}{\pi k}+U_0\left(1-\frac{x}{l}\right)e^{j\omega t}. \qquad (2.11)$$

The current function $i(x,t)$ can be determined by substitution of the relation (2.11) in the first equation from (2.1)

$$i(x,t)=\frac{2U_0}{Ll}\left\{\sum_{k=1}^{\infty}\left(\frac{a\pi k}{l}\right)^2\frac{e^{-\gamma_R t}(j\omega+\gamma_G)\cos(\pi kx/l)}{(j\omega-m_1)(j\omega-m_2)(\gamma_R+m_1)(\gamma_R+m_2)}+\right.$$

$$+\sum_{k=1}^{\infty}\left(\frac{a\pi k}{l}\right)^2\frac{\cos(\pi kx/l)}{m_1-m_2}\left(\frac{e^{m_1 t}}{(j\omega-m_1)(\gamma_R+m_1)}-\frac{e^{m_2 t}}{(j\omega-m_2)(\gamma_R+m_2)}\right)+$$

$$\left.+\frac{e^{-\gamma_R t}-e^{j\omega t}}{2(j\omega+\gamma_R)}\left(-1+2\gamma_\omega\sum_{k=1}^{\infty}\frac{l^2\cos(\pi kx/l)}{(a\pi k)^2-l^2\gamma_\omega}\right)\right\}. \qquad (2.12)$$

The formula (2.12) can be essentially simplified. The series with the multiplier $e^{-\gamma_R t}$ cancel, but the expression in the last round bracket can be summed up. As a result we obtain the following formula:

$$i(x,t)=-\frac{U_0 e^{-\gamma_R t}}{l\delta Z_0}+\frac{U_0 e^{j\omega t}}{Z_0\,\mathrm{sh}(\delta l)}\mathrm{ch}\delta(l-x)+$$

$$+\frac{2U_0}{lL}\sum_{k=1}^{\infty}\left(\frac{a\pi k}{l}\right)^2\frac{\cos(\pi kx/l)}{m_1-m_2}\left(\frac{e^{m_1 t}}{(j\omega-m_1)(\gamma_R+m_1)}-\right.$$

$$\left.-\frac{e^{m_2 t}}{(j\omega-m_2)(\gamma_R+m_2)}\right). \qquad (2.13)$$

Here the expressions

$$\delta=\sqrt{(R+j\omega L)(G+j\omega C)}\ \text{ and }\ Z_0=\sqrt{(R+j\omega L)/(G+j\omega C)}$$

identify the propagation coefficient of the electromagnetic wave and the line impedance.

To obtain the real solution of the problem (2.1) – (2.3) it is necessary to take the imaginary components of the formulas (2.11) and (2.13).

Let study the asymptotic properties of the solution (2.13) for the steady-state values of the current at the sending end of the line $x = 0$ when $t \to \infty$. As the roots $m_{1,2}$ of the characteristic equation have the negative imaginary component in case when $R \neq 0$ or $G \neq 0$, then under the condition $t \to \infty$ the last term of the expression (2.13) tends to zero and we obtain the solution of the following form

$$i(0,t) = -\frac{U_0 e^{-\gamma_R t}}{l\delta Z_0} + \frac{U_0 e^{j\omega t}}{Z_0 \mathrm{th}(\delta l)} = -\frac{U_0 e^{-\gamma_R t}}{l(R + j\omega L)} + I_0 e^{j\omega t},$$

where by I_0 is denoted the complex amplitude of the current.

Farther, if $R \neq 0$, then at the limit we obtain the solution

$$i(0,t) = I_0 e^{j\omega t}, \quad I_0 = \frac{U_0}{Z_0 \mathrm{th}(\delta l)} = \frac{U_0}{Z_{BX}}, \quad Z_{BX} = Z_0 \mathrm{th}(\delta l),$$

that coincides with the solution obtained by the complex amplitude method (CAM). In the case when $R = 0$ and $G \neq 0$ the steady-state solution is the following

$$i(0,t) = -\frac{U_0}{j\omega L l} + I_0 e^{j\omega t} = \frac{jU_0}{\omega L l} + I_0 e^{j\omega t}.$$

This solution already differs from the solution obtained by CAM on the constant component $\Delta I = U_0 / X_L$ that is determined only by inductive impedance $X_L = \omega L l$ and is independent of other lineal parameters.

Let's consider also the particular case of the solution (2.13) for ideal line $(R = G = 0)$ when $x = 0$. In this case $\gamma_R = \gamma_G = 0$, $\delta = j\omega / a$, $Z_0 = Z_B = \sqrt{L/C}$ and the roots of the characteristic equation have the form $m_{1,2} = \pm j(a\pi k / l) = \pm j(\pi k / \Delta)$, where $\Delta = l / a$ is the wave runtime along the line. Then the series from the (2.13) can be represented in the following form

$$\frac{2U_0}{lL}\sum_{k=1}^{\infty}\left(\frac{a\pi k}{l}\right)^2\frac{\cos(\pi kx/l)}{m_1-m_2}\left(\frac{e^{m_1 t}}{(j\omega-m_1)(\gamma_R+m_1)}-\frac{e^{m_2 t}}{(j\omega-m_2)(\gamma_R+m_2)}\right)=$$

$$=\frac{2U_0}{lL}\sum_{k=1}^{\infty}\frac{-\frac{\pi k}{\Delta}\sin\frac{\pi kt}{\Delta}+j\omega\cos\frac{\pi kt}{\Delta}}{\omega^2-\left(\frac{\pi k}{\Delta}\right)^2}.$$

Since $lL=\Delta Z_B$ then from (2.13) we obtain the real solution for ideal line

$$i(0,t)=\frac{U_0}{Z_B}\left[\frac{1}{\omega\Delta}-\operatorname{ctg}(\omega\Delta)\cos(\omega t)+2\omega\Delta\sum_{k=1}^{\infty}\frac{\cos\frac{\pi kt}{\Delta}}{(\omega\Delta)^2-(\pi k)^2}\right]. \quad (2.14)$$

The formula (2.14) represents the algebraic sum of three terms each of them being the periodical function with different periods. The first term is constant, the second one contains the function $\cos(\omega t)$ that is a periodical function with period $T_1=2\pi/\omega$ and the third term is represented as a series that is also a periodical function with period $T_2=2\Delta$. Therefore the current function $i(0,t)$ will be a periodical function with period T if there are two integer positive numbers k^* and n^* such as

$$T=k^*T_1=n^*T_2 \quad \text{or when } \omega=2\pi: \quad \frac{T_1}{T_2}=\frac{\pi}{\omega\Delta}=\frac{n^*}{k^*}=\frac{1}{2\Delta}.$$

Thus, if $\omega=2\pi$ and Δ is a rational number, than the solution $i(0,t)$ will be a periodical function with period $T=k^*=2n^*\Delta$. The formula (2.14) can be written in a closed form. By expansion in Fourier series it is easy to demonstrate that function $\cos\omega(t-\Delta)$ on the segment $t\in[0,2\Delta]$ can be represented in the form of series

$$\frac{\cos\omega(t-\Delta)}{\sin(\omega\Delta)}=\frac{1}{\omega\Delta}+2\omega\Delta\sum_{k=1}^{\infty}\frac{\cos\dfrac{\pi kt}{\Delta}}{(\omega\Delta)^2-(\pi k)^2},\quad t\in[0,\,2\Delta]. \qquad (2.15)$$

As it follows from (2.15) the function $\cos\omega(t-\Delta)$ is a periodical function with the period 2Δ, then for any t the sum of the series in (2.15) can be written as

$$\frac{1}{\omega\Delta}+2\omega\Delta\sum_{k=1}^{\infty}\frac{\cos\dfrac{\pi kt}{\Delta}}{(\omega\Delta)^2-(\pi k)^2}=\frac{\cos\omega(t-(2n-1)\Delta)}{\sin(\omega\Delta)},$$

$$t\in[2(n-1)\Delta,2n\Delta],\ n=1,2,3,...$$

and then (2.14) can be re-arranged to the form

$$i(0,t)=\frac{U_0}{Z_B}\left[\frac{\cos\omega(t-(2n-1)\Delta)}{\sin(\omega\Delta)}-\mathrm{ctg}(\omega\Delta)\cos(\omega t)\right], \qquad (2.16)$$

$$t\in[2(n-1)\Delta,2n\Delta],\ n=1,2,3,...$$

After some not complicated transformations we obtain the following representation for the formula (2.16):

$$i(0,t)=\frac{U_0}{Z_B}\left[\sin(\omega t)+2\frac{\sin\omega(n-1)\Delta\sin\omega(t-n\Delta)}{\sin(\omega\Delta)}\right], \qquad (2.17)$$

$$t\in[2(n-1)\Delta,2n\Delta],\ n=1,2,3,...$$

The identical expression for current function was obtained by means of method of characteristics in [89]. Specifically, for the quarter-wave line ($\Delta=1/4$, $\omega=2\pi$, $\sin(\omega\Delta)=1$), considering that $\cos\omega(t-(2n-1)\Delta)=$ $=(-1)^{n-1}\sin(2\pi t)$, one can obtain from (2.16) the quite simple solution

$$i(0,t)=\frac{U_0(-1)^{n-1}\sin(2\pi t)}{Z_B},\quad t\in[(n-1)/2,\,n/2],\,n=1,2,3,\ldots \quad (2.18)$$

From (2.13) we can obtain as well the solution for undistorting line ($\gamma_R=\gamma_G=\gamma$) when $x=0$ (here and later by the term "undistorting line" we understand the line with no distortions). In this case $\delta=(\gamma+j\omega)/a$, $\delta l=(\gamma+j\omega)\Delta$, $Z_0=Z_B=\sqrt{L/C}$, $lL=\Delta Z_B$ and the roots of the characteristic equation have the following form $m_{1,2}=-\gamma\pm j(a\pi k/l)=$ $=-\gamma\pm j(\pi k/\Delta)$, where $\Delta=l/a$ is the wave runtime along the line. Then the formula (2.13) at the point $x=0$ can be represented in the following form

$$i(0,t)=-\frac{U_0e^{-\gamma_R t}}{l\delta Z_0}+\frac{U_0e^{j\omega t}}{Z_0\mathrm{sh}(\delta l)}\mathrm{ch}\delta l+$$

$$+\frac{2U_0}{lL}\sum_{k=1}^{\infty}\left(\frac{a\pi k}{l}\right)^2\frac{1}{m_1-m_2}\left(\frac{e^{m_1t}}{(j\omega-m_1)(\gamma_R+m_1)}-\frac{e^{m_2t}}{(j\omega-m_2)(\gamma_R+m_2)}\right)=$$

$$=\frac{U_0e^{j\omega t}}{Z_B}\mathrm{cth}\Delta(\gamma+j\omega)-\frac{U_0e^{-\gamma t}}{Z_B(\gamma+j\omega)\Delta}-$$

$$-\frac{U_0e^{-\gamma t}}{Z_B\Delta}\sum_{k=1}^{\infty}\left(\frac{e^{j\pi kt/\Delta}}{\gamma+j(\omega-\pi k/\Delta)}+\frac{e^{-j\pi kt/\Delta}}{\gamma+j(\omega+\pi k/\Delta)}\right)=$$

$$=\frac{U_0e^{j\omega t}}{Z_B}\mathrm{cth}\Delta(\gamma+j\omega)-\frac{U_0e^{-\gamma t}}{Z_B\Delta}\sum_{k=-\infty}^{\infty}\frac{e^{j\pi kt/\Delta}}{\gamma+j(\omega-\pi k/\Delta)}. \quad (2.19)$$

By direct expansion in Fourier series it is easy to demonstrate that the series in formula (2.19) for any t can be written in the following final form:

$$\sum_{k=-\infty}^{\infty}\frac{e^{j\pi kt/\Delta}}{\gamma+j(\omega-\pi k/\Delta)}=\frac{2\Delta e^{(\gamma+j\omega)t}}{e^{2(n+1)(\gamma+j\omega)\Delta}-e^{2n(\gamma+j\omega)\Delta}}=$$

$$= \frac{2\Delta e^{(\gamma+j\omega)t} e^{-2(n+1)(\gamma+j\omega)\Delta}}{1-e^{-2(\gamma+j\omega)\Delta}}, \quad t \in [2n\Delta, 2(n+1)\Delta], \quad n = 0,1,2,...$$

Substituting this expression in formula (2.19) we obtain the final presentation for current at the sending end of the line

$$i(0,t) = \frac{U_0 e^{j\omega t}}{Z_B}\left(\text{cth}\Delta(\gamma + j\omega) - \frac{2e^{-2(n+1)(\gamma+j\omega)\Delta}}{1-e^{-2(\gamma+j\omega)\Delta}}\right), \tag{2.20}$$

$$t \in [2n\Delta, 2(n+1)\Delta], \quad n = 0,1,2,...$$

In particular, for quarter-wave line ($\Delta = 1/4$, $\omega = 2\pi$) from (2.20) we have the real solution

$$\text{cth}\Delta(\gamma + j\omega) = \text{th}(\gamma/4), \quad e^{-2(n+1)(\gamma+j\omega)\Delta} = \left(-e^{-\gamma/2}\right)^{n+1},$$

$$i(0,t) = \frac{U_0 \sin(2\pi t)}{Z_B}\left(\text{th}(\gamma/4) - \frac{2\left(-e^{-\gamma/2}\right)^{n+1}}{1+e^{-\gamma/2}}\right) =$$

$$= \frac{U_0 \sin(2\pi t)}{Z_B}\left(1 - 2e^{-\gamma/2}\,\frac{1-(-1)^n e^{-n\gamma/2}}{1+e^{-\gamma/2}}\right), \tag{2.21}$$

$$t \in [n/2, (n+1)/2], \quad n = 0,1,2,...,$$

that coincides with the solution obtained by method of characteristic [89].

Let's consider now the problem of determining of the unknown quantities in the open-circuited line with the given sinusoidal current at the sending end. Thus, it is necessary to determine the voltage $u(x,t)$ and current $i(x,t)$ functions satisfying the system of telegraph equations

$$L\frac{\partial i}{\partial t} + \frac{\partial u}{\partial x} + Ri = 0; \quad C\frac{\partial u}{\partial t} + \frac{\partial i}{\partial x} + Gu = 0 \text{ when } x \in (0,l), \quad t > 0 \tag{2.22}$$

and the following initial and boundary conditions:

$$u(x,0) = i(x,0) = 0, \;\; x \in [0,l]; \tag{2.23}$$

$$i(0,t) = I_0 \sin \omega t, \;\; i(l,t) = 0, \;\; t \geq 0. \tag{2.24}$$

In case of idling the boundary conditions are formulated in terms of current only. Therefore by elimination of the voltage function $u(x,t)$ from (2.22) – (2.24) we obtain the following boundary-value problem formulated with respect to current function $i(x,t)$:

$$LC\frac{\partial^2 i}{\partial t^2} + (LG + RC)\frac{\partial i}{\partial t} = \frac{\partial^2 i}{\partial x^2} - RGi$$

or

$$\frac{\partial^2 i}{\partial t^2} + (\gamma_R + \gamma_G)\frac{\partial i}{\partial t} = a^2 \frac{\partial^2 i}{\partial x^2} - \gamma_R \gamma_G i \text{ when } x \in (0,l), \;\; t > 0 \tag{2.25}$$

$$i(x,0) = \left.\frac{\partial i}{\partial t}\right|_{t=0} = 0, \;\; x \in [0,l]; \tag{2.26}$$

$$i(0,t) = I_0 e^{j\omega t}, \;\; i(l,t) = 0, \;\; t \geq 0. \tag{2.27}$$

The problem (2.25)-(2.27) also can be solved by means of Fourier series expansion method and its solution can be represented in the form

$$i(x,t) = 2I_0 \sum_{k=1}^{\infty} \left[\frac{(a\pi k)^2}{l^2 (m_1 - m_2)} \left(\frac{e^{m_2 t}}{j\omega - m_2} - \frac{e^{m_1 t}}{j\omega - m_1} \right) + \right.$$

$$\left. + \frac{l^2 \gamma_\omega e^{j\omega t}}{(a\pi k)^2 - l^2 \gamma_\omega} \right] \frac{\sin(\pi k x / l)}{\pi k} + I_0 \left(1 - \frac{x}{l}\right) e^{j\omega t}; \tag{2.28}$$

$$u(x,t) = \frac{2I_0}{Cl} \left\{ \sum_{k=1}^{\infty} \left(\frac{a\pi k}{l} \right)^2 \frac{e^{-\gamma_G t} (j\omega + \gamma_R) \cos(\pi k x / l)}{(j\omega - m_1)(j\omega - m_2)(\gamma_G + m_1)(\gamma_G + m_2)} + \right.$$

$$+\sum_{k=1}^{\infty}\left(\frac{a\pi k}{l}\right)^2\frac{\cos(\pi kx/l)}{m_1-m_2}\left(\frac{e^{m_1 t}}{(j\omega-m_1)(\gamma_G+m_1)}-\frac{e^{m_2 t}}{(j\omega-m_2)(\gamma_G+m_2)}\right)+$$

$$+\frac{e^{-\gamma_G t}-e^{j\omega t}}{2(j\omega+\gamma_G)}\left(-1+2\gamma_\omega\sum_{k=1}^{\infty}\frac{l^2\cos(\pi kx/l)}{(a\pi k)^2-l^2\gamma_\omega}\right)\Bigg\}. \qquad (2.29)$$

The formula (2.29) can be essentially simplified. The series, that contain as a factor $e^{-\gamma_G t}$, cancel and the expression in the last round bracket can be summed. As a result we obtain the following representation for voltage function:

$$u(x,t)=-\frac{I_0 Z_0 e^{-\gamma_G t}}{\delta l}+\frac{I_0 Z_0 e^{j\omega t}}{\mathrm{sh}(\delta l)}\mathrm{ch}\delta(l-x)+$$

$$+\frac{2I_0}{lC}\sum_{k=1}^{\infty}\left(\frac{a\pi k}{l}\right)^2\frac{\cos(\pi kx/l)}{m_1-m_2}\left(\frac{e^{m_1 t}}{(j\omega-m_1)(\gamma_G+m_1)}-\right.$$

$$\left.-\frac{e^{m_2 t}}{(j\omega-m_2)(\gamma_G+m_2)}\right). \qquad (2.30)$$

To obtain the real solution of the problem (2.22) – (2.24) it is necessary to take the imaginary components of the formulas (2.28) and (2.30).

Let's study the solution (2.30) at the sending end of the line ($x=0$) for the steady-state regime when $t\to\infty$. As the roots of the characteristic equation $m_{1,2}$ have the negative real component in case when $R\neq 0$ or $G\neq 0$, then under the condition $t\to\infty$ the last term of the expression (2.30) tends to zero and we obtain the solution of the following form

$$u(0,t)=-\frac{I_0 Z_0 e^{-\gamma_G t}}{\delta l}+\frac{I_0 Z_0 e^{j\omega t}}{\mathrm{th}(\delta l)}=-\frac{I_0 e^{-\gamma_G t}}{l(G+j\omega C)}+U_0 e^{j\omega t},$$

where by U_0 is denoted the complex amplitude of the voltage.

Farther, if $G\neq 0$, then at the limit we obtain the solution

$$u(0,t) = U_0 e^{j\omega t}, \quad U_0 = \frac{I_0 Z_0}{\text{th}(\delta l)} = Z_{BX} I_0, \quad Z_{BX} = \frac{Z_0}{\text{th}(\delta l)}.$$

This coincides with the solution obtained by CAM. In the case when $G = 0$ and $R \neq 0$ the steady-state solution is the following

$$u(0,t) = -\frac{I_0}{j\omega Cl} + U_0 e^{j\omega t} = \frac{jI_0}{\omega Cl} + U_0 e^{j\omega t}.$$

This solution already differs from the solution obtained by CAM on the constant component $\Delta U = I_0 X_C$, that is determined only by capacitance $X_C = 1/\omega Cl$ and is independent of other lineal parameters.

Let's consider also the particular case of the solution (2.30) for ideal line $(R = G = 0)$ when $x = 0$. In this case $\gamma_R = \gamma_G = 0$, $\delta = j\omega/a$, $Z_0 = Z_B = \sqrt{L/C}$ and the roots of the characteristic equation have the form $m_{1,2} = \pm j(a\pi k/l) = \pm j(\pi k/\Delta)$, where $\Delta = l/a$ is the wave runtime along the line. Then the series from the (2.30) can be represented in the form

$$\frac{2I_0}{lC}\sum_{k=1}^{\infty}\left(\frac{a\pi k}{l}\right)^2 \frac{\cos(\pi kx/l)}{m_1 - m_2}\left(\frac{e^{m_1 t}}{(j\omega - m_1)(\gamma_G + m_1)} - \frac{e^{m_2 t}}{(j\omega - m_2)(\gamma_G + m_2)}\right) =$$

$$= \frac{2I_0}{lC}\sum_{k=1}^{\infty}\frac{-\frac{\pi k}{\Delta}\sin\frac{\pi kt}{\Delta} + j\omega\cos\frac{\pi kt}{\Delta}}{\omega^2 - \left(\frac{\pi k}{\Delta}\right)^2}.$$

Since $lC = \Delta/Z_B$ then from (2.30) we obtain the real solution for ideal line

$$u(0,t) = I_0 Z_B\left[\frac{1}{\omega\Delta} - \text{ctg}(\omega\Delta)\cos(\omega t) + 2\omega\Delta\sum_{k=1}^{\infty}\frac{\cos\frac{\pi kt}{\Delta}}{(\omega\Delta)^2 - (\pi k)^2}\right]. \qquad (2.31)$$

The formula (2.31) represents the algebraic sum of three terms each of them being the periodical function with different periods. The first term is constant, the second one contains the function $\cos(\omega t)$ that is a periodical function with period $T_1 = 2\pi/\omega$ and the third term is represented as a series that is also a periodical function with period $T_2 = 2\Delta$. Therefore the voltage function $u(0,t)$ will be a periodical function with period T if there are two integer positive numbers k^* and n^* such as

$$T = k^* T_1 = n^* T_2 \qquad \text{or when } \omega = 2\pi: \qquad \frac{T_1}{T_2} = \frac{\pi}{\omega\Delta} = \frac{n^*}{k^*} = \frac{1}{2\Delta}.$$

Thus, if Δ is a rational number and $\omega = 2\pi$, than the solution $u(0,t)$ will be a periodical function with period $T = k^* = 2n^*\Delta$. The formula (2.31) can be written in a closed form. By expansion in Fourier series it is easy to demonstrate that function $\cos\omega(t-\Delta)$ on segment $t \in [0, 2\Delta]$ can be represented in the form of series

$$\frac{\cos\omega(t-\Delta)}{\sin(\omega\Delta)} = \frac{1}{\omega\Delta} + 2\omega\Delta\sum_{k=1}^{\infty}\frac{\cos\dfrac{\pi k t}{\Delta}}{(\omega\Delta)^2 - (\pi k)^2}, \quad t \in [0,\, 2\Delta]. \qquad (2.32)$$

Since $\cos\omega(t-\Delta)$ is a periodical function with period 2Δ, then for any t the sum of the series in (2.32) can be written as

$$\frac{1}{\omega\Delta} + 2\omega\Delta\sum_{k=1}^{\infty}\frac{\cos\dfrac{\pi k t}{\Delta}}{(\omega\Delta)^2 - (\pi k)^2} = \frac{\cos\omega(t-(2n-1)\Delta)}{\sin(\omega\Delta)},$$

$$t \in [2(n-1)\Delta, 2n\Delta],\ n = 1,2,3,...$$

Then (2.31) can be re-arranged to the form

$$u(0,t) = I_0 Z_B\left[\frac{\cos\omega(t-(2n-1)\Delta)}{\sin(\omega\Delta)} - \operatorname{ctg}(\omega\Delta)\cos(\omega t)\right], \qquad (2.33)$$

$$t \in [2(n-1)\Delta, 2n\Delta],\ n = 1,2,3,...$$

After some not complicated transformations we obtain the following representation for formula (2.33):

$$u(0,t) = I_0 Z_B \left[\sin(\omega t) + 2 \frac{\sin \omega(n-1)\Delta \sin \omega(t-n\Delta)}{\sin(\omega\Delta)} \right], \qquad (2.34)$$

$$t \in [2(n-1)\Delta, 2n\Delta],\ n = 1,2,3,...$$

Specifically, for the quarter-wave line ($\Delta = 1/4$, $\omega = 2\pi$, $\sin(\omega\Delta) = 1$), considering that $\cos\omega(t-(2n-1)\Delta) = (-1)^{n-1}\sin(2\pi t)$, one can obtain from (2.33) the following solution

$$u(0,t) = I_0 Z_B (-1)^{n-1} \sin(2\pi t), \quad t \in [(n-1)/2,\ n/2],\ n = 1,2,3,... \qquad (2.35)$$

Let's consider the particular case of the solution (2.30) for undistorting line ($\gamma_R = \gamma_G = \gamma$) when $x = 0$. In this case $\delta = (\gamma + j\omega)/a$, $\delta l = (\gamma + j\omega)\Delta$, $Z_0 = Z_B = \sqrt{L/C}$, $lC = \Delta / Z_B$ and the roots of the characteristic equation have the following form $m_{1,2} = -\gamma \pm j(a\pi k / l) = -\gamma \pm j(\pi k / \Delta)$, where $\Delta = l/a$ is the wave runtime along the line. Then the formula (2.30) when $x = 0$ can be represented in the form

$$u(0,t) = -\frac{I_0 Z_0 e^{-\gamma_G t}}{\delta l} + \frac{I_0 Z_0 e^{j\omega t}}{\mathrm{sh}(\delta l)} \mathrm{ch}\delta l +$$

$$+ \frac{2I_0}{lC} \sum_{k=1}^{\infty} \left(\frac{a\pi k}{l} \right)^2 \frac{1}{m_1 - m_2} \left(\frac{e^{m_1 t}}{(j\omega - m_1)(\gamma_G + m_1)} - \frac{e^{m_2 t}}{(j\omega - m_2)(\gamma_G + m_2)} \right) =$$

$$= I_0 Z_B e^{j\omega t} \mathrm{cth}\Delta(\gamma + j\omega) - \frac{I_0 Z_B e^{-\gamma t}}{(\gamma + j\omega)\Delta} -$$

$$- \frac{I_0 Z_B e^{-\gamma t}}{\Delta} \sum_{k=1}^{\infty} \left(\frac{e^{j\pi k t/\Delta}}{\gamma + j(\omega - \pi k/\Delta)} + \frac{e^{-j\pi k t/\Delta}}{\gamma + j(\omega + \pi k/\Delta)} \right) =$$

$$= I_0 Z_B e^{j\omega t} \operatorname{cth}\Delta(\gamma + j\omega) - \frac{I_0 Z_B e^{-\gamma t}}{\Delta} \sum_{k=-\infty}^{\infty} \frac{e^{j\pi k t/\Delta}}{\gamma + j(\omega - \pi k/\Delta)}. \qquad (2.36)$$

By direct expansion in Fourier series it is easy to demonstrate that the series in formula (2.36) for any t can be written in the following final form:

$$\sum_{k=-\infty}^{\infty} \frac{e^{j\pi k t/\Delta}}{\gamma + j(\omega - \pi k/\Delta)} = \frac{2\Delta e^{(\gamma + j\omega)t}}{e^{2(n+1)(\gamma + j\omega)\Delta} - e^{2n(\gamma + j\omega)\Delta}} =$$

$$= \frac{2\Delta e^{(\gamma + j\omega)t} e^{-2(n+1)(\gamma + j\omega)\Delta}}{1 - e^{-2(\gamma + j\omega)\Delta}}, \quad t \in [2n\Delta,\, 2(n+1)\Delta], \quad n = 0,1,2,...$$

Substituting this expression in formula (2.36) we obtain the final presentation for voltage function at the sending end of the line

$$u(0,t) = I_0 Z_B e^{j\omega t} \left(\operatorname{cth}\Delta(\gamma + j\omega) - \frac{2e^{-2(n+1)(\gamma + j\omega)\Delta}}{1 - e^{-2(\gamma + j\omega)\Delta}} \right), \qquad (2.37)$$

$$t \in [2n\Delta,\, 2(n+1)\Delta], \quad n = 0,1,2,...$$

In particular, for quarter-wave line when $\Delta = 1/4$, $\omega = 2\pi$ from (2.37) we have the real solution

$$\operatorname{cth}\Delta(\gamma + j\omega) = \operatorname{th}(\gamma/4), \quad e^{-2(n+1)(\gamma + j\omega)\Delta} = \left(-e^{-\gamma/2}\right)^{n+1},$$

$$u(0,t) = I_0 Z_B \sin(2\pi t) \left(\operatorname{th}(\gamma/4) - \frac{2\left(-e^{-\gamma/2}\right)^{n+1}}{1 + e^{-\gamma/2}} \right) =$$

$$= I_0 Z_B \sin(2\pi t) \left(1 - 2e^{-\gamma/2} \frac{1 - (-1)^n e^{-n\gamma/2}}{1 + e^{-\gamma/2}} \right), . \qquad (2.38)$$

$$t \in [n/2,\, (n+1)/2], \quad n = 0,1,2,...$$

Thus, the expressions for voltages at the sending end of the ideal and undistorting lines (2.35) and (2.38) are identical with the numerical solutions obtained by method of characteristic [89].

For pictorial presentation let's consider the graphical representation of the obtained solutions for degenerated cases and realize the parametric analysis of the losses effect on the transient and steady-state processes in the unloaded line [92]. The behavior in time of the voltage function at the sending end of the open-circuited quarter-wave line is presented on fig. 2.1 ($R = G = 0$ (*a*); $R = 0.48$, $G = 0$ (*b*); $R = 0.48$, $G = R/5$ (*c*); $R = G = 0.48$ (*d*); $R = 4.8$, $G = 0$ (*e*); $R = 4.8$, $G = R/5$ (*f*)). The steady-state sinusoidal regimes are formed only in the case when there is a leakage current through the line insulation ($G > 0$) and these regimes can be calculated by CAM (see fig. 2.1, *c*, *d*, *f*).

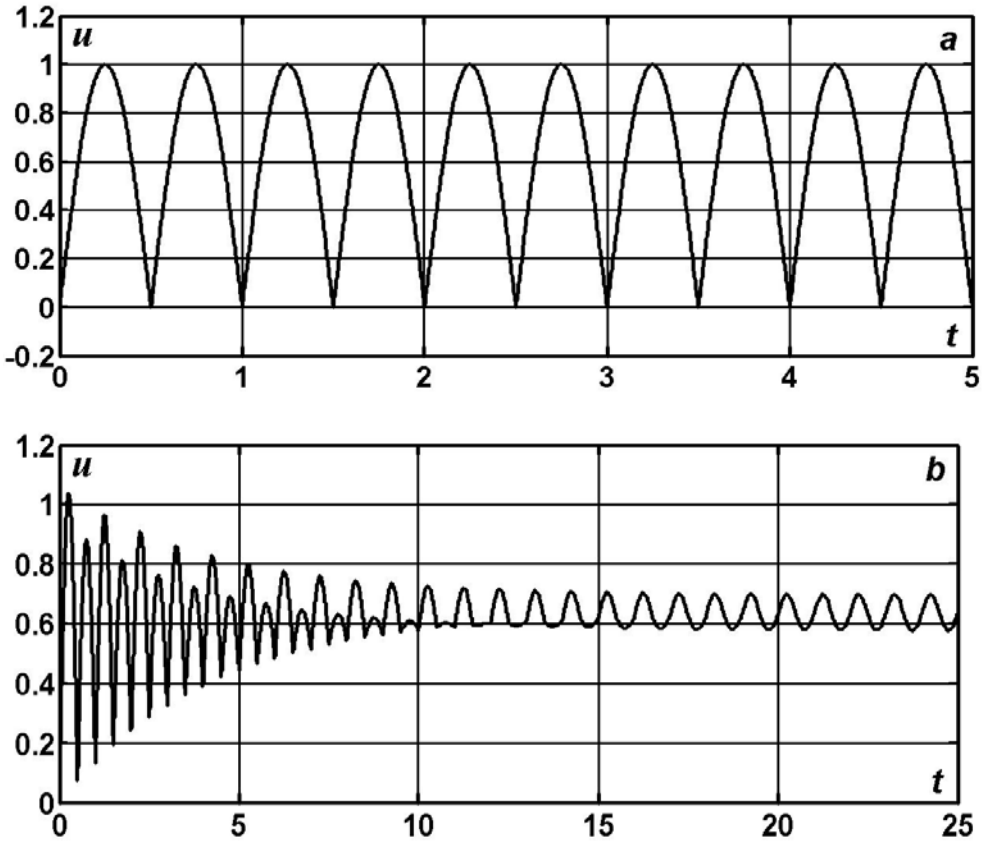

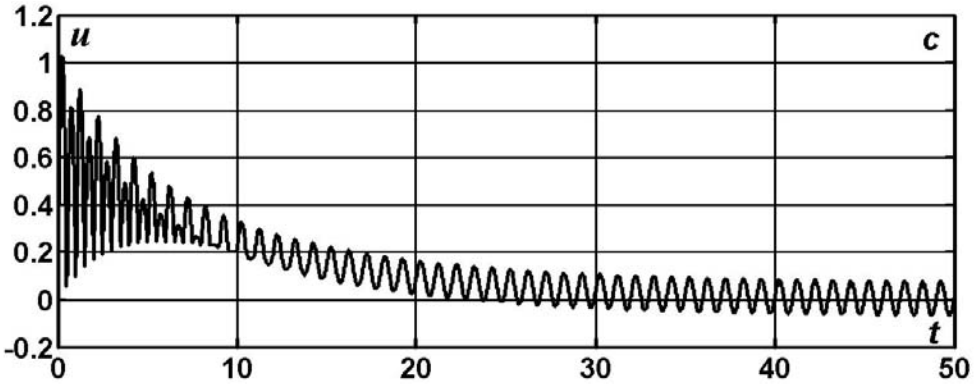

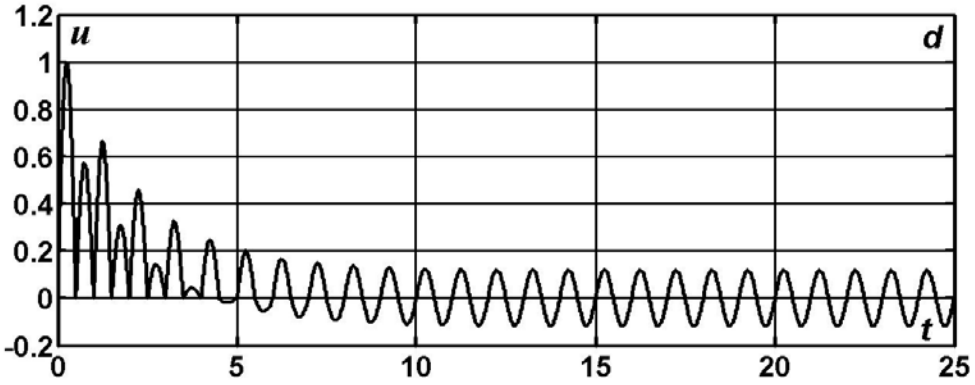

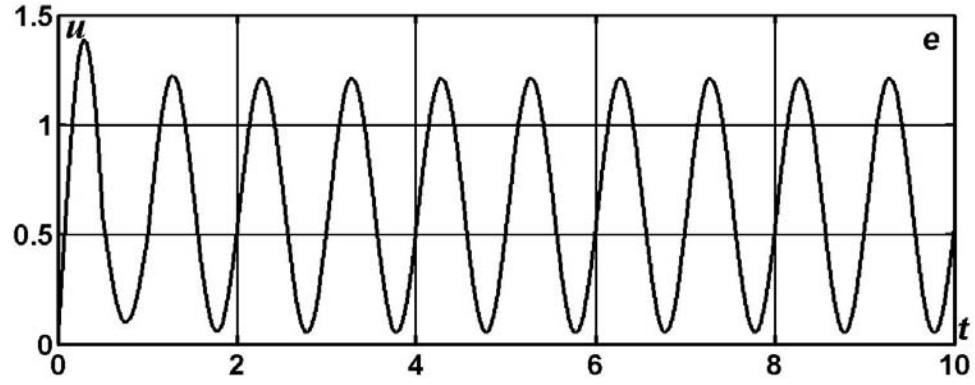

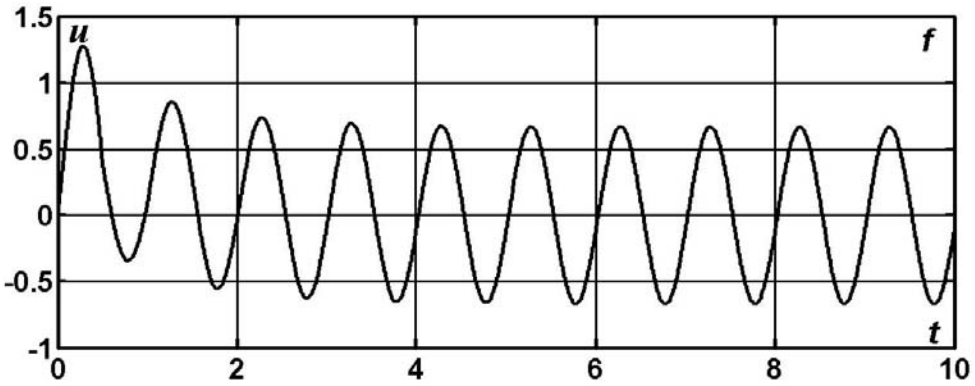

Fig. 2.1. The dynamics of the voltage function at the sending end of the open-circuited quarter-wave line when $R = G = 0$ (***a***); $R = 0.48$, $G = 0$ (***b***); $R = 0.48$, $G = R/5$ (***c***); $R = G = 0.48$ (***d***); $R = 4.8$, $G = 0$ (***e***); $R = 4.8$, $G = R/5$ (***f***).

In case of perfect insulation ($G = 0$) we obtain the displacement of voltages on the constant value that depends only on capacitance and is independent of the value of its active resistance $U_G = I_0 / X_C$. For more details see table 2.1, where the exact values of the voltages at the sending end of the open-circuited sinusoidal current line for different values of its length are presented. Similarly results we obtain for currents in a short-circuited sinusoidal voltage line when $R = 0$ (see table 2.2).

To surprise is the fact that for relatively short lines the steady-state values of the voltage under an idling regime are in small dependence on the level of resistance losses in the line. Highly remarkable is the fig. 2.2 where the voltage time diagrams for ideal line and for line with sufficiently great losses (R = 22.44 mΩ/km) are practically indistinguishable. The obtained results are recent and surely they require more sophisticated physical analysis and experimental validation. Let's remind that CAM is in principle unsuitable for calculation of such degenerated regimes because they are not sinusoidal.

Thus, represented here strongly valid solutions of the telegraph equations constrict even greater the class of problems that can be solved by means of symbolic method. To repeat or make use of results obtained here by classical deductive method it is necessary for user to possess a fund of knowledge in mathematical physics and some experience in the field. To achieve this object it is much easier to commercialize the computer-program **"Albatross"** (see [89, 90]) that executes with eases the analytical solutions with any accuracy rating and that is maximum simple in exploiting.

Thus, the general form of the exact solutions of the telegraph equations is presented for degenerated cases (short circuit and idling). The particular cases of the solutions for ideal and undistorting lines are considered in details that confirmed their complete concordance with the corresponding solutions obtained earlier by method of characteristics and by difference-characteristics algorithm **"Albatross"**.

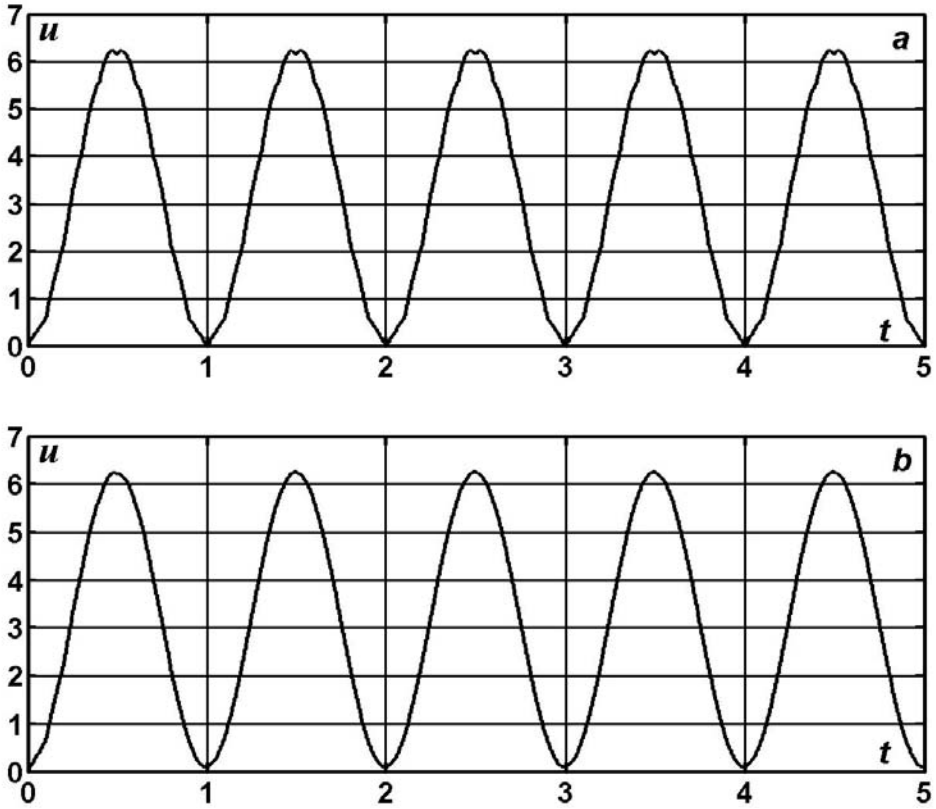

Fig. 2.2. The dynamics of the voltage function at the sending end of the open-circuited line of length l =0.05 when $R = G = 0$ (***a***); $R = 4.8$, $G = 0$ (***b***).

The constant component (unknown up to now) in the current and voltage functions for short-circuited and open-circuited lines connected to the sinusoidal voltage/current source was found out. If in the electric circuit with distributed reactive elements there are no losses on Joule–Lenz effect, then there is no possibility to generate the sinusoidal regime in it. In some cases the same regime doesn't appear even in the presence of losses in the open- circuited (short-circuited) lines.

Table 2.1. Steady-state voltages at the sending end of the open-circuited line with sinusoidal current.

R	G	$l = 0.05$	$l = 0.125$	$l = 0.25$	$l = 0.375$	$l = 0.5$	$l = 5$
0	0	6.2361; 0	2.2361; 0	1; 0	2.2361; –2	$\pm\infty$	$\pm\infty$
0.48	0	**3.1831**±3.0777	**1.2732**±1.0003	**0.6366**±0.0600	**0.4244**±1.0048	**0.3183**±8.3900	**0.0318**±1.2014
0.48	0.01	3.0777	1.0004	0.0612	1.0047	8.2203	1.1908
0.48	0.10	3.0774	1.0007	0.0724	1.0035	6.9572	1.1181
0.48	0.48	3.0694	1.0000	0.1194	1.0000	4.2464	1.0166
4.8	0	**3.1831**±3.0792	**1.2732**±1.0308	**0.6366**±0.5835	**0.4244**±1.2445	**0.3183**±1.3610	**0.0318**±1.1218
4.8	0.01	3.0793	1.0312	0.5845	1.2435	1.3598	1.1218
4.8	0.10	3.0801	1.0352	0.5934	1.2342	1.3492	1.1217
4.8	0.48	3.0767	1.0498	0.6297	1.2001	1.3068	1.1202

Table 2.2. Steady-state currents at the sending end of the short-circuited line with sinusoidal voltage.

R	G	$l = 0.05$	$l = 0.125$	$l = 0.25$	$l = 0.375$	$l = 0.5$	$l = 5$
0	0	6.2361; 0	2.2361; 0	1; 0	2.2361; –2	$\pm\infty$	$\pm\infty$
0	0.48	**3.1831**±3.0777	**1.2732**±1.0003	**0.6366**±0.0600	**0.4244**±1.0048	**0.3183**±8.3900	**0.0318**±1.2014
0.01	0.48	3.0777	1.0004	0.0612	1.0047	8.2203	1.1908
0.10	0.48	3.0774	1.0007	0.0724	1.0035	6.9572	1.1181
0.48	0.48	3.0694	1.0000	0.1194	1.0000	4.2464	1.0166
0	4.8	**3.1831**±3.0792	**1.2732**±1.0308	**0.6366**±0.5835	**0.4244**±1.2445	**0.3183**±1.3610	**0.0318**±1.1218
0.01	4.8	3.0793	1.0312	0.5845	1.2435	1.3598	1.1218
0.10	4.8	3.0801	1.0352	0.5934	1.2342	1.3492	1.1217
0.48	4.8	3.0767	1.0498	0.6297	1.2001	1.3068	1.1202

3. Method of characteristics for ideal and undistorting lines with lumped elements

The system of equations (1.1) is of hyperbolic type with finite velocity of electromagnetic disturbance propagation. If for the line parameters the condition of proportionality or undistorted wave condition $R = \gamma L$, $G = \gamma C$ takes place, then the general solution can be represented in the form of damped progressing waves with arbitrary shape and any localization ratio:

$$i = e^{-\gamma t}\psi(x \pm at);\ \ u = \pm e^{-\gamma t}\psi(x \pm at)/Z_B, \tag{3.1}$$

It results from (3.1) that the invariants of the original system (1.1) keep the constant values along the straight lines $dx/dt = \pm a$, called characteristics:

$$I^{\pm} \equiv e^{\gamma t}(i \pm u/Z_B) = const.$$

Let's remark, that the linear solitary waves during their propagation in the forward and reverse directions run through each other without interaction, this means that any set of them satisfies the original equations. Using these correlations (Riemannian invariants) it is easy to obtain the exact solution at arbitrary point x and time $t > 0$.

As an example let's consider the line with purely active load at the receiving end: $u = R_s i$ when $x = l$. The design domains and the wave-front configurations in the plane of variables xt are presented in the fig. 3.1. Starting from zero initial data when $t = 0$, the voltages and currents are also zero in the domain I, because the electromagnetic disturbance, propagating from the point $x = 0$ with constant velocity along the charge-free conductor, reaches the opposite end of the line $x = l$ after period of time $\Delta = l/a$.

Using the correlations on characteristics with negative slope $dx/dt = -a$: $I^{-} \equiv e^{\gamma t}(i_2 - u_2/Z_B) = i_1 - u_1/Z_B = 0$ and the boundary condition at the input of the linear circuit: $u_2 = U_0(t)$, we obtain $i_2 = U_0/Z_B$ when $x = 0;\ 0 < t \le 2\Delta$.

Let's note especially, that the current at the origin of the line in the initial stage (during the time required for wave double passing over the line length) is independent on the value of the dissipative factor $\gamma > 0$. In other

words the solution for ideal line coincides with the same for undistorting line over the time segment: $x = 0;\ 0 < t \le 2\Delta$.

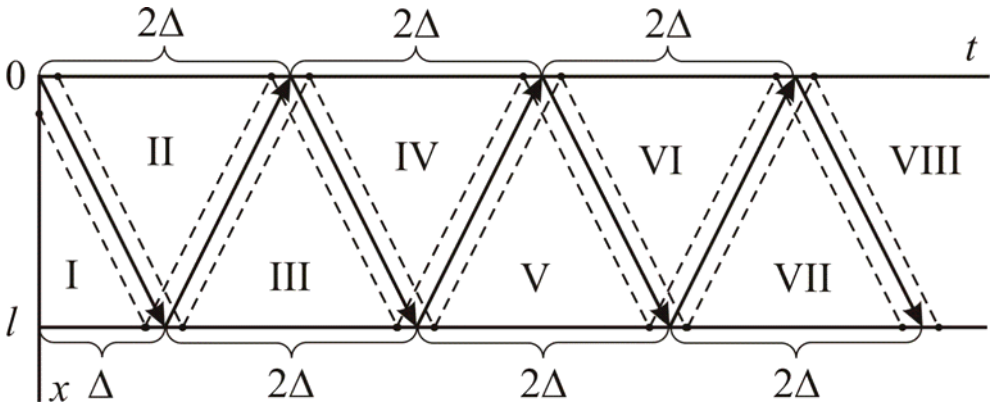

Fig. 3.1. The design domains and the wave-front configurations for uniform transmission line with *RLC* – circuit at the receiving end.

Using now the correlations on characteristics with positive slope $dx/dt = a$:

$$I^+ \equiv e^{\gamma t}(i_3 + u_3/Z_B) = e^{\gamma(t-\Delta)}\left[i_2(t-\Delta) + u_2(t-\Delta)/Z_B\right]$$

and the boundary condition $u_3 = R_S i_3$, we can determine the current

$$i_3 = \frac{Z_B}{Z_B + R_S} e^{-\gamma\Delta}\left[i_2(t-\Delta) + u_2(t-\Delta)/Z_B\right] \text{ when } x = l;\ \Delta < t \le 3\Delta.$$

From the correlation along the line $dx/dt = -a$:

$$I^- \equiv e^{\gamma t}(i_4 - u_4/Z_B) = e^{\gamma(t-\Delta)}\left[i_3(t-\Delta) - u_3(t-\Delta)/Z_B\right]$$

and the boundary condition at the input: $u_4 = U_0(t)$, we have

$$i_4 = U_0(t)/Z_B + e^{-\gamma\Delta}\left[i_3(t-\Delta) - u_3(t-\Delta)/Z_B\right] \text{ when } x = l;\ 2\Delta < t \le 4\Delta.$$

By using this not complicated procedure one can obtain the exact analytical solution for any space-time domain in the plane *xt*, as well as for any form of the input voltage (current). If, particularly, we assign the voltage in the complex form as $u = \exp(j\omega t) = \cos(\omega t) + j\sin(\omega t)$ when $x = 0$, then assigning the frequency $\omega = 0$ and separating the real component from the general solution, we obtain the solution for constant voltage $u = 1$. But if $\omega \neq 0$ and we separate the imaginary component of the solution, then we obtain the solution for sinusoidal voltage: $u = \sin(\omega t)$. Let's cite some exact solutions in the general form for different load regimes setting at the receiving end of the line $x = l$ boundary conditions of (1.3) type.

3.1. Active resistance at the end of the line

Using the boundary condition $u = R_s i$ when $x = l$ and introducing the following notations for dimensionless quantities: $Z_B = U_0 = 1$; $R = G = \gamma$; $z = \dfrac{R_S - Z_B}{R_S + Z_B}$; $E = e^{-(\gamma + j\omega)\Delta}$; $z_E = zE^2$, let's represent unsteady currents and voltages at the end points of the line as follows.

Starting point $x = 0$:

$$u_2 = e^{j\omega t};\ i_2 = e^{j\omega t} \text{ when } 0 < t \le 2\Delta;$$

$$u_4 = e^{j\omega t};\ i_4 = e^{j\omega t}(1 - 2z_E) \text{ when } 2\Delta < t \le 4\Delta;$$

$$u_6 = e^{j\omega t};\ i_6 = e^{j\omega t}\left[1 - 2z_E(1 - z_E)\right] \text{ when } 4\Delta < t \le 6\Delta;$$

$$u_8 = e^{j\omega t};\ i_8 = e^{j\omega t}\left[1 - 2z_E(1 - z_E + z_E^2)\right] = e^{j\omega t}\frac{1 - z_E - 2z_E^4}{1 + z_E}$$

$$\text{when } 6\Delta < t \le 8\Delta;$$

$$u_{10} = e^{j\omega t};\ i_{10} = e^{j\omega t}\left[1 - 2z_E(1 - z_E + z_E^2 - z_E^3)\right] = e^{j\omega t}\frac{1 - z_E + 2z_E^5}{1 + z_E}$$

$$\text{when } 8\Delta < t \le 10\Delta \text{ etc.}$$

The structure of the obtained solution makes it possible to write out the formulas for any arbitrary time interval

$$u_{2n} = e^{j\omega t}\,,\; i_{2n} = e^{j\omega t}\,\frac{1 - z_E - 2(-z_E)^n}{1 + z_E} \qquad (3.2)$$

when $2(n-1)\Delta < t \le 2n\Delta$, $n = 1, 2, 3, \ldots$

Receiving end $x = l$:

$i_1 = u_1 = 0$ when $0 < t \le \Delta$;

$u_3 = (1+z)e^{j\omega t}E$; $i_3 = (1-z)e^{j\omega t}E$ when $\Delta < t \le 3\Delta$;

$u_5 = (1+z)e^{j\omega t}E(1-z_E)$; $i_5 = (1-z)e^{j\omega t}E(1-z_E)$ when $3\Delta < t \le 5\Delta$;

$$u_7 = (1+z)e^{j\omega t}E(1 - z_E + z_E^2) = (1+z)e^{j\omega t}E\,\frac{1-(-z_E)^3}{1+z_E};$$

$$i_7 = (1-z)e^{j\omega t}E(1 - z_E + z_E^2) = (1-z)e^{j\omega t}E\,\frac{1-(-z_E)^3}{1+z_E}$$ when $5\Delta < t \le 7\Delta$;

$$u_9 = (1+z)e^{j\omega t}E(1 - z_E + z_E^2 - z_E^3) = (1+z)e^{j\omega t}E\,\frac{1-(-z_E)^4}{1+z_E};$$

$$i_9 = (1-z)e^{j\omega t}E(1 - z_E + z_E^2 - z_E^3) = (1-z)e^{j\omega t}E\,\frac{1-(-z_E)^4}{1+z_E}$$

when $7\Delta < t \le 9\Delta$;

$$u_{11} = (1+z)e^{j\omega t}E(1 - z_E + z_E^2 - z_E^3 + z_E^4) = (1+z)e^{j\omega t}E\,\frac{1-(-z_E)^5}{1+z_E};$$

$$i_{11} = (1-z)e^{j\omega t}E(1 - z_E + z_E^2 - z_E^3 + z_E^4) = (1-z)e^{j\omega t}E\,\frac{1-(-z_E)^5}{1+z_E}$$

when $9\Delta < t \le 11\Delta$ etc.

The formulas for any arbitrary time interval can be written out in this case too:

$$u_{2n+1} = (1+z)e^{-\gamma\Delta + j\omega(t-\Delta)}\,\frac{1-(-z_E)^n}{1+z_E};$$

$$i_{2n+1} = (1-z)e^{-\gamma\Delta + j\omega(t-\Delta)}\,\frac{1-(-z_E)^n}{1+z_E} \qquad (3.3)$$

when $(2n-1)\Delta < t \le (2n+1)\Delta$, $n = 1, 2, 3, \ldots$.

The solution corresponding to the input voltage $u = \sin(2\pi t)$ when $x = 0$ arrives in the form of imaginary component of the cited above formulas assigning $\omega = 2\pi$. These expressions look to be intricate, but they will become more complicate if we'll try to write out the real solution directly for boundary function $u = \sin(2\pi t)$.

Let's examine the asymptotic properties of the unknown functions when $t \to \infty$. In the case the parameter n in the formulas (3.2), (3.3) tends to infinity as well. The solution's behavior depends strongly on the parameter $z_E = zE^2$. If $|z_E| < 1$, then $(-z_E)^n \to 0$ and the solution takes the form of the periodical sinusoidal function with the period $T = 2\pi/\omega = 1/f = 1$:

$$u(t) = U_0 e^{j\omega t};\ U_0 = 1;\ i(t) = I_0 e^{j\omega t};\ I_0 = \frac{1 - z_E}{1 + z_E} \text{ when } x = 0 \qquad (3.4)$$

and

$$u(t) = U_1 e^{j\omega t};\ U_1 = \frac{1 + z}{1 + z_E} e^{-(\gamma + j\omega)\Delta};$$

$$i(t) = I_1 e^{j\omega t};\ I_1 = \frac{1 - z}{1 + z_E} e^{-(\gamma + j\omega)\Delta} \quad \text{when } x = l. \qquad (3.5)$$

After some transformations we obtain the asymptotic relations that coincide with the correlations obtained by CAM for steady-state (sinusoidal) regimes:

$$Z_0 = Z_B = \sqrt{\frac{L}{C}};\ \delta = \sqrt{(R + j\omega L)(G + j\omega C)} = (\gamma + j\omega)/a;\quad U_1 = R_S I_1;$$

$$Z_{BX} = Z_B \frac{R_S + Z_B \operatorname{th}(\delta l)}{Z_B + R_S \operatorname{th}(\delta l)};\ U_0 = Z_{BX} I_0;\ U_1 = U_0 \operatorname{ch}(\delta l) - Z_0 I_0 \operatorname{sh}(\delta l).$$

The condition $|z_E| < 1$ or $|z_E| = |zE^2| = |ze^{-2(\gamma + j\omega)\Delta}| = |ze^{-2\gamma\Delta}| < 1$ takes place when or $\gamma > 0$ or $|z| < 1$.

In case of short-circuited or open-circuited lines we have $\gamma = 0$, $z = \pm 1$ and, correspondingly, $|z_E| = 1$. Then when $t \to \infty$ the solution of (3.2), (3.3) doesn't tend to purely sinusoidal form. Transforming (3.2), (3.3) and taking

into consideration that $\gamma = 0$, $z = \pm 1$, it is easy to obtain the explicit formulas for real solutions for boundary condition $u(0,t) = \sin(\omega t)$. The solutions have the piecewise sinusoidal form given below.

Short-circuited ideal line:

$$i_{2n} = \frac{1}{\sin \omega\Delta}\left[\cos\omega(t-(2n-1)\Delta) - \cos\omega\Delta\cos\omega t\right]$$

$$\text{when } x = 0;\ 2(n-1)\Delta < t \le 2n\Delta. \tag{3.6}$$

$$i_{2n+1} = \frac{1}{\sin \omega\Delta}\left[\sin\omega t - \sin\omega(t-2n\Delta)\right]$$

$$\text{when } x = l;\ (2n-1)\Delta < t \le (2n+1)\Delta. \tag{3.7}$$

Open-circuited ideal line:

$$i_{2n} = \frac{1}{\cos \omega\Delta}\left[(-1)^{n-1}\sin\omega(t-(2n-1)\Delta) + \sin\omega\Delta\cos\omega t\right]$$

$$\text{when } x = 0,\ 2(n-1)\Delta < t \le 2n\Delta. \tag{3.8}$$

$$u_{2n+1} = \frac{1}{\cos \omega\Delta}\left[\sin\omega t - (-1)^{n}\sin\omega(t-2n\Delta)\right]$$

$$\text{when } x = l,\ (2n-1)\Delta < t \le (2n+1)\Delta. \tag{3.9}$$

The formula (3.6) coincides with the solution (2.16), obtained in the precedent paragraph by means of Fourier method. Using the formulas (3.2), (3.3) we'll write out some solutions for degenerated modes in sinusoidal voltage ideal and undistorting lines with the lengths l = 1/2;1/4;1/8; 3/8.

Ideal ($\gamma = 0$) short-circuited half-wave (l = ½) line:

$$z = -1;\ \Delta = 1/2;\ E = e^{-j\pi} = -1;\ z_E = -1;$$

$$u_{2n} = \sin(2\pi t);\ i_{2n} = \sin(2\pi t)\lim_{z_E \to -1}\frac{1 - z_E - 2(-z_E)^n}{1+z_E} = (2n-1)\sin(2\pi t)$$

$$\text{when } x = 0,\ n - 2\Delta < t \le n;$$

$$u_{2n+1} = 0;\ i_{2n+1} = 2\sin(2\pi(t-\Delta)) \lim_{z_E \to -1} \frac{1-(-z_E)^n}{1+z_E} = 2n\sin(2\pi(t-\Delta))$$

when $x = l,\ n - \Delta < t \le n + \Delta$.

Undistorting ($\gamma > 0$) short-circuited half-wave (l = ½) line:

$$z = -1;\ \Delta = 1/2;\quad E = e^{-\gamma/2 - j\pi} = -e^{-\gamma/2};\ z_E = -e^{-\gamma};$$

$$u_{2n} = \sin(2\pi t);\ i_{2n} = \frac{1+e^{-\gamma}-2e^{-\gamma n}}{1-e^{-\gamma}}\sin(2\pi t) \text{ when } x = 0,\ n - 2\Delta < t \le n;$$

$$u_{2n+1} = 0;\ i_{2n+1} = 2e^{-\gamma/2}\frac{1-e^{-\gamma n}}{1-e^{-\gamma}}\sin(2\pi(t-\Delta))$$

when $x = l,\ n - \Delta < t \le n + \Delta$.

Ideal ($\gamma = 0$) open-circuited have-wave (l = 1/2) line:

$$z = 1;\ \Delta = 1/2;\ E = e^{-j\pi} = -1;\ z_E = 1;$$

$$u_{2n} = \sin(2\pi t);\ i_{2n} = (-1)^{n-1}\sin(2\pi t) \text{ when } x = 0,\ n - 2\Delta < t \le n;$$

$$u_{2n+1} = \left(1-(-1)^n\right)\sin(2\pi(t-\Delta));\ i_{2n+1} = 0$$

when $x = l,\ n - \Delta < t \le n + \Delta$.

Undistorting ($\gamma > 0$) open-circuited have-wave (l = 1/2) line:

$$z = 1;\ \Delta = 1/2;\quad E = e^{-\gamma/2 - j\pi} = -e^{-\gamma/2};\ z_E = e^{-\gamma};$$

$$u_{2n} = \sin(2\pi t);\ i_{2n} = \frac{1-e^{-\gamma}-2(-1)^n e^{-\gamma n}}{1+e^{-\gamma}}\sin(2\pi t)$$

when $x = 0,\ n - 2\Delta < t \le n;$

$$u_{2n+1} = 2e^{-\gamma/2}\frac{1-(-1)^n e^{-n\gamma}}{1+e^{-\gamma}}\sin(2\pi(t-\Delta));\ i_{2n+1} = 0$$

when $x = l,\ n - \Delta < t \le n + \Delta$.

Ideal ($\gamma = 0$) short-circuited quarter -wave (l = 1/4) line:

$$z = -1;\ \Delta = 1/4;\quad E = e^{-j\pi/2} = -j;\ z_E = 1;$$

$$u_{2n} = \sin(2\pi t);\ i_{2n} = (-1)^{n-1}\sin(2\pi t)$$

when $x = 0,\ n/2 - 2\Delta < t \le n/2;$

$$u_{2n+1} = 0;\ i_{2n+1} = \left(1 - (-1)^n\right)\sin(2\pi(t-\Delta))$$

when $x = l,\ n/2 - \Delta < t \le n/2 + \Delta.$

Undistorting ($\gamma > 0$) short-circuited quarter -wave (l = 1/4) line:

$$z = -1;\ \Delta = 1/4;\quad E = e^{-\gamma/4 - j\pi/2} = -je^{-\gamma/4};\ z_E = e^{-\gamma/2};$$

$$u_{2n} = \sin(2\pi t);\ i_{2n} = \frac{1 - e^{-\gamma/2} - 2(-1)^n e^{-\gamma n/2}}{1 + e^{-\gamma/2}}\sin(2\pi t)$$

when $x = 0,\ n/2 - 2\Delta < t \le n/2;$

$$u_{2n+1} = 0;\ i_{2n+1} = 2e^{-\gamma/4}\,\frac{1 - (-1)^n e^{-\gamma n/2}}{1 + e^{-\gamma/2}}\sin(2\pi(t-\Delta))$$

when $x = l,\ n/2 - \Delta < t \le n/2 + \Delta.$

Ideal ($\gamma = 0$) open-circuited quarter -wave (l = 1/4) line:

$$z = 1;\ \Delta = 1/4;\quad E = e^{-j\pi/2} = -j;\ z_E = -1$$

$$u_{2n} = \sin(2\pi t);\ i_{2n} = \sin(2\pi t)\lim_{z_E \to -1}\frac{1 - z_E - 2(-z_E)^n}{1 + z_E} = (2n-1)\sin(2\pi t)$$

when $x = 0,\ n/2 - 2\Delta < t \le n/2;$

$$u_{2n+1} = 2\sin(2\pi(t-\Delta))\lim_{z_E \to -1}\frac{1 - (-z_E)^n}{1 + z_E} = 2(n+1)\sin(2\pi(t-\Delta));$$

$i_{2n+1} = 0$ when $x = l,\ n/2 - \Delta < t \le n/2 + \Delta.$

Undistorting ($\gamma > 0$) open-circuited quarter -wave (l = 1/4) line:

$$z = 1;\ \Delta = 1/4;\quad E = e^{-\gamma/4 - j\pi/2} = -je^{-\gamma/4};\ z_E = -e^{-\gamma/2}$$

$$u_{2n} = \sin(2\pi t)\,;\; i_{2n} = \frac{1 + e^{-\gamma/2} - 2e^{-\gamma n/2}}{1 - e^{-\gamma/2}} \sin(2\pi t)$$

when $x = 0,\ n/2 - 2\Delta < t \le n/2$;

$$u_{2n+1} = 2e^{-\gamma/4} \frac{1 - e^{-\gamma n/2}}{1 - e^{-\gamma/2}} \sin(2\pi(t - \Delta))\,;\; i_{2n+1} = 0$$

when $x = l,\ n/2 - \Delta < t \le n/2 + \Delta$.

Ideal ($\gamma = 0$) short-circuited line with the length l = 1/8:

$$z = -1;\ \Delta = 1/8;\ E = e^{-j\pi/4} = \sqrt{2}(1 - j)/2;\ z_E = j\,;$$

$$u_{2n} = \sin(2\pi t)\,;\; i_{2n} = \begin{cases} \sin(2\pi t), & n = 3, 7, 11, \ldots \\ \sqrt{5}\sin(2\pi t + \varphi);\ \mathrm{tg}(\varphi) = -2, & n = 4, 8, 12, \ldots \\ \sqrt{5}\sin(2\pi t + \varphi);\ \mathrm{tg}(\varphi + \pi) = 2, & n = 1, 5, 9, \ldots \\ \sin(2\pi t + \pi), & n = 2, 6, 10, \ldots \end{cases}$$

when $x = 0,\ n/4 - 2\Delta < t \le n/4$;

$$u_{2n+1} = 0\,;\; i_{2n+1} = \begin{cases} 0, & n = 4, 8, 12, \ldots \\ 2\sin(2\pi t - \pi/4), & n = 1, 5, 9, \ldots \\ 2\sqrt{2}\sin(2\pi t - \pi/2), & n = 2, 6, 10, \ldots \\ 2\cos(2\pi t + 3\pi/4), & n = 3, 7, 11, \ldots \end{cases}$$

when $x = l,\ n/4 - \Delta < t \le n/4 + \Delta$.

Undistorting ($\gamma > 0$) short-circuited line with the length l = 1/8:

$$z = -1;\ \Delta = 1/8;\ E = e^{-\gamma/8 - j\pi/4} = \sqrt{2}(1 - j)e^{-\gamma/8}/2;\ z_E = je^{-\gamma/4};$$

$$u_{2n} = \sin(2\pi t)\,;$$

$$i_{2n} = A\sin(2\pi t + \varphi);\ A = \left[\frac{1 + (e^{-\gamma/4} - 2e^{-\gamma n/4})^2}{1 + e^{-\gamma/2}}\right]^{1/2};$$

$$\varphi = \varphi_1 - \varphi_2;\ \mathrm{tg}\varphi_1 = 2e^{-\gamma n/4} - e^{-\gamma/4};\ \mathrm{tg}\varphi_2 = e^{-\gamma/4};\ n = 3, 7, 11, \ldots$$

$$i_{2n} = A\sin(2\pi t + \varphi);\ A = \left[\frac{(1+2e^{-\gamma n/4})^2 + e^{-\gamma/2}}{1+e^{-\gamma/2}}\right]^{1/2};$$

$$\varphi = \varphi_1 - \varphi_2;\ \operatorname{tg}\varphi_1 = -\frac{e^{-\gamma/4}}{1+2e^{-\gamma n/4}};\ \operatorname{tg}\varphi_2 = e^{-\gamma/4};\ n = 4, 8, 12, ...$$

$$i_{2n} = A\sin(2\pi t + \varphi);\ A = \left[\frac{1+(e^{-\gamma/4} + 2e^{-\gamma n/4})^2}{1+e^{-\gamma/2}}\right]^{1/2};$$

$$\varphi = \varphi_1 - \varphi_2;\ \operatorname{tg}\varphi_1 = -(2e^{-\gamma n/4} + e^{-\gamma/4});\ \operatorname{tg}\varphi_2 = e^{-\gamma/4};\ n = 1, 5, 9, ...$$

$$i_{2n} = A\sin(2\pi t + \varphi);\ A = \left[\frac{(1-2e^{-\gamma n/4})^2 + e^{-\gamma/2}}{1+e^{-\gamma/2}}\right]^{1/2};$$

$$\varphi = \varphi_1 - \varphi_2;\ \operatorname{tg}\varphi_1 = -\frac{e^{-\gamma/4}}{1-2e^{-\gamma n/4}};\ \operatorname{tg}\varphi_2 = e^{-\gamma/4};\ n = 2, 6, 10, ...$$

when $x = 0,\ n/4 - 2\Delta < t \le n/4;$

$u_{2n+1} = 0;$

$$i_{2n+1} = A\sin(2\pi t + \varphi - \pi/4);\ A = \frac{2e^{-\gamma/8}(1-e^{-\gamma n/4})}{\sqrt{1+e^{-\gamma/2}}};$$

$$\varphi = \varphi_1 - \varphi_2;\ \varphi_1 = 0;\ \operatorname{tg}\varphi_2 = e^{-\gamma/4};\ n = 4, 8, 12, ...$$

$$i_{2n+1} = A\sin(2\pi t + \varphi - \pi/4);\ A = 2e^{-\gamma/8}\sqrt{\frac{1+e^{-\gamma n/2}}{1+e^{-\gamma/2}}};$$

$$\varphi = \varphi_1 - \varphi_2;\ \operatorname{tg}\varphi_1 = e^{-\gamma n/4};\ \operatorname{tg}\varphi_2 = e^{-\gamma/4};\ n = 1, 5, 9, ...$$

$$i_{2n+1} = A\sin(2\pi t + \varphi - \pi/4);\ A = \frac{2e^{-\gamma/8}(1+e^{-\gamma n/4})}{\sqrt{1+e^{-\gamma/2}}};$$

$$\varphi = \varphi_1 - \varphi_2;\ \operatorname{tg}\varphi_1 = 0;\ \operatorname{tg}\varphi_2 = e^{-\gamma/4};\ n = 2, 6, 10, ...$$

$$i_{2n+1} = A\sin(2\pi t + \varphi - \pi/4);\ A = 2e^{-\gamma/8}\sqrt{\frac{1+e^{-\gamma n/2}}{1+e^{-\gamma/2}}};$$

$$\varphi = \varphi_1 - \varphi_2;\ \operatorname{tg}\varphi_1 = -e^{-\gamma n/4};\ \operatorname{tg}\varphi_2 = e^{-\gamma/4};\ n = 3, 7, 11, ...$$

when $x = l,\ n/4 - \Delta < t \le n/4 + \Delta.$

Ideal ($\gamma = 0$) open-circuited line with the length l = 1/8:

$$z = 1;\ \Delta = 1/8;\ E = e^{-j\pi/4} = \sqrt{2}(1-j)/2;\ z_E = -j$$

$$u_{2n} = \sin(2\pi t);\ i_{2n} = \begin{cases} \sin(2\pi t), & n = 3, 7, 11, ... \\ \sqrt{5}\sin(2\pi t + \varphi);\ \mathrm{tg}(\varphi) = 2, & n = 4, 8, 12, ... \\ \sqrt{5}\sin(2\pi t + \varphi);\ \mathrm{tg}(\varphi + \pi) = -2, & n = 1, 5, 9, ... \\ \sin(2\pi t + \pi), & n = 2, 6, 10, ... \end{cases}$$

when $x = 0,\ n/4 - 2\Delta < t \le n/4$;

$$u_{2n+1} = \begin{cases} 0, & n = 4, 8, 12, ... \\ 2\cos(2\pi t + 3\pi/4), & n = 1, 5, 9, ... \\ 2\sqrt{2}\sin(2\pi t - \pi/2), & n = 2, 6, 10, ... \\ 2\sin(2\pi t - \pi/4), & n = 3, 7, 11, ... \end{cases};\ i_{2n+1} = 0$$

when $x = l,\ n/4 - \Delta < t \le n/4 + \Delta$.

Undistorting ($\gamma > 0$) open-circuited line with the length l = 1/8:

$$z = 1;\ \Delta = 1/8;\ E = e^{-\gamma/8 - j\pi/4} = \sqrt{2}(1-j)e^{-\gamma/8}/2;\ z_E = -je^{-\gamma/4}$$

$$u_{2n} = \sin(2\pi t);$$

$$i_{2n} = A\sin(2\pi t + \varphi);\ A = \left[\frac{1 + (e^{-\gamma/4} - 2e^{-\gamma n/4})^2}{1 + e^{-\gamma/2}}\right]^{1/2};$$

$$\varphi = \varphi_1 - \varphi_2;\ \mathrm{tg}\varphi_1 = -2e^{-\gamma n/4} + e^{-\gamma/4};\ \mathrm{tg}\varphi_2 = -e^{-\gamma/4};\ n = 3, 7, 11, ...$$

$$i_{2n} = A\sin(2\pi t + \varphi);\ A = \left[\frac{(1 + 2e^{-\gamma n/4})^2 + e^{-\gamma/2}}{1 + e^{-\gamma/2}}\right]^{1/2};$$

$$\varphi = \varphi_1 - \varphi_2;\ \mathrm{tg}\varphi_1 = \frac{e^{-\gamma/4}}{1 + 2e^{-\gamma n/4}};\ \mathrm{tg}\varphi_2 = -e^{-\gamma/4};\ n = 4, 8, 12, ...$$

$$i_{2n} = A\sin(2\pi t + \varphi);\ A = \left[\frac{1+(e^{-\gamma/4}+2e^{-\gamma n/4})^2}{1+e^{-\gamma/2}}\right]^{1/2};$$

$$\varphi = \varphi_1 - \varphi_2;\ \ \mathrm{tg}\varphi_1 = 2e^{-\gamma n/4} + e^{-\gamma/4};\ \ \mathrm{tg}\varphi_2 = -e^{-\gamma/4};\ \ n = 1, 5, 9, ...$$

$$i_{2n} = A\sin(2\pi t + \varphi);\ A = \left[\frac{(1-2e^{-\gamma n/4})^2 + e^{-\gamma/2}}{1+e^{-\gamma/2}}\right]^{1/2};$$

$$\varphi = \varphi_1 - \varphi_2;\ \ \mathrm{tg}\varphi_1 = \frac{e^{-\gamma/4}}{1-2e^{-\gamma n/4}};\ \ \mathrm{tg}\varphi_2 = -e^{-\gamma/4};\ \ n = 2, 6, 10, ...$$

when $x = 0$, $n/4 - 2\Delta < t \le n/4$;

$i_{2n+1} = 0$;

$$u_{2n+1} = A\sin(2\pi t + \varphi - \pi/4);\ A = \frac{2e^{-\gamma/8}(1-e^{-\gamma n/4})}{\sqrt{1+e^{-\gamma/2}}};$$

$$\varphi = \varphi_1 - \varphi_2;\ \ \varphi_1 = 0;\ \ \mathrm{tg}\varphi_2 = -e^{-\gamma/4};\ \ n = 4, 8, 12, ...$$

$$u_{2n+1} = A\sin(2\pi t + \varphi - \pi/4);\ A = 2e^{-\gamma/8}\sqrt{\frac{1+e^{-\gamma n/2}}{1+e^{-\gamma/2}}};$$

$$\varphi = \varphi_1 - \varphi_2;\ \ \mathrm{tg}\varphi_1 = -e^{-\gamma n/4};\ \ \mathrm{tg}\varphi_2 = -e^{-\gamma/4};\ \ n = 1, 5, 9, ...$$

$$u_{2n+1} = A\sin(2\pi t + \varphi - \pi/4);\ A = \frac{2e^{-\gamma/8}(1+e^{-\gamma n/4})}{\sqrt{1+e^{-\gamma/2}}};$$

$$\varphi = \varphi_1 - \varphi_2;\ \ \mathrm{tg}\varphi_1 = 0;\ \ \mathrm{tg}\varphi_2 = -e^{-\gamma/4};\ \ n = 2, 6, 10, ...$$

$$u_{2n+1} = A\sin(2\pi t + \varphi - \pi/4);\ A = 2e^{-\gamma/8}\sqrt{\frac{1+e^{-\gamma n/2}}{1+e^{-\gamma/2}}};$$

$$\varphi = \varphi_1 - \varphi_2;\ \ \mathrm{tg}\varphi_1 = e^{-\gamma n/4};\ \ \mathrm{tg}\varphi_2 = -e^{-\gamma/4};\ \ n = 3, 7, 11, ...$$
$$\text{when } x = l,\ n/4 - \Delta < t \le n/4 + \Delta.$$

Ideal ($\gamma = 0$) short-circuited line with the length l = 3/8:

$$z = -1;\ \ \Delta = 3/8;\quad E = e^{-3j\pi/4} = -\sqrt{2}(1+j)/2;\ \ z_E = -j;$$

$$u_{2n} = \sin(2\pi t);\ i_{2n} = \begin{cases} \sqrt{5}\sin(2\pi t + \varphi);\ \mathrm{tg}(\varphi + \pi) = -2, & n = 3, 7, 11, ... \\ \sin(2\pi t + \pi), & n = 4, 8, 12, ... \\ \sin(2\pi t), & n = 1, 5, 9, ... \\ \sqrt{5}\sin(2\pi t + \varphi);\ \mathrm{tg}(\varphi) = 2, & n = 2, 6, 10, ... \end{cases}$$
$$\text{when } x = 0,\ 3n/4 - 2\Delta < t \le 3n/4;$$

$$u_{2n+1} = 0;\ i_{2n+1} = \begin{cases} 2\sqrt{2}\sin(2\pi t - \pi/2), & n = 4, 8, 12, ... \\ 2\cos(2\pi t - 3\pi/4), & n = 1, 5, 9, ... \\ 0, & n = 2, 6, 10, ... \\ 2\sin(2\pi t - 3\pi/4), & n = 3, 7, 11, ... \end{cases}$$
$$\text{when } x = l,\ 3n/4 - \Delta < t \le 3n/4 + \Delta.$$

Undistorting ($\gamma > 0$) short-circuited line with the length l = 3/8:

$$z = -1,\ \Delta = \frac{3}{8},\ \ E = e^{-3\gamma/8 - 3j\pi/4} = -\frac{\sqrt{2}}{2}(1+j)e^{-3\gamma/8},\ z_E = -je^{-3\gamma/4};$$

$$u_{2n} = \sin(2\pi t);$$

$$i_{2n} = A\sin(2\pi t + \varphi),\ A = \left[\frac{1 + (e^{-3\gamma/4} + 2e^{-3\gamma n/4})^2}{1 + e^{-3\gamma/2}}\right]^{1/2};$$

$$\varphi = \varphi_1 - \varphi_2;\ \ \mathrm{tg}\varphi_1 = 2e^{-3\gamma n/4} + e^{-3\gamma/4};\ \ \mathrm{tg}\varphi_2 = -e^{-3\gamma/4};\ \ n = 3, 7, 11, ...$$

$$i_{2n} = A\sin(2\pi t + \varphi),\ A = \left[\frac{(1 - 2e^{-3\gamma n/4})^2 + e^{-3\gamma/2}}{1 + e^{-3\gamma/2}}\right]^{1/2};$$

$$\varphi = \varphi_1 - \varphi_2;\ \ \mathrm{tg}\varphi_1 = \frac{e^{-3\gamma/4}}{1-2e^{-3\gamma n/4}};\ \ \mathrm{tg}\varphi_2 = -e^{-3\gamma/4};\ \ n = 4, 8, 12, ...$$

$$i_{2n} = A\sin(2\pi t + \varphi);\ A = \left[\frac{1+(e^{-3\gamma/4} - 2e^{-3\gamma n/4})^2}{1+e^{-3\gamma/2}}\right]^{1/2};$$

$$\varphi = \varphi_1 - \varphi_2;\ \ \mathrm{tg}\varphi_1 = e^{-3\gamma/4} - 2e^{-3\gamma n/4};\ \ \mathrm{tg}\varphi_2 = -e^{-3\gamma/4};\ \ n = 1, 5, 9, ...$$

$$i_{2n} = A\sin(2\pi t + \varphi);\ A = \left[\frac{(1+2e^{-3\gamma n/4})^2 + e^{-3\gamma/2}}{1+e^{-3\gamma/2}}\right]^{1/2};$$

$$\varphi = \varphi_1 - \varphi_2;\ \ \mathrm{tg}\varphi_1 = \frac{e^{-3\gamma/4}}{1+2e^{-3\gamma n/4}};\ \ \mathrm{tg}\varphi_2 = -e^{-3\gamma/4};\ \ n = 2, 6, 10, ...$$

when $x = 0,\ 3n/4 - 2\Delta < t \le 3n/4;$

$u_{2n+1} = 0;$

$$i_{2n+1} = A\sin(2\pi t + \varphi - \pi/4);\ A = \frac{2e^{-3\gamma/8}(1-e^{-3\gamma n/4})}{\sqrt{1+e^{-3\gamma/2}}};$$

$$\varphi = \varphi_1 - \varphi_2;\ \ \varphi_1 = 0;\ \ \mathrm{tg}\varphi_2 = -e^{-3\gamma/4};\ \ n = 4, 8, 12, ...$$

$$i_{2n+1} = A\sin(2\pi t + \varphi - \pi/4);\ A = 2e^{-3\gamma/8}\sqrt{\frac{1+e^{-3\gamma n/2}}{1+e^{-3\gamma/2}}};$$

$$\varphi = \varphi_1 - \varphi_2;\ \ \mathrm{tg}\varphi_1 = -e^{-3\gamma n/4};\ \ \mathrm{tg}\varphi_2 = -e^{-3\gamma/4};\ \ n = 1, 5, 9, ...$$

$$i_{2n+1} = A\sin(2\pi t + \varphi - \pi/4);\ A = \frac{2e^{-3\gamma/8}(1+e^{-3\gamma n/4})}{\sqrt{1+e^{-\gamma/2}}};$$

$$\varphi = \varphi_1 - \varphi_2;\ \ \mathrm{tg}\varphi_1 = 0;\ \ \mathrm{tg}\varphi_2 = -e^{-3\gamma/4};\ \ n = 2, 6, 10, ...$$

$$i_{2n+1} = A\sin(2\pi t + \varphi - \pi/4);\ A = 2e^{-3\gamma/8}\sqrt{\frac{1+e^{-3\gamma n/2}}{1+e^{-3\gamma/2}}};$$

$$\varphi = \varphi_1 - \varphi_2;\ \operatorname{tg}\varphi_1 = e^{-3\gamma n/4};\ \operatorname{tg}\varphi_2 = -e^{-3\gamma/4};\ n = 3, 7, 11, ...$$
$$\text{when } x = l,\ 3n/4 - \Delta < t \le 3n/4 + \Delta.$$

Ideal ($\gamma = 0$) open-circuited line with the length l = 3/8:

$$z = 1;\ \Delta = 3/8;\quad E = e^{-3j\pi/4} = -\sqrt{2}(1+j)/2;\ z_E = j$$

$$u_{2n} = \sin(2\pi t);\ i_{2n} = \begin{cases} \sqrt{5}\sin(2\pi t + \varphi);\ \operatorname{tg}(\varphi + \pi) = 2, & n = 3, 7, 11, ... \\ \sin(2\pi t + \pi), & n = 4, 8, 12, ... \\ \sin(2\pi t), & n = 1, 5, 9, ... \\ \sqrt{5}\sin(2\pi t + \varphi);\ \operatorname{tg}(\varphi) = -2, & n = 2, 6, 10, ... \end{cases}$$
$$\text{when } x = 0,\ 3n/4 - 2\Delta < t \le 3n/4;$$

$$u_{2n+1} = \begin{cases} 0, & n = 4, 8, 12, ... \\ 2\sin(2\pi t - 3\pi/4), & n = 1, 5, 9, ... \\ 2\sqrt{2}\sin(2\pi t - \pi/2), & n = 2, 6, 10, ... \\ 2\cos(2\pi t + \pi/4), & n = 3, 7, 11, ... \end{cases};\ i_{2n+1} = 0$$
$$\text{when } x = l,\ 3n/4 - \Delta < t \le 3n/4 + \Delta.$$

Undistorting ($\gamma > 0$) open-circuited line with the length l = 3/8:

$$z = 1;\ \Delta = 3/8;\ E = e^{-3\gamma/8 - 3j\pi/4} = -\sqrt{2}(1+j)e^{-3\gamma/8}/2;\ z_E = je^{-3\gamma/4};$$

$$u_{2n} = \sin(2\pi t);$$

$$i_{2n} = A\sin(2\pi t + \varphi),\ A = \left[\frac{1 + (e^{-3\gamma/4} + 2e^{-3\gamma n/4})^2}{1 + e^{-3\gamma/2}}\right]^{1/2};$$

$$\varphi = \varphi_1 - \varphi_2;\ \operatorname{tg}\varphi_1 = -(2e^{-3\gamma n/4} + e^{-3\gamma/4});\ \operatorname{tg}\varphi_2 = e^{-3\gamma/4};\ n = 3, 7, 11, ...$$

$$i_{2n} = A\sin(2\pi t + \varphi);\ A = \left[\frac{(1 - 2e^{-3\gamma n/4})^2 + e^{-3\gamma/2}}{1 + e^{-3\gamma/2}}\right]^{1/2};$$

$$\varphi = \varphi_1 - \varphi_2;\ \ \mathrm{tg}\varphi_1 = -\frac{e^{-3\gamma/4}}{1-2e^{-3\gamma n/4}};\ \ \mathrm{tg}\varphi_2 = e^{-3\gamma/4};\ \ n = 4, 8, 12, ...$$

$$i_{2n} = A\sin(2\pi t + \varphi);\ A = \left[\frac{1+(e^{-3\gamma/4} - 2e^{-3\gamma n/4})^2}{1+e^{-3\gamma/2}}\right]^{1/2};$$

$$\varphi = \varphi_1 - \varphi_2;\ \ \mathrm{tg}\varphi_1 = -e^{-3\gamma/4} + 2e^{-3\gamma n/4};\ \ \mathrm{tg}\varphi_2 = e^{-3\gamma/4};\ \ n = 1, 5, 9, ...$$

$$i_{2n} = A\sin(2\pi t + \varphi);\ A = \left[\frac{(1+2e^{-3\gamma n/4})^2 + e^{-3\gamma/2}}{1+e^{-3\gamma/2}}\right]^{1/2};$$

$$\varphi = \varphi_1 - \varphi_2;\ \ \mathrm{tg}\varphi_1 = -\frac{e^{-3\gamma/4}}{1+2e^{-3\gamma n/4}};\ \ \mathrm{tg}\varphi_2 = e^{-3\gamma/4};\ \ n = 2, 6, 10, ...$$

when $x = 0,\ 3n/4 - 2\Delta < t \le 3n/4;$

$$u_{2n+1} = A\sin(2\pi t + \varphi - \pi/4);\ A = \frac{2e^{-3\gamma/8}(1-e^{-3\gamma n/4})}{\sqrt{1+e^{-3\gamma/2}}};$$

$$\varphi = \varphi_1 - \varphi_2;\ \ \varphi_1 = 0;\ \ \mathrm{tg}\varphi_2 = e^{-3\gamma/4};\ \ n = 4, 8, 12, ...$$

$$u_{2n+1} = A\sin(2\pi t + \varphi - \pi/4);\ A = 2e^{-3\gamma/8}\sqrt{\frac{1+e^{-3\gamma n/2}}{1+e^{-3\gamma/2}}};$$

$$\varphi = \varphi_1 - \varphi_2;\ \ \mathrm{tg}\varphi_1 = e^{-3\gamma n/4};\ \ \mathrm{tg}\varphi_2 = e^{-3\gamma/4};\ \ n = 1, 5, 9, ...$$

$$u_{2n+1} = A\sin(2\pi t + \varphi - \pi/4);\ A = \frac{2e^{-3\gamma/8}(1+e^{-3\gamma n/4})}{\sqrt{1+e^{-\gamma/2}}};$$

$$\varphi = \varphi_1 - \varphi_2;\ \ \mathrm{tg}\varphi_1 = 0;\ \ \mathrm{tg}\varphi_2 = e^{-3\gamma/4};\ \ n = 2, 6, 10, ...$$

$$u_{2n+1} = A\sin(2\pi t + \varphi - \pi/4);\ A = 2e^{-3\gamma/8}\sqrt{\frac{1+e^{-3\gamma n/2}}{1+e^{-3\gamma/2}}};$$

$$\varphi = \varphi_1 - \varphi_2;\ \operatorname{tg}\varphi_1 = -e^{-3\gamma n/4};\ \operatorname{tg}\varphi_2 = e^{-3\gamma/4};\ n = 3, 7, 11, \ldots;$$

$$i_{2n+1} = 0$$
when $x = l,\ 3n/4 - \Delta < t \le 3n/4 + \Delta$.

3.2. Ideal capacity at the end of the line

Using the boundary condition $C_S du/dt = i$ when $x = l$ and introducing the following notations: $k = 1/C_S;\ t_m = t - m\Delta, m = 1,2,3,...$ we can represent nonstationary solution at the end points of the line in the form given below.

Starting point $x = 0$:

$$u_2 = e^{j\omega t};\ i_2 = e^{j\omega t} \text{ when } 0 < t \le 2\Delta;$$

$$u_4 = e^{j\omega t};\ i_4 = i_2 + \frac{2e^{-2\gamma\Delta}}{j\omega + k}\left[(j\omega - k)e^{j\omega t_2} + 2ke^{-kt_2}\right] \text{ when } 2\Delta < t \le 4\Delta;$$

$$u_6 = e^{j\omega t};\ i_6 = i_4 + \frac{2e^{-4\gamma\Delta}}{j\omega + k}\left[\frac{(j\omega - k)^2}{j\omega + k}e^{j\omega t_4} - 4k\left(kt_4 - \frac{j\omega}{j\omega + k}\right)e^{-kt_4}\right]$$
when $4\Delta < t \le 6\Delta$;

$$u_8 = e^{j\omega t};\ i_8 = i_6 + \frac{2e^{-6\gamma\Delta}}{j\omega + k}\left[\frac{(j\omega - k)^3}{(j\omega + k)^2}e^{j\omega t_6} + \right.$$

$$\left. + 4k\left(2k^2t_6^2 - 2\frac{k + 3j\omega}{j\omega + k}kt_6 + \frac{k^2 - 3\omega^2}{(j\omega + k)^2}\right)e^{-kt_6}\right] \text{ when } 6\Delta < t \le 8\Delta;$$

$$u_{10} = e^{j\omega t};\ i_{10} = i_8 + \frac{2e^{-8\gamma\Delta}}{j\omega + k}\left[\frac{(j\omega - k)^4}{(j\omega + k)^3}e^{j\omega t_8} - \right.$$

$$-\frac{8k}{3}\left(k^3t_8^3-3\frac{k+2j\omega}{j\omega+k}k^2t_8^2+3\frac{k^2+2j\omega k-3\omega^2}{(j\omega+k)^2}kt_8-\right.$$
$$\left.-3\frac{j\omega(k^2-\omega^2)}{(j\omega+k)^3}\right)e^{-kt_8}\Bigg] \text{ when } 8\Delta<t\le 10\Delta \text{ etc.}$$

Receiving end $x=l$:

$i_1=u_1=0$ when $0<t\le\Delta$;

$$u_3=\frac{2ke^{-\gamma\Delta}}{j\omega+k}\left(e^{j\omega t_1}-e^{-kt_1}\right);\ i_3=\frac{2e^{-\gamma\Delta}}{j\omega+k}\left(j\omega e^{j\omega t_1}+ke^{-kt_1}\right) \text{ when } \Delta<t\le 3\Delta;$$

$$u_5=u_3+\frac{2ke^{-3\gamma\Delta}}{j\omega+k}\left[\frac{j\omega-k}{j\omega+k}e^{j\omega t_3}+\left(2kt_3-\frac{j\omega-k}{j\omega+k}\right)e^{-kt_3}\right];$$

$$i_5=i_3+\frac{2e^{-3\gamma\Delta}}{j\omega+k}\left[\frac{j\omega(j\omega-k)}{j\omega+k}e^{j\omega t_3}-k\left(2kt_3-\frac{k+3j\omega}{j\omega+k}\right)e^{-kt_3}\right]$$
$$\text{when } 3\Delta<t\le 5\Delta;$$

$$u_7=u_5+\frac{2ke^{-5\gamma\Delta}}{j\omega+k}\left[\left(\frac{j\omega-k}{j\omega+k}\right)^2e^{j\omega t_5}-\right.$$
$$\left.-\left(2k^2t_5^2-\frac{4j\omega k}{j\omega+k}t_5+\left(\frac{j\omega-k}{j\omega+k}\right)^2\right)e^{-kt_5}\right];$$

$$i_7=i_5+\frac{2e^{-5\gamma\Delta}}{j\omega+k}\left[j\omega\left(\frac{k-j\omega}{j\omega+k}\right)^2e^{j\omega t_5}+\right.$$

$$\left.+k\left(2k^2t_5^2-\frac{4(2j\omega+k)}{j\omega+k}kt_5+\frac{k^2+2j\omega k-5\omega^2}{(j\omega+k)^2}\right)e^{-kt_5}\right] \text{ when } 5\Delta<t\le 7\Delta;$$

$$u_9 = u_7 + \frac{2ke^{-7\gamma\Delta}}{j\omega+k}\left[\left(\frac{j\omega-k}{j\omega+k}\right)^3 e^{j\omega t_7} + \right.$$

$$\left. + \frac{1}{3}\left(4k^3t_7^3 - 6\frac{3j\omega+k}{j\omega+k}k^2t_7^2 + \frac{6(k^2-3\omega^2)}{(j\omega+k)^2}kt_7 - 3\left(\frac{j\omega-k}{j\omega+k}\right)^3\right)e^{-kt_7}\right];$$

$$i_9 = i_7 + \frac{2e^{-7\gamma\Delta}}{j\omega+k}\left[j\omega\left(\frac{j\omega-k}{j\omega+k}\right)^3 e^{j\omega t_7} - \frac{k}{3}\left(4k^3t_7^3 - \frac{6(5j\omega+3k)}{j\omega+k}k^2t_7^2 + \right.\right.$$

$$\left.\left. + \frac{6(3k^2+8j\omega k-9\omega^2)}{(j\omega+k)^2}kt_7 - \frac{3k^3+15j\omega k^2-9\omega^2k-21j\omega^3}{(j\omega+k)^3}\right)e^{-kt_7}\right]$$

when $7\Delta < t \le 9\Delta$;

$$u_{11} = u_9 + \frac{2ke^{-9\gamma\Delta}}{j\omega+k}\left[\left(\frac{j\omega-k}{j\omega+k}\right)^4 e^{j\omega t_9} - \frac{1}{3}\left(2k^4t_9^4 - 8\frac{2j\omega+k}{j\omega+k}k^3t_9^3 + \right.\right.$$

$$\left.\left. + \frac{12(k^2+2j\omega k-3\omega^2)}{(j\omega+k)^2}k^2t_9^2 - \frac{24j\omega(k^2-\omega^2)}{(j\omega+k)^3}kt_9 + 3\left(\frac{j\omega-k}{j\omega+k}\right)^4\right)e^{-kt_9}\right];$$

$$i_{11} = i_9 + \frac{2e^{-9\gamma\Delta}}{j\omega+k}\left[j\omega\left(\frac{j\omega-k}{j\omega+k}\right)^4 e^{j\omega t_9} + \frac{k}{3}\left(2k^4t_9^4 - \frac{8(3j\omega+2k)}{j\omega+k}k^3t_9^3 + \right.\right.$$

$$+ 12\frac{3k^2+8j\omega k-7\omega^2}{(j\omega+k)^2}k^2t_9^2 - 24\frac{k^3+4j\omega k^2-5\omega^2k-4j\omega^3}{(j\omega+k)^3}kt_9 +$$

$$\left.\left. + \frac{3k^4+12j\omega k^3-42\omega^2k^2-12j\omega^3k+27\omega^4}{(j\omega+k)^4}\right)e^{-kt_9}\right]$$

when $9\Delta < t \le 11\Delta$ etc.

3.3. Ideal inductance at the end of the line

Using the boundary condition $u = L_S di/dt$ when $x = l$ and introducing the following notation: $k = 1/L_S$ we can represent nonstationary solution at the end points of the line in the form given below.

Starting point $x = 0$:

$u_2 = e^{j\omega t};\ i_2 = e^{j\omega t}$ when $0 < t \le 2\Delta$;

$$u_4 = e^{j\omega t};\ i_4 = i_2 - \frac{2e^{-2\gamma\Delta}}{j\omega + k}\left[(j\omega - k)e^{j\omega t_2} + 2ke^{-kt_2}\right] \text{ when } 2\Delta < t \le 4\Delta;$$

$$u_6 = e^{j\omega t};\ i_6 = i_4 + \frac{2e^{-4\gamma\Delta}}{j\omega + k}\left[\frac{(j\omega - k)^2}{j\omega + k}e^{j\omega t_4} - 4k\left(kt_4 - \frac{j\omega}{j\omega + k}\right)e^{-kt_4}\right]$$
when $4\Delta < t \le 6\Delta$;

$$u_8 = e^{j\omega t};\ i_8 = i_6 - \frac{2e^{-6\gamma\Delta}}{j\omega + k}\left[\frac{(j\omega - k)^3}{(j\omega + k)^2}e^{j\omega t_6} + \right.$$

$$\left. + 4k\left(2k^2t_6^2 - 2\frac{k + 3j\omega}{j\omega + k}kt_6 + \frac{k^2 - 3\omega^2}{(j\omega + k)^2}\right)e^{-kt_6}\right] \text{ when } 6\Delta < t \le 8\Delta;$$

$$u_{10} = e^{j\omega t};\ i_{10} = i_8 + \frac{2e^{-8\gamma\Delta}}{j\omega + k}\left[\frac{(j\omega - k)^4}{(j\omega + k)^3}e^{j\omega t_8} - \right.$$

$$- \frac{8k}{3}\left(k^3t_8^3 - 3\frac{k + 2j\omega}{j\omega + k}k^2t_8^2 + 3\frac{k^2 + 2j\omega k - 3\omega^2}{(j\omega + k)^2}kt_8 - \right.$$

$$\left.\left. - 3\frac{j\omega(k^2 - \omega^2)}{(j\omega + k)^3}\right)e^{-kt_8}\right] \text{ when } 8\Delta < t \le 10\Delta \text{ etc.}$$

Receiving end $x = l$:

$i_1 = u_1 = 0$ when $0 < t \le \Delta$;

$$u_3 = \frac{2e^{-\gamma\Delta}}{j\omega + k}\left(j\omega e^{j\omega t_1} + ke^{-kt_1}\right);\ i_3 = \frac{2ke^{-\gamma\Delta}}{j\omega + k}\left(e^{j\omega t_1} - e^{-kt_1}\right) \text{ when } \Delta < t \le 3\Delta;$$

$$u_5 = u_3 - \frac{2e^{-3\gamma\Delta}}{j\omega + k}\left[\frac{j\omega(j\omega - k)}{j\omega + k}e^{j\omega t_3} - k\left(2kt_3 - \frac{k + 3j\omega}{j\omega + k}\right)e^{-kt_3}\right];$$

$$i_5 = i_3 - \frac{2ke^{-3\gamma\Delta}}{j\omega + k}\left[\frac{j\omega - k}{j\omega + k}e^{j\omega t_3} + \left(2kt_3 - \frac{j\omega - k}{j\omega + k}\right)e^{-kt_3}\right]$$

when $3\Delta < t \le 5\Delta$;

$$u_7 = u_5 + \frac{2e^{-5\gamma\Delta}}{j\omega + k}\left[j\omega\left(\frac{k - j\omega}{j\omega + k}\right)^2 e^{j\omega t_5} + \right.$$

$$\left. + k\left(2k^2t_5^2 - \frac{4(2j\omega + k)}{j\omega + k}kt_5 + \frac{k^2 + 2j\omega k - 5\omega^2}{(j\omega + k)^2}\right)e^{-kt_5}\right];$$

$$i_7 = i_5 + \frac{2ke^{-5\gamma\Delta}}{j\omega + k}\left[\left(\frac{j\omega - k}{j\omega + k}\right)^2 e^{j\omega t_5} - \left(2k^2t_5^2 - \frac{4j\omega k}{j\omega + k}t_5 + \left(\frac{j\omega - k}{j\omega + k}\right)^2\right)e^{-kt_5}\right]$$

when $5\Delta < t \le 7\Delta$;

$$u_9 = u_7 - \frac{2e^{-7\gamma\Delta}}{j\omega + k}\left[j\omega\left(\frac{j\omega - k}{j\omega + k}\right)^3 e^{j\omega t_7} - \frac{k}{3}\left(4k^3t_7^3 - \frac{6(5j\omega + 3k)}{j\omega + k}k^2t_7^2 + \right.\right.$$

$$\left.\left. + \frac{6(3k^2 + 8j\omega k - 9\omega^2)}{(j\omega + k)^2}kt_7 - \frac{3k^3 + 15j\omega k^2 - 9\omega^2 k - 21j\omega^3}{(j\omega + k)^3}\right)e^{-kt_7}\right];$$

$$i_9 = i_7 - \frac{2ke^{-7\gamma\Delta}}{j\omega + k}\left[\left(\frac{j\omega - k}{j\omega + k}\right)^3 e^{j\omega t_7} + \right.$$

$$+\frac{1}{3}\left(4k^3t_7^3-6\frac{3j\omega+k}{j\omega+k}k^2t_7^2+\frac{6(k^2-3\omega^2)}{(j\omega+k)^2}kt_7-3\left(\frac{j\omega-k}{j\omega+k}\right)^3\right)e^{-kt_7}\Bigg]$$

when $7\Delta < t \le 9\Delta$;

$$u_{11}=u_9+\frac{2e^{-9\gamma\Delta}}{j\omega+k}\Bigg[j\omega\left(\frac{j\omega-k}{j\omega+k}\right)^4e^{j\omega t_9}+\frac{k}{3}\Bigg(2k^4t_9^4-\frac{8(3j\omega+2k)}{j\omega+k}k^3t_9^3+$$

$$+12\frac{3k^2+8j\omega k-7\omega^2}{(j\omega+k)^2}k^2t_9^2-24\frac{k^3+4j\omega k^2-5\omega^2k-4j\omega^3}{(j\omega+k)^3}kt_9+$$

$$+\frac{3k^4+12j\omega k^3-42\omega^2k^2-12j\omega^3k+27\omega^4}{(j\omega+k)^4}\Bigg)e^{-kt_9}\Bigg];$$

$$i_{11}=i_9+\frac{2ke^{-9\gamma\Delta}}{j\omega+k}\Bigg[\left(\frac{j\omega-k}{j\omega+k}\right)^4e^{j\omega t_9}-\frac{1}{3}\Bigg(2k^4t_9^4-8\frac{2j\omega+k}{j\omega+k}k^3t_9^3+$$

$$+\frac{12(k^2+2j\omega k-3\omega^2)}{(j\omega+k)^2}k^2t_9^2-\frac{24j\omega(k^2-\omega^2)}{(j\omega+k)^3}kt_9+3\left(\frac{j\omega-k}{j\omega+k}\right)^4\Bigg)e^{-kt_9}\Bigg]$$

when $9\Delta < t \le 11\Delta$ etc.

3.4. *RLC* – circuit at the end of the line

The boundary condition for *RLC* – circuit at the end of the line is of the form of (1.3). For some simplification let's consider the case of multiple roots of characteristic equation $L_Sk^2+(R_S+Z_B)k+1/C_S=0$, i.e. $4L_S=$ $=C_S(R_S+Z_B)^2$. Let's introduce the following notations: $k_\omega=j\omega+k$, $L_\omega=L_Sk_\omega^2$, $k=(R_S+Z_B)/(2L_S)$. Then the initial fragments of the nonstationary solution at the end points of the line can be written in the form given below.

Starting point $x=0$:

$u_2=e^{j\omega t}$; $i_2=e^{j\omega t}$ when $0<t\le 2\Delta$;

$u_4 = e^{j\omega t}$;

$$i_4 = i_2 - \frac{2e^{-2\gamma\Delta}}{L_\omega}\left[(L_\omega - 2j\omega)e^{j\omega t_2} - 2(kk_\omega t_2 - j\omega)e^{-kt_2}\right] \text{ when } 2\Delta < t \le 4\Delta;$$

$$u_6 = e^{j\omega t};\ i_6 = i_4 + \frac{2e^{-4\gamma\Delta}}{L_\omega^2}\left[(L_\omega - 2j\omega)^2 e^{j\omega t_4} - \frac{2}{3}\left(k^2 k_\omega^3 t_4^3 - \right.\right.$$

$$\left.\left. - 3k(k + 2j\omega)k_\omega^2 t_4^2 + 6k_\omega(kL_\omega - \omega^2)t_4 - 6j\omega(L_\omega - j\omega)\right)e^{-kt_4}\right]$$

when $4\Delta < t \le 6\Delta$;

$$u_8 = e^{j\omega t};\ i_8 = i_6 - \frac{2e^{-6\gamma\Delta}}{L_\omega^3}\left[(L_\omega - 2j\omega)^3 e^{j\omega t_6} - \frac{1}{15}\left(k^3 k_\omega^5 t_6^5 - \right.\right.$$

$$- 5k^2(2k + 3j\omega)k_\omega^4 t_6^4 + 10k(3kL_\omega + 2k^2 + 6j\omega k - 6\omega^2)k_\omega^3 t_6^3 -$$

$$- 30(3k(k + 2j\omega)L_\omega - 2j\omega^3)k_\omega^2 t_6^2 + 30(3kL_\omega^2 - 6\omega^2 L_\omega + 4j\omega^3)k_\omega t_6 -$$

$$\left.\left. - 30j\omega(3L_\omega^2 - 6j\omega L_\omega - 4\omega^2)\right)e^{-kt_6}\right] \text{ when } 6\Delta < t \le 8\Delta;$$

$$u_{10} = e^{j\omega t};\ i_{10} = i_8 + \frac{2e^{-8\gamma\Delta}}{L_\omega^4}\left[(L_\omega - 2j\omega)^4 e^{j\omega t_8} + \frac{1}{315}\left(k^4 k_\omega^7 t_8^7 - \right.\right.$$

$$- 7k^3(3k + 4j\omega)k_\omega^6 t_8^6 + 42k^2(2kL_\omega + 3k^2 + 8j\omega k - 6\omega^2)k_\omega^5 t_8^5 -$$

$$- 210k\left(2k(2k + 3j\omega)L_\omega + k^3 + 4j\omega k^2 - 6\omega^2 k - 4j\omega^3\right)k_\omega^4 t_8^4 +$$

$$+ 420\left(3k^2 L_\omega^2 + 4kL_\omega(k^2 + 3j\omega k - 3\omega^2) + 2\omega^4\right)k_\omega^3 t_8^3 -$$

$$- 1260\left(3k(k + 2j\omega)L_\omega^2 - 4j\omega^3 L_\omega - 2\omega^4\right)k_\omega^2 t_8^2 +$$

$$+2520\left(kL_\omega^3-3\omega^2L_\omega^2+4j\omega^3L_\omega+2\omega^4\right)k_\omega t_8-$$

$$-2520j\omega(L_\omega-j\omega)(L_\omega^2-2j\omega L_\omega-2\omega^2)\Big)e^{-kt_8}\Big]\ \text{when}\ 8\Delta<t\le10\Delta.$$

Receiving end $x=l$:

$i_1=u_1=0$ when $0<t\le\Delta$;

$$u_3=\frac{2e^{-\gamma\Delta}}{L_\omega}\left((L_\omega-j\omega)e^{j\omega t_1}-(kk_\omega t_1-j\omega)e^{-kt_1}\right);$$

$$i_3=\frac{2e^{-\gamma\Delta}}{L_\omega}\left(j\omega e^{j\omega t_1}+(kk_\omega t_1-j\omega)e^{-kt_1}\right)\ \text{when}\ \Delta<t\le3\Delta;$$

$$u_5=u_3+\frac{2e^{-3\gamma\Delta}}{L_\omega^2}\Big[(L_\omega-j\omega)(L_\omega-2j\omega)e^{j\omega t_3}+\frac{1}{3}\Big(k^2k_\omega^3t_3^3-$$

$$-3k(k+2j\omega)k_\omega^2t_3^2+3k_\omega(3kL_\omega-2\omega^2)t_3-3j\omega(3L_\omega-2j\omega)\Big)e^{-kt_3}\Big];$$

$$i_5=i_3-\frac{2e^{-3\gamma\Delta}}{L_\omega^2}\Big[j\omega(L_\omega-2j\omega)e^{j\omega t_3}+\frac{1}{3}\Big(k^2k_\omega^3t_3^3-$$

$$-3k(k+2j\omega)k_\omega^2t_3^2+3k_\omega(kL_\omega-2\omega^2)t_3-3j\omega(L_\omega-2j\omega)\Big)e^{-kt_3}\Big]$$

$$\text{when}\ 3\Delta<t\le5\Delta;$$

$$u_7=u_5+\frac{2e^{-5\gamma\Delta}}{L_\omega^3}\Big[(L_\omega-j\omega)(L_\omega-2j\omega)^2e^{j\omega t_5}-\frac{1}{30}\Big(k^3k_\omega^5t_5^5-$$

$$-5k^2(2k+3j\omega)k_\omega^4t_5^4+20k(2kL_\omega+k^2+3j\omega k-3\omega^2)k_\omega^3t_5^3-$$

$$-60(2k(k+2j\omega)L_\omega-j\omega^3)k_\omega^2t_5^2+30(5kL_\omega^2-8\omega^2L_\omega+4j\omega^3)k_\omega t_5-$$

$$-30j\omega(5L_\omega^2-8j\omega L_\omega-4\omega^2)\Big)e^{-kt_5}\Big];$$

$$i_7=i_5+\frac{2e^{-5\gamma\Delta}}{L_\omega^3}\Big[j\omega(L_\omega-2j\omega)^2e^{j\omega t_5}+\frac{1}{30}\Big(k^3k_\omega^5t_5^5-$$

$$-5k^2(2k+3j\omega)k_\omega^4t_5^4+20k(kL_\omega+k^2+3j\omega k-3\omega^2)k_\omega^3t_5^3-$$

$$-60(k(k+2j\omega)L_\omega-j\omega^3)k_\omega^2t_5^2+30(kL_\omega^2-4\omega^2L_\omega+4j\omega^3)k_\omega t_5-$$

$$-30j\omega(L_\omega-2j\omega)^2\Big)e^{-kt_5}\Big]\text{ when }5\Delta<t\le7\Delta;$$

$$u_9=u_7-\frac{2e^{-7\gamma\Delta}}{L_\omega^4}\Big[(L_\omega-j\omega)(L_\omega-2j\omega)^3e^{j\omega t_7}-\frac{1}{630}\Big(k^4k_\omega^7t_7^7-$$

$$-7k^3(3k+4j\omega)k_\omega^6t_7^6+21k^2(5kL_\omega+6k^2+16j\omega k-12\omega^2)k_\omega^5t_7^5-$$

$$-105k\Big(2(k+2j\omega)(k^2+2j\omega k-2\omega^2)+5kL_\omega(2k+3j\omega)\Big)k_\omega^4t_7^4+$$

$$+210\Big(9k^2L_\omega^2+10kL_\omega(k^2+3j\omega k-3\omega^2)+4\omega^4\Big)k_\omega^3t_7^3-$$

$$-630\Big(9k(k+2j\omega)L_\omega^2-10j\omega^3L_\omega-4\omega^4\Big)k_\omega^2t_7^2+$$

$$+630\Big(7kL_\omega^3-18\omega^2L_\omega^2+20j\omega^3L_\omega+8\omega^4\Big)k_\omega t_7-$$

$$-630j\omega\Big(7L_\omega^3-18j\omega L_\omega^2-20\omega^2L_\omega+8j\omega^3\Big)\Big)e^{-kt_7}\Big];$$

$$i_9=i_7-\frac{2e^{-7\gamma\Delta}}{L_\omega^4}\Big[j\omega(L_\omega-2j\omega)^3e^{j\omega t_7}+\frac{1}{630}\Big(k^4k_\omega^7t_7^7-$$

$$-7k^3(3k+4j\omega)k_\omega^6 t_7^6 + 21k^2(3kL_\omega + 6k^2 + 16j\omega k - 12\omega^2)k_\omega^5 t_7^5 -$$

$$-105k\left(2(k+2j\omega)(k^2+2j\omega k-2\omega^2)+3kL_\omega(2k+3j\omega)\right)k_\omega^4 t_7^4 +$$

$$+210\left(3k^2L_\omega^2 + 6kL_\omega(k^2+3j\omega k-3\omega^2)+4\omega^4\right)k_\omega^3 t_7^3 -$$

$$-630\left(3k(k+2j\omega)L_\omega^2 - 6j\omega^3 L_\omega - 4\omega^4\right)k_\omega^2 t_7^2 +$$

$$+630\left(kL_\omega^3 - 6\omega^2 L_\omega^2 + 12j\omega^3 L_\omega + 8\omega^4\right)k_\omega t_7 -$$

$$-630\,j\omega(L_\omega - 2j\omega)^3\Big)e^{-kt_7}\Big] \text{ when } 7\Delta < t \le 9\Delta \text{ etc.}$$

So, as it turned out, the formation of solution, the exact solution analysis and tabulation for undistorting lines (there is only wave dissipation and there is no wave dispersion) is enough laborious task. To make use of the given analytical solutions one must have certain grounding in mathematics. The design formulas look very intricate even at the initial stage of the transient process. So it is impossible to generalize them for the lines with arbitrary input voltage form, with variable (tunable) parameters, etc. Thus, only some elementary test problems can be solved by means of method of characteristics and Fourier method. However, these solutions are of methodical and practical importance, because they serve as a basis for comparative analysis and for posterior precision estimation of the numerical solutions.

Let's remark that the method of characteristics can be used for solving not only direct problems, but inverse problems (modeling the wave process in the reverse time from the present to the past) as well. The inverse problems of the mathematical physics with the irreversible energy dissipation are usually ill-defined because of input data instability.

Let's suppose that at some time moment $t = t_0$ the space distributions of the current and voltage in the line are known (are given): $i = i_0(x)$; $u = u_0(x)$, $x \in [0, l]$, as well as the boundary conditions at the end points when $t < t_0$: $u = \exp(j\omega t)$ when $x = 0$ and $u = R_s i$ when $x = l$. Now let's present the nonstationary solutions of (3.2), (3.3) in the reverse time. Starting from the initial state, the functions $i_0(x)$ and $u_0(x)$ generate two invariants $A(t)$ and $B(t)$ at the end points of the line:

$$A(t) = \left[u_0(x_l(t)) - Z_B i_0(x_l(t))\right] e^{\gamma(t_0 - t)},\ x_l(t) = l - a(t_0 - t),\ t_0 - \Delta < t \le t_0;$$
$$B(t) = \left[u_0(x_0(t)) + Z_B i_0(x_0(t))\right] e^{\gamma(t_0 - t)},\ x_0(t) = a(t_0 - t),\ t_0 - \Delta < t \le t_0.$$

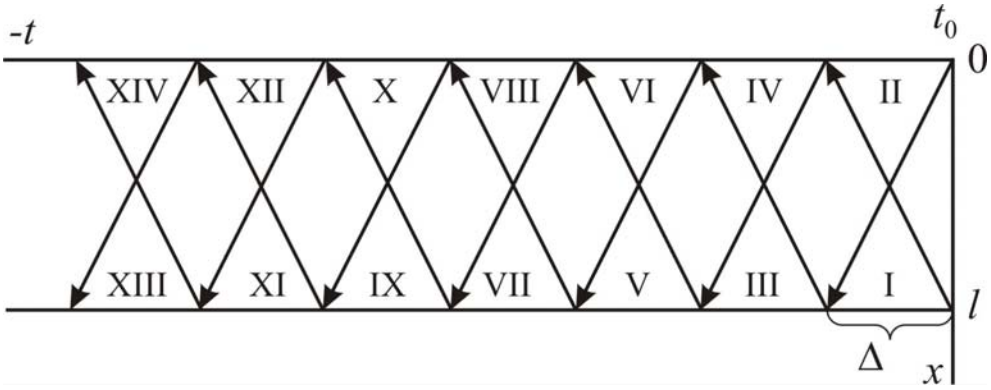

Fig. 3.2. The wave-front configurations in case of transient process in the reverse time.

Starting point $x = 0$ (fig. 3.2):

$$u_2 = e^{j\omega t};\ i_2 = -e^{j\omega t} + B(t) \text{ when } t_0 - \Delta < t \le t_0;$$

$$u_4 = e^{j\omega t};\ i_4 = -e^{j\omega t} + \frac{A(t+\Delta)e^{\gamma\Delta}}{z} \text{ when } t_0 - 2\Delta < t \le t_0 - \Delta;$$

$$u_6 = e^{j\omega t};\ i_6 = e^{j\omega t}\left[-1 + \frac{2}{z_E}\right] - \frac{B(t+2\Delta)e^{2\gamma\Delta}}{z} =$$

$$= e^{j\omega t}\,\frac{1 - z_E + \dfrac{2}{z_E}}{1 + z_E} - \frac{B(t+2\Delta)e^{2\gamma\Delta}}{z}$$

when $t_0 - 3\Delta < t \le t_0 - 2\Delta$;

$$u_8 = e^{j\omega t};\ i_8 = e^{j\omega t}\left[-1 + \frac{2}{z_E}\right] - \frac{A(t+3\Delta)e^{3\gamma\Delta}}{z^2} =$$

$$= e^{j\omega t}\,\frac{1 - z_E + \dfrac{2}{z_E}}{1 + z_E} - \frac{A(t+3\Delta)e^{3\gamma\Delta}}{z^2}$$

when $t_0 - 4\Delta < t \le t_0 - 3\Delta$;

$$u_{10} = e^{j\omega t};\ i_{10} = e^{j\omega t}\left[-1+\frac{2}{z_E}\left(1-\frac{1}{z_E}\right)\right] + \frac{B(t+4\Delta)e^{4\gamma\Delta}}{z^2} =$$

$$= e^{j\omega t}\,\frac{1-z_E-\dfrac{2}{z_E^2}}{1+z_E} + \frac{B(t+4\Delta)e^{4\gamma\Delta}}{z^2}$$

when $t_0 - 5\Delta < t \le t_0 - 4\Delta$;

$$u_{12} = e^{j\omega t};\ i_{12} = e^{j\omega t}\left[-1+\frac{2}{z_E}\left(1-\frac{1}{z_E}\right)\right] + \frac{A(t+5\Delta)e^{5\gamma\Delta}}{z^3} =$$

$$= e^{j\omega t}\,\frac{1-z_E-\dfrac{2}{z_E^2}}{1+z_E} + \frac{A(t+5\Delta)e^{5\gamma\Delta}}{z^3}$$

when $t_0 - 6\Delta < t \le t_0 - 5\Delta$;

$$u_{14} = e^{j\omega t};\ i_{14} = e^{j\omega t}\left[-1+\frac{2}{z_E}\left(1-\frac{1}{z_E}+\frac{1}{z_E^2}\right)\right] - \frac{B(t+6\Delta)e^{6\gamma\Delta}}{z^3} =$$

$$= e^{j\omega t}\,\frac{1-z_E+\dfrac{2}{z_E^3}}{1+z_E} - \frac{B(t+6\Delta)e^{6\gamma\Delta}}{z^3}$$

when $t_0 - 7\Delta < t \le t_0 - 6\Delta$ etc.

The structure of the obtained solution makes it possible to write out the formulas for any arbitrary time interval

$$u_{4m} = e^{j\omega t};$$

$$i_{4m} = e^{j\omega t}\,\frac{1-z_E-2\dfrac{(-1)^{m-1}}{z_E^{m-1}}}{1+z_E} + (-1)^{m-1}\,\frac{A(t+(2m-1)\Delta)e^{(2m-1)\gamma\Delta}}{z^m}$$

when $t_0 - 2m\Delta < t \le t_0 - (2m-1)\Delta,\ m = 1, 2, 3, \ldots$

$$u_{2(2m+1)} = e^{j\omega t};$$

$$i_{2(2m+1)} = e^{j\omega t}\,\frac{1 - z_E - 2\dfrac{(-1)^m}{z_E^m}}{1+z_E} + (-1)^m\,\frac{B(t+2m\Delta)e^{2m\gamma\Delta}}{z^m} \qquad (3.10)$$

when $t_0 - (2m+1)\Delta < t \le t_0 - 2m\Delta,\ m = 0, 1, 2, 3, \ldots$

Receiving end $x = l$:

$$u_1 = R_S i_1;\ i_1 = \frac{A(t)}{R_S - 1} \text{ when } t_0 - \Delta < t \le t_0;$$

$$u_3 = R_S i_3;\ i_3 = \frac{1}{R_S - 1}\left(\frac{2e^{j\omega t}}{E} - B(t+\Delta)e^{\gamma\Delta}\right)$$

when $t_0 - 2\Delta < t \le t_0 - \Delta$;

$$u_5 = R_S i_5;\ i_5 = \frac{2e^{j\omega t}}{(R_S - 1)E} - \frac{A(t+2\Delta)e^{2\gamma\Delta}}{z(R_S - 1)}$$

when $t_0 - 3\Delta < t \le t_0 - 2\Delta$;

$$u_7 = R_S i_7;\ i_7 = \frac{2e^{j\omega t}}{(R_S - 1)E}\left(1 - \frac{1}{z_E}\right) + \frac{B(t+3\Delta)e^{3\gamma\Delta}}{z(R_S - 1)} =$$

$$= \frac{2e^{j\omega t}}{(R_S - 1)E}\,\frac{z_E - \dfrac{1}{z_E}}{1+z_E} + \frac{B(t+3\Delta)e^{3\gamma\Delta}}{z(R_S - 1)}$$

when $t_0 - 4\Delta < t \le t_0 - 3\Delta$;

$$u_9 = R_S i_9;\ i_9 = \frac{2e^{j\omega t}}{(R_S - 1)E}\left(1 - \frac{1}{z_E}\right) + \frac{A(t+4\Delta)e^{4\gamma\Delta}}{z^2(R_S - 1)} =$$

$$= \frac{2e^{j\omega t}}{(R_S - 1)E}\,\frac{z_E - \dfrac{1}{z_E}}{1+z_E} + \frac{A(t+4\Delta)e^{4\gamma\Delta}}{z^2(R_S - 1)}$$

when $t_0 - 5\Delta < t \le t_0 - 4\Delta$;

$$u_{11} = R_S i_{11};\ i_{11} = \frac{2e^{j\omega t}}{(R_S - 1)E}\left(1 - \frac{1}{z_E} + \frac{1}{z_E^2}\right) - \frac{B(t+5\Delta)e^{5\gamma\Delta}}{z^2(R_S - 1)} =$$

$$= \frac{2e^{j\omega t}}{(R_S - 1)E} \frac{z_E + \frac{1}{z_E^2}}{1 + z_E} - \frac{B(t + 5\Delta)e^{5\gamma\Delta}}{z^2(R_S - 1)}$$

when $t_0 - 6\Delta < t \le t_0 - 5\Delta$;

$$u_{13} = R_S i_{13};\ i_{13} = \frac{2e^{j\omega t}}{(R_S - 1)E}\left(1 - \frac{1}{z_E} + \frac{1}{z_E^2}\right) - \frac{A(t + 6\Delta)e^{6\gamma\Delta}}{z^3(R_S - 1)} =$$

$$= \frac{2e^{j\omega t}}{(R_S - 1)E} \frac{z_E + \frac{1}{z_E^2}}{1 + z_E} - \frac{A(t + 6\Delta)e^{6\gamma\Delta}}{z^3(R_S - 1)}$$

when $t_0 - 7\Delta < t \le t_0 - 6\Delta$;

The formulas for any arbitrary time interval can be written out in this case too:

$u_{4m-1} = R_S i_{4m-1}$;

$$i_{4m-1} = \frac{2e^{j\omega t}}{(R_S - 1)E} \frac{z_E - \frac{(-1)^m}{z_E^{m-1}}}{1 + z_E} + (-1)^m \frac{B(t + (2m-1)\Delta)e^{(2m-1)\gamma\Delta}}{z^{m-1}(R_S - 1)}$$

when $t_0 - 2m\Delta < t \le t_0 - (2m-1)\Delta,\ m = 1, 2, 3, \ldots$

$u_{4m+1} = R_S i_{4m+1}$;

$$i_{4m+1} = \frac{2e^{j\omega t}}{(R_S - 1)E} \frac{z_E - \frac{(-1)^m}{z_E^{m-1}}}{1 + z_E} + (-1)^m \frac{A(t + 2m\Delta)e^{2m\gamma\Delta}}{z^m(R_S - 1)} \qquad (3.11)$$

when $t_0 - (2m+1)\Delta < t \le t_0 - 2m\Delta,\ m = 0, 1, 2, 3, \ldots$

Let's remark the expressions $1/z_E^m$ and $1/z^m$ in the formulas (3.10) and (3.11). Since for line with losses ($\gamma > 0$) we have $|z_E| < 1$ and for ideal line with loading $0 < R_S < \infty$ – $|z| < 1$, then these expressions tend to infinity when $m \to \infty$. Correspondingly, the currents and voltages will tend to infinity as well, but this means that the problem modeling the wave process

involution is ill-defined. In the strict sense, the solutions (3.10) and (3.11) are stable only in the case of ideal line ($\gamma = 0$) with short circuit or idling ($|z| = 1$).

Thus, the method of characteristics is of self-dependent importance, because by applying this method one can reconstruct (interpret) the initial wave image or input signal, that is extremely important for diagnostics and identification of the parameters of diverse electrotechnology and electroenergetics installations.

4. Moving capacitor discharge on long line with losses

The discharge on the ideal line of the moving with the steady speed capacitor was considered in [61]. Moving the voltage source with the speeds greater or lesser then the speed of the light, the authors attempted to discover the time delay effect within the limits of the linear electrodynamic model. As long as such effect didn't become apparent, the authors concluded that the obtained result is a good reason for disproof the special theory of relativity (STR).

In this paragraph by means of method of characteristics [89, 90] we examine the evolution of the nonstationary capacitor discharge on the long line. On the base of exact solutions of the boundary-value problems for telegraph equations it was established [76] that under some fixed relations between the capacity of the voltage source and the losses in the line, the electromagnetic energy distribution in the line is symmetric and independent of the speed of capacitor. It was discovered the effect of the speed enhancing of the electric capacity discharge under the speeds exceeding the speed of potential and current wave propagation in the line. The nonlinear problem of the discharge of capacitor, moving with steady acceleration (until the velocity of its motion reaches the electromagnetic wave velosity), was solved.

4.1. Solution of telegraph equations for undistorting line by means of method of characteristics

Let's consider the infinite twin-wire long line. Let the charged capacitor with the capacity C_n and potential U_0 is connected up to this line at the initial time moment $t = 0$ (fig. 4.1). Under contacting the current appears in the conductor and the potential will propagate in both directions from the

connection point with the speed *a*, that we'll take equal to 160000 km/sec (it is typical for cable lines).

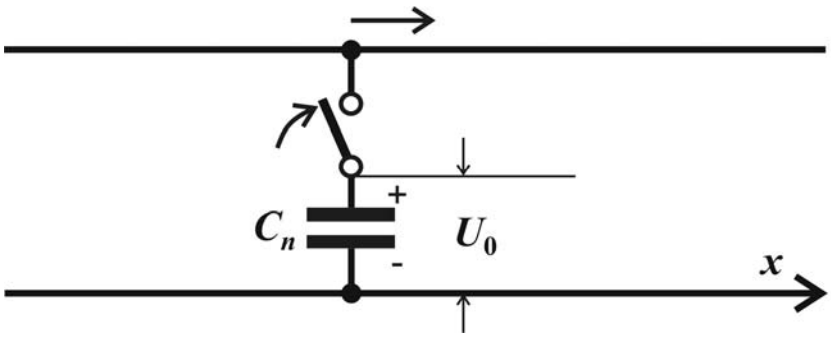

Fig. 4.1. The twin-wire long line with connected capacitor.

So, it requires to determine the voltage function $u(x,t)$ and the current function $i(x,t)$, $x \in (-\infty,\infty), t > 0$, satisfying the system of telegraph equations

$$L\frac{\partial i}{\partial t}+\frac{\partial u}{\partial x}+Ri=0; \qquad C\frac{\partial u}{\partial t}+\frac{\partial i}{\partial x}+Gu=0 \tag{4.1}$$

under the following initial and boundary conditions:

$$u(x,0)=i(x,0)=0, \ \ x\in(-\infty,\infty), \tag{4.2}$$

$$C_n\frac{du(0,t)}{dt}=i(0-0,t)-i(0+0,t) \ \text{ when } \ x=0, t>0. \tag{4.3}$$

In case of undistorting line ($R/L = G/C = \gamma$) the solution of the problem (4.1) – (4.3) can be obtained by the method of characteristics. [89, 90]. As it is considered the line with unrestricted length, than the potential and current waves are propagating to the left and to the right from the source without reflections. It means that for $x > 0$ along the characteristics $at + x = const$ the following relation takes place $Z_B\, i - u = 0$, where $Z_B = \sqrt{L/C}$ and $a = 1/\sqrt{LC}$ represent the impedance of the line and the velocity of the electromagnetic wave propagation correspondingly. At the same time for $x < 0$ along the characteristics $at - x = const$ the following relation takes place

$Z_B\, i + u = 0$. Now using these relations, let's eliminate the currents from the boundary condition (4.3). As a result we obtain the ordinary differential equation with respect to capacitor voltage

$$C_n \frac{du(0,t)}{dt} = -\frac{2}{Z_B} u(0,t), \;\; x = 0,\, t > 0, \;\; u(0,t) = U_0,$$

with the solution

$$u(0,t) = U_0 e^{-\lambda_0 t}, \;\; \lambda_0 = \frac{2}{C_n Z_B}, \;\; t \geq 0. \tag{4.4}$$

As can be seen, the capacitor voltage is independent on the losses in the line for which the proportionality condition $R/L = G/C = \gamma$ takes place.

The electrical energy, lumped in the capacitor, decreases in time by exponential law (just as the voltage) and can be calculated by formula

$$W_n(t) = \frac{C_n u^2}{2} = \frac{C_n U_0^2}{2} e^{-2\lambda_0 t} = \frac{U_0^2}{\lambda_0 Z_B} e^{-2\lambda_0 t}.$$

The solution of the initial equations (4.1) – (4.3) with boundary condition (4.4) using the method of characteristics can be written in the form

$$u(x,t) = i(x,t) = 0 \;\text{ when }\; x < -at \;\; or \;\; x > at;$$

$$u(x,t) = U_0 e^{-\lambda_0 t + (\lambda_0 - \gamma) x/a};\;\; i(x,t) = u(x,t)/Z_B \qquad \text{when} \qquad 0 < x < at; \tag{4.5}$$

$$u(x,t) = U_0 e^{-\lambda_0 t - (\lambda_0 - \gamma) x/a};\;\; i(x,t) = -u(x,t)/Z_B \qquad \text{when} \qquad -at < x < 0.$$

It can be seen from (4.5) that if the condition $\lambda_0 = \gamma$ takes place, then the potential distribution depends only on time in the perturbed domain and it is independent on the longitudinal coordinate *x*. The symmetrical character of the nonstationary process of wave propagation in the left and in the right from the capacity connection point is also evident. The solution (4.5) is valid also for ideal line when $\gamma = 0$:

$$u(x,t) = U_0 e^{-\lambda_0 (t - x/a)};\;\; i(x,t) = u(x,t)/Z_B \quad \text{when} \qquad 0 < x < at;$$

$$u(x,t) = U_0 e^{-\lambda_0 (t+x/a)};\ i(x,t) = -u(x,t)/Z_B \quad \text{when} \quad -at < x < 0\,.$$

So, the voltage jump on the characteristics $x = \pm at$ is equal to the initial potential value at the condenser: $\Delta U = U_0$. When $\gamma > 0$ the voltage jump monotone decreases in time by exponential law: $\Delta U = U_0\, e^{-\gamma t}$.

The evolution of the normalized with respect to U_0 voltages along the ideal and undistorting lines is represented in the fig. 4.2 – 4.4 for different time moments t = 1 (*a*); 2 (*b*); 3 (*c*); 4 (*d*) with diverse correlations between the value of capacitor C_n and the losses in the line γ.

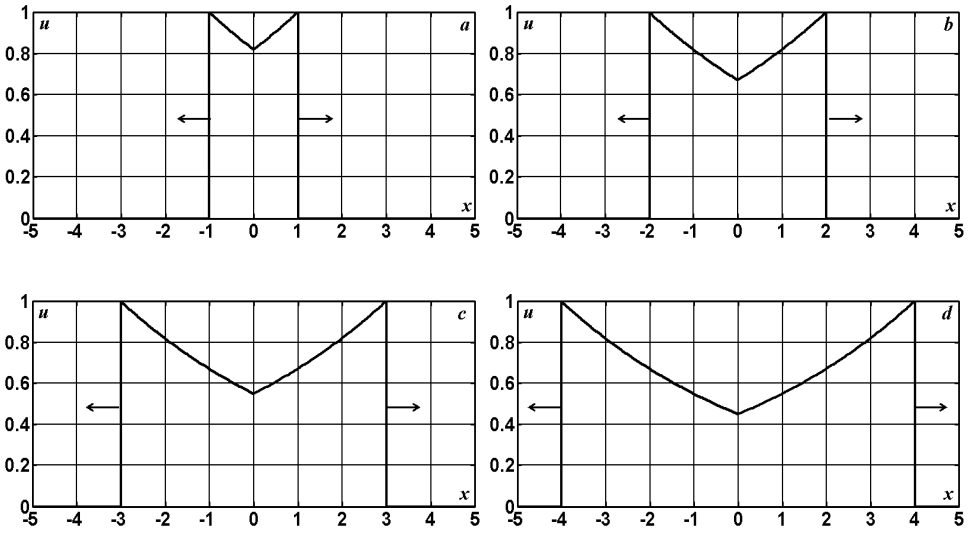

Fig. 4.2. The voltage distribution along the ideal line (γ = 0) for different time moments when C_n = 1, λ_0 = 2.

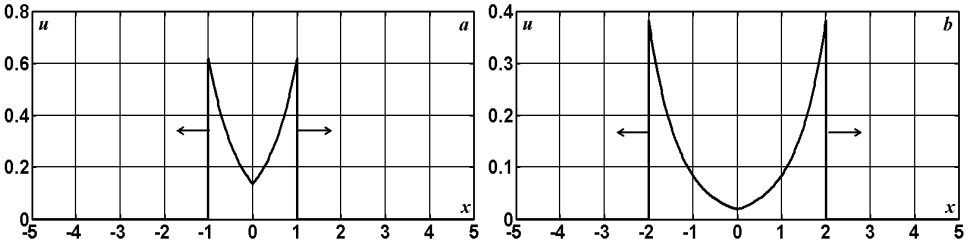

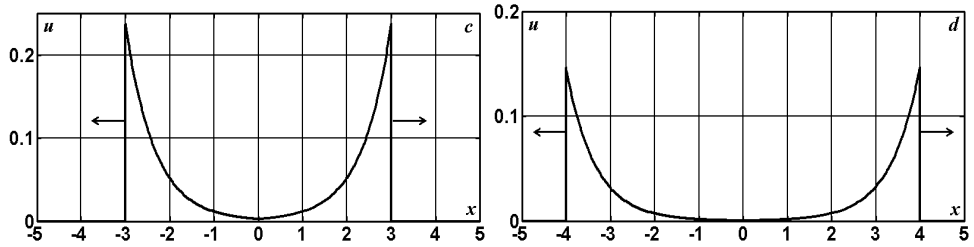

Fig. 4.3. The voltage distribution along the undistorting line ($\gamma = 0.48$) for different time moments when $C_n = 1$, $\lambda_0 = 2$.

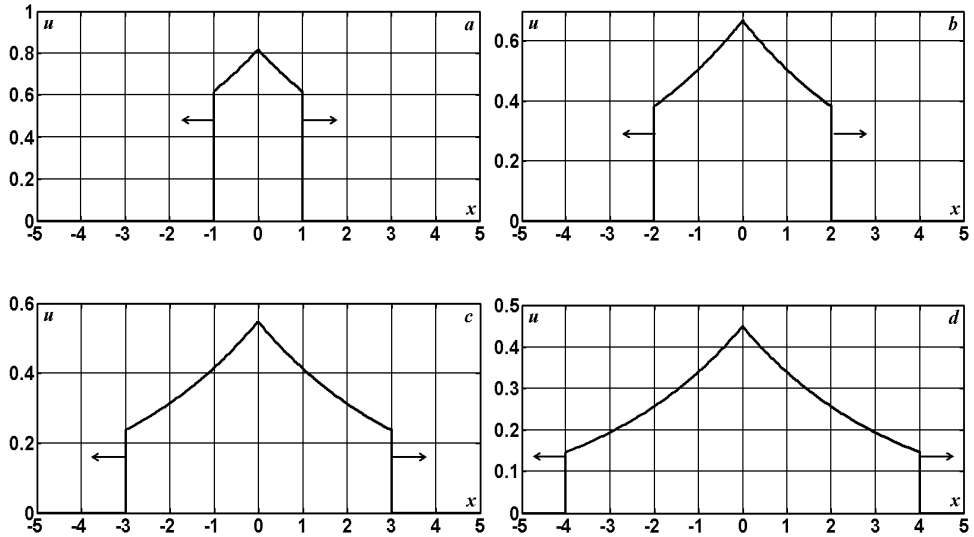

Fig. 4.4. The voltage distribution along the undistorting line ($\gamma = 0.48$) for different time moments when $C_n = 10$, $\lambda_0 = 0.2$.

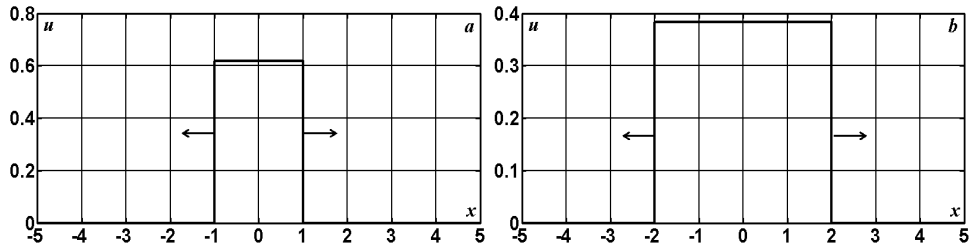

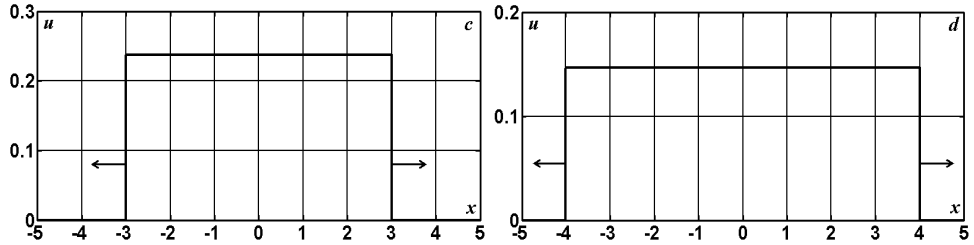

Fig. 4.5. The voltage distribution along the undistorting line ($\gamma = 0.48$) for different time moments when $C_n = 4.16667$, $\lambda_0 = \gamma = 0.48$.

The electromagnetic energy $W_q(t)$, accumulated in the distributed reactive elements till the time moment t, can be calculated by the formula [15, 34]

$$W_q(t) = \frac{1}{2}\int_{-at}^{at}\left(Li^2 + Cu^2\right)dx = \frac{C_n U_0^2}{2-\gamma C_n Z_B}\left(e^{-2\gamma t} - e^{-2\lambda_0 t}\right) =$$

$$= \frac{U_0^2}{(\lambda_0 - \gamma)Z_B}\left(e^{-2\gamma t} - e^{-2\lambda_0 t}\right).$$

Taking into consideration the conditioned of the Joule–Lenz effect irreversible losses of the active power in the line, the losses $W_p(t)$ in the line take the following form:

$$W_p(t) = \int_0^t \int_{-a\tau}^{a\tau}\left(Ri^2 + Gu^2\right)dx\,d\tau = \frac{U_0^2}{\lambda_0 Z_B}\left(1 - \frac{\lambda_0}{\lambda_0 - \gamma}e^{-2\gamma t} + \frac{\gamma}{\lambda_0 - \gamma}e^{-2\lambda_0 t}\right).$$

So the expression for the total energy in the line $W_l(t) = W_q(t) + W_p(t)$ is the following

$$W_l(t) = \frac{U_0^2}{\lambda_0 Z_B}\left(1 - e^{-2\lambda_0 t}\right) = W_n(0) - W_n(t) \qquad (4.6)$$

or

$$W(t) = W_l(t) + W_n(t) = W_n(0), \tag{4.7}$$

where $W(t)$ is the total energy.

4.2. Steady speed moving capacitor

Let's consider now the analogous problem but with the condition that the discharging capacitor is moving with steady speed $v \le a$ or $v > a$ to the right of the initial position. In this case the defining equations are to be integrated under the following boundary condition:

$$u(x_v(t),t) = U_0 e^{-\lambda_0 t}, \ \lambda_0 = \frac{2}{C_n Z_B}, \ x_v(t) = vt, \ t \ge 0. \tag{4.8}$$

Here $x_v(t)$ denotes the trajectory of the capacitor motion on the plane *Oxt* (fig. 4.6), that is the straight line *OA* in this case.

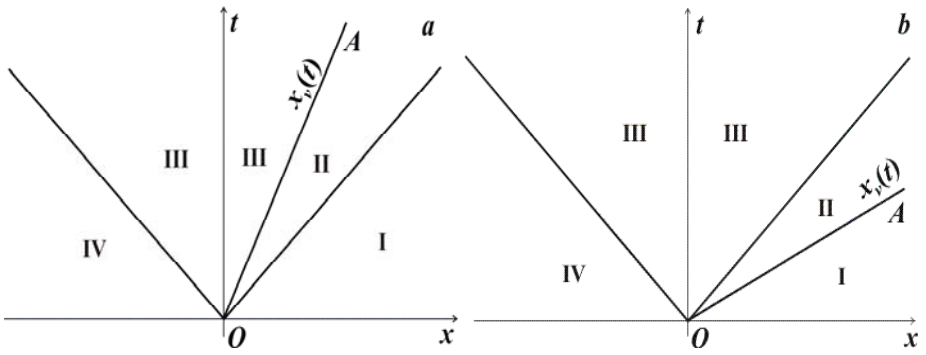

Fig. 4.6. The location of the solution regions on the plane *Oxt* when the capacitor is moving with steady speed $v \le a$ (***a***) and $v > a$ (***b***).

Let's describe the solution of this problem, defined by method of characteristics, in case when $v < a$ (fig. 4.6, *a*). The solution is zero in the domains I and IV, where the electromagnetic wave is not yet reached:

$$u(x,t) = i(x,t) = 0 \quad \text{when} \quad x < -at \quad \text{or} \quad x > at \tag{4.9}$$

Then we have the direct wave propagation (moving to the right) in the domain II:

$$u(x,t) = U_0 e^{-\gamma\frac{x-vt}{a-v}} e^{-\lambda_0\frac{at-x}{a-v}} = U_0 e^{-\frac{(\gamma-\lambda_0)x+(a\lambda_0-\gamma v)t}{a-v}}; \qquad (4.10)$$

$$i(x,t) = -u(x,t)/Z_B \quad \text{when} \quad -at < x < at$$

and the return wave propagation (moving to the left) in the domain III:

$$u(x,t) = U_0 e^{-\gamma\frac{vt-x}{a+v}} e^{-\lambda_0\frac{at+x}{a+v}} = U_0 e^{-\frac{(\lambda_0-\gamma)x+(a\lambda_0+\gamma v)t}{a+v}};$$

$$i(x,t) = -u(x,t)/Z_B \qquad \text{when} \qquad -at < x < vt\,. \qquad (4.11)$$

The electromagnetic energy, accumulated in the distributed reactive elements till the time moment t, can be calculated by the formula

$$W_q(t) = \frac{1}{2}\int_{-at}^{at}\left(Li^2 + Cu^2\right)dx = \frac{C_n U_0^2}{2-\gamma C_n Z_B}\left(e^{-2\gamma t} - e^{-2\lambda_0 t}\right) =$$

$$= \frac{U_0^2}{(\lambda_0-\gamma)Z_B}\left(e^{-2\gamma t} - e^{-2\lambda_0 t}\right),$$

and the total energy $W_0(t) = W_q(t) + W_n(t)$, accumulated in the distributed reactive elements and in the capacitor, takes the following form

$$W_0(t) = \frac{C_n U_0^2}{2-\gamma C_n Z_B}\left(e^{-2\gamma t} - \frac{\gamma C_n Z_B}{2}e^{-2\lambda_0 t}\right) =$$

$$= \frac{U_0^2}{(\lambda_0-\gamma)Z_B}\left(e^{-2\gamma t} - \frac{\gamma}{\lambda_0}e^{-2\lambda_0 t}\right). \qquad (4.12)$$

As it follows from (4.12), the total energy tends to zero with time in case of undistorting line ($\gamma > 0$), whereas it remains constant equal to capacitor energy at the initial time moment (4.7) in case of ideal line ($\gamma = 0$).

Thus, the moving capacitor discharges with the same speed as the fixed one in case when the speed of it's motion is less then the speed of the electromagnetic wave.

Now let's consider the solution in case when the capacitor is moving with the speed of electromagnetic wave $v = a$. It is the particular case of the solution (4.9) – (4.11). Here the domain II is missing. The solution is zero in the domains I and IV, where the electromagnetic wave is not yet reached. And we have the return wave propagation (moving to the left) in the domain III:

$$u(x,t) = U_0 e^{-\frac{(\lambda_0-\gamma)x+a(\lambda_0+\gamma)t}{2a}}; \quad i(x,t) = -u(x,t)/Z_B \quad \text{when} \quad -at < x < at$$

The distributions of voltage along the ideal and undistorting lines for the time moments t = 1; 2; 3; 4 when $v = 0.8 < a = 1$ are represented in the fig. 4.7 – 4.10. The wave pattern here has evidently asymmetrical form and the quantities of energy, that are taken off by the electromagnetic waves in the opposite directions, are essentially different.

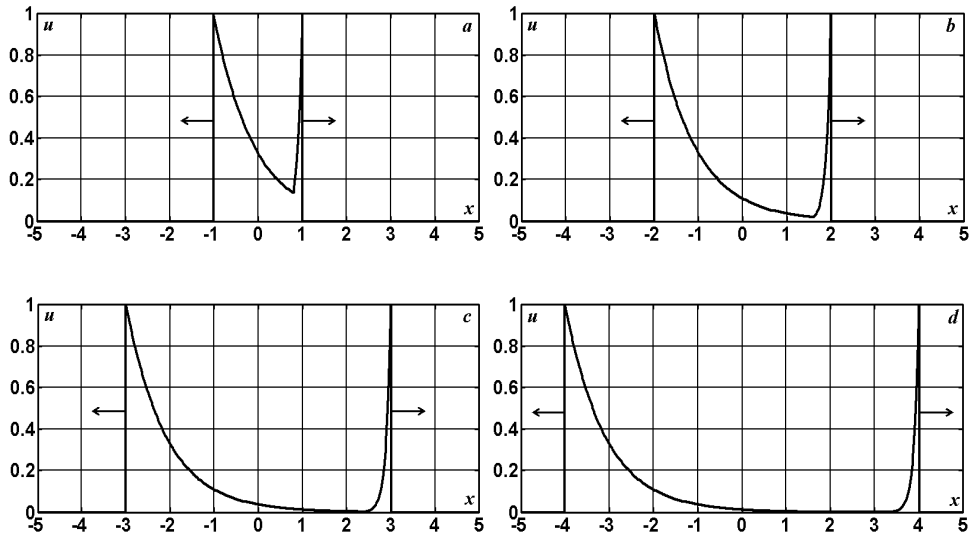

Fig. 4.7. The voltage distribution along the ideal line (γ = 0) for different time moments when C_n = 1, λ_0 = 2 and the steady speed v = 0.8 moving capacitor.

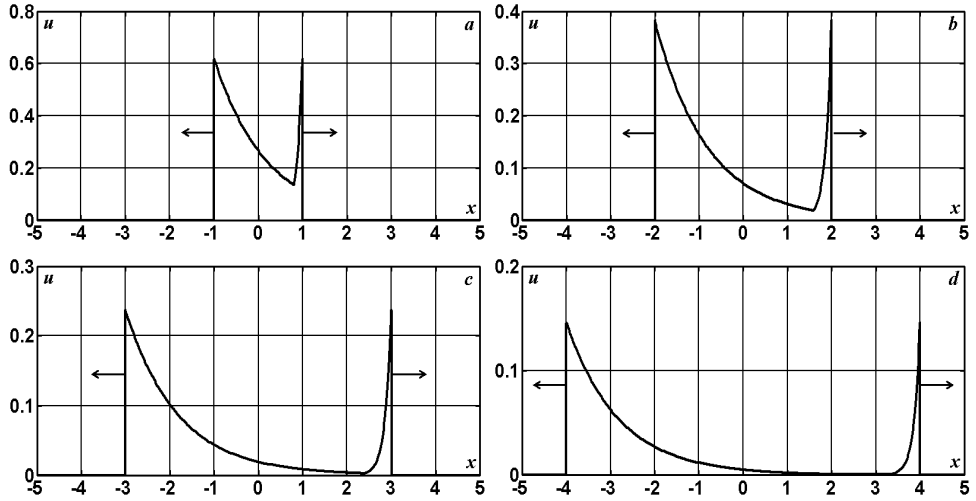

Fig. 4.8. The voltage distribution along the undistorting line ($\gamma = 0.48$) for different time moments when $C_n = 1$, $\lambda_0 = 2$ and the steady speed $v = 0.8$ moving capacitor.

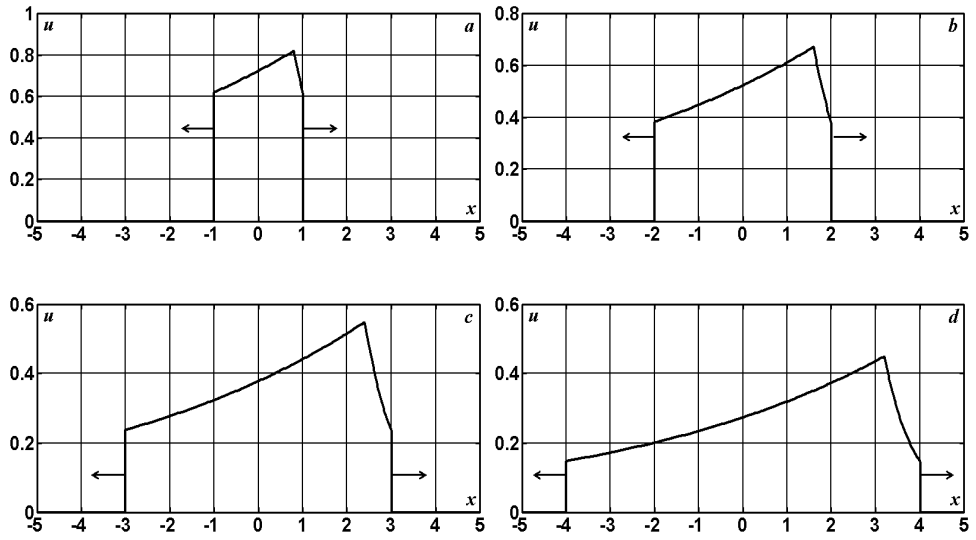

Fig. 4.9. The voltage distribution along the undistorting line ($\gamma = 0.48$) for different time moments when $C_n = 10$, $\lambda_0 = 0.2$ and the steady speed $v = 0.8$ moving capacitor.

Thus from the fig. 4.7 – 4.9 we see that the quantity of energy accumulated with time in the negative half plane $x < 0$ differs from energy in the

domain $x > 0$. Using the solution (4.9) – (4.11), let's obtain the quantitative estimation of this disbalance:

$$W_-(t) = \frac{1}{2}\int_{-at}^{0}\left(Li^2 + Cu^2\right)dx = \frac{U_0^2(a+v)}{2a(\lambda_0-\gamma)Z_B}\left(e^{-2\gamma t} - e^{-\frac{2(a\lambda_0+\gamma v)t}{a+v}}\right),$$

$$W_+(t) = \frac{1}{2}\int_{0}^{at}\left(Cu^2 + Li^2\right)dx =$$

$$= \frac{U_0^2}{2a(\lambda_0-\gamma)Z_B}\left((a+v)e^{-\frac{2(a\lambda_0+\gamma v)t}{a+v}} + (a-v)e^{-2\gamma t} - 2ae^{-2\lambda_0 t}\right).$$

Let's consider the difference between the energies $\Delta W(t) = W_+(t) - W_-(t)$:

$$\Delta W(t) = W_+(t) - W_-(t) =$$

$$= \frac{U_0^2}{a(\lambda_0-\gamma)Z_B}\left((a+v)e^{-\frac{2(a\lambda_0+\gamma v)t}{a+v}} - ve^{-2\gamma t} - ae^{-2\lambda_0 t}\right) =$$

$$= \frac{U_0^2}{adZ_B}e^{-\frac{2(a\lambda_0+\gamma v)t}{a+v}}\left[1 - \frac{v}{a+v}e^{2adt} - \frac{a}{a+v}e^{-2vdt}\right], \quad d = \frac{\lambda_0-\gamma}{a+v}. \qquad (4.13)$$

The derivative by parameter d of the expression in the square brackets of the formula (4.13) has the following signs:

$$F(d) = 1 - \frac{v}{a+v}e^{2adt} - \frac{a}{a+v}e^{-2vdt},$$

$$F_d' = -\frac{2avt}{a+v}\left[e^{2adt} - e^{-2vdt}\right] = \begin{cases} > 0, \text{ when } d < 0 \\ < 0, \text{ when } d > 0 \end{cases}.$$

Then the function $F(d)$ is convex and it reaches the maximum value equal to zero at the point $d = 0$. But this means that the function $F(d)$ possesses only nonpositive values for any values of the parameter d. Taking into consideration the sign of the coefficient $U_0^2/(adZ_B)$ in the formula (4.13), we obtain

$$\Delta W(t) > 0,\ W_-(t) < W_+(t) \quad \text{when} \quad \lambda_0 < \gamma,\ v \neq 0,$$

$$\Delta W(t) < 0,\ W_-(t) > W_+(t) \quad \text{when} \quad \lambda_0 > \gamma,\ v \neq 0,$$

$$\Delta W(t) = 0,\ W_-(t) = W_+(t) \quad \text{when} \quad \lambda_0 = \gamma \ \text{ or } \ v = 0.$$

So in case when $\lambda_0 = \gamma$ we observe the equal total energy storage in the left and in the right half planes. The formula (4.12) for total energy $W_0(t)$ in the line and in the capacitor in this case contains the indeterminate form 0/0, that can be disclosed by means of l'Hôpital rule

$$W_0(t) = \frac{U_0^2}{Z_B} \lim_{\gamma \to \lambda_0} \frac{e^{-2\gamma t} - e^{-2\lambda_0 t}}{\lambda_0 - \gamma} = \frac{U_0^2}{Z_B} \lim_{\gamma \to \lambda_0} \frac{-2te^{-2\gamma t}}{-1} = \frac{2U_0^2}{Z_B} te^{-2\lambda_0 t}. \qquad (4.14)$$

The voltage distribution along the line when $\lambda_0 = \gamma = 0.48$ is represented in the fig. 4.10 below. As the speed of wave attenuation in the line and the speed of the capacitor discharge are equal, then the voltage profiles get the symmetrical rectangular form (as in case of fixed capacitor).

Let's consider now the case of moving capacitor with the speed $v > a$ (fig. 4.6,*b*). In this case the energy in the line at the time moment t occupies the domain $[-at, vt]$, that is bigger then the domain $[-at, at]$ when $v \le a$. Hence, if the capacitor discharges with the previous speed $\lambda_0 = 2/(C_n Z_B)$, then in the ideal line we observe the greater then initial energy storage, that is the contradiction with the energy conservation law. Therefore let's assume that the capacitor discharges with another speed λ_v. This speed can be determined from the total energy conservation law in the ideal line. Let's write down the boundary conditions at the trajectory of the capacitor motion in the following form

$$u(x_v(t), t) = U_0 e^{-\lambda_v t},\ x_v(t) = vt,\ t \ge 0. \qquad (4.15)$$

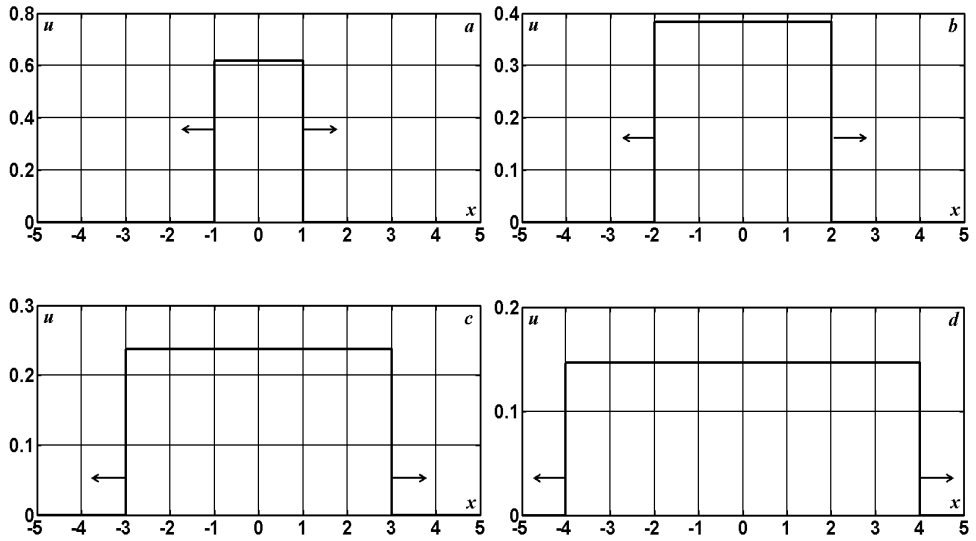

Fig. 4.10. The voltage distribution along the undistorting line ($\gamma = 0.48$) for different time moments when $C_n = 4.16667$, $\lambda_0 = \gamma = 0.48$, $v = const < a = 1$.

The solution of this problem when $v > a$ (fig. 4.6,*b*) we determine by means of method of characteristics. The solution is zero in the domains I and IV, where the electromagnetic wave is not yet reached. And we have the return wave propagation (moving to the left) in the domain III:

$$u(x,t) = U_0 e^{-\frac{(\lambda_v - \gamma)x + (a\lambda_v + \gamma v)t}{a+v}} = U_0 e^{-\gamma t} e^{-\frac{\lambda_v - \gamma}{a+v}(x+at)}; \qquad (4.16)$$

$$i(x,t) = -u(x,t)/Z_B \quad \text{when} \quad -at < x < at$$

Now we observe the propagation of two waves (direct and return) in the domain II. These waves are generated by boundary condition at the straight line *OA* (fig. 4.6,*b*):

$$u(x,t) = U_0 e^{-\gamma t}\left[e^{-\frac{\lambda_v - \gamma}{v-a}(x-at)} + e^{-\frac{\lambda_v - \gamma}{v+a}(x+at)} \right]; \qquad (4.17)$$

$$i(x,t)=\frac{U_0 e^{-\gamma t}}{Z_B}\left[e^{-\frac{\lambda_v-\gamma}{v-a}(x-at)}-e^{-\frac{\lambda_v-\gamma}{v+a}(x+at)}\right] \qquad \text{when} \qquad at<x<vt.$$

The energy, accumulated in the reactive elements in the line till the time moment t, can be calculated by formula

$$W_q(t)=\frac{1}{2}\int_{-at}^{vt}\left(Li^2+Cu^2\right)dx=\frac{vU_0^2}{a(\lambda_v-\gamma)Z_B}\left(e^{-2\gamma t}-e^{-2\lambda_v t}\right).$$

And the total energy takes the following form

$$W_0(t)=W_q(t)+W_n(t)=\frac{U_0^2}{(\lambda_v-\gamma)Z_B}\left[\frac{v}{a}e^{-2\gamma t}-\left(\frac{v}{a}-\frac{\lambda_v-\gamma}{\lambda_0}\right)e^{-2\lambda_v t}\right].$$

The total energy for ideal line $\gamma=0$ can be written down as

$$W_0(t)=\frac{U_0^2}{\lambda_v Z_B}\left[\frac{v}{a}-\left(\frac{v}{a}-\frac{\lambda_v}{\lambda_0}\right)e^{-2\lambda_v t}\right]=$$

$$=\frac{U_0^2}{(\lambda_v a/v)Z_B}\left[1-\left(1-\frac{\lambda_v a/v}{\lambda_0}\right)e^{-2\lambda_v t}\right]. \qquad (4.18)$$

It follows from (4.18) that to satisfy the energy conservation law, i.e. $\forall t>0$ the total energy to be equal to the initial energy in the capacitor $W_n(t)=U_0^2/(\lambda_0 Z_B)$, it is necessary to assign $\lambda_v a/v=\lambda_0$. This implies the following desired value for the speed of capacitor discharge $\lambda_v=\lambda_0 v/a$.

So, when moving with the speed greater than the electromagnetic wave speed, the capacitor discharges quicker then when $v\le a$.

As it follows from (4.16) – (4.17), the potential distribution depends only on the time in the disturbed domain and it is independent on the longitudinal coordinate x under the condition $\lambda_v=\gamma$ or $\lambda_0=a\gamma/v$, $C_n=$ $=2/(\lambda_0 Z_B)=2v/(a\gamma Z_B)$.

The distributions of voltage along the ideal and undistorting lines for the time moments t = 1; 2; 3; 4 when $v = 1.2 > a = 1$ are represented in the fig. 4.11 – 4.14.

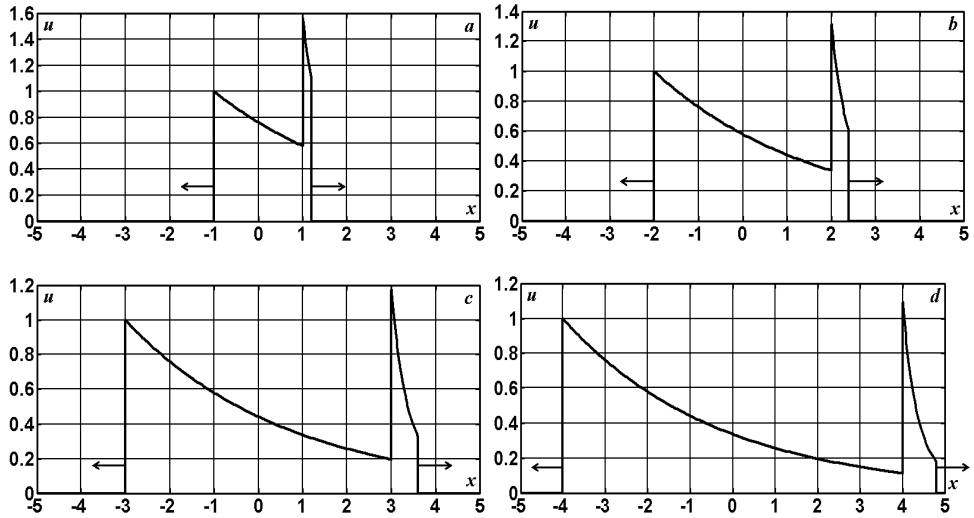

Fig. 4.11. The voltage distribution along the ideal line ($\gamma = 0$) for different time moments when $C_n = 4$, $\lambda_0 = 0.5$, $\lambda_v = 0.6$ and the steady speed $v = 1.2$ moving capacitor.

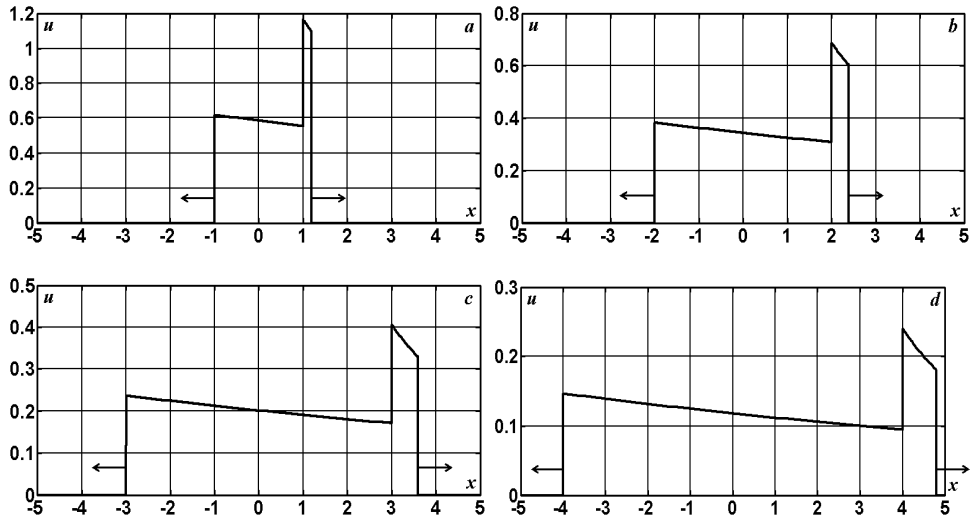

Fig. 4.12. The voltage distribution along the undistorting line ($\gamma = 0.48$) for different time moments when $C_n = 4$, $\lambda_0 = 0.5$, $\lambda_v = 0.6$ and the steady speed $v = 1.2$ moving capacitor.

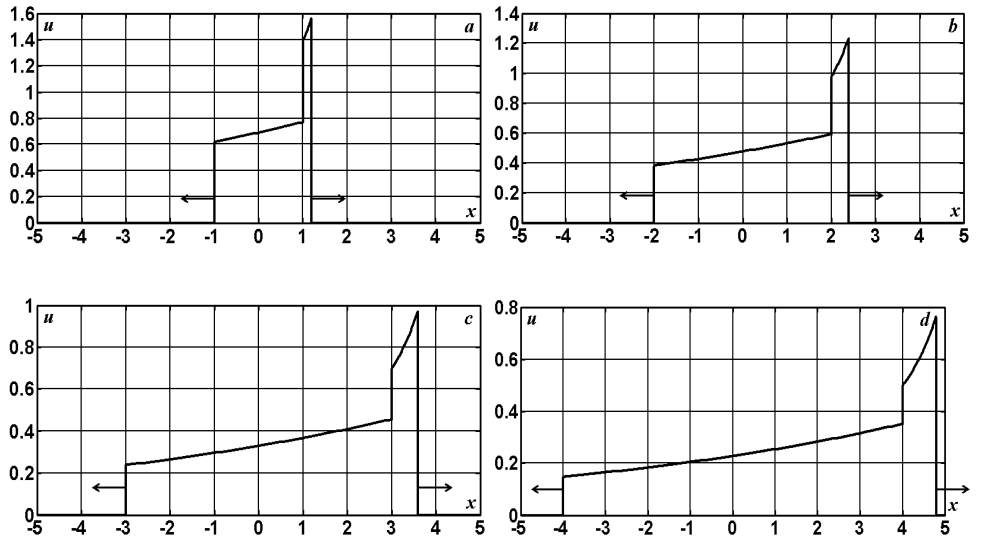

Fig. 4.13. The voltage distribution along the undistorting line ($\gamma = 0.48$) for different time moments when $C_n = 10$, $\lambda_0 = 0.2$, $\lambda_v = 0.24$ and the steady speed $v = 1.2$ moving capacitor.

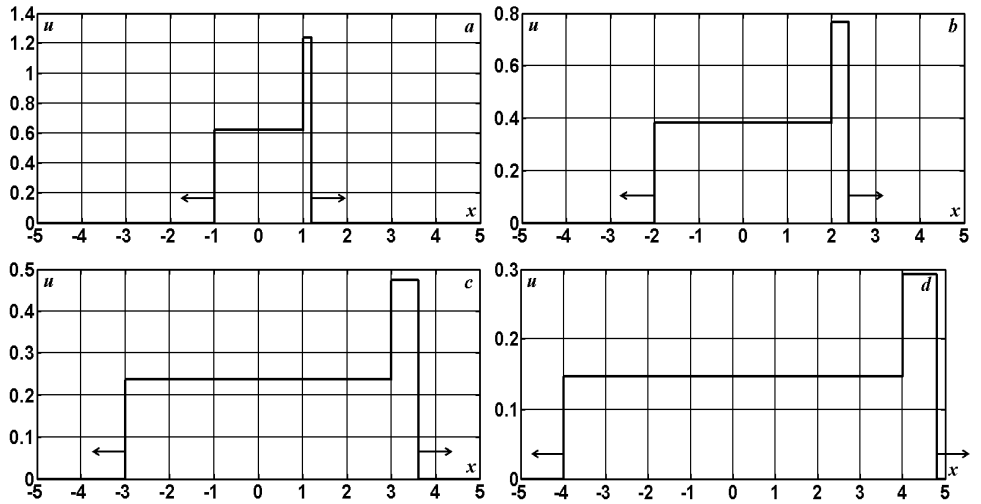

Fig. 4.14. The voltage distribution along the undistorting line ($\gamma = 0.48$) for different time moments when $C_n = 5$, $\lambda_0 = 0.4$, $\lambda_v = 0.48$ and the steady speed $v = 1.2$ moving capacitor.

Thus from the fig. 4.11 – 4.14 we see that the quantity of energy accumulated with time in the negative half plane $x < 0$ differs from energy in the domain $x > 0$. Indeed, using the solution (4.16) – (4.17), we obtain

$$W_-(t) = \frac{1}{2}\int_{-at}^{0}\left(Li^2 + Cu^2\right)dx = \frac{U_0^2(a+v)}{2a(\lambda_v - \gamma)Z_B}\left(e^{-2\gamma t} - e^{-\frac{2(a\lambda_v+\gamma v)t}{a+v}}\right),$$

$$W_+(t) = \frac{1}{2}\int_{0}^{vt}\left(Cu^2 + Li^2\right)dx =$$

$$= \frac{U_0^2}{2a(\lambda_v - \gamma)Z_B}\left((a+v)e^{-\frac{2(a\lambda_v+\gamma v)t}{a+v}} + (v-a)e^{-2\gamma t} - 2ve^{-2\lambda_v t}\right).$$

Let's consider the difference between the energies $\Delta W(t) = W_+(t) - W_-(t)$:

$$\Delta W(t) = W_+(t) - W_-(t) =$$

$$= \frac{U_0^2}{a(\lambda_v - \gamma)Z_B}\left((a+v)e^{-\frac{2(a\lambda_v+\gamma v)t}{a+v}} - ae^{-2\gamma t} - ve^{-2\lambda_v t}\right) =$$

$$= \frac{U_0^2}{adZ_B}e^{-\frac{2(a\lambda_v+\gamma v)t}{a+v}}\left[1 - \frac{a}{a+v}e^{2adt} - \frac{v}{a+v}e^{-2vdt}\right], \quad d = \frac{\lambda_v - \gamma}{a+v}. \qquad (4.19)$$

The derivative by parameter d of the expression in the square brackets of the formula (4.19) has the following signs

$$F(d) = 1 - \frac{a}{a+v}e^{2adt} - \frac{v}{a+v}e^{-2vdt},$$

$$F'_d = \frac{2t}{a+v}\left[v^2 e^{-2vdt} - a^2 e^{2adt}\right] = \begin{cases} > 0, \text{ при } d < \dfrac{\ln(v/a)}{(a+v)t} \\ < 0, \text{ при } d > \dfrac{\ln(v/a)}{(a+v)t} \end{cases}.$$

Then the function $F(d)$ is convex and it reaches the maximum positive value at the point $d = \dfrac{\ln(v/a)}{(a+v)t}$. But this means that the function $F(d)$ possesses both positive and negative values for different values of the parameter d. Taking into consideration the sign of the coefficient $U_0^2/(adZ_B)$ in the formula (4.19), we obtain that ΔW, as the function of parameter d, is decreasing function and it is equal to zero for $d = d_v$. The values d_v depend on time t and they can be determined as the roots of the transcendental equation $ae^{2adt} + ve^{-2vdt} = a + v$. Hence, we obtain

$$\Delta W(t) > 0,\ W_-(t) < W_+(t) \quad \text{when} \quad \lambda_v - \gamma < (a+v)d_v(t),$$

$$\Delta W(t) < 0,\ W_-(t) > W_+(t) \quad \text{when} \quad \lambda_v - \gamma > (a+v)d_v(t),$$

$$\Delta W(t) = 0,\ W_-(t) = W_+(t) \quad \text{when} \quad \lambda_v - \gamma = (a+v)d_v(t).$$

So, to obtain at any time moment t the equal total energy storage both in the positive and in the negative domains (that means the symmetry of the potential), the capacitor C_n must be variable (controllable) and must ensure the fulfillment of the condition: $\lambda_v = \gamma + (a+v)d_v(t)$.

4.3. Steady acceleration moving capacitor

Let's consider now the problem in which the discharging capacitor begins the motion with steady acceleration b and the initial speed v. But when its speed reaches the value a, at a later time the capacitor moves with this steady speed:

$$u(x_v(t),t) = U_0 e^{-\lambda_0 t},\ \lambda_0 = \frac{2}{C_n Z_B}, \tag{4.20}$$

$$x_v(t)=\begin{cases}\dfrac{bt^2}{2}+vt,\ 0\le t\le t_a\\ at,\ t>t_a\end{cases},\ t_a=\frac{a-v}{b},\ x_a=\frac{a^2-v^2}{2b},\ t\ge 0.$$

Here $x_v(t)$ denotes the trajectory of the capacitor motion on the plane *Oxt*, that is *OAB* on the fig. 4.15 and consists of two parts: at the part *OA* the curve $x_v(t)=\dfrac{bt^2}{2}+vt$ represents the parabola, and at the part *AB* it is a straight line $x_v(t)=at$.

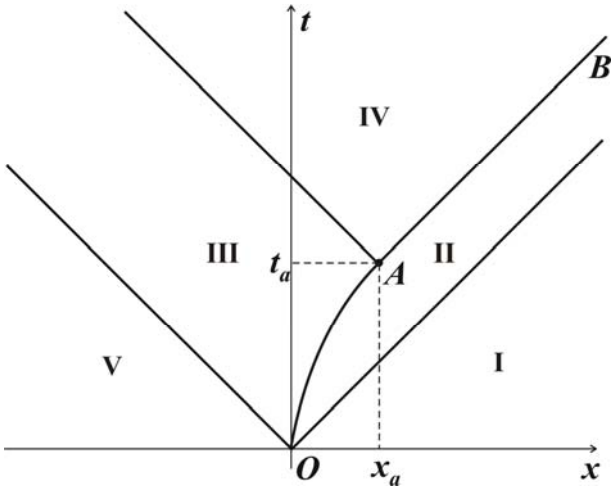

Fig. 4.15. The location of the solution regions on the plane *Oxt* when the capacitor is moving with steady acceleration right up till its speed reaches the electromagnetic wave speed *a*.

The solution of the problem, determined by method of characteristics, has the different form at every of five domains of the plane *Oxt* (fig. 4.15). The solution is zero in the domains I and V, where the electromagnetic wave is not yet reached. Then we have the direct wave propagation (moving to the right) in the domain II:

$$u(x,t)=U_0e^{-\gamma(t-t^+)}e^{-\lambda_0 t^+}=U_0e^{-\gamma t-(\lambda_0-\gamma)t^+},\ i(x,t)=u(x,t)/Z_B,\qquad(4.21)$$

$$t^+ = t^+(x,t) = \frac{a-v}{b}\left[1-\sqrt{1-\frac{2b(at-x)}{(a-v)^2}}\right]$$

when

$$\frac{bt^2}{2}+vt < x < at,\ 0 \le t \le t_a \quad \text{or} \quad a(t-t_a)+x_a < x < at,\ t > t_a .$$

And we have the return wave propagation (moving to the left) in the domain III:

$$u(x,t) = U_0 e^{-\gamma(t-t^-)} e^{-\lambda_0 t^-} = U_0 e^{-\gamma t-(\lambda_0-\gamma)t^-},\ i(x,t) = -u(x,t)/Z_B , \qquad (4.22)$$

$$t^- = t^-(x,t) = \frac{a+v}{b}\left[\sqrt{1+\frac{2b(at+x)}{(a+v)^2}}-1\right]$$

when

$$-at < x < \frac{bt^2}{2}+vt,\ 0 \le t \le t_a \quad \text{or} \quad -at < x < -a(t-t_a)+x_a ,\ t > t_a .$$

And we have also the return wave propagation (moving to the left) in the domain IV:

$$u(x,t) = U_0 e^{-\frac{(\gamma+\lambda_0)t}{2}} e^{-\frac{\lambda_0-\gamma}{2a}(x+at_a-x_a)},\ i(x,t) = -u(x,t)/Z_B \qquad (4.23)$$

when

$$-a(t-t_a)+x_a < x < a(t-t_a)+x_a ,\ t \ge t_a .$$

The distributions of voltage along the ideal and undistorting lines for the time moments t = 1.0; 2.0; 3.0; 4.0 when $v = 0$, $b = 0.5$ ($x_a = 1$, $t_a = 2$) are represented in the fig. 4.16 – 4.18.

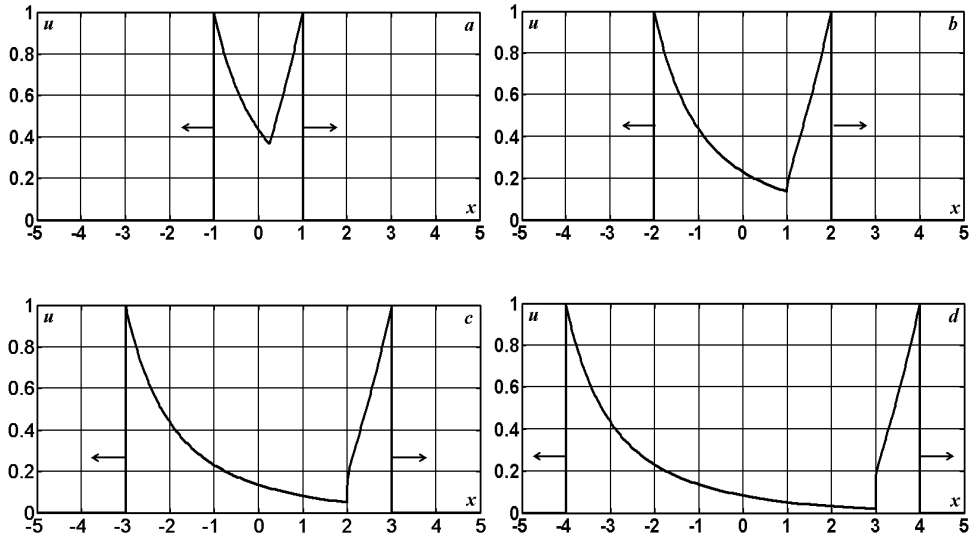

Fig. 4.16. The voltage distribution along the ideal line ($\gamma = 0$) for different time moments when $C_n = 1$, $\lambda_0 = 2$ and the steady acceleration $b = 0.5$ moving capacitor.

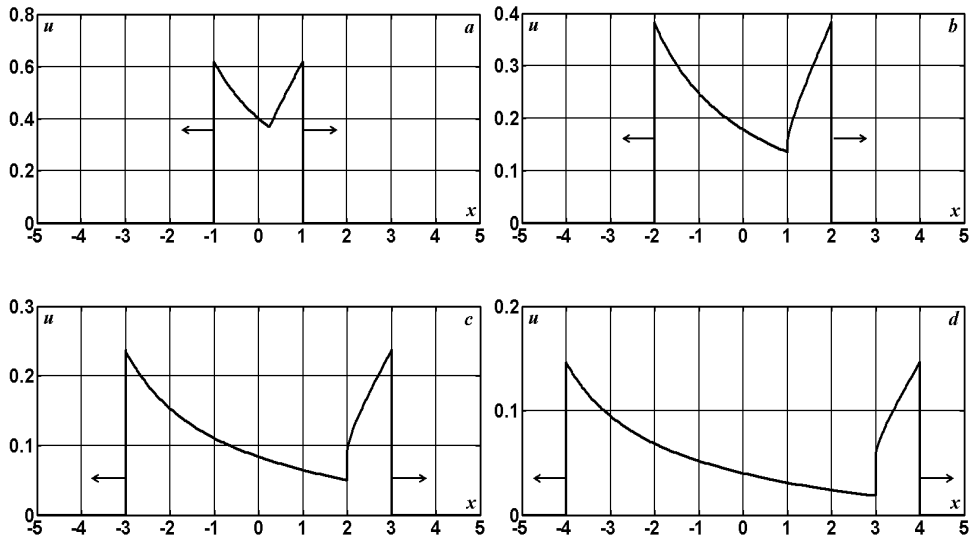

Fig. 4.17. The voltage distribution along the undistorting line ($\gamma = 0.48$) for different time moments when $C_n = 1$, $\lambda_0 = 2$ and the steady acceleration $b = 0.5$ moving capacitor.

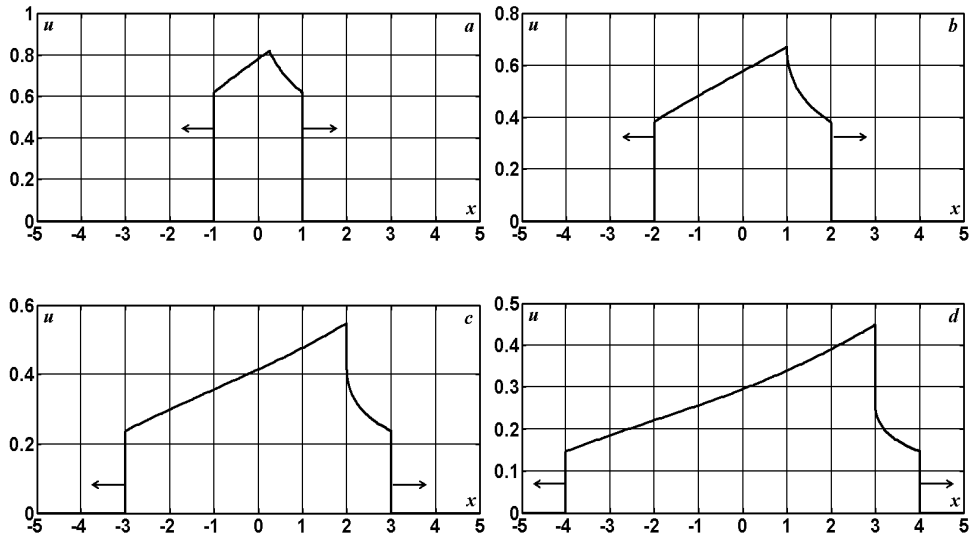

Fig. 4.18. The voltage distribution along the undistorting line ($\gamma = 0.48$) for different time moments when $C_n = 10$, $\lambda_0 = 0.2$ and the steady acceleration $b = 0.5$ moving capacitor.

How it follows from formulas (4.21) – (4.23) and fig. 4.16 – 4.18, the solution $u(x,t)$ is the continuous function of variable x till the time moment t_a, i.e. the time moment when the moving capacitor reaches the electromagnetic wave speed a. At a later time $t > t_a$ the function $u(x,t)$ endure the discontinuity (jump) at the points $x = a(t - t_a) + x_a$, i.e. along the straight line AB at the interface of domains II and IV (fig. 4.15). The value of this jump is the following

$$u(x+0,t) - u(x-0,t) = U_0 e^{-\gamma t}\left[e^{-(\lambda_0-\gamma)t_a} - e^{-(\lambda_0-\gamma)t/2}\right],$$

and it is equal to zero when $\lambda_0 = \gamma$.

The energy, accumulated in the line till time moment t, can be calculated by the formula that coincides with the formula for the case of steady speed moving capacitor when $v \le a$.

If not only wave dissipation, but the dispersion as well is presented, then the solution can not be presented in the form of decaying (d'Alemberian) solitons and the calculation must be effectuated by means of program Albatross. For the line with dispersion ($RC \neq GL$) the gradients of the wave field by x always will be nonzero and the symmetrical potential distribution

can't be achieved (fig. 4.19). As soon as the speed v exceeds the value of a, the solution becomes multiversion and the speed of discharge λ_v must be corrected in such a way as to ensure the observance of electromagnetic energy balance.

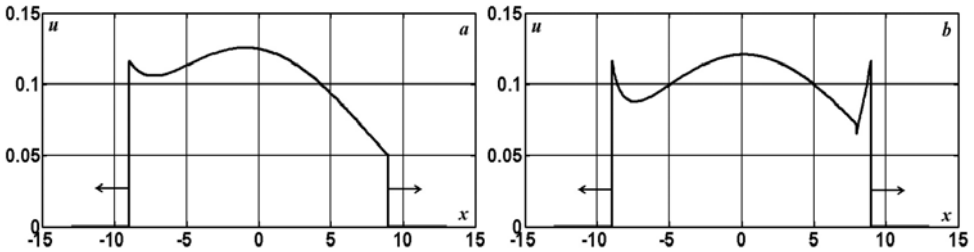

Fig. 4.19. The potential distribution for the time moment $t = 9.0$ along the line with losses $R = 0.48$, $G = 0$ when $C_n = 2$; $\lambda_0 = 1$; $v = 1.2$ (***a***); $b = 0.5$(***b***).

Thus, the dynamics of the capacitor discharge on the long line was analyzed by means of exact solutions of the telegraph equations. Under the some correlation between the capacitor of the voltage source and the losses in the line, the distribution of the total energy in the line becomes symmetrical and independent of the capacitor speed. It was discovered the effect of the speed enhancing of the electric capacity discharge under the speeds exceeding the speed of potential and current wave propagation in the line. The nonlinear problem of the steady acceleration moving capacitor was also solved.

5. The pulse mode power. Capacity or inductance connection to loaded continuous current line

It is well known, that the sudden alteration of the parameters of the line or of the receiver in the steady state electricity transmission leads to the rushes of both voltage (current) source power and active power consumed by loading at the transient stage of the process. Let's set a problem to carry out the exact quantitative analysis of nonstationary voltages and currents during the millisecond range. Another problem will be to determine the conditions in which the loading power reaches the maximal values under the pulse mode. Toward this end let's consider at first the momentary connection to the continuous voltage line of some passive one-ports in the form of

uncharged lumped capacity or inductance (we'll denote them as reactive power sources – RPS).

Let's consider undistorting line with the length *l*, that is connected to the continuous voltage source U_0 and closed on the resistance R_S. Let's suppose that the uncharged capacitor C_n is momentary paralleling at the point $x_n = l/2$ in the time moment $t = t^* > 0$ (fig. 5.1).

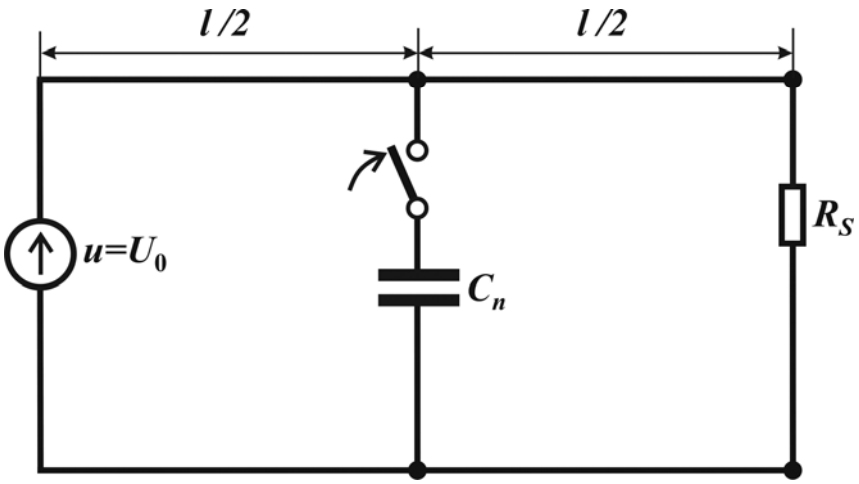

Fig. 5.1. Uncharged capacitor paralleling to the continuous current transmission line.

It requires to determine the voltage function $u(x,t)$ and current function $i(x,t)$, satisfying the system of telegraph equations

$$L\frac{\partial i}{\partial t}+\frac{\partial u}{\partial x}+Ri=0;\ C\frac{\partial u}{\partial t}+\frac{\partial i}{\partial x}+Gu=0,\ \ x\in[0,l],\ t>0 \qquad (5.1)$$

and the following initial and boundary conditions:

$$u(x,0)=i(x,0)=0,\ \ x\in[0,l], \qquad (5.2)$$

$$u(0,t)=U_0,\ \ u(l,t)=R_S i(l,t),\ \ t\geq 0, \qquad (5.3)$$

$$C_n\frac{du(x_n,t)}{dt}=i(x_n-0,t)-i(x_n+0,t),\quad t>t^*;\ u(x_n,t^*)=0. \qquad (5.4)$$

In the case of undistorting line: $R/L = G/C = \gamma$ the solution of the problem (5.1) – (5.4) can be find by method of characteristics [89, 90]. Till the time moment t^* the solution is determined in [89] and it has the following form

$$u_{2n}(t) = U_0\,,\; i_{2n}(t) = \frac{U_0}{Z_B}\left[1 + 2\sum_{j=1}^{n-1}(-z_\gamma)^j\right] = \frac{U_0\left[1 - z_\gamma - 2(-z_\gamma)^n\right]}{Z_B(1+z_\gamma)} \qquad (5.5)$$

when $x = 0\,,\; t \in [2(n-1)\Delta, 2n\Delta],\; n = 1,2,3,\ldots;$

$$u_{2n+1}(t) = (1+z)U_0 e^{-\gamma\Delta}\sum_{j=0}^{n-1}(-z_\gamma)^j = (1+z)U_0 e^{-\gamma\Delta}\frac{1-(-z_\gamma)^n}{1+z_\gamma},$$

$$i_{2n+1}(t) = \frac{(1-z)U_0 e^{-\gamma\Delta}}{Z_B}\sum_{j=0}^{n-1}(-z_\gamma)^j = \frac{(1-z)U_0 e^{-\gamma\Delta}}{Z_B}\frac{1-(-z_\gamma)^n}{1+z_\gamma} \qquad (5.6)$$

when $x = l\,,\; t \in [(2n-1)\Delta, (2n+1)\Delta],\; n = 1,2,3,\ldots.$

Here we use the following notations:

$$z = \frac{R_S - Z_B}{R_S + Z_B},\; z_\gamma = ze^{-2\gamma\Delta},\; Z_B = \sqrt{\frac{L}{C}},\; \Delta = l/a\;\; a = \frac{1}{\sqrt{LC}}. \qquad (5.7)$$

Let's suppose that the uncharged capacitor is connected to the middle point of the line in the time moment $t^* = 2n^*\Delta$. Then from the correlation on the characteristics $x \pm at = const$ for $t \in [t^*, t^* + \Delta/2]$ at the point $x_n = l/2$ we obtain

$$u(x_n - 0, t) + Z_B i(x_n - 0, t) =$$

$$= \left[u(0, t - \Delta/2) + Z_B i(0, t - \Delta/2)\right]e^{-\gamma\Delta/2} = \left[U_0 + Z_B i_{2n^*}\right]e^{-\gamma\Delta/2} \equiv A_0$$

$$u(x_n + 0, t) - Z_B i(x_n + 0, t) = \left[u(l, t - \Delta/2) - Z_B i(l, t - \Delta/2)\right]e^{-\gamma\Delta/2} =$$

$$= \left[u_{2n^*+1} - Z_B i_{2n^*+1}\right]e^{-\gamma\Delta/2} \equiv B_0\,. \qquad (5.8)$$

Then we add to these relations the voltage continuity condition and the differential equation (5.4):

$$u_n = u(x_n - 0, t) = u(x_n + 0, t),$$

$$C_n \frac{du_n}{dt} = i_n,\ i_n = i(x_n - 0, t) - i(x_n + 0, t). \tag{5.9}$$

Solving the equations (5.8) – (5.9) with regard to voltage and current values in the point x_n, we have

$$u_{n,0}(t) = \frac{A_0 + B_0}{2}\left[1 - e^{\lambda_n (t - t^*)}\right],\ i_{n,0-}(t) = \frac{A_0 - u_{n,0}(t)}{Z_B},$$

$$i_{n,0+}(t) = \frac{u_{n,0}(t) - B_0}{Z_B},\ i_{n,0}(t) = i_{n,0-}(t) - i_{n,0+}(t), \tag{5.10}$$

$$\lambda_n = -\frac{2}{C_n Z_B},\quad x = x_n, t \in [t^*, t^* + \Delta/2].$$

During this time interval $t \in [t^*, t^* + \Delta/2]$ at the end points of the line (till the wave from the capacitor draw-off point doesn't reach the ends) the solution remains as (5.5) – (5.6):

$$u_{0,0} = u(0, t) = U_0,$$

$$i_{0,0} = i(0, t) = i_{2(n^*+1)},\ x = 0, t \in [t^*, t^* + \Delta/2]; \tag{5.11}$$

$$u_{l,0} = u(l, t) = u_{2n^*+1},$$

$$i_{l,0} = i(l, t) = i_{2n^*+1},\ x = l, t \in [t^*, t^* + \Delta/2]. \tag{5.12}$$

During the next time interval $t \in [t^* + \Delta/2, t^* + \Delta]$ the wave from capacitor reaches the end points of the line and the solution becomes as follows

$$u_{0,1}(t) - Z_B i_{0,1}(t) = \left[u_{n,0}(t - \Delta/2) - Z_B i_{n,0-}(t - \Delta/2)\right] e^{-\gamma\Delta/2} \equiv D_1(t),$$

$$u_{0,1}(t) = U_0, \;\; i_{0,1}(t) = \left[U_0 - D_1(t)\right]/Z_B, \;\; x = 0; \qquad (5.13)$$

$$u_{l,1}(t) + Z_B i_{l,1}(t) = \left[u_{n,0}(t - \Delta/2) + Z_B i_{n,0+}(t - \Delta/2)\right] e^{-\gamma\Delta/2} \equiv E_1(t),$$

$$u_{l,1}(t) = R_S i_{l,1}(t),$$

$$u_{l,1}(t) = (1+z)E_1(t)/2, \;\; i_{l,1}(t) = (1-z)E_1(t)/(2Z_B), \;\; x = l. \qquad (5.14)$$

During the same interval $t \in [t^* + \Delta/2, t^* + \Delta]$ at the middle point of the line we have

$$A_1(t) = \left[U_0 + Z_B i_{0,0}(t - \Delta/2)\right] e^{-\gamma\Delta/2},$$

$$B_1(t) = \left[u_{l,0}(t - \Delta/2) - Z_B i_{l,0}(t - \Delta/2)\right] e^{-\gamma\Delta/2},$$

$$u_{n,1}(t) = u_{n,0}(t^* + \Delta/2) e^{\lambda_n (t - t^* - \Delta/2)} - \frac{\lambda_n}{2} \int_{t^* + \Delta/2}^{t} \left[A_1(\tau) + B_1(\tau)\right] e^{\lambda_n (t - \tau)} d\tau,$$

$$\lambda_n = -\frac{2}{C_n Z_B}, \; i_{n,1-}(t) = \frac{A_1(t) - u_{n,1}(t)}{Z_B}, \;\; i_{n,1+}(t) = \frac{u_{n,1}(t) - B_1(t)}{Z_B},$$

$$i_{n,1}(t) = i_{n,1-}(t) - i_{n,1+}(t), \;\; x = x_n, \; t \in [t^* + \Delta/2, t^* + \Delta]. \qquad (5.15)$$

During the next time interval $t \in [t^* + \Delta, t^* + 3\Delta/2]$ the solution at the end points of the line takes the form

$$u_{0,2}(t) - Z_B i_{0,2}(t) = \left[u_{n,1}(t - \Delta/2) - Z_B i_{n,1-}(t - \Delta/2)\right] e^{-\gamma\Delta/2} \equiv D_2(t),$$

$$u_{0,2}(t) = U_0, \;\; i_{0,2}(t) = \left[U_0 - D_2(t)\right]/Z_B, \;\; x = 0; \qquad (5.16)$$

$$u_{l,2}(t) + Z_B i_{l,2}(t) = \left[u_{n,1}(t - \Delta/2) + Z_B i_{n,1+}(t - \Delta/2)\right] e^{-\gamma\Delta/2} \equiv E_2(t),$$

$$u_{l,2}(t) = R_S i_{l,2}(t)\,,$$

$$u_{l,2}(t) = (1+z)E_2(t)/2\,,\ i_{l,2}(t) = (1-z)E_2(t)/(2Z_B)\,,\ x = l\,. \qquad (5.17)$$

During the same interval $t \in [t^*+\Delta, t^*+3\Delta/2]$ at the middle point of the line we obtain:

$$A_2(t) = \left[U_0 + Z_B i_{0,1}(t-\Delta/2)\right]e^{-\gamma\Delta/2}\,,$$

$$B_2(t) = \left[u_{l,1}(t-\Delta/2) - Z_B i_{l,1}(t-\Delta/2)\right]e^{-\gamma\Delta/2}\,,$$

$$u_{n,2}(t) = u_{n,1}(t^*+\Delta)e^{\lambda_n(t-t^*-\Delta)} - \frac{\lambda_n}{2}\int\limits_{t^*+\Delta}^{t}\left[A_2(\tau)+B_2(\tau)\right]e^{\lambda_n(t-\tau)}d\tau\,,$$

$$i_{n,2-}(t) = \frac{A_2(t)-u_{n,2}(t)}{Z_B},\ \ i_{n,2+}(t) = \frac{u_{n,2}(t)-B_2(t)}{Z_B},$$
$$i_{n,2}(t) = i_{n,2-}(t) - i_{n,2+}(t),\quad x = x_n,\ t \in [t^*+\Delta, t^*+3\Delta/2]\,. \qquad (5.18)$$

Proceeding in the same manner one can obtain the solutions for any time interval

$t \in [t^*+m\Delta/2, t^*+(m+1)\Delta/2]$, m = 1, 2, 3, …

$$u_{0,m}(t) - Z_B i_{0,m}(t) =$$

$$= \left[u_{n,m-1}(t-\Delta/2) - Z_B i_{n,(m-1)-}(t-\Delta/2)\right]e^{-\gamma\Delta/2} \equiv D_m(t)\,,$$

$$u_{0,m}(t) = U_0\,,\ \ i_{0,m}(t) = \left[U_0 - D_m(t)\right]/Z_B\,,\ x = 0\,; \qquad (5.19)$$

$$u_{l,m}(t) + Z_B i_{l,m}(t) =$$

$$= \left[u_{n,m-1}(t-\Delta/2) + Z_B i_{n,(m-1)+}(t-\Delta/2)\right]e^{-\gamma\Delta/2} \equiv E_m(t)\,,$$

$$u_{l,m}(t) = R_S i_{l,m}(t)\,,\; u_{l,m}(t) = (1+z)E_m(t)/2\,,$$

$$i_{l,m}(t) = (1-z)E_m(t)/(2Z_B)\,,\; x = l\,. \qquad (5.20)$$

During the same time interval at the middle point of the line we have the following relations

$$A_m(t) = \left[U_0 + Z_B i_{0,m-1}(t-\Delta/2)\right]e^{-\gamma\Delta/2}\,,$$

$$B_m(t) = \left[u_{l,m-1}(t-\Delta/2) - Z_B i_{l,m-1}(t-\Delta/2)\right]e^{-\gamma\Delta/2}\,,$$

$$u_{n,m}(t) = u_{n,m-1}(t^* + m\Delta/2)e^{\lambda_n(t-t^*-m\Delta/2)} -$$

$$-\frac{\lambda_n}{2}\int_{t^*+m\Delta/2}^{t}\left[A_m(\tau) + B_m(\tau)\right]e^{\lambda_n(t-\tau)}d\tau\,,$$

$$i_{n,m-}(t) = \frac{A_m(t) - u_{n,m}(t)}{Z_B}\,,\; i_{n,m+}(t) = \frac{u_{n,m}(t) - B_m(t)}{Z_B}\,,$$

$$i_{n,m}(t) = i_{n,m-}(t) - i_{n,m+}(t)\,,$$

$$x = x_n\,,\; t \in [t^* + m\Delta/2, t^* + (m+1)\Delta/2]\,. \qquad (5.21)$$

Using the obtained relations let's study at first the wave processes in the ideal line (R = G = 0), closed on impedance: $R_S = Z_B = 1$. Almost straight away after the commutation, the steady-state conditions with unit currents, voltages, generated and transmission capacities are formed. Let's suppose that the uncharged capacitor C_n is momentary connected at the point $x_n = l_n = l/2$ in the time moment t = 0.3125 corresponding to the 5 wave runs along the line length $l = 1/16$.

The dynamics of the power changes of the source, receiver and RPS is represented in the fig. 5.2 (curves 1-3) with consecutive doubling of the value C_n = 1(*a*); 2(*b*); 4(*c*); 8(*d*).. The increasing of this value is accompanied by disproportionate but monotonous increasing of the pure active load-

ing power during the transient process: P_1 = 3.13; 3.33; 3.50; 3.64, correspondingly.

Taking into account the losses in the continuous current line (fig. 5.3) we observe some decreasing of power rushes and nonlinear dependence of its maximal values on the values of the connected capacity: P_1 = 2.64; 2.68; 2.63; 2.5. Thus, as a first approximation the value C_n = 2 can be considered the optimal one in respect to reaching the ultimate loading power under the pulse mode and with capacitor connection at the middle point of the continuous current line.

If we move the point of capacity (C_n = 2) connection near the source $l_n = l/4$, then we get some increasing of the loading power: P_1 = 2.95 (fig. 5.4, *a*). However, the parametrical analysis makes it clear that the amplitude of oscillation of the active power can be raised no more than three-fold relatively to nominal level. It is interesting to mention, that these fluctuations can be eliminated, if the throttle with inductance L_m is connected to the line (independent of the point of its series connection $x_m = l_m$) simultaneously with capacity (fig. 5.4, *b-d*).

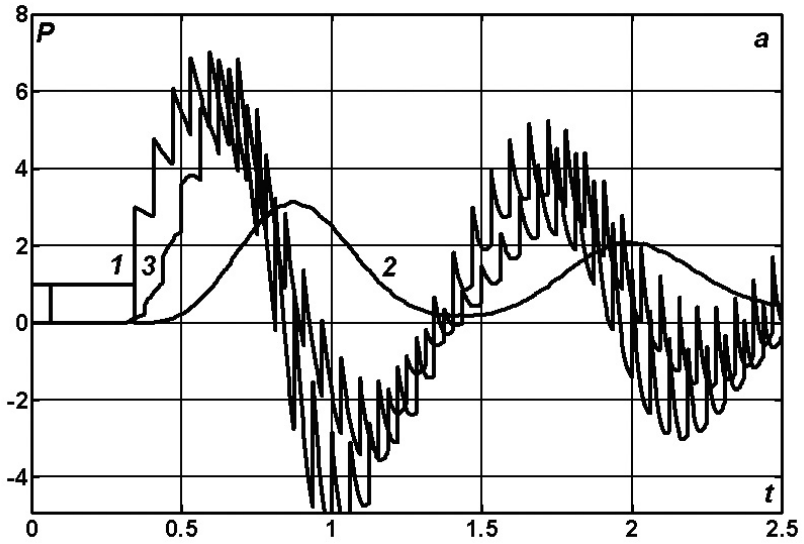

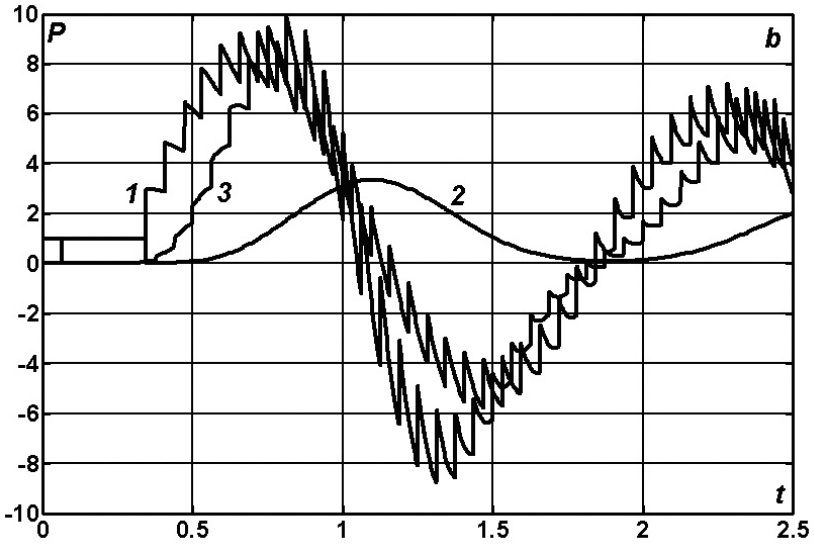

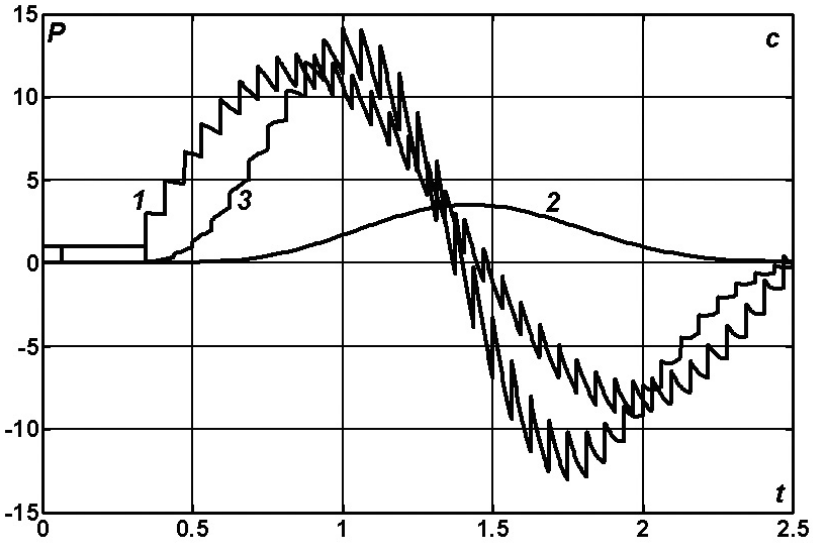

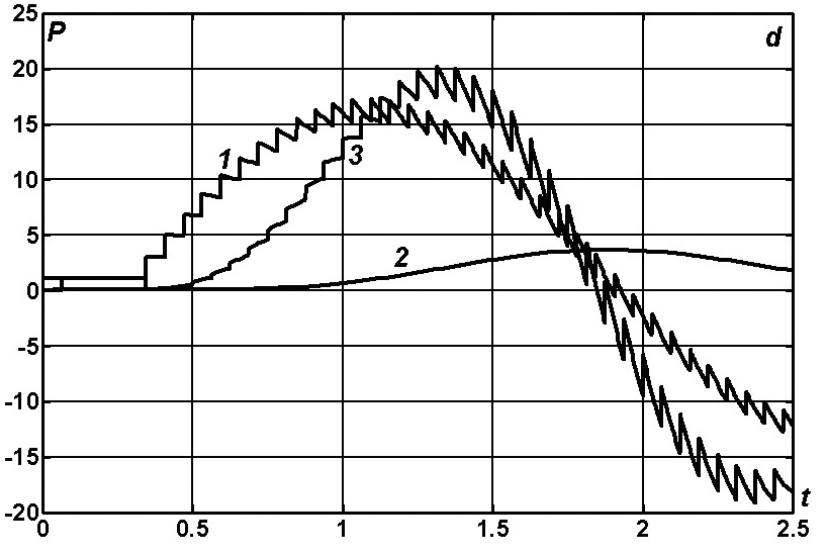

Fig. 5.2. Generator, loading and RPS power (curves 1-3) when $R = G = 0$; C_n = 1(***a***); 2(***b***); 4(***c***); 80(***d***).

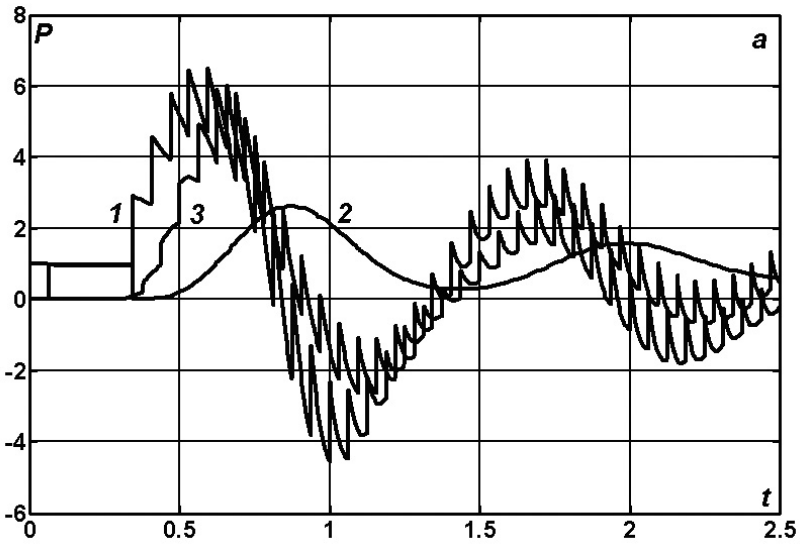

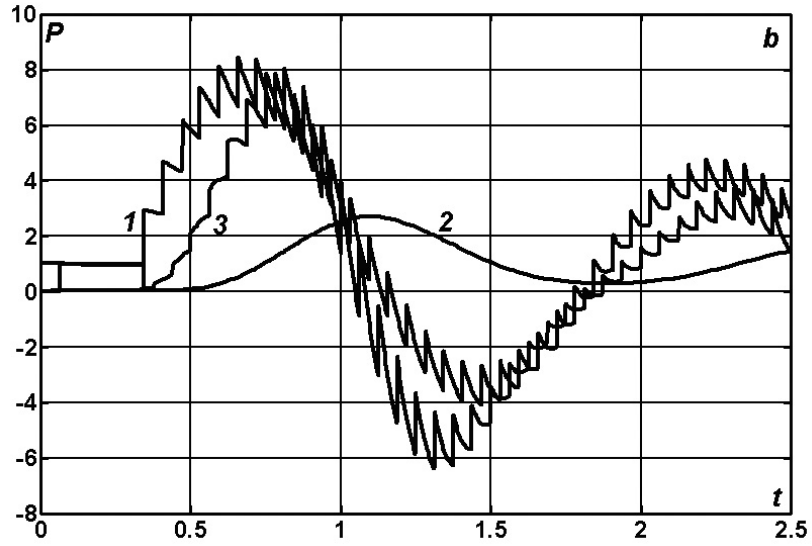

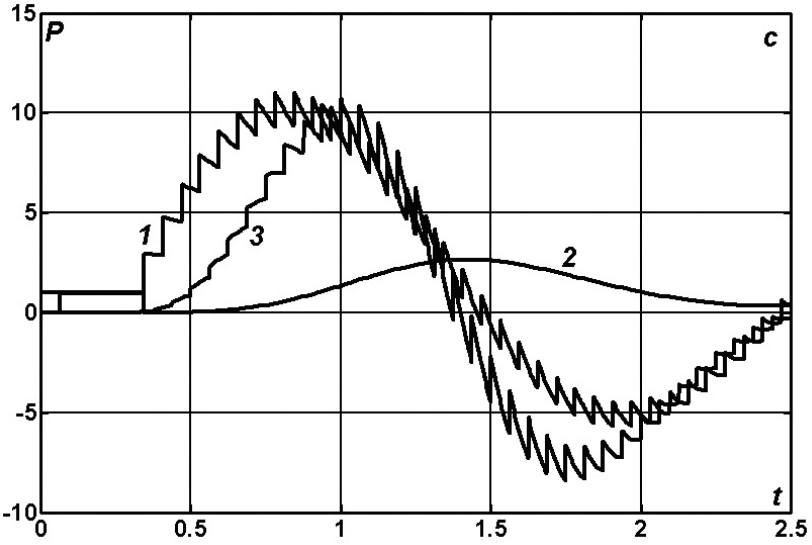

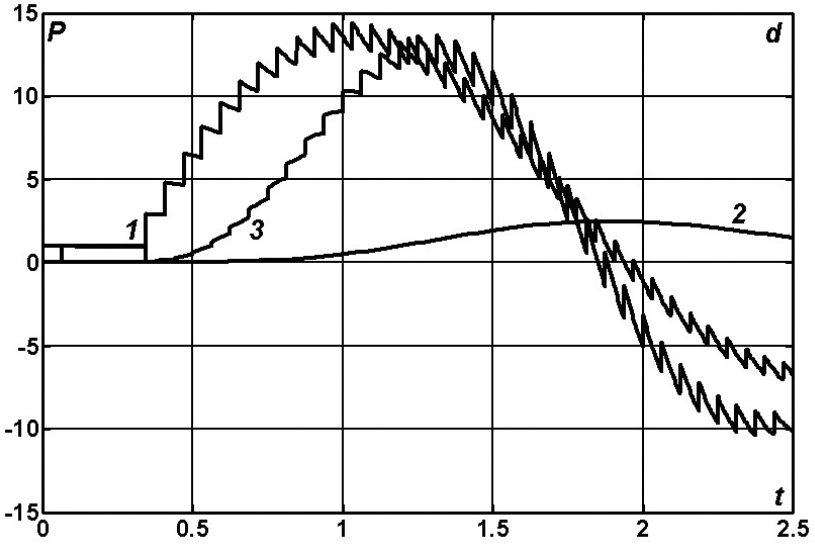

Fig. 5.3. Generator, loading and RPS power (curves 1-3) when $R = 7G = 0.48$; C_n = 1(***a***); 2(***b***); 4(***c***); 8(***d***).

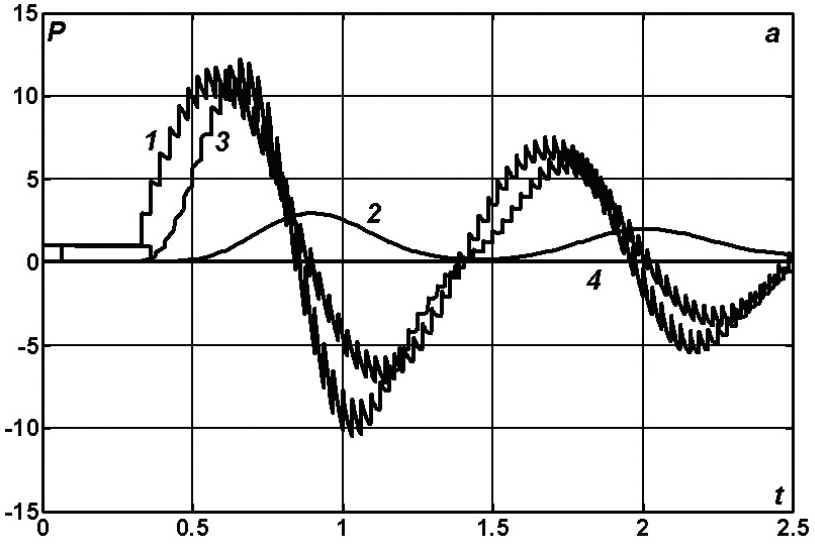

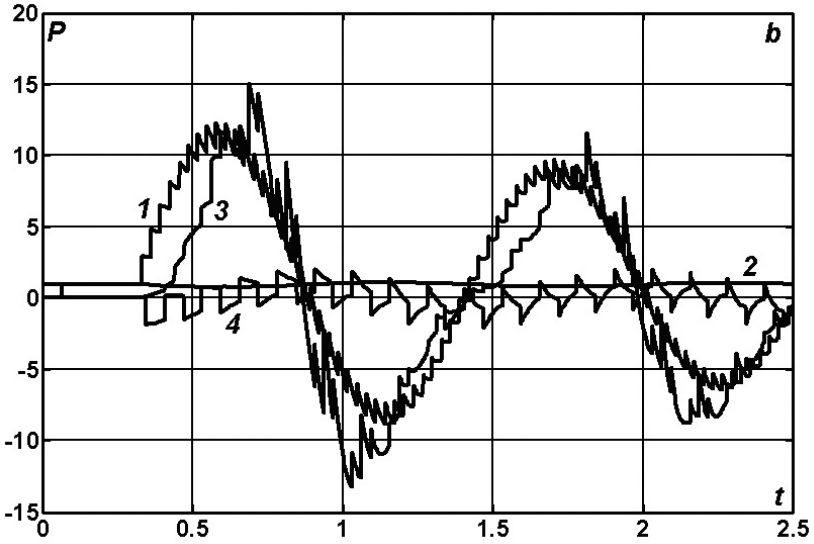

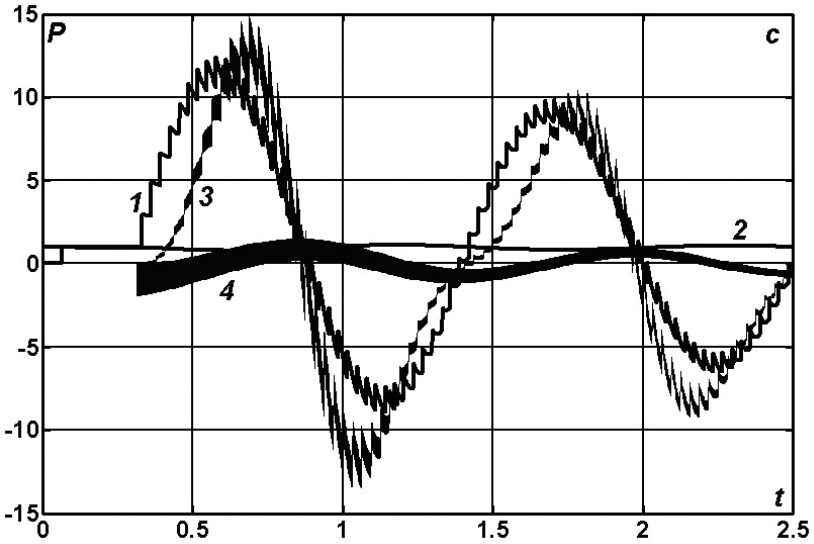

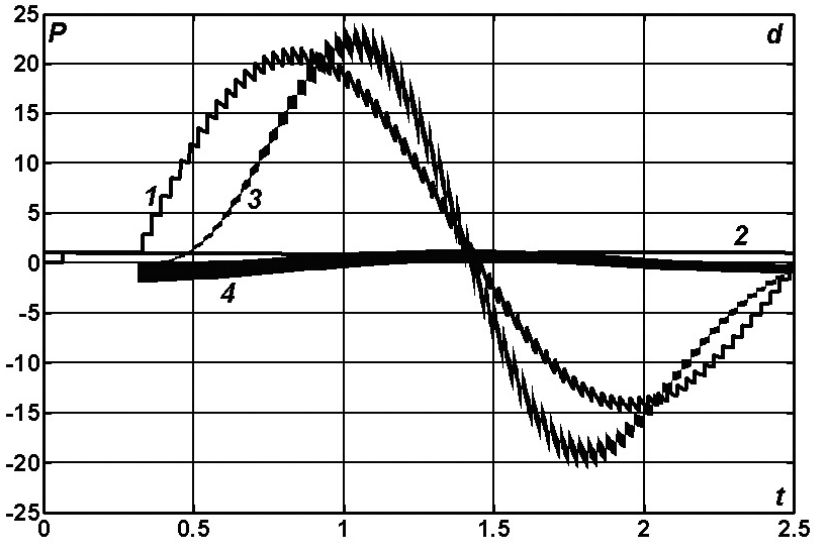

Fig. 5.4. Generator, loading and RPS power (curves 1-4) when $R = 7G = 0.48$; $C_n = 2$, $l_n = l/4$ (***a***); $C_n = L_m = 2$, $l_n = l/4$, $l_m = 3l/4$ (***b***); $C_n = L_m = 2$, $l_n = l_m = l/4$ (***c***); $C_n = L_m = 8$, $l_n = l_m = l/4$ (***d***).

6. Active and reactive powers of the long line

It is to mention that in the training and special literature there is no some common and strongly valid approach for the definition of the active and reactive power of the long line even in case of steady-state sinusoidal processes, not to mention the transient regimes. By means of complex amplitude method the total (apparent) power can be decomposed in two orthogonal components and so we can obtain their distribution along the whole circuit. However, at the same time it remains unclear what we must to interpret by reactive power of the whole line without resorting to its simplified representation as a lumped *RLC* – circuit [15, 56, 59]. Meanwhile, in respect to the mathematical physics the indetermination in the interpretation of the reactive power can be eliminated. The original equations of the electrical circuits theory are of hyperbolic type, but the energy integral (or the total electromagnetic energy conservation law) is well known and commonly used for such equations [95 – 98, 25 – 27].

6.1. The power under the sinusoidal regime

The electromagnetic power transmission in the long line by conduction currents can be described by well known telegraph equations that represent the Kirchhoff's law for closed contour formed by subcircuit with length *dx*:

$$L\frac{\partial i}{\partial t}+\frac{\partial u}{\partial x}+Ri=0;\;\; C\frac{\partial u}{\partial t}+\frac{\partial i}{\partial x}+Gu=0\,. \tag{6.1}$$

To obtain the unique solution the system (6.1) must be completed with initial and boundary conditions. Let's suppose that the electrical circuit at the initial time moment $t=0$ is connected to the external sinusoidal voltage source and its receiving end is closed on the load resistance $Z_S=R_S+jX_S$:

$$u=U_0e^{j\omega t} \text{ when } x=0\,; \quad u=Z_s i \text{ when } \quad x=l\,.$$

Let's derive the following integral identities transforming the equation (6.1) in the complex functions space. For that we multiply the first equation (6.1) by conjugated to current function i^*. The second equation we replace by conjugated one and multiply it by *u*. Now we sum up the obtained relations

$$L\frac{\partial i}{\partial t}i^*+C\frac{\partial u^*}{\partial t}u+\frac{\partial}{\partial x}(ui^*)+Rii^*+Guu^*=0$$

or

$$L\frac{\partial i}{\partial t}i^*+C\frac{\partial u^*}{\partial t}u+\frac{\partial}{\partial x}(ui^*)+R\left|i\right|^2+G\left|u\right|^2=0\,. \tag{6.2}$$

Let's write down one more expression conjugated to (6.2):

$$L\frac{\partial i^*}{\partial t}i+C\frac{\partial u}{\partial t}u^*+\frac{\partial}{\partial x}(u^*i)+R\left|i\right|^2+G\left|u\right|^2=0\,. \tag{6.3}$$

Now we sum up and subtract relations (6.2) and (6.3). After some transformations we obtain two identities:

$$\frac{1}{2}\frac{\partial}{\partial t}\left(L\left|i\right|^2+C\left|u\right|^2\right)+\frac{\partial}{\partial x}\left[\mathrm{Re}(ui^*)\right]+R\left|i\right|^2+G\left|u\right|^2=0; \qquad (6.4)$$

$$L\left(\frac{\partial i}{\partial t}i^*-\frac{\partial i^*}{\partial t}i\right)+C\left(\frac{\partial u^*}{\partial t}u-\frac{\partial u}{\partial t}u^*\right)+2j\frac{\partial}{\partial x}\left[\mathrm{Im}(ui^*)\right]=0. \qquad (6.5)$$

Let's suppose now that under the steady state regime when $t\to\infty$ the solution (as well as the input voltage) can be represented in the form of complex functions: $u(x,t)=U(x)e^{j\omega t}$ и $i(x,t)=I(x)e^{j\omega t}$. If the active values of voltages and currents are assigned as $U(x)=\left|U(x)\right|e^{j\varphi_u(x)}$; $I(x)=\left|I(x)\right|e^{j\varphi_i(x)}$, than in this case we have $\left|u(x,t)\right|=\left|U(x)\right|$ and $\left|i(x,t)\right|=\left|I(x)\right|$. Hence, $\mathrm{Re}(ui^*)$ from (6.4) and $\mathrm{Im}(ui^*)$ from (6.5) can be expressed by active power P and reactive power Q from the standpoint of the theoretical foundations of electrotechnology [15, 56, 59]:

$$ui^*=\left|U(x)\right|\cdot\left|I(x)\right|e^{j\varphi_u(x)}e^{-j\varphi_i(x)}=\left|U(x)\right|\cdot\left|I(x)\right|e^{j\varphi(x)};\ \varphi(x)=\varphi_u(x)-\varphi_i(x);$$

$$\mathrm{Re}(ui^*)=\left|U(x)\right|\cdot\left|I(x)\right|\cos\varphi(x)=P(x);$$

$$\mathrm{Im}(ui^*)=\left|U(x)\right|\cdot\left|I(x)\right|\sin\varphi(x)=Q(x).$$

Further we substitute the expressions $u(x,t)=U(x)e^{j\omega t}$ and $i(x,t)=I(x)e^{j\omega t}$ in (6.4) and (6.5), then we integrate by x on the interval $0\le x\le l$ and after some transformations we can obtain the following balance equations of active and reactive powers:

$$\int_0^l\left(R\left|I(x)\right|^2+G\left|U(x)\right|^2\right)dx=P(0)-P(l) \qquad (6.6)$$

and

$$\omega\int_0^l\left(L\left|I(x)\right|^2-C\left|U(x)\right|^2\right)dx=Q(0)-Q(l). \qquad (6.7)$$

So the left-hand members of the equalities (6.6) and (6.7) define correspondingly the active and reactive power of the long line. Computations can be continued by means of complex amplitude method:

$$Z_0 = \sqrt{\frac{R + j\omega L}{G + j\omega C}}\ ;\ \delta = \alpha + j\beta\ = \sqrt{(R + j\omega L)(G + j\omega C)}\ ;$$

$$Z_S = R_S + j\left(\omega L_S - \frac{1}{\omega C_S}\right);\ Z_{BX} = Z_0\,\frac{Z_S + Z_0\,\mathrm{th}(\delta l)}{Z_0 + Z_S\,\mathrm{th}(\delta l)};$$

$$U_0 = Z_{BX} I_0;\quad U_1 = Z_S I_1;\ U_1 = U_0\,\mathrm{ch}(\delta l) - Z_0 I_0\,\mathrm{sh}(\delta l);$$

$$S = UI^* = P + jQ = |U||I|\cos\varphi + j|U||I|\sin\varphi\,.$$

Here $\omega = 2\pi f$ is angle (circular) frequency; Z_0 is the complex (characteristic) impedance; δ, α, β are the propagation, attenuation and phase constants; Z_S, Z_{BX} are the load and input resistances; U_0, I_0, U_1, I_1 are the active values of the voltages and currents at the beginning and at the end of the line with the length l; S is the complex power with the active P and reactive Q components.

The solution at any point x of the interval [0, l] by means of complex amplitude method can be represented in the following form

$$U(x) = U_0\,\mathrm{ch}(\delta x) - Z_0 I_0\,\mathrm{sh}(\delta x);\quad Z_0 I(x) = -U_0\,\mathrm{sh}(\delta x) + Z_0 I_0\,\mathrm{ch}(\delta x)\,. \quad (6.8)$$

Let's substitute (6.8) in (6.6) and (6.7), then integrate by x. After some transformations we obtain the evident formulas banding together the source, receiver and long line powers:

$$2|Z_0|^2\,[P(0) - P(l)] = \left(R + G|Z_0|^2\right)\frac{\mathrm{sh}(\alpha l)}{\alpha}\left[\left(|U_0|^2 + |I_0 Z_0|^2\right)\mathrm{ch}(\alpha l) -\right.$$

$$\left. -2\,\mathrm{Re}\left(U_0 I_0^* Z_0^*\right)\mathrm{sh}(\alpha l)\right] + \left(R - G|Z_0|^2\right)\frac{\sin(\beta l)}{\beta}\left[\left(|I_0 Z_0|^2 - |U_0|^2\right)\cos(\beta l) +\right.$$

$$\left. +2\,\mathrm{Im}\left(U_0 I_0^* Z_0^*\right)\sin(\beta l)\right]\ ;$$

$$\frac{2|Z_0|^2}{\omega}[Q(0)-Q(l)]=\left(L-C|Z_0|^2\right)\frac{\mathrm{sh}(\alpha l)}{\alpha}\left[\left(|U_0|^2+|I_0Z_0|^2\right)\mathrm{ch}(\alpha l)-\right.$$

$$\left.-2\,\mathrm{Re}\left(U_0I_0^*Z_0^*\right)\mathrm{sh}(\alpha l)\right]+\left(L+C|Z_0|^2\right)\frac{\sin(\beta l)}{\beta}\left[\left(|I_0Z_0|^2-|U_0|^2\right)\cos(\beta l)+\right.$$

$$\left.+2\,\mathrm{Im}\left(U_0I_0^*Z_0^*\right)\sin(\beta l)\right]. \qquad (6.9)$$

In the case of undistorting line (when $Z_0=Z_B=\sqrt{L/C}$, $a=1/\sqrt{LC}$, $\delta=(\gamma+j\omega)/a$, $\gamma=R/L=G/C$), the correlation (6.9) becomes essentially simpler:

$$P(0)-P(l)=\mathrm{sh}(\gamma\Delta)\left[\left(Z_B|I_0|^2+|U_0|^2/Z_B\right)\mathrm{ch}(\gamma\Delta)-2\,\mathrm{Re}\left(U_0I_0^*\right)\mathrm{sh}(\gamma\Delta)\right];$$

$$Q(0)-Q(l)=\sin(\omega\Delta)\left[\left(Z_B|I_0|^2-|U_0|^2/Z_B\right)\cos(\omega\Delta)+2\,\mathrm{Im}\left(U_0I_0^*\right)\sin(\omega\Delta)\right]$$

.

If the load consists only of the active resistance $Z_S=R_S$, then it is easy to show that the reactive power at the receiving end of the line is zero and the balance equation can be reduced to the form

$$P(0)-P(l)=\frac{U_0^2}{Z_B}\frac{\left(1-e^{-2\gamma\Delta}\right)\left(1+z^2e^{-2\gamma\Delta}\right)}{1+2z_\gamma\cos(2\omega\Delta)+z_\gamma^2};$$

$$Q(0)=-\frac{U_0^2}{Z_B}\frac{z_\gamma\sin(2\omega\Delta)}{1+2z_\gamma\cos(2\omega\Delta)+z_\gamma^2};\ z_\gamma=ze^{-2\gamma\Delta};\ z=\frac{R_S-Z_B}{R_S+Z_B}.$$

In case when the undistorting line is closed on the matched load $R_S=Z_B$, then at the starting end of the transmission line we also obtain the zero reactive power $Q(0)=0$. In the absence of active losses in the line ($\gamma=0$), the generated power coincides with the transferred power: $P(l)=P(0)$.

It is quite difficult to give the real physical matter to the cited above computations, but even the fact of obtaining of the power balance equations as a sequent from the initial system (6.1) for steady state sinusoidal regime is important. The final formulas even for simple particular cases don't allow to make clear the nature of the reactive power and to give its pictorial physical interpretation.

It is to mention, that usually only the instantaneous power $p = iu$ and its mean value – active power P are admitted as physically valid by many authors [56]. The reactive power Q and the total (apparent) power S are considered only as a convenient design values for description of the energetic processes with sinusoidal currents and voltages solely. This is why we are going now to consider the instantaneous voltages and currents starting with commutation, i.e. from the zero initial state, right up to steady state stage of the electromagnetic oscillations in the linear circuit with distributed and lumped constants. This approach seems to be defensible and logical one, since nonstationary wave process precedes any steady state regime. But it is impossible from the instantaneous power a priori to mark out one or several reactive components in a unique and physically valid way. Even for periodical nonsinusoidal regimes such a problem is far from its resolution, although many authors have made an attempt to realize it [1, 4, 6, 29 – 31, 43].

6.2. The power under the nonsinusoidal regime

In case of steady state sinusoidal regimes the active component of the instantaneous power can be defined as a mean value during the oscillation period, but its reactive component can be calculated, for example, by the formula [56]:

$$Q = \frac{1}{\omega T}\int_0^T u\left(\frac{di}{dt}\right)dt = -\frac{1}{\omega T}\int_0^T i\left(\frac{du}{dt}\right)dt\,. \qquad (6.10)$$

However, these and other similar formulas are applicable only for lumped devices and do not assume any generalizations for systems with distributed parameters or for nonsinusoidal currents and voltages. Therefore, to obtain the energy integral, we'll use the approach generally accepted in the theory of linear hyperbolic equations [95 – 98, 25 – 27]. This approach is valid for any type of functions that are the solutions of the initial system (6.1).

Using the standard procedure we multiply the first equation (6.1) by i, the second equation – by u and then we sum up the obtained results

$$Li\frac{\partial i}{\partial t} + i\frac{\partial u}{\partial x} + Ri^2 + Cu\frac{\partial u}{\partial t} + u\frac{\partial i}{\partial x} + Gu^2 = 0$$

or

$$\frac{1}{2}\frac{\partial}{\partial t}(Li^2 + Cu^2) + Ri^2 + Gu^2 + \frac{\partial}{\partial x}(iu) = 0.$$

Now we integrate this expression in the domain $0 \le x \le l,\ \ 0 \le \tau \le t$. Taking into account zero initial data we obtain the following integral identity:

$$\int_0^t\int_0^l \left(Ri^2 + Gu^2\right)dx\,d\tau + \frac{1}{2}\int_0^l \left(Li^2 + Cu^2\right)dx =$$

$$= \int_0^t [i(0,\tau)u(0,\tau) - i(l,\tau)u(l,\tau)]\,d\tau. \qquad (6.11)$$

The left-hand member of the energy balance equation represents the sum of its active (irreversible converting to the heat) and reactive (reversible) components, but the right-hand member – the difference between the source energy and receiver energy. It is easy to verify, that all members in (6.11), as a physical quantities, have the same dimension – the joule (J).

Thus, if the instantaneous currents and voltages are the solutions of the initial system (6.1), then they satisfy the conservation law (6.11) as well. Since under the zero initial and boundary conditions the integral identity (6.11) holds only for trivial solution $i \equiv u \equiv 0$, then, taking into account the Fredholm alternative, it follows the proof of the unicity theorem with the assumption of solution's existence.

So, if the distribution in space and time of the voltages and currents is known, then the irreversible losses of the active power in the line can be defined from (6.11) as follows

$$P(t) = \int_0^l \left(Ri^2 + Gu^2\right)dx \ , \qquad (6.12)$$

and the current total energy (storing in the distributed reactive elements of the line) at time point $t > 0$ can be calculated by the formula

$$W(t) = W_{\text{м}}(t) + W_{\text{э}}(t) = \frac{1}{2}\int_0^l \left(Li^2 + Cu^2\right)dx \, . \qquad (6.13)$$

Let's differentiate the relation (6.11) by time variable and obtain

$$\int_0^l \left(Ri^2 + Gu^2\right)dx + \frac{1}{2}\frac{d}{dt}\int_0^l \left(Li^2 + Cu^2\right)dx = i(0,t)u(0,t) - i(l,t)u(l,t)$$

or taking into account (6.12), (6.13)

$$P(t) + \frac{d}{dt}W(t) = i(0,t)u(0,t) - i(l,t)u(l,t) \, .$$

If we suppose that all components here are periodical functions, than calculation of the mean values during the time interval $[0,T]$ gives

$$\frac{1}{T}\int_0^T P(t)dt + \frac{1}{T}\left[W(T) - W(0)\right] = \frac{1}{T}\int_0^T i(0,t)u(0,t)dt - \frac{1}{T}\int_0^T i(l,t)u(l,t)dt \, . \qquad (6.14)$$

Taking into account that $W(T) = W(0)$, we get the generator and loading active powers balance equation

$$P_a = P(0) - P(l) = \frac{1}{T}\int_0^T P(t)dt \, . \qquad (6.15)$$

Particularly, under the steady state sinusoidal regime with the period $T = 2\pi/\omega$ with

$$u(x,t) = U(x)\sin(\omega t + \varphi_u(x)), \quad i(x,t) = I(x)\sin(\omega t + \varphi_i(x)) \, ,$$

where $U(x)$ and $I(x)$ are voltage and current amplitude active values, after the direct integration in (6.14), we obtain

$$P_a = \int_0^l \left[RI^2(x) + GU^2(x)\right]dx;\ P(0) = I(0)U(0)\cos\varphi(0);$$

$$P(l) = I(l)U(l)\cos\varphi(l);\ \varphi(x) = \varphi_u(x) - \varphi_i(x).$$

Then the relation (6.15) takes the form

$$\int_0^l \left[RI^2(x) + GU^2(x)\right]dx = P(0) - P(l),$$

that coincides with (6.6).

To obtain the analogous expressions for reactive power (in case of arbitrary periodical functions) we differentiate the first equation from (6.1) by time and multiply it by i. Then the second equation we multiply by $\partial u/\partial t$ and sum up the obtained results

$$Li\frac{\partial^2 i}{\partial t^2} + i\frac{\partial}{\partial x}\left(\frac{\partial u}{\partial t}\right) + Ri\frac{\partial i}{\partial t} + C\left(\frac{\partial u}{\partial t}\right)^2 + \frac{\partial u}{\partial t}\frac{\partial i}{\partial x} + Gu\frac{\partial u}{\partial t} = 0$$

or

$$\frac{1}{2}\frac{\partial}{\partial t}(Ri^2 + Gu^2) + Li\frac{\partial^2 i}{\partial t^2} + C\left(\frac{\partial u}{\partial t}\right)^2 + \frac{\partial}{\partial x}\left(i\frac{\partial u}{\partial t}\right) = 0.$$

Let's integrate the last expression in the domain $0 \le x \le l$:

$$\frac{1}{2}\frac{d}{dt}\int_0^l \left(Ri^2 + Gu^2\right)dx + \int_0^l \left[Li\frac{\partial^2 i}{\partial t^2} + C\left(\frac{\partial u}{\partial t}\right)^2\right]dx =$$

$$= i(0,t)\frac{du(0,t)}{dt} - i(l,t)\frac{du(l,t)}{dt}.$$

Calculating the mean values on the time interval $[0,T]$, we obtain

$$\frac{1}{2T}\left[P(T)-P(0)\right]+\frac{1}{T}\int_0^T\int_0^l\left[Li\frac{\partial^2 i}{\partial t^2}+C\left(\frac{\partial u}{\partial t}\right)^2\right]dx\,dt=$$

$$=\frac{1}{T}\int_0^T i(0,t)\frac{du(0,t)}{dt}dt-\frac{1}{T}\int_0^T i(l,t)\frac{du(l,t)}{dt}dt\,.$$

Since $P(T)=P(0)$ we can obtain the reactive power balance equation using the notations from (6.10):

$$\frac{1}{T}\int_0^T\int_0^l\left[Li\frac{\partial^2 i}{\partial t^2}+C\left(\frac{\partial u}{\partial t}\right)^2\right]dx\,dt=-\omega\left[Q(0)-Q(l)\right]. \qquad (6.16)$$

Now we apply to the left-hand member of the relation (6.16) the formula of integration by parts. Then the double integral can be transformed to the form

$$\frac{1}{T}\int_0^T\int_0^l\left[Li\frac{\partial^2 i}{\partial t^2}+C\left(\frac{\partial u}{\partial t}\right)^2\right]dx\,dt=\frac{1}{T}\int_0^l i\frac{\partial i}{\partial t}\Big|_{t=0}^{T}dx-$$

$$-\frac{1}{T}\int_0^T\int_0^l\left[L\left(\frac{\partial i}{\partial t}\right)^2-C\left(\frac{\partial u}{\partial t}\right)^2\right]dx\,dt\,.$$

Let's mention that for periodical solution with period T the member $i\partial i/\partial t\big|_{t=0}^{T}$ is equal to zero. Therefore, under the pure active loading at the receiving end $u=R_S\,i$ according to (6.10) we obtain the zero reactive power: $Q(l)=0$.

Now from (6.16) we can obtain the relation between the reactive powers of the source, receiver and long line

$$\frac{1}{\omega T}\int_0^T\int_0^l\left[L\left(\frac{\partial i}{\partial t}\right)^2-C\left(\frac{\partial u}{\partial t}\right)^2\right]dx\,dt=Q(0)-Q(l)\,. \qquad (6.17)$$

This relation comes out right for any periodical solution of the problem. In case of sinusoidal regime we get the formula

$$\omega\int_0^l\left[LI^2(x)-CU^2(x)\right]dx=Q(0)-Q(l)\,, \qquad (6.18)$$

that coincides with (6.7).

6.3. Numerical examples

Let's consider now the numerical examination of some energy characteristics of the steady state electricity transmission with sinusoidal and non-sinusoidal currents and voltages. For simplicity and clearness we use the dimensionless quantities $L = C = Z_B = \lambda = a = T = f = 1$ and consider the undistorting line (because for this kind of line it is easy to obtain the exact solution in case of both transient and steady sate regimes for arbitrary forms of acting voltage or current) [75, 90]. Let's the homogeneous line with parameters $l = 3\lambda/8$; $R = G = 0.48$ is instantaneously connected to the sinusoidal voltage source: $u = \sin(2\pi ft)$, and its receiving end $x = l$ is closed on the active resistance: $u = R_S\, i$.

The lines with the wave lengths λ /8, 3λ /8, 5λ /8,… are notable by two main reasons. The first reason is that the active losses (calculated by complex amplitude method) under the idling in such lines coincide with the same under the short circuit. And the second one is that the generator reactive powers under these two degenerated regimes are equal by their absolute values but are opposite by their signs. The reactive power is zero under the natural power regime (progressing waves) when $R_S = 1$. It is accepted that in this case the line is balanced in accordance with reactive power as long as the power of its magnetic field coincides with the power of its electrical field. [4, 6].

As it was mentioned above, the nonstationary wave process precedes to any steady state regime, so the calculations we'll realize in the same order. Fig. 6.1 shows the changes in time of the total source power $S_0(t)$ =

$i(0,t)u(0,t)$ and of the instantaneous active power losses in the line $P(t)$ (curves 1;2) from the commutation moment under the variation of the load resistance: $R_S = \infty$ (*a*); 0 (*b*); 1 (*c*). The constant, distinguished by number 3, corresponds to the active component (calculated by complex amplitude method) of the difference between the source power and receiver power, that coincides exactly with the mean steady value, calculated by formula (6.15): $P_a = 0.1726$ (*a*); 0.1726 (*b*); 0.1512 (*c*).

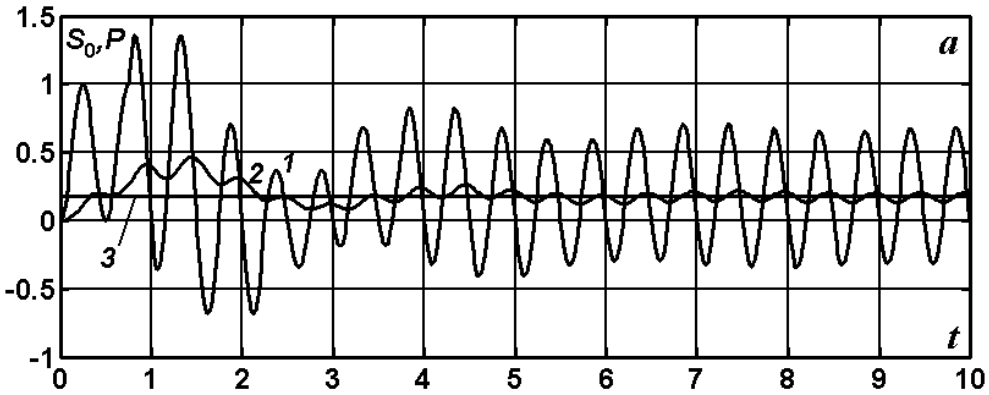

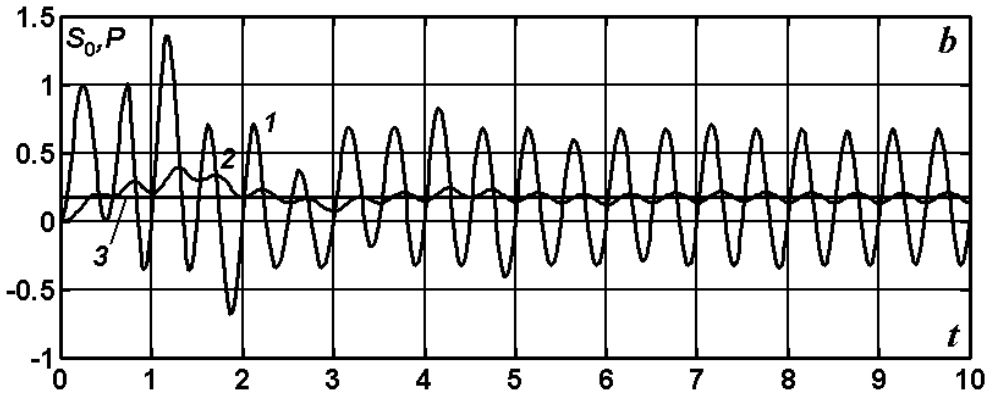

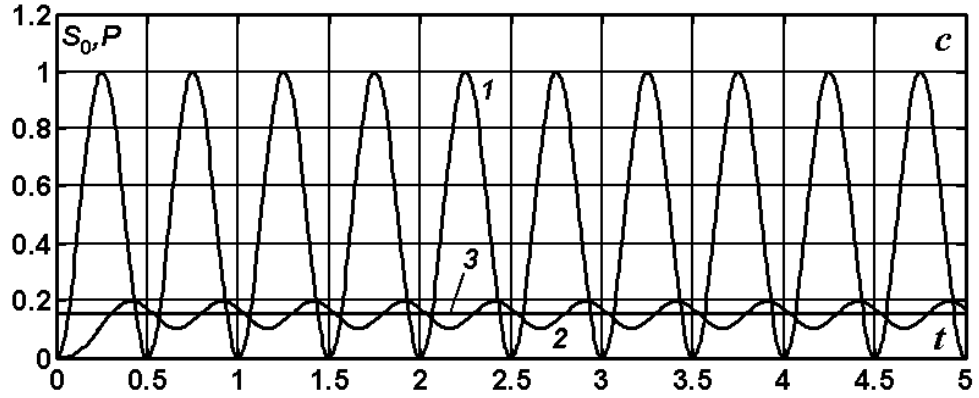

Fig. 6.1. The dynamics of the total source power and the active power losses in the line (curves 1;2) when $R = G = 0.48$ and variation of the load resistance: $R_S = \infty$ (***a***); 0 (***b***); 1 (***c***).

For numerical analysis of the exchange electromagnetic processes between the sinusoidal voltage source and the line with lumped reactivities let's consider fig. 6.2**,** where the instantaneous powers of the magnetic and electrical fields in the line $Q_{\text{м}}(t)$ and $Q_{\text{э}}(t)$ are represented. These quantities are calculated as a derivatives by time variable of the energy functions $W_{\text{м}}(t)$ and $W_{\text{э}}(t)$ (curves 1;2). The constant, distinguished by number 3, corresponds to the reactive power of the source (calculated by complex amplitude method), that coincides exactly with the value, calculated by formula (6.18) for sinusoidal currents and voltages.

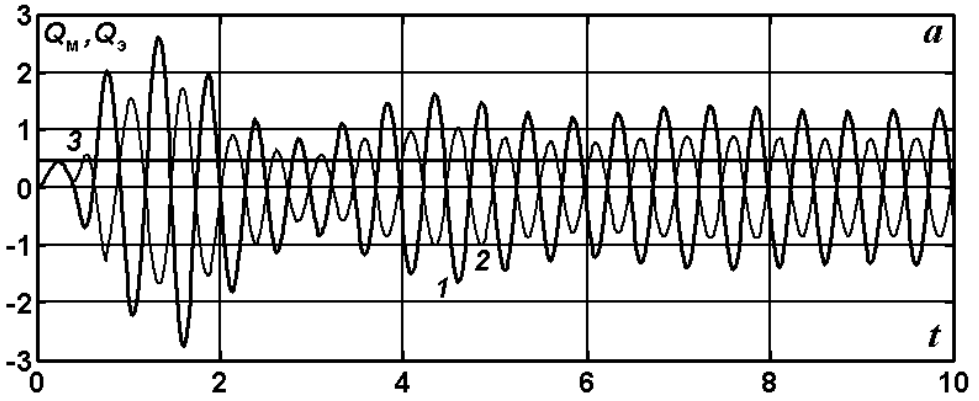

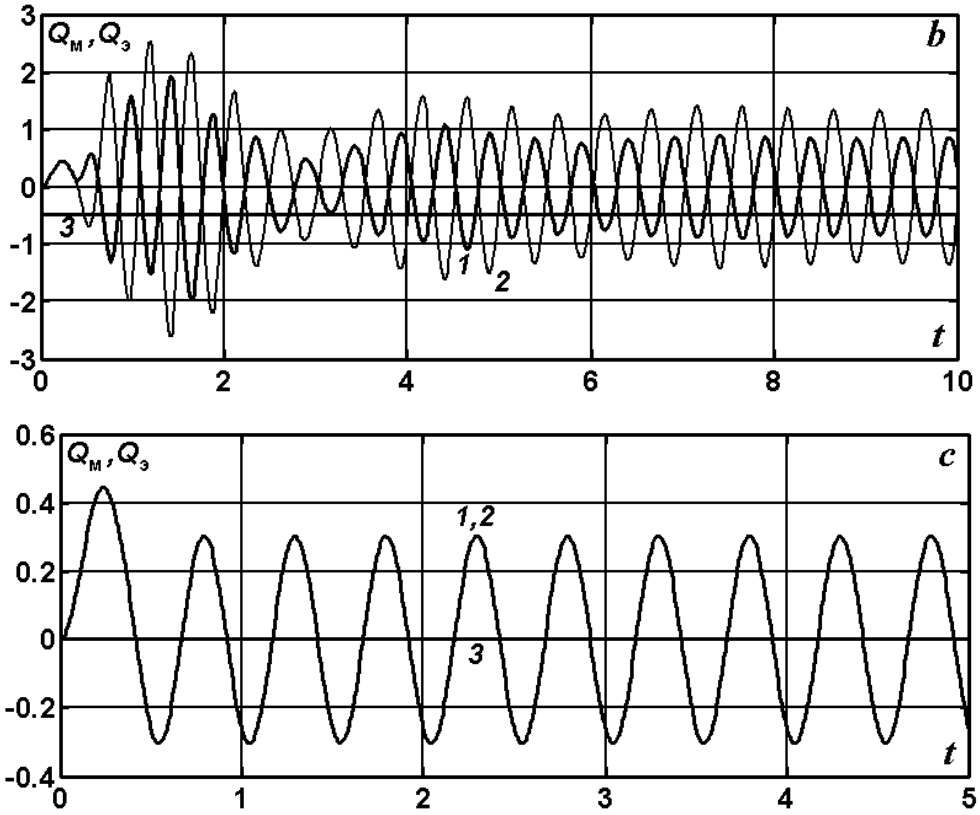

Fig. 6.2. The instantaneous powers of the magnetic and electrical fields in the line when $R = G = 0.48$ and variation of the load resistance: $R_S = \infty$ (***a***); 0 (***b***); 1 (***c***).

One can pay attention to the full coincidence, i.e. zero disbalance between the instantaneous powers of the magnetic and electrical fields in the undistorting line with the matched load $R_S = 1$. It seems to be more difficult the case when the amplitudes and the phases of the instantaneous powers don't coincide not only during the transient process but during the steady state regime as well. In this case the estimation of the reactive power in the form of one number gives only approximate qualitative idea about the electromagnetic energy circulation in the linear circuit. For example, let's consider the reactive power at the starting end of the transmission line under the idling regime: $Q_0 = 0.4693$ (curve 3 in fig. 6.2, *a*) and $Q_0 = -0.4693$ under the short-circuit regime (curve 3 in fig. 6.2, *b*). The comparison makes it clear that the power of the magnetic field in the first case prevail over the power of the electric field, whereas in the second case the situation is ex-

actly opposite. Indeed, the figures show that the corresponding periodical functions exchange their amplitude values.

The dynamics of the total power of the source and the active power losses in the short-circuited line (curves 1;2) when $R = 0$; $G = 0.48$ (*a*); 0 (*b*) are presented in the fig. 6.3. The constant, distinguished by number 3, corresponds to $P_a = 0.1082$ (*a*); 0.0 (*b*).

The instantaneous powers of the magnetic and electrical fields in the short-circuited line are represented in the fig. 6.4. The constants, distinguished by number 3, correspond to $Q_0 = -0.4906$ (*a*); -0.5 (*b*), determined by formula (6.18). For given variants the solutions in the steady state regime present periodical piecewise sinusoidal functions (see fig. 6.5) and the complex amplitude method is inapplicable in this case in principle.

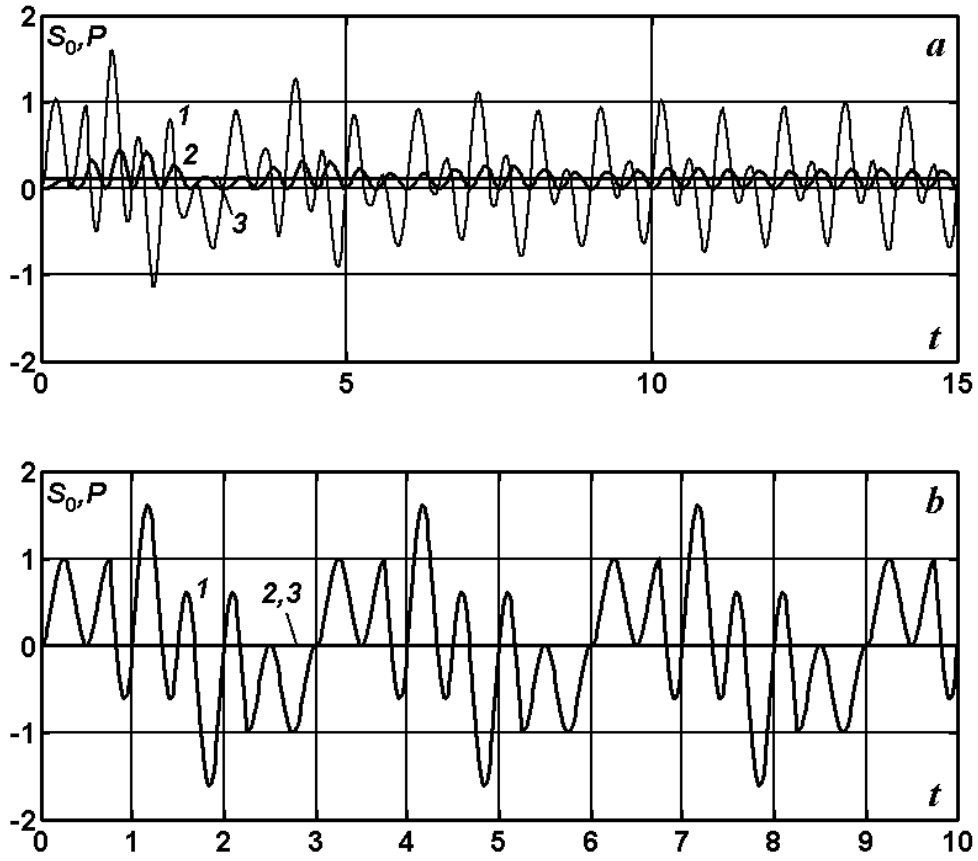

Fig. 6.3. The dynamics of the total source power and the active power losses in the short-circuited line (curves 1;2) when $R = 0$; $G = 0.48$ (***a***); 0 (***b***).

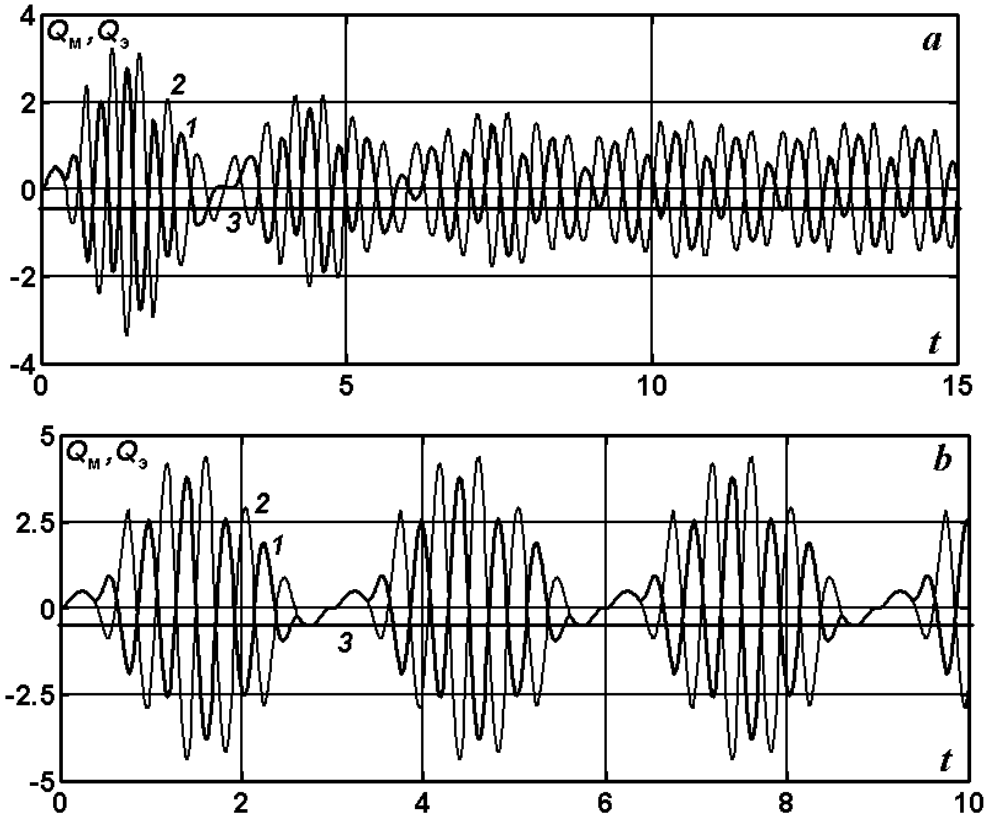

Fig. 6.4. The instantaneous powers of the magnetic and electrical fields in the short-circuited line (curves 1;2) when $R = 0$; $G = 0.48$ (***a***); 0 (***b***).

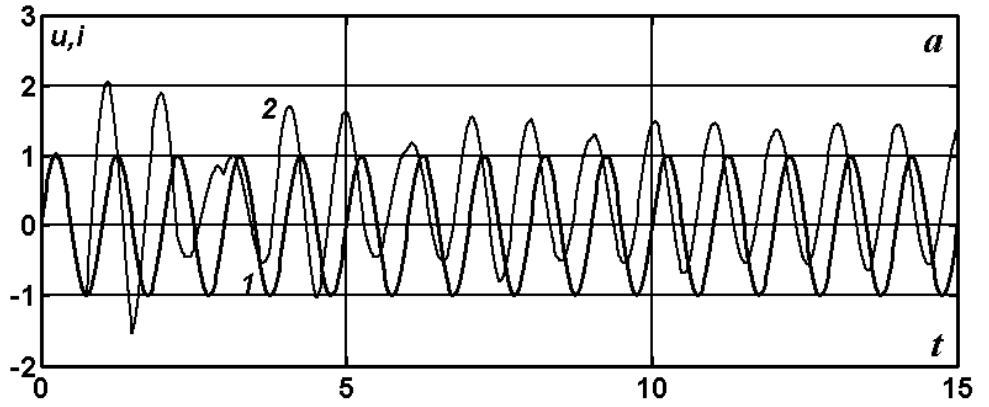

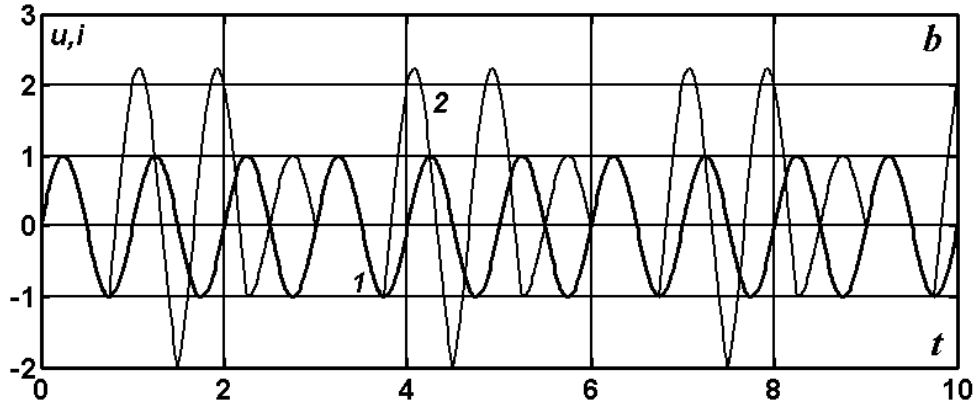

Fig. 6.5. The instantaneous voltages and currents (curves 1;2) at the input of the short-circuited line when $R = 0$; $G = 0.48$ (***a***); 0 (***b***).

If irreversible losses of the active power in the line can be described as before by means of its mean value, then the disbalance between the instantaneous powers of the magnetic and electrical fields (defined by formula (6.18) as one real number) hardly can give the exhaustive information about the exchange electromagnetic processes in the transmission line. When comparing the graphical charts in the fig. 6.2,*b* and fig. 6.4, it is easy to notice that the behavior in time of the magnetic and electric fields in the short-circuited line are strongly different both in quantity and in quality. At the same time their integral characteristics in the form of reactive power values (6.18) differ only in second-third significant digit.

If we assign the input voltages in the trapezium form, sufficiently closed to the rectangular one (fig. 6.6), then the corresponding values of the reactive power slightly increase: $Q_0 = -0.626$ (*a*); -0.636 (*b*), but the difference between them remains negligible as before. Under the periodical input voltages of the triangular form the reactive power in the considering cases decreases in half: $Q_0 = -0.314$ (*a*); -0.318 (*b*).

The generation and transmission by the multiwire lines of the big energy fluxes leads to more complicated situation with the reactive power. It becomes more complex to estimate correctly nonstationary disbalance between the powers of the magnetic and electric fields in the transient process under the alert conditions like a short circuit, unexpected load faults or load rises and so on. Obviously, for adequate description of the electromagnetic processes and phenomenon in the real circuits it is nevertheless necessary to use the instantaneous powers of the magnetic and electrical fields of the line.

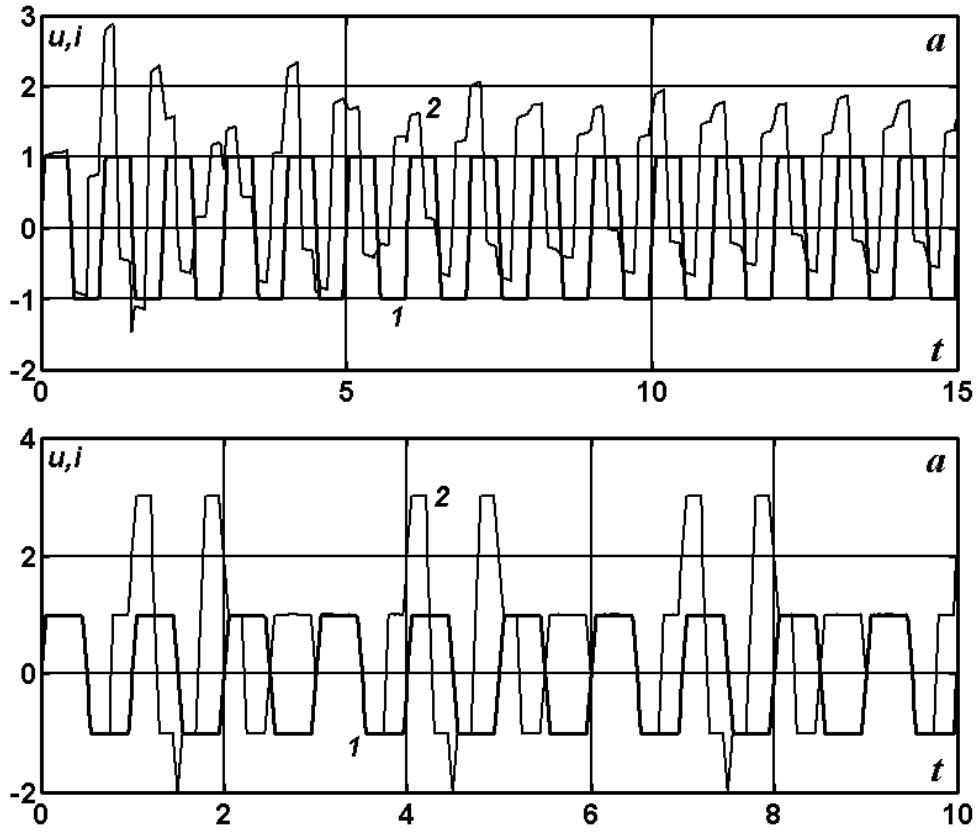

Fig. 6.6. The instantaneous voltages and currents (curves 1;2) at the input of the short-circuited line when $R = 0$; $G = 0.48$ (***a***); 0 (***b***).

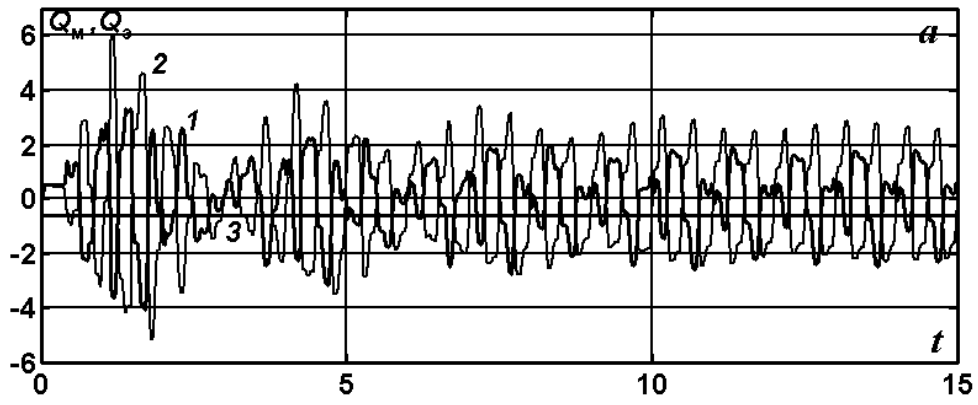

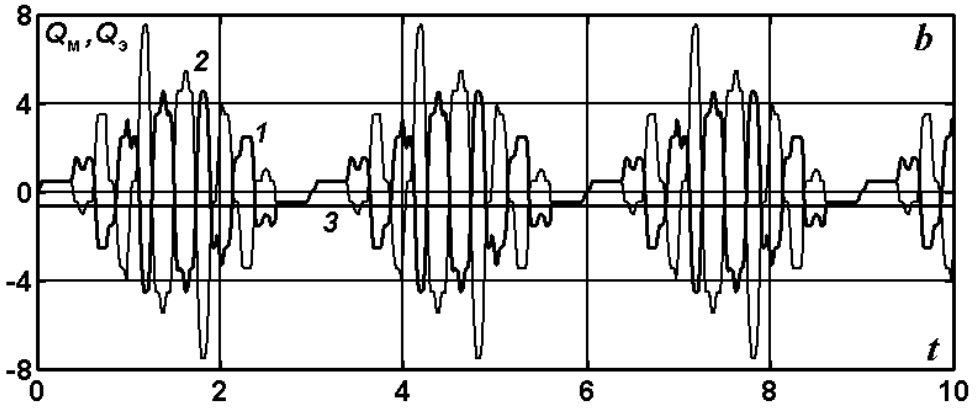

Fig. 6.7. The instantaneous powers of the magnetic and electrical fields in the short-circuited line (curves 1;2) when $R = 0$; $G = 0.48$ (***a***); 0 (***b***).

7. The finite-difference scheme: principle of creation and theoretical foundation

Let's consider the problem (1.1)-(1.3) for telegraph equations on the interval $x \in [0, l]$ when $t \geq 0$ with zero initial data:

$$L\frac{\partial i}{\partial t} + \frac{\partial u}{\partial x} + Ri = 0; \;\; C\frac{\partial u}{\partial t} + \frac{\partial i}{\partial x} + Gu = 0; \tag{7.1}$$

$$u(0,t) = U_0(t), \; u(l,t) = Di(l,t), \; t > 0. \tag{7.2}$$

Here D is an integro-differential operator that, according to the boundary condition (1.3), has the following form

$$Di(t) = R_s i(t) + L_s \frac{di(t)}{dt} + \frac{1}{C_s}\int_0^t i(\tau)d\tau. \tag{7.3}$$

In order to create the finite-difference scheme we use the grid-characteristic method as follows. At first on the interval $[0, l]$ we generate the uniform grid with integer and half-integer indexes:

$$x_m = mh,\ m = \overline{0,N};\ x_{m-1/2} = x_m - h/2,\ m = \overline{1,N};\ h = l/N\,.$$

The uniform grid is generated over the time coordinate with the step τ also with integer and half-integer indexes: $t_n = n\tau$, $t_{n+1/2} = t_n + \tau/2$, n = 0,1,2,…

Then we integrate the equations (7.1) by the cell $Q = [x_{m-1}, x_m] \times [t_n, t_{n+1}]$ of the two-dimensional grid. So we obtain the integral relations along the boundary of the cell Q

$$L\int_{x_{m-1}}^{x_m}\left[i(x,t_{n+1}) - i(x,t_n)\right]dx + \int_{t_n}^{t_{n+1}}\left[u(x_m,t) - u(x_{m-1},t)\right]dt + R\iint_Q i(x,t)\,dt\,dx = 0\,;$$

$$C\int_{x_{m-1}}^{x_m}\left[u(x,t_{n+1}) - u(x,t_n)\right]dx + \int_{t_n}^{t_{n+1}}\left[i(x_m,t) - i(x_{m-1},t)\right]dt + G\iint_Q u(x,t)\,dt\,dx = 0\,.$$

Now the one-dimensional integrals we approximate by means of quadrature midpoint rule or rectangle rule, but two-dimensional integrals – by the formula with weights α and β. As a result we obtain

$$\begin{aligned} &L\frac{i_{m-1/2}^{n+1} - i_{m-1/2}^{n}}{\tau} + \frac{u_m^{n+1/2} - u_{m-1}^{n+1/2}}{h} + \alpha i_{m-1/2}^{n+1} + (R-\alpha) i_{m-1/2}^{n} = 0\,; \\ &C\frac{u_{m-1/2}^{n+1} - u_{m-1/2}^{n}}{\tau} + \frac{i_m^{n+1/2} - i_{m-1}^{n+1/2}}{h} + \beta u_{m-1/2}^{n+1} + (G-\beta) u_{m-1/2}^{n} = 0\,. \end{aligned} \tag{7.4}$$

The following notations are used here

$$i_{m\pm1/2}^{n} = i(x_m \pm h/2, t_n),\ \ i_m^{n+1/2} = i(x_m, t_n + \tau/2)\,.$$

The values $i_m^{n+1/2}$ и $u_m^{n+1/2}$ at the half-integer time layer can be expressed from (7.4) through the variables $i_{m\pm1/2}^{n}$ and $u_{m\pm1/2}^{n}$. We'll use the relations on the characteristics with positive and negative slopes:

$$u_m^{n+1/2} + Z_B i_m^{n+1/2} = u_{m-1/2}^n + Z_B i_{m-1/2}^n;\ u_m^{n+1/2} - Z_B i_m^{n+1/2} = u_{m+1/2}^n - Z_B i_{m+1/2}^n.$$

Solving this system we obtain the following correlations

$$\begin{aligned} i_m^{n+1/2} &= \frac{u_{m-1/2}^n - u_{m+1/2}^n}{2Z_B} + \frac{i_{m-1/2}^n + i_{m+1/2}^n}{2}; \\ u_m^{n+1/2} &= \frac{u_{m-1/2}^n + u_{m+1/2}^n}{2} + Z_B \frac{i_{m-1/2}^n - i_{m+1/2}^n}{2}. \end{aligned} \tag{7.5}$$

So, the finite difference equations, that approximate (7.1), have the form of relations (7.4), (7.5). The boundary values $i_m^{n+1/2}$ and $u_m^{n+1/2}$ take the form

$$u_0^{n+1/2} = U_0(t_{n+1/2}),\ i_0^{n+1/2} = \left(U_0(t_{n+1/2}) - u_{1/2}^n\right)/Z_B + i_{1/2}^n; \tag{7.6}$$

$$\left(D_h + Z_B\right) i_N^{n+1/2} = u_{N-1/2}^n + Z_B i_{N-1/2}^n,\ u_N^{n+1/2} = D_h i_N^{n+1/2},$$

where D_h is the finite-difference approximation for the integro-differential operator D from (7.3). The operator D_h can be represented in the following form

$$D_h i_N^{n+1/2} = R_S i_N^{n+1/2} + L_S \frac{i_N^{n+1/2} - i_N^{n-1/2}}{\tau} + \frac{1}{C_S} \sum_{k=1}^{n} \frac{i_N^{n+1/2} + i_N^{n-1/2}}{2} \tau.$$

Then the boundary values at the right end $i_N^{n+1/2}$ and $u_N^{n+1/2}$ can be written in the explicit form

$$\begin{aligned} u_N^{n+1/2} &= \frac{1}{B_S + Z_B}\left[Z_B F_S + B_S\left(u_{N-1/2}^n + Z_B i_{N-1/2}^n\right)\right]; \\ i_N^{n+1/2} &= \frac{1}{B_S + Z_B}\left[-F_S + \left(u_{N-1/2}^n + Z_B i_{N-1/2}^n\right)\right]; \end{aligned} \tag{7.7}$$

$$B_S = R_S + \frac{L_S}{\tau} + \frac{\tau}{C_S};\ F_S = \left(-\frac{L_S}{\tau} + \frac{\tau}{2C_S} \right) i_N^{n-1/2} + \frac{1}{C_S} \sum_{k=1}^{n-1} \frac{i_N^{n+1/2} + i_N^{n-1/2}}{2} \tau .$$

The weighting coefficients α, β and the time-step τ in (7.4), (7.5) must be chosen in such a way as to ensure the minimal effect of the dispersion and dissipation phenomenon of the finite difference scheme. In order to determine the optimal values of the parameters α, β and τ we apply the first differential approximation method for finite difference relations. Using (7.5) we eliminate the values $i_m^{n+1/2}$, $u_m^{n+1/2}$ from the (7.4) and write out the obtained relations in the non-index form:

$$\begin{gathered} (L + \alpha\tau) i_t + u_{\dot{x}} + Ri - \frac{hLa}{2} i_{\bar{x}x} = 0; \\ (C + \beta\tau) u_t + i_{\dot{x}} + Gu - \frac{hCa}{2} u_{\bar{x}x} = 0. \end{gathered} \tag{7.8}$$

So the first differential approximation for this scheme has the following form

$$(L + \alpha\tau) \left(\frac{\partial i}{\partial t} + \frac{\tau}{2} \frac{\partial^2 i}{\partial t^2} \right) + \frac{\partial u}{\partial x} + Ri - \frac{hLa}{2} \frac{\partial^2 i}{\partial x^2} = 0;$$

$$(C + \beta\tau) \left(\frac{\partial u}{\partial t} + \frac{\tau}{2} \frac{\partial^2 u}{\partial t^2} \right) + \frac{\partial i}{\partial x} + Gu - \frac{hCa}{2} \frac{\partial^2 u}{\partial x^2} = 0.$$

These differential equations are approximated by finite-difference equations (7.8) with second order of accuracy by h and τ.

The original telegraph equations for the line with losses are equivalent to the following:

$$\frac{\partial^2 i}{\partial x^2} = LC \frac{\partial^2 i}{\partial t^2} + (LG + RC) \frac{\partial i}{\partial t} + RGi;$$

$$\frac{\partial^2 u}{\partial x^2} = LC\frac{\partial^2 u}{\partial t^2} + (LG + RC)\frac{\partial u}{\partial t} + RGu.$$

Taking into account above representations the first differential approximation can be transformed to the form:

$$L\frac{\partial i}{\partial t} + \frac{\partial u}{\partial x} + Ri + \alpha\tau\frac{\partial i}{\partial t} + \frac{L\tau}{2}\frac{\partial^2 i}{\partial t^2} - \frac{Lah}{2}\frac{\partial^2 i}{\partial x^2} = 0;$$

$$C\frac{\partial u}{\partial t} + \frac{\partial i}{\partial x} + Gu + \beta\tau\frac{\partial u}{\partial t} + \frac{C\tau}{2}\frac{\partial^2 u}{\partial t^2} - \frac{Cah}{2}\frac{\partial^2 u}{\partial x^2} = 0.$$

This implies that the weighting coefficients α, β should be chosen in such a way as to minimize (desirable to zero) differential additions to the original equations:

$$\alpha\tau\frac{\partial i}{\partial t} + \frac{L\tau}{2}\frac{\partial^2 i}{\partial t^2} - \frac{Lah}{2}\left[LC\frac{\partial^2 i}{\partial t^2} + (LG + RC)\frac{\partial i}{\partial t} + RGi\right] \to 0;$$

$$\beta\tau\frac{\partial u}{\partial t} + \frac{C\tau}{2}\frac{\partial^2 u}{\partial t^2} - \frac{Cah}{2}\left[LC\frac{\partial^2 u}{\partial t^2} + (LG + RC)\frac{\partial u}{\partial t} + RGu\right] \to 0.$$

After collecting terms we obtain

$$\frac{\partial^2 i}{\partial t^2}\left(\frac{L\tau}{2} - \frac{Lh}{2a}\right) + \frac{\partial i}{\partial t}\left[\alpha\tau - \frac{Lah}{2}(LG + RC)\right] - \frac{Lah}{2}RGi \to 0;$$

$$\frac{\partial^2 u}{\partial t^2}\left(\frac{C\tau}{2} - \frac{Ch}{2a}\right) + \frac{\partial u}{\partial t}\left[\beta\tau - \frac{Cah}{2}(LG + RC)\right] - \frac{Cah}{2}RGu \to 0.$$

One can readily see that when $\tau = h/a$ and

$$\alpha = \frac{hLa}{2\tau}(LG + RC) = \frac{La^2}{2}(LG + RC) = \frac{1}{2}\left(R + \frac{LG}{C}\right);$$

$$\beta = \frac{hCa}{2\tau}(LG + RC) = \frac{Ca^2}{2}(LG + RC) = \frac{1}{2}\left(G + \frac{CR}{L}\right)$$

the coefficients of time derivatives become zero, but the remaining members do not contain the derivatives and tend to zero with first order when $h \to 0$. The coefficients α and β can be represented as: $\alpha = L\gamma$, $\beta = C\gamma$, $\gamma = (\gamma_G + \gamma_R)/2$, $\gamma_R = R/L$, $\gamma_G = G/C$. Hence, the proposed scheme with the weights minimizes not only the dissipation, but the difference dispersion of the numerical solution as well. The finite-difference relations (7.4), (7.5) can be generalized for the case when the line lineal parameters change along the longitudinal coordinate *x* and for the case of the multiwire lines with the branchpoints, lumped elements and other complicative factors. In case of heterogeneous line the space coordinate *x* partition to the elementary cells must be realized in such a way as to fulfill the condition $\tau = h_{m\text{-}1/2}/a_{m\text{-}1/2} = const$ for any index *m*. The approximation for the boundary conditions of the type (7.2) and for more general forms is in detail described in [86 – 90].

The numerous numerical experiments and comparisons with analytical solutions have demonstrated that the accuracy of the numerical solutions constitutes no less then three-four significant digits even in the vicinity of the wave fronts (strong discontinuities). A priori and a posteriori accuracy estimations and some other theoretical aspects of the developed method will be considered in the next paragraphs.

8. Stability of computational scheme

Let's prove the stability of the finite-difference scheme (7.4)-(7.7), (7.8) by initial data taking into account zero boundary conditions. In this order we write down the finite-difference scheme for new unknown functions *r* and *s*, that are known as Riemannian invariants of the system (7.1) and can be expressed through currents and voltages as follows: $r = u + Z_B i$, $s = u - Z_B i$. The system of equations (7.1) written in invariants takes the form

$$\begin{aligned} &\frac{\partial r}{\partial t} + a\frac{\partial r}{\partial x} + \frac{\gamma_G + \gamma_R}{2}r + \frac{\gamma_G - \gamma_R}{2}s = 0; \\ &\frac{\partial s}{\partial t} - a\frac{\partial s}{\partial x} + \frac{\gamma_G - \gamma_R}{2}r + \frac{\gamma_G + \gamma_R}{2}s = 0. \end{aligned} \qquad (8.1)$$

The finite-difference scheme (7.8) in terms of r and s when $\alpha = L\gamma$, $\beta = C\gamma$ gets the following form

$$(1+\gamma\tau)r_t^n + ar_{\dot{x}}^n - \frac{ha}{2} r_{\bar{x}x}^n + \gamma r^n + \frac{\gamma_G - \gamma_R}{2} s^n = 0;$$

$$(1+\gamma\tau)s_t^n - as_{\dot{x}}^n - \frac{ha}{2} s_{\bar{x}x}^n + \gamma s^n + \frac{\gamma_G - \gamma_R}{2} r^n = 0$$

or

$$\begin{aligned} &(1+\gamma\tau)r_t^n + ar_{\bar{x}}^n + \gamma r^n + \frac{\gamma_G - \gamma_R}{2} s^n = 0; \\ &(1+\gamma\tau)s_t^n - as_x^n + \gamma s^n + \frac{\gamma_G - \gamma_R}{2} r^n = 0. \end{aligned} \tag{8.2}$$

The equations (8.2) are written for internal nodes $x_{m\text{-}1/2}$, $m = \overline{1, N}$. In order that the first equation to be correctly formulated the value $r_{-1/2}^n$ is required. This value we determine from the zero boundary condition (7.6) $u_0^{n+1/2} = 0$. So we have $r_0^{n+1/2} + s_0^{n+1/2} = 0$ and $s_0^{n+1/2} = s_{1/2}^n$ or $r_0^{n+1/2} = r_{-1/2}^n = s_{1/2}^n$. In the second equation the value $s_{N+1/2}^n$ is required. This value we determine from the boundary condition (7.7) when $L_S = 1/C_S = 0$. Then at the right-hand end we have only active loading: $u_N^{n+1/2} = R_S i_N^{n+1/2}$ or in the invariants $s_N^{n+1/2} = -zr_N^{n+1/2}$, $z = (R_S - Z_B)/(R_S + Z_B)$, $|z| \le 1$. From the relations on characteristics: $s_N^{n+1/2} = s_{N+1/2}^n$ и $r_N^{n+1/2} = r_{N-1/2}^n$ we get the condition $s_{N+1/2}^n = -zr_{N-1/2}^n$. Consequently, the homogeneous boundary conditions for the scheme (8.2) take the following form

$$r_{-1/2}^n = s_{1/2}^n;\ s_{N+1/2}^n = -zr_{N-1/2}^n. \tag{8.3}$$

Let's write down the scheme (8.2) in the operator form

$$By_t^n + (\widetilde{A} + D)y^n = 0, \tag{8.4}$$

where

$$B = (1+\gamma\tau)E,\ y = \begin{pmatrix} r \\ s \end{pmatrix},\ \widetilde{A}y = \begin{pmatrix} ar_{\bar{x}}^n \\ -as_x^n \end{pmatrix},\ Dy = \frac{1}{2}\begin{pmatrix} 2\gamma & \gamma_G - \gamma_R \\ \gamma_G - \gamma_R & 2\gamma \end{pmatrix}.$$

As the operator $(\widetilde{A} + D)$ in (8.4) is not self-conjugated, then to prove the stability we use the theorem 4, part II, §2 [98].

Theorem.

Let in two-layer finite-difference scheme

$$By_t^n + Ay^n = 0 \tag{8.5}$$

the operators A and B are independent on n, $B = B^* > 0$ and the operator A^{-1} exists. Then the condition

$$A^{-1} \geq \frac{\tau}{1+\rho} B^{-1} \tag{8.6}$$

is sufficient for stability of the scheme (8.5) with the constant $\rho \geq 1$ in the energetic space H_B. The same condition is necessary for stability in H_B with the constant $\rho \leq 1$. The condition

$$A^{-1} \geq 0.5\tau B^{-1} \tag{8.7}$$

is necessary and sufficient for stability of the scheme (8.5) with the constant $\rho = 1$ in the energetic space H_B.

Let's notice that if $B = dE$ ($d > 0$), then the condition (8.7) is equivalent to

$$(Ay, y) \geq \frac{\tau}{2d}\|Ay\|^2. \tag{8.8}$$

Let' introduce the following scalar product and norm

$$(r,s)=\sum_{k=1}^{N} r_{k-1/2}s_{k-1/2}h,\ \ \|r\|^2=(r,r).$$

The operator A from (8.8) for the scheme (8.4) gets the form $A=\widetilde{A}+D$ when $d=1+\gamma\tau$. Therefore at first we obtain the estimation of the type (8.8) for the operator $\widetilde{A}$. For that we apply the following two finite-difference formulas [102]

$$w_{\bar{x}}w=0.5\left[\left(w^2\right)_{\bar{x}}+h\left(w_{\bar{x}}\right)^2\right];\quad -w_x w=0.5\left[-\left(w^2\right)_x+h\left(w_x\right)^2\right].$$

Now we sum up these formulas by all internal nodes of the grid $x_{m\text{-}1/2}$, $m=\overline{1,N}$ and get

$$(w_{\bar{x}},w)=\sum_{m=1}^{N} w_{m-1/2,\bar{x}}w_{m-1/2}h=0.5h\sum_{m=1}^{N}(w_{m-1/2,\bar{x}})^2h-w_{-1/2}^2+w_{N-1/2}^2=$$

$$=0.5h\|w_{\bar{x}}\|^2-w_{-1/2}^2+w_{N-1/2}^2;$$

$$-(w_x,w)=\sum_{m=1}^{N} w_{m-1/2,x}w_{m-1/2}h=0.5h\sum_{m=1}^{N}(w_{m-1/2,x})^2h+w_{1/2}^2-w_{N+1/2}^2=$$

$$=0.5h\|w_x\|^2+w_{1/2}^2-w_{N+1/2}^2.$$

Now we consider and transform the expression $(\widetilde{A}y,y)$

$$(\widetilde{A}y,y)=a(r_{\bar{x}}^n,r)-a(s_x^n,s)=$$

$$=0.5ah\left[\|r_{\bar{x}}\|^2+\|s_x\|^2\right]+0.5a\left(s_{1/2}^2-r_{-1/2}^2\right)+0.5a\left(r_{N-1/2}^2-s_{N+1/2}^2\right)=$$

$$=0.5(h/a)\left\|\widetilde{A}y\right\|^2+0.5a\left(s_{1/2}^2-r_{-1/2}^2\right)+0.5a\left(r_{N-1/2}^2-s_{N+1/2}^2\right). \qquad (8.9)$$

From the boundary condition (8.3) we have

$$s_{1/2}^2 = r_{-1/2}^2 \text{ and } r_{N-1/2}^2 - s_{N+1/2}^2 = (1-z^2) r_{N-1/2}^2 \geq 0 \ (|z| \leq 1).$$

Then from (8.9) it follows

$$(\widetilde{A}y, y) \geq \frac{h}{2a} \left\| \widetilde{A}y \right\|^2 . \tag{8.10}$$

Now we return to the estimation (8.8) for operator $A = \widetilde{A} + D$, that has the form

$$\left((\widetilde{A} + D)y, y \right) \geq \frac{\tau}{2d} \left\| (\widetilde{A} + D)y \right\|^2 . \tag{8.11}$$

Let's estimate the norm $\left\| (\widetilde{A} + D)y \right\|^2$

$$\left\| (\widetilde{A} + D)y \right\|^2 \leq \left\| \widetilde{A}y \right\|^2 + \left\| Dy \right\|^2 + 2(\widetilde{A}y, Dy) . \tag{8.12}$$

The first member in the right-hand part of the (8.12) can be estimated by formula (8.10). The second member $\left\| Dy \right\|^2$, that contains the symmetric matrix D from (8.4), can be estimated by maximal eigenvalue of this matrix $\lambda_{\max}(D) = \max(\gamma_R, \gamma_G)$

$$\left\| Dy \right\|^2 \leq \lambda_{\max}(D)(Dy, y) . \tag{8.13}$$

To estimate the third member from the (8.12) we apply the inequalities (8.10), (8.13) and ε-inequality: $2ab \leq a^2 / \varepsilon + \varepsilon b^2, \varepsilon > 0$

$$2(\widetilde{A}y, Dy) \leq \frac{1}{\varepsilon} \left\| \widetilde{A}y \right\|^2 + \varepsilon \left\| Dy \right\|^2 \leq \frac{2a}{\varepsilon h} (\widetilde{A}y, y) + \varepsilon \lambda_{\max}(D)(Dy, y) . \tag{8.14}$$

Using the inequalities (8.10), (8.13) and (8.14), from (8.12) we obtain

$$\left\| (\widetilde{A} + D)y \right\|^2 \leq \frac{2a}{h} (\widetilde{A}y, y) + \lambda_{\max}(D)(Dy, y) + \frac{2a}{\varepsilon h} (\widetilde{A}y, y) +$$

$$+\varepsilon\lambda_{\max}(D)(Dy,y)=\frac{2a(1+\varepsilon)}{\varepsilon h}(\widetilde{A}y,y)+(1+\varepsilon)\lambda_{\max}(D)(Dy,y).$$

Now we choose the parameter ε from the condition of equality of the coefficients

$$\frac{2a(1+\varepsilon)}{\varepsilon h}=(1+\varepsilon)\lambda_{\max}(D),\ \ \varepsilon=\frac{2a}{h\lambda_{\max}(D)}.$$

Then we get the following estimation

$$\left\|(\widetilde{A}+D)y\right\|^2\le\left(\frac{2a}{h}+\lambda_{\max}(D)\right)\left((\widetilde{A}+D)y,y\right). \qquad (8.15)$$

Substituting the inequality (8.15) in the stability condition (8.11), we obtain

$$\left((\widetilde{A}+D)y,y\right)-\frac{\tau}{2d}\left\|(\widetilde{A}+D)y\right\|^2\ge$$

$$\ge\left(\frac{1}{\lambda_{\max}(D)+2a/h}-\frac{\tau}{2d}\right)\left\|(\widetilde{A}+D)y\right\|^2\ge 0.$$

Hence, the condition

$$\tau\le\frac{1}{\frac{a}{h}+\lambda_{\max}(D)/2-\gamma}=\frac{h}{a+[\lambda_{\max}(D)/2-\gamma]h}=$$

$$=\frac{h}{a-h\min(\gamma_R,\gamma_G)/2}\ \text{ or }\ \frac{\tau a}{h}\le\frac{1}{1-h\min(\gamma_R,\gamma_G)/(2a)} \qquad (8.16)$$

is sufficient for stability of the finite-difference scheme (8.2), (8.3) by initial data in the space L_2.

Let's obtain also the necessary condition of stability for the finite-difference scheme (7.8)

$$(L+\alpha\tau)i^n_{m,t}+u^n_{m,\dot{x}}+Ri^n_m-\frac{hLa}{2}i^n_{m,\bar{x}x}=0;$$
$$(C+\beta\tau)u^n_{m,t}+i^n_{m,\dot{x}}+Gu^n_m-\frac{hCa}{2}u^n_{m,\bar{x}x}=0. \tag{8.17}$$

Substituting the values $\alpha=L\gamma$, $\beta=C\gamma$, $\gamma=(\gamma_G+\gamma_R)/2$, $\gamma_R=R/L$, $\gamma_G=G/C$ in (8.17), we rewrite it in the form

$$(1+\gamma\tau)i^n_{m,t}+\frac{1}{L}u^n_{m,\dot{x}}+\gamma_R i^n_m-\frac{ha}{2}i^n_{m,\bar{x}x}=0;$$
$$(1+\gamma\tau)u^n_{m,t}+\frac{1}{C}i^n_{m,\dot{x}}+\gamma_G u^n_m-\frac{ha}{2}u^n_{m,\bar{x}x}=0. \tag{8.18}$$

Now we apply the spectral stability criterion (Neumann criterion). We will find the solution of the equations (8.18) in the harmonics form with the phase φ

$$y=\begin{pmatrix} i \\ u \end{pmatrix}=y_0 q^n e^{j\varphi x_m}. \tag{8.19}$$

Substituting (8.19) in (8.18) we get the system of two equations with the matrix A

$$q^n e^{j\varphi x_m} A y_0=0; \tag{8.20}$$

$$A=\begin{pmatrix} \frac{1+\gamma\tau}{\tau}(q-1)+\gamma_R+\frac{2a}{h}\sin^2\frac{\varphi h}{2} & \frac{j}{Lh}\sin\varphi h \\ \frac{j}{Ch}\sin\varphi h & \frac{1+\gamma\tau}{\tau}(q-1)+\gamma_G+\frac{2a}{h}\sin^2\frac{\varphi h}{2} \end{pmatrix}.$$

For existence of the nontrivial solution of the form (8.19), it is required that the matrix A determinant to be equal to zero. Expanding this determinant, we obtain the equation with regard to parameter q. The value of this parameter is equal to the norm of the transition operator from the layer with number n to the layer n+1.

$$\left[\frac{1+\gamma\tau}{\tau}(q-1)+\left(\gamma+\frac{2a}{h}\sin^2\frac{\varphi h}{2}\right)\right]^2+\frac{a^2}{h^2}\sin^2\varphi h+$$

$$+\left(\gamma_R+\frac{2a}{h}\sin^2\frac{\varphi h}{2}\right)\left(\gamma_G+\frac{2a}{h}\sin^2\frac{\varphi h}{2}\right)-\left(\gamma+\frac{2a}{h}\sin^2\frac{\varphi h}{2}\right)^2= \tag{8.21}$$

$$=\left[\frac{1+\gamma\tau}{\tau}(q-1)+\left(\gamma+\frac{2a}{h}\sin^2\frac{\varphi h}{2}\right)\right]^2+\frac{a^2}{h^2}\sin^2\varphi h-\frac{(\gamma_R-\gamma_G)^2}{4}=0.$$

In case of undistorting line ($\gamma_R=\gamma_G=\gamma$) this equation takes sufficiently simple form

$$\left[\frac{1+\gamma\tau}{\tau}(q-1)+\left(\gamma+\frac{2a}{h}\sin^2\frac{\varphi h}{2}\right)\right]^2+\frac{a^2}{h^2}\sin^2\varphi h=0.$$

Its roots are the following

$$\frac{1+\gamma\tau}{\tau}(q_{1,2}-1)=-\left(\gamma+\frac{2a}{h}\sin^2\frac{\varphi h}{2}\right)\pm j\frac{a}{h}\left|\sin\varphi h\right|. \tag{8.22}$$

According to the spectral stability criterion, the finite-difference scheme is instable if there exists such values of the phase φ for which $|q|>1$. From (8.22) yields

$$|q|^2-1=\frac{\gamma\tau}{1+\gamma\tau}\left(\frac{\gamma\tau}{1+\gamma\tau}-2\right)+\frac{4a\tau/h}{1+\gamma\tau}\cdot\frac{a\tau/h-1}{1+\gamma\tau}\sin^2\frac{\varphi h}{2}>0.$$

Solving this inequality, we obtain the necessary stability condition

$$\frac{\tau a}{h}>\frac{1}{1-\gamma h/(2a)}. \tag{8.23}$$

It is easy to see that this condition coincides with the sufficient condition (8.16) when $\gamma_R=\gamma_G=\gamma$.

For line with losses, the roots of the equation (8.21) have the following form

$$\frac{1+\gamma\tau}{\tau}(q_{1,2}-1) = -\left(\gamma + \frac{2a}{h}\sin^2\frac{\varphi h}{2}\right) \pm$$

$$\pm\sqrt{-\frac{a^2}{h^2}\sin^2\varphi h + \frac{(\gamma_R-\gamma_G)^2}{4}} = 0\,. \qquad (8.24)$$

To obtain the necessary stability condition in this case we are to demonstrate that there exists at least one value of the phase φ, for which $|q|>1$. Therefore, we will consider the value φ that makes the radical expression in (8.24) be equal to zero

$$\sin^2\varphi h = \frac{h^2(\gamma_R-\gamma_G)^2}{4a^2};\ \sin^2\frac{\varphi h}{2} = 0.5\left(1+\sqrt{1-\frac{h^2(\gamma_R-\gamma_G)^2}{4a^2}}\right).$$

Then the roots of (8.24) are real and multiple and the inequality $|q|>1$ leads to the stability condition

$$\frac{\tau a}{h} > \frac{2}{1+\sqrt{1-\frac{h^2(\gamma_R-\gamma_G)^2}{4a^2}}-\frac{\gamma h}{a}}\,. \qquad (8.25)$$

It is easy to notice that the condition (8.25) coincides with (8.23) when $\gamma_R = \gamma_G = \gamma$.

9. A posteriori analysis of the numerical solutions accuracy

To have some test problem we'll consider the nonstationary problem about the motion of the potential and current rectangular wave along the half-infinite line with strong dissipation and dispersion: $U_0 = L = C = 1$;

$R = 2$; $G = 0$. In [15, 60] one finds the exact analytical solution of this problem in the form of the zero order Bessel function of the first kind. The solution is $i(x,t) = J_0\left(0.5Rj\sqrt{t^2 - x^2}\right)e^{-0.5Rt}$ when $t > x$ and $i(x, t) = 0$ when $t \le x$. It is to mention that the motion of the current jump with the steady speed $a = 1$ is identified here in the explicit manner. So the solution appears to be a heavy test for every numerical scheme. Nevertheless, the design finite-difference formulas (7.4) - (7.7) ensure the accuracy till two significant digits even on the very coarse grid with 5 partitions per length and time unit (these corresponds to 300000 km and 1 s in a real scale).

It is easy to see from the time diagrams at the fixed space points: $x = 1$; 3; 5 (curves 1–3 in the fig. 9.1), that the structure of the finite-difference functions is such, that independent of the grid step the exact solution is in the gripe of them and the residual between them tends to zero under the grid refinement. The increasing of the number of the grid points by an order results in increasing of the number of significant digits in the numerical solution by the unit at least. The approximate solution on the sufficiently long time interval (50 s) is visual indistinguishable from exact one when $\tau = h = 0.02$ (fig. 9.1, *b*).

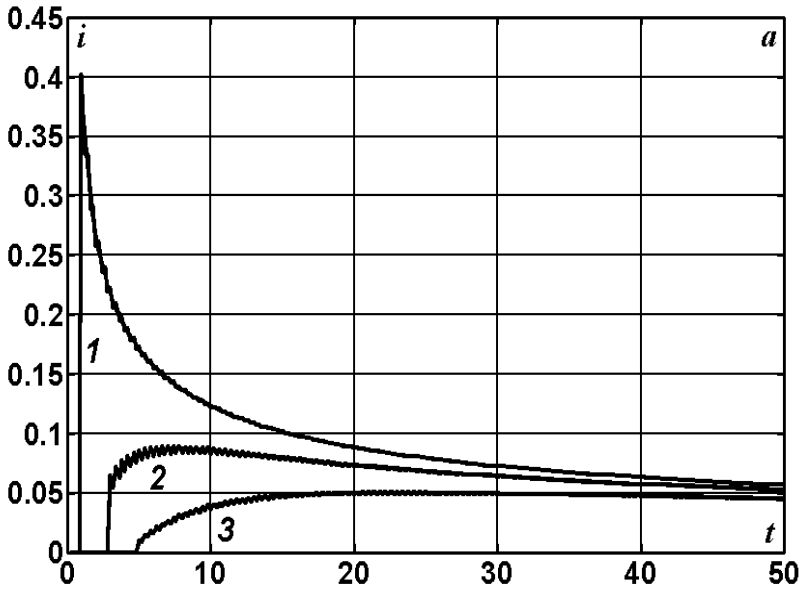

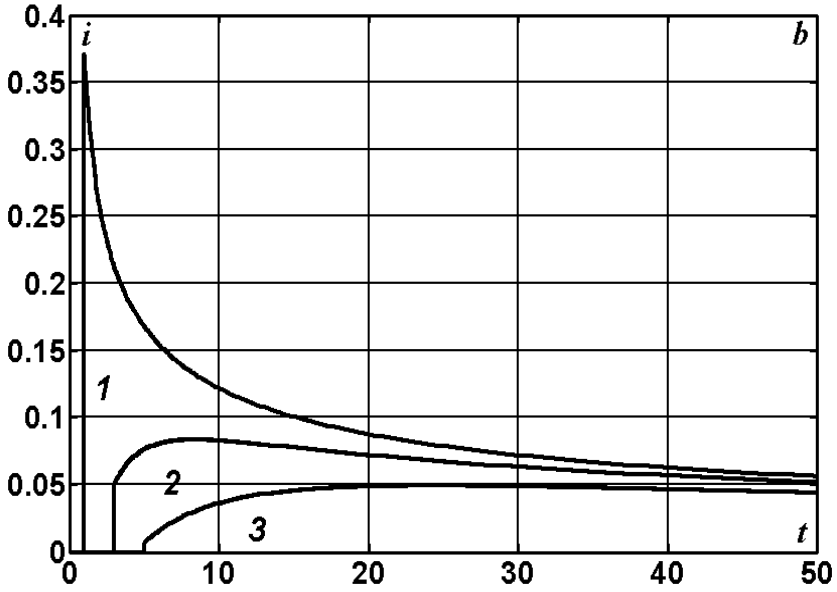

Fig. 9.1. Currents dynamics at the points x = 1; 3; 5 (curves 1-3) in the direct voltage line with losses in cases of 5 (***a***) and 50 (***b***) partitions per length unit.

Let's apply now to another source [48]. Here we find the investigation of the degenerated and loading regimes in the direct voltage circuit with distributed losses: $U_0 = 1$ V; L = 0.77 μH/m; C = 2.9 nF/m; R = 48 mΩ /m; G = 0.4 mS/m; l =341 m; Z_B = 16.29 Ω; a = 211619 km/s; Δ = 1.61 μs. The investigation is fulfilled by means of operator method with help of Laplace transformation and the expansion theorem. The considered here load resistance is: $R_S = 0$ (short-circuit); ∞ (idling); 15 Ω. After transformation to the relative units by formulas (1.4), we obtain R = 1.0045; G = 2.2226; $R_S = 0.9205$. These values discover unnaturally big cable shunt conductance, because for high-current lines and data transmission systems we usually have $R \geq G$.

The voltage and current oscillograms in in the short-circuited), open-ended and loaded lines are represented in the fig. 9.2. These calculations correspond to partitioning of the computational domain in 100 of elementary cells. The desired functions discontinuity propagation is not followed specially in the computational scheme, but nevertheless, it clearly recognizes even fine details of the wave motion, all jumps are extremely accurate and exactly correspond to the arrival moments of the direct and reflected waves to the point of observation. Let's consider now the pure active load

($R_S = 0.9205$) that is closed to the matched load for direct current line ($R_S = 1$). In this case the amplitude of the wave reflected from the receiver numerically is present in the third digit, but it is too small to be visually watched in the time diagrams. The analogous wave presentation from [48] is correct from qualitative point of view but it can not be used as a test because of its smearing (it seems to be so because of using of the smoothing Lanczos sigma-factors with the object to cancel the Gibbs oscillations in the resultant discontinuous solution).

The transient process, that appears when the short-circuited line is connected to the direct voltage, can be calculated and rechecked by the Fourier variable separation method [75, 90]. As a result of its applying one gets the following voluminous expression for current:

$$i(x,t) = -U_0 \left\{ \frac{e^{-\gamma_R t}}{lR} - \frac{\mathrm{ch}\delta(l-x)}{Z_0 \mathrm{sh}(\delta l)} + \frac{2e^{-\alpha t}}{lL} \times \right.$$

$$\left. \times \sum_{k=1}^{\infty} \frac{\cos(\pi k x / l)}{\beta_k \gamma_k} \left[(\alpha\gamma_G - \gamma_k)\mathrm{sh}\beta_k t + \beta_k \gamma_G \mathrm{ch}\beta_k t \right] \right\}, \qquad (9.1)$$

where

$$\gamma_R = R/L;\ \gamma_G = G/C;\ \delta = \sqrt{RG} = \sqrt{\gamma_R \gamma_G}\ / a;\ Z_0 = \sqrt{R/G}\ ;$$

$$\alpha = 0.5(\gamma_R + \gamma_G)\ ;\ \beta_k = 0.5\sqrt{(\gamma_R - \gamma_G)^2 - \left(\frac{2a\pi k}{l}\right)^2}\ ;\ \gamma_k = \gamma_R \gamma_G + \left(\frac{a\pi k}{l}\right)^2 .$$

To obtain as sensitive results as in fig. 9.2 by applying the above formulas it is necessary here to sum up as minimum 1000 of members. This is caused by the slow convergence of the Fourier series in the vicinity of the desired functions jumps.

Let's mention another source [110], where it was made an attempt to solve the nonstationary problem about the instantaneous connection to the direct voltage source $u = U_0$ (when $x = 0$) of the cable with the lumped capacity at the end: L = 31.2 mH/km; C = 0.25 μF /km; R = 1.88 Ω/km; G = 0; l = 320 km ; $Z_B = 353.27$ Ω; a = 11323 km/s; Δ = 28.3 ms; $C_s = Cl$ = = 80 μF. if we assume the unit to be the wave length with the frequency f =

= 50 Hz: λ = 226.45 km, then in the dimensionless form we obtain: $l = C_s = \Delta = 1.4131$; $R = 1.2051$.

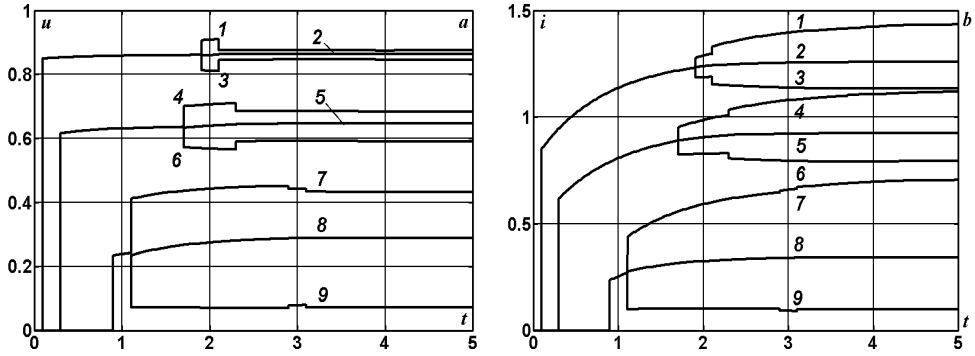

Fig. 9.2. The dynamics of voltages (***a***) and currents (***b***) at the points $x = 0.1$ (curves 1-3); 0.3 (4-6); 0.9 (7-9) in the short-circuited (1;4;7), open-ended (3; 6; 9) and loaded on pure active resistance (2;5;8) lines.

The changes in time of the voltage and current (curves 1; 2) at the charging capacitor in the line without losses $R = G = 0$ are represented in fig. 9.3,*a*. The superposition of the direct and reflected waves leads to the forming of enough complicated nonstationary picture. The electric energy accumulated in the capacity returns back in the line approximately every 7 wave runs along the circuit. It arrives that in the absence of active losses in the connecting wires it is impossible theoretically to charge the ideal condenser because the wave process here does not steady or it steadies infinitely long. The grid solutions are calculated with use of 100 of nodes along the line length and it was found quite enough to repeat the exact solution obtained by method of characteristics. Let's denote $k = -1/C_S$, $t_m = k(t - m\Delta)$, $m = 1,2,3,\ldots$. Then the voltages and currents at the end of the line during the underwritten time intervals can be represented as follows

$$
\begin{aligned}
&i_1 = u_1 = 0 \text{ when } 0 < t \le \Delta;\\
&u_3 = 2 - 2e^{t_1};\ i_3 = 2e^{t_1} \text{ when } \Delta < t \le 3\Delta;\\
&u_5 = -2 + u_3 + 2(1 - 2t_3)e^{t_3};\ i_5 = i_3 + 2(1 + 2t_3)e^{t_3} \text{ when } 3\Delta < t \le 5\Delta; \quad (9.2)\\
&u_7 = 2 + u_5 - 2(1 + 2t_5^2)e^{t_5};\ i_7 = i_5 + 2(1 + 4t_5 + 2t_5^2)e^{t_5} \text{ when } 5\Delta < t \le 7\Delta
\end{aligned}
$$

etc.

As can be seen from formulas (9.2) (these formulas can be continued on the plane *xt* with no limit), tracking from the zero initial state switching wave process has the pronounced oscillatory character and does not manifest any asymptotic properties.

Taking into account the real active losses in the cable without the current insulation leakage we obtain the sufficiently rapid stabilization of voltage on the condenser till the nomination level and the charging current decreasing till zero (see fig. 9.3,*b*). The voltage curve coincides qualitative with the same from the source but we can not say the same about the calculated current oscillogram. The method applied in [110] does not take into consideration high-frequency components of the transient process and gives incorrect results even for asymptotic values of the desired functions that can be easily calculated by complex amplitude method. In steady state regime under the conditions $R > G = 0$ we always obtain the unit voltage and zero current in the whole line.

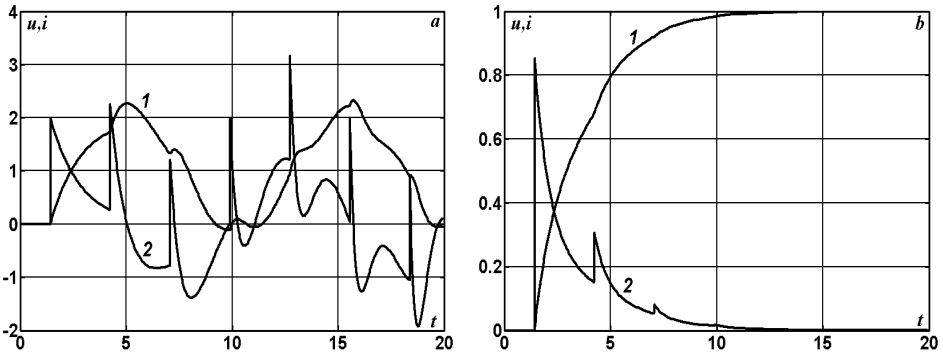

Fig. 9.3. The rectangular wave fall on the lumped capacity C_S = 80 μF, connected to the receiving end of the cable with length l = 320 km when R = 0 (***a***); 1.88 Ω/km (***b***).

Since, when connecting the ideal line with distributed and lumped reactive elements to the direct voltage, the regime does not steady then the same regime hardly can appear under the sinusoidal input voltage (fig. 9.4,*a*). As a result of continuous bilateral interchange of energy between the infinite power generator and the line reactive elements the wave process is developed by very complex script, that from the qualitative point of view reminds of aperiodic regime, but is not it. If to calculate the steady state electricity transmission regime in the absence of losses on the Joule–Lenz effect one applies formally the complex amplitude method, then obtained voltage and current amplitudes will not represent the real values (see curves 3 and 4).

In the line with losses the wave process represented in the fig. 9.4, *b* later then 100…200 ms after commutation practically comes to the steady state stage, when the voltage and current amplitudes can be calculated by complex amplitude method. This fact gives one more confirmation of the correctness of calculations by the "albatross" method.

The evident shortage of experimental data for transient electromagnetic processes forces to the inaccessible articles. In the experiments [66], traced as early as 1959, some nonstationary processes have been researched. The process was caused by capacitor discharge with $C_S = 0.5\mu\text{F}$ on the cable with length $l = 0.8$ km with lineal parameters: L = 0.125 mH/km; C = 0.31 μF/km; Δ = 5 μs. The capacitor discharge can be modeled by the following boundary conditions:

$$C_S \frac{du}{dt} = i \quad \text{when} \quad x = 0, t \geq 0; \; u = U_0 \quad \text{when} \quad x = t = 0.$$

The theoretical calculations in [66] have been effectuated by traveling wave method without taking into consideration the losses in the line. The results of these numerical experiments are reproduced in fig. 9.5, 9.6 for short-circuited and opened cable correspondingly. However, the cited article author assertion about acceptable conformity between the computational and experimental data seems to be highly disputable. It is indeed necessary to repeat the similar experiments at the more qualitative level using the modern measuring equipment.

If we set the active losses in the cable equal to the same from the previous example (R = 1.88 Ω/km) then, owing to moderate length of the line (l = 0.8 km), the wave process in it does not steady even after 35 wave runs along the line length (see fig. 9.7).

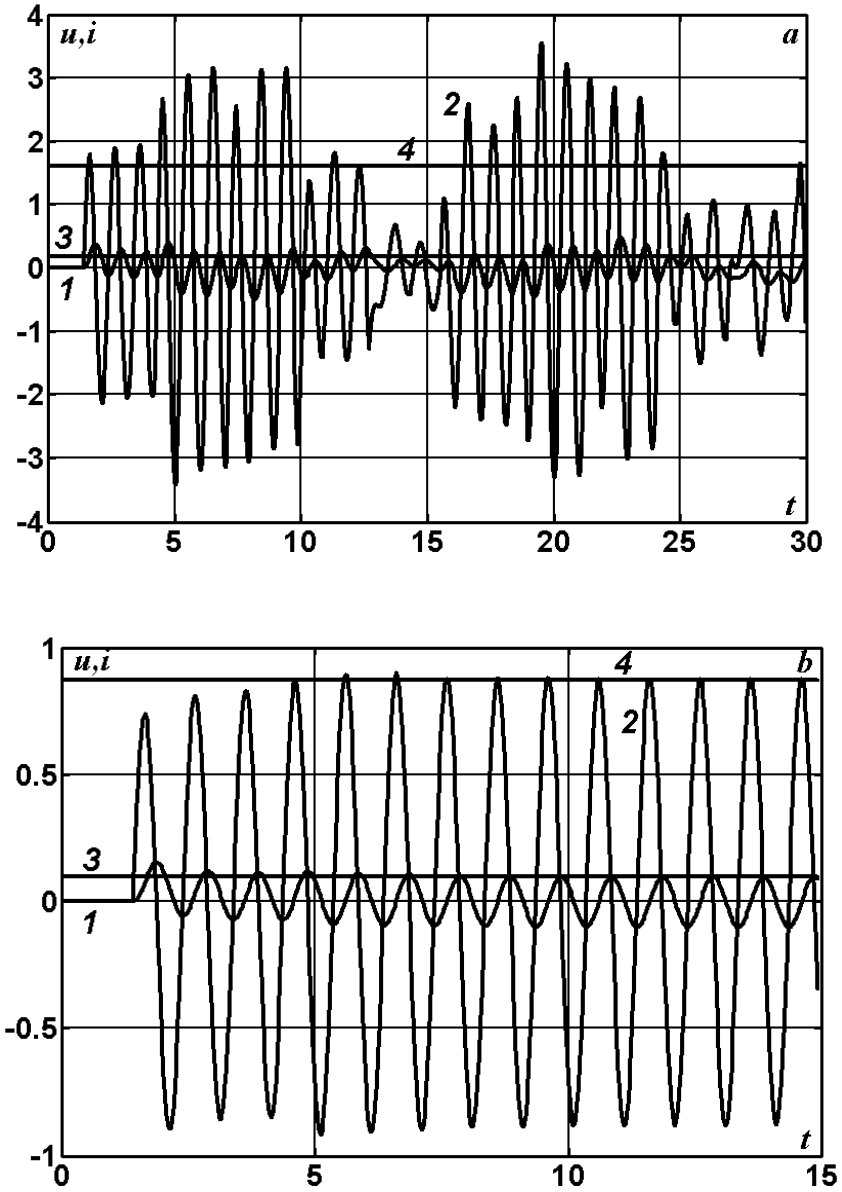

Fig. 9.4. The sinusoidal wave fall on the lumped capacity C_S = 80 μF, connected to the receiving end of the cable with the length l = 320 km when R = 0 (***a***); 1.88 Ω/km (***b***).

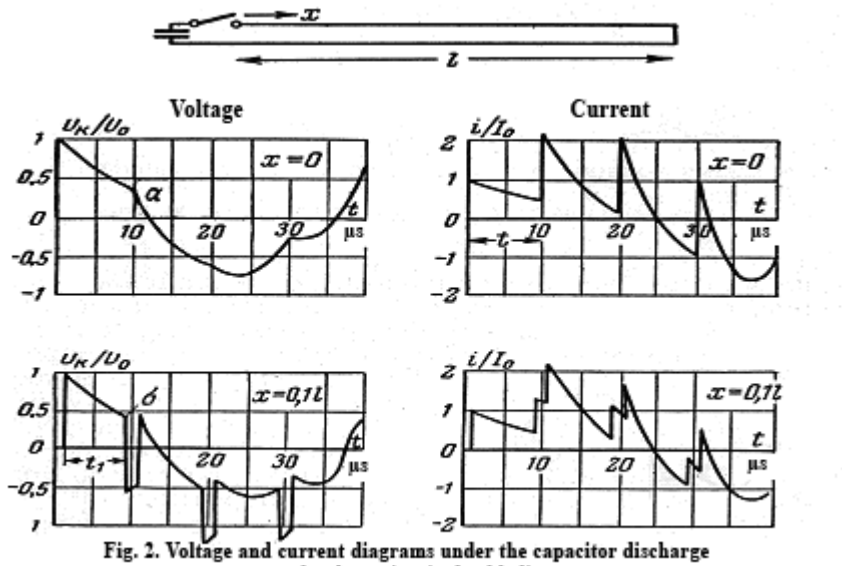

Fig. 2. Voltage and current diagrams under the capacitor discharge on the short-circuited cable line
l = 800 m; Z_C = 20 Ω; R = 0; G = 0; U_0 = m/μs; C_k = 0.5 μF.

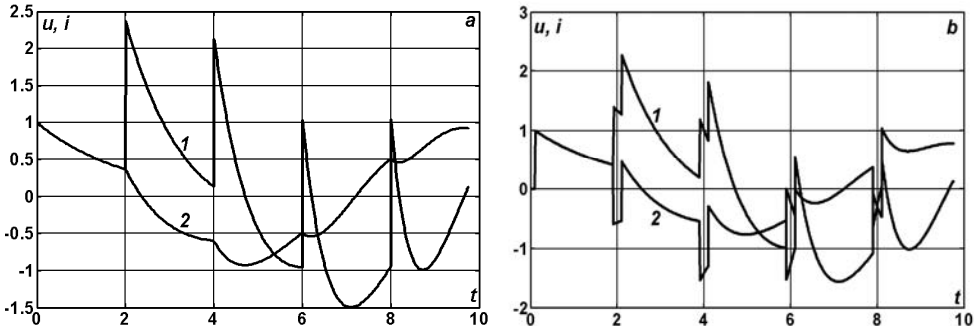

Fig. 9.5. Voltage and current diagrams (curves 1;2) at the points x = 0 (***a***); l/10 (***b***) under the capacitor discharge C_S = 0.5 μF on the ideal short-circuited cable line with the length l =0.8 km.

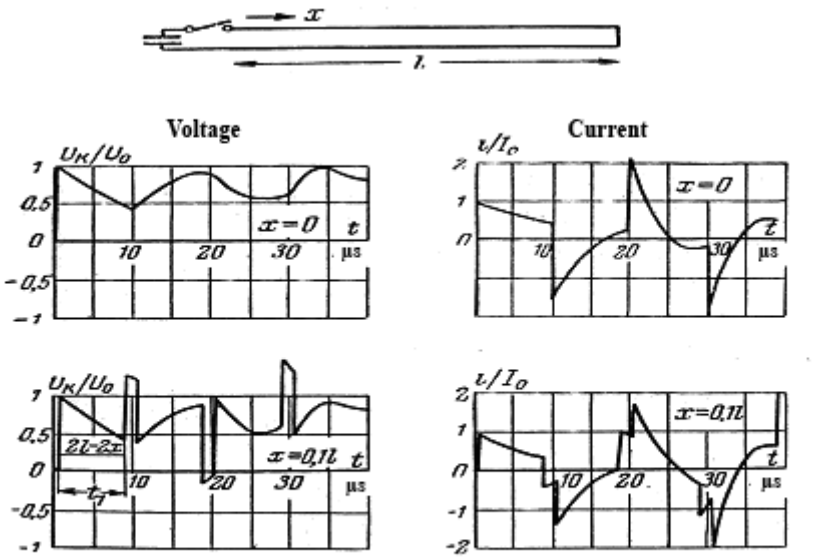

Fig. 7. Voltage and current diagrams under the capacitor discharge on the open-ended cable line
l = 800 m; Z_C = 20 Ω; R = 0; G = 0; U_0 = m/μs; C_k = 0.5 μF.

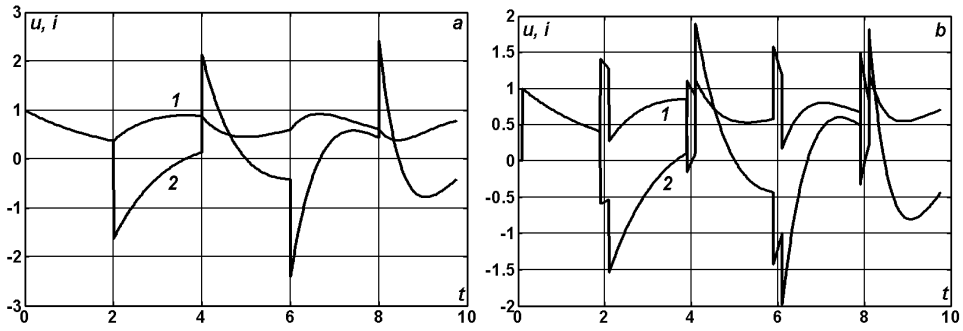

Fig. 9.6. Voltage and current diagrams (curves 1;2) at the points x = 0 (***a***); l/10 (***b***) under the capacitor discharge C_S = 0.5 μF on the ideal open-ended cable line with the length l =0.8 km.

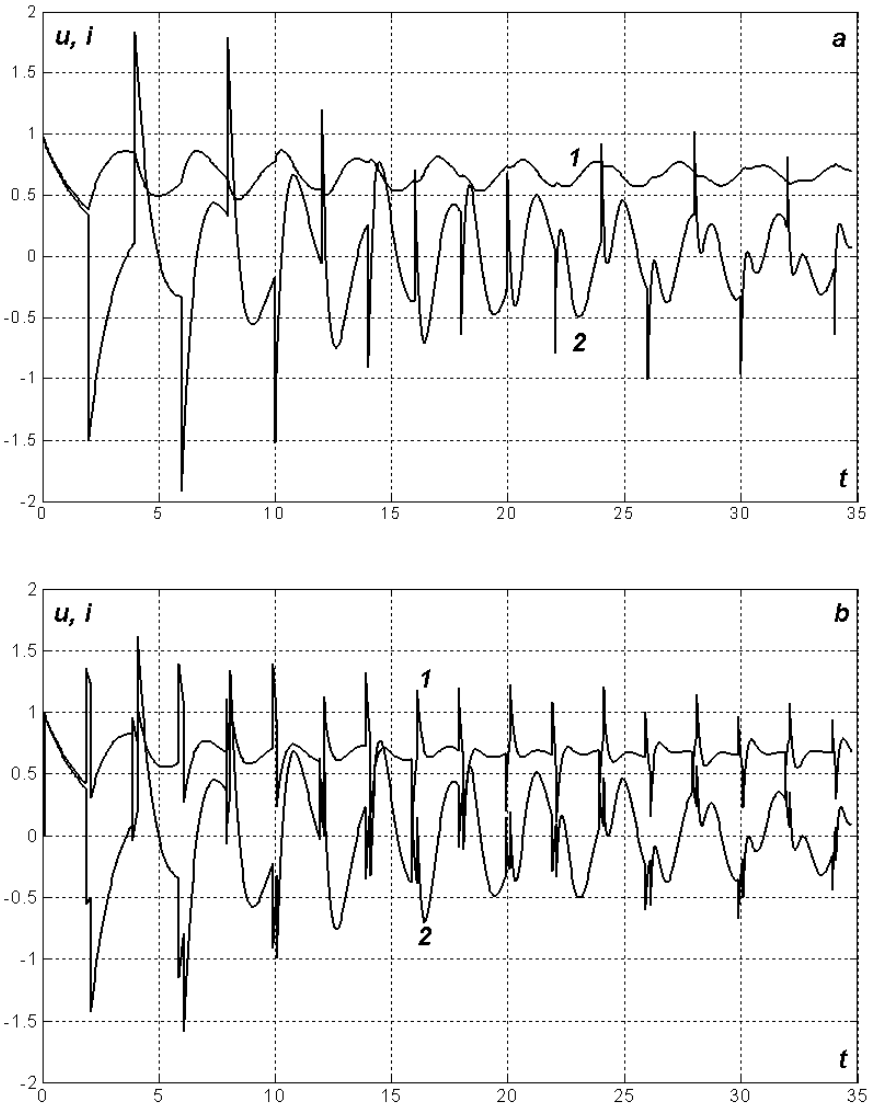

Fig. 9.7. Voltage and current diagrams (curves 1;2) at the points $x = 0$ (***a***); $l/10$ (***b***) under the capacitor discharge $C_S = 0.5$ μF on the open-ended cable line with the length $l = 0.8$ km and the losses: $R = 1.88$ Ω/km, $G = 0$.

As a test problem let's consider also the reflection of the rectangular potential and current wave from the *RL* – circuit connected to the end of the line. The aerial circuit with the length $l = 100$ km with the wave resistance $Z_B = 500$ Ω and the speed of wave propagation $a = 300000$ km/s has at the end the *RL* – load that consists of parallel connected active resistance $R_S =$

700 Ω and inductance L_S = 0.1 H (see fig. 9.8). The line is connected to the direct voltage source U_0 = 30 kV. It is required to obtain the voltage and current distribution diagrams along the line for the time moment when the reflected from the end of the line wave reaches the midpoint of the line [15].

Fig. 9.8. Uncharged line with *RL* – circuit connection to the direct voltage.

In the dimensionless variables we have $U_0 = l = Z_B = a$ =1; R_S = 1.4; L_S = 0.6. The boundary conditions can be written as

$$u = U_0(t) \text{ when } x = 0; t > 0;$$

$$i = i_1 + i_2; u = R_s i_1; u = L_s \frac{di_2}{dt} \text{ when } x = l, t > 0.$$

The distribution of voltages and currents along the line for time moment t = 1.5 is represented in fig 9.9 when $G = R/5$; R = 0 (*a*); 0.048 (*b*); 0.48 (*c*); 4.8 (*d*). The diagrams in the fig. 9.9,*a* exactly repeat the results obtained for ideal line in [15]. In the presence of losses in the line distorts the profile of direct and reflected from the end of the line wave right up to beyond recognition when R = 4.8 (see fig. 9.9,*d*).

Voltage and current time diagrams at the point of connection of active-inductive load are represented in the fig 9.10 for ideal line of direct (*a*) and sinusoidal voltages with commercial frequency f = 50 H (*b*). During the initial stage of the nonstationary process the results are closely related, but already after several wave runs along the line length (1…2 ms in real time scale) the difference between the comparing functions becomes evident. These differences between the direct and alternating current lines are pro-

nounced when the losses are present in the line (see fig. 9.11) and in the first circuit the regime steadies quickly.

Therefore, only in very rough approximation the results of calculations for the line with sinusoidal voltage at the head end can be replaced by the same for the line with direct voltage.

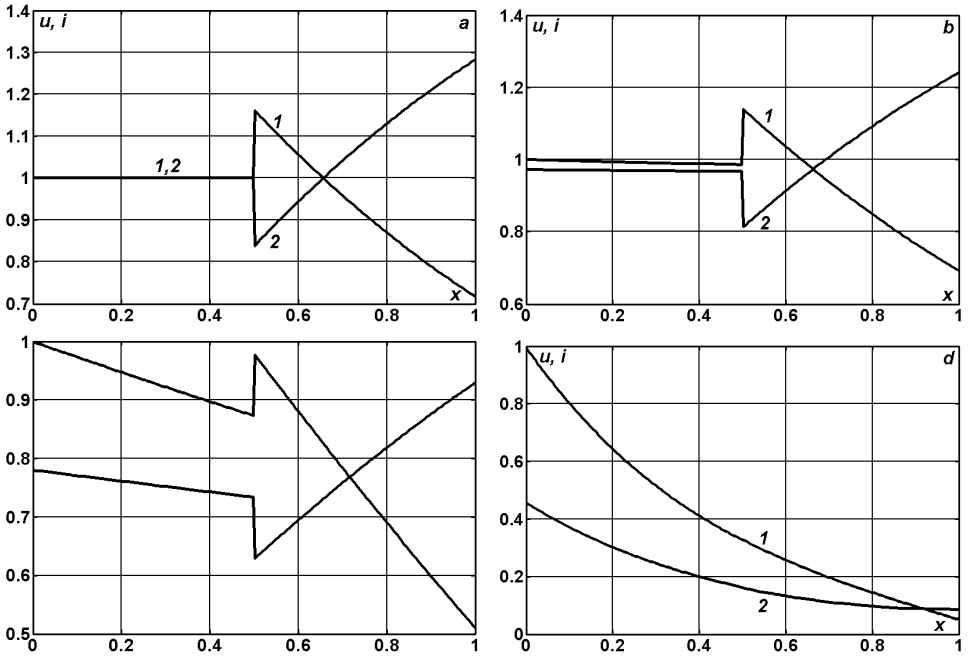

Fig. 9.9. Voltage and current (curves 1;2) distribution diagrams along the line with *RL* – circuit for $t = 1.5$ when $G = R/5$, $G = R/5$, $R = 0$ (***a***); 0.048 (***b***); 0.48 (***c***); 4.8 (***d***).

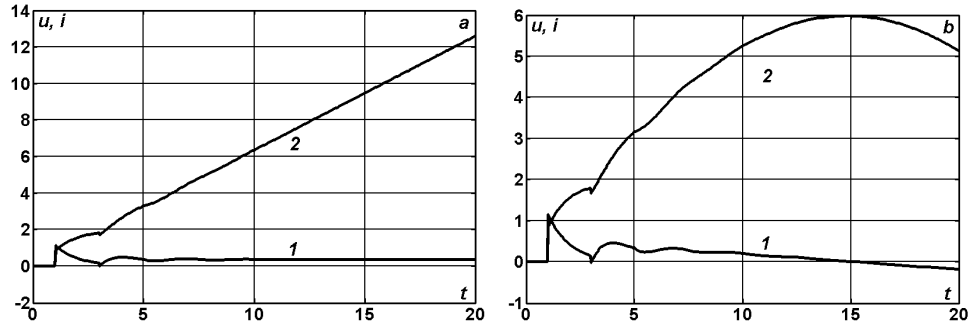

Fig. 9.10. Voltages and currents (curves 1;2) at the receiving end of the ideal direct voltage (***a***) and alternating voltage (***b***) lines.

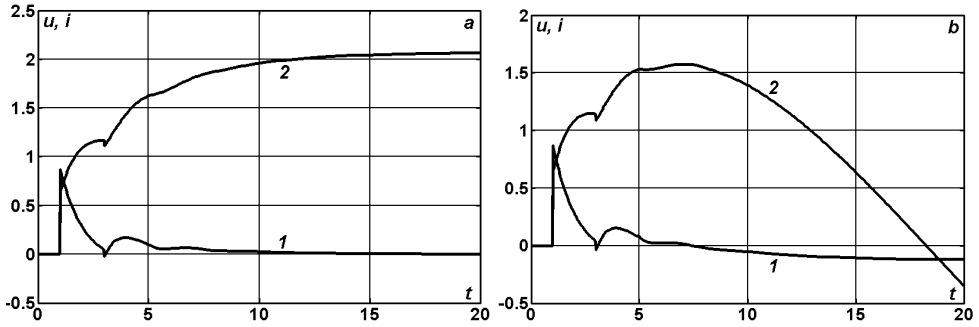

Fig. 9.11. Voltages and currents (curves 1;2) at the receiving end of the ideal direct voltage (***a***) and alternating voltage (***b***) lines when R= 0.48, $G = R/5$.

The travelling waves in the line appear most often under the external electromagnetic fields action, for example, under the lightning stroke [59]. Let's set the initial current distribution as a two positive half-periods of the sinusoid with amplitude 1 and 0.5, as it is depicted in the fig. 9.12,*a*. The left-hand end of the line we consider as short-circuited and the right-hand end – opened.

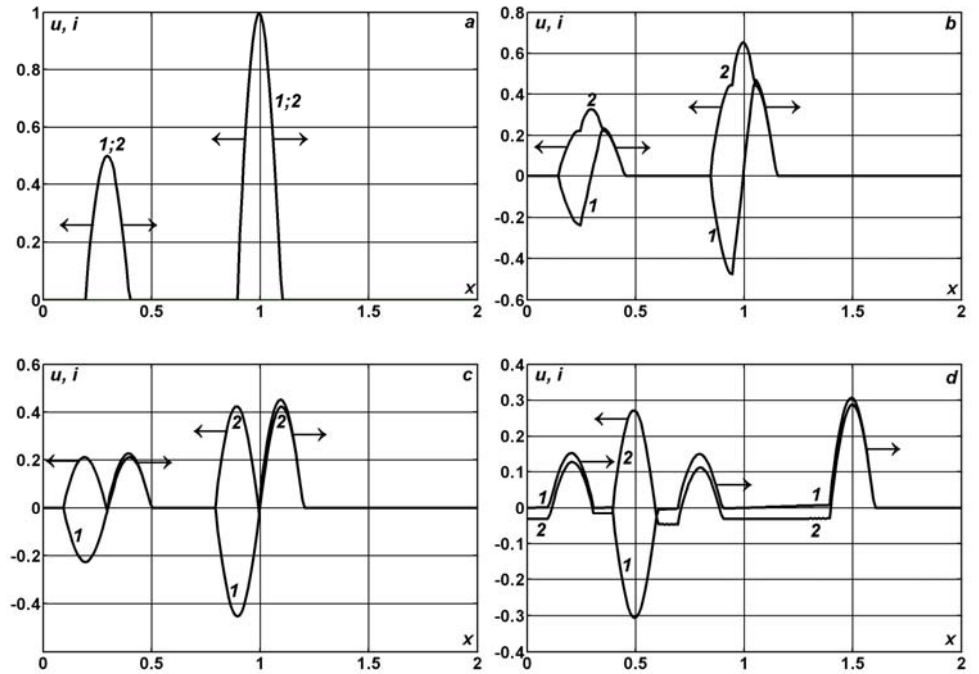

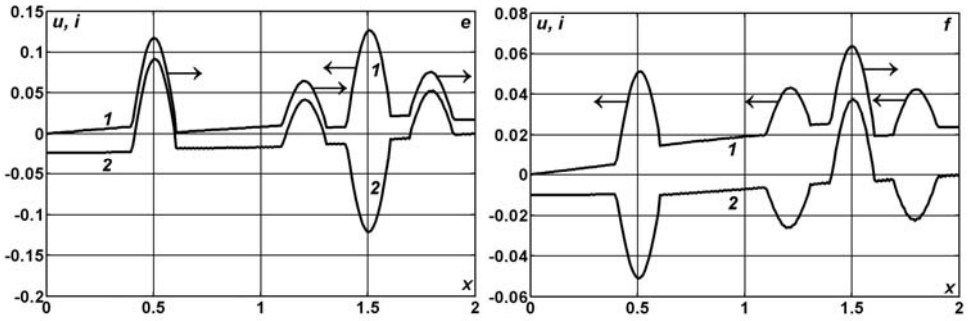

Fig. 9.12. Traveling waves in the line with open right-hand end and short-circuited left-hand end.

Either of two initial electromagnetic perturbations generates in twos waves of current and potential with equal amplitudes and opposite directions. The evolution of the wave motion represented in fig. 9.12,*b-f* achieves that the linear (d'Alemberian) solitary waves interpenetrate but do not interact. As a result of irreversible power losses in the line ($R = 2$, $G = 0$) the amplitude of the single pulses gradually decreases till zero.

So the approaches and analytical methods stated in [15, 48, 59, 60, 66, 110] together with Fourier method, method of characteristics and complex amplitude method have very restricted range of application and do not permit further generalizations for lines with arbitrary losses and with arbitrary form of the input voltage, tunable parameters, etc. Only elementary test problems can be solved by means of these methods. But such problems are of methodical and practical importance, because they serve as a base for comparative analysis and a posteriori accuracy estimation of the numerical solutions (see the table 9.1).

Table 9.1. The comparative characteristics of the methods for computation of the transient and steady state processes in the electrical circuits with distributed and lumped parameters.

Method and its age	Accuracy	Range of application
1. Complex amplitude method is more then 100 years old	absolute	Steady state sinusoidal regimes in a piecewise-homogeneous circuits with nonzero losses
2. The Fourier method is about 200 years old	absolute	Transient and steady state processes in an alternating current opened lines and in an alternating voltage short-circuited lines with arbitrary losses

Method and its age	Accuracy	Range of application
3. Method of characteristics (of traveling waves) is more then 250 years old	absolute	Transient and steady state processes in a piecewise-homogeneous ideal and undistorting circuits with variable (by time) lumped parameters
4. The universal grid-characteristics method "Albatross" is more then 10 years old	From three-four significant digits and more	Transient and steady state processes in a non-homogeneous parametrical circuits with arbitrary losses and another complicative factors

10. Emergency and postemergency states caused by instantaneous changes of load parameters in the overhead transmission line 500 kV

The power supply security and the quality of the delivered electric power take on special significance in the state of the art. Towards this end the isolated automatic and protection subsystems are stipulated in a power supply systems as their basic elements. The necessary condition of their reliable performance is the learning of limit regimes including the emergency states that depend on the design features and on topology of protected areas.

The perturbations that decrease the quality of voltage can appear both under the transmission of power and under the distribution of power. Because of the considerable length the overhead transmission lines are subjected to atmospheric forcing. The diverse types of discharges of the atmospheric electricity (lightning) become a reason of different perturbations, swings, undervoltage, power outage. The duration and the degree of perturbations depend on the circuit structure and on time that is necessary for its reconfiguration. The reasons of overvoltage caused by lightning strokes usually are considered as external with respect to the electric mains. Another type of perturbations appears during the electric mains administration under the load droppings or unexpected load pickups. The last type of perturbations is very infrequent, because usually the large-scale loads are gradually connected to the electric mains. But this does not relate to unexpected load dropping, that usually is a result of the emergency situations like the short-circuit or the break in the line. The current maximal value during the transient electromagnetic processes can in dozens and hundreds of times exceed its nominal value. The maximal possible overvoltage under the different nonstationary regimes constitutes several tens of its nominal value.

10.1. Transient processes caused by instantaneous change of load resistance

The exact solution for the homogeneous line with the active resistance R_S at the receiving end

$$u = R_S i \text{ when } x = l, t > 0, \tag{10.1}$$

and with sinusoidal voltage at the input

$$u = U_0 \sin(\omega t) \text{ when } x = 0, t > 0 \tag{10.2}$$

was obtained in [89, 93]. This solution at the steady regime has the following form

$$i(t) = \frac{U_0 A_0}{Z_B} \sin(\omega t + \varphi_0) \text{ when } x = 0, t > 0, \tag{10.3}$$

$$\operatorname{tg}\varphi_0 = \frac{2z_\gamma \sin 4\pi\Delta}{1 - z_\gamma^2}, \; A_0 = \frac{\sqrt{1 - 2z_\gamma^2 \cos 8\pi\Delta + z_\gamma^4}}{1 + 2z_\gamma \cos 4\pi\Delta + z_\gamma^2}, \tag{10.4}$$

$$u(t) = U_0 A_1 (1 + z) \sin(\omega t + \varphi_1),$$

$$i(t) = \frac{U_0 A_1}{Z_B} (1 - z) \sin(\omega t + \varphi_1) \text{ when } x = l, t > 0, \tag{10.5}$$

$$\operatorname{tg}\varphi_1 = \frac{z_\gamma - 1}{z_\gamma + 1} \operatorname{tg} 2\pi\Delta, \; A_1 = \frac{e^{-\gamma\Delta}}{\sqrt{1 + 2z_\gamma \cos 4\pi\Delta + z_\gamma^2}}. \tag{10.6}$$

The following notations have been used above

$$z = \frac{R_S - Z_B}{R_S + Z_B}, z_\gamma = z e^{-2\gamma\Delta}, \; R_S = Z_B \frac{1 + z}{1 - z}, Z_B = \frac{1}{aC},$$

$$\gamma = \frac{R}{L} = \frac{G}{C}, a = \frac{1}{\sqrt{LC}}, \Delta = \frac{l}{a}.$$

Let's suppose that till the initial time moment $t = 0$ the steady state regime has been generated in the line. This regime can be described by the formulas (10.3) – (10.6). Then the sudden (stepwise) change of the load R_S happens at the time moment $t = 0$. Let's find the solution of this problem on time interval $t \in [0, t^*]$, $t^* = (2n^* + 1)\Delta$. Thus, the boundary condition at the right-hand end of the line takes the form

$$u = R_S^* i \text{ when } x = l, \quad t \in [0, t^*] . \tag{10.7}$$

If the load R_S^* is equal to zero or

$$z^* = \frac{R_S^* - Z_B}{R_S^* + Z_B} = -1,$$

then the short-circuited regime is realized. If ever $R_S^* = \infty$ or $z^* = 1$, then the idling regime is realized.

The solution of this problem is found by the method of characteristics that is described in detail in [89]. At the input of the line the steady state solution (10.3)–(10.6) remains, until the reflected from the loaded end wave reaches the input (see fig. 10.1).

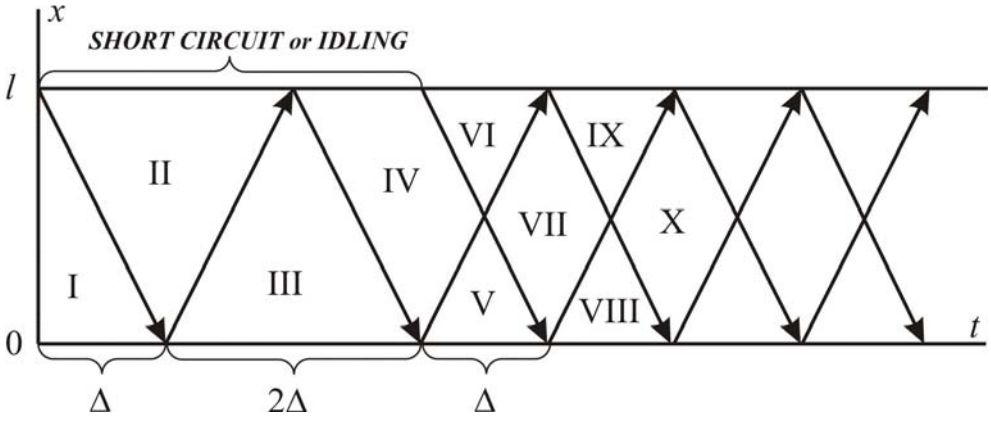

Fig. 10.1. Computational domains and configurations of the wave fronts under the instantaneous change of the load resistance.

Hence, when $x = 0, t \in [0, \Delta]$ we have

1. $u_{-1}(t) = U_0 \sin(\omega t)$, $i_{-1}(t) = \dfrac{U_0 A_0}{Z_B} \sin(\omega t + \varphi_0) = \dfrac{U_0}{Z_B} i_{ct}(t)$

when $x = 0, t \in [0, \Delta]$.

Then at the right-hand end of the line when $x = l, t \in [0, 2\Delta]$

2. $u_0(t) = \dfrac{(1 + z^*)e^{-\gamma\Delta}}{2} U_0 \left[\sin \omega(t - \Delta) + i_{ct}(t - \Delta)\right]$,

$$i_0(t) = \frac{(1 - z^*)e^{-\gamma\Delta}}{2} \frac{U_0}{Z_B} \left[\sin \omega(t - \Delta) + i_{ct}(t - \Delta)\right]$$

when $x = l, t \in [0, 2\Delta]$.

3. $u_1(t) = U_0 \sin(\omega t)$,

$$i_1(t) = \frac{U_0}{Z_B} \left[\sin(\omega t) - z_\gamma^* \left(\sin \omega(t - 2\Delta) + i_{ct}(t - 2\Delta)\right)\right]$$

when $x = 0, t \in [\Delta, 3\Delta]$.

4. $u_2(t) = \dfrac{(1 + z^*)e^{-\gamma\Delta}}{2} U_0 \left[2 \sin \omega(t - \Delta) - z_\gamma^* \left(\sin \omega(t - 3\Delta) + i_{ct}(t - 3\Delta)\right)\right]$

$$i_2(t) = \frac{(1 - z^*)e^{-\gamma\Delta}}{2} U_0 \left[2 \sin \omega(t - \Delta) - z_\gamma^* \left(\sin \omega(t - 3\Delta) + i_{ct}(t - 3\Delta)\right)\right]$$

when $x = l, t \in [2\Delta, 4\Delta]$.

5. $u_3(t) = U_0 \sin(\omega t)$,

$$i_3(t) = \frac{U_0}{Z_B} \left[\sin(\omega t) - 2 z_\gamma^* \sin \omega(t - 2\Delta) + (z_\gamma^*)^2 \left(\sin \omega(t - 4\Delta) + i_{ct}(t - 4\Delta)\right)\right]$$

when $x = 0, t \in [3\Delta, 5\Delta]$.

6. $u_4(t) = \dfrac{(1 + z^*)e^{-\gamma\Delta}}{2} U_0 \left[2 \sin \omega(t - \Delta) - 2 z_\gamma^* \sin \omega(t - 3\Delta) + \right.$

$$\left. + (z_\gamma^*)^2 \left(\sin \omega(t - 5\Delta) + i_{ct}(t - 5\Delta)\right)\right],$$

$$i_4(t)=\frac{(1-z^*)e^{-\gamma\Delta}}{2}U_0\Big[2\sin\omega(t-\Delta)-2z_\gamma^*\sin\omega(t-3\Delta)+$$

$$+(z_\gamma^*)^2\left(\sin\omega(t-5\Delta)+i_{ct}(t-5\Delta)\right)\Big]$$

when $x=l,\ t\in[4\Delta,6\Delta]$.

7. $u_5(t)=U_0\sin(\omega t)$,

$$i_5(t)=\frac{U_0}{Z_B}\Big[\sin(\omega t)-2z_\gamma^*\sin\omega(t-2\Delta)+2(z_\gamma^*)^2\sin\omega(t-4\Delta)-$$

$$-(z_\gamma^*)^3\left(\sin\omega(t-6\Delta)+i_{ct}(t-6\Delta)\right)\Big]$$

when $x=0,\ t\in[5\Delta,7\Delta]$.

The cited above formulas can be represented in the general form

$u_{2n-1}(t)=U_0\sin(\omega t)$,

$$i_{2n-1}(t)=\frac{U_0}{Z_B}\left[\sin(\omega t)+2\sum_{j=1}^{n-1}(-z_\gamma^*)^j\sin\omega(t-2j\Delta)+\right.$$

$$\left.+(-z_\gamma^*)^n\left(\sin\omega(t-2n\Delta)+i_{ct}(t-2n\Delta)\right)\right] \qquad (10.8)$$

when $x=0,\ t\in[(2n-1)\Delta,(2n+1)\Delta],\ n=1,2,...,n*$.

$$u_{2n}(t)=\frac{(1+z^*)e^{-\gamma\Delta}}{2}U_0\left[2\sum_{j=0}^{n-1}(-z_\gamma^*)^j\sin\omega(t-(2j+1)\Delta)+\right.$$

$$\left.+(-z_\gamma^*)^n\left(\sin\omega(t-(2n+1)\Delta)+i_{ct}(t-(2n+1)\Delta)\right)\right],$$

$$i_{2n}(t)=\frac{(1-z^*)e^{-\gamma\Delta}}{2}\frac{U_0}{Z_B}\left[2\sum_{j=0}^{n-1}(-z_\gamma^*)^j\sin\omega(t-(2j+1)\Delta)+\right.$$

$$+(-z_\gamma^*)^n\left(\sin\omega(t-(2n+1)\Delta)+i_{cl}(t-(2n+1)\Delta)\right)\Bigg] \qquad (10.9)$$

when $x=l,\ t\in[2n\Delta,2(n+1)\Delta],\ n=0,1,...,(n*-1)$.

If at the time moment $t^*=(2n*+1)\Delta$ the previous load is restored, then the subsequent solution has the form

$$u^*_{2m-1}(t)=U_0\sin(\omega t),$$

$$i^*_{2m-1}(t)=\frac{U_0}{Z_B}\Bigg[\sin(\omega t)+2\sum_{j=1}^{m-1}(-z_\gamma)^j\sin\omega(t-2j\Delta)+$$

$$+(-z_\gamma)^m\left(\sin\omega(t-2m\Delta)+i_{nA}(t-2m\Delta)\right)\Bigg] \qquad (10.10)$$

when $x=0,\ t\in[t^*+(2m-1)\Delta,\ t^*+(2m+1)\Delta],\ m=1,2,...$.

$$u^*_{2m}(t)=\frac{(1+z)e^{-\gamma\Delta}}{2}U_0\Bigg[2\sum_{j=0}^{m-1}(-z_\gamma)^j\sin\omega(t-(2j+1)\Delta)+$$

$$+(-z_\gamma)^m\left(\sin\omega(t-(2m+1)\Delta)+i_{nA}(t-(2m+1)\Delta)\right)\Bigg],$$

$$i^*_{2m}(t)=\frac{(1-z)e^{-\gamma\Delta}}{2}\frac{U_0}{Z_B}\Bigg[2\sum_{j=0}^{m-1}(-z_\gamma)^j\sin\omega(t-(2j+1)\Delta)+$$

$$+(-z_\gamma)^m\left(\sin\omega(t-(2m+1)\Delta)+i_{nA}(t-(2m+1)\Delta)\right)\Bigg] \qquad (10.11)$$

when $x=l,\ t\in[t^*+2m\Delta,\ t^*+2(m+1)\Delta],\ m=0,1,2....$

Here by i_{nA} is denoted the current function at the input of the line $x=0$ during the time interval $t\in[t^*-\Delta,\ t^*+\Delta]$

$$i_{nA}(t)=\begin{cases}\dfrac{Z_B}{U_0}i_{2n^*-1}(t), & t\in[t^*-\Delta,t^*]\\ \dfrac{Z_B}{U_0}i_{2n^*+1}(t), & t\in[t^*,t^*+\Delta]\end{cases}.$$

10.2. Comparison of calculated results and full-scale test for half-wave line 500 kV

Let's consider the three-phase overhead transmission line 500 kV Volgograd – Lipetsk (556 km) – Arzamas (1572 km) – Shagol (2858 km) without intermediate connections with total wave distance 173º [22], that determines the wave-length as $\lambda = 2858 \times 360^\circ / 173^\circ = 5947.28$ km and the speed of electromagnetic disturbance propagation along the as $a = \lambda f = 297364$ km/s with the frequency f =50 H (the oscillation period $\Delta = \lambda / a = 1/f = 20$ ms; the time of the wave run along the line length $\Delta_l = l/a = 9.61$ ms). If we do not take into consideration the interference of the wires in the homogeneous line and set its equivalent wave resistance as $Z_B = 278\ \Omega$ [4], then we obtain following lineal reactive parameters: $L = 0.9348$ mH /km; C =12.10 nF/km; $Ll = 2.67$ H; $Cl = 34.58$ μF; $X_L = 133.5\ \Omega$; $X_C = 578.37\ \Omega$. If $l = \lambda$, then $X_L = X_C = Z_B$. The active resistance and conduction we set as $R = 22.44$ mΩ/km; $G = 41.47$ nS/km, that corresponds to the phase consisted of three wires of the type AC 450/51 [70].

Starting from these values of the initial parameters we determine the complex wave resistance $Z_0 = 278.25 - j9.0927\ \Omega$. It is easy to certain that under the character for high-current lines lineal parameters ($CR > LG$) the angle of the complex number Z_0 always gets the negative value, that implies the capacitive nature of the wave resistance.

In the line loaded on the resistance Z_0 (that usually is used as a matched load) the return (reflected) waves are missing when the whole energy is propagated in it by the direct wave [4]. However, it does not follow from this that just in the case of the steady state process of travelling waves the minimal losses are realized [89]. For example, in the homogeneous line with the length $l = 0.15\lambda$ the efficiency is 92.10% under the action on the matched load $Z_S = Z_0 = 278.25 - j9.0927\ \Omega$., whereas under the unmatched load of the capacitive nature $Z_S = 278 + j278\ \Omega$ we obtain the efficiency equal to 93.73%, but for all that the active power of 40% from natural is transferred in it.

We assume that the amplitude of the phase voltage is equal $U_0 = 525\sqrt{2/3} = 428.66$ kV and the natural power of the sinusoidal voltage line $u = U_0 \sin(2\pi f t)$ possesses the value $P_н = U_0^2/(2Z_B) = 330.5$ MW. Thus during the travelling waves regime at the sending end of the three-phase line 500 kV it is generated about 1 GW of the power. If we now will use the formulas (1.4), then in the dimensionless form we'll obtain $U_0 = f = L = C = Z_B = \lambda = a = \Delta = 2P_н = 1$; $Z_0 = 1.0009 - j0.0327$; $l = 173°/360° = R = 7G = \Delta_l = Cl = Ll = 0.4805$.

Let's consider at first the steady state processes of the power transfer and realize the comparative analysis of the calculated and experimental data. In fig. 10.2 it is shown the dependence of the losses on the line length when transferring the natural power $П = 1 - P_1/P_0$, where P_0, P_1 are the generated and transmission powers (curves 1;2), as well as during the idling $П_{xx} = P_0/P_н$ (curve 3). The losses in the loaded half-wave line with the parameters $R = 7G = 0.48$ come to 23%, that practically coincides with the full-scale test results represented in [22]. Let's remind that in the experiment from 1967 the losses of the active power come to 225 kW (the part of them being the crown losses) when at the sending end (hydroelectric power station) it was 985 kW. The case with R =0.74, G = 0 (*b*) corresponds to $R = 34$ mΩ/km. With these values of the lineal active resistance of the three wires AC 300/66 (that are used also in the lines of the type 500 kV), the losses exceed 30%, that contradict with experimental data [22].

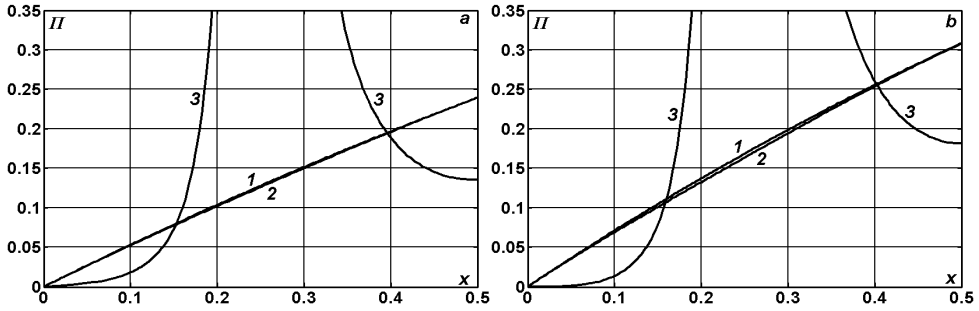

Fig. 10.2. Line length x dependence of the power losses when transferring the natural power $П = 1 - P_1/P_0$ (curves1;2) and when idling $П_{xx} = P_0/P_н$ (curve 3) for $R = 7G = 0.48$(***a***); R =0.74, G = 0(***b***).

Comparing the curves 1 and 3 we can conclude that the losses under the pure active load $Z_S = Z_B$ =1 are nevertheless lower than in the case of the

line with matched load equal to complex wave resistance: $Z_S = Z_0$. However these distinctions are sufficiently small for every line length and they can be neglected. As we see the relative losses under the natural power transfer (or the power closed to natural) almost linear depend on the line length and the value of these losses is sufficiently sensible to the variations of the parameter R. It is appropriate to mention here that the idling losses for half-wave line without supplementary connections come to 13.66%, i.e. the half from the losses under the natural power transfer.

Now we will mention another source where the design losses come to 13% under the natural power transfer in the projected half-wave line 750 kV Surgut – Chornobyl [46]. It is easy to determine that in this case for the line without supplementary connections the inequality $R \leq 12$ mΩ/km must be hold at the minimum. If we will take in consideration the inevitable crown losses (0.5…1% on every 1000 km of the power transmission line) then the parameter R can not exceed 9…11 mΩ/km. The idling losses in this case can be only 6 %. The decrease of active power losses in the wires due to the increase of their wave resistance ($Z_B = 278$ Ω) is inadmissible, as it will involve inevitably the decrease of the natural power value.

The connection to the half-wave line of 3…4 shunt reactors makes it possible to decrease the idling losses, if the location and parameters of the reactors are selected in the optimal manner. As regards the possibility of the losses decrease under the natural power transfer, to obtain the same impressive effect seems hardly possibly. The losses can be decreased no more then on 2…3% in this case, but the question remains for another investigation.

The distribution along the line of the active (*a*) and reactive (*b*) powers is represented in fig. 10.3 under the natural power regime (curves 1;2) and prior to natural power regime (curves 3-5). The curve 6 corresponds to the idling in the line, when the load is disconnected. The load resistance Z_S is selected here in such a way that at the end of the line (Shagol) to have 760, 506, 430, 260 MW as in the experiment [22].

The decreasing of the load resistance Z_S results in the gradual rise of the active power (right up to the regime of natural power transfer) and in reduction of the reactive power that is maximal under the standing wave regime (idling). The minimal values of the reactive power at the generator connection point can be observed when $Z_S = Z_B$. In this case the power factor of the pure active load is equal to 1 (by definition) and it is closed to 1 near the source. This means that the bilateral interchange of the electromagnetic energy between the generator and the receiver is missing practically. Under the matched load $Z_S = Z_0$ the distribution of the reactive power along the line is of linear character and constitutes $Q_0 = -32.30$ MVA at the sending

end and $Q_1 = -24.85$ MVA at the receiving end. Whereas when $Z_S = Z_B$ we have correspondingly $Q_0 = -8.60$ MVA and $Q_1 = 0$.

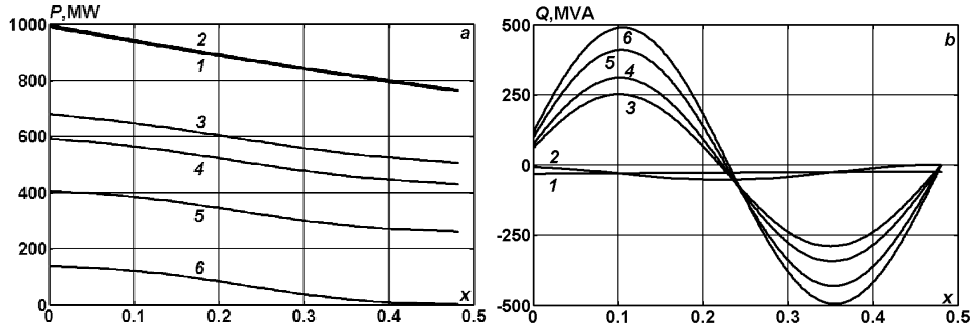

Fig. 10.3. Distribution along the line of the active (*a*) and reactive (*b*) powers when $R = 7G = 0.48$ and the load resistance variations $Z_S = Z_0$ (curve 1); Z_B (curve 2); $1.676Z_B$ (curve 3); $2.025Z_B$ (curve 4); $3.535Z_B$ (curve 5); ∞ (curve 6).

The diagrams of voltage modulus (*a*) and current modulus (*b*) are represented in fig. 10.4 when $R = 7G = 0.48$ and the load resistance variations $Z_S = Z_0$ (curve 1); Z_B (curve 2); $1.676\,Z_B$ (curve 3); $2.025\,Z_B$ (curve 4); $3.535\,Z_B$ (curve 5); ∞ (curve 6).The voltage (current) losses under the natural power transfer come to 12%, that fill in the experimental data [22].

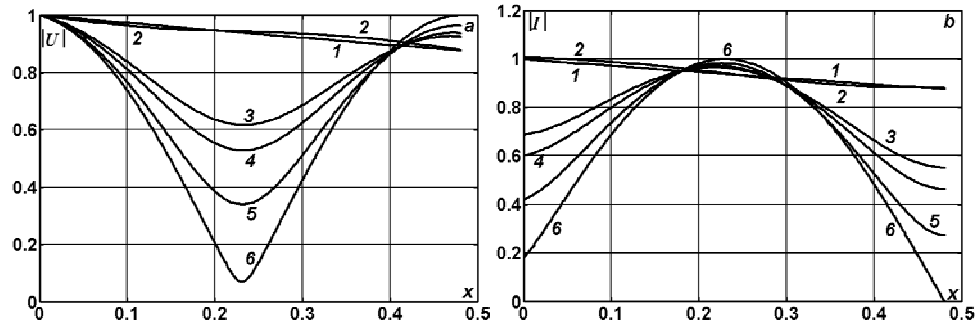

Fig. 10.4. Distribution along the line of the voltage modulus (***a***) and current modulus (***b***) when $R = 7G = 0.48$ and the load resistance variations $Z_S = Z_0$ (curve 1); Z_B (curve 2); $1.676Z_B$ (curve 3); $2.025Z_B$ (curve 4); $3.535Z_B$ (curve 5); ∞ (curve 6).

Under the steady state regime the maximal in absolute value voltages and currents (in dependence on wave distance) appear or in idling or in short-circuit of the receiving end (fig. 10.5). The minimal values of the volt-

ages and currents in the transmission line appear under the matched load in the line (curves 1;2).

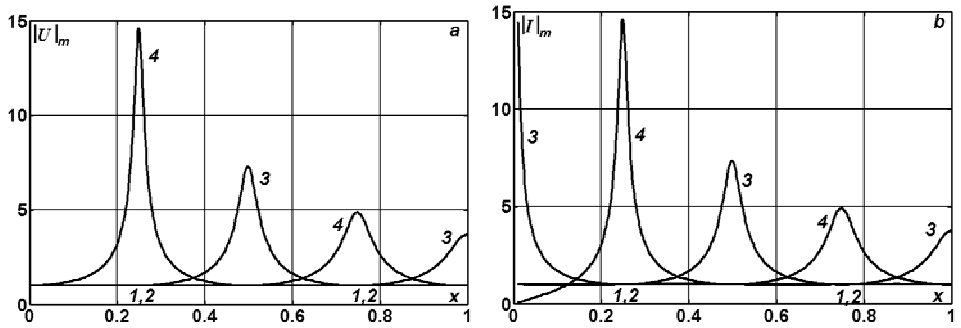

Fig. 10.5. The maximal in absolute values of voltage (***a***) and current (***b***) dependence on the line length x when $R = 7G = 0.48$ and the load resistance variations $Z_S = Z_0$; (curve 1); Z_B (curve 2); 0 (curve 3); ∞ (curve 4).

In the table 10.1 besides the maximal voltages $|U|_{\mathrm{m}}$, that can be observed in the line when $x = x_{\mathrm{m}}$, the phase displacements δ between voltages at the end points are represented, as well as the power factors of the source ($\cos\varphi_0$) and the critical values of the pure active load Z_S, that ensure the maximum of the transmission power and efficiency. The mentioned parameters of the steady state process quite essentially depend on the length l and resistance Z_S. It is sufficient to pay attention to the fact that the angle δ for half-wave line ($l = \lambda/2$) varies from $+0.9995\pi$ when $Z_S = Z_0 = 1.0009 - j0.0327$ till -0.9993π when $Z_S = Z_B = 1$. The maximal overvoltage values for the line with the length that is closed to half-wave consist from 5.2 till 7.3 of nominal values. Also we can not ignore the differences in the second-third significant digit of the transmission power and efficiency values in the lines with the length that slightly or strongly differs from half-wave. In many cases the regime with maximal transmission (generated) power or maximal efficiency can not be realized in practice. It seems to have only some theoretical importance, but it is not exactly so. Anyway the information about the extreme regimes enlarges essentially the traditional ideas about the electromagnetic power transfer along the long lines and proves to be useful for analyzing of the emergency and postemergency states, caused by instantaneous changes of the load parameters.

Table 10.1. The influence of the line length l and load resistance Z_S on the electricity transmission parameters under the steady state regime when $R = 7G = 0.48$.

l	Z_S	P_0	P_1	η	$\lvert I_0 \rvert$	cosφ$_0$	$\lvert U_1 \rvert$	δ	$\lvert U \rvert_m$	x_m
556 km 0.0935λ	∞	0.0076	0.0000	0.0000	0.6658	0.0228	1.2011	-0.0054π	1.2011	0.0935
	0	0.0659	-0.0000	-0.0000	1.4977	0.0881	0.0000	-0.9876π	1.0000	0.0000
	Z_0	0.4990	0.4741	0.9500	0.9986	0.9995	0.9747	-0.1871π	1.0000	0.0000
	1	0.4853	0.4614	0.9506	0.9709	0.9998	0.9606	-0.1840π	1.0000	0.0000
	0.6677	0.5306	0.4964	0.9357	1.1204	0.9471	0.8142	-0.2414π	1.0000	0.0000
	1.9662	0.3253	0.3122	0.9596	0.7814	0.8328	1.1080	-0.1064π	1.1091	0.0850
743.5 km λ/8	∞	0.0179	0.0000	0.0000	0.9994	0.0358	1.4131	-0.0109π	1.4131	0.1250
	0	0.0504	0.0000	0.0000	0.9977	0.1010	0.0000	-0.5000π	1.0000	0.0000
	Z_0	0.4990	0.4660	0.9338	0.9986	0.9995	0.9663	-0.2501π	1.0000	0.0000
	1	0.4840	0.4524	0.9347	0.9686	0.9995	0.9512	-0.2451π	1.0000	0.0000
	1.0023	0.4840	0.4524	0.9348	0.9686	0.9994	0.9523	-0.2448π	1.0000	0.0000
	1.6817	0.4272	0.4024	0.9420	0.9723	0.8786	1.1633	-0.1732π	1.1652	0.1140

l	Z_S	P_0	P_1	η	$\lvert I_0\rvert$	cosφ$_0$	$\lvert U_1\rvert$	δ	$\lvert U\rvert_m$	x_m
	∞	**7.2945**	**0.0000**	**0.0000**	**14.5921**	**0.9998**	**14.5786**	**-0.5039π**	**14.5786**	**0.2500**
	0	0.0341	-0.0000	-0.0000	0.0683	0.9990	0.0000	1.0000π	1.0000	0.0000
1487 km	Z_0	0.4990	0.4351	0.8719	0.9986	0.9995	0.9338	-0.5003π	1.0000	0.0000
λ/4	1	0.4978	0.4348	0.8736	0.9974	0.9981	0.9326	-0.4905π	1.0000	0.0000
	14.6337	3.6627	1.8164	0.4959	7.3320	0.9991	7.2911	-0.4968π	7.2912	0.2490
	1.0010	0.4982	0.4352	0.8736	0.9983	0.9981	0.9335	-0.4905π	1.0000	0.0000
	∞	**2.8030**	**0.0000**	**0.0000**	**8.5913**	**0.6525**	**8.6163**	**-0.7862π**	**8.6163**	**0.2643**
	0	0.0349	-0.0000	-0.0000	0.1161	0.6016	0.0000	1.0000π	1.0038	0.0140
1572 km	Z_0	0.4990	0.4317	0.8651	0.9986	0.9995	0.9301	-0.5289π	1.0000	0.0000
0.2643λ	1	0.5003	0.4336	0.8668	1.0025	0.9982	0.9313	-0.5192π	1.0000	0.0000
	8.6159	2.2422	1.3450	0.5999	4.8428	0.9260	4.8142	-0.6390π	4.8144	0.2628
	0.9616	0.4837	0.4193	0.8668	0.9696	0.9978	0.8980	-0.5182π	1.0000	0.0000
	∞	0.1169	0.0000	0.0000	0.9961	0.2346	1.3977	-0.9676π	1.3977	0.3750
	0	0.0854	0.0000	0.0000	1.0010	0.1707	0.0000	-0.5000π	1.4045	0.1245
2230.5 km	Z_0	0.4990	0.4063	0.8142	0.9986	0.9995	0.9023	-0.7504π	1.0000	0.0000
3λ/8	1	0.5125	0.4176	0.8150	1.0255	0.9994	0.9139	-0.7450π	1.0000	0.0000
	0.9990	0.5124	0.4176	0.8150	1.0255	0.9994	0.9135	-0.7449π	1.0000	0.0000
	0.8541	0.5061	0.4133	0.8167	1.0255	0.9869	0.8402	-0.7240π	1.0454	0.1160

l	Z_S	P_0	P_1	η	$\lvert I_0\rvert$	$\cos\varphi_0$	$\lvert U_1\rvert$	δ	$\lvert U\rvert_m$	x_m
2858 km 0.4805λ	∞	0.0683	0.0000	0.0000	0.1784	0.7653	0.9986	-0.9949π	1.0000	0.0000
	0	**2.0170**	**0.0000**	**0.0000**	**5.5904**	**0.7216**	**0.0000**	**0.8712π**	**5.6034**	**0.2300**
	***Z*₀**	**0.4990**	**0.3834**	**0.7684**	**0.9986**	**0.9995**	**0.8766**	**-0.9615π**	**1.0000**	**0.0000**
	1	**0.5028**	**0.3864**	**0.7685**	**1.0057**	**1.0000**	**0.8791**	**-0.9602π**	**1.0000**	**0.0000**
	0.1789	1.4433	0.8094	0.5608	3.0869	0.9351	0.5381	-0.8732π	3.0566	0.2300
	0.9724	0.5134	0.3946	0.7686	1.0269	0.9999	0.8760	-0.9593π	1.0000	0.0000
2974 km λ/2	∞	0.0679	0.0000	0.0000	0.1360	0.9990	0.9907	0.9999π	1.0000	0.0000
	0	3.6643	-0.0000	-0.0000	7.3302	0.9998	0.0000	0.5000π	7.2893	0.2495
	***Z*₀**	**0.4990**	**0.3794**	**0.7602**	**0.9986**	**0.9995**	**0.8719**	**0.9995π**	**1.0000**	**0.0000**
	1	**0.4998**	**0.3800**	**0.7603**	**0.9996**	**1.0000**	**0.8718**	**-0.9993π**	**1.0000**	**0.0000**
	0.1364	1.8665	0.8994	0.4818	3.7332	0.9999	0.4954	-0.9968π	3.6788	0.2495
	1.0018	0.4991	0.3795	0.7603	0.9982	1.0000	0.8720	-0.9993π	1.0000	0.0000
3093 km 0.5200λ	∞	0.0697	0.0000	0.0000	0.1906	0.7317	0.9979	0.9942π	1.0072	0.0195
	0	2.0259	0.0000	0.0000	5.2305	0.7747	0.0000	0.2862π	5.2390	0.2695
	Z_0	0.4990	0.3752	0.7519	0.9986	0.9995	0.8671	0.9594π	1.0000	0.0000
	1	0.4967	0.3736	0.7521	0.9934	1.0000	0.8643	0.9608π	1.0000	0.0000
	0.1912	1.3541	0.7337	0.5418	2.8512	0.9498	0.5297	0.8853π	2.8172	0.2695
	1.0304	0.4860	0.3655	0.7521	0.9720	0.9999	0.8679	0.9617π	1.0000	0.0000

The series of emergency regimes in the loaded half-wave line executed in [22] showed the comparative high stability of the line with respect to dynamical changes. The internal overvoltages at the diverse substations do not exceed the predicted insulation level of the overhead lines 500 kV. The maximal registered overvoltage factor under the transient process with short circuit duration 130…190 ms comes to 1.75…1.95. Let's check the correspondence of these experimental data with the theoretical calculations based on the exact solutions of the corresponding boundary-value problems for telegraph equations in the dynamical formulation.

Let's model at first the sudden change-over of the receiving end of the half-wave line from idling to short circuit with duration $\Delta t = 6.5$ (130 ms). The calculation results are shown in the fig. 10.6 as a time dependences of voltage (*a*) and power (*b*) at the sending and receiving ends of the line. The curves 2 and 3 correspond to the voltages at the substations Lipetsk and Arzamas. As it easy to observe from diagrams, the overvoltages at the substation Arzamas (see curve 3) during the short-circuited (with duration only130 ms) stage practically reach the multiplicity 5.6 that is characteristically for the steady state regime under the assumption that the short circuit is of infinite duration. After transferring to the idling regime the sixfold overvoltages appear at the switchpoint (Shagol substation). But these overvoltages attenuate quickly (curve 4).

The maximal overvoltage multiplicity at the Arzamas substation under the short circuit in the loaded transmission line ($R_S = 1$) remains the same as in the unloaded line (fig. 10.7). The maximal voltages in the loaded line at the postemergency stage with duration around the 20 ms (the time equal to double wave runs along the line length) reach value 4 and the transmission power hits form two pronounced peaks with the amplitude 9. The situation with the overvoltages at the middle of the half-wave line remains approximate the same if the power take-of will increase or will decrease by changing the load resistance R_S. The variation of the length and of the lineal parameters of the line in the limits of 10…20% leads to the overvoltage multiplicity not less then 5 under the short-circuited regime. The interference between the wires in the three-phase transmission system can be considered among the second order effects, because it does not influence practically upon the overvoltage multiplicity in the faulty phase under the steady state and under the transient processes as well. The studies on this question lie ahead.

If the short circuit point will be replaced at Arzamas substation (fig. 10.8), then the maximal overvoltages will arise at Lipetsk substation and

they will be equal only to 1.6, that coincides with experimental data [22]. Here we must to mention that this maximal value occurs at the beginning of the nonstationary process and it is greater then steady-state value (the last one is equal to 1). In this case the voltage and power jumps at the point of load connection are not to be observed and the process of power transmission practically returns to the original state in 20 ms after short circuit elimination.

Let's suppose now that at the same place the short-term break with duration $\Delta t = 3$ (60 ms) has happened. From the fig. 10.9 we see that the maximal overvoltage values, as well as the power hits, appear at the point of loading. The aftereffect of the emergency event is felt only during the 20 ms time interval, after that the system "forgets" the event. Thus, the break in the middle of the half-wave line can have more grave consequences then the short circuit at its end.

Concerning so quick system restoring let's mention the following. From the formulas for current and voltage (10.10) – (10.11) one can see that the influence on the active solution for the current i_{nA} during the short circuit action decreases in time, because it is multiplied by the factor $\left(z_\gamma\right)^m = \left(ze^{-2\gamma\Delta}\right)^m$. In this concrete case the influence vanishes very fast, because $R_S = 1$ or $z = 0$. For undistorting line when $z = 0$ the solution restores after 19.22 ms (the time equal to double wave runs along the line length) as if it wasn't prehistory. This is possible because in this case the regime of wave propagation without reflection is realized. In case of the line with arbitrary losses the solution also "forgets" the emergency state but not so quickly as in previous case.

Thus, the electric power transmission by long lines has some particular features including the emergency regimes. The proposed approach gives the possibility to model the real emergency situations and to determine the steady and impulsive values of voltages and currents at the most weak points of the electrical circuit.

Thus, it is presented the strategy of calculation for transient processes caused by instantaneous changes of the resistance load at the receiving end of the half-wave transmission line. The comparison of the calculating data and full-scale experiment data for half-wave line 500 kV discovers their satisfactory coordination with the experimental data for steady state regime. The calculating overvoltage multiplicity under the short circuit at the point of load connection with duration 130 ms and under the circuit break at the middle of the half-wave line with duration 60 ms comes to 6 nominal values, that is contrary to the full-scale experiment results [22].

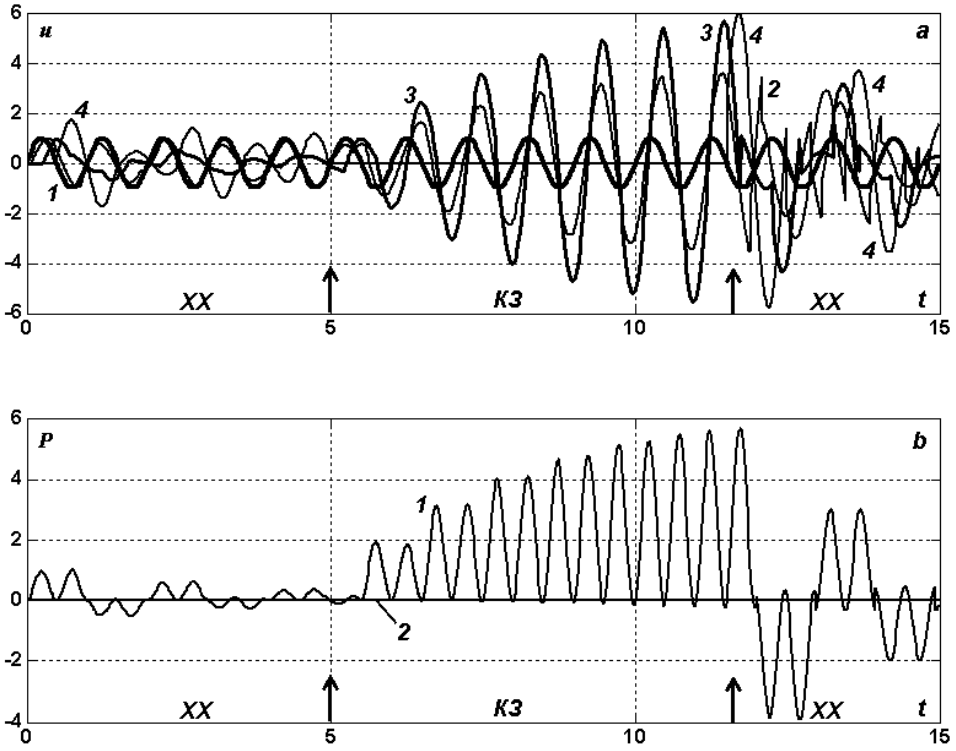

Fig. 10.6. Voltages (***a***) and powers (***b***) in the unloaded transmission line ($R_S = \infty$) under the short circuit with duration Δt = 6.5 (130 ms) at the receiving end l = 0.4805 (2858 km).

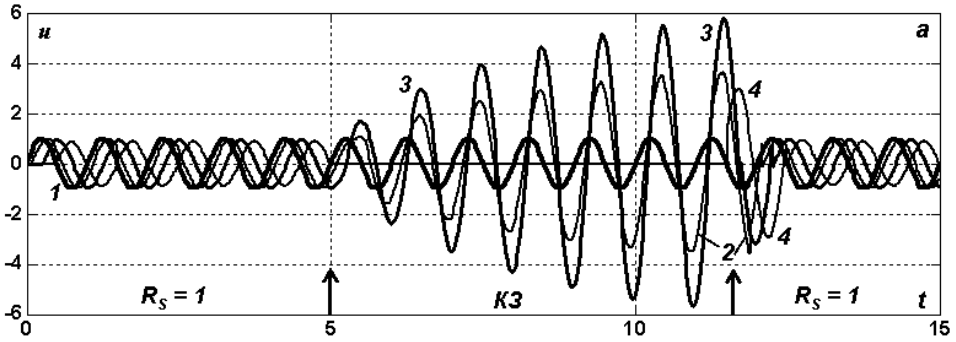

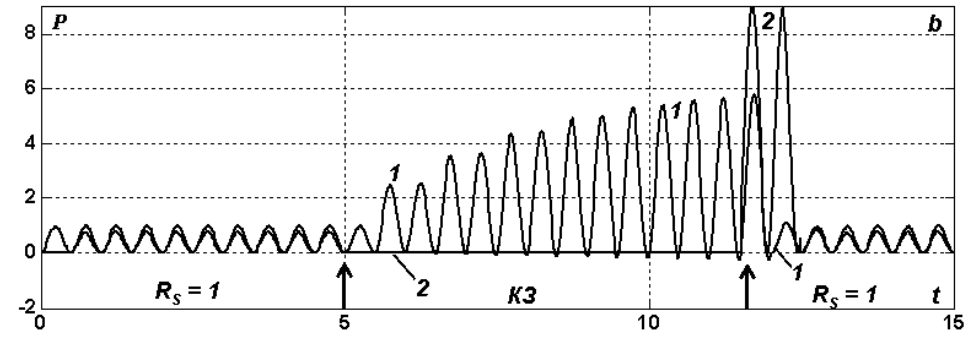

Fig. 10.7. Voltages (***a***) and powers (***b***) in the loaded transmission line (R_S = 1) under the short circuit with duration 6.5 (130 ms) at the point of load connection l = 0.4805 (2858 km).

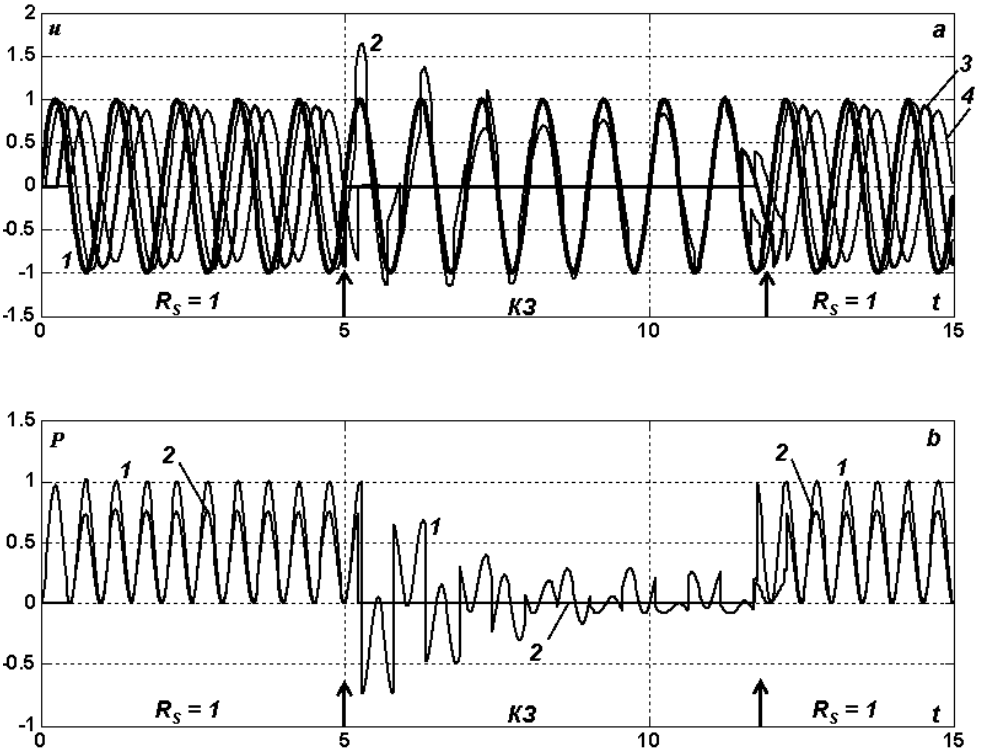

Fig. 10.8. Voltages (***a***) and powers (***b***) in the loaded transmission line (R_S = 1) under the short circuit with duration 7 (140 ms) at the point x = 0.2643 (1572 km).

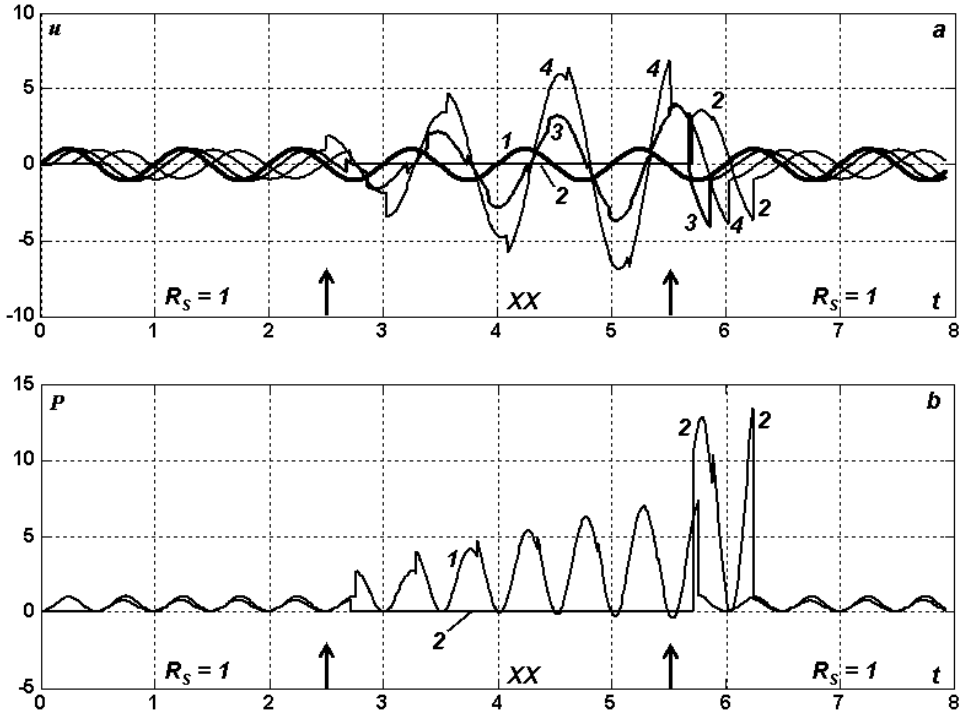

Fig. 10.9. Voltages (***a***) and powers (***b***) in the loaded transmission line (R_S = 1) under its break (idling) with duration (60 ms) at the point x = 0.2643 (1572 km).

CHAPTER II

TRANSMISSION POWER AND EFFICIENCY INCREASE BY MEANS OF "BUCKING OUT" SYSTEMS

11. Maximal steady-state voltages and currents in homogeneous alternating current transmission line

Let's consider the problem of determination of the maximal by R_s steady-state values of voltages and currents in the long line with the generator at the left-hand end and with the active load R_s at the right-hand end. The currents and voltages satisfy the telegraph equations

$$L\frac{\partial i}{\partial t}+\frac{\partial u}{\partial x}+Ri=0;\ C\frac{\partial u}{\partial t}+\frac{\partial i}{\partial x}+Gu=0. \qquad (11.1)$$

At the ends of the line we have the following boundary conditions:

$$u(0,t)=U_0\exp(j\omega t);\ u(l,t)=R_s i(l,t). \qquad (11.2)$$

For the steady-state regime the solution for current $I(x)$ and voltage $U(x)$ complexes can be obtained by complex amplitude method (CAM)

$$I(x)=\frac{U_0}{Z_0}\cdot\frac{R_s\mathrm{sh}\delta(l-x)+Z_0\mathrm{ch}\delta(l-x)}{R_s\mathrm{ch}\delta l+Z_0\mathrm{sh}\delta l};$$

$$U(x)=U_0\frac{R_s\mathrm{ch}\delta(l-x)+Z_0\mathrm{sh}\delta(l-x)}{R_s\mathrm{ch}\delta l+Z_0\mathrm{sh}\delta l}. \qquad (11.3)$$

Here Z_0 is the complex wave (characteristic) resistance; δ is propagation coefficient; $\delta=\alpha+j\beta$; α, β are the attenuation and phase constants.

The square of the modulus of the current complex can be determined from the relation

$$|I(x)|^2 = I(x)I^*(x) = \frac{U_0^2}{|Z_0|^2}\left|\frac{\mathrm{sh}\delta(l-x)}{\mathrm{ch}\delta l}\right|^2 \cdot \left\{R_s^2 + 2R_s\,\mathrm{Re}\left[Z_0\,\mathrm{cth}\delta(l-x)\right]+\right.$$

$$\left.+\left|Z_0\,\mathrm{cth}\delta(l-x)\right|^2\right\} \cdot \left\{R_s^2 + 2R_s\,\mathrm{Re}\left[Z_0\,\mathrm{th}(\delta l)\right]+\left|Z_0\,\mathrm{th}\delta l\right|^2\right\}^{-1}. \quad (11.4)$$

The maximal values of $|I(x)|^2$ by R_s can be determined by the examination of the derivative $d|I(x)|^2 / dR_s$. The derivative sign is determined by the values of the following quadratic trinomial:

$$\frac{d|I(x)|^2}{dR_s} = K\left\{R_s^2\left(\mathrm{Re}\left[Z_0\,\mathrm{th}(\delta l)\right]-\mathrm{Re}\left[Z_0\,\mathrm{cth}(\delta(l-x))\right]\right)+\right.$$

$$+R_s\left(\left|Z_0\,\mathrm{th}(\delta l)\right|^2-\left|Z_0\,\mathrm{cth}(\delta(l-x))\right|^2\right)+$$

$$\left.+\left|Z_0\,\mathrm{th}(\delta l)\right|^2\mathrm{Re}\left[Z_0\,\mathrm{cth}(\delta(l-x))\right]-\left|Z_0\,\mathrm{cth}(\delta(l-x))\right|^2\mathrm{Re}\left[Z_0\,\mathrm{th}(\delta l)\right]\right\} =$$

$$= K\left\{aR_s^2 + bR_s + c\right\}; \quad (11.5)$$

$$a = \mathrm{Re}\left[Z_0\,\mathrm{th}(\delta l)\right]-\mathrm{Re}\left[Z_0\,\mathrm{cth}(\delta(l-x))\right];\ b = \left|Z_0\,\mathrm{th}(\delta l)\right|^2-\left|Z_0\,\mathrm{cth}(\delta(l-x))\right|^2;$$

$$c = \left|Z_0\,\mathrm{th}(\delta l)\right|^2\mathrm{Re}\left[Z_0\,\mathrm{cth}(\delta(l-x))\right]-\left|Z_0\,\mathrm{cth}(\delta(l-x))\right|^2\mathrm{Re}\left[Z_0\,\mathrm{th}(\delta l)\right];$$

$$K = \frac{2U_0^2}{|Z_0|^2}\left|\frac{\mathrm{sh}\delta(l-x)}{\mathrm{ch}\delta l}\right|^2 \cdot \left\{R_s^2 + 2R_s\,\mathrm{Re}\left[Z_0\,\mathrm{th}(\delta l)\right]+\left|Z_0\,\mathrm{th}\delta l\right|^2\right\}^{-2} > 0.$$

Let's note that the following inequalities are equivalent

$$a < 0 \Leftrightarrow \frac{\mathrm{Re}\left[Z_0\,\mathrm{th}(\delta l)\right]}{\mathrm{Re}\left[Z_0\,\mathrm{cth}(\delta(l-x))\right]} < 1;\ b < 0 \Leftrightarrow \frac{\left|\mathrm{th}(\delta l)\right|^2}{\left|\mathrm{cth}(\delta(l-x))\right|^2} < 1;$$

$$c < 0 \Leftrightarrow \frac{\left|\text{th}(\delta l)\right|^2}{\left|\text{cth}(\delta(l-x))\right|^2} < \frac{\text{Re}\left[Z_0 \text{th}(\delta l)\right]}{\text{Re}\left[Z_0 \text{cth}(\delta(l-x))\right]}. \qquad (11.6)$$

We consider at first the case of ideal line: $R = G = 0$; $\delta = j\omega/a$; $a = 1/\sqrt{LC}$; $Z_0 = Z_B = \sqrt{L/C}$. Then in equation (11.5) the following expressions become equal to zero:

$$\text{Re}\left[Z_0 \text{th}(\delta l)\right] = Z_B \,\text{Re}\left[j\text{tg}(\omega\Delta)\right] = 0;$$

$$\text{Re}\left[Z_0 \text{cth}(\delta(l-x))\right] = Z_B \,\text{Re}\left[j\text{ctg}(\omega(\Delta - \Delta_x))\right] = 0 \Rightarrow a = c = 0$$

and the derivative $d\left|I(x)\right|^2 / dR_s$ takes the form of linear function with respect to load resistance R_s

$$\frac{d\left|I(x)\right|^2}{dR_s} = KR_s Z_B \left(\left|\text{tg}(\omega\Delta)\right|^2 - \left|\text{ctg}(\omega(\Delta - \Delta_x))\right|^2\right).$$

Here we denote by Δ, Δ_x the time of electromagnetic wave run along the line length l and along the interval $[0, x]$ correspondingly.

As $R_s \in [0, \infty)$ and the derivative is a linear function yields $\left|I(x)\right|^2$ is monotone function and the maximal values of the current modulus for ideal line are reached at the extremities of the interval $[0, \infty)$, i.e. when $R_s = 0$ (i.e. short circuit is realized) or when $R_s = \infty$ (i.e. in case of idling in the line).

Let's consider now the case of undistorting line: $R/L = G/C = \gamma$; $\delta = (\gamma + j\omega)/a$; $a = 1/\sqrt{LC}$; $Z_0 = Z_B = \sqrt{L/C}$. Then

$$\text{Re}\left[Z_0 \text{th}(\delta l)\right] = Z_B \frac{\text{sh}(2\gamma\Delta)}{\text{ch}(2\gamma\Delta) + \cos(2\omega\Delta)};$$

$$\left|Z_0 \text{th}(\delta l)\right|^2 = Z_B^2 \frac{\text{ch}(2\gamma\Delta) - \cos(2\omega\Delta)}{\text{ch}(2\gamma\Delta) + \cos(2\omega\Delta)};$$

$$\mathrm{Re}\left[Z_0\mathrm{cth}(\delta(l-x))\right]=Z_B\,\frac{\mathrm{sh}(2\gamma(\Delta-\Delta_x))}{\mathrm{ch}(2\gamma(\Delta-\Delta_x))-\cos(2\omega(\Delta-\Delta_x))};$$

$$\left|Z_0\mathrm{cth}(\delta(l-x))\right|^2=Z_B^2\,\frac{\mathrm{ch}(2\gamma(\Delta-\Delta_x))+\cos(2\omega(\Delta-\Delta_x))}{\mathrm{ch}(2\gamma(\Delta-\Delta_x))-\cos(2\omega(\Delta-\Delta_x))}$$

and the formula (11.5) can be represented in the form

$$\frac{d\left|I(x)\right|^2}{dR_s}=K_1\left\{\widetilde{a}Z_BR_S^2+\widetilde{b}Z_B^2R_S+\widetilde{c}Z_B^3\right\};\qquad(11.7)$$

$$K_1=K\left[\mathrm{ch}(2\gamma\Delta)+\cos(2\omega\Delta)\right]^{-1}\left[\mathrm{ch}(2\gamma(\Delta-\Delta_x))-\cos(2\omega(\Delta-\Delta_x))\right]^{-1}>0;$$

$$\widetilde{a}=\mathrm{sh}(2\gamma\Delta_x)-\mathrm{sh}(2\gamma(\Delta-\Delta_x))\cos(2\omega\Delta)-\mathrm{sh}(2\gamma\Delta)\cos(2\omega(\Delta-\Delta_x));$$

$$\widetilde{b}=-2\left[\mathrm{ch}(2\gamma(\Delta-\Delta_x))\cos(2\omega\Delta)+\mathrm{ch}(2\gamma\Delta)\cos(2\omega(\Delta-\Delta_x))\right];$$

$$\widetilde{c}=-\mathrm{sh}(2\gamma\Delta_x)-\mathrm{sh}(2\gamma(\Delta-\Delta_x))\cos(2\omega\Delta)-\mathrm{sh}(2\gamma\Delta)\cos(2\omega(\Delta-\Delta_x)).$$

Let's note that the signs of the coefficients a and $\widetilde{a}$, b and $\widetilde{b}$, c and $\widetilde{c}$ coincide. Now we will prove that the quadratic trinomial in (11.7) at the interval $R_s\in[0,\infty)$ can possess only positive or only negative values, or it has only one positive root in case when $\widetilde{a}>0$.

First of all, if the discriminant $\widetilde{d}=\widetilde{b}^2-4\widetilde{a}\widetilde{c}<0$, then the expression (11.7) possesses only positive or only negative values in dependence on the sign of $\widetilde{a}$. If the discriminant is non-negative, then the equation $\widetilde{a}Z_BR_S^2+\widetilde{b}Z_B^2R_S+\widetilde{c}Z_B^3=0$ has real roots. Let's consider the case $\widetilde{a}<0$ and $a<0$. Then from (11.6) we have $\dfrac{\mathrm{Re}\left[Z_0\mathrm{th}(\delta l)\right]}{\mathrm{Re}\left[Z_0\mathrm{cth}(\delta(l-x))\right]}<1$. As $\widetilde{c}=\widetilde{a}-2\mathrm{sh}(2\gamma\Delta_x)$, then $\widetilde{c}<0$ and $c<0$. So from (11.6) we obtain

$$\frac{\left|\mathrm{th}(\delta l)\right|^2}{\left|\mathrm{cth}(\delta(l-x))\right|^2}<\frac{\mathrm{Re}\left[Z_0\mathrm{th}(\delta l)\right]}{\mathrm{Re}\left[Z_0\mathrm{cth}(\delta(l-x))\right]}.$$

Combining these two inequalities, we have $\dfrac{\left|\text{th}(\delta l)\right|^2}{\left|\text{cth}(\delta(l-x))\right|^2} < 1$, and so $\widetilde{b} < 0$ and $b < 0$. Thus if the coefficient *a* is negative, then *b* and *c* are negative too and the both roots of the quadratic equation are negative.

Further, let $\widetilde{c} > 0$. The from $\widetilde{a} = \widetilde{c} + 2\text{sh}(2\gamma\Delta_x)$ we obtain that $\widetilde{a} > 0$. From (11.6) it follows

$$\frac{\text{Re}\left[Z_0\,\text{th}(\delta l)\right]}{\text{Re}\left[Z_0\,\text{cth}(\delta(l-x))\right]} > 1;\ \frac{\left|\text{th}(\delta l)\right|^2}{\left|\text{cth}(\delta(l-x))\right|^2} > \frac{\text{Re}\left[Z_0\,\text{th}(\delta l)\right]}{\text{Re}\left[Z_0\,\text{cth}(\delta(l-x))\right]}.$$

Then $\dfrac{\left|\text{th}(\delta l)\right|^2}{\left|\text{cth}(\delta(l-x))\right|^2} > 1$ and correspondingly $b > 0$ and $\widetilde{b} > 0$. Thus we obtain that if the coefficient *c* is positive, then *a* and *b* are positive too and the both roots of the quadratic equation are also negative. It remains to consider the case when $\widetilde{a} > 0$ and $\widetilde{c} < 0$. In this case independent on the sign of the coefficient $\widetilde{b}$ the quadratic equation has one positive and one negative root.

Hence, we have demonstrated that the quadratic trinomial in formula (11.7) at the interval $R_s \in [0,\infty)$ can possess only positive or only negative values, or it has only one positive root in case when $\widetilde{a} > 0$. In these cases the modulus $\left|I(x)\right|^2$ is either monotone function by R_s, or nonmonotonic but concave function for any values of *x* and *l* at the interval $R_s \in [0,\infty)$. This implies that the maximal values of the current modulus for undistorting line are reached at the extremities of the interval $[0,\infty)$, i.e. when $R_s = 0$, (i.e. short circuit is realized) or when $R_s = \infty$ (i.e. in case of idling in the line).

In case of line with arbitrary losses $(R/L \neq G/C)$ the behavior of the modulus $\left|I(x)\right|^2$ as a function of R_s is more complicated, i.e. there are local maximums for $0 < R_s < \infty$. This is why it is impossible to prove mathematically rigorous the affirmation obtained above for ideal and undistorting lines. However, the affirmation remains correct in this case too. This fact is justified by contl curves that are represented in the fig. 11.1, when *R* = 0.48,

$G = R/7$. We use here the dimensionless load parameter $z = \dfrac{R_s - Z_B}{R_s + Z_B}$, that possesses the value z = -1 under the short circuit and the value z = 1 under the idling. As it is seen from the figure the maximal values are reached for different line lengths l when $z = \pm 1$.

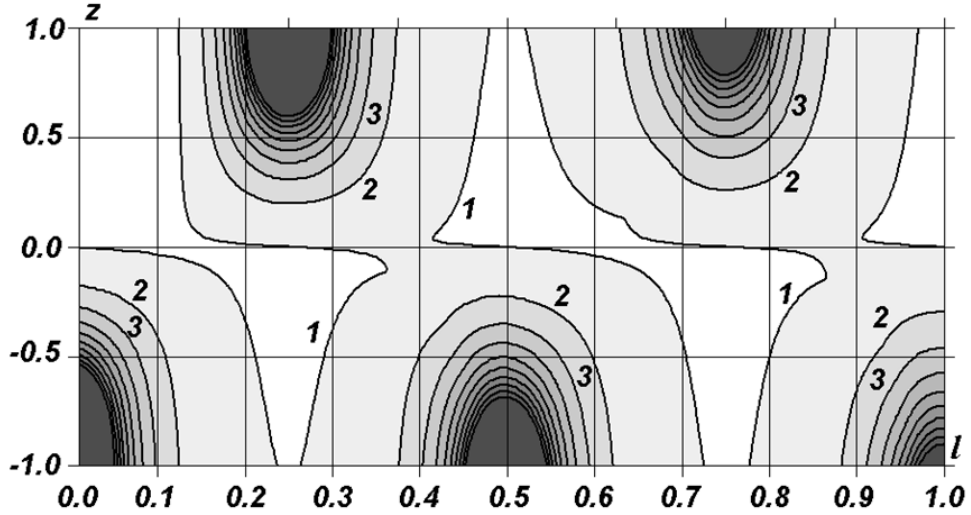

Fig. 11.1. Contl curves $\max\limits_{x}\left|I(x)\right|^2$ for different values of the line lengths l and of the load resistance z.

Let's consider now the analogous problem for modulus of voltage complex $\left|U(x)\right|$.

The square of modulus of voltage complex can be determined as follows

$$\left|U(x)\right|^2 = U(x)U^*(x) = U_0^2\left|\frac{\mathrm{ch}\delta(l-x)}{\mathrm{ch}\delta l}\right|^2 \cdot \left\{R_s^2 + 2R_s\,\mathrm{Re}\left[Z_0\,\mathrm{th}\delta(l-x)\right] + \right.$$

$$\left. + \left|Z_0\,\mathrm{th}\delta(l-x)\right|^2 \right\} \cdot \left\{R_s^2 + 2R_s\,\mathrm{Re}\left[Z_0\,\mathrm{th}(\delta l)\right] + \left|Z_0\,\mathrm{th}\delta l\right|^2\right\}^{-1}. \quad (11.8)$$

The maximal values of $\left|U(x)\right|^2$ by R_s can be determined by the examination of the derivative $d\left|U(x)\right|^2 / dR_s$. The derivative sign is determined by the following quadratic trinomial:

$$\frac{d|U(x)|^2}{dR_s} = K\Big\{R_s^2\left(\mathrm{Re}[Z_0\,\mathrm{th}(\delta l)] - \mathrm{Re}[Z_0\,\mathrm{th}(\delta(l-x))]\right) +$$

$$+ R_s\left(|Z_0\,\mathrm{th}(\delta l)|^2 - |Z_0\,\mathrm{th}(\delta(l-x))|^2\right) +$$

$$+|Z_0\,\mathrm{th}(\delta l)|^2\,\mathrm{Re}[Z_0\,\mathrm{th}(\delta(l-x))] - |Z_0\,\mathrm{th}(\delta(l-x))|^2\,\mathrm{Re}[Z_0\,\mathrm{th}(\delta l)]\Big\} =$$

$$= K\{aR_S^2 + bR_S + c\}; \qquad (11.9)$$

$$a = \mathrm{Re}[Z_0\,\mathrm{th}(\delta l)] - \mathrm{Re}[Z_0\,\mathrm{th}(\delta(l-x))];\ b = |Z_0\,\mathrm{th}(\delta l)|^2 - |Z_0\,\mathrm{th}(\delta(l-x))|^2;$$

$$c = |Z_0\,\mathrm{th}(\delta l)|^2\,\mathrm{Re}[Z_0\,\mathrm{th}(\delta(l-x))] - |Z_0\,\mathrm{th}(\delta(l-x))|^2\,\mathrm{Re}[Z_0\,\mathrm{th}(\delta l)];$$

$$K = 2U_0^2\left|\frac{\mathrm{ch}\delta(l-x)}{\mathrm{ch}\delta l}\right|^2 \cdot \left\{R_s^2 + 2R_s\,\mathrm{Re}\left[Z_0\,\mathrm{th}(\delta l)\right] + |Z_0\,\mathrm{th}\delta l|^2\right\}^{-2} > 0.$$

Let's note that the following inequalities are equivalent

$$a < 0 \Leftrightarrow \frac{\mathrm{Re}[Z_0\,\mathrm{th}(\delta l)]}{\mathrm{Re}[Z_0\,\mathrm{th}(\delta(l-x))]} < 1;\ b < 0 \Leftrightarrow \frac{|\mathrm{th}(\delta l)|^2}{|\mathrm{th}(\delta(l-x))|^2} < 1;$$

$$c < 0 \Leftrightarrow \frac{|\mathrm{th}(\delta l)|^2}{|\mathrm{th}(\delta(l-x))|^2} < \frac{\mathrm{Re}[Z_0\,\mathrm{th}(\delta l)]}{\mathrm{Re}[Z_0\,\mathrm{th}(\delta(l-x))]}. \qquad (11.10)$$

We consider at first the case of ideal line: $R = G = 0$; $\delta = j\omega/a$; $a = 1/\sqrt{LC}$; $Z_0 = Z_B = \sqrt{L/C}$. Then from (11.9) we obtain

$$\mathrm{Re}[Z_0\,\mathrm{th}(\delta l)] = Z_B\,\mathrm{Re}[j\mathrm{tg}(\omega\Delta)] = 0;$$

$$\mathrm{Re}[Z_0\,\mathrm{th}(\delta(l-x))] = Z_B\,\mathrm{Re}[j\mathrm{tg}(\omega(\Delta-\Delta_x))] = 0 \Rightarrow a = c = 0$$

and the derivative $d|U(x)|^2 / dR_s$ takes the form of linear function with respect to load resistance R_s

$$\frac{d|U(x)|^2}{dR_s} = KR_s Z_B \left(|\mathrm{tg}(\omega\Delta)|^2 - |\mathrm{tg}(\omega(\Delta - \Delta_x))|^2 \right).$$

As $R_s \in [0,\infty)$ and the derivative is a linear function yields $|U(x)|^2$ is monotone function and the maximal values of the voltage modulus for ideal line are reached at the extremities of the interval $[0,\infty)$, i.e. when $R_s = 0$ (i.e. short circuit is realized) or when $R_s = \infty$ (i.e. in case of idling in the line).

Let's consider now the case of undistorting line: $R/L = G/C = \gamma$; $\delta = (\gamma + j\omega)/a$; $a = 1/\sqrt{LC}$; $Z_0 = Z_B = \sqrt{L/C}$. Then

$$\mathrm{Re}[Z_0 \mathrm{th}(\delta l)] = Z_B \frac{\mathrm{sh}(2\gamma\Delta)}{\mathrm{ch}(2\gamma\Delta) + \cos(2\omega\Delta)};$$

$$|Z_0 \mathrm{th}(\delta l)|^2 = Z_B^2 \frac{\mathrm{ch}(2\gamma\Delta) - \cos(2\omega\Delta)}{\mathrm{ch}(2\gamma\Delta) + \cos(2\omega\Delta)};$$

$$\mathrm{Re}[Z_0 \mathrm{th}(\delta(l-x))] = Z_B \frac{\mathrm{sh}(2\gamma(\Delta - \Delta_x))}{\mathrm{ch}(2\gamma(\Delta - \Delta_x)) + \cos(2\omega(\Delta - \Delta_x))};$$

$$|Z_0 \mathrm{th}(\delta(l-x))|^2 = Z_B^2 \frac{\mathrm{ch}(2\gamma(\Delta - \Delta_x)) - \cos(2\omega(\Delta - \Delta_x))}{\mathrm{ch}(2\gamma(\Delta - \Delta_x)) + \cos(2\omega(\Delta - \Delta_x))}$$

and the formula (11.9) can be represented in the following form

$$\frac{d|U(x)|^2}{dR_s} = K_1 \left\{ \tilde{a} Z_B R_S^2 + \tilde{b} Z_B^2 R_S + \tilde{c} Z_B^3 \right\}; \qquad (11.11)$$

$$K_1 = K[\mathrm{ch}(2\gamma\Delta) + \cos(2\omega\Delta)]^{-1} [\mathrm{ch}(2\gamma(\Delta - \Delta_x)) + \cos(2\omega(\Delta - \Delta_x))]^{-1} > 0;$$

$$\widetilde{a} = \mathrm{sh}(2\gamma\Delta_x) - \mathrm{sh}(2\gamma(\Delta-\Delta_x))\cos(2\omega\Delta) + \mathrm{sh}(2\gamma\Delta)\cos(2\omega(\Delta-\Delta_x));$$

$$\widetilde{b} = 2\left[\mathrm{ch}(2\gamma\Delta)\cos(2\omega(\Delta-\Delta_x)) - \mathrm{ch}(2\gamma(\Delta-\Delta_x))\cos(2\omega\Delta)\right];$$

$$\widetilde{c} = -\mathrm{sh}(2\gamma\Delta_x) - \mathrm{sh}(2\gamma(\Delta-\Delta_x))\cos(2\omega\Delta) + \mathrm{sh}(2\gamma\Delta)\cos(2\omega(\Delta-\Delta_x)).$$

Let's note that the signs of the coefficients a and $\widetilde{a}$, b and $\widetilde{b}$, c and $\widetilde{c}$ coincide. Now we will prove that the quadratic trinomial in (11.11) at the interval $R_S \in [0,\infty)$ can possess only positive or only negative values, or it has only one positive root in case when $\widetilde{a} > 0$.

First of all, if the discriminant $\widetilde{d} = \widetilde{b}^2 - 4\widetilde{a}\widetilde{c} < 0$, then the expression (11.11) possesses only positive or only negative values in dependence on the sign of $\widetilde{a}$. If the discriminant is non-negative, then the equation $\widetilde{a}Z_B R_S^2 + \widetilde{b}Z_B^2 R_S + \widetilde{c}Z_B^3 = 0$ has real roots. Let's consider the case $\widetilde{a} < 0$ and $a < 0$. Then from (11.10) we have $\dfrac{\mathrm{Re}[Z_0\mathrm{th}(\delta l)]}{\mathrm{Re}[Z_0\mathrm{th}(\delta(l-x))]} < 1$. As $\widetilde{c} = \widetilde{a} - 2\mathrm{sh}(2\gamma\Delta_x)$, then $\widetilde{c} < 0$ and $c < 0$. So from (11.10) we obtain

$$\frac{\left|\mathrm{th}(\delta l)\right|^2}{\left|\mathrm{th}(\delta(l-x))\right|^2} < \frac{\mathrm{Re}[Z_0\mathrm{th}(\delta l)]}{\mathrm{Re}[Z_0\mathrm{th}(\delta(l-x))]}.$$

Combining these two inequalities, we have $\dfrac{\left|\mathrm{th}(\delta l)\right|^2}{\left|\mathrm{th}(\delta(l-x))\right|^2} < 1$, and so $\widetilde{b} < 0$ and $b < 0$. Thus if the coefficient a is negative, then b and c are negative too and the both roots of the quadratic equation are negative.

Further, let $\widetilde{c} > 0$. The from $\widetilde{a} = \widetilde{c} + 2\mathrm{sh}(2\gamma\Delta_x)$ we obtain that $\widetilde{a} > 0$. From (11.10) it follows

$$\frac{\mathrm{Re}[Z_0\mathrm{th}(\delta l)]}{\mathrm{Re}[Z_0\mathrm{th}(\delta(l-x))]} > 1; \quad \frac{\left|\mathrm{th}(\delta l)\right|^2}{\left|\mathrm{th}(\delta(l-x))\right|^2} > \frac{\mathrm{Re}[Z_0\mathrm{th}(\delta l)]}{\mathrm{Re}[Z_0\mathrm{th}(\delta(l-x))]}.$$

Then $\dfrac{\left|\text{th}(\delta l)\right|^2}{\left|\text{cth}(\delta(l-x))\right|^2} > 1$ and correspondingly $b > 0$ and $\widetilde{b} > 0$. Thus we obtain that if the coefficient *c* is positive, then *a* and *b* are positive too and the both roots of the quadratic equation are also negative. It remains to consider the case when $\widetilde{a} > 0$ and $\widetilde{c} < 0$. In this case independent on the sign of the coefficient $\widetilde{b}$ the quadratic equation has one positive and one negative root.

Hence, we have demonstrated that the quadratic trinomial in formula (11.11) at the interval $R_s \in [0,\infty)$ can possess only positive or only negative values, or it has only one positive root in case when $\widetilde{a} > 0$. In these cases the modulus $\left|U(x)\right|^2$ is either monotone function by R_s, or nonmonotonic but concave function for any values of *x* and *l* at the interval $R_s \in [0,\infty)$. This implies that the maximal values of the current modulus for undistorting line are reached at the extremities of the interval $[0,\infty)$, i.e. when $R_s = 0$, (i.e. short circuit is realized) or when $R_s = \infty$ (i.e. in case of idling in the line).

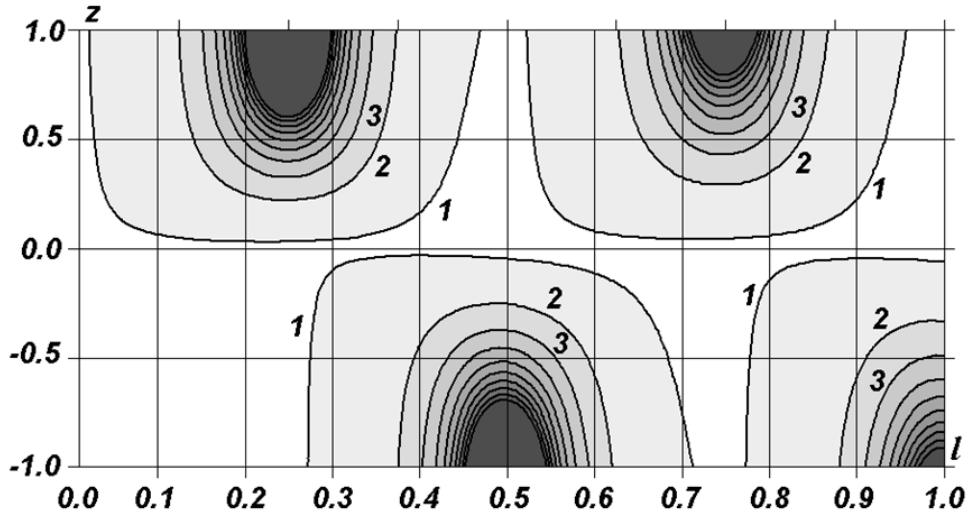

Fig. 11.2. Contl curves $\max\limits_x \left|U(x)\right|^2$ for different values of the line lengths *l* and of the load resistance *z*.

In case of line with arbitrary losses $(R/L \neq G/C)$ the behavior of the modulus $|U(x)|^2$ as a function of R_s is more complicated, i.e. there are local maximums for $0 < R_S < \infty$. This is why it is impossible to prove mathematically rigorous the affirmation obtained above for ideal and undistorting lines. However, the affirmation remains correct in this case too. This fact is justified by contl curves that are represented in the fig. 11.2, when $R = 0.48$, $G = R/7$. We use here the dimensionless load parameter $z = \dfrac{R_S - Z_B}{R_S + Z_B}$, that possesses the value $z = -1$ under the short circuit and the value $z = 1$ under the idling. As it is seen from the figure the maximal values are reached for different line lengths l when $z = \pm 1$.

12. Maximal transmission power and efficiency in alternating voltage line

12.1. Calculation of losses under traveling-wave and mixed-wave modes

The analytical solutions for generated power, transmission power and efficiency in cases of ideal and undistorting lines have been obtained in [89, 90]. Now we are going to determine the conditions in which the active load at the receiving end consumes maximal power under the steady-state regime. Let's show at first that for any line length the efficiency of the alternating voltage line with arbitrary losses is always greater under the pure active load $Z_S = R_S = Z_B$ (i.e. the line is in the traveling-wave mode) then when the line is closed on matched (active-reactive) load that is equal to complex wave resistance $Z_S = Z_0$ (i.e. the line is in the mixed-wave mode). The small exceptions are the short lines with large values of the lineal parameters R and G. However, the differences between the efficiencies in these two cases are very slight and come to fraction of a percent.

The dependence of the efficiency and of the transmission power on the line length x are represented in the fig. 12.1 and fig. 12.2 when $Z_S = Z_B$ (curve 1); Z_0 (curve 2) and $R = 0.48$, $G = R/5$ (*a*); $R = 0.48$, $G = 0$ (*b*); $R = 4.8$, $G = R/5$(*c*); $R = 4.8$, $G = 0$ (*d*).

The data cited in the table 12.1 represent the power losses in the line with pure active load that is equal to the wave resistance of the ideal line: $Z_S = R_S = Z_B$. Under such load the quasisteady wave process occurs. This process is closed to traveling-wave regime and the efficiency value of the half-wave line is maximal possible. It is to mention that even in the line with

complex matched load $Z_S = Z_0$ under the traveling-wave mode (natural power) the losses turn out to be a little greater [91].

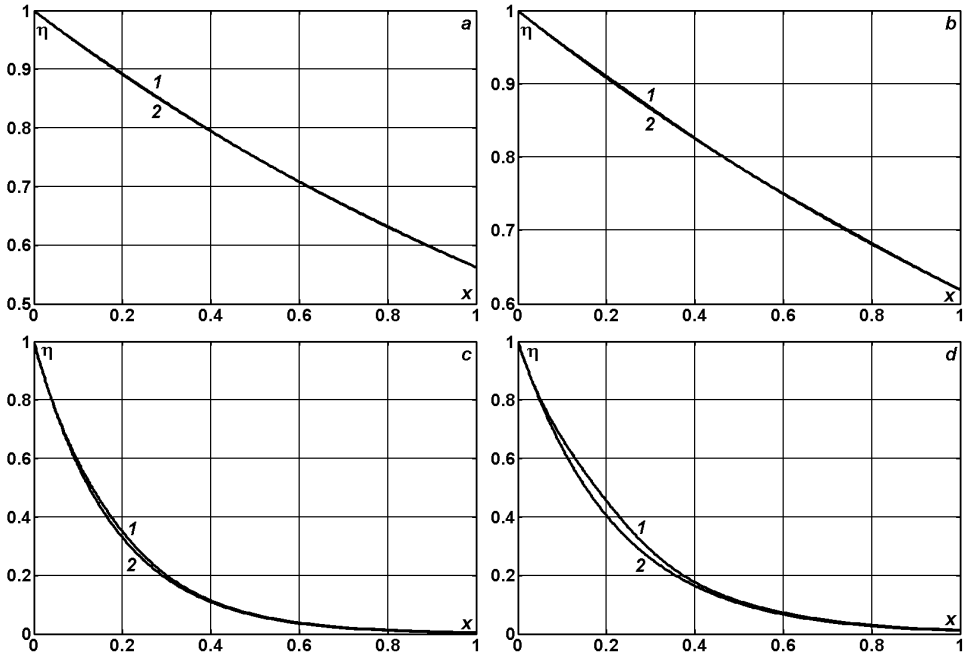

Fig. 12.1. Efficiency depending on the line length x when $Z_S = Z_B$ (curve 1); Z_0 (curve 2) and $R = 0.48$, $G = R/5$ (***a***); $R = 0.48$, $G = 0$ (***b***); $R = 4.8$, $G = R/5$(***c***); $R = 4.8$, $G = 0$ (***d***).

Now we will consider the power losses in the alternating voltage line with the length closed to half-wave with frequency 50 Hz and will compare them with published calculation and experimental data for lines of this type. As may be seen from presented results for the alternating voltage line with length $l = 2858$ km the losses come to 24.48%, that is with 1.64% greater then in the [22]. As is well known in the experiment from 1968, concerning the 985 MW power transfer, the losses in the half-wave three-phase line 500 kV come to 225 MW (22.84%). If we neglect the insulation leakage current ($G = 0$), then the losses decrease till 20.85%. The total coincidence between the calculating and experimental data can be reached if we set $G = 32$ nS/km. However, such a comparison can hardly be considered as a correct one because of some reasons. The first reason is that the interference between the wires was ignored. The second one is that in this experiment the half-wave overhead line 500 kV was evidently working under the mixed-wave mode, but not under the traveling-wave mode. This fact is confirmed

by the amplitude value that is equal to 1.07 kA at the beginning of the line with the voltage 525 kV. It is possible to get the increasing of transmission power under the mixed-wave mode but the relative losses in this case will increase too.

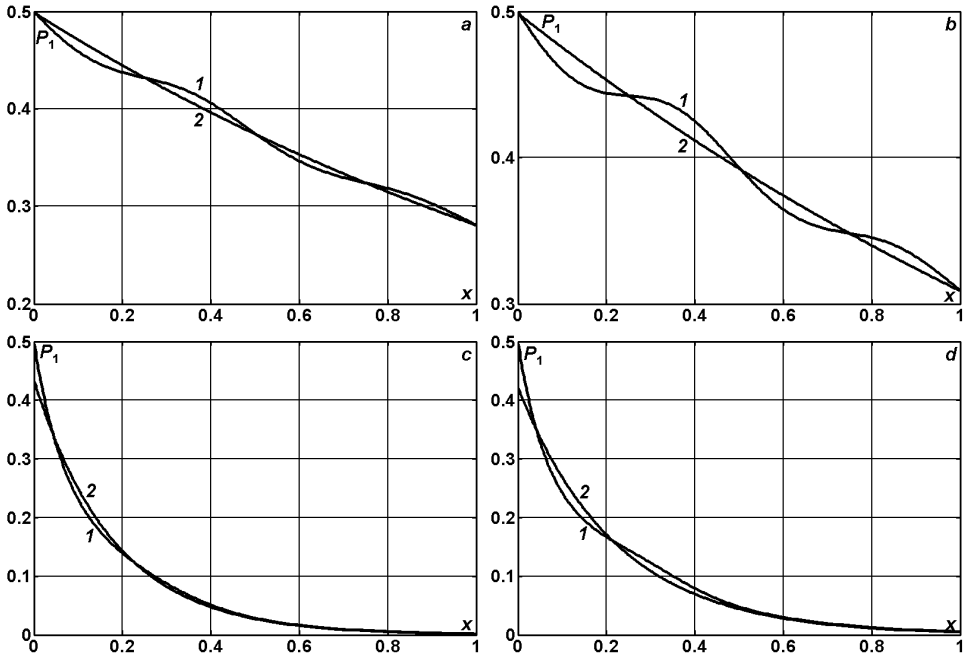

Fig. 12.2. Transmission power depending on the line length x when $Z_S = Z_B$ (curve 1); Z_0 (curve 2) and $R = 0.48$, $G = R/5$ (***a***); $R = 0.48$, $G = 0$ (***b***); $R = 4.8$, $G = R/5$(***c***); $R = 4.8$, $G = 0$ (***d***).

Let's apply to another source where the losses in the half-wave alternating and direct voltage lines are considered [46]. As it is established in [46], to obtain for design line 700 kV Surgut – Chernobyl (3000 km) the power losses about 13%, the inequality $R \leq 12$ mΩ/km must to hold at least. The violation of this condition gives rise to the losses that are always greater then 13%.

For comparison the power losses in case of direct current are represented in the last column of the table 12.1. As can be seen the losses in this case are always lower then in case of alternating voltage of the energy source. Only for undistorting lines, when $RC = GL$ (only the dissipation occurs but the dispersion is missing completely), these results coincide. But in high-current electrical circuits $RC > GL$, as a rule, and so the differences

between the efficiency in alternating and direct voltage lines can reach several percents.

Table 12.1. Power losses for different line lengths *l*, longitudinal active resistances R and insulation shunt admittances *G* in case when $Z_S = Z_B$.

l	*R*, mΩ/km	*G,* nS/km	ΔP, %	$\Delta \Pi$, %
0.0516 λ	22	62	2.91	2.91
302 km	22	0	2.42	2.42
0.0949 λ	22	62	5.27	5.26
556 km	22	0	4.37	4.36
0.2684 λ	22	62	14.18	13.91
1572 km	22	0	11.85	11.41
0.4880 λ	22	62	24.48	23.38
2858 km	22	0	20.85	18.98
0.5123 λ 3000 km	22	62	25.53	24.34
	22	0	21.77	19.74
	12	**0**	**12.91**	**12.15**
	12	175	24.17	24.17
	22	311	38.85	38.85

The changes of the average (dimensionless) values of the generated and transmission power *P* (curves 1, 2), efficiency η (curve 3), power factors ($\cos\varphi$) of the source and the receiver (curves 4, 5) depending on the line length *x* are represented in the fig.12.3 in case when $Z_S = Z_0$ (*a*); Z_B (*b*); $R = 0.48$, *G*=*R*/5. As can be seen from the diagrams the transmission power and the efficiency monotone decrease with increasing of the line length, but the generated power remains practically steady with slight (in limits of 1…3 %) fluctuations in case when $Z_S = Z_B$.

In the fig. 12.4 the line length *x* dependence of the investigated values is represented when $Z_S = Z_B + j\omega L_S$ (*a*); $Z_B - j/(\omega C_S)$ (*b*); L_S =1/8 (0.66 H); C_S =1/5 (15.23 μF); R = 0.48; $G = R/5$**.** The presence of the reactive elements in the load resistance results in dramatic change of the input circuit resistance and, as implication, all values characterizing the alternating current power transfer experience oscillations in dozens of percents. For the half-wave line the transmission power and efficiency are maximal when the load at the receiving end is pure active.

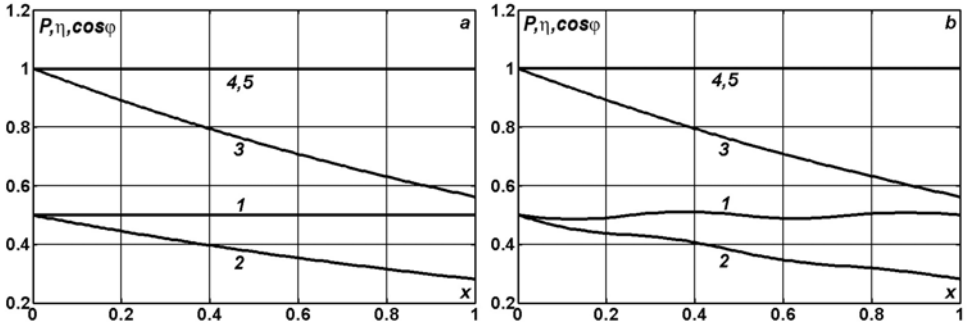

Fig. 12.3. Line length dependence of generated and transmission power, efficiency and power factors of source and receiver when $Z_S = Z_0$ (***a***); $Z_S = Z_B$(***b***); R = 0.48; $G = R/5$.

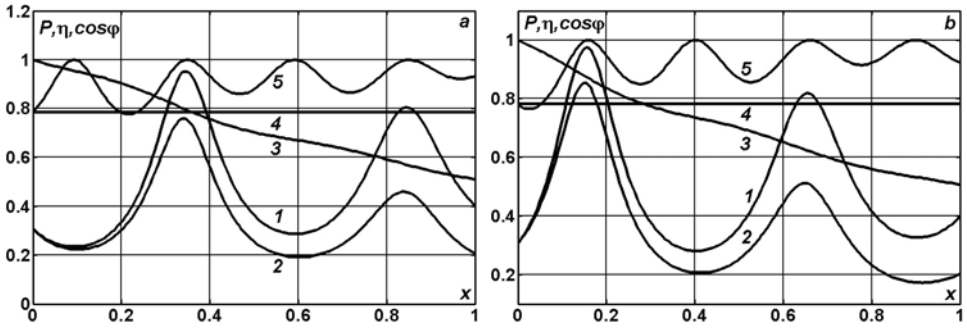

Fig. 12.4. Line length dependence of generated and transmission power, efficiency and power factors of source and of receiver when $Z_S = Z_B + j\omega L_S$ (***a***); $Z_S = Z_B - j/(\omega C_S)$ (***b***); L_S =1/8; C_S =1/5; R = 0.48; $G = R/5$.

12.2. Pure active load critical resistances

For direct current line with nonzero lineal resistance ($R>0$) and ideal insulation ($G = 0$) the maximal power consumption reaches in case when the condition $R_S = R\,l$ is fulfilled, i.e. when the active load resistance is equal to the total resistance of the line (the Lenz-Bott theorem) [15, 34]. In this case the efficiency of the line is independent on its length and is equal to 0.5. It is not so for alternating voltage lines even in case of relative short lines: $l \sim \lambda/16$. The question about limit values of the transmission power dependence on the alternating voltage line length was raised in [60] but it had not any future development.

Let's remind [89, 90] the formulas for exact determination of average steady values of generated power (P_0), transmission power (P_1) and efficiency (η) in alternating voltage line with pure active load with the resistance $R_S \geq 0$. They have the following form

$$P_1 = \frac{1}{2}\mathrm{Re}(U_1 I_1^*) = \frac{1}{2}|I_1|^2\,\mathrm{Re}(Z_S) = \frac{R_S}{2}|I_1|^2 = \frac{U_0^2 R_S}{2|R_S \mathrm{ch}\delta l + Z_0 \mathrm{sh}\delta l|^2};$$

$$P_0 = \frac{1}{2}\mathrm{Re}(U_0 I_0^*) = \frac{U_0}{2}\mathrm{Re}(I_0) = \frac{U_0}{2}\mathrm{Re}\left(\frac{1}{Z_{BX}}\right) = \frac{U_0^2\,\mathrm{Re}(Z_{BX})}{2|Z_{BX}|^2};$$

$$\eta = \frac{P_1}{P_0} = \frac{R_S|Z_{BX}|^2}{|R_S \mathrm{ch}\delta l + Z_0 \mathrm{sh}\delta l|^2\,\mathrm{Re}(Z_{BX})};$$

$$Z_{BX} = Z_0\,\frac{R_S \mathrm{ch}\delta l + Z_0 \mathrm{sh}\delta l}{R_S \mathrm{sh}\delta l + Z_0 \mathrm{ch}\delta l}.$$

Let's set the following problem: to determine the values of resistance $R_S \geq 0$ at the receiving end of the sinusoidal voltage line which ensure the maximal values of generated power, transmission power and efficiency. If we test the indicated functions for extremum, then we obtain for resistance R_S the following expressions:

$$\max_{R_S} P_0 \text{ is reached at } R_{0k}.$$

The value R_{0k} is determined through the real roots $R_{0k}^{\pm}$ of the quadratic equation

$$R_S^2\,\mathrm{Re}(\mathrm{ch}^2\delta l) + R_S\,\mathrm{Re}(Z_0 \mathrm{sh}2\delta l) + \mathrm{Re}(Z_0^2 \mathrm{sh}^2\delta l) = 0:$$

$$R_{0k}^{\pm} = \frac{-\mathrm{Re}(Z_0 \mathrm{sh}\delta l \mathrm{ch}\delta l) \pm \mathrm{Im}(Z_0 \mathrm{sh}\delta l \mathrm{ch}\delta^* l)}{\mathrm{Re}(\mathrm{ch}^2\delta l)}.$$

These roots can be either with opposite signs or both negative. This is way the value R_{0k} is determined by formula

$$R_{0k} = \begin{cases} R_{0k}^{+}, & \text{если } R_{0k}^{+} > 0 \\ R_{0k}^{-}, & \text{если } R_{0k}^{-} > 0 \\ 0, & \text{если } \mathrm{Re}\left(\mathrm{ch}^2 \delta l\right) > 0 \\ \infty, & \text{если } \mathrm{Re}\left(\mathrm{ch}^2 \delta l\right) < 0 \end{cases}.$$

$$\max_{R_S} P_1 \text{ is reached at } R_{1k} = \left| Z_0 \mathrm{th} \delta l \right|;$$

The maximal value of efficiency $\max_{R_S} \eta$ is reached at

$$R_\eta = |Z_0| \sqrt{\frac{\mathrm{Re}\left(Z_0 \mathrm{sh}\delta l \mathrm{ch}\delta^* l\right)}{\mathrm{Re}\left(Z_0 \mathrm{sh}\delta^* l \mathrm{ch}\delta l\right)}}, \text{ if } \mathrm{Re}\left(Z_0 \mathrm{sh}\delta l \mathrm{ch}\delta^* l\right)\mathrm{Re}\left(Z_0 \mathrm{sh}\delta^* l \mathrm{ch}\delta l\right) >= 0.$$

$$\text{If } \mathrm{Re}\left(Z_0 \mathrm{sh}\delta l \mathrm{ch}\delta^* l\right)\mathrm{Re}\left(Z_0 \mathrm{sh}\delta^* l \mathrm{ch}\delta l\right) < 0, \text{ then } R_\eta = 0 \text{ when}$$
$$\mathrm{Re}\left(Z_0 \mathrm{sh}\delta l \mathrm{ch}\delta^* l\right) < 0 \text{ and } R_\eta = \infty \text{ when } \mathrm{Re}\left(Z_0 \mathrm{sh}\delta l \mathrm{ch}\delta^* l\right) > 0.$$

In the fig. 12.5 we can see the changes of generated and transmission powers, efficiency and power factors of the source and receiver (curves 1–5) depending on parameter z when l = 0.0516 (Balashov substation); R = 0.48(*a*); 4.8(*b*); $G = R/5$; $Z_S = R_S$. The represented diagrams visual demonstrate that the maximal values of all examined functions are reached at the different values of the load resistance R_S. With increasing of the losses in the line we observe the "dispersal" of the critical resistances for generated and transmission powers, whereas the maximum points of efficiency and of power factor remain practically fixed. Thus, by variation of the parameter R_S one can gain a clear idea of power flow for any interval of the line length. This information in turn gives the possibility to choose the optimal regime starting from some criteria or posed purposes.

Fig. 12.6 illustrates the generated and transmission powers, efficiency and power factors of the source and receiver depending on parameter z when $Z_S = R_S - j/(\omega C_S)$; C_S =1 (17.57 μF). Here and below we assume that $R = 0.48$, $G = R/5$. The longitudinal compensation of the load parame-

ters for this line length increases the maximal transmission power, but it decreases efficiency and $\cos\varphi$.

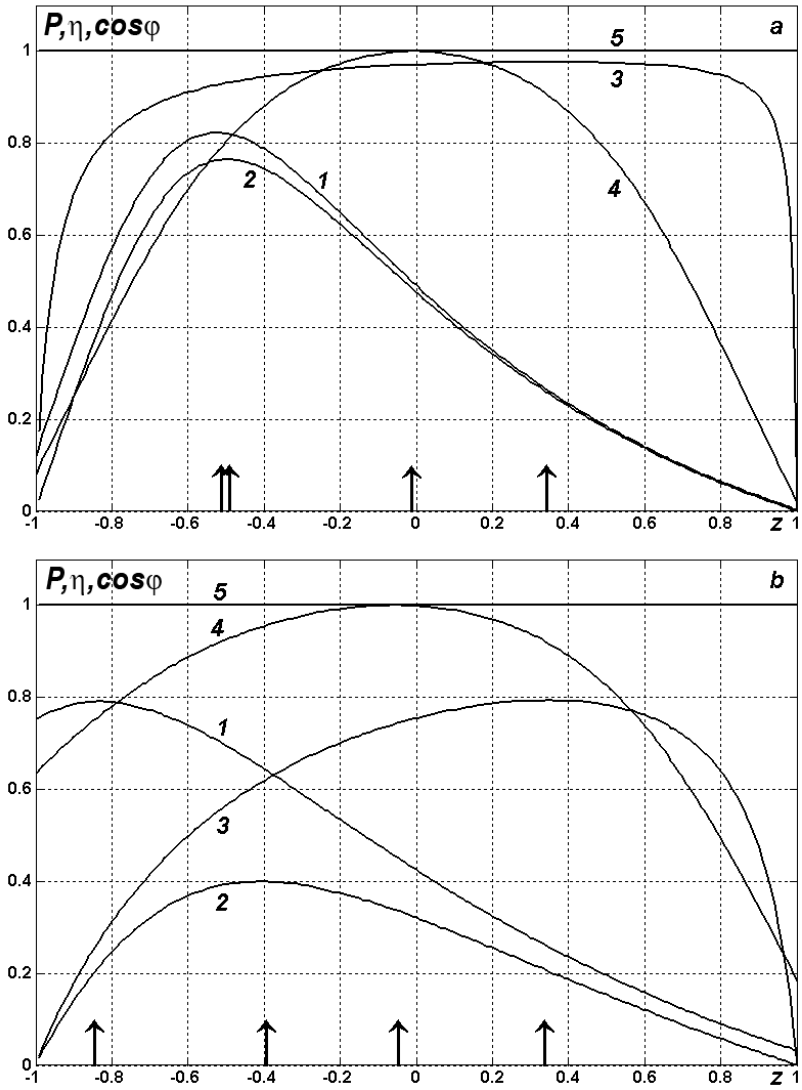

Fig. 12.5. Generated power, transmission power, efficiency and power factors of source and of receiver depending on load resistance R_S when l = 0.0516; R = 0.48(***a***); 4.8(***b***); $G = R/5$; $Z_S = R_S$.

The generated power, maximal transmission power, efficiency and critical resistance z_{1k} depending on the line length are represented in the fig. 12.7 (curves 1 – 4 correspondingly). The increasing (decreasing) of the transmis-

sion power as line length changes always is accompanied by the decreasing (increasing) of efficiency. For quarter-wave line the power maximum is reached under the regime closed to idling ($R_S = 13.93 Z_B$), but for half-wave line – under the regime closed to short circuit ($R_S = 0.14 Z_B$).

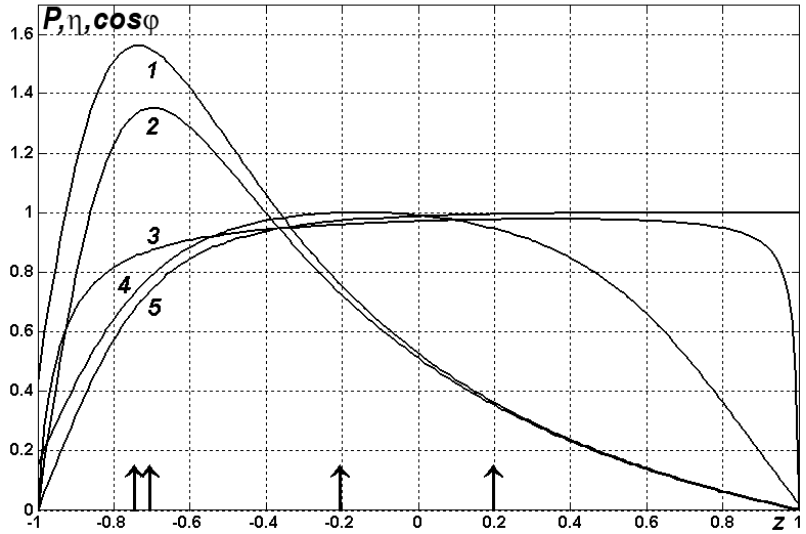

Fig. 12.6. Generated power, transmission power, efficiency and power factors of source and of receiver depending on load resistance R_S when l = 0.0516; R = 0.48; $G = R/5$; $Z_S = R_S - j/(\omega C_S)$; C_S =1.

Generated power, transmission power, maximal efficiency and critical resistance z_η depending on the line length are represented in the fig. 12.8. It is especially visible here that the maximal efficiency not in the least corresponds to the maximal transmission power. Thus, it is necessary to tell the difference between the different regimes of line working: under maximal transmission power, efficiency, power factor and maximal watt-hour efficiency of the sinusoidal voltage generator.

If load parameters and line parameters are independent on time, then calculation of steady-state regime in e electrical circuit by symbolic method does not constitute a complicated problem. The situation changes radically in case when such dependence exists. Even slight parameter changes in time, voltage jumps or jumps of the feeding generator frequency give rise to appearance of nonsinusoidal current components that can not be determined by using the steady-state regime equations in hyperbolic functions. Fourier expansion of the input signal and another approaches for nonsinusoidal regimes calculation seem to be unpromising and inefficient.

The complex amplitude method potential is far from being exhausted, but the field of its application is a priori restricted in limits of sinusoidal steady-state regimes.

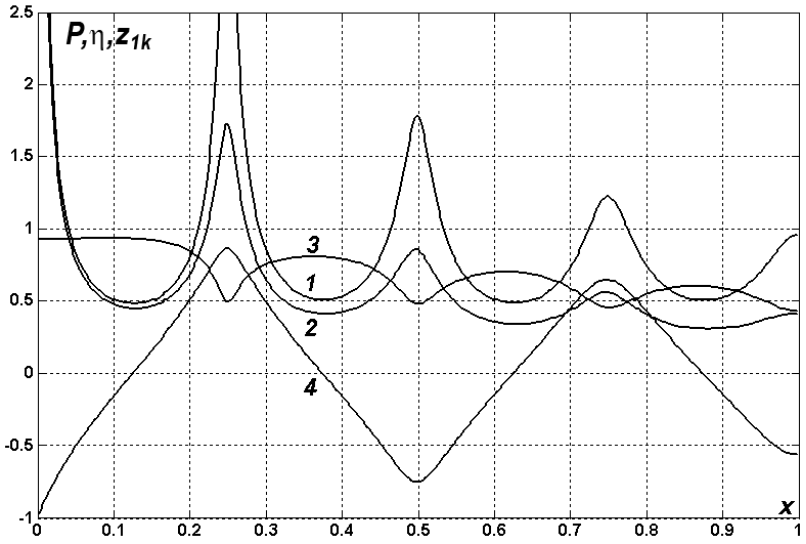

Fig. 12.7. Generated power (1), maximal transmission power (2), efficiency (3) and critical resistance z_{1k} (4) depending on the line length x when $R = 0.48$; $G = R/5$.

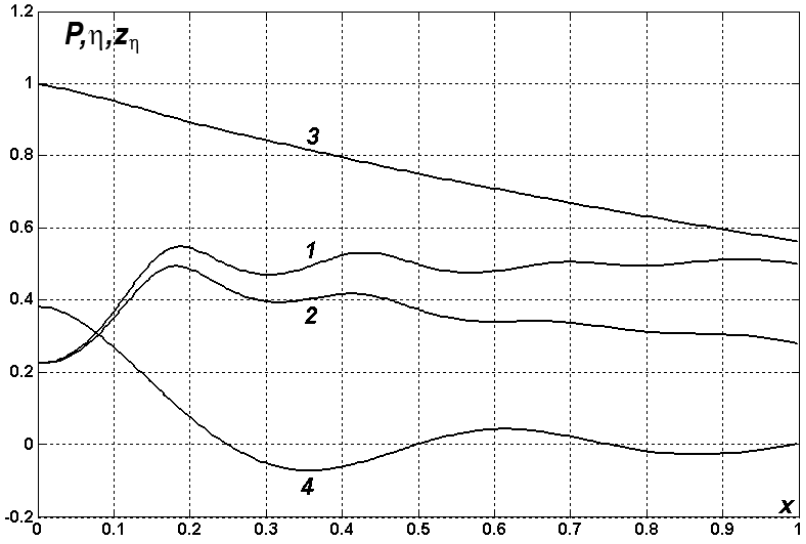

Fig. 12.8. Generated power (1), transmission power (2), maximal efficiency (3) and critical resistance z_η (4) depending on the line length x when $R = 0.48$; $G = R/5$.

13. Load parameters compensation with the object of transmission power and efficiency increasing

For compensation of the reactive power consumed by loads (asynchronous motors, electrolysis installations; etc.) and by electrical system elements usually the transverse included capacitor banks, synchronous condensers and synchronous motors are used. These "bucking out" systems are destined for electrical customer ensuring with the reactive power with desired voltage values, as well as for active power losses decreasing in elements of electric mains.

Controlled "bucking out" systems (controllable capacitor banks, synchronous condensers and motors with automatic excitation control) are used also as an automatic voltage control systems in electric mains. The power and the location of the "bucking out" systems are usually defined by technical and economic indices obtained from calculations.

The reactive power compensation at present is of no small importance factor that allows to settle a problem of energy-saving at small, medium and large-scale enterprises. In opinion of main experts in domain the energy resources part (in particular, electric power) comes to 30-40% from the cost of production. This is enough forcible argument to necessitate the analysis and auditing of power consumption and to elaborate some reactive power compensation procedure.

The most of electrical consumers are the electric machines (transformers, arc welding equipment) in which the alternating magnetic flux is connected with windings. As a consequence, in the windings under the alternating current the reactive electromotive forces are induced. These electromotive forces cause the phase displacement (φ) between voltage and current. This phase displacement usually increases, but cosφ decreases under the small load. For example, if cosφ of alternating current engine under full loading is equal to 0,75-0,80, then under small loading it is equal to 0,20-0,40. Small-loaded transformers also have low values of cosφ. Thus, if the reactive power compensation is not applied, then the resulting cosφ of the energetic system will be low and the load current will increase with the same active power consumption from the electric main. Correspondingly, the application of the reactive power compensation (using the automatic capacitor installations) results in decreasing of the consumable current. This decreasing comes to 30-50% depending on values of cosφ and, correspondingly, it leads to decreasing of the conductive wires heating and insulation aging.

It is accepted that by compensation of parameters of the line with any length it is possible to impart the properties characteristic to the half-wave line. With other words, any line can be adjusted to the half-wave length. The idea of adjustment is known for a long time however it does not get yet some practical application. The investigations in the field have shown that the application of the adjusted electric mains is advisable for lines with lengths 1500 – 3500 km. The adjustment to the half-wave is realized by adjusting devices. The adjusting schemes are picked out in such a way as to ensure the minimal consumption of the adjusting devices under the given flow capacity.

However, some strict theoretical foundation and comprehensive quantitative analysis of the reactive power compensation processes are missing in the textbooks and special literature. Thus we will try to fill up this gap.

Let's formulate the following problem. Is it possible to compensate the pure active load in such a way as to increase simultaneously both the efficiency and the transmission power? If yes, then what values the reactive resistance must possess and what quantitative effect can be reached?

Fig. 13.1. Alternating voltage line with active R_S and reactive X_S load at receiving end.

If the load at the end of the line has active and reactive components (see fig. 13.1), then the equations of steady-state process in the hyperbolic functions (1.5) take the form

$$Z_S = R_S + j\left(\omega L_S - \frac{1}{\omega C_S}\right) = R_S + jX_S;$$

$$Z_0 = \sqrt{\frac{R + j\omega L}{G + j\omega C}}\ ;\ \delta = \sqrt{(R + j\omega L)(G + j\omega C)}\ ;$$

$$U_0 = Z_{BX} I_0;\quad U_1 = Z_S I_1;\ Z_{BX} = Z_0 \frac{Z_S + Z_0 \mathrm{th}(\delta l)}{Z_0 + Z_S \mathrm{th}(\delta l)}; \qquad (13.1)$$

$$U_1 = U_0 \mathrm{ch}(\delta l) - Z_0 I_0 \mathrm{sh}(\delta l);$$

$$I_1 = -\frac{U_0}{Z_0}\mathrm{sh}(\delta l) + I_0 \mathrm{ch}(\delta l) = \frac{U_0}{Z_0 \mathrm{sh}(\delta l) + Z_S \mathrm{ch}(\delta l)};$$

$$S = UI^* = |U||I|\cos\varphi + j|U||I|\sin\varphi.$$

The active power of the load can be written in the following form

$$P_1 = \frac{1}{2}\mathrm{Re}\left(U_1 I_1^*\right) = \frac{1}{2}\mathrm{Re}\left(Z_S I_1 I_1^*\right) = \frac{1}{2}|I_1|^2\ \mathrm{Re}\left(Z_S\right) = \frac{R_S}{2}|I_1|^2. \quad (13.2)$$

To determine the maximal value P_1 with respect to the load parameters X_S and R_S it is necessary to solve the system of two equations

$$\frac{\partial P_1(X_S, R_S)}{\partial X_S} = 0,\quad \frac{\partial P_1(X_S, R_S)}{\partial R_S} = 0.$$

After the differentiation the system gets the form

$$R_S|I_1|\frac{\partial |I_1|}{\partial X_S} = 0,\quad |I_1|\left(|I_1| + 2R_S\frac{\partial |I_1|}{\partial R_S}\right) = 0. \qquad (13.3)$$

Now it is easy to see that we need to solve the following system of equations

$$\frac{\partial |I_1|}{\partial X_S} = 0,\quad |I_1| + 2R_S\frac{\partial |I_1|}{\partial R_S} = 0. \qquad (13.4)$$

Let's consider the first equation from (13.4). After differentiation of the modulus $|I_1|$, we obtain the equation form which we determine the optimal value for X_S:

$$X_{S,k} = \frac{\mathrm{Im}\left(Z_0^* \mathrm{sh}(\gamma^* l)\mathrm{ch}(\gamma l)\right)}{\left|\mathrm{ch}(\gamma l)\right|^2}. \qquad (13.5)$$

Solving the second equation from (13.4) we obtain the explicit expression for optimal value for R_S depending on parameter value X_S:

$$R_S^2 = X_S^2 + \left|Z_0 \mathrm{th}(\gamma l)\right|^2 - \frac{2X_S}{\left|\mathrm{ch}(\gamma l)\right|^2} \mathrm{Im}\left(Z_0^* \mathrm{sh}(\gamma^* l)\mathrm{ch}(\gamma l)\right). \qquad (13.6)$$

Now let's determine the values of the load parameters X_S and R_S, for which the efficiency ($\eta = P_1 / P_0$) reaches its maximal value. As

$$P_1 = R_S |I_1|^2 \text{ and } P_0 = U_0 \,\mathrm{Re}(I_0) = U_0 (I_0 + I_0^*)/2,$$

then

$$\eta = \frac{R_S Z_0 Z_0^*}{\mathrm{Re}\left[Z_0^* (Z_0 \mathrm{ch}\gamma l + Z_S \mathrm{sh}\gamma l)(Z_S^* \mathrm{ch}\gamma^* l + Z_0^* \mathrm{sh}\gamma^* l)\right]}.$$

To obtain the maximal value of efficiency it is necessary to solve the following system of equations

$$\frac{\partial \eta(X_S, R_S)}{\partial X_S} = 0, \quad \frac{\partial \eta(X_S, R_S)}{\partial R_S} = 0. \qquad (13.7)$$

Let's consider the first equation from (13.7). After differentiation and some simplifications we obtain the equation form which we determine the optimal value for X_S:

$$X_{S,\eta} = \frac{\mathrm{Im}\left[Z_0^*\left(Z_0^*|\mathrm{sh}(\gamma l)|^2 - Z_0|\mathrm{ch}(\gamma l)|^2\right)\right]}{2\,\mathrm{Re}\left(Z_0^*\mathrm{sh}(\gamma l)\mathrm{ch}(\gamma^* l)\right)}. \qquad (13.8)$$

Solving the second equation from (13.7) we obtain the explicit expression for optimal value for R_S depending on parameter value X_S:

$$R_S^2 = X_S^2 + \frac{X_S\,\mathrm{Im}(Z_0^2)|\mathrm{sh}(\gamma l)|^2 + |Z_0|^2\,\mathrm{Re}\left(Z_0^*\mathrm{sh}(\gamma^* l)\mathrm{ch}(\gamma l)\right)}{\mathrm{Re}\left(Z_0^*\mathrm{sh}(\gamma l)\mathrm{ch}(\gamma^* l)\right)}. \qquad (13.9)$$

It is natural to choose the wave resistance of the line $R_S = Z_B$ as an active load, because the efficiency reaches its maximal value (with respect to variation of R_S) exactly under such resistance. The efficiency depending on line length is represented in the fig. 13.2 when $R = 0.48$, $G = R/5$(*a*); $R = 0.48$, $G = 0$(*b*); $R = 1.205$, $G = R/5$(*c*); $R = G = 1.205$(*d*); $R = 4.8$, $G = R/5$(*e*); $R = 4.8$, $G = 0$(*f*). The curve 1 is obtained in case when the reactive load resistance is zero $X_S = 0$, and the curve 2 corresponds to $X_S = X_{S,\eta}$ (the case when the efficiency is maximal for given line length).

As it can be seen from diagrams some evident efficiency increasing can be reached by means of longitudinal compensation of the load parameters only at the interval $0 < x < 0.25$ under the sufficiently large values of the lineal resistance and zero leakage $R = 4.8$, $G = 0$ (see fig. 13.2, *f*). If the load is connected to the undistorting line (see fig. 13.2, *d*), then the both curves coincide and it is impossible to get any efficiency refinement.

The diagrams in the fig. 13.3 show that the optimal (critical) resistance $X_{S,\eta}$ is changing within wide limits, but it always remains positive, hence it is of inductive nature. Under the not great losses ($R = 22$ mΩ /km) the resistance of the compensative reactive element is equal to zero for half-wave line (see fig. 13.3, *a, b*).

Let's consider now the changes in transmission power under the reactive resistance $X_S = X_{S,\eta}$ connected to the pure active load. The corresponding dependences on the line length of the P_1 are represented in the fig. 13.4. We must mention especially the intervals along the line length for which the load active power turned out to be higher under the longitudinal compensation. It is easy to note that the optimal line length here turns out to be the line with the length approximately equal to 0.3, for which the increasing of the function P_1 is maximal.

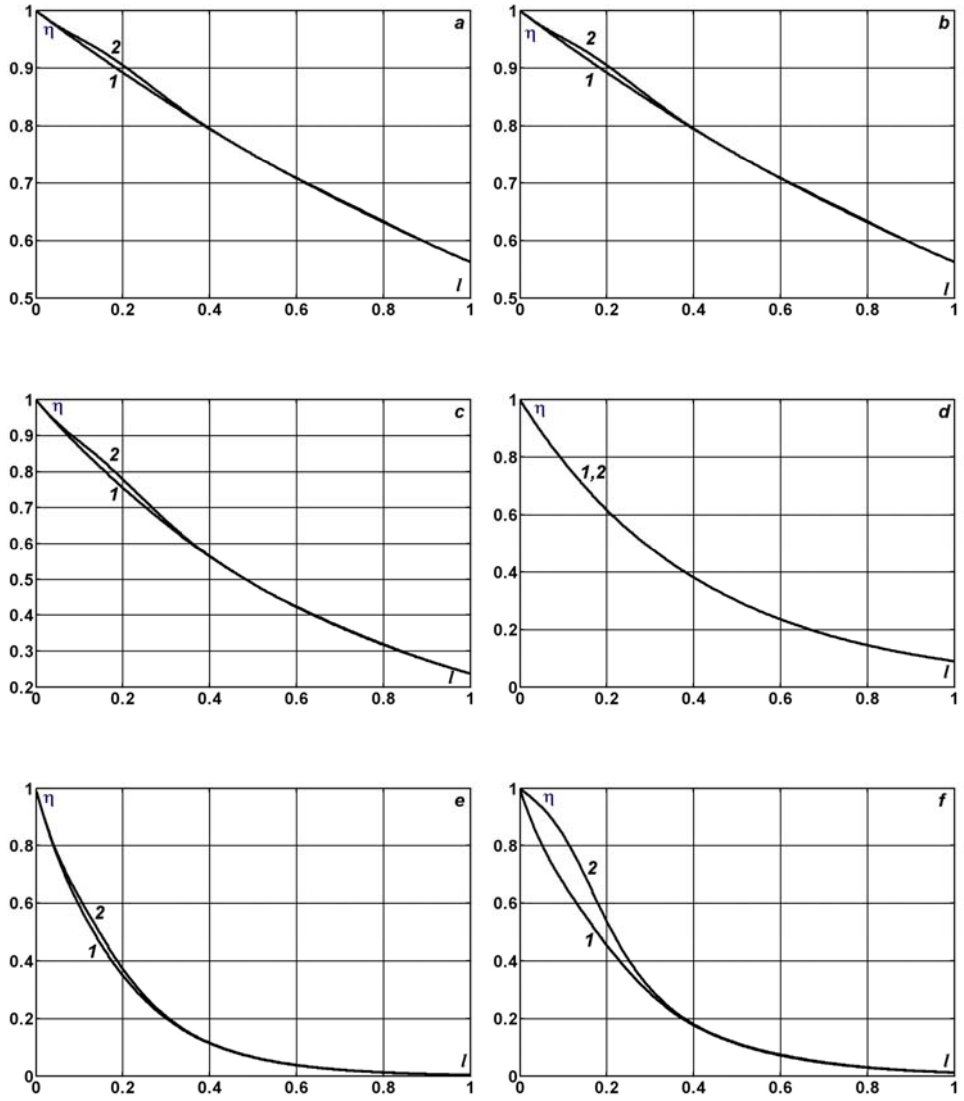

Fig. 13.2. $\eta(X_S = 0)$ (1) and $\eta(X_S = X_{S,\eta})$ (2) depending on line length when $R_S = Z_B$ and $R = 0.48$, $G = R/5$(***a***); $R = 0.48$, $G = 0$(***b***); $R = 1.205$, $G = R/5$(***c***); $R = G = 1.205$(***d***); $R = 4.8$, $G = R/5$(***e***); $R = 4.8$, $G = 0$(***f***).

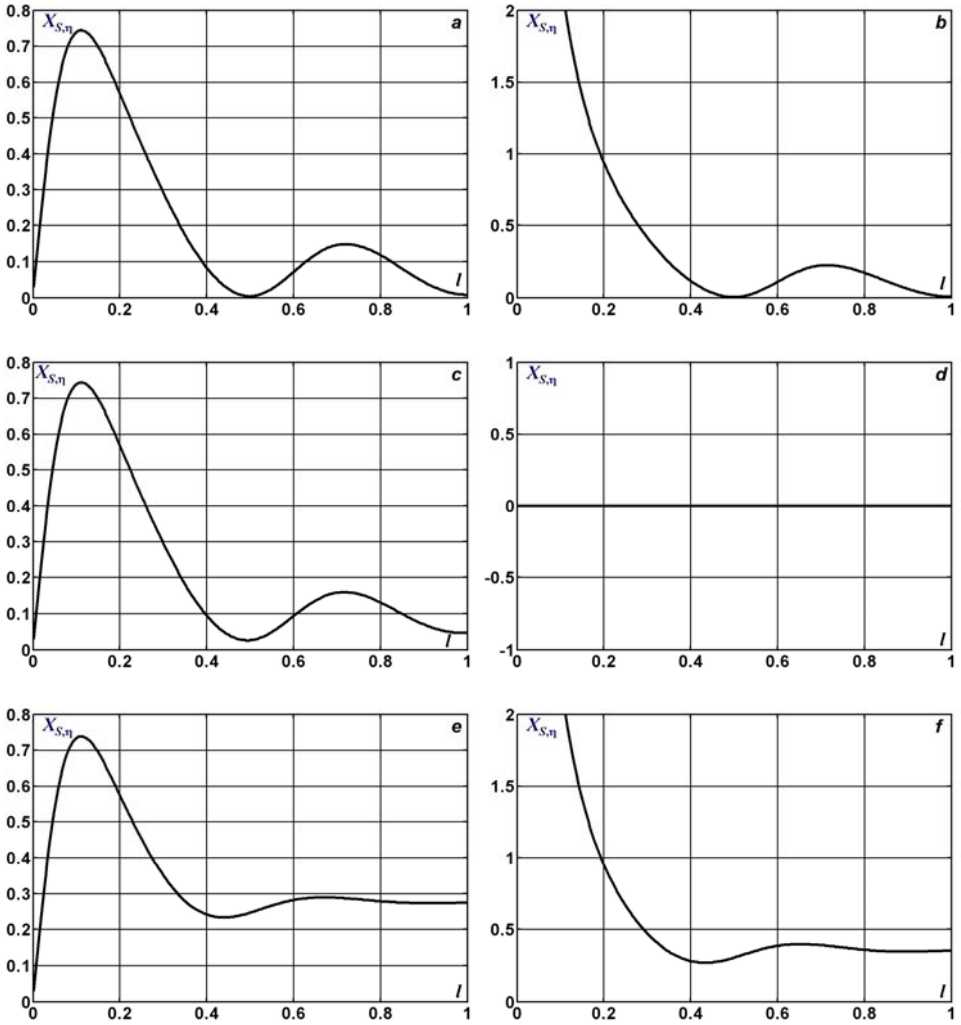

Fig. 13.3. $X_{S,\eta}$ depending on line length when $R_S = Z_B$ and $R = 0.48$, $G = R/5$(***a***); $R = 0.48$, $G = 0$(***b***); $R = 1.205$, $G = R/5$(***c***); $R = G = 1.205$(***d***); $R = 4.8$, $G = R/5$(***e***); $R = 4.8$, $G = 0$(***f***).

The changes of the input resistance for above mentioned variants are represented in the fig. 13.5, where the curve 1 represents the modulus and curve 2 – argument of the complex function. Here we note also that in the vicinity of the point $x = 0.3$ the modulus of the input resistance decreases that results in passing current increasing and then in transmission power increasing.

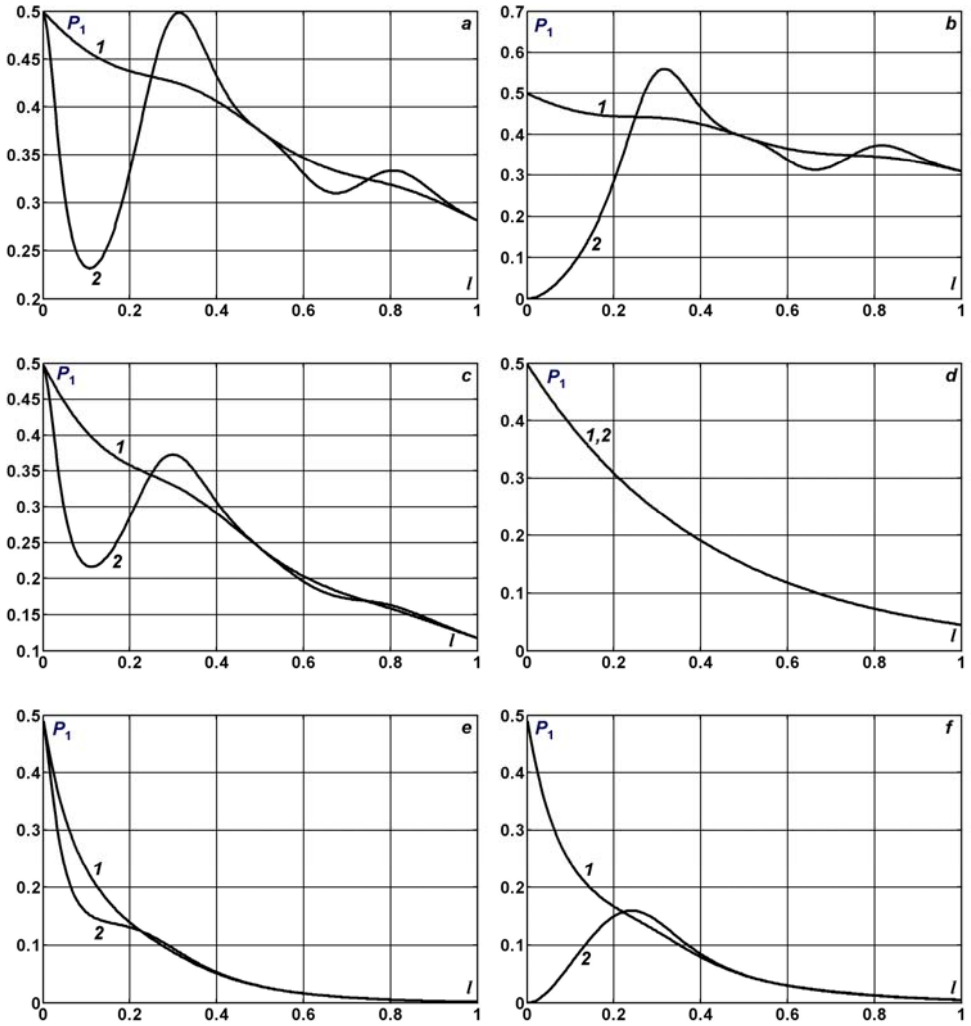

Fig. 13.4. $P_1(X_S = 0)$ (1) and $P_1(X_S = X_{S,\eta})$ (2) depending on line length when $R_S = Z_B$ and $R = 0.48$, $G = R/5$(***a***); $R = 0.48$, $G = 0$(***b***); $R = 1.205$, $G = R/5$(***c***); $R = G = 1.205$(***d***); $R = 4.8$, $G = R/5$(***e***); $R = 4.8$, $G = 0$(***f***).

Let's determine the resistance $X_S = X_{S,k}$, under which the transmission power is maximal. At the same time let's clarify how the efficiency will change. The maximal transmission power depending on the line length is represented in the fig. 13.6. Straight away one can mention that integrally the power can be increased even for undistorting line with the exception of the cases when the load is connected to the receiving ends of the quarter-wave or half-wave lines. The dependence of $X_{S,k}$ on line length here is alter-

nating-sign (see fig. 13.7). The capacitive nature of the reactive resistance ($X_{S,k} < 0$) takes turn to inductive one ($X_{S,k} > 0$) in a parts of line that are equal to 0.25.

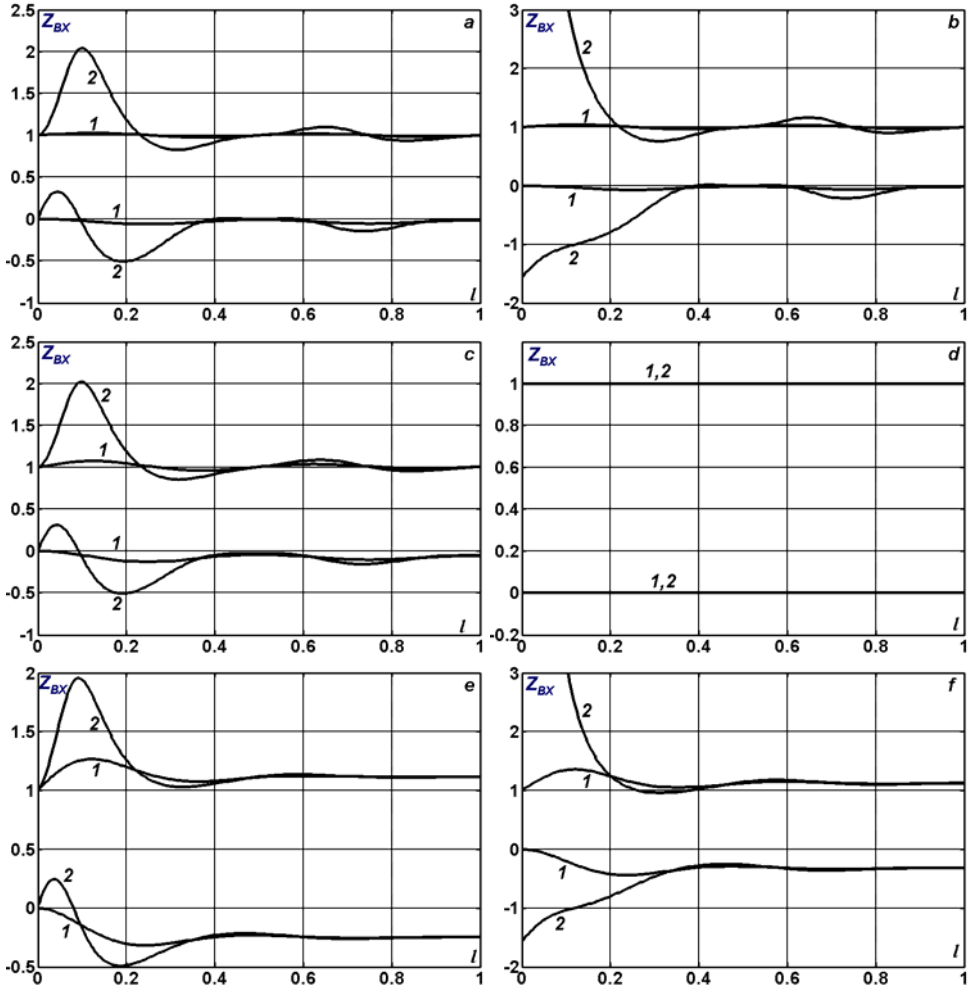

Fig. 13.5. Z_{BX} ($X_S = 0$) (1) and Z_{BX} ($X_S = X_{S,\eta}$) (2) depending on line length when $R_S = Z_B$ and $R = 0.48$, $G = R/5$(***a***); $R = 0.48$, $G = 0$(***b***); $R = 1.205$, $G = R/5$(***c***); $R = G = 1.205$(***d***); $R = 4.8$, $G = R/5$(***e***); $R = 4.8$, $G = 0$(***f***).

The efficiency depending on line length represented in the fig. 13.8 shows that only in the vicinity of the point $x = 0.25$ we can mention its slight increasing. Minimum points at this figure correspond to maximum points in the fig. 13.5. Thus, the maximal increasing of the transmission power always is accompanied by efficiency decreasing (sometimes till the inadmis-

sible down level). The same correlation can be observed at the diagrams represented in the fig. 13.9. Here we have the input resistance Z_{BX} depending on line length.

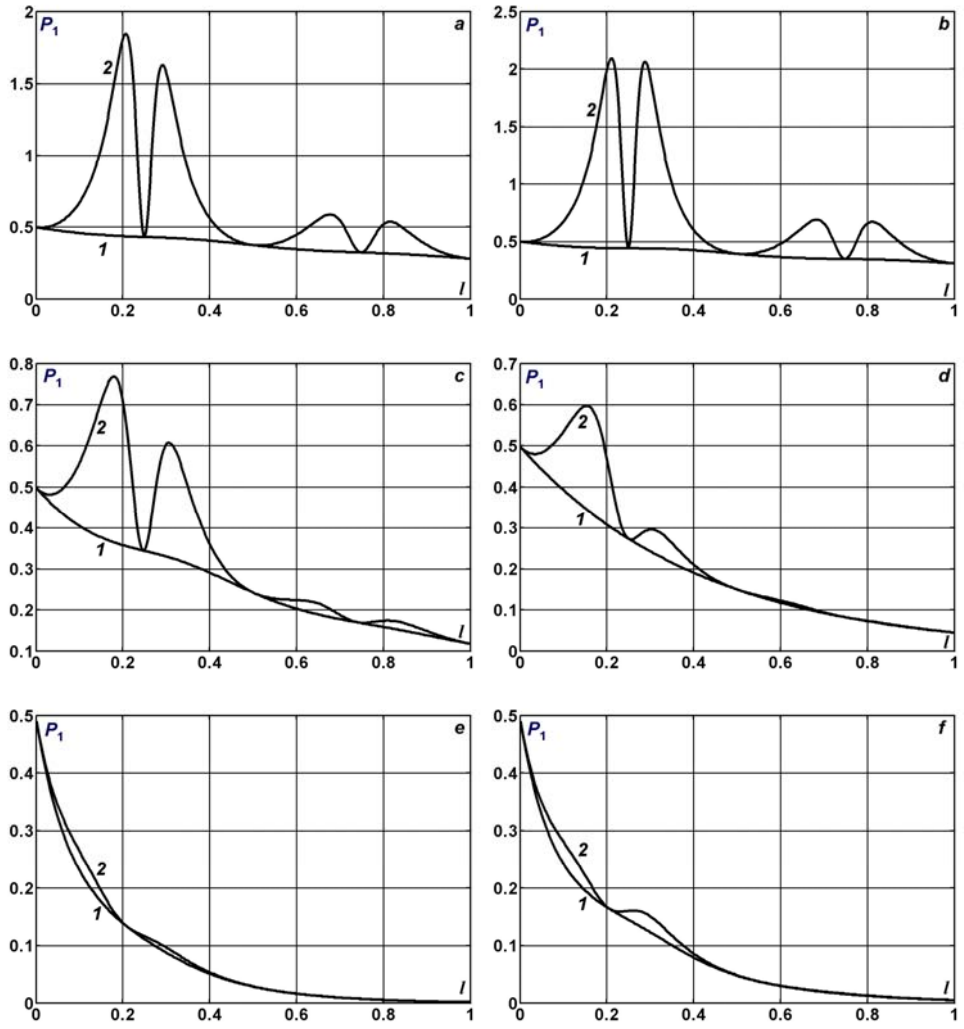

Fig. 13.6. $P_1(X_S = 0)$ (1) and $P_1(X_S = X_{S,k})$ (2) depending on line length when $R_S = Z_B$ and $R = 0.48$, $G = R/5$(***a***); $R = 0.48$, $G = 0$(***b***); $R = 1.205$, $G = R/5$(***c***); $R = G = 1.205$(***d***); $R = 4.8$, $G = R/5$(***e***); $R = 4.8$, $G = 0$(***f***).

To have more complete presentation about possibilities of transmission power increasing with respect to variation of complex load resistance $Z_S = R_S + jX_S$ the contl curves of the function $P_1(z, X_S)$ are shown in the fig. 13.10

for different segments of the line length. Let's remind that $z = (R_S - Z_B)/(R_S + Z_B)$. Analyzing the represented results we can conclude that the pure active load connected to the quarter-wave or to half-wave line can not be compensated in such a way as to increase the power in it.

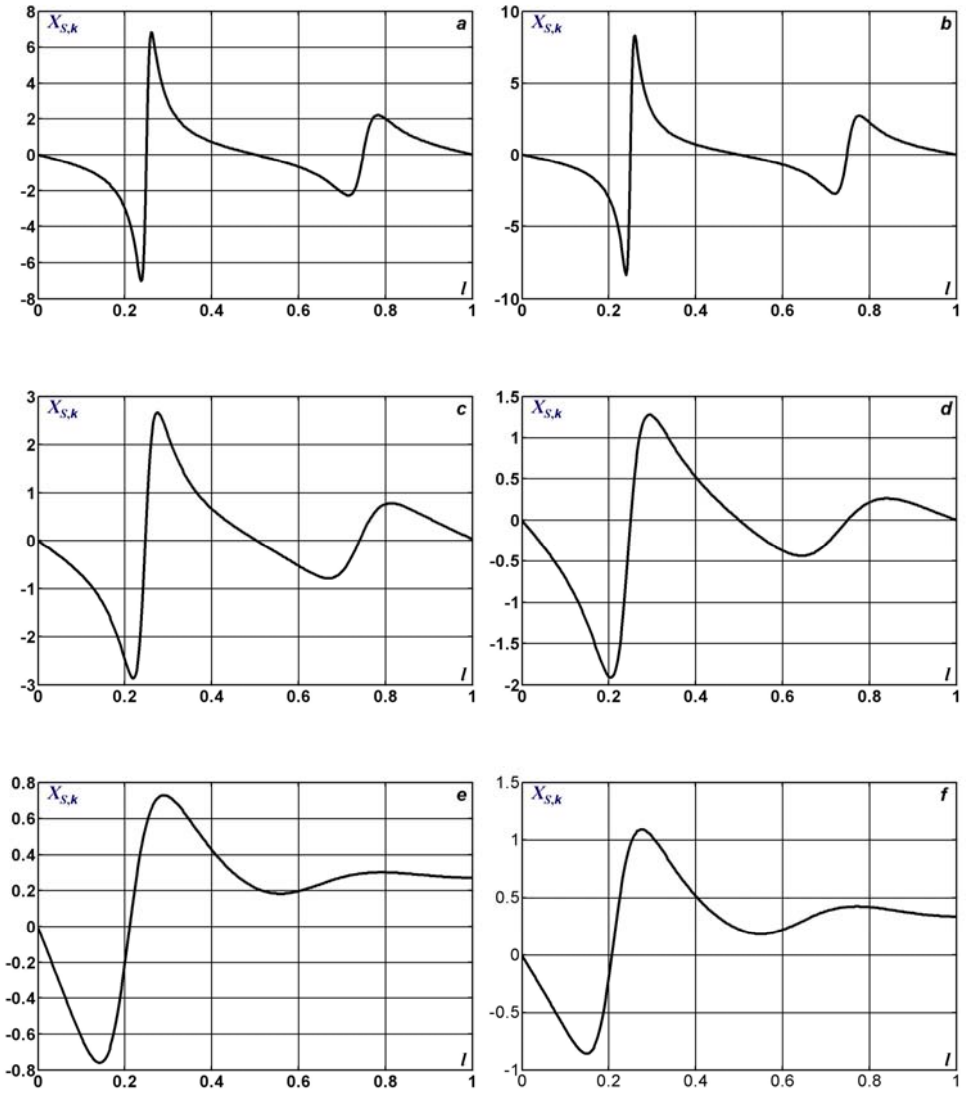

Fig. 13.7. $X_{S,k}$ depending on line length when $R_S = Z_B$ and $R = 0.48$, $G = R/5$(***a***); $R = 0.48$, $G = 0$(***b***); $R = 1.205$, $G = R/5$(***c***); $R = G = 1.205$(***d***); $R = 4.8$, $G = R/5$(***e***); $R = 4.8$, $G = 0$(***f***).

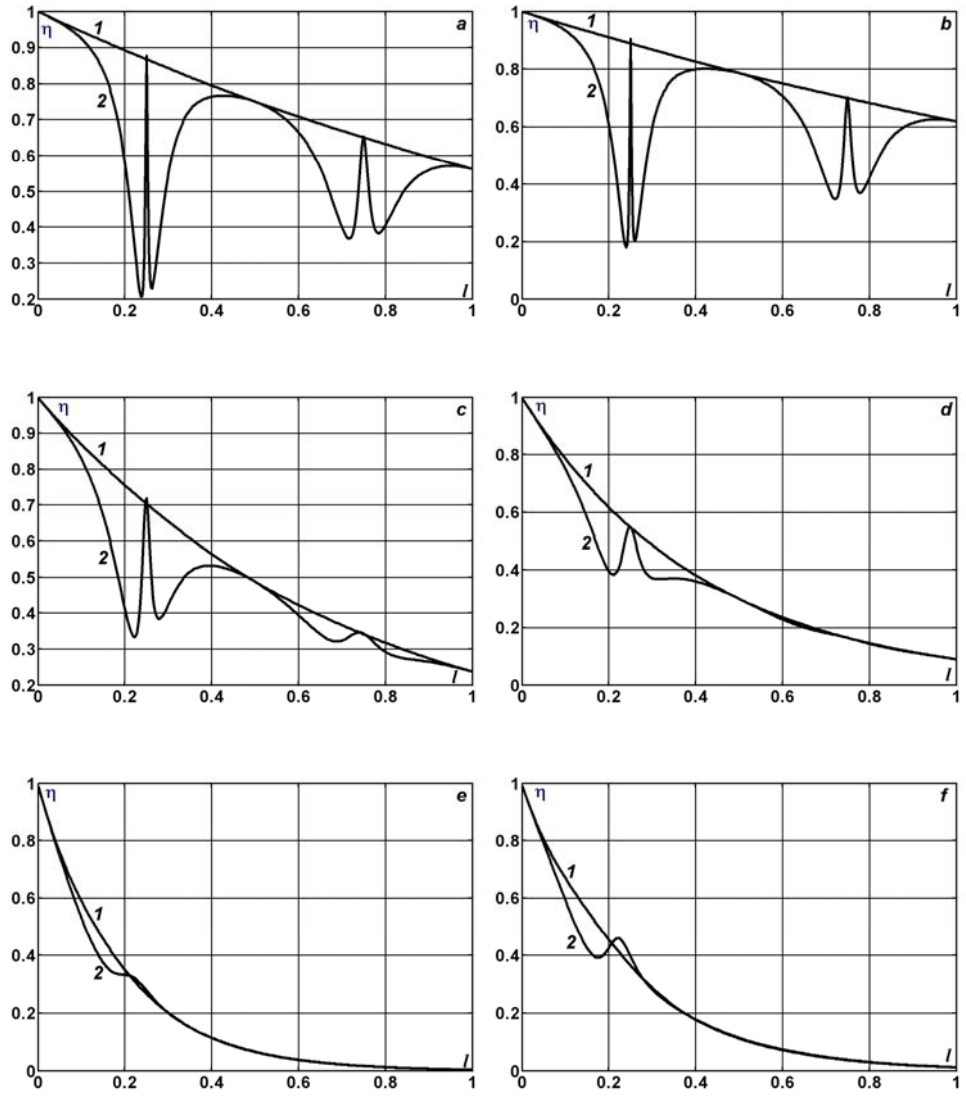

Fig. 13.8. $\eta(X_S = 0)$ (1) and $\eta(X_S = X_{S,k})$ (2) depending on line length when $R_S = Z_B$ and $R = 0.48$, $G = R/5$(***a***); $R = 0.48$, $G = 0$(***b***); $R = 1.205$, $G = R/5$(***c***); $R = G = 1.205$(***d***); $R = 4.8$, $G = R/5$(***e***); $R = 4.8$, $G = 0$(***f***).

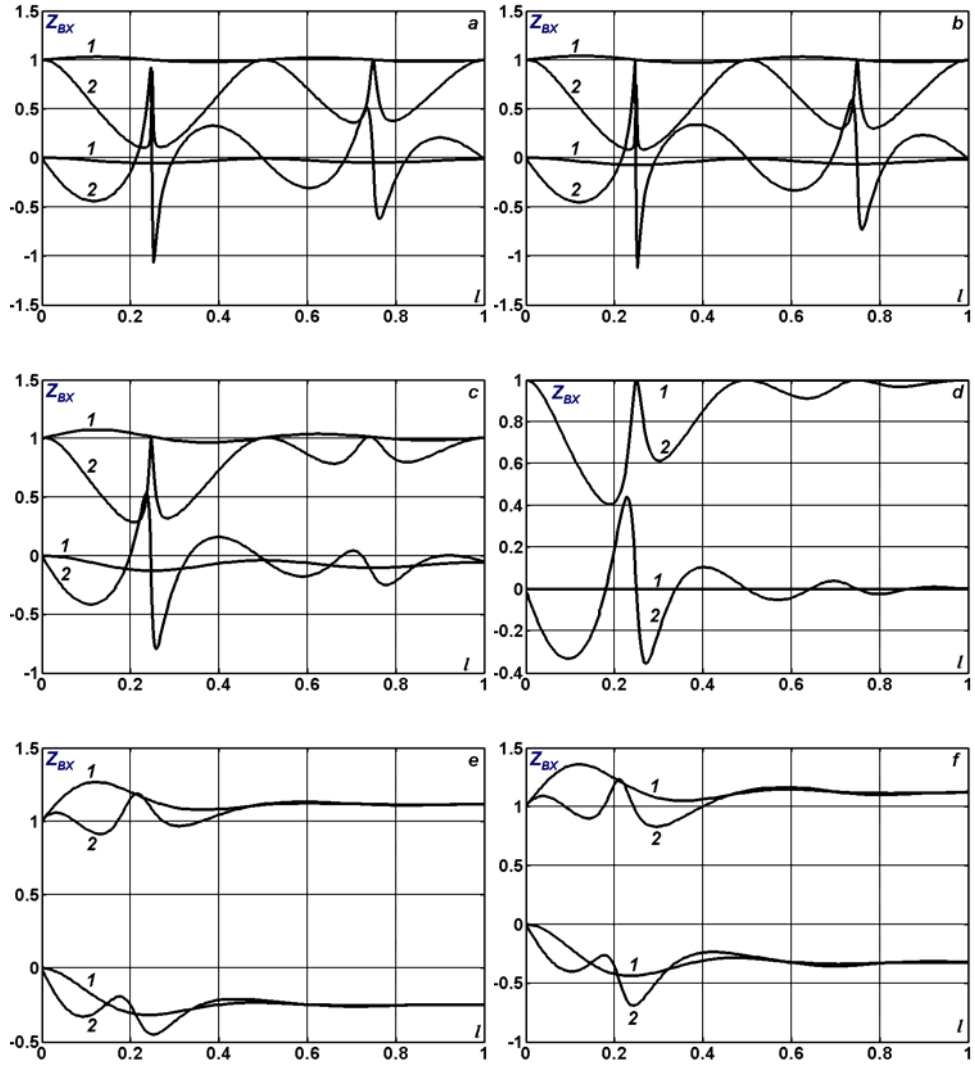

Fig. 13.9. Z_{BX} ($X_S = 0$) (1) and Z_{BX} ($X_S = X_{S,k}$) (2) depending on line length when $R_S = Z_B$ and $R = 0.48$, $G = R/5$(***a***); $R = 0.48$, $G = 0$(***b***); $R = 1.205$, $G = R/5$(***c***); $R = G = 1.205$(***d***); $R = 4.8$, $G = R/5$(***e***); $R = 4.8$, $G = 0$(***f***).

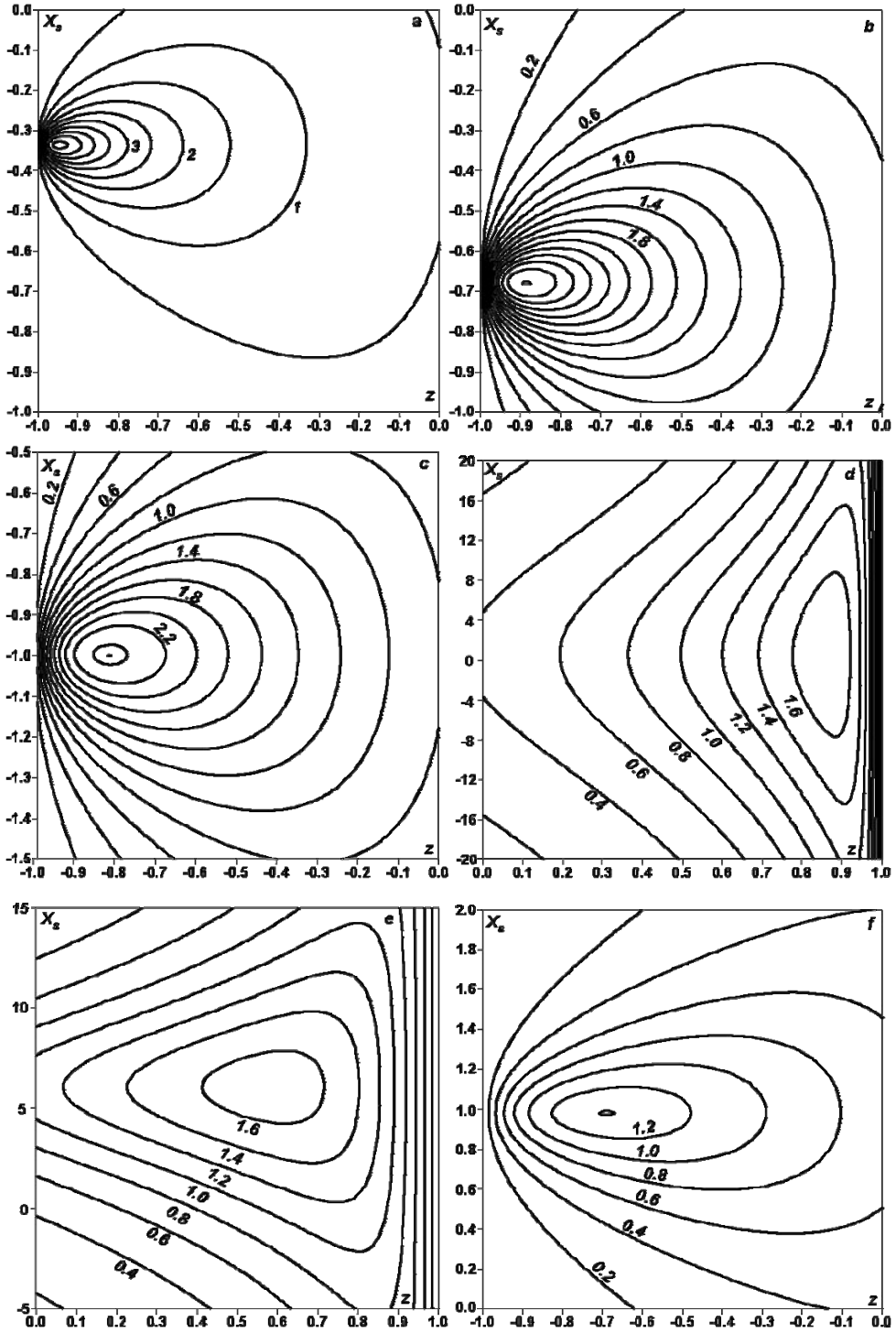
a
b
c
d
e
f
z

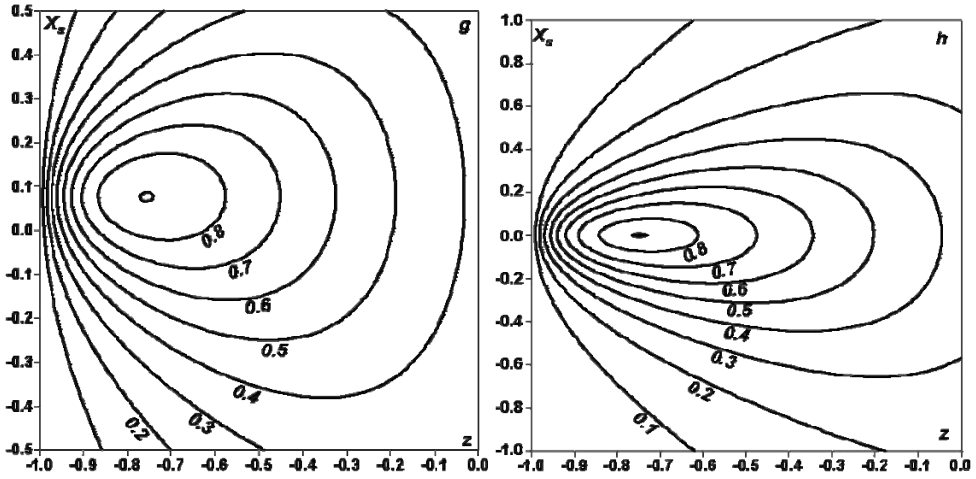

Fig. 13.10. Transmission power depending on complex load resistance when R = 0.48, $G = R/5$; l = 0.0516 (***a***);0.0949 (***b***); 0.125 (***c***); 0.25(***d***); 0.2684(***e***); 0.375(***f***); 0.488(***g***); 0.5(***h***).

14. Line parameters longitudinal compensation

Let's formulate the problem with the similar nature (see previous section): how to compensate the parameters of the line with pure active load at the receiving end for the purpose of increasing the efficiency and the transmission power simultaneously?

Let the reactive power source with complex resistance $Z_n = R_n + jX_n$ (see fig.14.1) is connected to the line cleaving at the point $x = l_n$. Then the steady-state regime equations in hyperbolic functions (1.5) take the form

$$Z_S = R_S + j\left(\omega L_S - \frac{1}{\omega C_S}\right) = R_S + jX_S;$$

$$Z_{BX} = Z_0 \frac{Z_S \mathrm{ch}(\delta l) + Z_0 \mathrm{sh}(\delta l) + \dfrac{Z_n}{Z_0}\mathrm{ch}(\delta l_n) B_n}{Z_S \mathrm{sh}(\delta l) + Z_0 \mathrm{ch}(\delta l) + \dfrac{Z_n}{Z_0}\mathrm{sh}(\delta l_n) B_n} = Z_0 \frac{A + Z_n B}{\widetilde{A} + Z_n \widetilde{B}};$$

$$B_n = Z_S \mathrm{sh}\delta(l - l_n) + Z_0 \mathrm{ch}\delta(l - l_n);$$

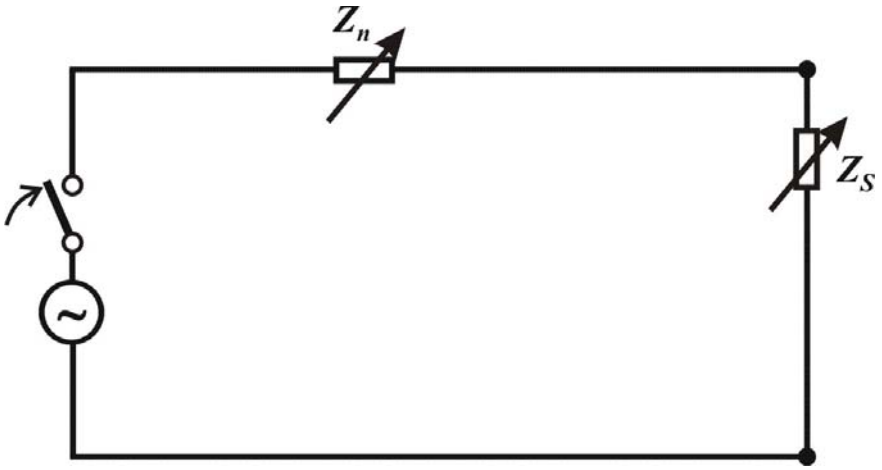

Fig. 14.1. The alternating voltage line with pure active load R_S at the receiving end and the reactive load X_n, connected to the line cleaving.

$$A = Z_S \mathrm{ch}(\delta l) + Z_0 \mathrm{sh}(\delta l);\ \widetilde{A} = Z_S \mathrm{sh}(\delta l) + Z_0 \mathrm{ch}(\delta l);$$

$$B = \frac{\mathrm{ch}(\delta l_n)}{Z_0} B_n;\ \ \widetilde{B} = \frac{\mathrm{sh}(\delta l_n)}{Z_0} B_n;$$

$$U_0 = Z_{BX} I_0; U_1 = Z_S I_1; U_n = Z_n I_n; U_n = U_n^- - U_n^+; \qquad (14.1)$$

$$I_n = U_0 \left(\frac{\mathrm{ch}(\delta l_n)}{Z_{BX}} - \frac{\mathrm{sh}(\delta l_n)}{Z_0} \right);$$

$$I_1 = \frac{Z_0 I_n}{Z_S \mathrm{sh}\delta(l - l_n) + Z_0 \mathrm{ch}\delta(l - l_n)} = \frac{U_0}{A + Z_n B}.$$

Let's consider the case when $Z_S = R_S = Z_B$ and $R_n = 0$, $Z_n = jX_n$. Then the load active power can be written as follows

$$P_1 = \frac{1}{2} \mathrm{Re}\left(U_1 I_1^*\right) = \frac{Z_B}{2} I_1 I_1^* = \frac{Z_B U_0^2}{2(A + Z_n B)(A + Z_n B)^*}. \qquad (14.2)$$

As to determine the values of the compensating load $Z_n = jX_n$ and its location l_n (the values that ensure the maximal active power $P_{1,k}$ values), we are to solve the system of two equations

$$\frac{\partial P_1(X_n, l_n)}{\partial X_n} = 0, \quad \frac{\partial P_1(X_n, l_n)}{\partial l_n} = 0 .$$

These equations after differentiation and some simplifications take the form

$$X_n |B|^2 - \mathrm{Im}(BA^*) = 0, \quad \mathrm{Im}\left[\frac{\partial B}{\partial l_n} (A + Z_n B)^* \right] = 0 . \qquad (14.3)$$

From the first equation now we obtain the explicit expression for optimal value of the X_n depending on the parameter l_n:

$$X_n = \frac{\mathrm{Im}(BA^*)}{|B|^2} . \qquad (14.4)$$

Substituting this expression in the second equation we obtain the transcendental equation with respect to unknown l_n

$$\mathrm{Im}\left[\frac{\partial B}{\partial l_n} \left(A^* - \frac{j\,\mathrm{Im}(BA^*)}{|B|^2} B^* \right) \right] = \mathrm{Re}(AB^*)\,\mathrm{Im}\left[\frac{1}{B} \frac{\partial B}{\partial l_n} \right] = 0 .$$

Taking into account that $\mathrm{Re}(AB^*) \neq 0$, we can write down

$$\mathrm{Im}\left[\frac{1}{B} \frac{\partial B}{\partial l_n} \right] = \mathrm{Im}\left[\frac{\delta}{\mathrm{ch}(\delta l_n)} \frac{Z_S \mathrm{ch}\delta(2l_n - l) - Z_0 \mathrm{sh}\delta(2l_n - l)}{Z_S \mathrm{sh}\delta(l - l_n) + Z_0 \mathrm{ch}\delta(l - l_n)} \right] = 0 . \qquad (14.5)$$

Thus, to calculate the maximal value P_1 it is necessary to determine the value $l_{n,k}$ as a solution of the nonlinear equation (14.5). Than from the relation (14.4) we can determine the optimal value $X_{n,k}$ and from (14.2) – the maximal value $P_{1,k}$.

Let's note that the equation (14.5) possesses several roots. The values of these roots give only extreme values (i.e. maximal and minimal) of P_1. Therefore we are to find all roots of the equation (14.5) at first and then to choose the value of the root $l_{n,k}$, that ensure the global maximum of the P_1.

Now we will consider the problem of determination of the maximal value η of the efficiency and of the transmission power. The efficiency can be represented in the following form:

$$\eta = \frac{P_1}{P_0} = \frac{\mathrm{Re}\left(U_1 I_1^*\right)}{\mathrm{Re}\left(U_0 I_0^*\right)} = \frac{Z_B I_1 I_1^*}{U_0^2 \,\mathrm{Re}(1/Z_{BX})} =$$

$$= \frac{Z_B |Z_0|^2}{\mathrm{Re}\left[Z_0 (A + jX_n B)(\widetilde{A} + jX_n \widetilde{B})^*\right]}. \qquad (14.6)$$

As to determine the values of the compensating load $Z_n = jX_n$ and its location l_n (the values that ensure the maximal active power $P_{1,k}$ values), we are to solve the system of two equations

$$\frac{\partial \eta(X_n, l_n)}{\partial X_n} = 0, \quad \frac{\partial \eta(X_n, l_n)}{\partial l_n} = 0.$$

These equations after differentiation and some simplifications take the form

$$2\,\mathrm{Re}\left(Z_0 B \widetilde{B}^*\right) X_n - \mathrm{Im}\left[Z_0 (B\widetilde{A}^* - \widetilde{B}^* A)\right] = 0;$$

$$\mathrm{Re}\left\{ Z_0 \left[X_n \frac{\partial (B\widetilde{B}^*)}{\partial l_n} + j\left(\widetilde{A}^* \frac{\partial B}{\partial l_n} - A \frac{\partial \widetilde{B}^*}{\partial l_n} \right) \right] \right\} = 0. \qquad (14.7)$$

From the first equation now we obtain the explicit expression for optimal value of the X_n depending on the distance l_n:

$$X_n = \frac{\mathrm{Im}\left[Z_0 (\widetilde{A}^* B - A \widetilde{B}^*)\right]}{2\,\mathrm{Re}\left(Z_0 B \widetilde{B}^*\right)}. \qquad (14.8)$$

Substituting this expression in the second equation we obtain the transcendental equation with respect to unknown l_n

$$\mathrm{Re}\left\{ Z_0 \left[\frac{\mathrm{Im}\left[Z_0 (\widetilde{A}^* B - A\widetilde{B}^*) \right]}{2\,\mathrm{Re}\left(Z_0 B \widetilde{B}^* \right)} \frac{\partial (B\widetilde{B}^*)}{\partial l_n} + j \left(\widetilde{A}^* \frac{\partial B}{\partial l_n} - A \frac{\partial \widetilde{B}^*}{\partial l_n} \right) \right] \right\} = 0 . \qquad (14.9)$$

Thus, to calculate the maximal value η it is necessary to determine the value $l_{n,\eta}$ as a solution of the nonlinear equation (14.9). Then from the relation (14.8) we can determine the optimal value $X_{n,\eta}$ and from (14.6) – the maximal value η.

Let's note that the equation (14.8) possesses several roots. The values of these roots give only extreme values (i.e. maximal and minimal) of η. Therefore we are to find all roots of the equation (14.9) at first and then to choose the value of the root $l_{n,\eta}$, that ensure the global maximum of the η.

On the basis of obtained exact solutions let's carry out the parametrical analysis of the considered circuit with pure active load $R_S = Z_B$ under the variation of the line lineal parameters R, G and its length. It seems to be of fundamental importance the fact, that efficiency increasing due to the longitudinal compensation is possible only for the lines with wave dispersion (see fig. 14.2). As it follows from diagrams in the fig. 14.2, *b, f,* the increasing of the efficiency of the line with compensated reactive parameters is so much the better when the dispersion is greater. In case when there is only the wave dissipation in the line, the effect of efficiency increasing is not to be observed at all (see fig. 14.2, *d*).

The diagrams in fig. 14.3 show that the reactive resistance of the reactive power sources is positive and so it has purely inductive nature. The absence of the leakage current through the insulation changes quite greatly the nonlinear dependence of the compensating element reactive resistance on line length (see fig. 14.3, *b, f*).

The information about the location of the reactive power sources depending on the line length is represented in the fig. 14.4. The coordinate of the optimal reactive power source connection at the interval $l/\lambda < (0.15\text{-}0.2)$ represents the linear function, but it can hardly be said about the transmission power.

The diagrams in the fig. 14.5 give the negative answer for the main question relative to transmission power increasing by means of inductive element (that increases the efficiency) connected to the line. The power de-

creases in all considered cases and in case of short lines with great dispersion it decreases till inadmissible down level (see fig. 14.5 *b, f*).

The diagrams in the fig. 14.6 give the idea about input resistance of the compensated electrical circuit depending on the line length. The curves 1 and 3 represent the modules but curves 2 and 4 – the arguments of the complexes. The fluctuations of the input resistance become progressively less when line length increases.

Now let's increase the transmission power to the limit value for every line interval and study the efficiency in these cases. The curves 2 in the fig. 14.7 correspond to the series reactive power source as before. For line with small losses the transmission power can be increased approximately in 4 times (see fig. 17, *a, b*). For undistorting line this increasing is double. But when the losses are sufficiently great, the difference between these considered cases becomes insignificant.

How it was to be expected, the reactive power source has a capacitance nature because its reactive resistance is negative for any line length ($X_{n,\eta}<0$). The presence of the leakage current through the insulation does not influence so greatly as in case of inductive reactive power source connected to the line (see fig. 14.8).

It is interesting to observe the $l_{n,k}$ depending on the line length (see fig. 14.9). For short lines the optimal location changes by linear low, then it becomes stabilized at constant level.

The transmission power increasing is accompanied by efficiency decreasing. For the lines with relatively small losses the efficiency decreases approximately in 2 times, but under the rise of the losses this decreasing becomes not so evident (see fig. 14.10).

The diagrams of the electrical circuit input resistance depending on the length l are represented in the fig. 14.11. The longitudinal capacity connection stipulates for input resistance decreasing and transmission power increasing. This effect comes out under the capacity connection to any point of the long line, but we obtain different values of the transmission power increasing even under the optimal value of the parameter X_n.

The effect of the transmission power increasing is possible as well under the longitudinal connection of the inductance, but only at the points distant from the sending end more than on the distance equal to $\lambda/4$ (see fig. 14.12-14.16). The efficiency in this case is always less in comparison with homogeneous line. The efficiency becomes especially small for lines with length closed to the quarter-wave line.

The contl curves for maximal values of the transmission power and for efficiency depending on the value and on the location of the longitudinal

compensation X_n in the line with the length $l = \lambda$ are represented in the fig. 14.17 and 14.18.

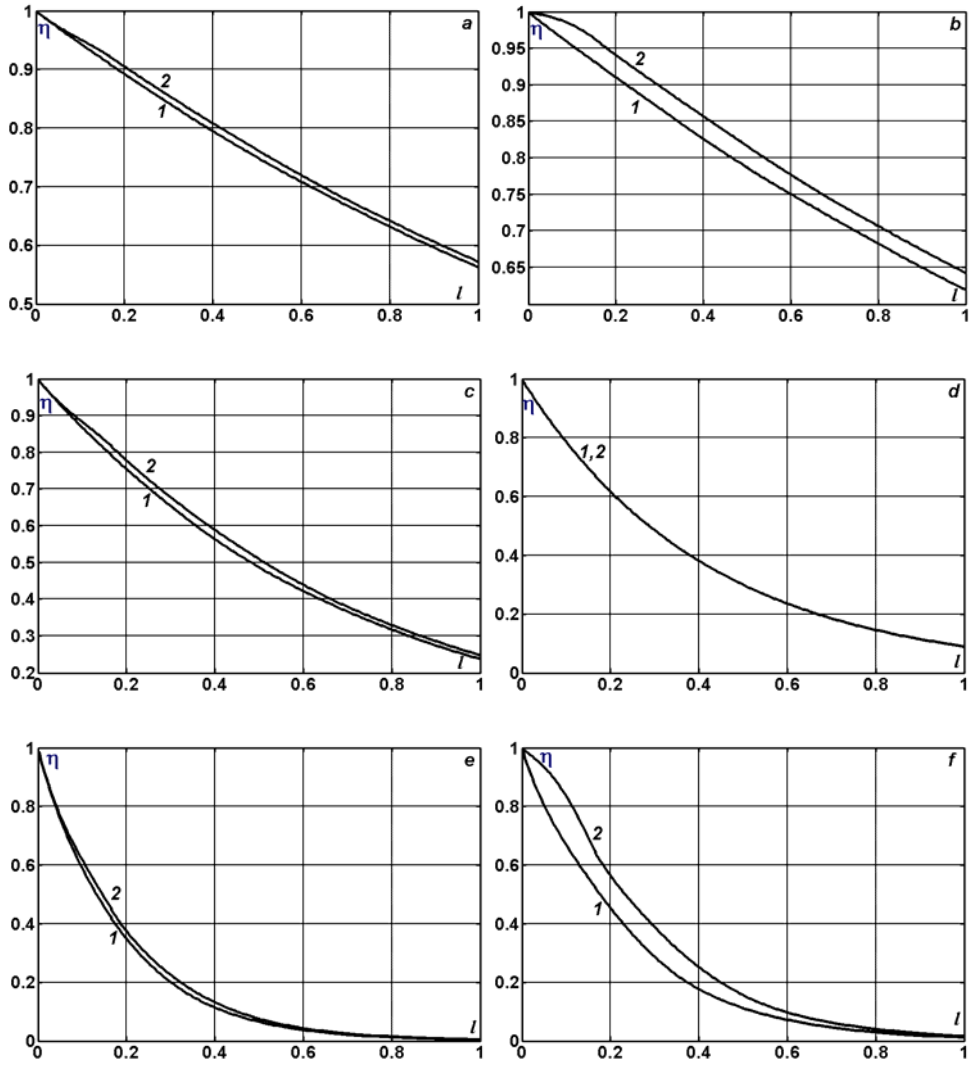

Fig. 14.2. $\eta(X_n = 0)$ (1) and η $(X_n = X_{n,\eta})$ (2) depending on the line length when $R_S = Z_B$ and $R = 0.48$, $G = R/5$(***a***); $R = 0.48$, $G = 0$(***b***); $R = 1.205$, $G = R/5$(***c***); $R = G = 1.205$(***d***); $R = 4.8$, $G = R/5$(***e***); $R = 4.8$, $G = 0$(***f***).

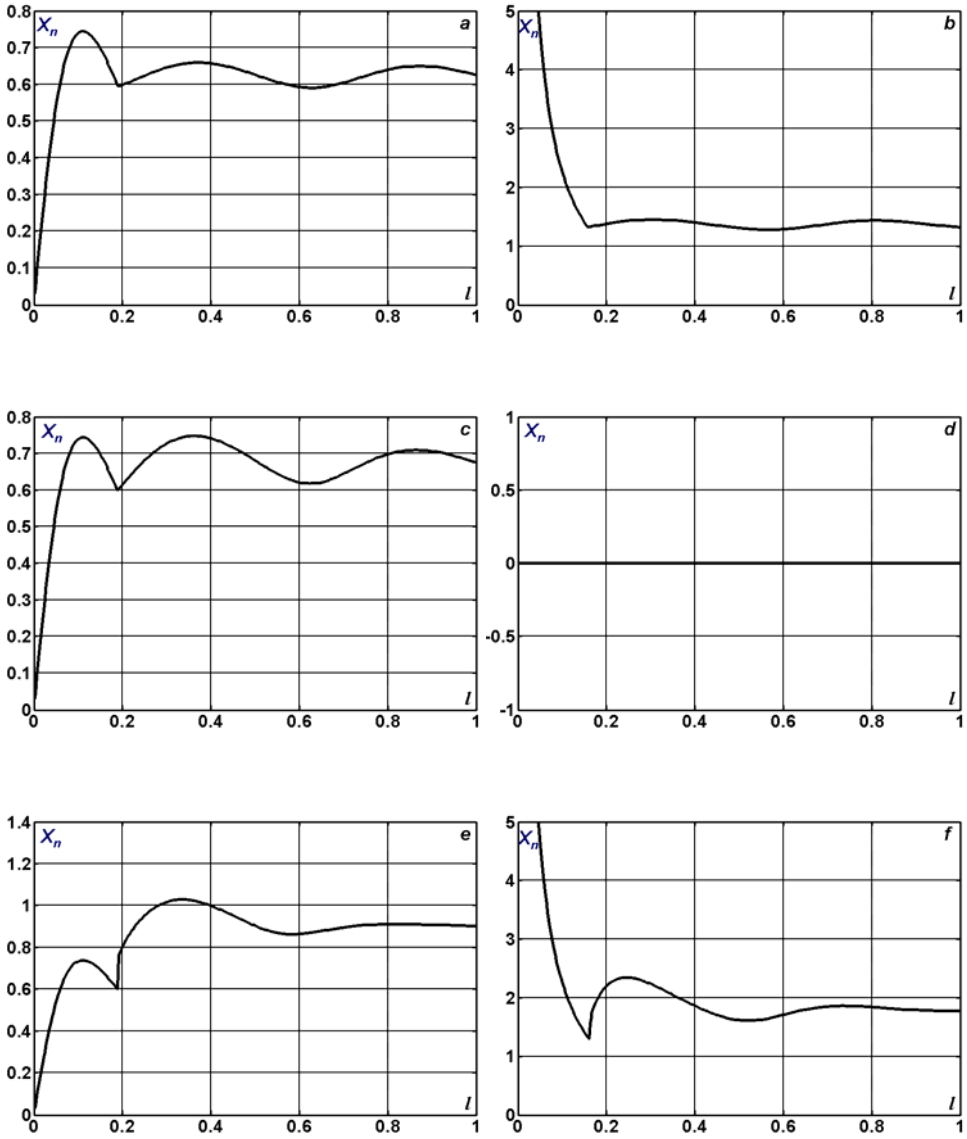

Fig. 14.3. $X_{n,\eta}$ depending on the line length when $R_S = Z_B$ and $R = 0.48$, $G = R/5$(***a***); $R = 0.48$, $G = 0$(***b***); $R = 1.205$, $G = R/5$(***c***); $R = G = 1.205$(***d***); $R = 4.8$, $G = R/5$(***e***); $R = 4.8$, $G = 0$(***f***).

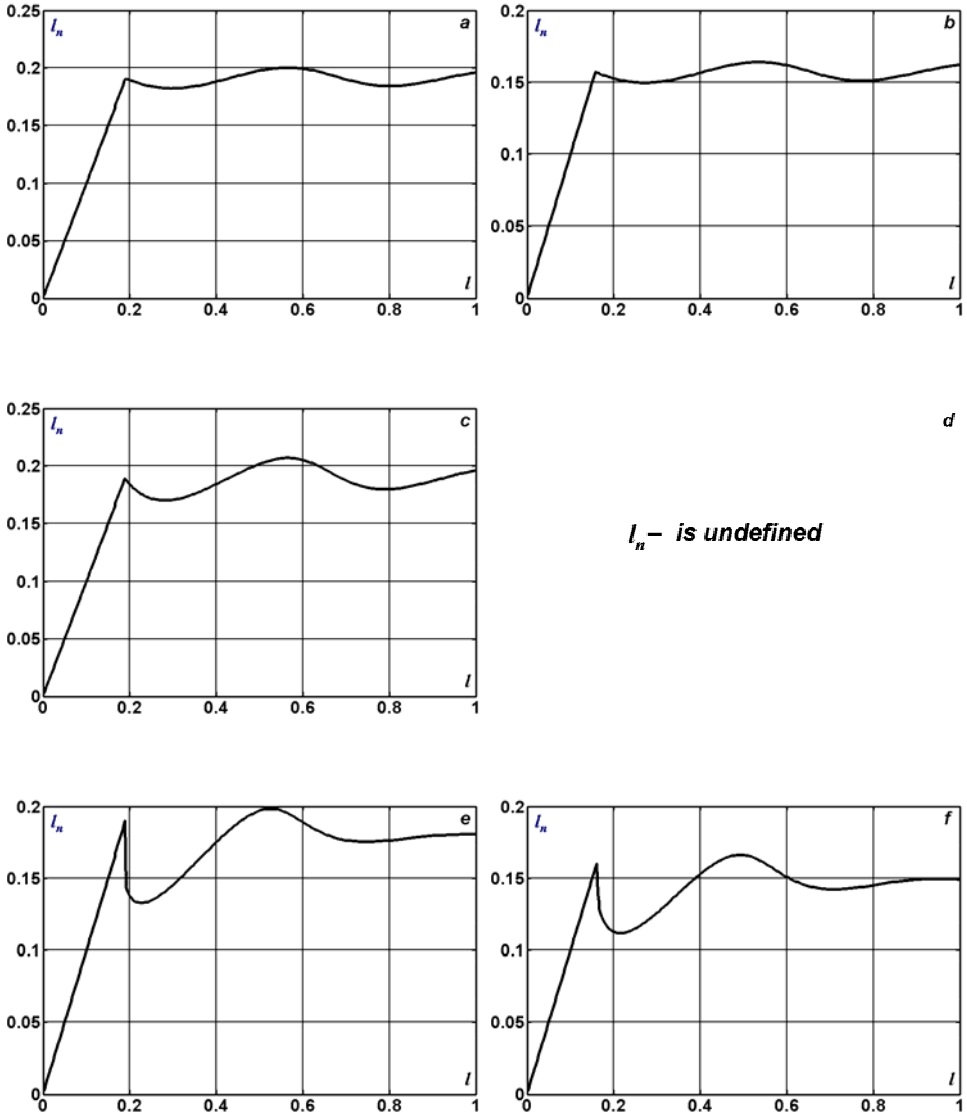

Fig. 14.4. $l_{n,\eta}$ depending on the line length when $R_S = Z_B$ and $R = 0.48$, $G = R/5$(***a***); $R = 0.48$, $G = 0$(***b***); $R = 1.205$, $G = R/5$(***c***); $R = G = 1.205$(***d***); $R = 4.8$, $G = R/5$(***e***); $R = 4.8$, $G = 0$(***f***).

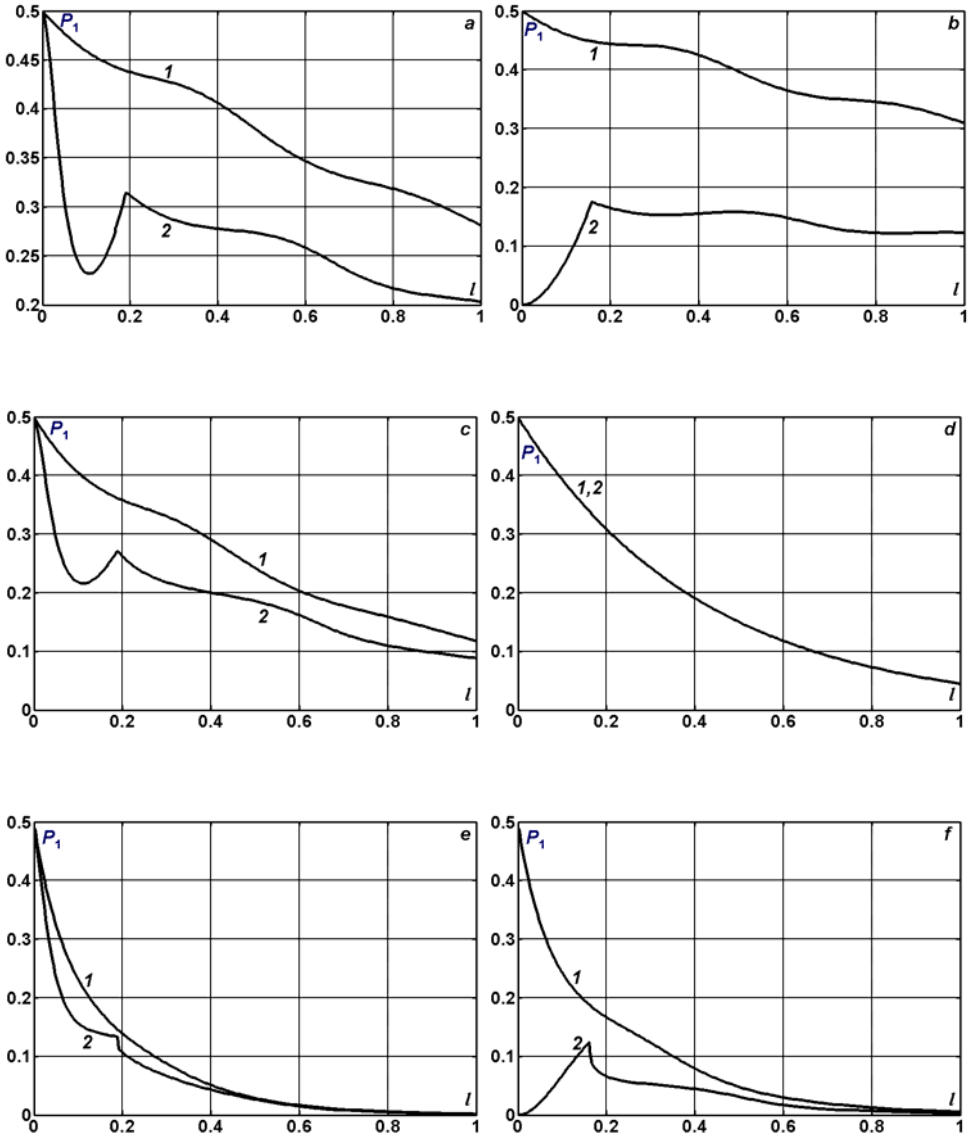

Fig. 14.5. $P1(X_n = 0)$ (1) and $P1(X_n = X_{n,\eta})$ (2) depending on the line length when $R_S = Z_B$ and $R = 0.48$, $G = R/5$(***a***); $R = 0.48$, $G = 0$(***b***); $R = 1.205$, $G = R/5$(***c***); $R = G = 1.205$(***d***); $R = 4.8$, $G = R/5$(***e***); $R = 4.8$, $G = 0$(***f***).

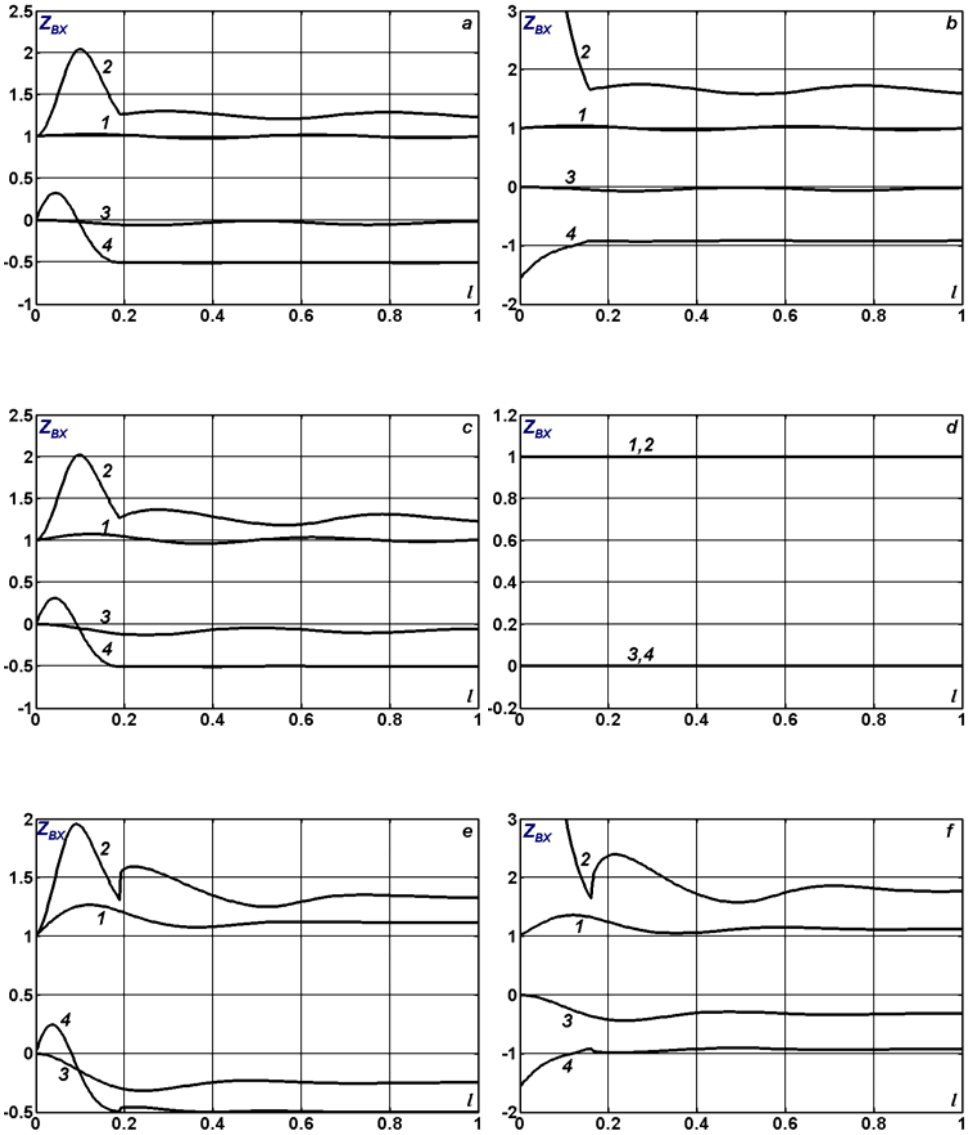

Fig. 14.6. $|Z_{BX}|$ (1), $\arg(Z_{BX})$ (3) ($X_n = 0$) and $|Z_{BX}|$ (2), $\arg(Z_{BX})$ (4) ($X_n = X_{n\eta}$) depending on the line length when $R_S = Z_B$ and $R = 0.48$, $G = R/5$(***a***); $R = 0.48$, $G = 0$(***b***); $R = 1.205$, $G = R/5$(***c***); $R = G = 1.205$(***d***); $R = 4.8$, $G = R/5$(***e***); $R = 4.8$, $G = 0$(***f***).

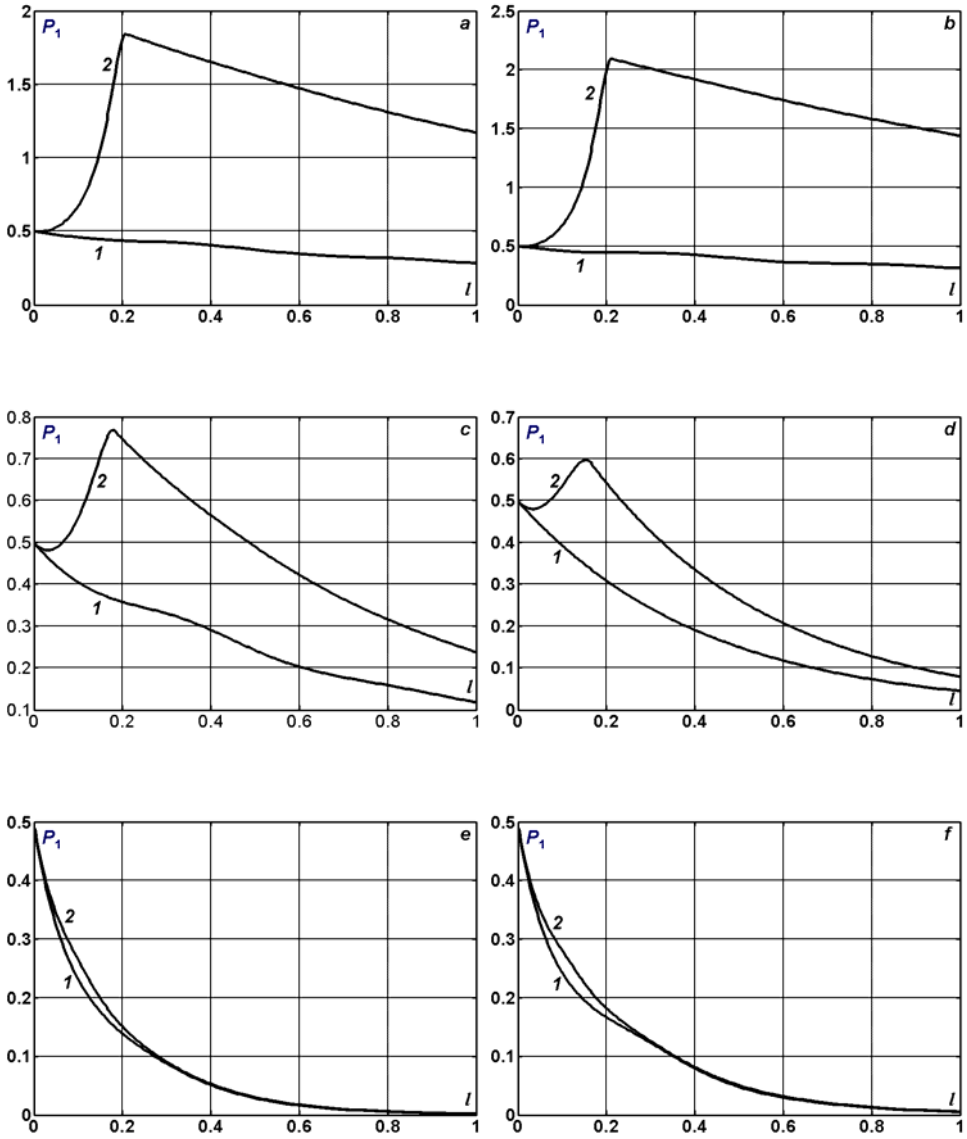

Fig. 14.7. $P1(X_n = 0)$ (1) and $P1(X_n = X_{n,\mathbf{k}} < 0)$ (2) depending on the line length when $R_S = Z_B$ and $R = 0.48$, $G = R/5$(***a***); $R = 0.48$, $G = 0$(***b***); $R = 1.205$, $G = R/5$(***c***); $R = G = 1.205$(***d***); $R = 4.8$, $G = R/5$(***e***); $R = 4.8$, $G = 0$(***f***).

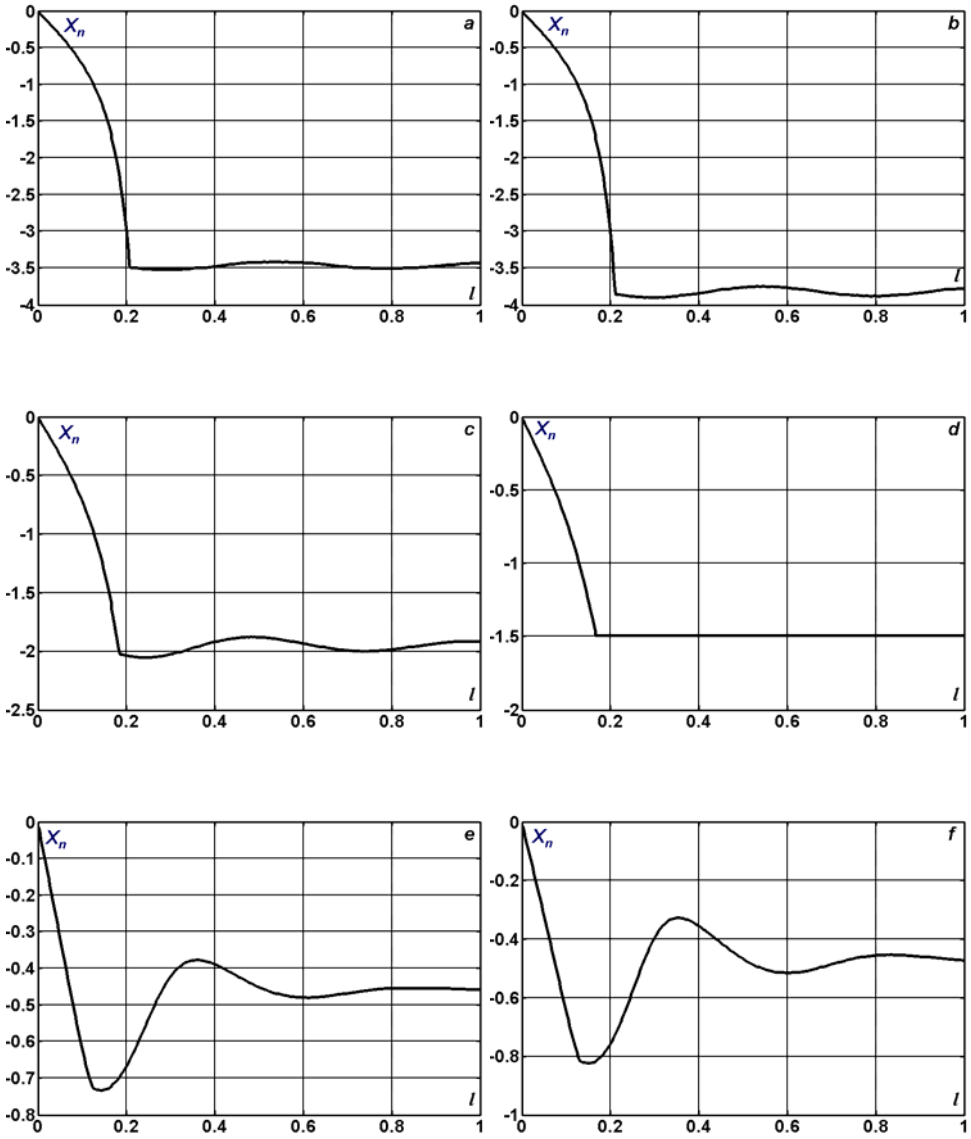

Fig. 14.8. $X_{n,k}<0$ depending on the line length when $R_S = Z_B$ and $R = 0.48$, $G = R/5$(***a***); $R = 0.48$, $G = 0$(***b***); $R = 1.205$, $G = R/5$(***c***); $R = G = 1.205$(***d***); $R = 4.8$, $G = R/5$(***e***); $R = 4.8$, $G = 0$(***f***).

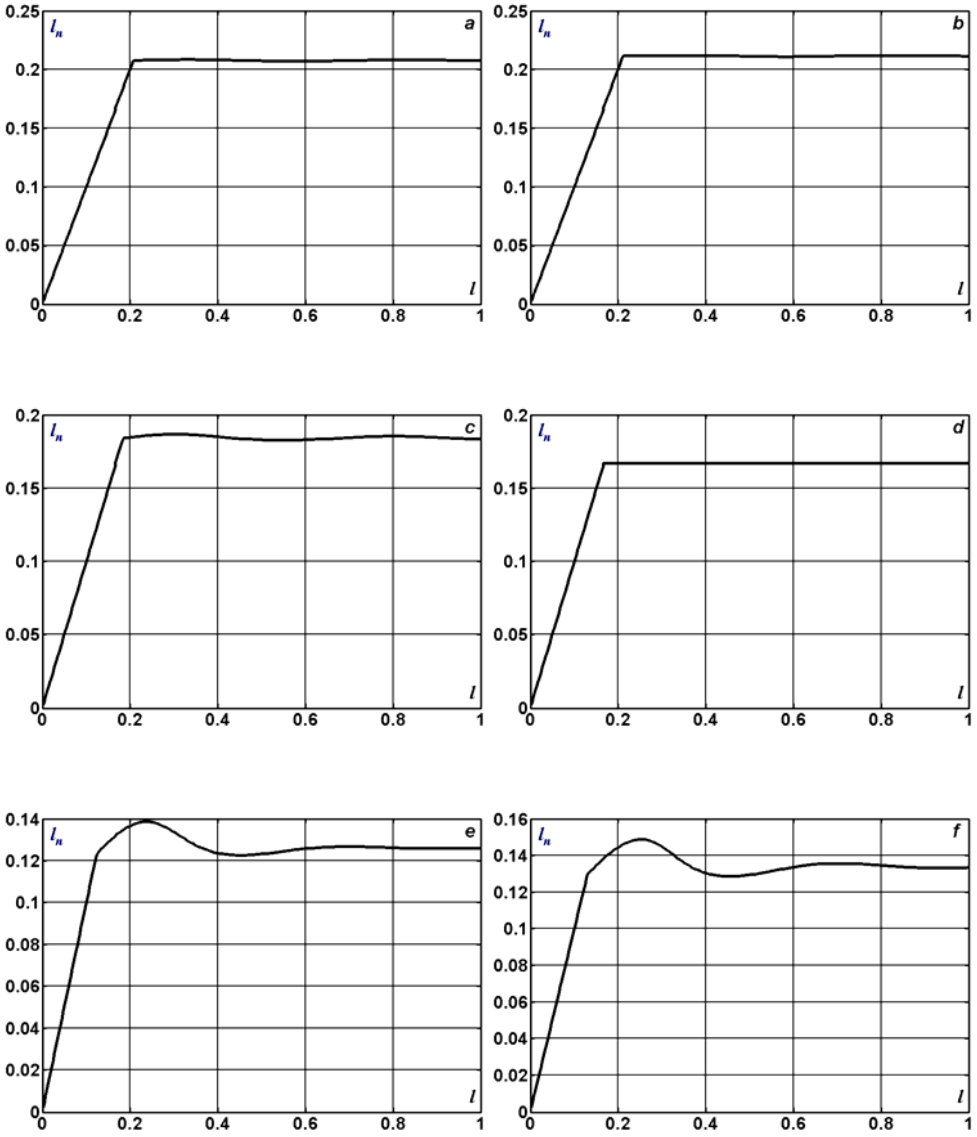

Fig. 14.9. $l_{n,k}$ depending on the line length when $R_S = Z_B$ and $R = 0.48$, $G = R/5$(***a***); $R = 0.48$, $G = 0$(***b***); $R = 1.205$, $G = R/5$(***c***); $R = G = 1.205$(***d***); $R = 4.8$, $G = R/5$(***e***); $R = 4.8$, $G = 0$(***f***).

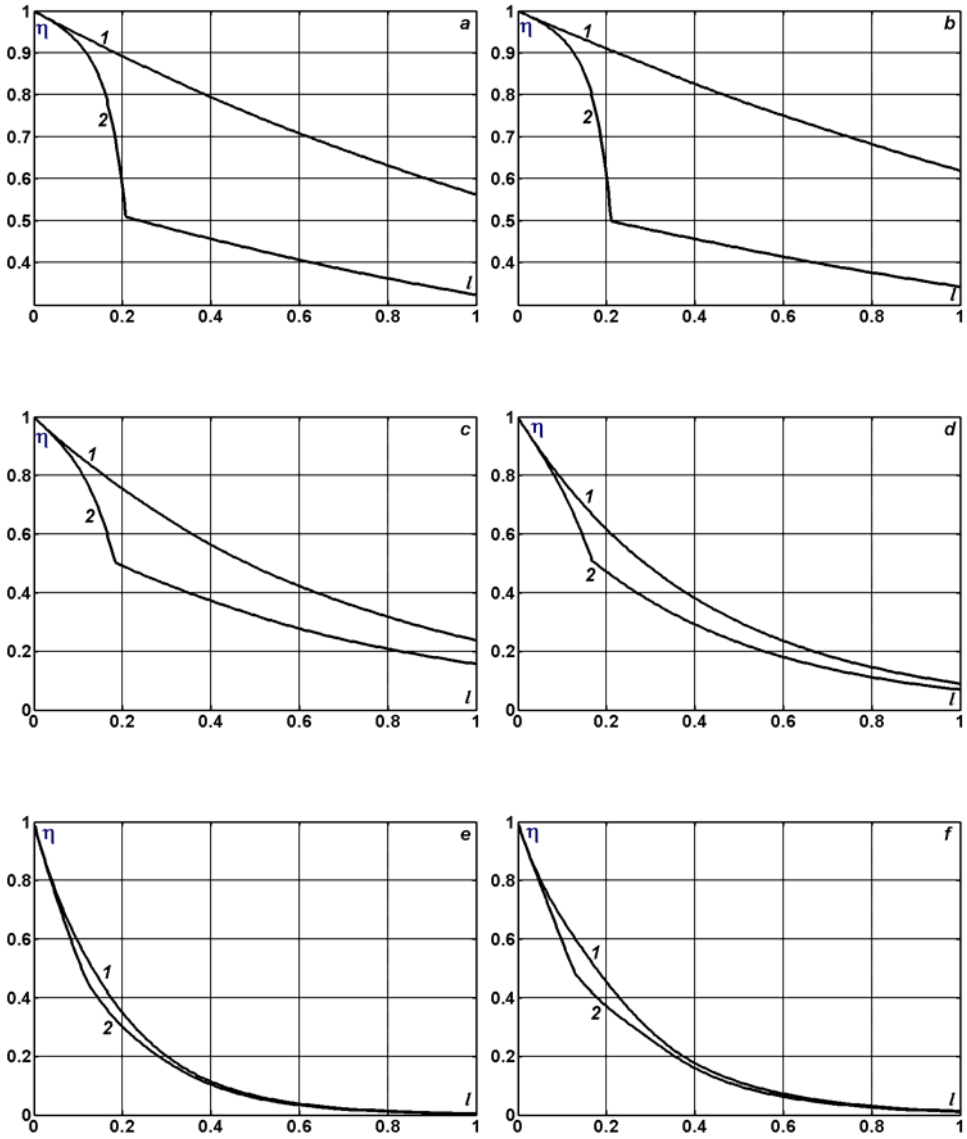

Fig. 14.10. $\eta(X_n = 0)$ (1) and η $(X_n = X_{n,k} < 0)$ (2) depending on the line length when $R_S = Z_B$ and $R = 0.48$, $G = R/5$(***a***); $R = 0.48$, $G = 0$(***b***); $R = 1.205$, $G = R/5$(***c***); $R = G = 1.205$(***d***); $R = 4.8$, $G = R/5$(***e***); $R = 4.8$, $G = 0$(***f***).

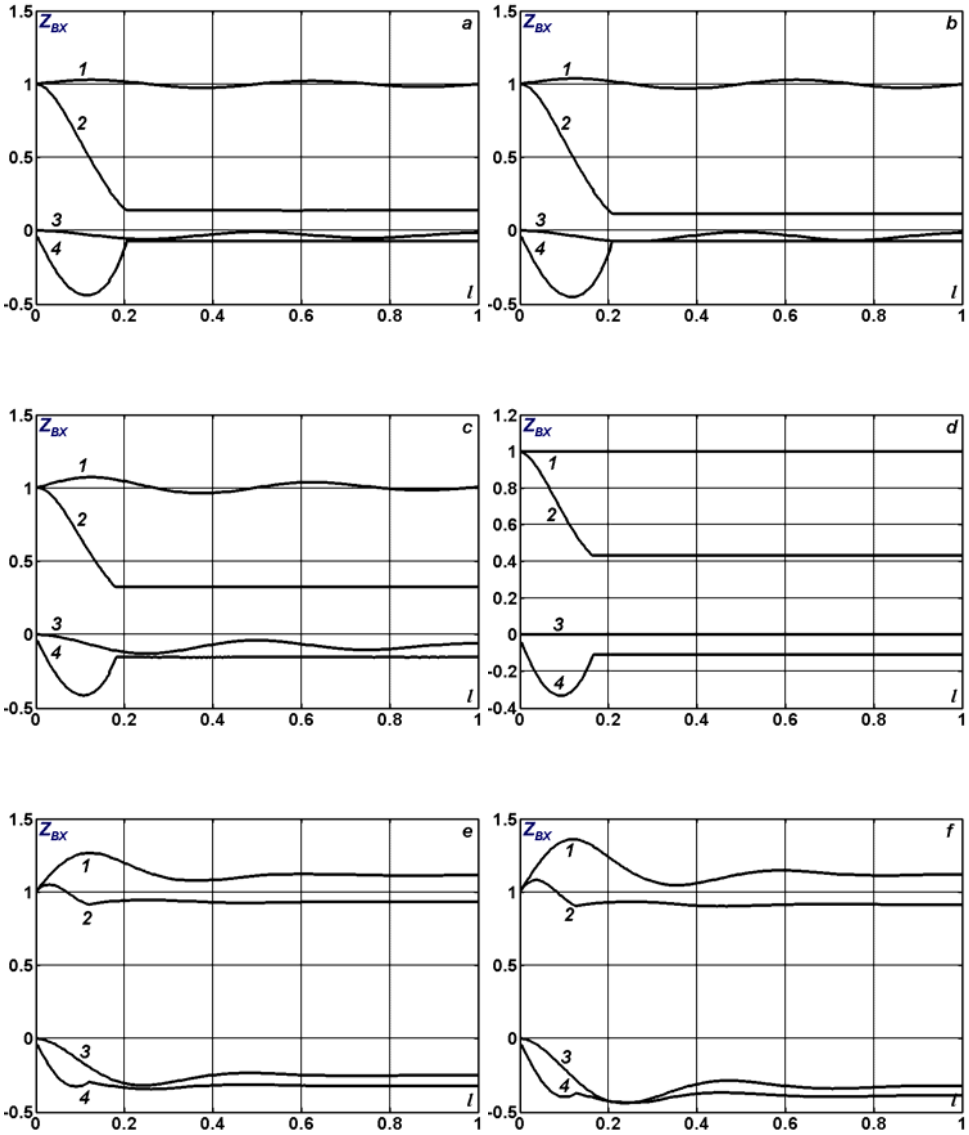

Fig. 14.11. $|Z_{BX}|$ (1), $\arg(Z_{BX})$ (3) ($X_n = 0$) and $|Z_{BX}|$ (2), $\arg(Z_{BX})$ (4) ($X_n = X_{n,\mathbf{k}} < 0$) depending on the line length when $R_S = Z_B$ and $R = 0.48$, $G = R/5$(***a***); $R = 0.48$, $G = 0$(***b***); $R = 1.205$, $G = R/5$(***c***); $R = G = 1.205$(***d***); $R = 4.8$, $G = R/5$(***e***); $R = 4.8$, $G = 0$(***f***).

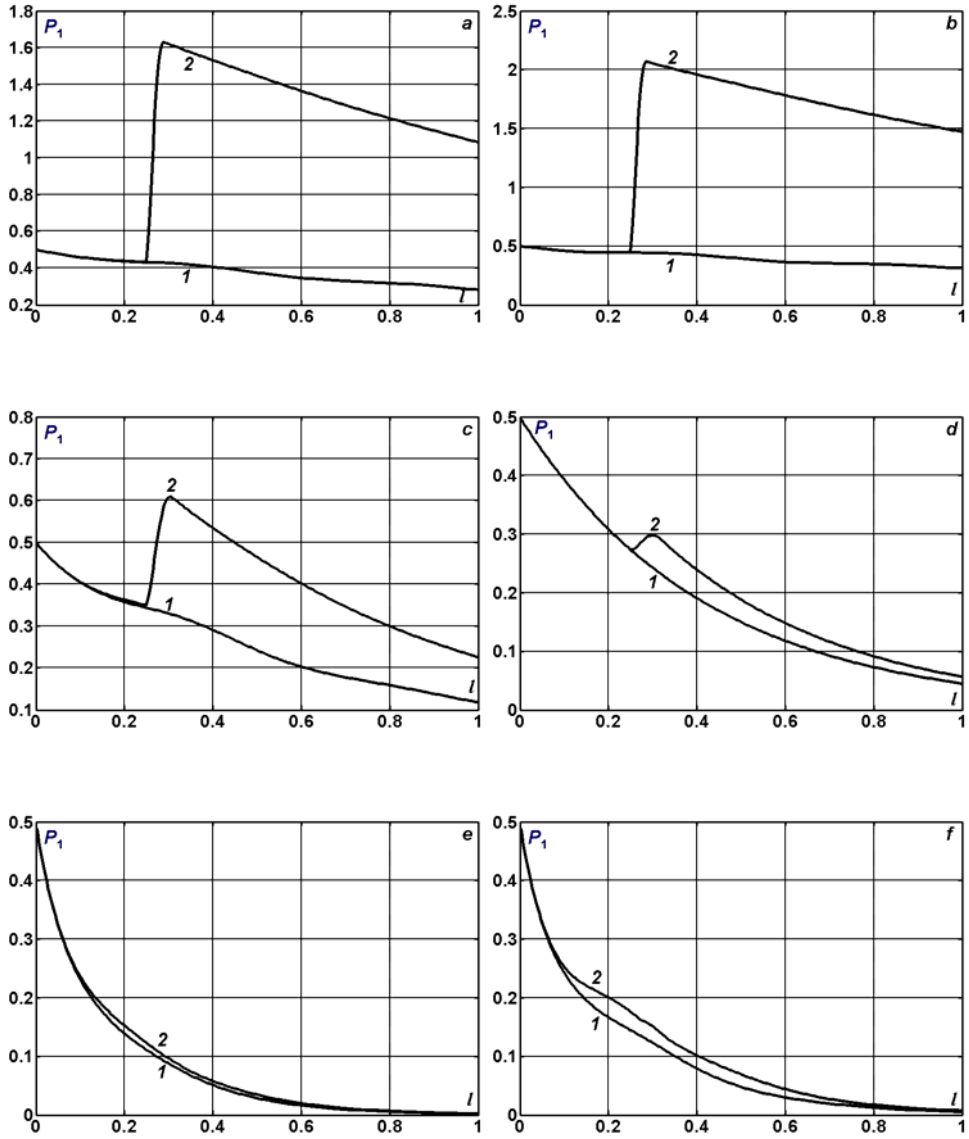

Fig. 14.12. P1(X_n = 0) (1) and P1($X_n = X_{n,k} > 0$) (2) depending on the line length when $R_S = Z_B$ and$R$ = 0.48, $G = R/5$(***a***); R = 0.48, G = 0(***b***); R = 1.205, $G = R/5$(***c***); $R = G$ = 1.205(***d***); R = 4.8, $G = R/5$(***e***); R = 4.8, G = 0(***f***).

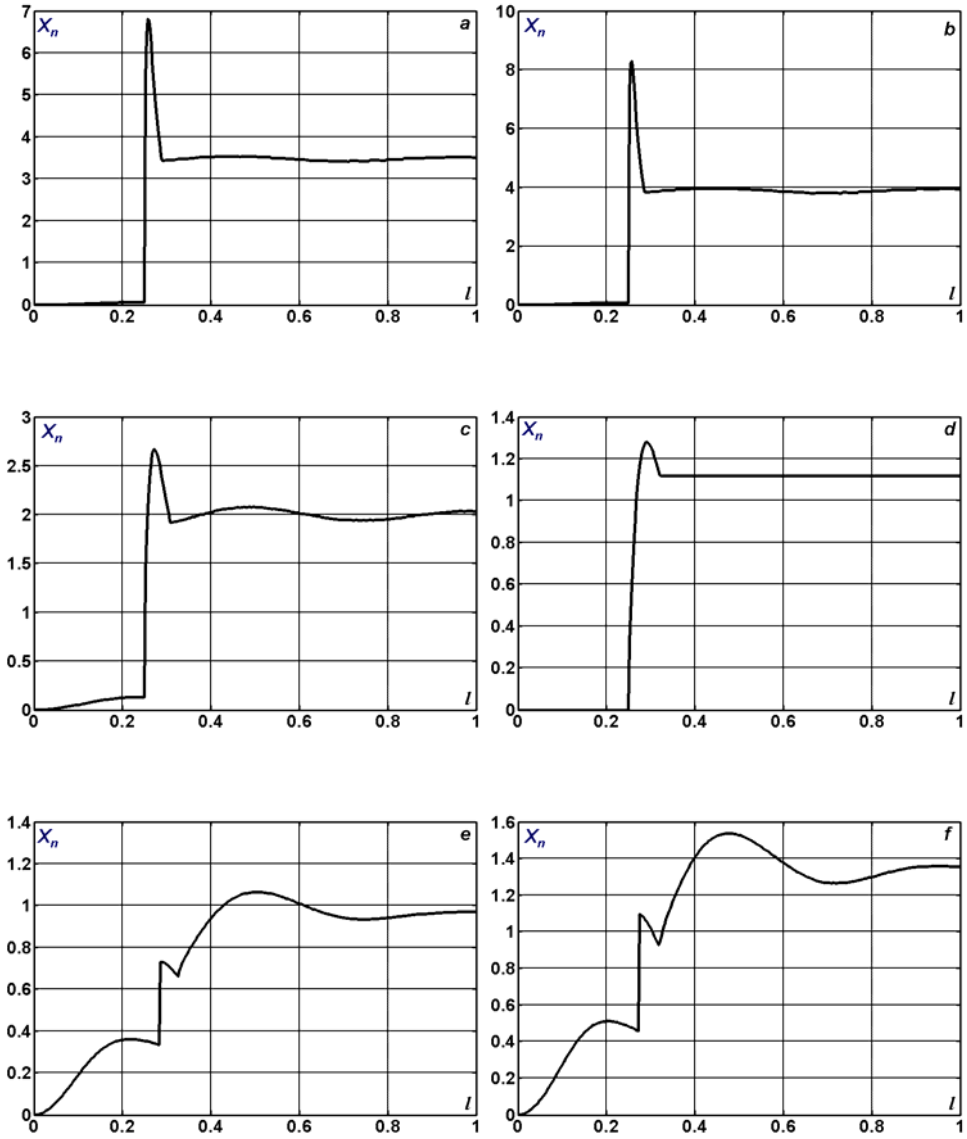

Fig. 14.13. $X_{n,\boldsymbol{k}} > 0$ depending on the line length when $R_S = Z_B$ and $R = 0.48$, $G = R/5$(***a***); $R = 0.48$, $G = 0$(***b***); $R = 1.205$, $G = R/5$(***c***); $R = G = 1.205$(***d***); $R = 4.8$, $G = R/5$(***e***); $R = 4.8$, $G = 0$(***f***).

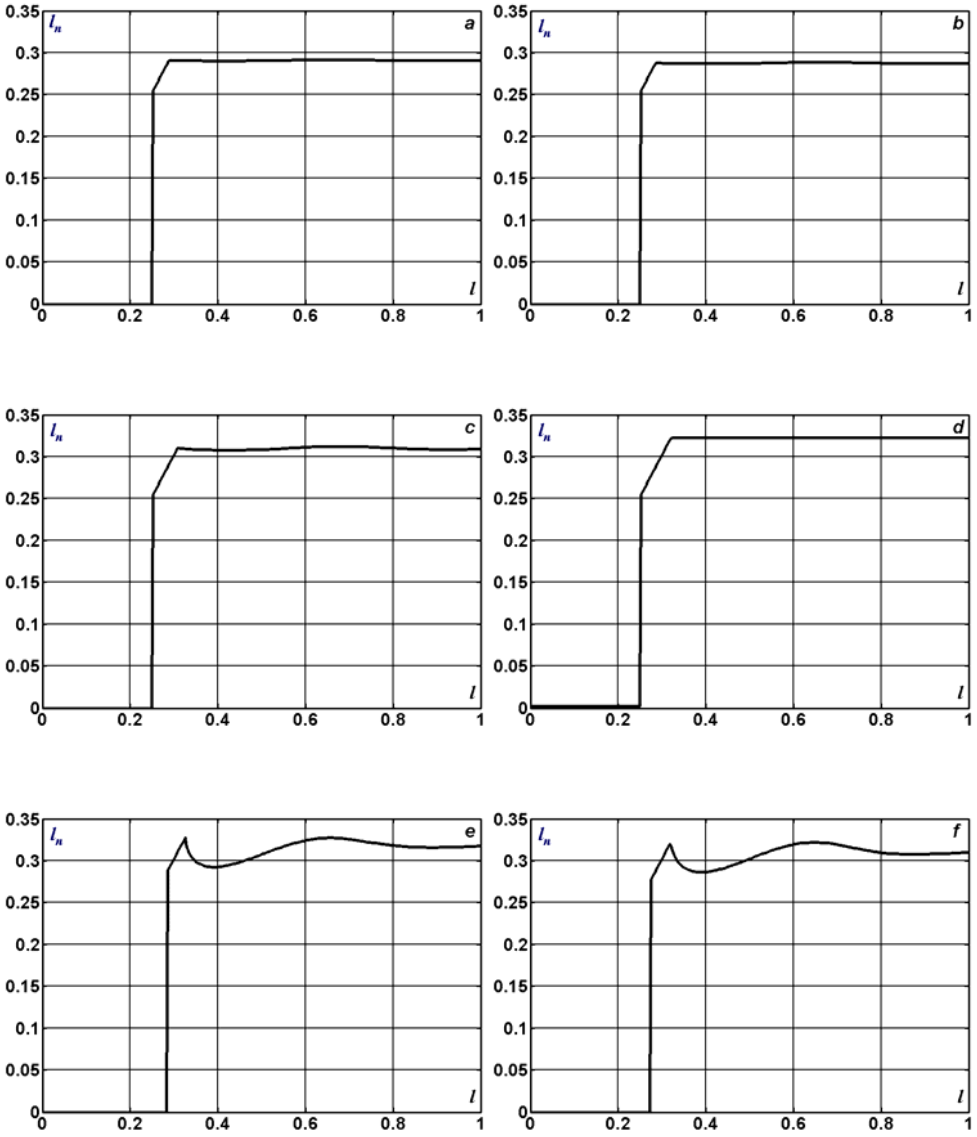

Fig. 14.14. $l_{n,k}$ depending on the line length when $R_S = Z_B$ and $R = 0.48$, $G = R/5$(***a***); $R = 0.48$, $G = 0$(***b***); $R = 1.205$, $G = R/5$(***c***); $R = G = 1.205$(***d***); $R = 4.8$, $G = R/5$(***e***); $R = 4.8$, $G = 0$(***f***).

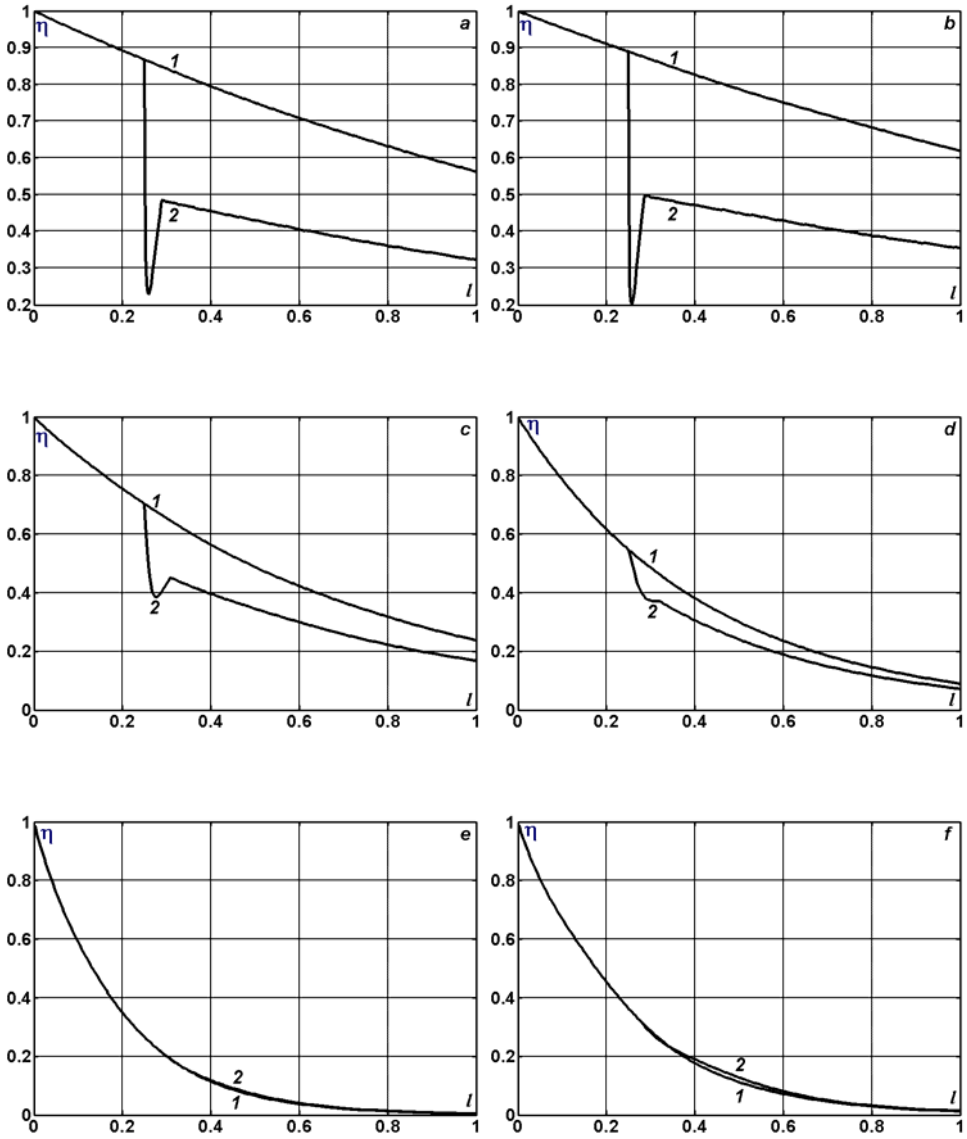

Fig. 14.15. $\eta(X_n = 0)$ (1) and η ($X_n = X_{n,k}>0$) (2) depending on the line length when $R_S = Z_B$ and R = 0.48, $G = R/5$(***a***); R = 0.48, G = 0(***b***); R = 1.205, $G = R/5$(***c***); $R = G$ = 1.205(***d***); R = 4.8, $G = R/5$(***e***); R = 4.8, G = 0(***f***).

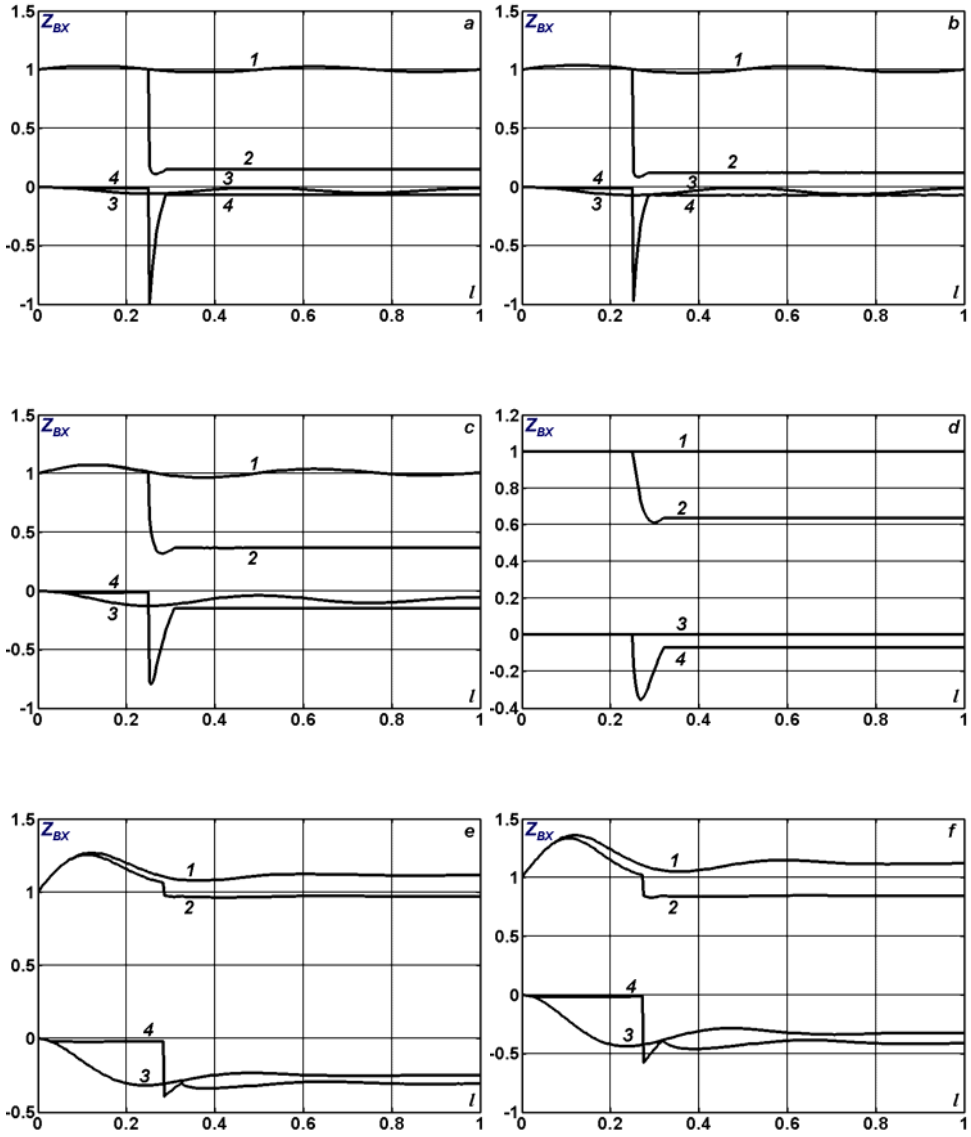

Fig. 14.16. $|Z_{BX}|$(1), $\arg(Z_{BX})$(3) (X_n = 0) and $|Z_{BX}|$(2), $\arg(Z_{BX})$(4) (X_n = $X_{n,k}$>0) depending on the line length when $R_S = Z_B$ and R = 0.48, $G = R/5$(***a***); R = 0.48, G = 0(***b***); R = 1.205, $G = R/5$(***c***); $R = G$ = 1.205(***d***); R = 4.8, $G = R/5$(***e***); R = 4.8, G = 0(***f***).

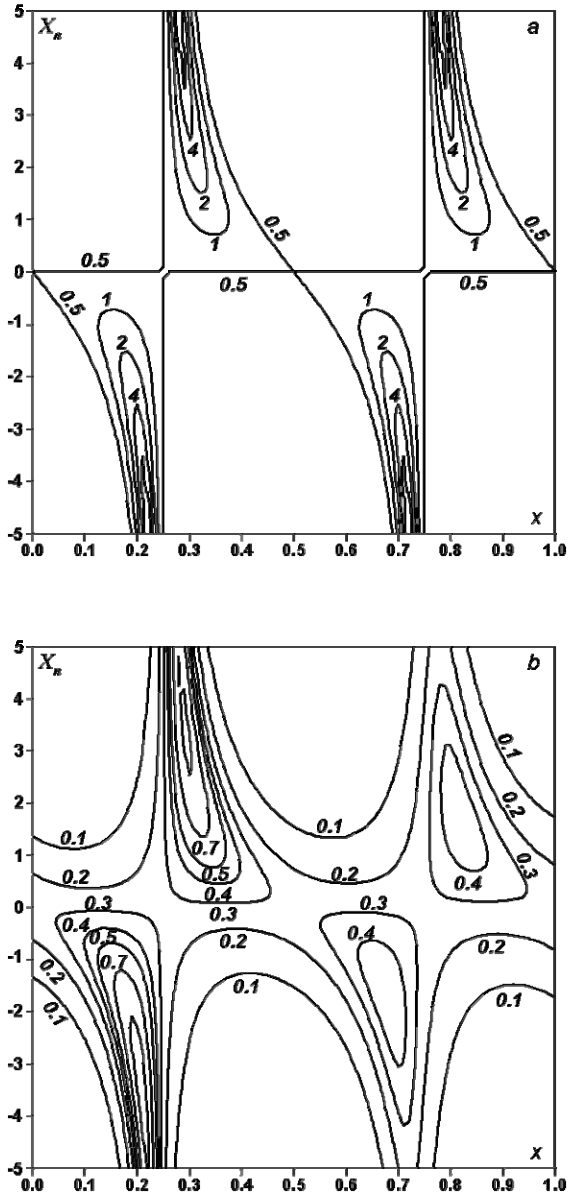

Fig. 14.17. The transmission power depending on the value and on the location of the longitudinal compensating reactive element X_n when l = 1.0; R = 0 (***a***); 0.48 (***b***); $G = R/5$.

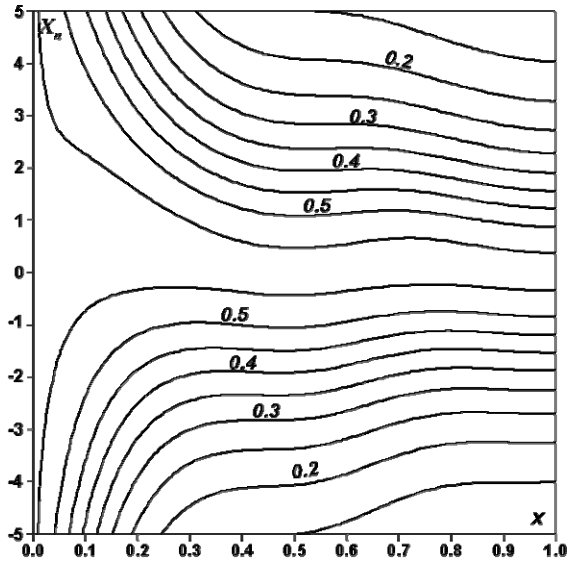

Fig. 14.18. The efficiency depending on the value and on the location of the longitudinal compensating reactive element X_n when $l = 1.0$; $R = 0.48$, $G = R/5$.

15. Line parameters transverse compensation

Let at the point $x = l_n$ the reactive power source with complex resistance $Z_n = R_n + jX_n$ is parallel-connected to the line with length l (see fig. 15.1).

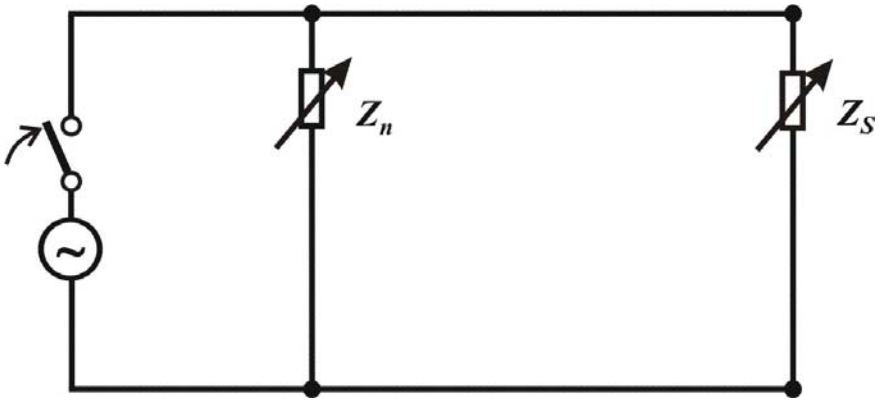

Fig. 15.1. The alternating voltage line with active load R_S at the receiving end and the reactive load X_n, parallel-connected to the line.

Then the steady-state regime equations in hyperbolic functions (1.5) take the form

$$Z_S = R_S + j\left(\omega L_S - \frac{1}{\omega C_S}\right) = R_S + jX_S;$$

$$Z_{BX} = Z_0 \frac{Z_S \mathrm{ch}(\delta l) + Z_0 \mathrm{sh}(\delta l) + \dfrac{Z_0}{Z_n}\mathrm{sh}(\delta l_n) A_n}{Z_S \mathrm{sh}(\delta l) + Z_0 \mathrm{ch}(\delta l) + \dfrac{Z_0}{Z_n}\mathrm{ch}(\delta l_n) A_n} = Z_0 \frac{AZ_n + D}{\widetilde{A} Z_n + \widetilde{D}};$$

$$A_n = Z_S \mathrm{ch}\delta(l - l_n) + Z_0 \mathrm{sh}\delta(l - l_n);$$

$$A = Z_S \mathrm{ch}(\delta l) + Z_0 \mathrm{sh}(\delta l);\ \ \widetilde{A} = Z_S \mathrm{sh}(\delta l) + Z_0 \mathrm{ch}(\delta l);$$

$$D = Z_0 \mathrm{sh}(\delta l_n) A_n;\ \ \widetilde{D} = Z_0 \mathrm{ch}(\delta l_n) A_n;$$

$$U_0 = Z_{BX} I_0; U_1 = Z_S I_1; U_n = Z_n I_n; I_n = I_n^- - I_n^+; \qquad (15.1)$$

$$I_n = U_0\left(\frac{\mathrm{ch}(\delta l_n)}{Z_{BX}} - \frac{\mathrm{sh}(\delta l_n)}{Z_0}\right) = \frac{I_0\left(Z_0 \mathrm{ch}(\delta l_n) - Z_{BX} \mathrm{sh}(\delta l_n)\right)}{Z_0};$$

$$I_1 = \frac{Z_0 I_n}{Z_S \mathrm{sh}(\delta l_n) + Z_0 \mathrm{ch}(\delta l_n)} = \frac{U_0 Z_n}{AZ_n + D}.$$

Let's consider the case when $Z_S = R_S = \mathrm{Z}_B$ and $R_n = 0$, $Z_n = jX_n$. Then the load active power can be written as follows

$$P_1 = \frac{1}{2}\mathrm{Re}\left(U_1 I_1^*\right) = \frac{Z_B}{2} I_1 I_1^* = \frac{Z_B U_0^2}{2} \frac{Z_n Z_n^*}{(AZ_n + D)(AZ_n + D)^*}. \qquad (15.2)$$

As to determine the values of the compensating load $Z_n = jX_n$ and its location l_n (the values that ensure the maximal active power $P_{1,k}$ values), we are to solve the system of two equations

$$\frac{\partial P_1(X_n, l_n)}{\partial X_n} = 0, \quad \frac{\partial P_1(X_n, l_n)}{\partial l_n} = 0 .$$

These equations after differentiation and some simplifications take the form

$$X_n \operatorname{Im}(AD^*) - |D|^2 = 0, \quad \operatorname{Re}\left[\frac{\partial D}{\partial l_n}(AZ_n + D)^*\right] = 0 . \tag{15.3}$$

From the first equation now we obtain the explicit expression for optimal value of the X_n depending on the parameter l_n:

$$X_n = \frac{|D|^2}{\operatorname{Im}(AD^*)} . \tag{15.4}$$

Substituting this expression in the second equation we obtain the transcendental equation with respect to unknown l_n

$$\operatorname{Re}\left[\frac{\partial D}{\partial l_n}\left(\frac{jA|D|^2}{\operatorname{Im}(AD^*)} + D\right)^*\right] = 0 . \tag{15.5}$$

Thus, to calculate the maximal value P_1 it is necessary to determine the value $l_{n,k}$ as a solution of the nonlinear equation (15.5). Than from the relation (15.4) we can determine the optimal value $X_{n,k}$ and from (15.2) – the maximal value $P_{1,k}$.

Let's note that the equation (15.5) possesses several roots. The values of these roots give only extreme values (i.e. maximal and minimal) of P_1. Therefore we are to find all roots of the equation (15.5) at first and then to choose the value of the root $l_{n,k}$, that ensure the global maximum of the P_1.

Now we will consider the problem of determination of the maximal value η of the efficiency and of the transmission power. The efficiency can be represented in the following form

$$\eta = \frac{P_1}{P_0} = \frac{\mathrm{Re}\left(U_1 I_1^*\right)}{\mathrm{Re}\left(U_0 I_0^*\right)} = \frac{Z_B I_1 I_1^*}{U_0^2 \,\mathrm{Re}(1/Z_{BX})} =$$

$$= \frac{Z_B X_n^2}{\mathrm{Re}\left[(j\widetilde{A}X_n + \widetilde{D})(jAX_n + D)^* / Z_0\right]}. \qquad (15.6)$$

As to determine the values of the compensating load $Z_n = jX_n$ and its location l_n (the values that ensure the maximal efficiency values), we are to solve the system of two equations

$$\frac{\partial \eta(X_n, l_n)}{\partial X_n} = 0, \quad \frac{\partial \eta(X_n, l_n)}{\partial l_n} = 0.$$

These equations after differentiation and some simplifications take the form

$$X_n \,\mathrm{Im}\left[Z_0(A\widetilde{D}^* - \widetilde{A}^* D)\right] - 2\,\mathrm{Re}\left(Z_0^* \widetilde{D} D^*\right) = 0;$$

$$\mathrm{Re}\left\{\frac{1}{Z_0}\left[\frac{1}{X_n}\frac{\partial(D^*\widetilde{D})}{\partial l_n} + j\left(A\frac{\partial \widetilde{D}}{\partial l_n} + \widetilde{A}\frac{\partial D^*}{\partial l_n}\right)\right]\right\} = 0. \qquad (15.7)$$

From the first equation now we obtain the explicit expression for optimal value of the X_n depending on the l_n:

$$\frac{1}{X_n} = \frac{\mathrm{Im}\left[Z_0(A\widetilde{D}^* - \widetilde{A}^* D)\right]}{2\,\mathrm{Re}\left(Z_0^* \widetilde{D} D^*\right)}. \qquad (15.8)$$

Substituting this expression in the second equation (15.7) we obtain the transcendental equation with respect to unknown l_n

$$\mathrm{Re}\left\{\frac{1}{Z_0}\left[\frac{\mathrm{Im}\left[Z_0(A\widetilde{D}^* - \widetilde{A}^* D)\right]}{2\,\mathrm{Re}\left(Z_0^* \widetilde{D} D^*\right)}\frac{\partial(D^*\widetilde{D})}{\partial l_n} + j\left(A\frac{\partial \widetilde{D}}{\partial l_n} + \widetilde{A}\frac{\partial D^*}{\partial l_n}\right)\right]\right\} = 0. \qquad (15.9)$$

Thus, to calculate the maximal value η it is necessary to determine the value $l_{n,\eta}$ as a solution of the nonlinear equation (15.9). Then from the relation (15.8) we can determine the optimal value $X_{n,\eta}$ and from (15.6) – the maximal value η.

Let's note that the equation (15.8) possesses several roots. The values of these roots give only extreme values (i.e. maximal and minimal) of η. Therefore we are to find all roots of the equation (15.9) at first and then to choose the value of the root $l_{n,\eta}$, that ensure the global maximum of the η.

Now we will consider the efficiency of the line with matched active load when the compensation of its reactive elements ensures the maximal values for efficiency (fig. 15.2). Let's mention that the qualitative and quantitative data using in the diagrams in the fig. 15.2 – 15.5 are similar with the same data obtained for the line under the reactive parameters longitudinal compensation (see fig. 14.2 – 14.6). As in the case of longitudinal compensation the efficiency increasing here is achieved by connection to the line of the reactive power source with inductive resistance. However, at the same time the decreasing of the active power consumption is observed always (see fig. 15.5).

The results on transverse capacitive compensation with the object of increasing the power transmitted in pure active load turn out to be rather unexpected (see fig. 15.7 – 15.11). It arrives that the reactive power source with optimal capacitive resistance must be located at the sending end of the line independently of line length and of losses (see fig. 15.9). As a result the power of receiver can be increased in dozens of times including the case of undistorting line (see fig. 15.7, *d*). The power increasing in this case also is accompanied by efficiency decreasing. The efficiency decreasing runs down to disastrous down level for lines with great losses (see fig. 15.10, *e*, *f*).

The transmission power increasing can be achieved also by means of inductive transverse compensation but only for lines with length greater then a quarter-wave (see fig. 15.12 – 15.16). The power increasing in this case is not as impressive as in case of capacitive transverse compensation, but the efficiency does not decline so greatly. Moreover, for the lines with great active losses (in order of 220 mΩ/km) we obtain the simultaneous (although not very significant) efficiency increasing (see fig. 15.15, *e*, *f*).

The contl curves for maximal values of the transmission power and for efficiency depending on the value and on the location of the transverse compensation X_n in the line with the length $l = \lambda$ are represented in the fig. 15.17 and 15.18. These diagrams can serve in a sense of a navigator when choos-

ing the parameters of the passive compensators reasoning from the technical requirements and restrictions.

The practical implementation of the reactive power sources (mainly bank of capacitors and reactors) frequently purposes entirely different objects (not the increasing of active transmission power). However, the suggested approach to the quantitative analysis of the consequences of reactive power sources connection to the trunk and distribution transmission lines gives the possibility to enlarge essentially the present notions about the role and real potentialities of the different compensating elements.

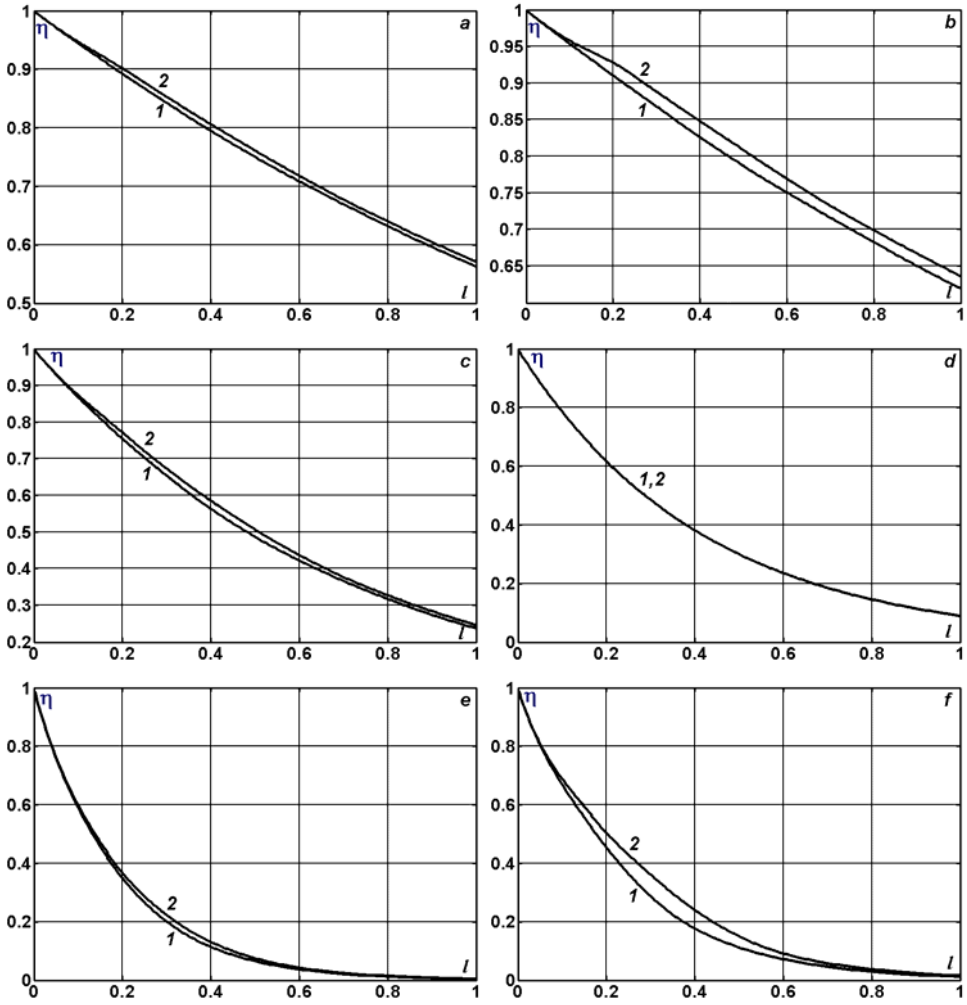

Fig. 15.2. $\eta(X_n^{-1}=0)$ (1) and η $(X_n^{-1}=X_{n,\eta}^{-1})$ (2) depending on the line length when $R_S = Z_B$ and R = 0.48, $G = R/5$(***a***); R = 0.48, G = 0(***b***); R = 1.205, $G = R/5$(***c***); $R = G$ = 1.205(***d***); R = 4.8, $G = R/5$(***e***); R = 4.8, G = 0(***f***).

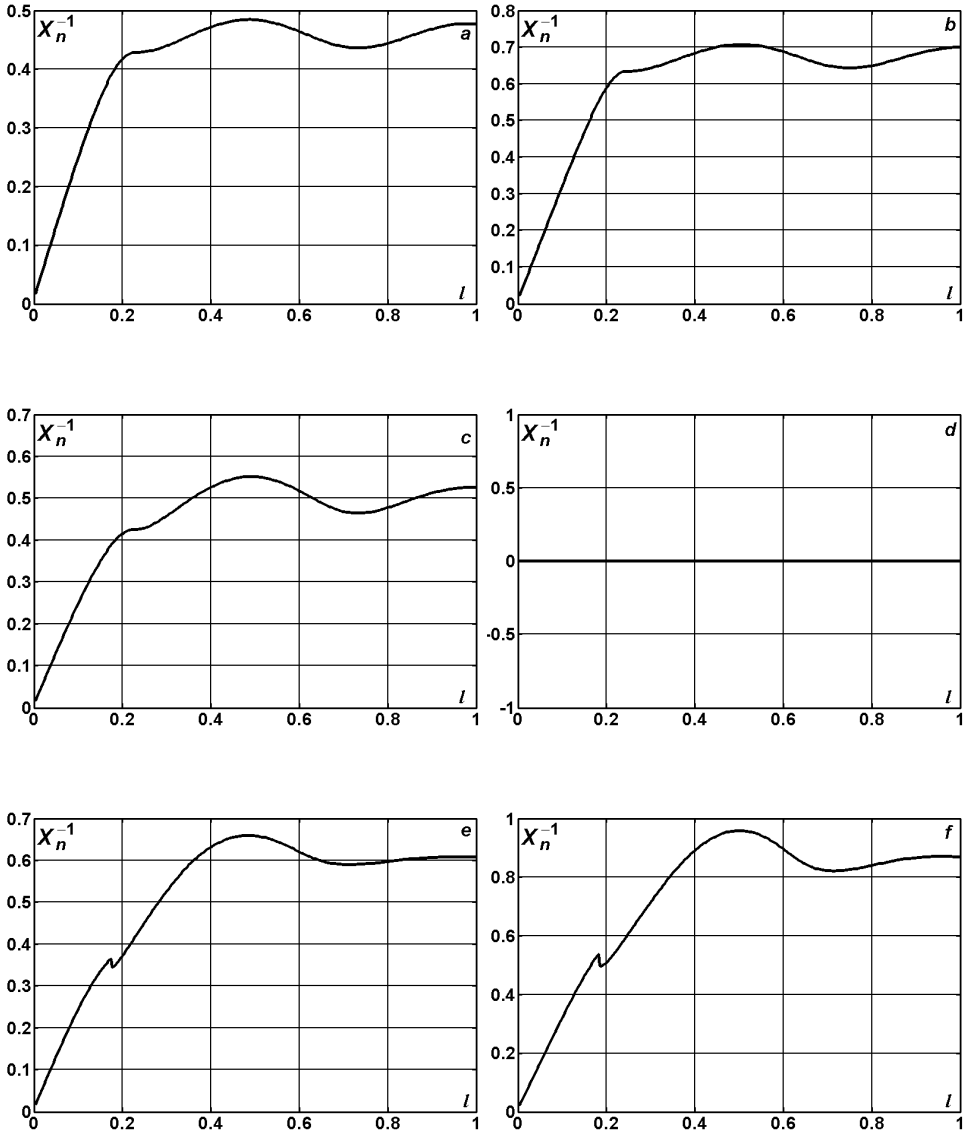

Fig. 15.3. $X_{n,\eta}^{-1}$ depending on the line length when $R_S = Z_B$ and $R = 0.48$, $G = R/5$(***a***); $R = 0.48$, $G = 0$(***b***); $R = 1.205$, $G = R/5$(***c***); $R = G = 1.205$(***d***); $R = 4.8$, $G = R/5$(***e***); $R = 4.8$, $G = 0$(***f***).

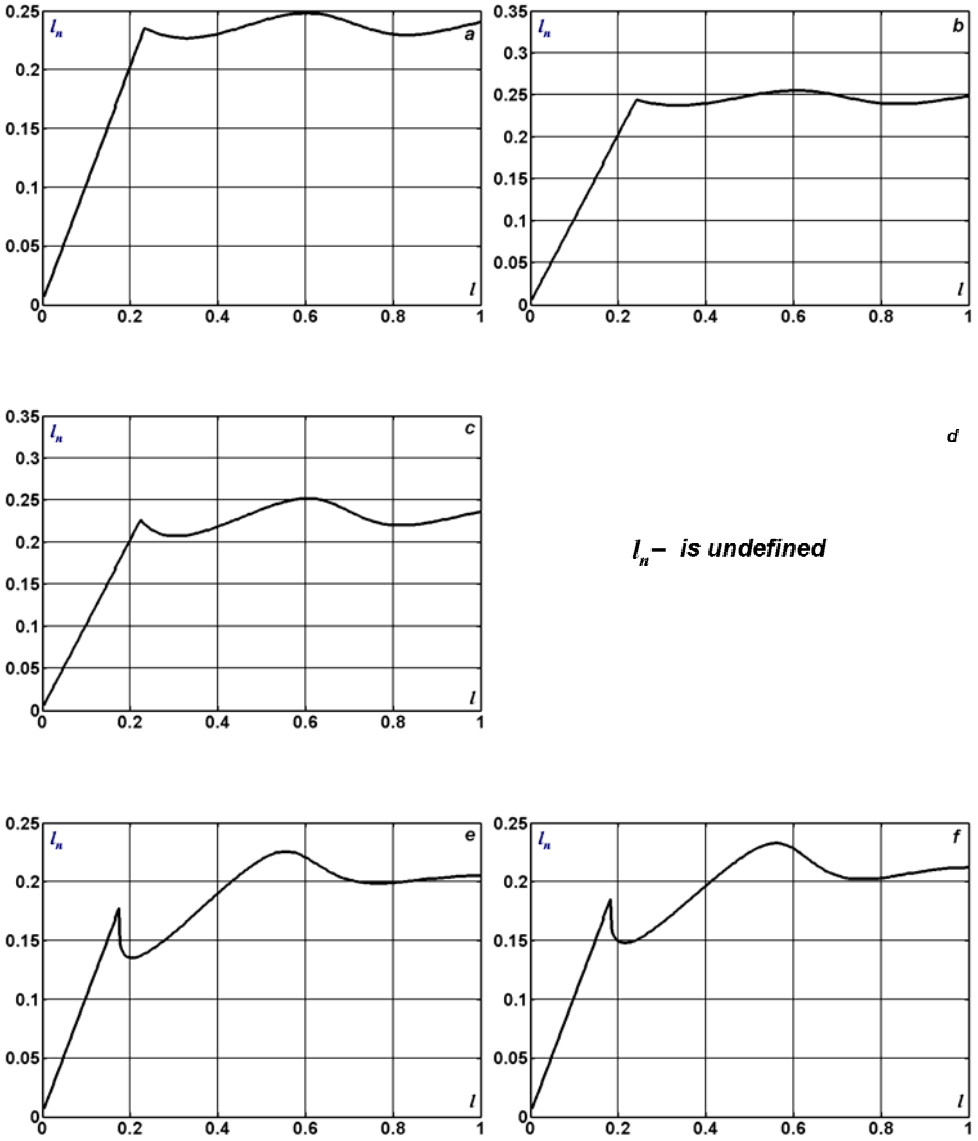

Fig. 15.4. $l_{n,\eta}$ depending on the line length when $R_S = Z_B$ and $R = 0.48$, $G = R/5$(***a***); $R = 0.48$, $G = 0$(***b***); $R = 1.205$, $G = R/5$(***c***); $R = G = 1.205$(***d***); $R = 4.8$, $G = R/5$(***e***); $R = 4.8$, $G = 0$(***f***).

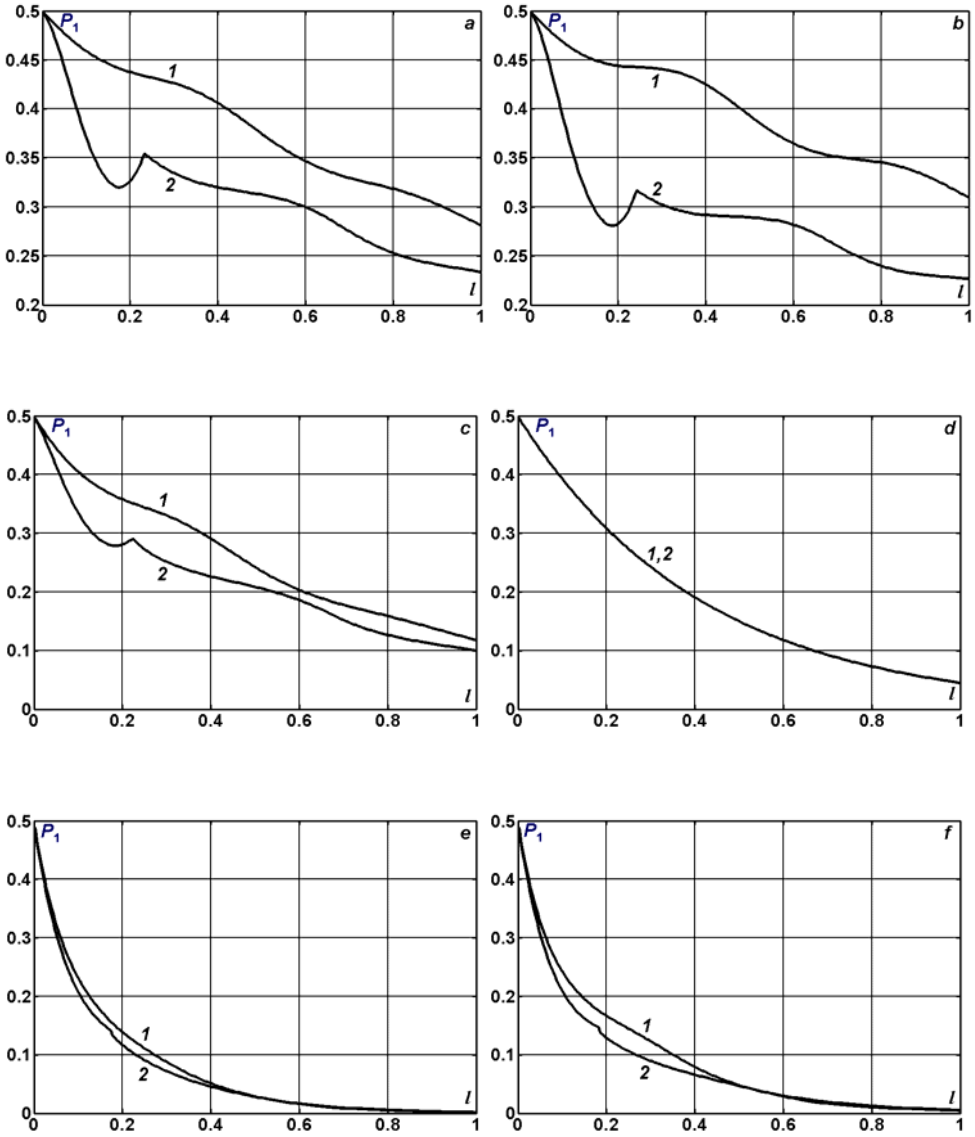

Fig. 15.5. $P_1(X_n^{-1}=0)$ (1) and $P_1(X_n^{-1}=X_{n,\eta}^{-1})$ (2) depending on the line length when $R_S = Z_B$ and R = 0.48, $G = R/5$(***a***); R = 0.48, G = 0(***b***); R = 1.205, $G = R/5$(***c***); $R = G$ = 1.205(***d***); R = 4.8, $G = R/5$(***e***); R = 4.8, G = 0(***f***).

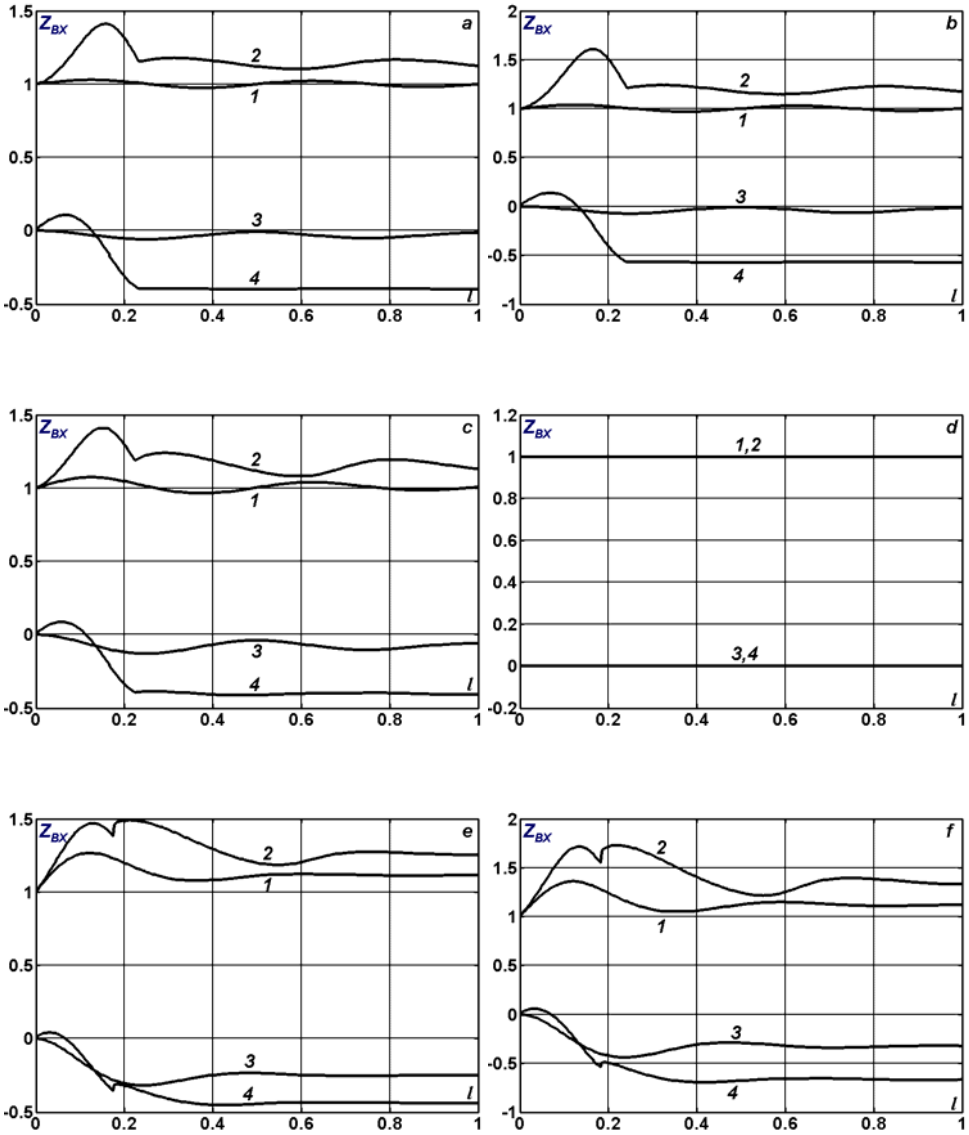

Fig. 15.6. $|Z_{BX}|$(1), $\arg(Z_{BX})$(3) ($X_n^{-1}=0$) and $|Z_{BX}|$(2), $\arg(Z_{BX})$(4) ($X_n^{-1}=X_{n,\eta}^{-1}$)depending on the line length when $R_S = Z_B$ and R = 0.48, $G = R/5$(***a***); R = 0.48, G = 0(***b***); R = 1.205, $G = R/5$(***c***); $R = G$ = 1.205(***d***); R = 4.8, $G = R/5$(***e***); R = 4.8, G = 0(***f***).

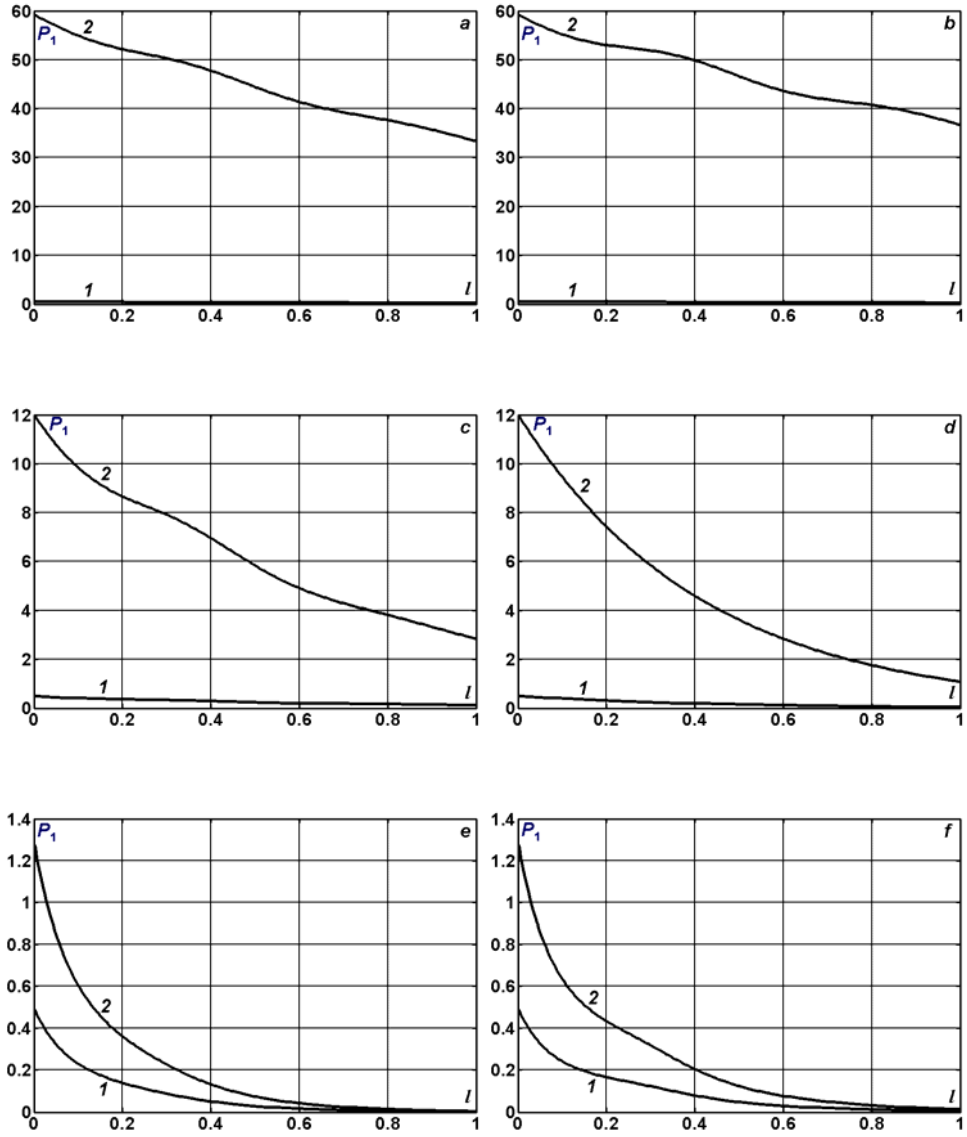

Fig. 15.7. $P_1(X_n^{-1}=0)$ (1) and $P_1(X_n^{-1}=X_{n,k}^{-1}<0)$ (2) depending on the line length when $R_S = Z_B$ and R = 0.48, $G = R/5$(***a***); R = 0.48, G = 0(***b***); R = 1.205, $G = R/5$(***c***); $R = G$ = 1.205(***d***); R = 4.8, $G = R/5$(***e***); R = 4.8, G = 0(***f***).

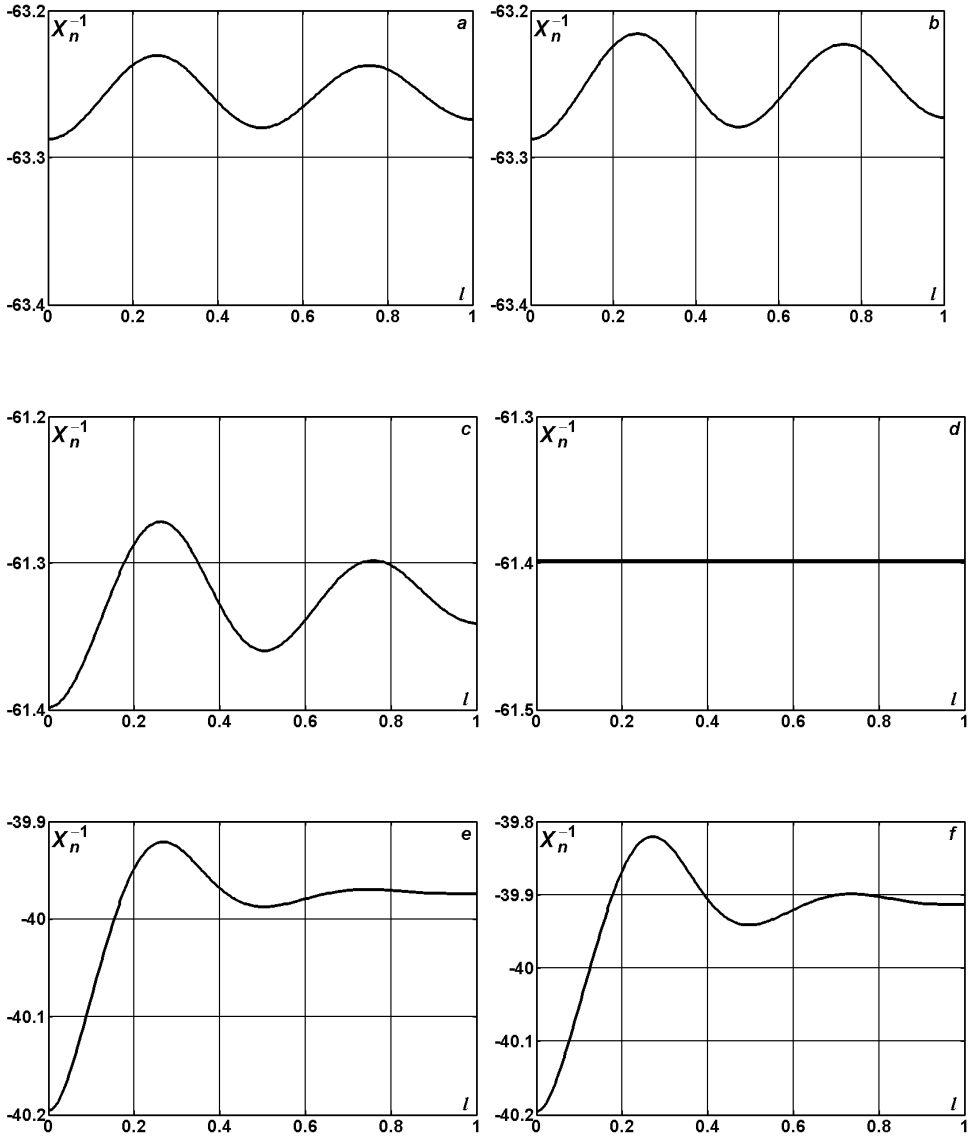

Fig. 15.8. $X_{n,\boldsymbol{k}}^{-1} < 0$ depending on the line length when $R_S = Z_B$ and $R = 0.48$, $G = R/5$(***a***); $R = 0.48$, $G = 0$(***b***); $R = 1.205$, $G = R/5$(***c***); $R = G = 1.205$(***d***); $R = 4.8$, $G = R/5$(***e***); $R = 4.8$, $G = 0$(***f***).

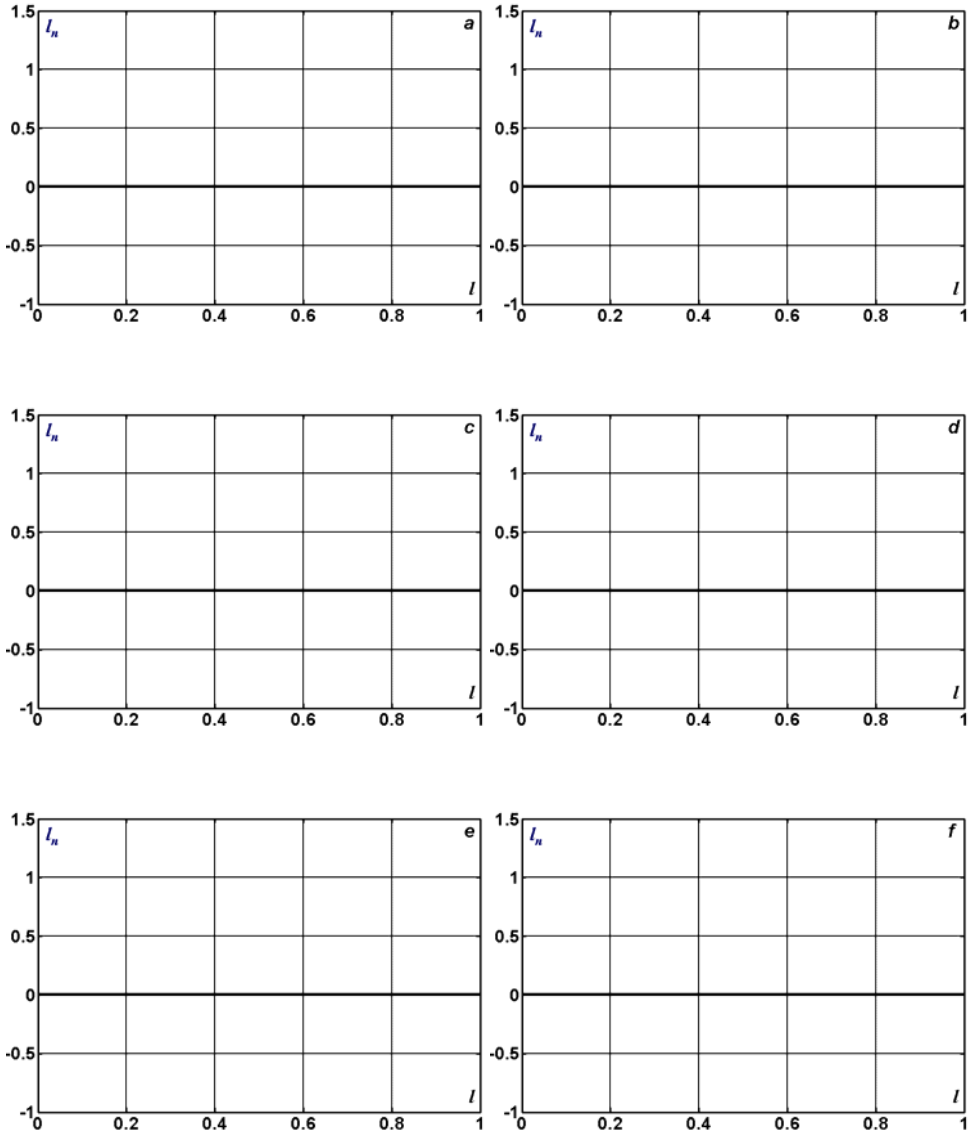

Fig. 15.9. $l_{n,k}$ depending on the line length when $R_S = Z_B$ and $R = 0.48$, $G = R/5$(***a***); $R = 0.48$, $G = 0$(***b***); $R = 1.205$, $G = R/5$(***c***); $R = G = 1.205$(***d***); $R = 4.8$, $G = R/5$(***e***); $R = 4.8$, $G = 0$(***f***).

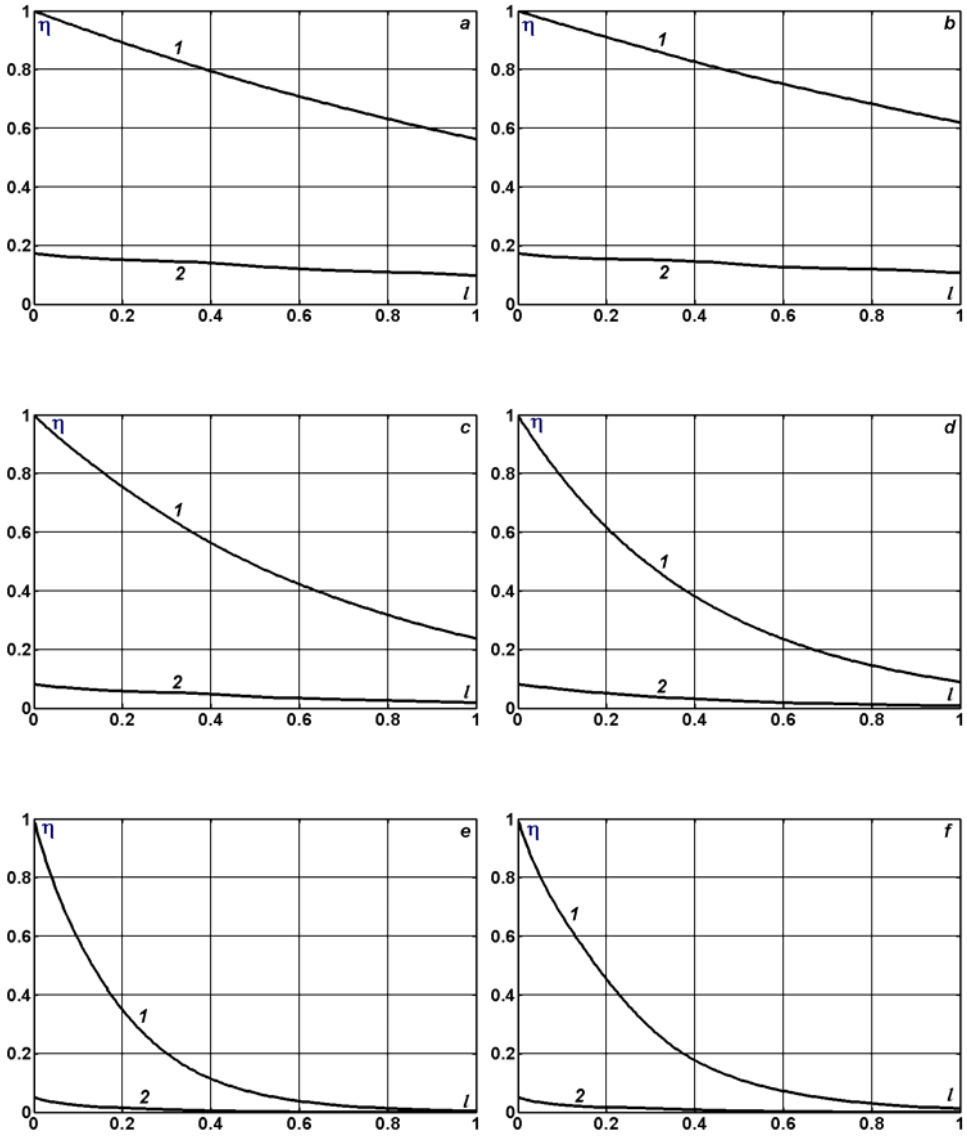

Fig. 15.10. $\eta(X_n^{-1}=0)$ (1) and η $(X_n^{-1}=X_{n,\boldsymbol{k}}^{-1}<0)$ (2) depending on the line length when $R_S = Z_B$ and R = 0.48, $G = R/5$(***a***); R = 0.48, G = 0(***b***); R = 1.205, $G = R/5$(***c***); $R = G$ = 1.205(***d***); R = 4.8, $G = R/5$(***e***); R = 4.8, G = 0(***f***).

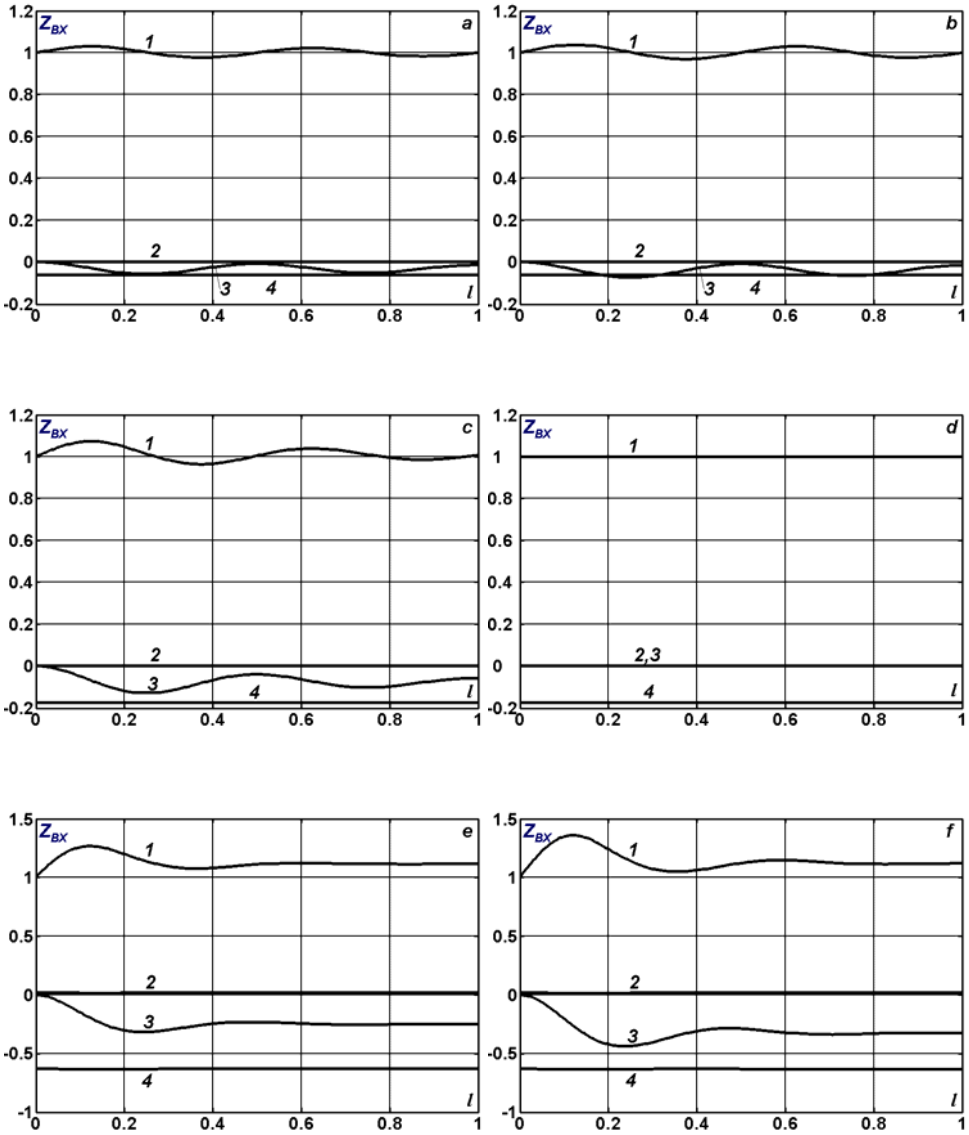

Fig. 15.11. $|Z_{BX}|$(1), $\arg(Z_{BX})$(3) ($X_n^{-1}=0$) and $|Z_{BX}|$(2), $\arg(Z_{BX})$(4) ($X_n^{-1}=X_{n,\boldsymbol{k}}^{-1}<0$)depending on the line length when $R_S = Z_B$ and R = 0.48, G = R/5(***a***); R = 0.48, G = 0(***b***); R = 1.205, G = R/5(***c***); R = G = 1.205(***d***); R = 4.8, G = R/5(***e***); R = 4.8, G = 0(***f***).

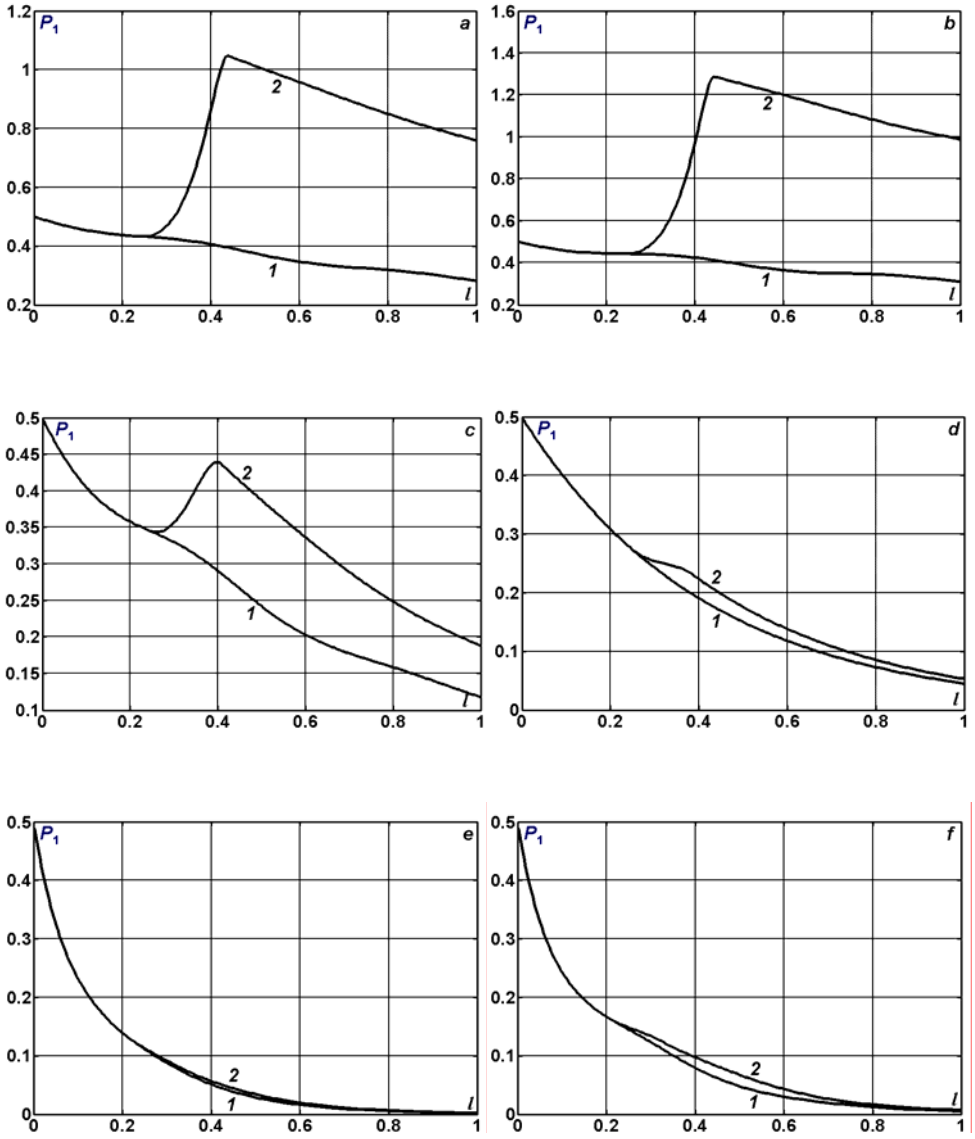

Fig. 15.12. $P_1(X_n^{-1}=0)$ (1) and $P_1(X_n^{-1}=X_{n,k}^{-1}>0)$ (2) depending on the line length when $R_S = Z_B$ and R = 0.48, $G = R/5$(***a***); R = 0.48, G = 0(***b***); R = 1.205, $G = R/5$(***c***); $R = G$ = 1.205(***d***); R = 4.8, $G = R/5$(***e***); R = 4.8, G = 0(***f***).

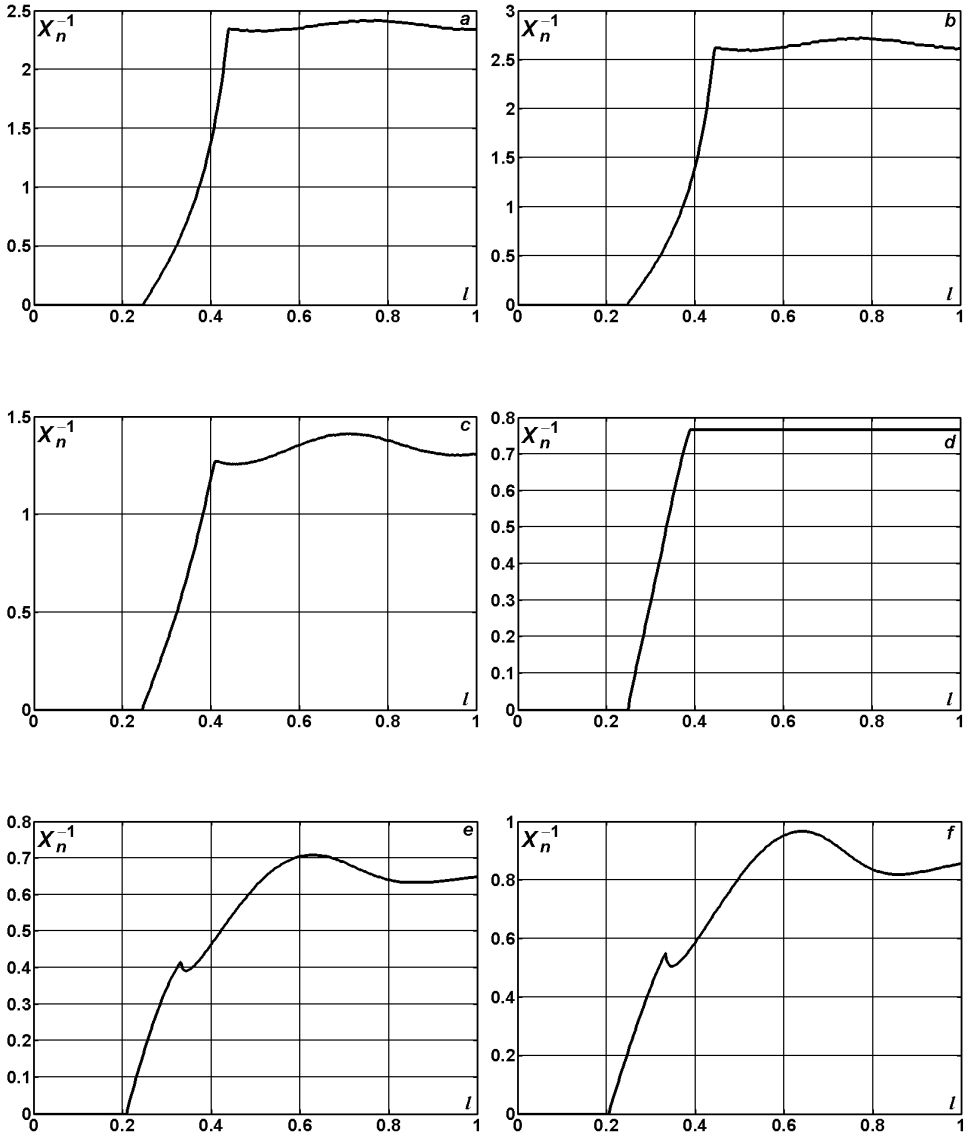

Fig. 15.13. $X_{n,\boldsymbol{k}}^{-1} > 0$ depending on the line length when $R_S = Z_B$ and R = 0.48, G = R/5(***a***); R = 0.48, G = 0(***b***); R = 1.205, G = R/5(***c***); R = G = 1.205(***d***); R = 4.8, G = R/5(***e***); R = 4.8, G = 0(***f***).

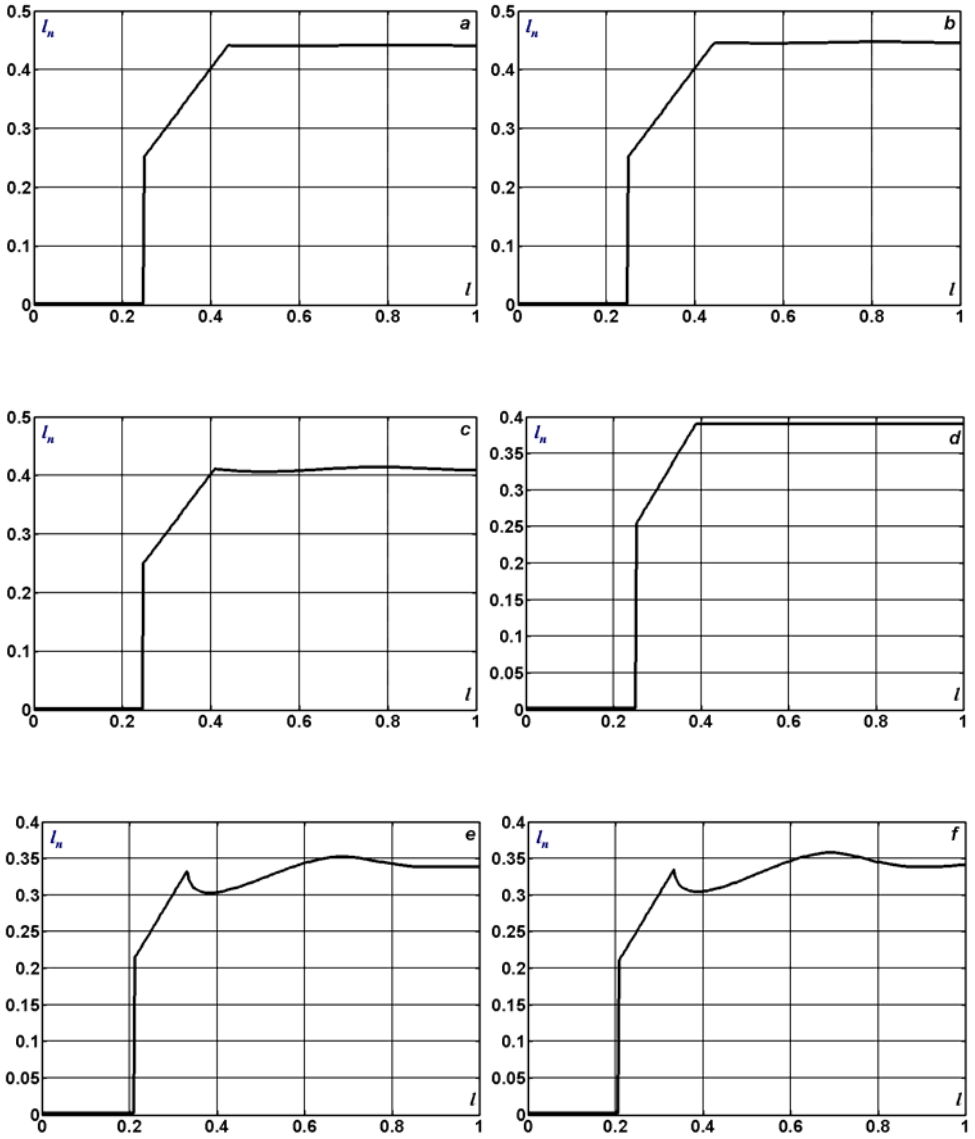

Fig. 15.14. $l_{n,k}$ depending on the line length when $R_S = Z_B$ and $R = 0.48$, $G = R/5$(***a***); $R = 0.48$, $G = 0$(***b***); $R = 1.205$, $G = R/5$(***c***); $R = G = 1.205$(***d***); $R = 4.8$, $G = R/5$(***e***); $R = 4.8$, $G = 0$(***f***).

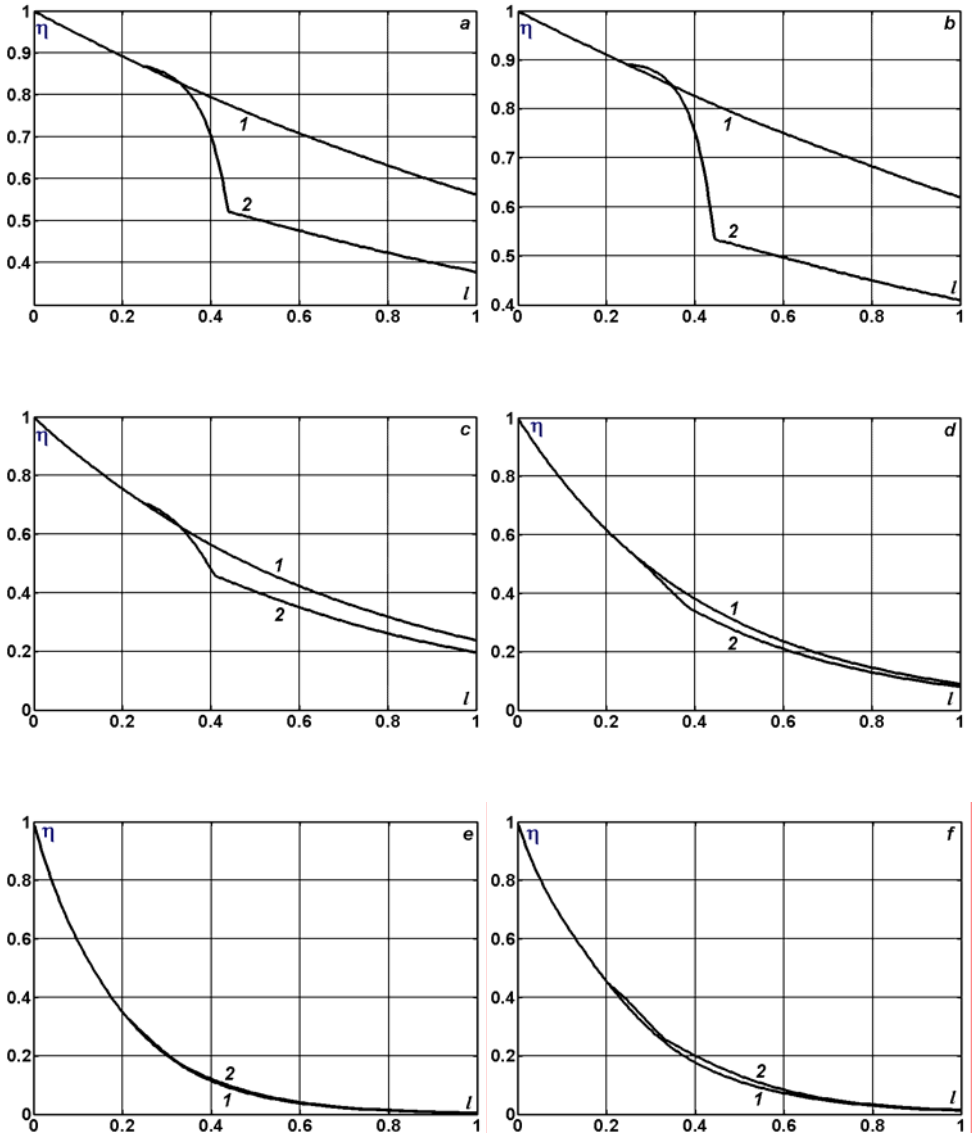

Fig. 15.15. $\eta(X_n^{-1}=0)$ (1) and η ($X_n^{-1}=X_{n,k}^{-1}>0$) (2) depending on the line length when $R_S = Z_B$ and R = 0.48, $G = R/5$(***a***); R = 0.48, G = 0(***b***); R = 1.205, $G = R/5$(***c***); $R = G = 1.205$(***d***); R = 4.8, $G = R/5$(***e***); R = 4.8, G = 0(***f***).

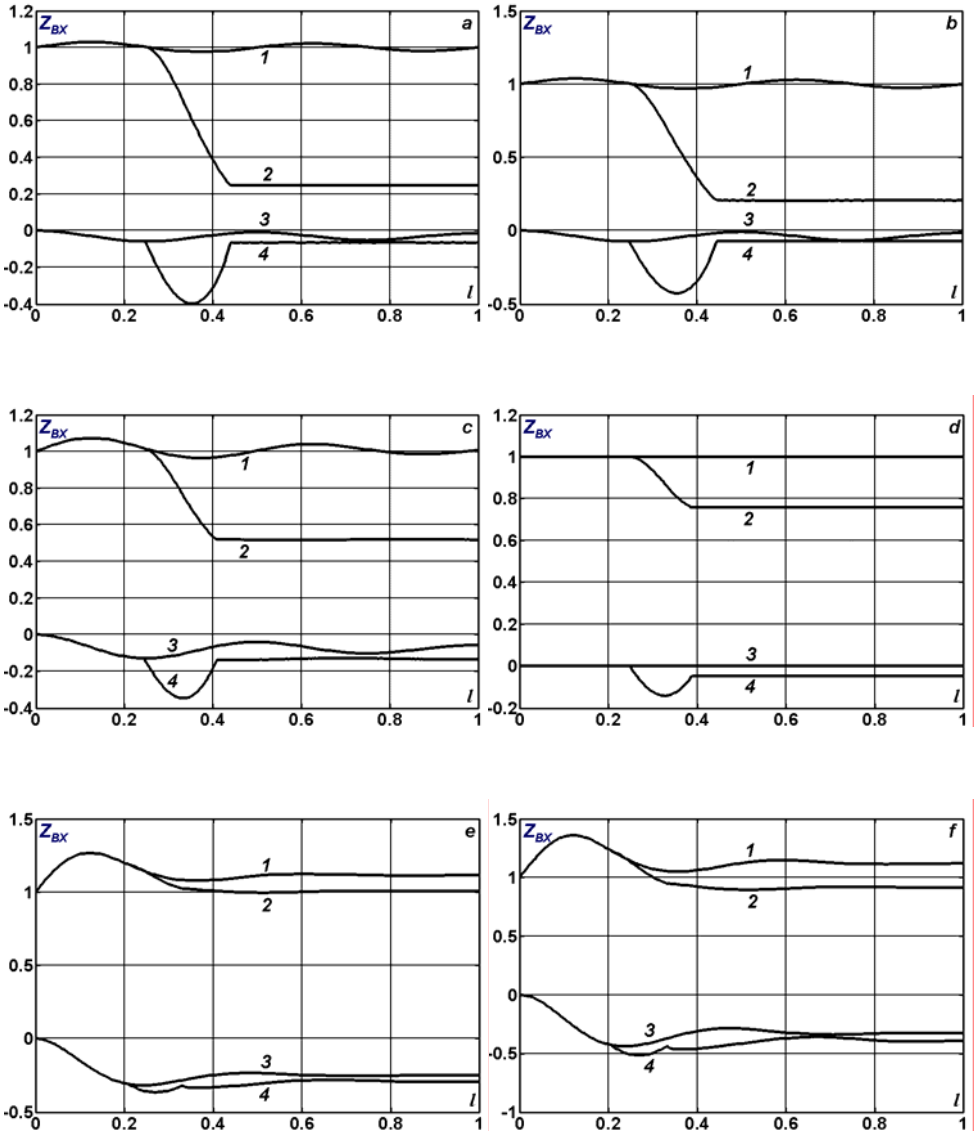

Fig. 15.16. $|Z_{BX}|$(1), $\arg(Z_{BX})$(3) ($X_n^{-1}=0$) and $|Z_{BX}|$(2), $\arg(Z_{BX})$(4) ($X_n^{-1}=X_{n,\boldsymbol{k}}^{-1}>0$)depending on the line length when $R_S = Z_B$ and R = 0.48, G = R/5(***a***); R = 0.48, G = 0(***b***); R = 1.205, G = R/5(***c***); R = G = 1.205(***d***); R = 4.8, G = R/5(***e***); R = 4.8, G = 0(***f***).

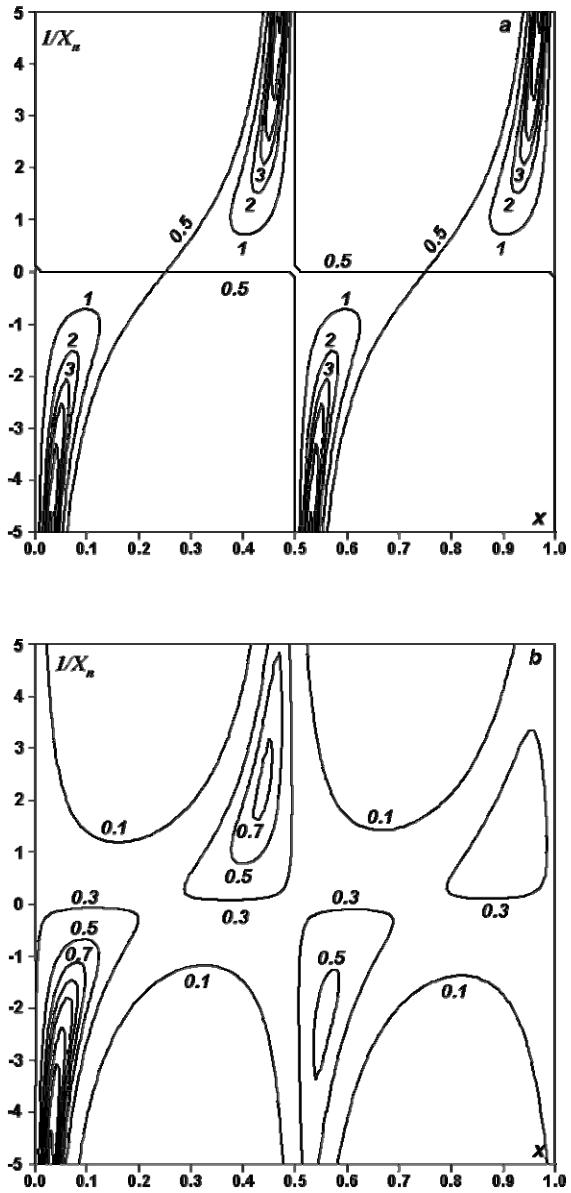

Fig. 15.17. The transmission power depending on the value and on the location of the transverse compensating reactive element X_n when l = 1.0; R = 0 (***a***); 0.48(***b***); $G = R/5$.

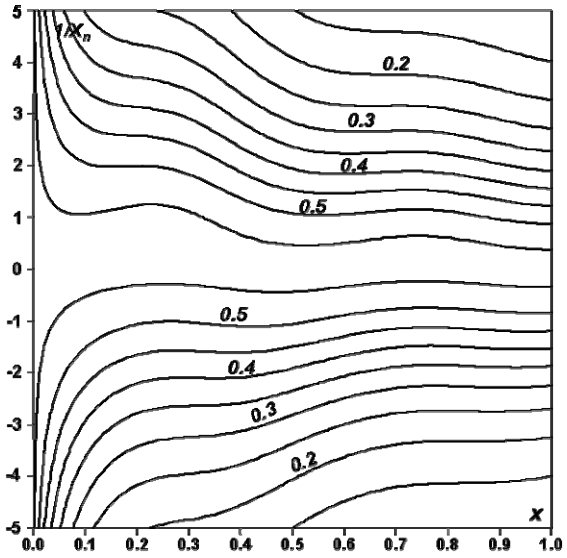

Fig. 15.18. The efficiency depending on the value and on the location of the transverse compensating reactive element X_n when $l = 1.0$; $R = 0.48$; $G = R/5$.

16. How to tune the quarter-wave line to the half-wave regime

Controlled "bucking out" systems or compensating systems (controllable capacitor banks, synchronous condensers and motors with automatic excitation control) are used as an automatic voltage control systems in electric mains.

It is accepted that by compensation of parameters of the line with any length it is possible to impart the characteristic properties of the half-wave line. The idea of adjustment is known for a long time however it does not get yet some practical application. The investigations in the field have shown that the application of the adjusted electric mains is advisable for lines with lengths 1500 – 3500 km. The adjustment to the half-wave is realized by adjusting devices. The adjusting schemes are picked out in such a way as to ensure the minimal consumption of the adjusting devices under the given flow capacity [19, 36].

In this connection we will consider the problem of imparting of characteristic properties of the half-wave line to the quarter-wave line by means of lumped elements (throttles, reactors, banks of capacitors) [74].

16.1. Steady-state regime equations

Let's consider the homogeneous line with length $l = \lambda / 4$ closed to the lumped resistance R_S and consisting from the N parts with lengths l_k, $k = \overline{1, N}$; $l = \sum_{k=1}^{N} l_k$. At the junction points of these parts there parallel or series connected the lumped elements with complex resistances Z_{n1} and Z_{n2} (as it is shown in the fig. 16.1). It is known [89], that .the expression for the power at the receiving end of the ideal half-wave line has the form $P_1 = 0.5U_0^2 / R_S$, i.e. it is in inverse proportion with the load resistance that means the increasing of the power consumption under the parallel electrical customers connection. At the same time for the quarter-wave line we have the opposite picture: $P_1 = 0.5R_S U_0^2$, i.e. the power is directly proportional with the load resistance. In this case the extraction of power at this point must be done by means of series electrical customers connections that are impossible in practice.

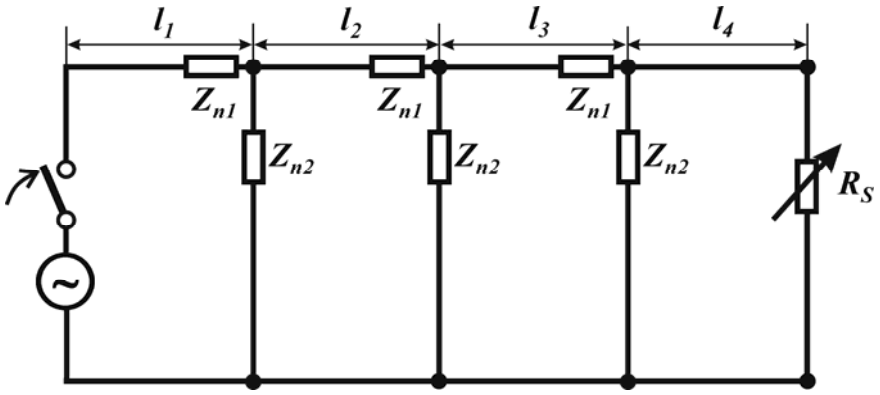

Fig. 16.1. Homogeneous alternating voltage line with series and parallel equidistant connected lumped elements.

Now let's consider the problem of lumped elements connection to the quarter-wave line with purpose to change the nature of load power dependence on the parameter R_S. Since we consider the steady-state regime in the electrical sinusoidal voltage circuit with amplitude U_0, then we can use the symbolic method [59].

Let's denote the complex amplitudes of voltages and currents at the input and output of the electrical circuit by U_0, I_0, U_{N+1}, I_{N+1}, and at the points of lumped elements connection – as follows:

$$U_k(x_k - 0) = U_k^{(1)},\ U_k(x_k + 0) = U_k^{(2)},\ I_k(x_k - 0) = I_k^{(1)},$$

$$I_k(x_k + 0) = I_k^{(2)},\ k = \overline{1,N},\ x_k = \sum_{i=1}^{k} l_i,\ x_1 = l_1,\ x_2 = l_1 + l_2, \ldots$$

In case of homogeneous line with parameters *L*, *C*, *R*, *G* without lumped elements, the solution of the problem at the interval $x \in [0, l]$ has the following form

$$U_0 = Z_{BX} I_0, U_{N+1} = Z_S I_{N+1}, Z_S = R_S, \tag{16.1}$$

$$I_{N+1} = -\frac{U_0}{Z_C}\mathrm{sh}(\delta l) + I_0 \mathrm{ch}(\delta l) = \frac{I_0}{Z_C}\left(Z_C \mathrm{ch}(\delta l) - Z_{BX}\mathrm{sh}(\delta l)\right) =$$

$$= \frac{I_0 Z_0}{Z_S \mathrm{sh}(\delta l) + Z_0 \mathrm{ch}(\delta l)} = \frac{U_0}{Z_S \mathrm{ch}(\gamma l) + Z_0 \mathrm{sh}(\delta l)}, \tag{16.2}$$

$$Z_{BX} = Z_0 \frac{Z_S \mathrm{ch}(\delta l) + Z_0 \mathrm{sh}(\delta l)}{Z_S \mathrm{sh}(\delta l) + Z_0 \mathrm{ch}(\delta l)}, \tag{16.3}$$

$$Z_0 = \sqrt{\frac{R + j\omega L}{G + j\omega C}},\ \delta = \sqrt{(R + j\omega L)(G + j\omega C)}. \tag{16.4}$$

Here Z_{BX}, Z_0 are the input and wave resistances of the line, δ is the propagation factor, Z_H is the load resistance, $\omega = 2\pi f$, f is generator supply frequency.

The solution for the line with *N* connected lumped elements we will obtain in the following manner. Let's suppose that all series connected complex resistances possess the same value Z_{n1}, and those parallel connected – Z_{n2}. Then the conjugation conditions at the points x_k take the form

$$U_k^{(1)} - U_k^{(2)} = Z_{n1} I_k^{(1)}, \quad U_k^{(2)} = Z_{n2}\left(I_k^{(1)} - I_k^{(2)}\right), k = 1,...N. \quad (16.5)$$

To solve the problem with the conjugation conditions (16.5) let's introduce the notion of the input resistance $Z_{BX}^{(k)}$ for parts of the line $x \in [x_k, l], k = \overline{1,N}$. Then the complexes of voltages and currents at the points $x = x_k + 0$ will be connected by relations

$$U_k^{(2)} = Z_{BX}^{(k)} I_k^{(2)}, \quad (16.6)$$

$$Z_{BX}^{(k)} = Z_0 \frac{Z_n^{(k+1)} \mathrm{ch}(\delta l_{k+1}) + Z_0 \mathrm{sh}(\delta l_{k+1})}{Z_n^{(k+1)} \mathrm{sh}(\delta l_{k+1}) + Z_0 \mathrm{ch}(\delta l_{k+1})}, k = \overline{1,N}; Z_n^{(N+1)} = Z_S. \quad (16.7)$$

At the points $x = x_k - 0$ from (16.5) we obtain

$$U_k^{(1)} = Z_n^{(k)} I_k^{(1)}, \quad (16.8)$$

$$Z_n^{(k)} = Z_{n1}^{(k)} + \left(\frac{1}{Z_{BX}^{(k)}} + \frac{1}{Z_{n2}^{(k)}}\right)^{-1}, \quad k = \overline{1,N}. \quad (16.9)$$

The currents and voltages values at the left and at the right of the points x_k and at the ends of the line are connected by the recurrence relations

$$U_k^{(2)} = \left(1 - \frac{Z_{n1}^{(k)}}{Z_n^{(k)}}\right) U_k^{(1)}, \; I_k^{(1)} = \left(1 + \frac{Z_{BX}^{(k)}}{Z_{n2}^{(k)}}\right) I_k^{(2)}, \quad k = \overline{1,N}, \quad (16.10)$$

$$I_1^{(1)} = \frac{I_0 Z_0}{Z_0 \mathrm{ch}(\delta l_1) + Z_n^{(1)} \mathrm{sh}(\delta l_1)} = \frac{U_0}{Z_0 \mathrm{sh}(\delta l_1) + Z_n^{(1)} \mathrm{ch}(\delta l_1)}, \quad (16.11)$$

$$I_{N+1} = \frac{I_N^{(2)} Z_0}{Z_0 \mathrm{ch}(\delta l_{N+1}) + Z_S \mathrm{sh}(\delta l_{N+1})}. \quad (16.12)$$

Combining the formulas (16.10)-(16.12), we obtain the current at the output of the line expressed by initial voltage

$$I_{N+1} = I_0 (Z_0)^{N+1} \left\{ [Z_0 \mathrm{ch}(\delta l_{N+1}) + Z_S \mathrm{sh}(\delta l_{N+1})] \times \right.$$

$$\left. \times \prod_{k=1}^{N} \left[\left(1 + Z_{BX}^{(k)} / Z_{n2}^{(k)} \right) \left(Z_0 \mathrm{ch}(\delta l_k) + Z_n^{(k)} \mathrm{sh}(\delta l_k) \right) \right] \right\}^{-1}, \qquad (16.13)$$

$$I_0 = \frac{U_0}{Z_{BX}}, \quad Z_{BX} = Z_0 \frac{Z_n^{(1)} \mathrm{ch}(\delta l_1) + Z_0 \mathrm{sh}(\delta l_1)}{Z_n^{(1)} \mathrm{sh}(\delta l_1) + Z_0 \mathrm{ch}(\delta l_1)}. \qquad (16.14)$$

The generator power and the load power can be calculated by formulas

$$P_0 = \frac{1}{2} \mathrm{Re}\left(U_0^* I_0 \right) = \frac{1}{2} \mathrm{Re}\left(U_0 I_0^* \right) = \frac{U_0^2}{2} \mathrm{Re}\left(\frac{1}{Z_{BX}} \right),$$

$$P_1 = \frac{1}{2} \mathrm{Re}\left(U_{N+1}^* I_{N+1} \right) = \frac{1}{2} \mathrm{Re}\left(U_{N+1} I_{N+1}^* \right) =$$

$$= \frac{|I_{N+1}|^2 \mathrm{Re}(Z_S)}{2} = \frac{R_S |I_{N+1}|^2}{2}. \qquad (16.15)$$

The obtained formulas (16.6)–(16.15) give the possibility to realize the parametrical analysis lumped elements connection influence on the distribution of voltages, currents and power along the line.

16.2. Numerical results

Let's consider the homogeneous quarter-wave line with parameters: l = 1/4; $C = L = 1$. The diagrams in the fig. 16.2, 16.3 represent the load power P_1 and generator power P_0 depending on the dimensionless parameter $z = (R_S - 1)/(R_S + 1)$ for the lines with length l = 1/2 (curve 1) and l = 1/4 (curve 2) without insertions. Then for quarter-wave line we consider the insertions at the points $x_k = k/(4(N+1))$, $k = \overline{1, N}$ of the series connected complex

resistances $Z_{n1} = (R + j\omega L)/(4N)$ and of the parallel connected complex resistances $Z_{n2} = 4N/(G + j\omega C)$: $N = 2$ (3), $N = 4$ (4), $N = 6$ (5), $N = 8$ (6) $N = 10$ (7).

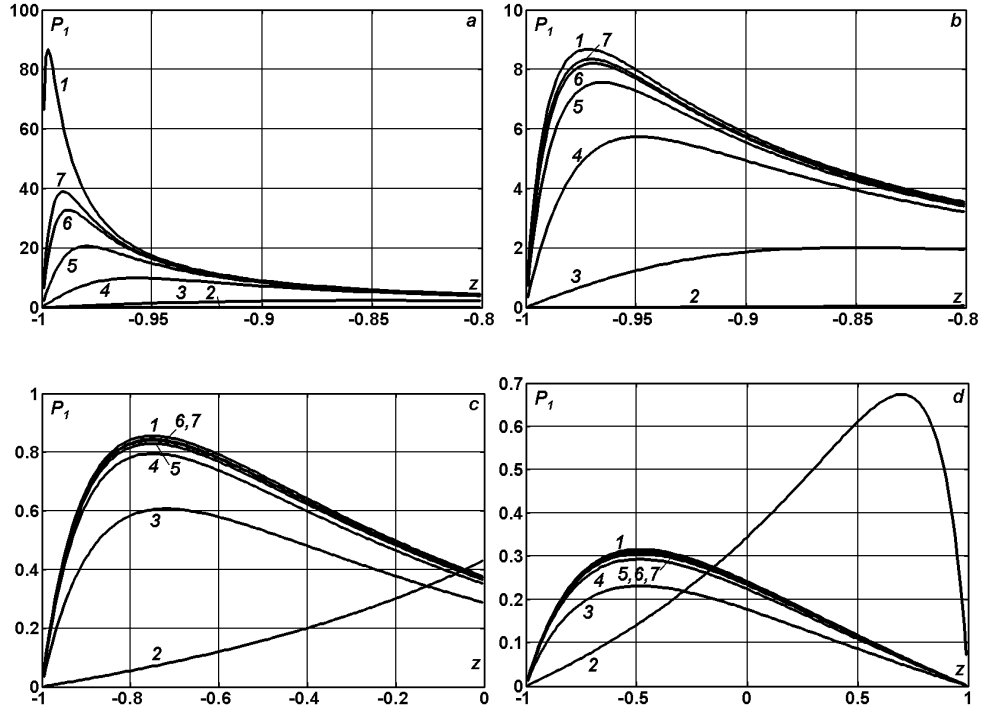

Fig 16.2. Transmission power depending on load resistance when $G = R/5$, $R =$ 0.0048 (***a***); 0.048 (***b***);0.48 (***c***); 1.205 (***d***).

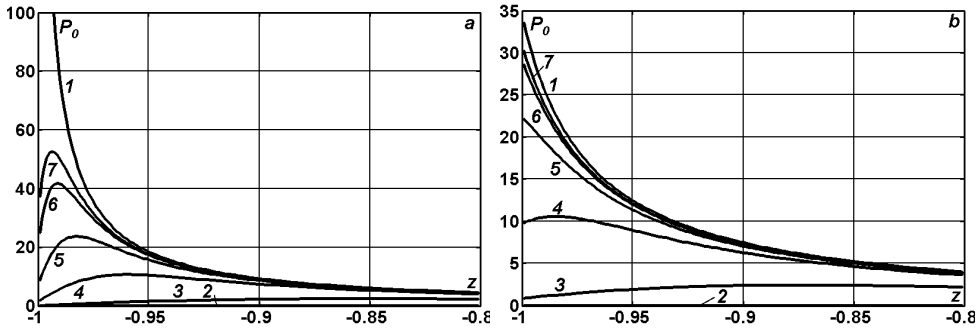

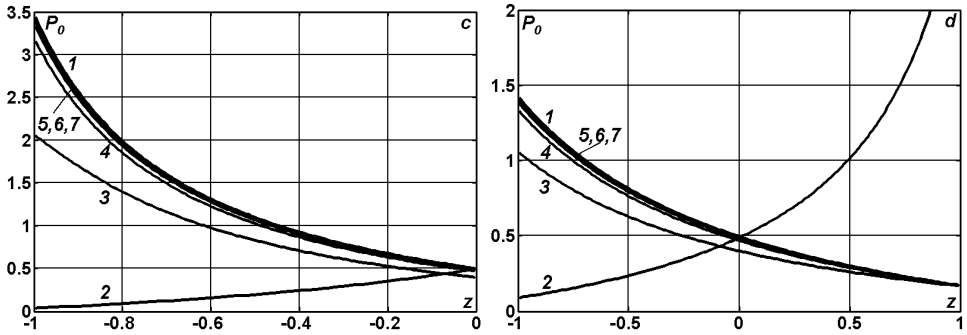

Fig 16.3. Generated power depending on load resistance when $G = R/5$, $R = 0.0048$ (***a***); 0.048 (***b***);0.48 (***c***); 1.205 (***d***).

The presented results show that the compensation by means of resistances Z_{n1}, Z_{n2} with nonzero active components makes it possible to transform the quarter-wave line to the half-wave line when even 8 … 10 supplementary elements are connected. At the same time the nature of voltage distribution along the compensated quarter-wave line is at most approximated to the same for half-wave line (see fig. 16.4).

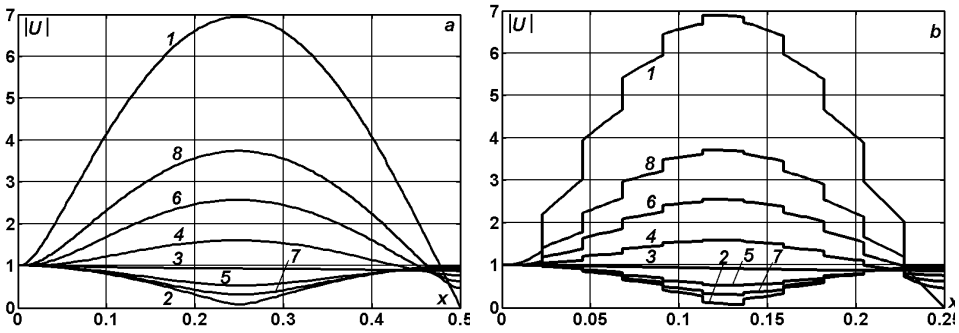

Fig 16.4. Voltage modulus depending on line length for half-wave line (***a***) and for quarter-wave line (***b***) with 10 lumped elements with resistances $Z_{n1} = (R+j\omega L)/40$, $Z_{n2} = 40/(G+j\omega C)$ when $R = 0.48$, $G = R/5$ and $R_S = 0$ (curve 1); ∞ (2); 1 (3); 1/2 (4); 2 (5); 1/4 (6); 4 (7); 1/8 (8).

At the same time if we will try to compensate the line by means of pure active resistances (throttles and condensers), then (as it is seen from diagrams in the fig. 16.5–16.8) the quarter-wave line (curves 2 – 7) can be approximated to the half-wave line (curve 1) only qualitatively. However this result turns out to be acceptable from the practice point of view.

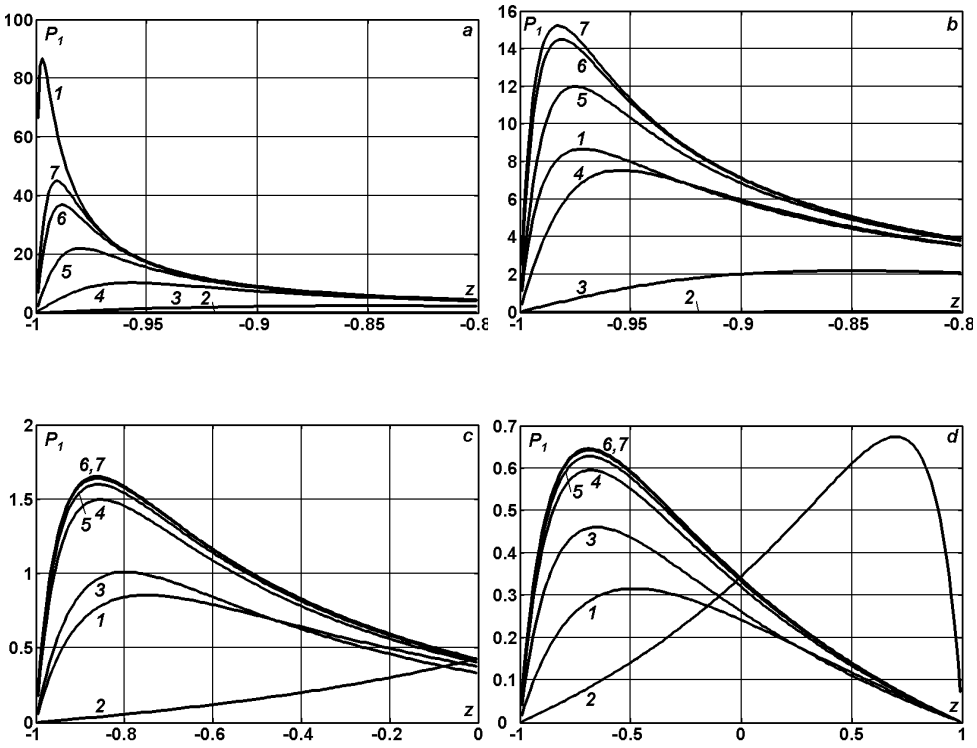

Fig 16.5. Transmission power depending on load resistance when $G = R/5$, $R = 0.0048$ (***a***); 0.048 (***b***); 0.48 (***c***); 1.205 (***d***) and $Z_{n1} = j\omega L/(4N)$ and $Z_{n2} = -j4N/(\omega C)$.

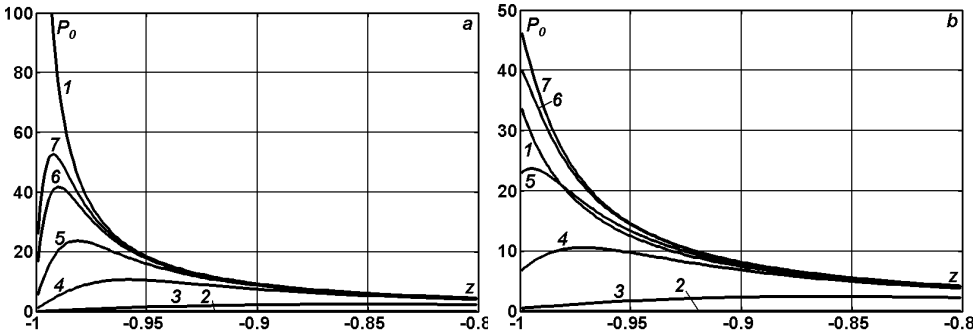

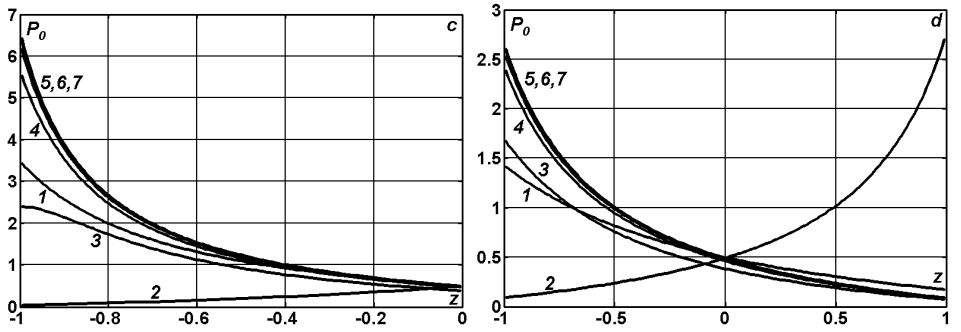

Fig 16.6. Generated power depending on load resistance when $G = R/5$, $R = 0.0048$ (***a***); 0.048 (***b***);0.48 (***c***); 1.205 (***d***) and $Z_{n1} = j\omega L/(4N)$ and $Z_{n2} = -j4N/(\omega C)$.

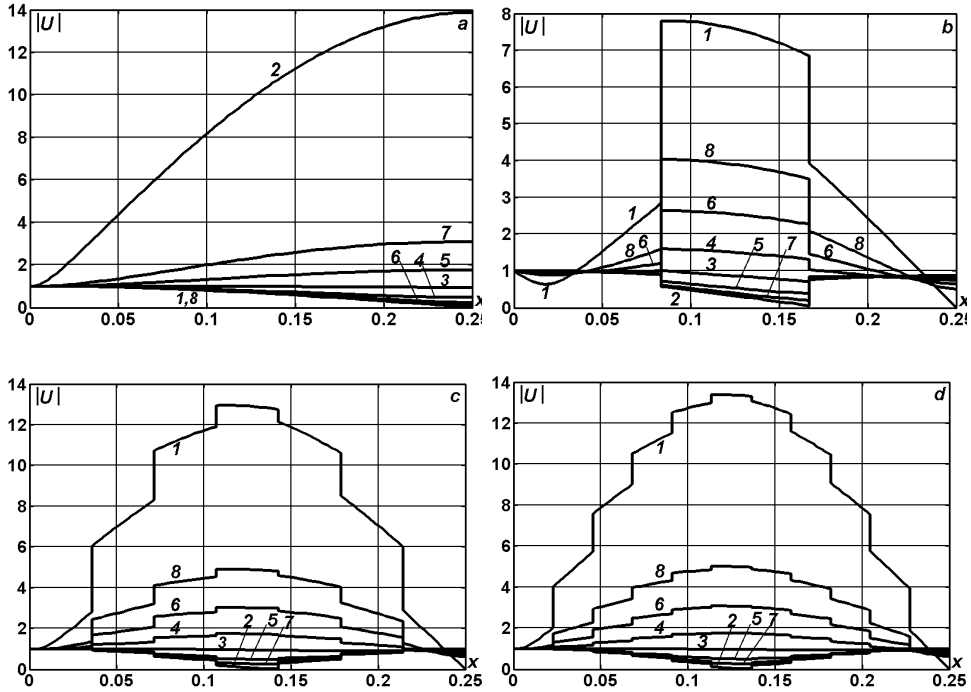

Fig 16.7. Voltage modulus distribution for quarter-wave line (***a***), with two (N=2) (***b***), with six (N=6) (***c***) and with ten (N=10) (***d***) compensating elements with resistances $Z_{n1} = j\omega L/(4N)$, $Z_{n2} = -j4N/(\omega C)$ when $R = 0.48$, $G = R/5$ and $R_S =$ 0 (curve 1); ∞ (2); 1 (3); 1/2 (4); 2 (5); 1/4 (6); 4 (7); 1/8 (8).

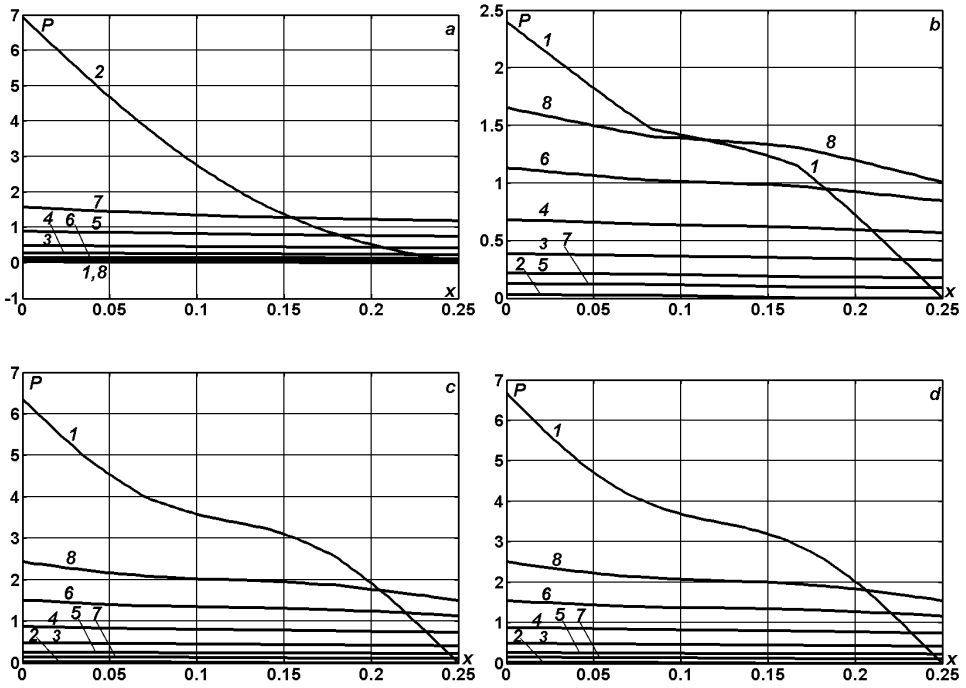

Fig 16.8. The active power distribution along the quarter-wave line (***a***), with two (N=2) (***b***), with six (N=6) (***c***) and with ten (N=10) (***d***) compensating elements with resistances $Z_{n1} = j\omega L/(4N)$, $Z_{n2} = -j4N/(\omega C)$ when R = 0.48, $G = R/5$ and $R_S = 0$ (curve1); ∞ (2); 1 (3); 1/2 (4); 2 (5); 1/4 (6); 4 (7); 1/8 (8).

Thus, the analytical formulas and the numerical results for steady-state power transmission process calculations in the piecewise-homogeneous loaded and unloaded alternating voltage transmission line are cited and represented. The throttles and bank of capacitors connections to the quarter-wave line allow us to fetch its properties to the half-wave line properties.

17. Idling and natural power transfer loss saving by means of shunt reactors and reactive power sources

The “losses control problem” has had, for a long-time, a cult-like status among the power engineering community. A significant amount of forces from the scientific, technological and civil-engineering communities is dedicated to solving this problem. The loss saving within a small fraction of a percent is usually considered to be a major achievement in this domain.

The main factors, that determine the losses during its transmission by means of alternating or continuous current, are active longitudinal resistance $R(x,t)$ and shunt admittance of insulation $G(x,t)$. However, both wave dissipation and wave dispersion are present in high-current electric circuits. In particular, this circumstance can be used for component redistribution of the quasi-steady electromagnetic processes: decreasing the power of magnetic field in favor of increasing the power of electric field. As a consequence, the idling and natural power transfer losses saving can be reached

17.1. The steady-state regime in the homogeneous transmission line with lumped LC – circuits

Let's consider the connection to the line of the "bucking out" systems in the form of shunt reactors and the bank of capacitors (fig. 17.1). As long as we consider the steady-state regime in the electric circuit with sinusoidal current, we apply the symbolic method [59] to solve the telegraph equations.

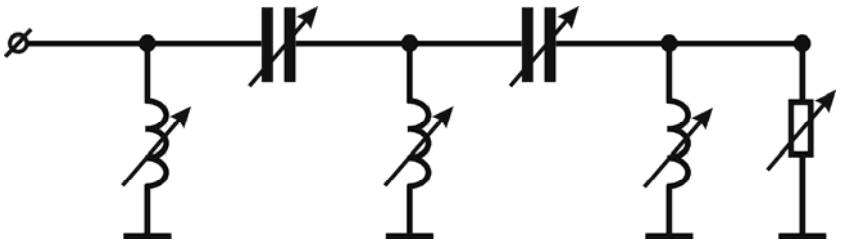

Fig. 17.1. Shunt reactors and reactive power sources connection to the transmission line.

Let's denote the complex voltage and current amplitudes at the sending end and output end of the electric circuit by U_0, I_0, U_N, I_N and at the points of connection of lumped elements by

$$U_k(x_k - 0) = U_k^{(1)},\ U_k(x_k + 0) = U_k^{(2)},\ I_k(x_k - 0) = I_k^{(1)},$$

$$I_k(x_k + 0) = I_k^{(2)},\ k = \overline{1, N-1},$$

$$x_k = \sum_{i=1}^{k} l_i,\ x_1 = l_1,\ x_2 = l_1 + l_2, \ldots,\ x_N = l.$$

In case of homogeneous transmission line with parameters *L*, *C*, *R*, *G* without lumped elements the problem solution at interval $x \in [0, l]$ takes the following form

$$U_0 = Z_{BX} I_0, U_N = Z_S I_N, Z_S = R_S, \tag{17.1}$$

$$I_N = -\frac{U_0}{Z_0}\mathrm{sh}(\delta l) + I_0 \mathrm{ch}(\delta l) = \frac{I_0}{Z_0}\left(Z_0 \mathrm{ch}(\delta l) - Z_{BX}\mathrm{sh}(\delta l)\right) =$$

$$= \frac{I_0 Z_0}{Z_S \mathrm{sh}(\delta l) + Z_0 \mathrm{ch}(\delta l)} = \frac{U_0}{Z_S \mathrm{ch}(\delta l) + Z_0 \mathrm{sh}(\delta l)}, \tag{17.2}$$

$$Z_{BX} = Z_0 \frac{Z_S \mathrm{ch}(\delta l) + Z_0 \mathrm{sh}(\delta l)}{Z_S \mathrm{sh}(\delta l) + Z_0 \mathrm{ch}(\delta l)}, \tag{17.3}$$

$$Z_0 = \sqrt{\frac{R + j\omega L}{G + j\omega C}}, \ \delta = \sqrt{(R + j\omega L)(G + j\omega C)}\,. \tag{17.4}$$

Here Z_{BX}, Z_0 are the input resistance and the impedance (wave resistance) of the line, γ is the propagation factor, Z_S is the load resistance, $\omega = 2\pi f$, f is the frequency of the feeding generator.

The solution for the line with (*N*-1) lumped elements is obtained by us in the following manner: Let's denote the resistances of the series reactive power sources by $Z_{n1}^{(k)}$, and the resistances of the connected in parallel shunt reactors by $Z_{n2}^{(k)}$. Then, the conjugation constraints for the reactive power sources in the points x_k take the form

$$U_k^{(1)} - U_k^{(2)} = Z_{n1}^{(k)} I_k^{(1)}, \quad I_k^{(1)} = I_k^{(2)}, \ Z_{n2}^{(k)} = \infty, k = 1,..., N-1 \tag{17.5}$$

and the following one, for the shunt reactors

$$U_k^{(1)} = U_k^{(2)}, \quad U_k^{(2)} = Z_{n2}^{(k)}\left(I_k^{(1)} - I_k^{(2)}\right), \ Z_{n1}^{(k)} = 0, k = 1,..., N-1\,. \tag{17.6}$$

To solve the problem with conjugation constraints (17.5) and (17.6) let's introduce the concepts of input resistance $Z_{BX}^{(k)}$ for the parts of the line $x \in [x_k, l]$, $k = \overline{1, N-1}$. Then, the complexes of the voltages and of the currents at the points $x = x_k + 0$ will be related by formulas

$$U_k^{(2)} = Z_{BX}^{(k)} I_k^{(2)}, \tag{17.7}$$

$$Z_{BX}^{(k)} = Z_0 \frac{Z_n^{(k+1)} \mathrm{ch}(\delta l_{k+1}) + Z_0 \mathrm{sh}(\delta l_{k+1})}{Z_n^{(k+1)} \mathrm{sh}(\delta l_{k+1}) + Z_0 \mathrm{ch}(\delta l_{k+1})}, k = \overline{0, N-1}; Z_n^{(N)} = Z_S. \tag{17.8}$$

From (17.5) and (17.6) at the points $x = x_k - 0$ we'll have

$$U_k^{(1)} = Z_n^{(k)} I_k^{(1)} \quad k = \overline{1, N-1}, \tag{17.9}$$

where $Z_n^{(k)} = Z_{n1}^{(k)} + Z_{BX}^{(k)}$ for reactive power sources and $Z_n^{(k)} = \dfrac{Z_{n2}^{(k)} Z_{BX}^{(k)}}{Z_{n2}^{(k)} + Z_{BX}^{(k)}}$ for shunt reactors.

The current and voltage values at the left and at the right of the points x_k and at the ends of the line are in the following recurrence relations

$$I_1^{(1)} = \frac{I_0 Z_0}{Z_0 \mathrm{ch}(\delta l_1) + Z_n^{(1)} \mathrm{sh}(\delta l_1)}, I_0 = U_0 / Z_{BX}^{(0)}, U_1^{(1)} = Z_n^{(1)} I_1^{(1)}, \tag{17.10}$$

$$U_k^{(2)} = \left(1 - \frac{Z_{n1}^{(k)}}{Z_n^{(k)}}\right) U_k^{(1)}, \; I_k^{(1)} = \left(1 + \frac{Z_{BX}^{(k)}}{Z_{n2}^{(k)}}\right) I_k^{(2)}, \quad k = \overline{1, N-1}, \tag{17.11}$$

$$I_k^{(1)} = \frac{I_{k-1}^{(2)} Z_0}{Z_0 \mathrm{ch}(\delta l_k) + Z_n^{(k)} \mathrm{sh}(\delta l_k)}, U_k^{(1)} = Z_n^{(k)} I_k^{(1)}, \quad k = \overline{2, N-1}, \tag{17.12}$$

$$I_N = \frac{I_{N-1}^{(2)} Z_0}{Z_0 \mathrm{ch}(\delta l_N) + Z_S \mathrm{sh}(\delta l_N)}, U_N = Z_S I_N. \tag{17.13}$$

Combining the formulas (17.10) – (17.13), we obtain the formula for current at the output expressed through the initial voltage

$$I_N = I_0 (Z_0)^N \left\{ [Z_0 \mathrm{ch}(\delta l_N) + Z_S \mathrm{sh}(\delta l_N)] \times \right.$$

$$\left. \times \prod_{k=1}^{N-1} \left[\left(1 + Z_{BX}^{(k)} / Z_{n2}^{(k)} \right) \left(Z_0 \mathrm{ch}(\delta l_k) + Z_n^{(k)} \mathrm{sh}(\delta l_k) \right) \right] \right\}^{-1}, \qquad (17.14)$$

$$I_0 = \frac{U_0}{Z_{BX}^{(0)}}, \quad Z_{BX}^{(0)} = Z_0 \frac{Z_n^{(1)} \mathrm{ch}(\delta l_1) + Z_0 \mathrm{sh}(\delta l_1)}{Z_n^{(1)} \mathrm{sh}(\delta l_1) + Z_0 \mathrm{ch}(\delta l_1)}. \qquad (17.15)$$

The generator power and the loading power can be calculated using the formulas

$$P_0 = \frac{1}{2} \mathrm{Re}\left(U_0^* I_0 \right) = \frac{1}{2} \mathrm{Re}\left(U_0 I_0^* \right) = \frac{U_0^2}{2} \mathrm{Re}\left(\frac{1}{Z_{BX}^{(0)}} \right),$$

$$P_1 = \frac{1}{2} \mathrm{Re}\left(U_N^* I_N \right) = \frac{1}{2} \mathrm{Re}\left(U_N I_N^* \right) = \frac{|I_N|^2 \, \mathrm{Re}(Z_S)}{2} = \frac{R_S |I_N|^2}{2}. \qquad (17.16)$$

The obtained relations (17.6) – (17.16) allow us to carry out the parametric analysis of the influence of connecting lumped elements on the voltage and current distributions as well as on the power losses along the whole line

$$\Pi = \frac{P_0 - P_1}{P_H}, \quad P_H = \frac{U_0^2}{2 Z_B}.$$

17.2. The results of numerical experiments regarding loss minimization

Let's consider a homogeneous (without additional connections) line with dimensionless parameters $C = L = 2P_{\text{н}} = 1$; $R = 0.48$; $G = R/7$. Let the line be closed on the load with complex resistance Z_S. At first, we construct the functional dependences of the active and reactive source power (generator) on the length of the open-ended line without losses $R = G = 0$ (*a*) and with losses $R = 7G = 0.48$ (*b*). As can be seen on graphic representation (see fig. 17.2), the active losses in the neighborhood of the quarter-wave line

without loading ($Z_S = \infty$) reach peak values, whereas the active losses for half-wave line are relatively not too large and constitute only 13.58% comparing with natural power $P_{\text{H}} = 0.5$. In case when there is a matched load in the line $Z_S = Z_0 = 1.0009 - j0.0327$ then the active power losses are equal to 24.75%, but when the load is purely active $Z_S = Z_B = 1$ then the losses are slightly smaller and constitute 24.65%. However, the losses during the idling must be minimally half as great as during the natural power transmission [3, 4, 8]. Therefore, let's consider the problem of losses minimization by connecting the "bucking out" systems in the form of shunt reactors and reactive power sources in the line.

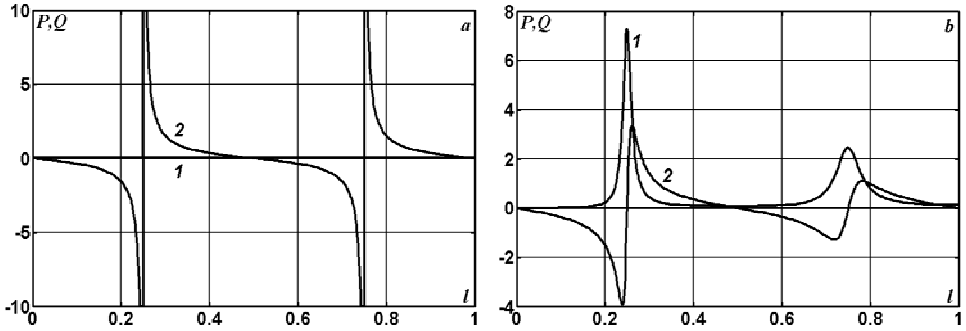

Fig. 17.2. Active and reactive powers of generator (curves 1, 2) depending on the length of open-ended line when $R = G = 0$ (*a*); $R = 7G = 0.48$ (*b*).

The parallel connection to the line of the ideal shunt reactor makes it possible to reduce the idling losses up to 2.28% if the inductances and their locations will be chosen as in the table 17.1. At the same time, the serial connection to the line of the bank of capacitors with capacitances C_n does not give some appreciable result. In case of the 1/4-wave or 1/8-wave lines (the tables 17.2 and 17.3), the connection of only two reactors results in a decrease of losses up to 1.97% and 0.89% respectively. Let's remember that the dimensionless value $L_n = 1$ corresponds to $L_n = 5.56$ H with the reactor power $Q_n = \dfrac{U_0^2}{2\omega L_n} = 330.5$ MVAr and the phase voltage $U_0 = 525\sqrt{2/3} = 428.66$ kV.

All foregoing results bring out clearly the evident advantages of the shunt reactors in comparison with reactive power sources from the standpoint of solving the problem of idling losses minimization and confirm the conclusions stated by G. Alexandrov in [3, 4, 59].

Table 17.1. The idling losses in dependence of the number, location and parameters of the reactors or reactive power sources connected to the half-wave transmission line.

Number	x_k	L_n	P_0/P_H, %	x_k	C_n	P_0/P_H, %
1	0.25	∞	13.58	0.25	∞	13.58
1	0.22638	0.00245	6.74	0.46029	0.11817	13.53
2	0.15533 0.36912	0.09390 0.04890	4.27	0.45535 0.47161	0.24704 0.15124	13.53
3	0.11292 0.24922 0.41186	0.15969 0.12447 0.10067	3.40	0.00000 0.00000 0.49621	0.57724 0.61198 0.96338	13.43
4	0.08841 0.18948 0.30489 0.43314	0.21997 0.18807 0.16192 0.14649	3.00	0.00000 0.00115 0.48868 0.50000	0.56071 0.67903 0.93410 0.48271	13.49
5	0.07706 0.16118 0.24786 0.34926 0.45146	0.25316 0.25289 0.22467 0.18798 0.21637	2.28	0.00000 0.00001 0.00001 0.00021 0.00052	1.08447 0.45487 1.49851 0.91257 0.39859	13.11

Nevertheless in some articles [40, 41, 90] it is pointed out at some undesirable consequences in exploiting of overhead transmission line 500…1150 kV, equipped with shunt reactors, under the abnormal (asymmetrical, unbalanced, open-phase operating) regimes. The utilization of the shunt reactors distinctly complicates the processes of commutation of overhead transmission lines and can give rise to resonance conditions resulting from the presence of line capacitance and reactor inductance. Hence, it is necessary to calculate the transient processes caused by short-term open-phase operating energization (de-energization) of overhead high-voltage transmission lines. Now we are going to consider this problem in detail using the exact formulation of the initial boundary-value problem for telegraph equations. It is also necessary to carry out careful comparative study of efficiency and controllability of shunt reactors of different embodiment controlled by means of magnetic bias circuits or by means of a transformer type compensator. This kind of study allows to determine the preferred possibilities for utilization of these reactors in the overhead high-voltage transmission lines of different purpose and embodiment [40, 41, 90].

Table 17.2. The idling losses in dependence of the number, location and parameters of the reactors or reactive power sources connected to the quarter-wave transmission line.

Number	x_k	L_n	P_0/P_H, %	x_k	C_n	P_0/P_H, %
1	0.125	∞	1458.9	0.125	∞	1458.9
1	0.16217	0.10119	2.87	0.00000	0.48387	60.20
2	0.09568 0.19773	0.20777 0.19691	1.97	0.00000 0.00000	1.51370 0.94687	85.52
3	0.06786 0.13912 0.21276	0.30754 0.29372 0.28677	1.75	0.03246 0.03246 0.07716	1.60984 0.00253 0.01658	0.26
4	0.05314 0.11014 0.16520 0.22073	0.38617 0.37512 0.41541 0.36984	1.67	0.00000 0.00650 0.00650 0.01499	0.42379 0.02427 0.17994 0.32825	0.13
5	0.04413 0.08972 0.13610 0.18218 0.22719	0.47755 0.48316 0.45735 0.49357 0.47919	1.62	0.00129 0.00129 0.00159 0.01429 0.14792	0.24725 0.16917 0.43684 0.12460 0.01353	0.29

Table 17.3. The idling losses in dependence of the number, location and parameters of the reactors or reactive power sources connected to the 1/8-wave transmission line.

Number	x_k	L_n	P_0/P_H, %	x_k	C_n	P_0/P_H, %
1	0.06	∞	3.58	0.25	∞	3.58
1	0.08293	0.25119	1.01	0.00000	0.63404	2.29
2	0.04953 0.09976	0.43598 0.43173	0.89	0.00000 0.00000	0.37061 0.41082	1.09
3	0.03527 0.07101 0.10698	0.61837 0.61225 0.60959	0.86	0.00000 0.00000 0.00000	0.33919 0.23981 0.34709	0.53
4	0.02792 0.05573 0.08342 0.11119	0.78128 0.80428 0.78987 0.79797	0.85	0.00431 0.00431 0.00438 0.00459	0.11847 0.19833 0.19509 0.16596	0.18
5	0.02235 0.04433 0.06712 0.09034 0.11338	1.00494 1.00472 0.93802 0.96340 0.95189	0.84	0.00007 0.00008 0.00017 0.00017 0.02523	0.15397 0.12380 0.15445 0.14623 0.17232	0.09

For visual demonstration, let's represent some of the obtained results for determination of optimal power and location of shunt reactors in the graphical form. The distributions along the half-wave line of the active (curves 1, 2) and reactive (3, 4) power are presented in fig. 17.3 (*a*). The distributions of voltage modulus (curves 1, 2) and current modulus (3, 4) are presented in fig. 17.3 (*b*). All results in fig. 17.3 are obtained in case when $R = 7G = 0.48$ for five shunt reactors providing the minimal value for idling losses. The curves 1, 3 hereinafter correspond to homogeneous line without additional lumped elements.

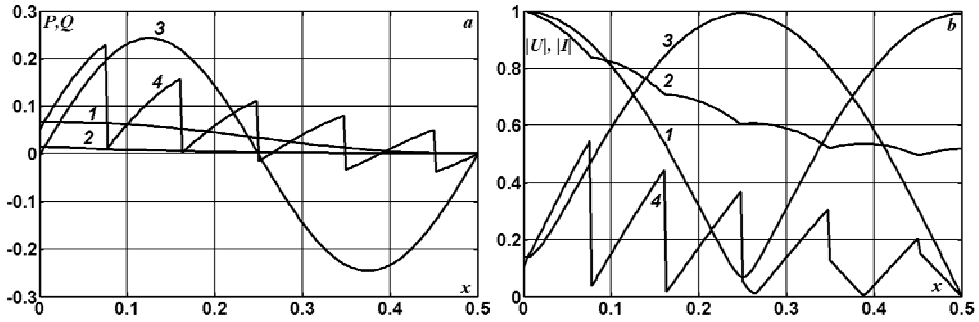

Fig. 17.3. The distribution along the half-wave line of the active (curves 1, 2) and reactive (curves 3, 4) power (***a***), voltage modulus (curves 1, 2) and current modulus (curves 3, 4) (***b***) when $R = 7G = 0.48$ for five shunt reactors connected to the line.

The physical meaning of the obtained results at the qualitative level is sufficiently evident. In the line with connected reactors, we obtain the voltage equalization along the line and simultaneous decreasing of modulus current. Due to this fact, a decrease of the power of the magnetic field and an increase of the power of the electric field takes place in the whole line. Let's remember that the total losses in the wires are determined by two components: active (ohmic) losses Ri^2 and the losses caused by leakage of current through imperfect isolation Gu^2. Since $R > G$, then the redistribution of the electromagnetic field components makes it possible to minimize the total losses. The same effect can not be achieved in case of undistorting line, because we have here $R = G$ in dimensionless form. This example of the comparative analysis of computational results serves as a good illustration of the evident advantages provided by the transfer to dimensionless variables [49].

It is considered, that the half-wave line has such a remarkable property as the equilibrium by reactive power. In consequence, there is no need to install additional "bucking out" systems for its functioning [19, 22, 36, 104].

Let's examine this case and see if it is possible to increase simultaneously the power transfer and efficiency using the shunt reactors, selecting their powers and locations in some optimal manner.

Because of obvious reasons, the problem of searching the optimal parameters of "bucking out" systems, with the scope of wire losses decreasing during the natural power transfer, is much more complicated. Hereinafter we consider the half-wave line with losses, closed on pure active load $Z_S = Z_B = 1$, because in this case the efficiency is is higher, but not too much, than in case of progressing wave regime when the space wave transfers the energy in the matched load: $Z_S = Z_0 = 1.0009 - j0.0327$. Let's perform this search by means of configuration method in the space of variables x_k, L_n without any restrictions on reactors location or on maximal values of the voltages along the whole line.

Connection to the half-wave line of 3…4 reactors makes it possible to decrease the active losses with more than 3%, if at the same time there are no restrictions upon the voltage drops along the line (table 17.4). The further increase in the number of "bucking out" systems does not contribute to an increase of efficiency.

Table 17.4. The maximal values of the power transfer and efficiency in dependence on the number, location and parameters of the reactors.

Number	x_k	L_n	P_1	η, %
1	0.25	∞	0.38000	76.033
1	0.27921	0.35344	0.38618	77.237
2	0.23540 0.43754	0.28354 0.42204	0.39166	78.331
3	0.19028 0.32904 0.50000	0.36976 0.34469 0.36019	0.39568	79.136
4	0.17687 0.28016 0.33871 0.49976	0.48660 0.84034 0.49917 0.43407	0.39594	79.188

Let's consider now the fig. 17.4, where we have the distribution along the half-wave line of the active (curves 1, 2) and reactive (curves 3, 4) power (***a***), voltage modulus (curves 1, 2) and current modulus (curves 3, 4) (***b***) for four shunt reactors connected to the line, the last one being "clasped" to the receiver. The presented results show that the decrease of the losses is

accompanied, unfortunately, by reactive an increase of power the whole line and, especially, at its starting end. Here the generator begins to consume the reactive power (see curve 4) that is always extremely undesirable, because this leads to its rapid deterioration.

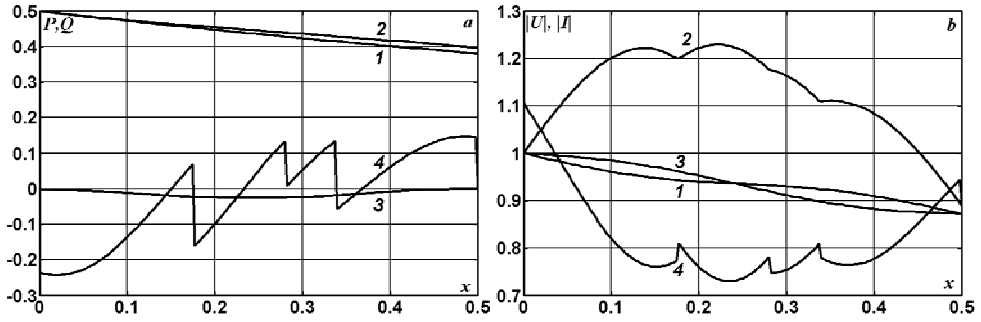

Fig. 17.4. The distributions along the half-wave line of the active (curves 1, 2) and reactive (curves 3, 4) power (***a***), voltage modulus (curves 1, 2) and current modulus (curves 3, 4) (***b***) for four shunt reactors connected to the line.

The situation improves drastically if we limit to 1.05 the maximal value of the voltage modulus in the line (table 17.5, fig.17.5). Taking into account the 5% restriction on voltage exceeding in the line, the effect from connection of shunt reactors decreases up to 1.8%, but the first reactor, "clasped" to the voltage source, forces the generator not to consume but to return the reactive power in the line (Q = 0.04 when $x = 0$). The obtained profit in efficiency is enough good.

Table 17.5. The maximal values of the power transfer and efficiency in dependence on location and inductance values of the four shunt reactors under the restriction: $\max\limits_{x\in[0,l]}|U(x)| \le 1.05$.

Number	x_k	L_n	P_1	η, %
1	0.25	∞	0.38000	76.033
4	0.00153 0.16895 0.29023 0.47255	0.61539 0.82961 0.71337 0.78460	0.38912	77.824

If we will suppose that the insulation of the half-wave line is ideal (G = 0), than in such a line (with stronger wave dispersion) the effect intensifies

up to 2% in comparison with homogeneous line (table 17.6). For loaded undistorting line (R = G and only the wave dissipation exists) it is impossible to decrease the losses as well as in the idling regime.

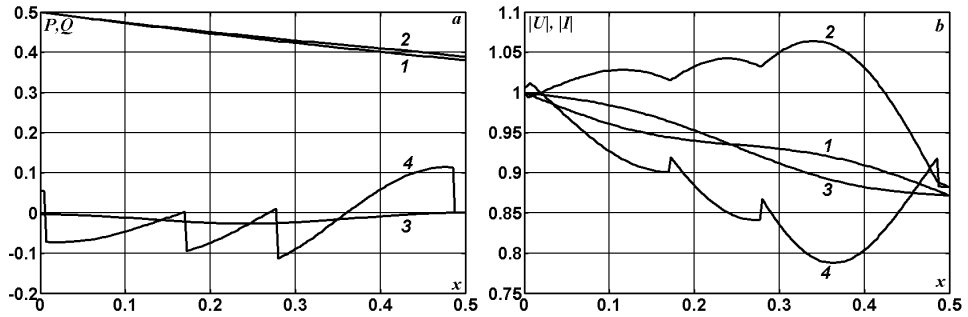

Fig. 17.5. The distributions along the line of the active (curves 1, 2) and reactive (curves 3, 4) power (***a***), voltage modulus (curves 1, 2) and current modulus (curves 3, 4) (***b***) for four shunt reactors connected to the line under the restriction: $\max_{x\in[0,l]}|U(x)| \le 1.05$.

Thus, the calculation relations for voltage, current, active and reactive power determination for the steady-state regime in the alternating voltage circuit with distributed and lumped parameters are obtained. The connection of the shunt reactors and reactive power sources in the form of the bank of capacitors makes it possible the decrease of idling losses in a several times for lines with different length.

Table 17.6. The maximal values of the power transfer and efficiency in dependence on location and inductance values of the four shunt reactors in case of half-wave line with ideal insulation (G = 0) and under the restriction: $\max_{x\in[0,l]}|U(x)| \le 1.05$.

Number	x_k	L_n	P_1	η, %
1	0.25	∞	0.39326	78.690
4	0.00003 0.15256 0.28372 0.46822	0.92998 0.82858 0.84911 0.73522	0.40340	80.680

The efficiency in the half-wave line at the natural power transfer can be increased more then on 3% in case when there are no restrictions on the

voltage exceeding or on 1.8% when the voltage exceeding are restricted by limiting value of 1.05. The connection of the "bucking out" systems in the undistorting line does not give rise to decrease the losses in the line.

18. Decomposition method for calculation of two generators optimal action under general loads

As it was shown in [90] the nature of active power take-off in the alternating voltage line essentially depends on load location. For simplicity and clearness we will consider at first the line without losses with purely active load nodes (fig. 18.1). If we connect the load at the points $x = \lambda/2, \lambda, 3\lambda/2,\ldots$, then the transmission power is in inverse proportion to the resistance R_S , but at the points $x = \lambda/4, 3\lambda/4, 5\lambda/4,\ldots$ this dependence is directly proportional (it is of linear nature). This means that at the mentioned points of the circuit with the alternating voltage source of unlimited power it is possible to realize the unlimited power take-off under the regimes approximated to the idling or short circuit. It is to note, that in the line with distributed active losses ($R > 0$) the unlimited power take-off is impossible (even from the theoretical point of view). In case when the load nodes are located at the points $x = \lambda/8, 3\lambda/8, 5\lambda/8,\ldots$, the maximal possible power at this nodes is equal to natural power (that is reached under $R_S = Z_B$).

In this way, every point of the alternating voltage circuit can be identified by its strongly association with individual functional dependence between the transmission power and the load resistance R_S. Thus, the nature of power take-off in the sinusoidal current circuit changes radically in the equal intervals of length $\lambda/8$. This fact fundamentally distinguishes this kind of line from the direct current line. It is naturally, that the realization of the system interconnection in USA is scheduled to put into practice by means of backbone direct current transmission lines used as the main method of separation of synchronously acting subsystems.

The structure of interregional and regional interconnections of the electric mains in accordance with Conceptual Design of the USA Electricity System for 2010 – 2030 is represented in the fig. 18.2. The dimensions and the geographical location of the main electrical producers and main electrical customers in USA admit to realize not only the ring structure of intersystem tie, but the star structures as well. Due to this fact, the two-way customer supply is preserved since it is presupposed to place the main power-supply sources at the system nodes [33].

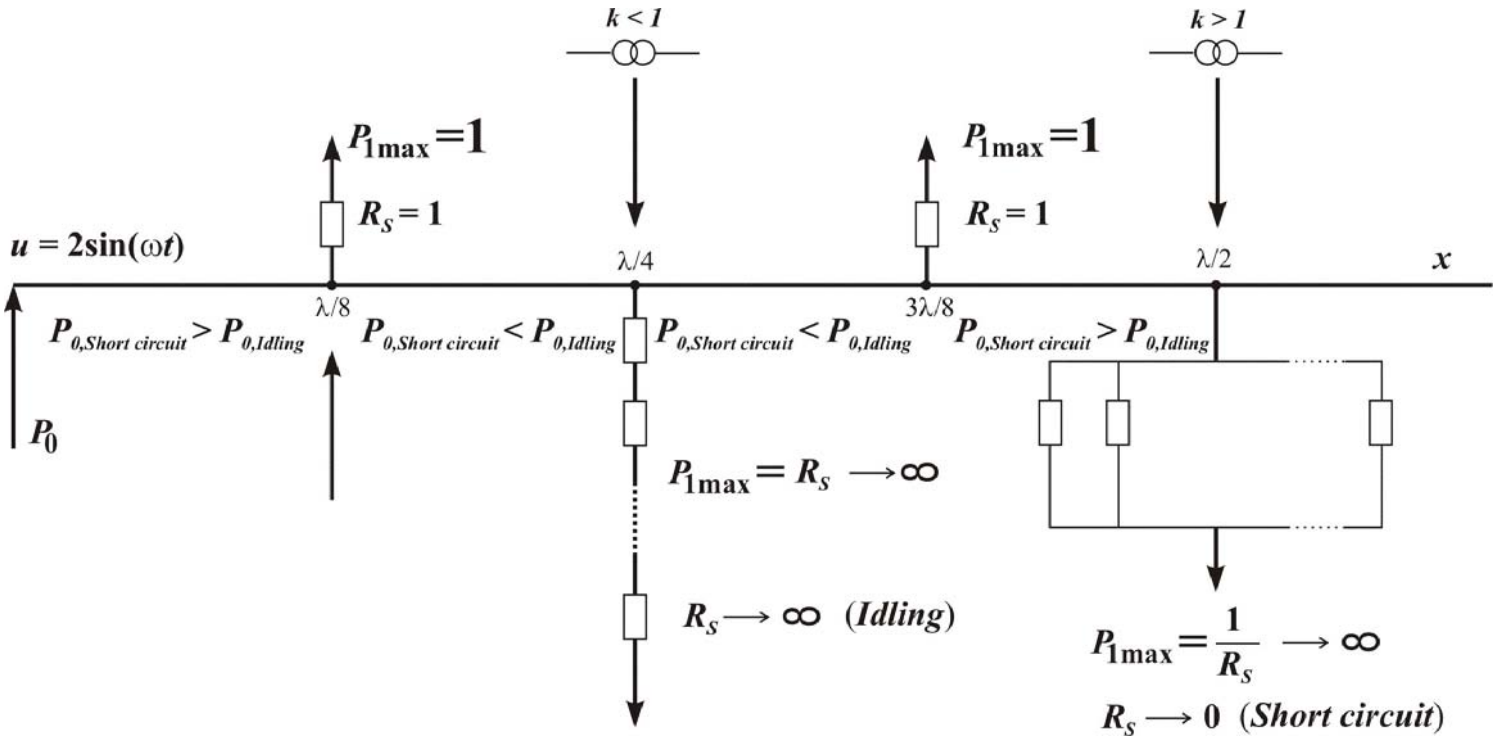

Fig. 18.1. “Anatomy ” of alternating voltage line.

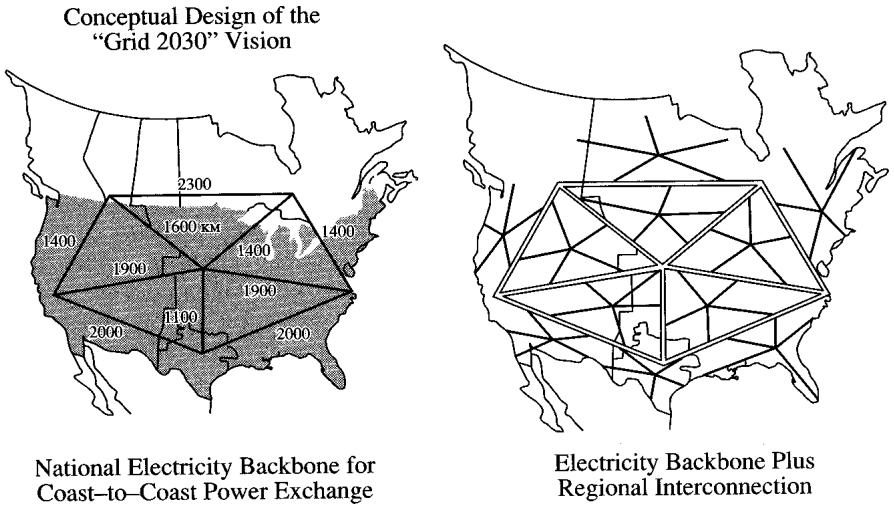

Fig. 18.2. The structure of interregional and regional interconnections of the electric mains in accordance with Conceptual Design of the USA Electricity System for 2010 – 2030.

Let's consider at first the simplest circuit with two generators and five load nodes located as it is shown in the fig. 18.3. Let's suppose that the alternating voltage sources possess the unlimited power and their action on general loads is not necessarily synchronized. In accordance with complex amplitude method the currents and voltages at the ends points of the homogeneous line with length l are connected by the relations

$$U_2 = U_1 \mathrm{ch}\delta l - Z_0 I_1 \mathrm{sh}\delta l \,;\; Z_0 I_2 = -U_1 \mathrm{sh}\delta l + Z_0 I_1 \mathrm{ch}\delta l \qquad (18.1)$$

or

$$U_1 = U_2 \mathrm{ch}\delta l + Z_0 I_2 \mathrm{sh}\delta l \,;\; Z_0 I_1 = U_2 \mathrm{sh}\delta l + Z_0 I_2 \mathrm{ch}\delta l \,. \qquad (18.2)$$

Here by $Z_0 = \sqrt{\dfrac{R + j\omega L}{G + j\omega C}}$, $\delta = \sqrt{(R + j\omega L)(G + j\omega C)}$ we denote the wave resistance (impedance) and the propagation factor in the line and by U_1, I_1, U_2, I_2 – the voltages and currents at the left-hand and right-hand ends of the line.

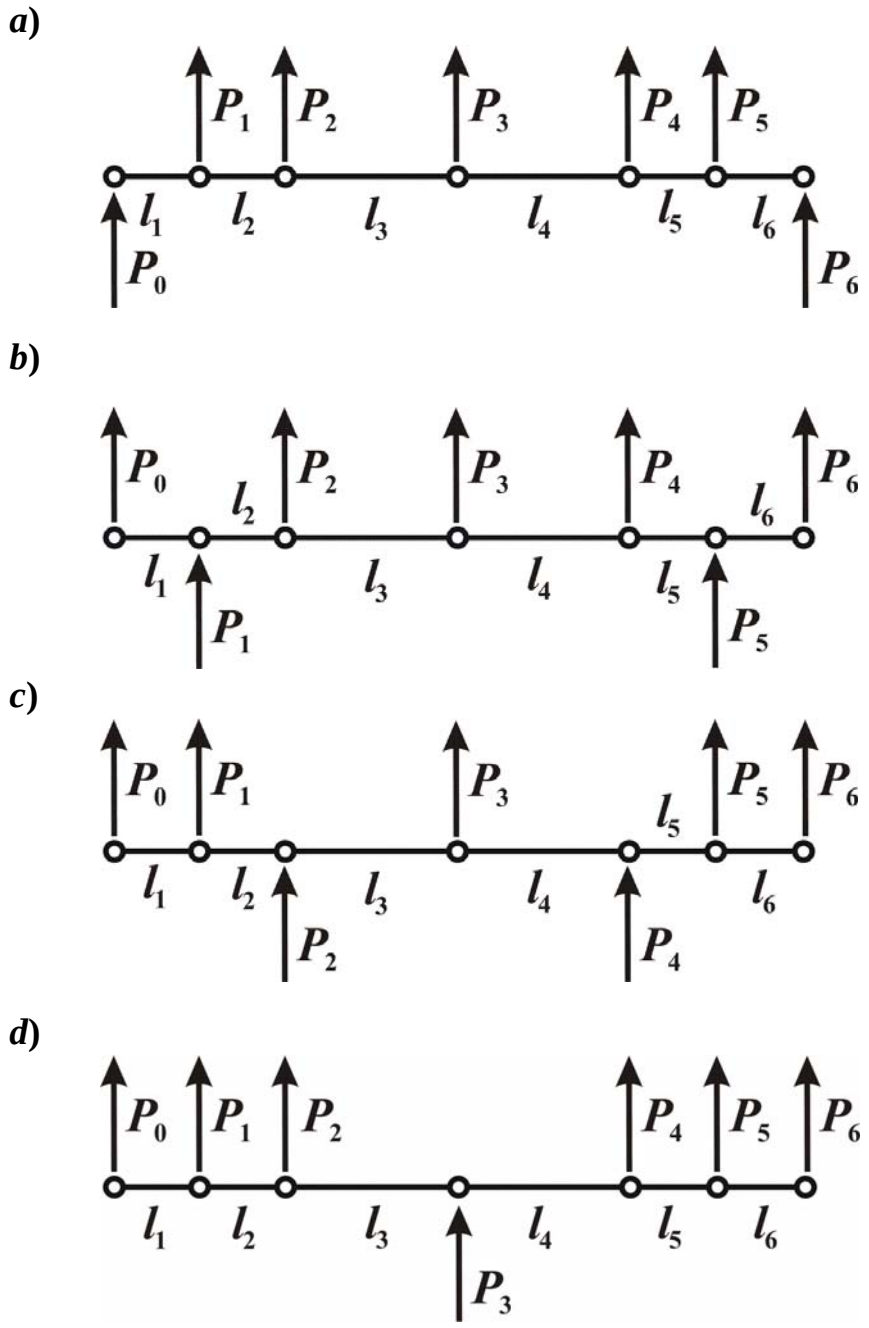

Fig. 18.3. Scheme of generator nodes and load nodes location in alternating voltage circuit.

Let's denote the lengths of the parts of non-homogeneous line by l_k, and the points of conjunction – by x_k: $x_k = \sum_{i=1}^{k} l_i$, $k = \overline{1,6}$, $x_0 = 0, x_6 = l$. The lineal parameters of the part of the line with number k we denote by L_k, C_k, R_k, G_k, the wave resistances and the propagation factors – by $Z_{0,k}, \gamma_k$. Let's suppose that all loads with complex resistance $Z_{n,k}$ at the conjunction points are parallel-connected. Then the voltage at the conjunction points of the sectional line is a continuous function, whereas the current has discontinuity of the first kind. Let's denote the voltage and current at the node with number k by U_k, $I_k^- = I(x_k - 0)$, $I_k^+ = I(x_k + 0)$. For the line with six heterogeneous sections we are to determine 19 unknowns: 7 voltages U_k at the nodes x_k, $k = \overline{0,6}$, 2 currents at the ends of the line $I_0^+ = I_0$, $I_6^- = I_6$ and 10 currents at the conjunction points $I_k^-, I_k^+, k = \overline{1,5}$. For unique determination of these unknowns it is necessary to construct the system of 19 equations. This system consists of twelve equations of the type (18.1), (18.2), five equations for load and two values of voltage at the generation points. Now we will cite these equations in accordance with the scheme in the fig. 18.3, a, where by $\widetilde{U}_0, \widetilde{U}_6$ are denoted given voltages at the points x_0 and x_6:

$$U_0 = \widetilde{U}_0;\ Z_{0,1} I_1^- = -U_0 \mathrm{sh}\delta_1 l_1 + Z_{0,1} I_0 \mathrm{ch}\delta_1 l_1;$$

$$Z_{0,1} I_0 = U_1 \mathrm{sh}\delta_1 l_1 + Z_{0,1} I_1^- \mathrm{ch}\delta_1 l_1;\ U_1 = Z_{n,1}(I_1^- - I_1^+);$$

$$Z_{0,2} I_2^- = -U_1 \mathrm{sh}\delta_2 l_2 + Z_{0,2} I_1^+ \mathrm{ch}\delta_2 l_2;$$

$$Z_{0,2} I_1^+ = U_2 \mathrm{sh}\delta_2 l_2 + Z_{0,2} I_2^- \mathrm{ch}\delta_2 l_2;$$

$$U_2 = Z_{n,2}(I_2^- - I_2^+);\ Z_{0,3} I_3^- = -U_2 \mathrm{sh}\delta_3 l_3 + Z_{0,3} I_2^+ \mathrm{ch}\delta_3 l_3;$$

$$Z_{0,3} I_2^+ = U_3 \mathrm{sh}\delta_3 l_3 + Z_{0,3} I_3^- \mathrm{ch}\delta_3 l_3;\ U_3 = Z_{n,3}(I_3^- - I_3^+); \qquad (18.3)$$

$$Z_{0,4}I_4^- = -U_3\mathrm{sh}\delta_4 l_4 + Z_{0,4}I_3^+\mathrm{ch}\delta_4 l_4;$$

$$Z_{0,4}I_3^+ = U_4\mathrm{sh}\delta_4 l_4 + Z_{0,4}I_4^-\mathrm{ch}\delta_4 l_4;\ U_4 = Z_{n,4}(I_4^- - I_4^+);$$

$$Z_{0,5}I_5^- = -U_4\mathrm{sh}\delta_5 l_5 + Z_{0,5}I_4^+\mathrm{ch}\delta_5 l_5;$$

$$Z_{0,5}I_4^+ = U_5\mathrm{sh}\delta_5 l_5 + Z_{0,5}I_5^-\mathrm{ch}\delta_5 l_5;\ U_5 = Z_{n,5}(I_5^- - I_5^+);$$

$$Z_{0,6}I_6^- = -U_5\mathrm{sh}\delta_6 l_6 + Z_{0,6}I_5^+\mathrm{ch}\delta_6 l_6;$$

$$Z_{0,6}I_5^+ = U_6\mathrm{sh}\delta_6 l_6 + Z_{0,6}I_6\mathrm{ch}\delta_6 l_6;\ U_6 = \widetilde{U}_6.$$

Let's form the vector $\bar{y}$ from unknowns in the following order:

$$\bar{y} = (U_0, I_0, I_1^-, U_1, I_1^+, I_2^-, U_2, I_2^+, I_3^-, U_3, I_3^+,$$

$$I_4^-, U_4, I_4^+, I_5^-, U_5, I_5^+, I_6, U_6)^T.$$

Then the system (18.3) can be written in the matrix form

$$A\bar{y} = \bar{F}, \tag{18.4}$$

where the vector $\bar{F} = (\widetilde{U}_0, 0,0,0,0,0,0,0,0,0,0,0,0,0,0,0,0,0,\widetilde{U}_6)$, and the matrix A has a simple tridiagonal structure. In the general case the system with such a matrix can be written in the following form

$$b_0 y_0 + c_0 y_1 = F_0;$$

$$a_i y_{i-1} + b_i y_i + c_i y_{i+1} = F_i,\ i = \overline{1, n-1}; \tag{18.5}$$

$$a_n y_{n-1} + b_n y_n = F_n.$$

Such systems can be solved efficiently by means of sweep method [101]. The recurrence relations of this method are the followings:

$$\alpha_0 = \frac{-c_0}{b_0}, \quad \beta_0 = \frac{F_0}{b_0};$$

$$\alpha_i = \frac{-c_i}{b_i + a_i\alpha_{i-1}}, i = \overline{1, n-1}; \quad \beta_i = \frac{F_i - a_i\beta_{i-1}}{b_i + a_i\alpha_{i-1}}, i = \overline{1, n}; \qquad (18.6)$$

$$y_n = \beta_n;\ y_i = \alpha_i y_{i+1} + \beta_i, i = n-1, n-2, \ldots 1, 0.$$

However, for the system (18.3) we can obtain the solution in the explicit form as recurrence formulas. At first we will solve the problem with one generator at the left end and with given loads $Z_{n,k}$ at all other nodes. Let' the line with length l consists of N sections with lengths l_k and with parameters L_k, C_k, R_k, G_k, $Z_{0,k}$, δ_k, $k = \overline{1, N}$. Let's denote the voltages and currents at the node with number k by U_k, $I_k^- = I(x_k - 0)$, $I_k^+ = I(x_k + 0)$, $k = \overline{0, N}$. Then at every section with number k the relations of type (18.1) – (18.2) take place. These relations connect the currents and voltages at the ends of the line

$$Z_{0,k} I_{k-1}^+ = U_k \mathrm{sh}\delta_k l_k + Z_{0,k} I_k^- \mathrm{ch}\delta_k l_k;$$

$$U_{k-1} = U_k \mathrm{ch}\delta_k l_k + Z_{0,k} I_k^- \mathrm{sh}\delta_k l_k, k = \overline{1, N}. \qquad (18.7)$$

At the right-hand end of the line $x_N = l$ and at the conjunction nodes $x_k = \sum_{i=1}^{k} l_i, k = \overline{1, (N-1)}$ the following conditions are fulfilled

$$U_N = Z_{S,N}^- I_N^-, \ Z_{S,N}^- = Z_{n,N},$$

$$U_k = Z_{n,k}(I_k^- - I_k^+), k = \overline{1, (N-1)}. \qquad (18.8)$$

The solution of the system (18.7), (18.8) with the condition at the left-hand end $U_0 = \widetilde{U}_0$ can be obtained in the following manner. From the equation for the last section

$$Z_{0,N} I_{N-1}^{+} = U_N \mathrm{sh}\delta_N l_N + Z_{0,N} I_N^{-} \mathrm{ch}\delta_N l_N ;$$

$$U_{N-1} = U_N \mathrm{ch}\delta_N l_N + Z_{0,N} I_N^{-} \mathrm{sh}\delta_N l_N$$

and the boundary condition $U_N = Z_{S,N}^{-} I_N^{-}$ we eliminate U_N and calculate the ratio: $U_{N-1} / I_{N-1}^{+} = Z_{BX,N}^{+}$. In this way we obtain the expression for input resistance $Z_{BX,N}^{+}$ for the last section of the line $x \in [x_{N-1}, x_N]$, that includes the resistance at the right-hand end and the parameters of this section

$$Z_{BX,N}^{+} = Z_{0,N} \frac{Z_{0,N} \mathrm{sh}\delta_N l_N + Z_{S,N}^{-} \mathrm{ch}\delta_N l_N}{Z_{0,N} \mathrm{ch}\delta_N l_N + Z_{S,N}^{-} \mathrm{sh}\delta_N l_N}. \qquad (18.9)$$

Thus, we obtain the relation between the voltage U_{N-1} and the current I_{N-1}^{+}

$$U_{N-1} = Z_{BX,N}^{+} I_{N-1}^{+}. \qquad (18.10)$$

Then applying (18.10) we eliminate I_{N-1}^{+} from the conjunction condition (18.8) at the node x_{N-1}, calculate the ratio between U_{N-1} and I_{N-1}^{-}. In this way we obtain the relation between the voltage U_{N-1} and current I_{N-1}^{-}

$$U_{N-1} / I_{N-1}^{-} = Z_{S,N-1}^{-} = \frac{Z_{BX,N}^{+} Z_{n,N-1}}{Z_{BX,N}^{+} + Z_{n,N-1}}; \qquad (18.11)$$

$$U_{N-1} = Z_{S,N-1}^{-} I_{N-1}^{-}. \qquad (18.12)$$

Now we pass on to the section $x \in [x_{N-2}, x_{N-1}]$. From the equations for this section

$$Z_{0,N-1}I^{+}_{N-2} = U_{N-1}\mathrm{sh}\delta_{N-1}l_{N-1} + Z_{0,N-1}I^{-}_{N-1}\mathrm{ch}\delta_{N-1}l_{N-1};$$

$$U_{N-2} = U_{N-1}\mathrm{ch}\delta_{N-1}l_{N-1} + Z_{0,N-1}I^{-}_{N-1}\mathrm{sh}\delta_{N-1}l_{N-1},$$

using the condition (18.12) $U_{N-1} = Z^{-}_{S,N-1}I^{-}_{N-1}$, we eliminate U_{N-1} and calculate the ratio $U_{N-2}/I^{+}_{N-2} = Z^{+}_{BX,N-1}$. In this way we get the expression for input voltage $Z^{+}_{BX,N-1}$, corresponding to the last two sections of the line $x \in [x_{N-2}, x_N]$:

$$Z^{+}_{BX,N-1} = Z_{0,N-1}\frac{Z_{0,N-1}\mathrm{sh}\delta_{N-1}l_{N-1} + Z^{-}_{S,N-1}\mathrm{ch}\delta_{N-1}l_{N-1}}{Z_{0,N-1}\mathrm{ch}\delta_{N-1}l_{N-1} + Z^{-}_{S,N-1}\mathrm{sh}\delta_{N-1}l_{N-1}}. \quad (18.13)$$

Thus, we obtain the following relation between the voltage U_{N-2} and the current I^{+}_{N-2}:

$$U_{N-2} = Z^{+}_{BX,N-1}I^{+}_{N-2}. \quad (18.14)$$

Then applying (18.14) we eliminate I^{+}_{N-2} from the conjunction condition (18.8) at the node x_{N-2}, calculate the ratio between U_{N-2} and I^{-}_{N-2}. So we obtain the relation between the voltage U_{N-2} and current I^{-}_{N-2}:

$$U_{N-2}/I^{-}_{N-2} = Z^{-}_{S,N-2} = \frac{Z^{+}_{BX,N-1}Z_{n,N-2}}{Z^{+}_{BX,N-1} + Z_{n,N-2}}; \quad (18.15)$$

$$U_{N-2} = Z^{-}_{S,N-2}I^{-}_{N-2}. \quad (18.16)$$

If we continue in this manner, we obtain the recurrence formulas for voltages and currents for any section. Thus, for section with number *k* these formulas get the form

$$Z^{+}_{BX,k} = Z_{0,k}\frac{Z_{0,k}\mathrm{sh}\delta_k l_k + Z^{-}_{S,k}\mathrm{ch}\delta_k l_k}{Z_{0,k}\mathrm{ch}\delta_k l_k + Z^{-}_{S,k}\mathrm{sh}\delta_k l_k};$$

$$U_{k-1} = Z^{+}_{BX,k} I^{+}_{k-1},\ k = \overline{1,N};\ Z^{-}_{S,k-1} = \frac{Z^{+}_{BX,k} Z_{n,k-1}}{Z^{+}_{BX,k} + Z_{n,k-1}};$$

$$U_{k-1} = Z^{-}_{S,k-1} I^{-}_{k-1},\ k = \overline{2,(N+1)}. \qquad (18.17)$$

The solution of the problem for currents and voltages is formed by consecutive calculations by formulas (18.17), starting with known voltage value at the left-hand end of the line $U_0 = \widetilde{U}_0$.

Now we will consider the problem with the generator at the right-hand end and with given loads $Z_{n,k}$ at all other nodes and with the boundary condition at the left-hand end $U_0 = -Z^{+}_{S,0} I^{+}_0 = -Z_{n,0} I^{+}_0$. By repeating the transformations described above for the problem with the generator at the left-hand end, we obtain the formulas analogous to (18.17)

$$Z^{-}_{BX,k} = Z_{0,k}\frac{Z_{0,k}\mathrm{sh}\delta_k l_k + Z^{+}_{S,k-1}\mathrm{ch}\delta_k l_k}{Z_{0,k}\mathrm{ch}\delta_k l_k + Z^{+}_{S,k-1}\mathrm{sh}\delta_k l_k};$$

$$U_k = -Z^{-}_{BX,k} I^{-}_k,\ k = \overline{1,N};\ Z^{+}_{S,k} = \frac{Z^{-}_{BX,k} Z_{n,k}}{Z^{-}_{BX,k} + Z_{n,k}};$$

$$U_k = -Z^{+}_{S,k} I^{+}_k,\ k = \overline{1,(N-1)}. \qquad (18.18)$$

Now by means of formulas (18.17) and (18.18) one can obtain the solution of problems for the nodes represented in the fig. 18.3,a. By formulas (18.17) we get the solution of the problem for generator at the left-hand end and with the condition $U_6 = 0$ or $Z^{-}_{S,6} = 0$, that is equivalent with the short-circuit of the right-hand end. And by formulas (18.18) we solve the problem for generator at the right-hand end and with condition $U_0 = 0$ or $Z^{+}_{S,0} = 0$, i.e. with short-circuited left-hand end. By virtue of linearity of the defining equations, the solution of the original problem turns out to be the

sum of solutions of two problems with one acting generator and short-circuited end.

The solution of the problems for nodes configurations represented in the fig. 18.3, *b-d* can be obtained analogically. The line is divided in tree sections: the first section – from the left-hand loaded end to the first generator, the second – the section between two generators, and the third – from the second generator to the right-hand loaded end. From the structure of the equations (18.7), (18.8) it is clear that at every section the solution is independent on other sections. Thus, the problem can be solved by means of formulas (18.17), (18.18) for each of three sections.

As an example we will consider the calculation of the generators active power and the loads for the problems schematically represented in the fig 18.3. We set that at each line section the lineal parameters are the same (R = 0.48, $G = R/7$), and all load resistances coincide with wave resistance of the line: $Z_{S,k} = Z_0$. The voltage at the left-hand generator always is equal to unit, but at the right-hand generator it has the form $U = e^{j\delta}$, where δ is phase displacement. The total line length is equal to half-wave length l = 0.5, and $2l_1 = 2l_2 = l_3 = l_4 = 2l_5 = 2l_6 = 1/8$.

In the tables 18.1–18.3 there are represented the values of generated P_{gen} and transmission P_{tran} powers, efficiency (η) and power factor ($\cos\varphi$) for two parallel acting sources under the general loads (the generator powers are printed in bold). For the first variant of generator and load nodes location the maximal total power consumption P_{tran} = 1.0622 is reached under the synchronous action of generators (δ =0), whereas the maximal efficiency equal to 89.28% is reached when $\delta = 2\pi/3$, but it corresponds to smaller transmission: P_{tran} = 0.9219.

If the nodes are placed as in the second variant, then the limiting values of transmission power as well as of the efficiency are obtained under the synchronous action of generators. The transmission power increases (in comparison with the previous variant) in two and a half times: P_{tran} = 2.6338, and the efficiency increases up to 93.26%. In the third variant the efficiency remains approximately the same, but the transmission power goes down till the value P_{tran} = 2.0554.

In the table 18.4 there are represented the values of generated and transmission powers in case when the second generator is disconnected. Here the most winning variant for limiting efficiency is the second one, but for maximal transmission power – the third one.

Table 18.1. Generated and transmission powers for the scheme represented in the fig. 18.3, *a*.

δ	$\frac{P_0}{\cos\varphi_0}$	$\frac{P_1}{\cos\varphi_1}$	$\frac{P_2}{\cos\varphi_2}$	$\frac{P_3}{\cos\varphi_3}$	$\frac{P_4}{\cos\varphi_4}$	$\frac{P_5}{\cos\varphi_5}$	$\frac{P_6}{\cos\varphi_6}$	P_{gen}	P_{tran}	η
-2π/3	**0.4013**	0.2101	0.0610	0.0716	0.2592	0.3200	**0.6314**	1.0327	0.9219	0.8928
	0.6987	0.9995	0.9995	0.9995	0.9995	0.9995	**0.9013**			
-π/2	**0.4145**	0.1795	0.0553	0.1432	0.2843	0.3064	**0.6802**	1.0947	0.9687	0.8849
	0.6492	0.9995	0.9995	0.9995	0.9995	0.9995	**0.8830**			
-π/3	**0.4633**	0.1659	0.0804	0.2148	0.2786	0.2758	**0.6934**	1.1567	1.0155	0.8779
	0.6486	0.9995	0.9995	0.9995	0.9995	0.9995	**0.8464**			
-π/6	**0.5346**	0.1729	0.1293	0.2672	0.2438	0.2364	**0.6675**	1.2021	1.0497	0.8732
	0.6843	0.9995	0.9995	0.9995	0.9995	0.9995	**0.7960**			
0	**0.6094**	0.1987	0.1892	0.2864	0.1892	0.1987	**0.6094**	1.2188	1.0622	0.8716
	0.7384	0.9995	0.9995	0.9995	0.9995	0.9995	**0.7384**			
π/6	**0.6675**	0.2364	0.2438	0.2672	0.1293	0.1729	**0.5346**	1.2021	1.0497	0.8732
	0.7960	0.9995	0.9995	0.9995	0.9995	0.9995	**0.6843**			
π/3	**0.6934**	0.2758	0.2786	0.2148	0.0804	0.1659	**0.4633**	1.1567	1.0155	0.8779
	0.8464	0.9995	0.9995	0.9995	0.9995	0.9995	**0.6486**			
π/2	**0.6802**	0.3064	0.2843	0.1432	0.0553	0.1795	**0.4145**	1.0947	0.9687	0.8849
	0.8830	0.9995	0.9995	0.9995	0.9995	0.9995	**0.6492**			
2π/3	**0.6314**	0.3200	0.2592	0.0716	0.0610	0.2101	**0.4013**	1.0327	0.9219	0.8928
	0.9013	0.9995	0.9995	0.9995	0.9995	0.9995	**0.6987**			

Table 18.2. Generated and transmission powers for the scheme represented in the fig. 18.3, *b*.

δ	$\frac{P_0}{\cos\varphi_0}$	$\frac{P_1}{\cos\varphi_1}$	$\frac{P_2}{\cos\varphi_2}$	$\frac{P_3}{\cos\varphi_3}$	$\frac{P_4}{\cos\varphi_4}$	$\frac{P_5}{\cos\varphi_5}$	$\frac{P_6}{\cos\varphi_6}$	P_{gen}	P_{tran}	η
-2π/3	0.4822	**0.9782**	0.1747	0.1798	0.4549	**0.9308**	0.4822	1.9089	1.7739	92.92
	0.9995	**0.8853**	0.9995	0.9995	0.9995	**0.9999**	0.9995			
-π/2	0.4822	**1.1344**	0.2064	0.3596	0.5300	**1.0796**	0.4822	2.2140	2.0605	93.07
	0.9995	**0.9026**	0.9995	0.9995	0.9995	**0.9980**	0.9995			
-π/3	0.4822	**1.2832**	0.2815	0.5395	0.5617	**1.2358**	0.4822	2.5191	2.3472	93.18
	0.9995	**0.9351**	0.9995	0.9995	0.9995	**0.9994**	0.9995			
-π/6	0.4822	**1.3849**	0.3798	0.6711	0.5416	**1.3575**	0.4822	2.7424	2.5570	93.24
	0.9995	**0.9670**	0.9995	0.9995	0.9995	**0.9990**	0.9995			
0	0.4822	**1.4121**	0.4751	0.7193	0.4751	**1.4121**	0.4822	2.8241	2.6338	93.26
	0.9995	**0.9893**	0.9995	0.9995	0.9995	**0.9893**	0.9995			
π/6	0.4822	**1.3575**	0.5416	0.6711	0.3798	**1.3849**	0.4822	2.7424	2.5570	93.24
	0.9995	**0.9990**	0.9995	0.9995	0.9995	**0.9670**	0.9995			
π/3	0.4822	**1.2358**	0.5617	0.5395	0.2815	**1.2832**	0.4822	2.5191	2.3472	93.18
	0.9995	**0.9994**	0.9995	0.9995	0.9995	**0.9351**	0.9995			
π/2	0.4822	**1.0796**	0.5300	0.3596	0.2064	**1.1344**	0.4822	2.2140	2.0605	93.07
	0.9995	**0.9980**	0.9995	0.9995	0.9995	**0.9026**	0.9995			
2π/3	0.4822	**0.9308**	0.4549	0.1798	0.1747	**0.9782**	0.4822	1.9089	1.7739	92.92
	0.9995	**0.9999**	0.9995	0.9995	0.9995	**0.8853**	0.9995			

Table 18.3. Generated and transmission powers for the scheme represented in the fig. 18.3, *c*.

δ	$\frac{P_0}{\cos\varphi_0}$	$\frac{P_1}{\cos\varphi_1}$	$\frac{P_2}{\cos\varphi_2}$	$\frac{P_3}{\cos\varphi_3}$	$\frac{P_4}{\cos\varphi_4}$	$\frac{P_5}{\cos\varphi_5}$	$\frac{P_6}{\cos\varphi_6}$	P_{gen}	P_{tran}	η
-2π/3	0.3194	0.3305	**1.1829**	0.1889	**0.4960**	0.3305	0.3194	1.6789	1.4887	0.8867
	0.9995	0.9995	**0.8354**	0.9995	**0.7229**	0.9995	0.9995			
-π/2	0.3194	0.3305	**1.3239**	0.3778	**0.5308**	0.3305	0.3194	1.8546	1.6776	0.9046
	0.9995	0.9995	**0.9099**	0.9995	**0.9032**	0.9995	0.9995			
-π/3	0.3194	0.3305	**1.3586**	0.5667	**0.6717**	0.3305	0.3194	2.0303	1.8665	0.9193
	0.9995	0.9995	**0.9627**	0.9995	**0.9934**	0.9995	0.9995			
-π/6	0.3194	0.3305	**1.2778**	0.7050	**0.8812**	0.3305	0.3194	2.1590	2.0048	0.9286
	0.9995	0.9995	**0.9910**	0.9995	**1.0000**	0.9995	0.9995			
0	0.3194	0.3305	**1.1030**	0.7556	**1.1030**	0.3305	0.3194	2.2060	2.0554	0.9317
	0.9995	0.9995	**0.9996**	0.9995	**0.9996**	0.9995	0.9995			
π/6	0.3194	0.3305	**0.8812**	0.7050	**1.2778**	0.3305	0.3194	2.1590	2.0048	0.9286
	0.9995	0.9995	**1.0000**	0.9995	**0.9910**	0.9995	0.9995			
π/3	0.3194	0.3305	**0.6717**	0.5667	**1.3586**	0.3305	0.3194	2.0303	1.8665	0.9193
	0.9995	0.9995	**0.9934**	0.9995	**0.9627**	0.9995	0.9995			
π/2	0.3194	0.3305	**0.5308**	0.3778	**1.3239**	0.3305	0.3194	1.8546	1.6776	0.9046
	0.9995	0.9995	**0.9032**	0.9995	**0.9099**	0.9995	0.9995			
2π/3	0.3194	0.3305	**0.4960**	0.1889	**1.1829**	0.3305	0.3194	1.6789	1.4887	0.8867
	0.9995	0.9995	**0.7229**	0.9995	**0.8354**	0.9995	0.9995			

Table 18.4. Generated and transmission powers when one generator is disconnected.

$\frac{P_0}{\cos\varphi_0}$	$\frac{P_1}{\cos\varphi_1}$	$\frac{P_2}{\cos\varphi_2}$	$\frac{P_3}{\cos\varphi_3}$	$\frac{P_4}{\cos\varphi_4}$	$\frac{P_5}{\cos\varphi_5}$	$\frac{P_6}{\cos\varphi_6}$	P_{gen}	P_{tran}	η
0.5485	0.2514	0.1553	0.0478	0.0148	0.0191	**0.0000**	0.5485	0.4885	89.05
0.8132	0.9995	0.9995	0.9995	0.9995	0.9995				
0.4822	**1.0303**	0.3021	0.1000	0.0378	**0.0000**	0.0353	1.0303	0.9575	92.93
0.9995	**0.9680**	0.9995	0.9995	0.9995		0.9995			
0.3194	0.3305	**1.0968**	0.2254	**0.0000**	0.0596	0.0576	1.0968	0.9925	90.49
0.9995	0.9995	**0.9099**	0.9995		0.9995	0.9995			
0.0716	0.0741	0.1119	**0.6081**	0.1119	0.0741	0.0716	0.6081	0.5151	84.71
0.9995	0.9995	0.9995	**0.7363**	0.9995	0.9995	0.9995			

Table 18.5. Reactive resistances for the scheme represented in the fig. 18.4

δ	X_{n1}	X_{n7}
$-2\pi/3$	-1.2168	-1.6477
$-\pi/2$	-1.0296	-1.3828
$-\pi/3$	-0.9195	-1.1460
$-\pi/6$	-0.8777	-0.9849
0	-0.8985	-0.8985
$\pi/6$	-0.9849	-0.8777
$\pi/3$	-1.1460	-0.9195
$\pi/2$	-1.3828	-1.0296
$2\pi/3$	-1.6477	-1.2168

Thus, the generator locations and the order of their synchronization (determined by the phase displacement δ) influence sufficiently on power flows in the alternating voltage circuit. Even under the synchronized action of two generators the load power P_3, placed at the equal distances from them, changes approximately in 3 times: from 0.2864 to 0.7556. In this way it becomes clear that the line action under the lumped loads can hardly be optimal one as from point of view of limiting efficiency values ensuring as well as of maximal transmission power values reaching. The main question here is the following: is it possible to set the load parameters in such a way as to increase the transmission power and the efficiency simultaneously? Yes, of course. For example, when Z_n = {0.8048; 1.3031; 0.9124; 1.3016; 0.8047} we obtain P_{tran} = 2.6369 and the efficiency equal to 93.47%.

If the scheme of location of generator and load nodes has more complicated topology (for example, as in the fig. 18.2), then the problem must be decomposed in the subproblems of the type considered above. The situation becomes greatly complicated if we consider the restricted (limited) generators powers. This problem still lies ahead to be formulated correctly and to be solved by means of tensor analysis methods for electrical circuits [57, 58].

As it follows from the table 18.1 the power factors of generators are wide of unit. This means the inadmissibly large reactive power values. Let's remember that under the power factor less then 0.7071 the reactive power becomes even greater then generated active power.

Let's formulate the problem of minimization of generator nodes reactive power. For that let's place the "bucking-out" systems (compensative elements) in the immediate vicinity of the voltage sources (see fig. 18.4). We suppose that the distances l_1 and l_8 are infinitesimal.

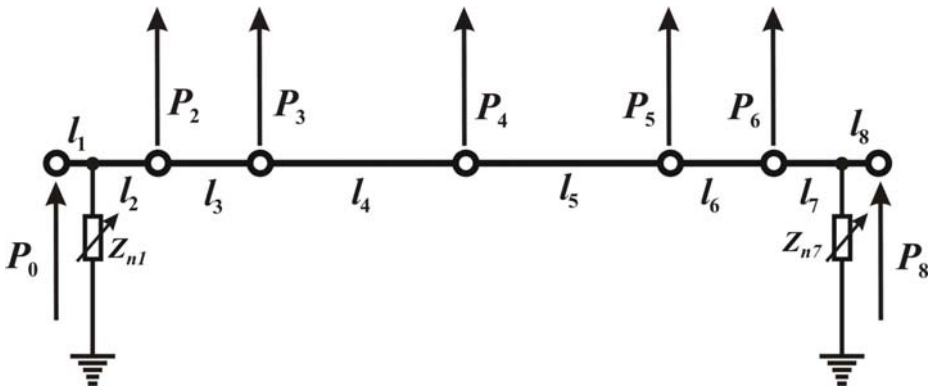

Fig. 18.4. Connection of "bucking out" systems with resistances $Z_{n1} = jX_{n1}$ and $Z_{n7} = jX_{n7}$ with purpose to increase generator power factor till 1.

In this case the electrical circuit consists of 9 nodes and the system of equations (18.3) gets the form of system with 25 equations

$$U_0 = \widetilde{U}_0;\ Z_{0,1}I_1^- = -U_0\mathrm{sh}\delta_1 l_1 + Z_{0,1}I_0\mathrm{ch}\delta_1 l_1;$$

$$Z_{0,1}I_0 = U_1\mathrm{sh}\delta_1 l_1 + Z_{0,1}I_1^-\mathrm{ch}\delta_1 l_1;\ U_1 = Z_{n,1}(I_1^- - I_1^+);$$

$$Z_{0,2}I_2^- = -U_1\mathrm{sh}\delta_2 l_2 + Z_{0,2}I_1^+\mathrm{ch}\delta_2 l_2;\ Z_{0,2}I_1^+ = U_2\mathrm{sh}\delta_2 l_2 + Z_{0,2}I_2^-\mathrm{ch}\delta_2 l_2;$$

$$U_2 = Z_{n,2}(I_2^- - I_2^+);\ Z_{0,3}I_3^- = -U_2\mathrm{sh}\delta_3 l_3 + Z_{0,3}I_2^+\mathrm{ch}\delta_3 l_3;$$

$$Z_{0,3}I_2^+ = U_3\mathrm{sh}\delta_3 l_3 + Z_{0,3}I_3^-\mathrm{ch}\delta_3 l_3;\ U_3 = Z_{n,3}(I_3^- - I_3^+);$$

$$Z_{0,4}I_4^- = -U_3\mathrm{sh}\delta_4 l_4 + Z_{0,4}I_3^+\mathrm{ch}\delta_4 l_4;$$

$$Z_{0,4}I_3^+ = U_4\mathrm{sh}\delta_4 l_4 + Z_{0,4}I_4^-\mathrm{ch}\delta_4 l_4;\ U_4 = Z_{n,4}(I_4^- - I_4^+);$$

$$Z_{0,5}I_5^- = -U_4\mathrm{sh}\delta_5 l_5 + Z_{0,5}I_4^+\mathrm{ch}\delta_5 l_5; \qquad (18.19)$$

$$Z_{0,5}I_4^+ = U_5\mathrm{sh}\delta_5 l_5 + Z_{0,5}I_5^-\mathrm{ch}\delta_5 l_5;\ U_5 = Z_{n,5}(I_5^- - I_5^+);$$

$$Z_{0,6}I_6^- = -U_5\mathrm{sh}\delta_6 l_6 + Z_{0,6}I_5^+\mathrm{ch}\delta_6 l_6;$$

$$Z_{0,6}I_5^+ = U_6\mathrm{sh}\delta_6 l_6 + Z_{0,6}I_6^-\mathrm{ch}\delta_6 l_6;\ U_6 = Z_{n,6}(I_6^- - I_6^+);$$

$$Z_{0,7}I_7^- = -U_6\mathrm{sh}\delta_7 l_7 + Z_{0,7}I_6^+\mathrm{ch}\delta_7 l_7;$$

$$Z_{0,7}I_6^+ = U_7\mathrm{sh}\delta_7 l_7 + Z_{0,7}I_7^-\mathrm{ch}\delta_7 l_7;\ U_7 = Z_{n,7}(I_7^- - I_7^+);$$

$$Z_{0,8}I_8^- = -U_7\mathrm{sh}\delta_8 l_8 + Z_{0,8}I_7^+\mathrm{ch}\delta_8 l_8;$$

$$Z_{0,8}I_7^+ = U_8\mathrm{sh}\delta_8 l_8 + Z_{0,8}I_8\mathrm{ch}\delta_8 l_8;\ U_8 = \widetilde{U}_8.$$

When $l_1 \to 0$ and $l_8 \to 0$ from relations (18.1), (18.2) we obtain the evident equalities: $I_1^- = I_0$, $U_1 = U_0$ and $I_7^+ = I_8$, $U_8 = U_7$. If we eliminate from (18.19) the unknowns I_0, I_1^-, U_1, I_8, I_7^+ and U_7, then we obtain the new system for 19 remained desired functions

$$U_0 = \widetilde{U}_0;\ Z_{0,2}I_2^- = -U_0\mathrm{sh}\delta_2 l_2 + Z_{0,2}I_1^+\mathrm{ch}\delta_2 l_2;$$

$$Z_{0,2}I_1^+ = U_2\mathrm{sh}\delta_2 l_2 + Z_{0,2}I_2^-\mathrm{ch}\delta_2 l_2;$$

$$U_2 = Z_{n,2}(I_2^- - I_2^+);\ Z_{0,3}I_3^- = -U_2\mathrm{sh}\delta_3 l_3 + Z_{0,3}I_2^+\mathrm{ch}\delta_3 l_3;$$

$$Z_{0,3}I_2^+ = U_3\mathrm{sh}\delta_3 l_3 + Z_{0,3}I_3^-\mathrm{ch}\delta_3 l_3;\ U_3 = Z_{n,3}(I_3^- - I_3^+);$$

$$Z_{0,4}I_4^- = -U_3\mathrm{sh}\delta_4 l_4 + Z_{0,4}I_3^+\mathrm{ch}\delta_4 l_4;$$

$$Z_{0,4}I_3^+ = U_4\mathrm{sh}\delta_4 l_4 + Z_{0,4}I_4^-\mathrm{ch}\delta_4 l_4;\ U_4 = Z_{n,4}(I_4^- - I_4^+);$$

$$Z_{0,5}I_5^- = -U_4\mathrm{sh}\delta_5 l_5 + Z_{0,5}I_4^+\mathrm{ch}\delta_5 l_5; \qquad (18.20)$$

$$Z_{0,5}I_4^+ = U_5\mathrm{sh}\delta_5 l_5 + Z_{0,5}I_5^-\mathrm{ch}\delta_5 l_5;\ U_5 = Z_{n,5}(I_5^- - I_5^+);$$

$$Z_{0,6}I_6^- = -U_5\mathrm{sh}\delta_6 l_6 + Z_{0,6}I_5^+\mathrm{ch}\delta_6 l_6;$$

$$Z_{0,6}I_5^+ = U_6\mathrm{sh}\delta_6 l_6 + Z_{0,6}I_6^-\mathrm{ch}\delta_6 l_6;\ U_6 = Z_{n,6}(I_6^- - I_6^+);$$

$$Z_{0,7}I_7^- = -U_6\mathrm{sh}\delta_7 l_7 + Z_{0,7}I_6^+\mathrm{ch}\delta_7 l_7;$$

$$Z_{0,7}I_6^+ = U_8\mathrm{sh}\delta_7 l_7 + Z_{0,7}I_7^-\mathrm{ch}\delta_7 l_7;\ U_8 = \widetilde{U}_8.$$

Let's mention that the system (18.20) does not contain the current values I_0 and I_8, corresponding to the end points of the line. Thus the procedure of reactive power compensation can be realized in the following manner. At first we solve the system (18.20) by described above method. Then from the correlations between currents and voltages at the ends of the line

$$U_0 = Z_{n,1}(I_0 - I_1^+);\ U_8 = Z_{n,7}(I_7^- - I_8) \qquad (18.21)$$

we determine the resistances of the compensative elements in accordance with the condition of equality to zero of the generated active power:

$$Q_0 = \mathrm{Im}(U_0 I_0^*) = 0 \ \text{ and } \ Q_8 = \mathrm{Im}(U_8 I_8^*) = 0. \qquad (18.22)$$

Now using the (18.21) we eliminate I_0 and I_8 and solve the obtained equations with regard to $Z_{n1} = jX_{n1}$ and $Z_{n7} = jX_{n7}$. In this way we obtain the explicit relations for reactive resistances of the compensative elements:

$$X_{n1} = -\frac{\mathrm{Re}\left[U_0 U_0^*\right]}{\mathrm{Im}\left[U_0 (I_1^+)^*\right]};\ X_{n7} = \frac{\mathrm{Re}\left[U_8 U_8^*\right]}{\mathrm{Im}\left[U_8 (I_7^-)^*\right]}. \qquad (18.23)$$

Then from the (18.21) we determine the currents I_0 and I_8, that give the zero value for generators reactive power.

The reactive resistances, under which the generator power factors are equal to 1, are represented in the table 18.5. The reactive resistances here are of capacitive nature and under the synchronous action of the generators they get the equal values owing to symmetrical location of the loading nodes with respect to the middle of the line. If we remove the load locations moving them near the first generator (see table 18.6), then the compensative element for the second generator becomes of capacitive nature and the resistance values change in an order depending on the synchronization angle δ (see table 18.6).

Reducing the distance between the generators in 100 times (approximately 30 km in the real scale) we obtain the acceptable energy datum for power transmission only under $\delta = 0$, when the line efficiency and the source power factor consist of more then three of nines (see table 18.7). If we try formally to apply the formulas (18.23) to determine the reactive resistance of compensative elements, then we get the unwarrantable great inductance values (see table 18.7), that has no any practical meaning. It is to mention, that under the unmatched load resistances ($Z_S = Z_0/2$) the efficiency decreases slightly (in a third digit) and the power factors approximate to 1, so the compensative elements connection becomes unwarranted (see table 18.8).

Let's mention that variation of the values Z_{n1} and Z_{n7} does not change the values of the loads active powers because the currents and the voltages in the line do not depend on the current values at the generators I_0 and I_8, but depend on current values I_1^+ and I_7^- at the input of compensative elements. The values of generators active powers also do not depend on I_0 and I_8 and, correspondingly, on Z_{n1} and Z_{n7} in view of following reasons. The generators active powers are calculated by the formulas

$$P_0 = \mathrm{Re}(U_0 I_0^*) \text{ and } P_8 = \mathrm{Re}(U_8 I_8^*). \qquad (18.24)$$

Let's express from (18.21) the values I_0 and I_8 through the I_1^+, I_7^- and introduce them in (18.24). Then we get

Table 18.6. Generated and transmission powers for the scheme represented in the fig 18.3, *a* when $l_1 = 1/64$; $l_2 = 1/64$; $l_3 = 1/32$; $l_4 = 1/32$; $l_5 = 1/64$; $l_6 = 25/64$.

δ	$\frac{P_0}{\cos\varphi_0}$	$\frac{P_1}{\cos\varphi_1}$	$\frac{P_2}{\cos\varphi_2}$	$\frac{P_3}{\cos\varphi_3}$	$\frac{P_4}{\cos\varphi_4}$	$\frac{P_5}{\cos\varphi_5}$	$\frac{P_6}{\cos\varphi_6}$	P_{gen}	P_{tran}	η	X_{n1}	X_{n7}
-	**0.7240**	0.2713	0.1214	0.0160	0.1442	0.2838	**0.5440**	1.2681	0.8367	0.6598	-	0.5040
2π/3	**0.4832**	0.9995	0.9995	0.9995	0.9995	0.9995	**0.4808**					
-π/2	**0.9048**	0.2533	0.1097	0.0632	0.2819	0.4691	**0.7747**	1.6795	1.1772	0.7010	-	0.5241
	0.5267	0.9995	0.9995	0.9995	0.9995	0.9995	**0.6304**					
-π/3	**1.1354**	0.2537	0.1286	0.1409	0.4173	0.6249	**0.9554**	2.0909	1.5655	0.7487	-	0.6206
	0.6040	0.9995	0.9995	0.9995	0.9995	0.9995	**0.7645**					
-π/6	**1.3542**	0.2724	0.1730	0.2284	0.5141	0.7095	**1.0378**	2.3920	1.8974	0.7932	-	0.8519
	0.6912	0.9995	0.9995	0.9995	0.9995	0.9995	**0.8704**					
0	**1.5025**	0.3043	0.2310	0.3022	0.5464	0.7002	**0.9997**	2.5022	2.0840	0.8329	-	1.4035
	0.7725	0.9995	0.9995	0.9995	0.9995	0.9995	**0.9420**					
π/6	**1.5406**	0.3409	0.2870	0.3426	0.5055	0.5995	**0.8514**	2.3920	2.0754	0.8676	-	2.8484
	0.8376	0.9995	0.9995	0.9995	0.9995	0.9995	**0.9794**					
π/3	**1.4582**	0.3724	0.3261	0.3386	0.4023	0.4344	**0.6327**	2.0909	1.8738	0.8962	-	5.3665
	0.8803	0.9995	0.9995	0.9995	0.9995	0.9995	**0.9893**					
π/2	**1.2775**	0.3904	0.3378	0.2915	0.2646	0.2491	**0.4020**	1.6795	1.5333	0.9130	-	3.8100
	0.8948	0.9995	0.9995	0.9995	0.9995	0.9995	**0.9506**					
2π/3	**1.0468**	0.3900	0.3189	0.2137	0.1292	0.0933	**0.2213**	1.2681	1.1451	0.9030	-	1.7887
	0.8678	0.9995	0.9995	0.9995	0.9995	0.9995	**0.6207**					

Table 18.7. Generated and transmission powers for the scheme represented in the fig 18.3, *a* when l_1 = 1/6400; l_2 = 1/6400; l_3 = 1/3200; l_4 = 1/3200; l_5 = 1/6400; l_6 = 25/6400.

δ	$\frac{P_0}{\cos\varphi_0}$	$\frac{P_1}{\cos\varphi_1}$	$\frac{P_2}{\cos\varphi_2}$	$\frac{P_3}{\cos\varphi_3}$	$\frac{P_4}{\cos\varphi_4}$	$\frac{P_5}{\cos\varphi_5}$	$\frac{P_6}{\cos\varphi_6}$	P_{gen}	P_{tran}	η	X_{n1}	X_{n7}
-	**17.3157**	0.4532	0.4106	0.3346	0.2709	0.2435	**11.9751**	29.2907	1.7128	0.0585	-	-0.0204
2π/3	**0.6037**	0.9995	0.9995	0.9995	0.9995	0.9995	**0.4384**					
-π/2	**18.9623**	0.4682	0.4397	0.3891	0.3469	0.3288	**14.5703**	33.5326	1.9728	0.0588	-	-0.0298
	0.7878	0.9995	0.9995	0.9995	0.9995	0.9995	**0.6560**					
-π/3	**16.3671**	0.4834	0.4690	0.4437	0.4228	0.4139	**12.9236**	29.2907	2.2327	0.0762	-	-0.0573
	0.9187	0.9995	0.9995	0.9995	0.9995	0.9995	**0.8289**					
-π/6	**10.2254**	0.4946	0.4906	0.4837	0.4782	0.4759	**7.4764**	17.7018	2.4230	0.1369	-	-0.1937
	0.9881	0.9995	0.9995	0.9995	0.9995	0.9995	**0.9452**					
0	**2.1830**	0.4988	0.4987	0.4985	0.4984	0.4984	**0.3119**	2.4949	2.4927	0.9991	8.9105	35.9921
	0.9997	0.9995	0.9995	0.9995	0.9995	0.9995	**0.9990**					
π/6	**5.6054**	0.4950	0.4911	0.4840	0.4778	0.4751	**8.3544**	13.9598	2.4230	0.1736	-	-0.3062
	0.9109	0.9995	0.9995	0.9995	0.9995	0.9995	**0.9814**					
π/3	**11.0526**	0.4840	0.4699	0.4442	0.4221	0.4125	**14.4961**	25.5487	2.2327	0.0874	-	-0.0706
	0.7864	0.9995	0.9995	0.9995	0.9995	0.9995	**0.8986**					
π/2	**12.6993**	0.4690	0.4408	0.3897	0.3461	0.3272	**17.0913**	29.7905	1.9728	0.0662	-	-0.0336
	0.6048	0.9995	0.9995	0.9995	0.9995	0.9995	**0.7545**					
2π/3	**10.1041**	0.4539	0.4115	0.3352	0.2702	0.2421	**15.4447**	25.5487	1.7128	0.0670	-	-0.0218
	0.3811	0.9995	0.9995	0.9995	0.9995	0.9995	**0.5590**					

Table 18.8. Generated and transmission powers for the scheme represented in the fig 18.3, *a* when $l_1 = 1/6400$; $l_2 = 1/6400$; $l_3 = 1/3200$; $l_4 = 1/3200$; $l_5 = 1/6400$; $l_6 = 25/6400$ when $Z_S = Z_0/2$.

δ	$\frac{P_0}{\cos\varphi_0}$	$\frac{P_1}{\cos\varphi_1}$	$\frac{P_2}{\cos\varphi_2}$	$\frac{P_3}{\cos\varphi_3}$	$\frac{P_4}{\cos\varphi_4}$	$\frac{P_5}{\cos\varphi_5}$	$\frac{P_6}{\cos\varphi_6}$	P_{gen}	P_{tran}	η	X_{n1}	X_{n7}
-	**19.1048**	0.9053	0.8195	0.6678	0.5414	0.4875	**12.0517**	31.1565	3.4215	0.1098	-	-0.0206
2π/3	**0.6375**	0.9995	0.9995	0.9995	0.9995	0.9995	**0.4439**					
-π/2	**20.8811**	0.9352	0.8776	0.7765	0.6932	0.6580	**14.5167**	35.3978	3.9405	0.1113	-	-0.0303
	0.8107	0.9995	0.9995	0.9995	0.9995	0.9995	**0.6604**					
-π/3	**18.4161**	0.9656	0.9362	0.8855	0.8446	0.8276	**12.7404**	31.1565	4.4595	0.1431	-	-0.0588
	0.9303	0.9995	0.9995	0.9995	0.9995	0.9995	**0.8319**					
-π/6	**12.3703**	0.9882	0.9797	0.9656	0.9550	0.9509	**7.1987**	19.5690	4.8395	0.2473	-	-0.2038
	0.9905	0.9995	0.9995	0.9995	0.9995	0.9995	**0.9465**					
0	**4.3636**	0.9970	0.9963	0.9954	0.9949	0.9949	**0.6234**	4.9870	4.9785	0.9983	8.5716	42.9267
	0.9999	0.9995	0.9995	0.9995	0.9995	0.9995	**0.9998**					
π/6	**3.4586**	0.9897	0.9817	0.9668	0.9535	0.9477	**8.6301**	12.0886	4.8395	0.4003	-	-0.2833
	0.8208	0.9995	0.9995	0.9995	0.9995	0.9995	**0.9797**					
π/3	**9.0002**	0.9682	0.9398	0.8876	0.8420	0.8220	**14.6759**	23.6761	4.4595	0.1884	-	-0.0684
	0.7289	0.9995	0.9995	0.9995	0.9995	0.9995	**0.8952**					
π/2	**10.7765**	0.9383	0.8817	0.7789	0.6902	0.6515	**17.1409**	27.9174	3.9405	0.1411	-	-0.0331
	0.5478	0.9995	0.9995	0.9995	0.9995	0.9995	**0.7497**					
2π/3	**8.3115**	0.9079	0.8231	0.6699	0.5388	0.4819	**15.3646**	23.6761	3.4215	0.1445	-	-0.0216
	0.3239	0.9995	0.9995	0.9995	0.9995	0.9995	**0.5532**					

$$I_0 = I_1^+ + U_0 / Z_{n,1};\ P_0 = \mathrm{Re}(U_0 I_0^*) = \mathrm{Re}\left[U_0 (I_1^+ + U_0 / Z_{n,1})^*\right] =$$

$$= \mathrm{Re}\left[U_0 (I_1^+)^*\right] + \mathrm{Re}\left[U_0 U_0^* / Z_{n,1}^*\right] =$$

$$= \mathrm{Re}\left[U_0 (I_1^+)^*\right] + |U_0|^2 \mathrm{Re}\left[1 / Z_{n,1}^*\right] . \qquad (18.25)$$

If the compensative elements resistance is purely reactive, i.e. $Z_{n,1} = jX_{n,1}$, then the second member in the (18.25) is equal to zero and we obtain $P_0 = \mathrm{Re}\left[U_0 (I_1^+)^*\right]$, i.e. the generator active power depends only on I_1^+ and does not depend on I_0 and $Z_{n,1}$. For the right-hand generator we obtain the analogical result owing to relation $I_8 = I_7^- + U_8 / Z_{n,7}$.

Now at last let's consider the model of two sinusoidal voltage sources synchronous action ($\delta = 0$) under the general active-reactive load in the form of lumped *RL* – circuit: $Z_n = 40 + j{\cdot}20\ \Omega$. We will use the following parameters values: $U_0 = U_2 = 27.5$ kV; $l = 40$ km; $Z_B = 387.7\ \Omega$; $a = 299\,883$ km/s; $R = 0.2\ \Omega$/km; $G = 56$ nS/km. The variable x in the table 18.9 denotes the distance from the receiver to the left-hand generator. Such given data are characteristic for traction circuit of the railway alternating current electrified transport where the moving load (electric locomotive) can change not only in time, but can move in space with determined velocity.

All alternating current electrical receivers are, as a rule, consumers of active and of reactive powers at the same time, at that only the electric power station generators serve as an active power sources. The presence of the reactive elements in the moving load causes the power factor decrease and, correspondingly, generated reactive power increase, which often is comparable with generated active power.

In the considered variant the origin generators power factors vary from 0.87 to 0.91, but the generated reactive power forms nearly 50% from the active power. Connection of the capacitive nature compensative elements with the power equal to the reactive power of the supply generators eliminates completely the phase displacement between the current and voltage.

As it follows from presented results, the greatest losses of the active and the reactive powers as well as of the phase voltage occur in case when the receiver is equidistant from the sources. The voltage decrease at the load in this case reaches $\Delta U = 2$ kV, that is with 7% greater then nominal value (fig. 18.5). This is the reason to calculate the losses of active and of reactive

powers even for so short lines (l = 40 km) by exact formulas presented in the paragraph 6.

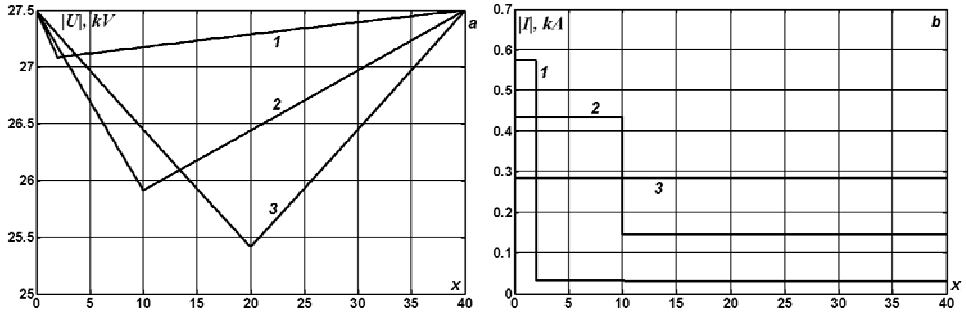

Fig. 18.5. Voltage and current modules distribution along line under the load Z_n = 40 + j·20 Ω located at the points x = 2; 10; 20 km (curves 1-3).

The location of unmatched active-inductive load Z_n = 40 + j·20 Ω influences essentially on the reactive power value, which changes more then in 6 times: Q_l =0.1010 MVAr when x =2 km and Q_l = 0.6165 MVAr when x = 20 km. If the load has matched capacitive nature $Z_n = Z_0$ = 399.56 – j·88.69 Ω, then this energy datum becomes less in an order and the voltage fluctuations are marked only in second significant digit (table 18.10). The match of the load insures the efficiency greater than 99%, independently on its location between two supply substations.

If we double the longitudinal active resistance and the transverse leakance: R = 0.4 Ω /km; G = 120 nS/km, then we obtain the results represented in the tables 18.11, 18.12. When x = 20 km the voltage at the load decreases till 24.46 kV, and the thrust loading decreases till 6 MW, whereas in the previous variant it comes to 6.46 MW.

In the table 18.13 we represent the calculations for the case when l = = 50 km; Z_n = 530 + j·460 Ω; R = 0.364 Ω/km; G = 0, and the load consumes approximately 0.4 MW of the active power and 0.35 MVAr of reactive power. In this case the losses of power and of phase voltage are insignificant and they can be neglected. Only the generated reactive power depends essentially on the load location. In this case it is necessary to regulate compensative elements resistances (as to compensate the generated reactive power).

Table 18.9. Synchronous action of two generators under the general load with resistance $Z_n = 40 + j \cdot 20\ \Omega$ when $R = 0.2\ \Omega$/km; $G = 56$ nS/km.

x, km	$\frac{P_0}{\cos\varphi_0}$, MW	$\frac{P_1}{\cos\varphi_1}$, MW	$\frac{P_2}{\cos\varphi_2}$, MW	P_l, MW	η	Q_0, MVAr	Q_1, MVAr	Q_2, MVAr	Q_l, MVAr	$\lvert U_1 \rvert$, kV	X_{n0}, Ω	X_{n2}, Ω
2	**7.0353**	7.3357	**0.3708**	0.0704	0.9905	**3.5987**	3.6678	**0.1701**	0.1010	27.08	-105	-2222
	0.8903	0.8944	**0.9089**									
4	**6.5415**	7.1398	**0.7273**	0.1291	0.9822	**3.4277**	3.5699	**0.3629**	0.2207	26.72	-110	-1042
	0.8858	0.8944	**0.8948**									
6	**6.0774**	6.9722	**1.0730**	0.1782	0.9751	**3.2502**	3.4861	**0.5570**	0.3210	26.40	-116	-679
	0.8818	0.8944	**0.8876**									
8	**5.6395**	6.8310	**1.4104**	0.2189	0.9689	**3.0677**	3.4155	**0.7519**	0.4041	26.14	-123	-503
	0.8784	0.8944	**0.8824**									
10	**5.2243**	6.7142	**1.7419**	0.2520	0.9638	**2.8816**	3.3571	**0.9472**	0.4717	25.91	-131	-399
	0.8756	0.8944	**0.8785**									
12	**4.8289**	6.6206	**2.0699**	0.2783	0.9597	**2.6928**	3.3103	**1.1426**	0.5252	25.73	-140	-331
	0.8734	0.8944	**0.8755**									
14	**4.4503**	6.5489	**2.3967**	0.2981	0.9565	**2.5021**	3.2744	**1.3381**	0.5657	25.59	-151	-283
	0.8717	0.8944	**0.8731**									
16	**4.0860**	6.4983	**2.7243**	0.3120	0.9542	**2.3099**	3.2491	**1.5333**	0.5941	25.49	-164	-247
	0.8705	0.8944	**0.8715**									
18	**3.7335**	6.4681	**3.0548**	0.3203	0.9528	**2.1167**	3.2341	**1.7282**	0.6109	25.43	-179	-219
	0.8699	0.8944	**0.8704**									
20	**3.3905**	6.4581	**3.3905**	0.3230	0.9524	**1.9228**	3.2291	**1.9228**	0.6165	25.41	-197	-197
	0.8699	0.8944	**0.8699**									

Table 18.10. Synchronous action of two generators under the general load with resistance $Z_n = Z_0 = 399.56 - j \cdot 88.69\ \Omega$ when $R = 0.2\ \Omega$/km; $G = 56$ nS/km.

x, km	$\frac{P_0}{\cos\varphi_0}$, MW	$\frac{P_1}{\cos\varphi_1}$, MW	$\frac{P_2}{\cos\varphi_2}$, MW	P_l, MW	η	Q_0, MVAr	Q_1, MVAr	Q_2, MVAr	Q_l, MVAr	$\lvert U_1 \rvert$, kV	X_{n0}, Ω	X_{n2}, Ω
2	**0.8573**	0.9011	**0.0455**	0.0017	0.9981	**-0.2088**	-0.2000	**-0.0303**	-0.0391	27.49	1811	12461
	0.9716	0.9762	**0.8321**									
4	**0.8122**	0.9004	**0.0906**	0.0025	0.9972	**-0.1973**	-0.1998	**-0.0401**	-0.0375	27.48	1917	9434
	0.9717	0.9762	**0.9146**									
6	**0.7671**	0.8997	**0.1358**	0.0032	0.9965	**-0.1861**	-0.1997	**-0.0497**	-0.0361	27.47	2031	7613
	0.9718	0.9762	**0.9391**									
8	**0.7220**	0.8991	**0.1809**	0.0038	0.9958	**-0.1753**	-0.1996	**-0.0591**	-0.0349	27.46	2157	6393
	0.9718	0.9762	**0.9505**									
10	**0.6769**	0.8986	**0.2260**	0.0043	0.9953	**-0.1648**	-0.1995	**-0.0685**	-0.0339	27.45	2295	5516
	0.9716	0.9762	**0.9569**									
12	**0.6318**	0.8982	**0.2711**	0.0047	0.9948	**-0.1545**	-0.1994	**-0.0779**	-0.0330	27.44	2447	4855
	0.9714	0.9762	**0.9611**									
14	**0.5867**	0.8979	**0.3162**	0.0050	0.9945	**-0.1445**	-0.1993	**-0.0872**	-0.0324	27.44	2617	4336
	0.9710	0.9762	**0.9640**									
16	**0.5416**	0.8977	**0.3613**	0.0052	0.9942	**-0.1346**	-0.1993	**-0.0966**	-0.0319	27.44	2809	3916
	0.9705	0.9762	**0.9661**									
18	**0.4965**	0.8975	**0.4063**	0.0053	0.9941	**-0.1249**	-0.1992	**-0.1059**	-0.0316	27.43	3027	3570
	0.9698	0.9762	**0.9677**									
20	**0.4514**	0.8975	**0.4514**	0.0054	0.9940	**-0.1154**	-0.1992	**-0.1154**	-0.0315	27.43	3277	3277
	0.9689	0.9762	**0.9689**									

Table 18.11. Synchronous action of two generators under the general load with resistance $Z_n = 40 + j \cdot 20\ \Omega$ when $R = 0.4\ \Omega$/km; $G = 120$ nS/km.

x, km	$\frac{P_0}{\cos\varphi_0}$, MW	$\frac{P_1}{\cos\varphi_1}$, MW	$\frac{P_2}{\cos\varphi_2}$, MW	P_l, MW	η	Q_0, MVAr	Q_1, MVAr	Q_2, MVAr	Q_l, MVAr	$\lvert U_1 \rvert$, kV	X_{n0}, Ω	X_{n2}, Ω
2	**6.9901**	7.2202	**0.3688**	0.1387	0.9812	**3.5508**	3.6101	**0.1676**	0.1083	26.87	-106	-2256
	0.8916	0.8944	**0.9104**									
4	**6.4641**	6.9325	**0.7191**	0.2508	0.9651	**3.3433**	3.4662	**0.3535**	0.2306	26.33	-113	-1070
	0.8882	0.8944	**0.8974**									
6	**5.9785**	6.6920	**1.0559**	0.3423	0.9513	**3.1390**	3.3460	**0.5374**	0.3304	25.87	-120	-704
	0.8854	0.8944	**0.8912**									
8	**5.5271**	6.4932	**1.3826**	0.4164	0.9397	**2.9383**	3.2466	**0.7196**	0.4112	25.48	-129	-525
	0.8830	0.8944	**0.8870**									
10	**5.1048**	6.3316	**1.7023**	0.4755	0.9301	**2.7411**	3.1658	**0.9004**	0.4758	25.16	-138	-420
	0.8810	0.8944	**0.8840**									
12	**4.7073**	6.2036	**2.0180**	0.5217	0.9224	**2.5475**	3.1018	**1.0804**	0.5261	24.91	-148	-350
	0.8795	0.8944	**0.8816**									
14	**4.3305**	6.1067	**2.3323**	0.5562	0.9165	**2.3571**	3.0533	**1.2601**	0.5638	24.71	-160	-300
	0.8783	0.8944	**0.8798**									
16	**3.9711**	6.0387	**2.6478**	0.5801	0.9124	**2.1695**	3.0194	**1.4398**	0.5899	24.57	-174	-263
	0.8776	0.8944	**0.8785**									
18	**3.6259**	5.9985	**2.9668**	0.5942	0.9099	**1.9845**	2.9992	**1.6201**	0.6053	24.49	-191	-233
	0.8772	0.8944	**0.8777**									
20	**3.2920**	5.9852	**3.2920**	0.5989	0.9090	**1.8015**	2.9926	**1.8015**	0.6104	24.46	-210	-210
	0.8772	0.8944	**0.8772**									

Table 18.12. Synchronous action of two generators under the general load with resistance $Z_n = Z_0 = 399.56 - j \cdot 88.69\ \Omega$ when $R = 0.4\ \Omega$/km; $G = 120$ nS/km.

x, km	$\frac{P_0}{\cos\varphi_0}$, MW	$\frac{P_1}{\cos\varphi_1}$, MW	$\frac{P_2}{\cos\varphi_2}$, MW	P_l, MW	η	Q_0, MVAr	Q_1, MVAr	Q_2, MVAr	Q_l, MVAr	$\lvert U_1\rvert$, kV	X_{n0}, Ω	X_{n2}, Ω
2	**0.7242**	0.7601	**0.0390**	0.0032	0.9959	**-0.2831**	-0.2779	**-0.0343**	-0.0395	27.48	1336	11024
	0.9314	0.9392	**0.7509**									
4	**0.6861**	0.7589	**0.0771**	0.0044	0.9943	**-0.2677**	-0.2775	**-0.0479**	-0.0381	27.45	1412	7887
	0.9316	0.9392	**0.8491**									
6	**0.6481**	0.7578	**0.1151**	0.0054	0.9929	**-0.2526**	-0.2771	**-0.0614**	-0.0370	27.43	1497	6155
	0.9317	0.9392	**0.8823**									
8	**0.6100**	0.7569	**0.1532**	0.0063	0.9917	**-0.2379**	-0.2768	**-0.0748**	-0.0360	27.42	1589	5054
	0.9316	0.9392	**0.8986**									
10	**0.5719**	0.7561	**0.1913**	0.0071	0.9907	**-0.2235**	-0.2765	**-0.0881**	-0.0351	27.40	1692	4291
	0.9314	0.9392	**0.9082**									
12	**0.5338**	0.7554	**0.2293**	0.0077	0.9899	**-0.2093**	-0.2762	**-0.1014**	-0.0344	27.39	1807	3730
	0.9310	0.9392	**0.9146**									
14	**0.4957**	0.7549	**0.2674**	0.0082	0.9892	**-0.1953**	-0.2761	**-0.1146**	-0.0339	27.38	1936	3299
	0.9304	0.9392	**0.9191**									
16	**0.4577**	0.7546	**0.3055**	0.0086	0.9888	**-0.1816**	-0.2759	**-0.1279**	-0.0335	27.38	2083	2958
	0.9295	0.9392	**0.9225**									
18	**0.4196**	0.7544	**0.3435**	0.0088	0.9885	**-0.1680**	-0.2759	**-0.1411**	-0.0332	27.37	2251	2679
	0.9284	0.9392	**0.9250**									
20	**0.3816**	0.7543	**0.3816**	0.0088	0.9884	**-0.1545**	-0.2758	**-0.1545**	-0.0332	27.37	2447	2447
	0.9269	0.9392	**0.9269**									

Table 18.13. Synchronous action of two generators under the general load with resistance $Z_n = 530 + j \cdot 460\ \Omega$ when $R = 0.364\ \Omega/km$; $G = 0$.

x, km	$\frac{P_0}{\cos\varphi_0}$, MW	$\frac{P_1}{\cos\varphi_1}$, MW	$\frac{P_2}{\cos\varphi_2}$, MW	P_l, MW	η	Q_0, MVAr	Q_1, MVAr	Q_2, MVAr	Q_l, MVAr	$\lvert U_1\rvert$, kV	X_{n0}, Ω	X_{n2}, Ω
2.5	**0.3858**	0.4055	**0.0203**	0.0006	0.9984	**0.3095**	0.3519	**-0.0079**	-0.0503	27.45	-1222	47867
	0.7800	0.7552	**0.9320**									
5	**0.3648**	0.4042	**0.0405**	0.0012	0.9971	**0.2915**	0.3508	**0.0097**	-0.0496	27.41	-1297	-38962
	0.7813	0.7552	**0.9725**									
7.5	**0.3440**	0.4031	**0.0607**	0.0017	0.9959	**0.2736**	0.3498	**0.0273**	-0.0490	27.37	-1382	-13865
	0.7827	0.7552	**0.9122**									
10	**0.3234**	0.4021	**0.0808**	0.0021	0.9948	**0.2557**	0.3490	**0.0448**	-0.0485	27.34	-1479	-8439
	0.7844	0.7552	**0.8746**									
12.5	**0.3028**	0.4013	**0.1009**	0.0024	0.9940	**0.2379**	0.3483	**0.0623**	-0.0480	27.31	-1589	-6067
	0.7863	0.7552	**0.8509**									
15	**0.2823**	0.4006	**0.1210**	0.0027	0.9933	**0.2202**	0.3477	**0.0798**	-0.0477	27.29	-1717	-4737
	0.7885	0.7552	**0.8347**									
17.5	**0.2620**	0.4001	**0.1411**	0.0029	0.9927	**0.2026**	0.3473	**0.0973**	-0.0474	27.27	-1867	-3885
	0.7911	0.7552	**0.8231**									
20	**0.2417**	0.3998	**0.1611**	0.0031	0.9923	**0.1850**	0.3470	**0.1148**	-0.0472	27.26	-2044	-3293
	0.7942	0.7552	**0.8144**									
22.5	**0.2215**	0.3995	**0.1812**	0.0032	0.9921	**0.1674**	0.3468	**0.1323**	-0.0471	27.25	-2259	-2858
	0.7978	0.7552	**0.8076**									
25	**0.2013**	0.3995	**0.2013**	0.0032	0.9920	**0.1498**	0.3467	**0.1498**	-0.0470	27.25	-2524	-2524
	0.8022	0.7552	**0.8022**									

CHAPTER III

TRANSIENT AND STEADY-SATE REGIMES UNDER THE IDEAL TRANSFORMERS CONNECTED TO THE LINE

The connection to the line of the ideal transformers (when sinks or additional electromagnetic energy sources are missed) is considered in this chapter. There are for the first time formulated the problems connected with the increase of transmission power and of efficiency by means of transformers. The methods of these problems solving are indicated.

19. Transformer connection to an arbitrary point of line

The exact solution for undistorting line with linear parameters $R = \gamma L$, $G = \gamma C$ in accordance with method of characteristics can be represented in the form of traveling waves with dissipative factor

$$i = e^{-\gamma t}\psi(x \pm at);\ \ u = \pm e^{-\gamma t}\psi(x \pm at)/Z_B\,. \qquad (19.1)$$

It follows from (19.1) that the invariants of the original hyperbolic system of equations (1.1) keep the constant values along the straight lines $dx/dt = \pm a$, called characteristics

$$I^{\pm} \equiv e^{-\gamma t}(i \pm aCu) = const\,.$$

Let's obtain the exact solution for homogeneous line with resistance R_S at the receiving end

$$u = R_S i \ \text{ when } \ x = l,\ t > 0\ . \qquad (19.2)$$

Consider the case when at the input of the line the voltage is given as an arbitrary function of time

$$u = u_0(t) \text{ when } x = 0, t > 0 . \tag{19.3}$$

Now let the ideal transformer is connected to the point of the line with the coordinate $x = x_n = \varepsilon l$, $0 < \varepsilon < 1$. This connection can be simulated by the following boundary conditions:

$$u^+ = -ku^-, \; i^+ = -i^- / k^*, \tag{19.4}$$

where k and k^* are the transformer ratios (or turns ratios).

We will consider only the case when these ratios are equal: $k = k^*$. Then at the point $x = x_n$ the continuity condition of power instantaneous values by space coordinate *x* is fulfilled:

$$i^- u^- = i^+ u^+ \text{ when } x = x_n .$$

It means that at the connection point the additional energy source or its sink is missed.

Using the relations on characteristics with positive and negative slopes $dx/dt = \pm a$ and the conjunction condition (19.4) at the point $x = l_1$ for $0 \le t < \min(\Delta_1, \Delta_2) = t_{1,1}$, we obtain the system of four equations with respect to four unknowns i^-, i^+, u^-, u^+

$$i^+ - aCu^+ = 0; \; i^- + aCu^- = 0;$$

$$i^- = -ki^+, \quad u^+ = -ku^-,$$

from which the zero solution results

$$i^+ = u^+ = i^- = u^- = 0.$$

Here we denote by $\Delta_1, \Delta_2, \Delta = \Delta_1 + \Delta_2 = l/a$ the times of electromagnetic wave run along the line intervals with lengths $l_1 = \varepsilon l, l_2 = (1-\varepsilon)l$ and *l* correspondingly.

Further we use the relations on characteristics with negative slope $dx/dt = -a$, the zero initial data $i = u = 0$ when $t = 0$, the values $i^+ = u^+ = i^- = u^- = 0$ when $x = l_1$ and the boundary condition (19.3). As a result at the left-hand end of the line $x = 0$ we get the system of two equations with respect to two unknown functions

$$i - aCu = 0; \quad u = u_0,$$

the solution of which can be easily determined

$$i_1^0 = aCu_0, u_1^0 = u_0 \text{ when } x = 0, 0 < t \le 2\Delta_1 = t_{0,1}.$$

Evidently, at the points $x = l, 0 < t < \Delta = t_{l,1}$ we have the trivial solution under the zero initial data

$$i_1^l = u_1^l = 0.$$

To obtain the solution for $x = 0$, $t > t_{0,1}$ and $x = l$, $t > t_{l,1}$ it is necessary to consider the solution behavior when $x = l_1$.

Using the relations on characteristics with positive and negative slopes $dx/dt = \pm a$ and the conjunction condition (19.4) at the point $x = l_1$ for $0 \le t < \min(\Delta_1, \Delta_2) = t_{1,1}$, we obtain the system of four equations with respect to four unknowns i^-, i^+, u^-, u^+:

$$\begin{aligned} i^+ - aCu^+ &= \left(i_1^l(t-\Delta_2) - aCu_1^l(t-\Delta_2)\right)e^{-\gamma\Delta_2} \equiv B_1^+(t); \\ i^- + aCu^- &= \left(i_1^0(t-\Delta_1) + aCu_1^0(t-\Delta_1)\right)e^{-\gamma\Delta_1} \equiv B_1^-(t); \\ i^- &= -ki^+, \quad u^+ = -ku^-. \end{aligned} \qquad (19.5)$$

This system reduces to the system of two equations

$$i^+ + kaCu^- = B_1^+(t),$$

$$-ki^{+} + aCu^{-} = B_1^{-}(t). \tag{19.6}$$

Now we can obtain the desired functions when $x = l_1$, $t_{1,1} \le t < \min(t_{0,1} + \Delta_1, t_{l,1} + \Delta_2) = t_{1,2}$:

$$i_1^{+} = \frac{1}{1+k^2}\left[B_1^{+}(t) - kB_1^{-}(t)\right], \quad i_1^{-} = -ki_1^{+},$$

$$u_1^{-} = \frac{1}{aC(1+k^2)}\left[B_1^{-}(t) + kB_1^{+}(t)\right], \quad u_1^{+} = -ku_1^{-}. \tag{19.7}$$

Let's determine the solution when $x = 0$, $t_{0,1} \le t < t_{0,2}$ and $x = l$, $t_{l,1} \le t < t_{l,2}$. According to the relations on characteristics $dx/dt = \pm a$ and the boundary conditions (19.2), (19.3) we get the system of two equations with respect to two unknowns:

$$x = 0: \quad i - aCu = \left(i_1^{-}(t - \Delta_1) - aCu_1^{-}(t - \Delta_1)\right)e^{-\gamma\Delta_1} \equiv A_2^0(t);$$

$$u = u_0(t). \tag{19.8}$$

$$x = l: \quad i + aCu = \left(i_1^{+}(t - \Delta_2) + aCu_1^{+}(t - \Delta_2)\right)e^{-\gamma\Delta_2} \equiv A_2^l(t);$$

$$u = R_S i. \tag{19.9}$$

Solving the systems (19.8) and (19.9) we determine the unknown functions i_2^0, u_2^0 at the time interval $t_{0,1} \le t < t_{1,1} + \Delta_1 = t_{0,2}$ and i_2^l, u_2^l for $t_{l,1} \le t < t_{1,1} + \Delta_2 = t_{l,2}$:

$$u_2^0 = u_0(t), \quad i_2^0 = aCu_2^0 + A_2^0(t), \tag{19.10}$$

$$i_2^0 = \frac{1}{1+aCR_S}A_2^l(t), \quad u_2^l = \frac{R_S}{1+aCR_S}A_2^l(t). \tag{19.11}$$

Further, using the relations on characteristics with positive and negative slopes $dx/dt = \pm a$ and the conjunction condition (19.4) at the point $x = l_1$ for $0 \le t < \min(\Delta_1, \Delta_2) = t_{1,1}$, we get the system of four equations with respect to four unknowns i^-, i^+, u^-, u^+:

$$i^+ - aCu^+ = \left(i_2^l(t-\Delta_2) - aCu_2^l(t-\Delta_2)\right)e^{-\gamma\Delta_2} \equiv B_2^+(t);$$

$$i^- + aCu^- = \left(i_2^0(t-\Delta_1) + aCu_2^0(t-\Delta_1)\right)e^{-\gamma\Delta_1} \equiv B_2^-(t);$$

$$i^- = -ki^+, \quad u^+ = -ku^-. \tag{19.12}$$

From this system we obtain the solution when $x = l_1$ for $t_{1,2} \le t < \min(t_{0,2} + \Delta_1, t_{l,2} + \Delta_2) = t_{1,3}$:

$$i_2^+ = \frac{1}{1+k^2}\left[B_2^+(t) - kB_2^-(t)\right], \quad i_2^- = -ki_2^+,$$

$$u_2^- = \frac{1}{aC(1+k^2)}\left[B_2^-(t) + kB_2^+(t)\right], \quad u_2^+ = -ku_2^-. \tag{19.13}$$

Now let's determine the solution when $x = 0$, $t_{0,2} \le t < t_{0,3}$ and $x = l$, $t_{l,2} \le t < t_{l,3}$. According to the relations on characteristics $dx/dt = \pm a$ and the boundary conditions (19.2), (19.3) we obtain the system of two equations with respect to two unknowns:

$$x = 0: \quad i - aCu = \left(i_2^-(t-\Delta_1) - aCu_2^-(t-\Delta_1)\right)e^{-\gamma\Delta_1} \equiv A_3^0(t);$$

$$u = u_0(t). \tag{19.14}$$

$$x = l: \quad i + aCu = \left(i_2^+(t-\Delta_2) + aCu_2^+(t-\Delta_2)\right)e^{-\gamma\Delta_2} \equiv A_3^l(t);$$

$$u = R_S i. \tag{19.15}$$

Solving the systems (19.14) and (19.15) we determine the unknown functions i_3^0, u_3^0 for $t_{0,2} \le t < t_{1,2} + \Delta_1 = t_{0,3}$ and i_3^l, u_3^l for $t_{l,2} \le t < t_{1,2} + \Delta_2 = t_{l,3}$:

$$u_3^0 = u_0(t), \quad i_3^0 = aCu_3^0 + A_3^0(t), \tag{19.16}$$

$$i_3^0 = \frac{1}{1 + aCR_S} A_3^l(t), \quad u_3^l = \frac{R_S}{1 + aCR_S} A_3^l(t) \ . \tag{19.17}$$

Continuing this procedure we can obtain the solution for any time moment $t > 0$.

As an example let's cite some exact solutions for undistorting line with parameters: $L = C = a = Z_B = 1$; $l_1 = 0.35\Delta$; $\gamma \ge 0$ under the sinusoidal voltage of the feeding generator: $u_0 = \sin(2\pi t)$.

19.1. Current and voltage at the sending end of the line $x = 0$:

$u_1^0 = i_1^0 = \sin t_0$ when $0 < t \le 0.7\Delta$; $t_0 = 2\pi t$,

$u_2^0 = \sin t_0$, $i_2^0 = i_1^0 + 2yE^7 \sin t_7$

when $0.7\Delta < t \le 1.4\Delta$; $t_7 = 2\pi(t - 0.7\Delta)$,

$u_3^0 = \sin t_0$; $i_3^0 = i_2^0 + 2y^2E^{14} \sin t_{14}$

when $1.4\Delta < t \le 2.0\Delta$; $t_{14} = 2\pi(t - 1.4\Delta)$,

$u_4^0 = \sin t_0$; $i_4^0 = i_3^0 - 2z(1 - y^2)E^{20} \sin t_{20}$

when $2.0\Delta < t \le 2.1\Delta$; $t_{20} = 2\pi(t - 2.0\Delta)$,

$u_5^0 = \sin t_0$; $i_5^0 = i_4^0 + 2y^3E^{21} \sin t_{21}$

when $2.1\Delta < t \le 2.7\Delta$; $t_{21} = 2\pi(t - 2.1\Delta)$,

$u_6^0 = \sin t_0$; $i_6^0 = i_5^0 - 4zy(1 - y^2)E^{27} \sin t_{27}$

when $2.7\Delta < t \le 2.8\Delta$; $t_{27} = 2\pi(t - 2.7\Delta)$,

$$u_7^0 = \sin t_0;\ i_7^0 = i_6^0 + 2y^4 E^{28} \sin t_{28}$$
$$\text{when } 2.8\Delta < t \le 3.3\Delta;\ t_{28} = 2\pi(t - 2.8\Delta),$$

$$u_8^0 = \sin t_0;\ i_8^0 = i_7^0 - 2z^2 y(1-y^2) E^{33} \sin t_{33}$$
$$\text{when } 3.3\Delta < t \le 3.4\Delta;\ t_{33} = 2\pi(t - 3.3\Delta),$$

$$u_9^0 = \sin t_0;\ i_9^0 = i_8^0 - 6zy^2(1-y^2) E^{34} \sin t_{34}$$
$$\text{when } 3.4\Delta < t \le 3.5\Delta;\ t_{34} = 2\pi(t - 3.4\Delta),$$

$$u_{10}^0 = \sin t_0;\ i_{10}^0 = i_9^0 + 2y^5 E^{35} \sin t_{35}$$
$$\text{when } 3.5\Delta < t \le 4.0\Delta;\ t_{35} = 2\pi(t - 3.5\Delta),$$

$$u_{11}^0 = \sin t_0;\ i_{11}^0 = i_{10}^0 - 2z^2(1-y^2)(3y^2 - 1) E^{40} \sin t_{40}$$
$$\text{when } 4.0\Delta < t \le 4.1\Delta;\ t_{40} = 2\pi(t - 4.0\Delta),$$

$$u_{12}^0 = \sin t_0;\ i_{12}^0 = i_{11}^0 - 8zy^3(1-y^2) E^{41} \sin t_{41}$$
$$\text{when } 4.1\Delta < t \le 4.2\Delta;\ t_{41} = 2\pi(t - 4.1\Delta),$$

$$u_{13}^0 = \sin t_0;\ i_{13}^0 = i_{12}^0 + 2y^6 E^{42} \sin t_{42}$$
$$\text{when } 4.2\Delta < t \le 4.6\Delta;\ t_{42} = 2\pi(t - 4.2\Delta),$$

$$u_{14}^0 = \sin t_0;\ i_{14}^0 = i_{13}^0 - 2z^3 y^2(1-y^2) E^{46} \sin t_{46}$$
$$\text{when } 4.6\Delta < t \le 4.7\Delta;\ t_{46} = 2\pi(t - 4.6\Delta),$$

$$u_{15}^0 = \sin t_0;\ i_{15}^0 = i_{14}^0 - 6z^2 y(1-y^2)(2y^2 - 1) E^{47} \sin t_{47}$$
$$\text{when } 4.7\Delta < t \le 4.8\Delta;\ t_{47} = 2\pi(t - 4.7\Delta),$$

$$u_{16}^0 = \sin t_0;\ i_{16}^0 = i_{15}^0 - 10zy^4(1-y^2) E^{48} \sin t_{48}$$
$$\text{when } 4.8\Delta < t \le 4.9\Delta;\ t_{48} = 2\pi(t - 4.8\Delta),$$
$$u_{17}^0 = \sin t_0;\ i_{17}^0 = i_{16}^0 + 2y^7 E^{49} \sin t_{49}$$
$$\text{when } 4.9\Delta < t \le 5.3\Delta;\ t_{49} = 2\pi(t - 4.9\Delta),$$

$u_{18}^0 = \sin t_0;\ i_{18}^0 = i_{17}^0 - 4z^3 y(1-y^2)(2y^2-1)E^{53}\sin t_{53}$

when $5.3\Delta < t \le 5.4\Delta;\ t_{53} = 2\pi(t-5.3\Delta)$,

$u_{19}^0 = \sin t_0;\ i_{19}^0 = i_{18}^0 - 4z^2 y^2(1-y^2)(5y^2-3)E^{54}\sin t_{54}$

when $5.4\Delta < t \le 5.5\Delta;\ t_{54} = 2\pi(t-5.4\Delta)$,

$u_{20}^0 = \sin t_0;\ i_{20}^0 = i_{19}^0 - 12zy^5(1-y^2)E^{55}\sin t_{55}$

when $5.5\Delta < t \le 5.6\Delta;\ t_{55} = 2\pi(t-5.5\Delta)$,

$u_{21}^0 = \sin t_0;\ i_{21}^0 = i_{20}^0 + 2y^8 E^{56}\sin t_{56}$

when $5.6\Delta < t \le 5.9\Delta;\ t_{56} = 2\pi(t-5.6\Delta)$,

$u_{22}^0 = \sin t_0;\ i_{22}^0 = i_{21}^0 - 2z^4 y^3(1-y^2)E^{59}\sin t_{59}$

when $5.9\Delta < t \le 6.0\Delta;\ t_{59} = 2\pi(t-5.9\Delta)$.,

Here $z = \dfrac{R_S - Z_B}{R_S + Z_B}$, $y = \dfrac{k^2-1}{k^2+1}$, $y_z = y(1+z)$, $E = e^{-\gamma\Delta/10}$.

19.2. Current and voltage at the end of the line $x = l$:

$u_2^l = i_2^l = 0$ when $0 < t \le 1.0\Delta$,

$u_2^l = \dfrac{1+z}{1-z} i_2^l;\ i_2^l = (1-z)\sqrt{1-y^2}E^{10}\sin t_{10}$

when $1.0\Delta < t \le 1.7\Delta;\ t_{10} = 2\pi(t-1.0\Delta)$,

$u_3^l = \dfrac{1+z}{1-z} i_3^l;\ i_3^l = i_2^l + (1-z)y\sqrt{1-y^2}E^{17}\sin t_{17}$

when $1.7\Delta < t \le 2.3\Delta;\ t_{17} = 2\pi(t-1.7\Delta)$,

$u_4^l = \dfrac{1+z}{1-z} i_4^l;\ i_4^l = i_3^l + (1-z)zy\sqrt{1-y^2}E^{23}\sin t_{23}$

when $2.3\Delta < t \le 2.4\Delta;\ t_{23} = 2\pi(t-2.3\Delta)$,

$$u_5^l = \frac{1+z}{1-z} i_5^l;\ i_5^l = i_4^l + (1-z)y^2\sqrt{1-y^2}E^{24}\sin t_{24}$$

when $2.4\Delta < t \le 3.0\Delta;\ t_{24} = 2\pi(t-2.4\Delta)$,

$$u_6^l = \frac{1+z}{1-z} i_6^l;\ i_6^l = i_5^l + (1-z)z\sqrt{1-y^2}(2y^2-1)E^{30}\sin t_{30}$$

when $3.0\Delta < t \le 3.1\Delta;\ t_{30} = 2\pi(t-3.0\Delta)$,

$$u_7^l = \frac{1+z}{1-z} i_7^l;\ i_7^l = i_6^l + (1-z)y^3\sqrt{1-y^2}E^{31}\sin t_{31}$$

when $3.1\Delta < t \le 3.6\Delta;\ t_{31} = 2\pi(t-3.1\Delta)$,

$$u_8^l = \frac{1+z}{1-z} i_8^l;\ i_8^l = i_9^l + (1-z)z^2y^2\sqrt{1-y^2}E^{36}\sin t_{36}$$

when $3.6\Delta < t \le 3.7\Delta;\ t_{36} = 2\pi(t-3.6\Delta)$,

$$u_9^l = \frac{1+z}{1-z} i_9^l;\ i_9^l = i_8^l + (1-z)zy\sqrt{1-y^2}(3y^2-2)E^{37}\sin t_{37}$$

when $3.7\Delta < t \le 3.8\Delta;\ t_{37} = 2\pi(t-3.7\Delta)$,

$$u_{10}^l = \frac{1+z}{1-z} i_{10}^l;\ i_{10}^l = i_9^l + (1-z)y^4\sqrt{1-y^2}E^{28}\sin t_{38}$$

when $3.8\Delta < t \le 4.3\Delta;\ t_{38} = 2\pi(t-3.8\Delta)$,

$$u_{11}^l = \frac{1+z}{1-z} i_{11}^l;\ i_{11}^l = i_{10}^l + (1-z)z^2y\sqrt{1-y^2}(3y^2-2)E^{43}\sin t_{43}$$

when $4.3\Delta < t \le 4.4\Delta;\ t_{43} = 2\pi(t-4.3\Delta)$,

$$u_{12}^l = \frac{1+z}{1-z} i_{12}^l;\ i_{12}^l = i_{11}^l + (1-z)zy^2\sqrt{1-y^2}(4y^2-3)E^{44}\sin t_{44}$$

when $4.4\Delta < t \le 4.5\Delta;\ t_{44} = 2\pi(t-4.4\Delta)$,

$$u_{13}^l = \frac{1+z}{1-z} i_{13}^l;\ i_{13}^l = i_{12}^l + (1-z)y\sqrt{1-y^2}E^{45}\sin t_{45}$$

when $4.5\Delta < t \le 4.9\Delta;\ t_{45} = 2\pi(t-4.5\Delta)$,

$$u_{14}^{l}=\frac{1+z}{1-z}i_{14}^{l};\ i_{14}^{l}=i_{13}^{l}+(1-z)z^{3}y^{3}\sqrt{1-y^{2}}E^{49}\sin t_{49}$$

when $4.9\Delta < t \le 5.0\Delta$; $t_{49}=2\pi(t-4.9\Delta)$,

$$u_{15}^{l}=\frac{1+z}{1-z}i_{15}^{l};$$

$$i_{15}^{l}=i_{16}^{l}+(1-z)z^{2}\sqrt{1-y^{2}}(6y^{4}-6y^{2}+1)E^{50}\sin t_{50}$$

when $5.0\Delta < t \le 5.1\Delta$; $t_{50}=2\pi(t-5.0\Delta)$,

$$u_{16}^{l}=\frac{1+z}{1-z}i_{16}^{l};\ i_{16}^{l}=i_{15}^{l}+(1-z)zy^{3}\sqrt{1-y^{2}}(5y^{2}-4)E^{51}\sin t_{51}$$

when $5.1\Delta < t \le 5.2\Delta$; $t_{51}=2\pi(t-5.1\Delta)$,

$$u_{17}^{l}=\frac{1+z}{1-z}i_{17}^{l};\ i_{17}^{l}=i_{16}^{l}+(1-z)y^{6}\sqrt{1-y^{2}}E^{52}\sin t_{52}$$

when $5.2\Delta < t \le 5.6\Delta$; $t_{52}=2\pi(t-5.2\Delta)$,

$$u_{18}^{l}=\frac{1+z}{1-z}i_{18}^{l};\ i_{18}^{l}=i_{17}^{l}+(1-z)z^{3}y^{2}\sqrt{1-y^{2}}(4y^{2}-3)E^{56}\sin t_{56}$$

when $5.6\Delta < t \le 5.7\Delta$; $t_{56}=2\pi(t-5.6\Delta)$,

$$u_{19}^{l}=\frac{1+z}{1-z}i_{19}^{l};$$

$$i_{19}^{l}=i_{18}^{l}+(1-z)z^{2}y\sqrt{1-y^{2}}(10y^{4}-12y^{2}+3)E^{57}\sin t_{57}$$

when $5.7\Delta < t \le 5.8\Delta$; $t_{57}=2\pi(t-5.7\Delta)$,

$$u_{20}^{l}=\frac{1+z}{1-z}i_{20}^{l};\ i_{20}^{l}=i_{19}^{l}+(1-z)zy^{4}\sqrt{1-y^{2}}(6y^{2}-5)E^{58}\sin t_{58}$$

when $5.8\Delta < t \le 5.9\Delta$; $t_{58}=2\pi(t-5.8\Delta)$,

$$u_{21}^{l}=\frac{1+z}{1-z}i_{21}^{l};\ i_{21}^{l}=i_{20}^{l}+(1-z)y^{7}\sqrt{1-y^{2}}E^{59}\sin t_{59}$$

when $5.9\Delta < t \le 6.0\Delta$; $t_{59}=2\pi(t-5.9\Delta)$.

19.3. Quasisteady-state current and voltage forms for undistorting line

Let's obtain the closed formulas for currents, voltages and for average power in the steady-state regime (so named quasisteady-state forms) applying the following approach. Let's suppose that the wave propagation process starts at the infinitely far in time point $t = -\infty$, and by the time moment $t = 0$ the wave motion becomes already steady-state. We will look for the solution at the beginning of the line $x = 0$ and at the end of the line $x = l$ in the following form

$$x = 0: \; u(0,t) = u_0(t) = U \sin 2\pi t, \; i(0,t) = A_1 \sin(2\pi t + \varphi_1) \tag{19.18}$$

$$x = l: \; u(t) = R_S A_2 \sin(2\pi t + \varphi_2), \; i(t) = A_2 \sin(2\pi t + \varphi_2). \tag{19.19}$$

Here U is given amplitude of the sinusoidal voltage, A_1, A_2 and φ_1, φ_2 are unknown amplitudes and phases. These unknown values we will determine starting from the condition that after the wave (19.18) reflection from the receiving end $x = l$ and after wave (19.19) reflection from the loaded end $x = 0$ the current forms remain permanent sinusoidal. But it is necessary to take into account the appearance of the waves reflected from the conjunction point $x = x_n = \varepsilon l = l_1, \; 0 < \varepsilon < 1$.

According to the formulas (19.5) the values i^-, i^+, u^- and u^+ can be determined from the system

$$\begin{gathered} i^+ - aCu^+ = \left(i^l(t - \Delta_2) - aCu^l(t - \Delta_2)\right)e^{-\gamma\Delta_2} \equiv B^+(t); \\ i^- + aCu^- = \left(i^0(t - \Delta_1) + aCu^0(t - \Delta_1)\right)e^{-\gamma\Delta_1} \equiv B^-(t); \\ i^- = -ki^+, \quad u^+ = -ku^-. \end{gathered} \tag{19.20}$$

Here we denote by $\Delta_1, \Delta_2, \Delta = \Delta_1 + \Delta_2 = l/a$ the times of electromagnetic wave run along the line intervals with lengths $l_1 = \varepsilon l, l_2 = (1 - \varepsilon)l$ and l correspondingly.

This system reduces to the system of two equations

$$i^+ + kaCu^- = B^+(t), \; -ki^+ + aCu^- = B^-(t). \tag{19.21}$$

Solving the last system we obtain the solution when $x = l_1 = \varepsilon l$:

$$i^+ = \frac{1}{1+k^2}\left[B^+(t) - kB^-(t)\right], \quad i^- = -ki^+,$$

$$u^- = \frac{1}{aC(1+k^2)}\left[B^-(t) + kB^+(t)\right], \quad u^+ = -ku^-. \qquad (19.22)$$

Substituting the expressions (19.18), (19.19) in the (19.20) we get

$$B^+(t) = A_2(1 - aCR_S)\sin(2\pi(t - \Delta_2) + \varphi_2)e^{-\gamma\Delta_2};$$

$$B^-(t) = \left[A_1 \sin(2\pi(t - \Delta_1) + \varphi_1) + aCU \sin(2\pi(t - \Delta_1))\right]e^{-\gamma\Delta_1}.$$

In accordance with the (19.22) we obtain

$$i^+(t) = \frac{1}{1+k^2}\left[A_2(1 - aCR_S)\sin(2\pi(t - \Delta_2) + \varphi_2)\right]e^{-\gamma\Delta_2} -$$

$$- \frac{k}{1+k^2}\left[A_1 \sin(2\pi(t - \Delta_1) + \varphi_1) + aCU \sin(2\pi(t - \Delta_1))\right]e^{-\gamma\Delta_1};$$

$$i^-(t) = -ki^+(t);$$

$$u^-(t) = \frac{1}{aC(1+k^2)}\left[A_1 \sin(2\pi(t - \Delta_1) + \varphi_1) + \right.$$

$$\left. + aCU \sin(2\pi(t - \Delta_1))\right]e^{-\gamma\Delta_1} +$$

$$+ \frac{k}{aC(1+k^2)} A_2(1 - aCR_S)U \sin(2\pi(t - \Delta_2) + \varphi_2)e^{-\gamma\Delta_2};$$

$$u^+(t) = -ku^-(t). \qquad (19.23)$$

Further, we determine the current and voltage at the points $x = 0$ and $x = l$ by formulas (19.8), (19.9)

$$x = 0: \quad i = aCu + \left(i^{-}(t - \Delta_1) - aCu^{-}(t - \Delta_1)\right)e^{-\gamma\Delta_1};$$

$$u = u_0(t). \tag{19.24}$$

$$x = l: \quad i + aCu = \left(i^{+}(t - \Delta_2) + aCu^{+}(t - \Delta_2)\right)e^{-\gamma\Delta_2};$$

$$u = R_S i. \tag{19.25}$$

Thus, after two reflections the current at the sending end of the line $x = 0$ takes the form

$$i(t) = aCU \sin 2\pi t -$$

$$-\frac{2k}{1+k^2} A_2 e^{-\gamma\Delta}(1 - aCR_S)\sin(2\pi(t - \Delta) + \varphi_2) +$$

$$+\left[\frac{k^2 - 1}{k^2 + 1} A_1 \sin(2\pi(t - 2\Delta_1) + \varphi_1) +\right.$$

$$\left. + aCU \frac{k^2 - 1}{k^2 + 1}\sin(2\pi(t - 2\Delta_1))\right] e^{-2\gamma\Delta_1}. \tag{19.26}$$

It is convenient to introduce the following notations

$$z = \frac{R_S - Z_B}{R_S + Z_B},\ z_\gamma = ze^{-2\gamma\Delta},\ k = \operatorname{tg}\frac{\alpha}{2},$$

$$y = \frac{k^2 - 1}{k^2 + 1} = -\cos\alpha,\ \frac{2k}{k^2 + 1} = \sqrt{1 - y^2} = \sin\alpha, \tag{19.27}$$

$$y_\gamma = ye^{-\gamma\Delta},\ y_{z\gamma} = y_\gamma(1 + z) = y(1 + z)e^{-\gamma\Delta}\ .$$

Then the formula (19.26) can be rewritten in the form

$$i(t) = aCU \sin 2\pi t + \frac{2z \sin\alpha}{1-z} A_2 e^{-\gamma\Delta} \sin(2\pi(t-\Delta)+\varphi_2) +$$

$$+ \cos\alpha\left[A_1 \sin(2\pi(t-2\Delta_1)+\varphi_1) +\right.$$

$$\left. + aCU \sin(2\pi(t-2\Delta_1))\right] e^{-2\gamma\Delta_1}. \qquad (19.28)$$

At the right-hand end of the line $x = l$ from (19.25) we obtain

$$i(t) = -\frac{k^2-1}{k^2+1} \cdot \frac{1-aCR_s}{1+aCR_s} A_2 e^{-2\gamma\Delta_2} \sin(2\pi(t-2\Delta_2)+\varphi_2) -$$

$$- \frac{2k}{1+k^2} \cdot \frac{1}{1+aCR_s}\left[A_1 \sin(2\pi(t-\Delta)+\varphi_1) +\right.$$

$$\left. + aCU \sin(2\pi(t-\Delta))\right] e^{-\gamma\Delta}.$$

Or taking into consideration the notations (19.27) finally we get

$$i(t) = -z\cos\alpha A_2 e^{-2\gamma\Delta_2} \sin(2\pi(t-2\Delta_2)+\varphi_2) -$$

$$- \frac{(1-z)\sin\alpha}{2}\left[A_1 \sin(2\pi(t-\Delta)+\varphi_1) +\right.$$

$$\left. + aCU \sin(2\pi(t-\Delta))\right] e^{-\gamma\Delta}. \qquad (19.29)$$

Now to determine the parameters A_1, A_2, φ_1, φ_2 we equate the relations (19.18), (19.19) with (19.28), (19.29):

$$A_1 \sin(2\pi t + \varphi_1) = aCU \sin 2\pi t +$$

$$+ \frac{2z \sin\alpha}{1-z} A_2 e^{-\gamma\Delta} \sin(2\pi(t-\Delta)+\varphi_2) +$$

$$+\cos\alpha\left[A_1\sin(2\pi(t-2\Delta_1)+\varphi_1)+aCU\sin(2\pi(t-2\Delta_1))\right]e^{-2\gamma\Delta_1};$$

$$A_2\sin(2\pi t+\varphi_2)=-z\cos\alpha A_2 e^{-2\gamma\Delta_2}\sin(2\pi(t-2\Delta_2)+\varphi_2)-$$

$$-\frac{(1-z)\sin\alpha}{2}\left[A_1\sin(2\pi(t-\Delta)+\varphi_1)+aCU\sin(2\pi(t-\Delta))\right]e^{-\gamma\Delta}.$$

As these equalities are to fulfill for any t, then equating the coefficients of $\sin 2\pi t$ with the coefficients of $\cos 2\pi t$, we obtain the following system of four equations with respect to unknowns A_1, A_2, φ_1, φ_2:

$$A_1\cos\varphi_1=aCU+\frac{2z\sin\alpha}{1-z}A_2e^{-\gamma\Delta}\cos(2\pi\Delta-\varphi_2)-$$

$$-\cos\alpha A_1e^{-2\gamma\Delta_1}\cos(4\pi\Delta_1-\varphi_1)-aCUe^{-2\gamma\Delta_1}\cos\alpha\cos(4\pi\Delta_1);$$

$$A_1\sin\varphi_1=-\frac{2z\sin\alpha}{1-z}A_2e^{-\gamma\Delta}\sin(2\pi\Delta-\varphi_2)+$$

$$+\cos\alpha A_1e^{-2\gamma\Delta_1}\sin(4\pi\Delta_1-\varphi_1)+aCUe^{-2\gamma\Delta_1}\cos\alpha\sin(4\pi\Delta_1);$$

$$A_2\cos\varphi_2=-z\cos\alpha A_2e^{-2\gamma\Delta_2}\cos(4\pi\Delta_2-\varphi_2)-$$

$$-\frac{1-z}{2}\sin\alpha A_1e^{-\gamma\Delta}\cos(2\pi\Delta-\varphi_1)-$$

$$-aCU\frac{1-z}{2}\sin\alpha e^{-\gamma\Delta}\cos(2\pi\Delta);\qquad(19.30)$$

$$A_2\sin\varphi_2=z\cos\alpha A_2e^{-2\gamma\Delta_2}\sin(4\pi\Delta_2-\varphi_2)+$$

$$+\frac{1-z}{2}\sin\alpha A_1e^{-\gamma\Delta}\sin(2\pi\Delta-\varphi_1)+$$

$$+ aCU\frac{1-z}{2}\sin\alpha e^{-\gamma\Delta}\sin(2\pi\Delta).$$

After the notations

$$y_1 = A_1/(aCU)\sin\varphi_1,\ y_2 = A_1/(aCU)\cos\varphi_1,$$

$$y_3 = A_2/(aCU)\sin\varphi_2,\ y_4 = A_2/(aCU)\cos\varphi_2\ ,$$

the system (19.30) transforms to the following system of linear algebraic equations

$$G\,\bar{y} = \bar{F}\,, \tag{19.31}$$

where

$$G = \begin{pmatrix} Y_{s1} & 1+Y_{c1} & D\sin 2\pi\Delta & D\cos 2\pi\Delta \\ 1+Y_{c1} & -Y_{s1} & D\cos 2\pi\Delta & -D\sin 2\pi\Delta \\ -B\sin 2\pi\Delta & -B\cos 2\pi\Delta & zY_{s2} & 1+zY_{c2} \\ -B\cos 2\pi\Delta & B\sin 2\pi\Delta & 1+zY_{c2} & -zY_{s2} \end{pmatrix};$$

$$\bar{y} = (y_1, y_2, y_3, y_4)^T;\ \bar{F} = (1-Y_{c1},\ Y_{s1},\ B\cos 2\pi\Delta,\ -B\sin 2\pi\Delta)^T;$$

$$B = \frac{z-1}{2}e^{-\gamma\Delta}\sin\alpha = \frac{\sqrt{1-y^2}\,(z-1)}{2}e^{-\gamma\Delta};$$

$$D = \frac{2z\sin\alpha}{z-1}e^{-\gamma\Delta} = \frac{2z\sqrt{1-y^2}}{z-1}e^{-\gamma\Delta};$$

$$Y_{s1} = e^{-2\gamma\Delta_1}\cos\alpha\sin 4\pi\Delta_1 = -ye^{-2\gamma\Delta_1}\sin 4\pi\Delta_1;$$

$$Y_{c1} = e^{-2\gamma\Delta_1}\cos\alpha\cos 4\pi\Delta_1 = -ye^{-2\gamma\Delta_1}\cos 4\pi\Delta_1;$$

$$Y_{s2} = e^{-2\gamma\Delta_2}\cos\alpha\sin 4\pi\Delta_2 = -ye^{-2\gamma\Delta_2}\sin 4\pi\Delta_2;$$

$$Y_{c2} = e^{-2\gamma\Delta_2}\cos\alpha\cos 4\pi\Delta_2 = -ye^{-2\gamma\Delta_2}\cos 4\pi\Delta_2 .$$

The solution of the system (19.31) can be represented in the form

$$y_1 = A_1\sin\varphi_1 =$$

$$= \frac{2aCU}{Zn}\Big[z_\gamma\sin 4\pi\Delta + \left(e^{-2\gamma\Delta_1} + zz_\gamma e^{-2\gamma\Delta_2}\right)\cos\alpha\sin 4\pi\Delta_1 +$$

$$+ z_\gamma\cos^2\alpha\sin 4\pi(\Delta_1-\Delta_2)\Big];$$

$$y_2 = A_1\cos\varphi_1 =$$

$$= \frac{aCU}{Zn}\Big[1 - z_\gamma^2 + y_\gamma^2\left(z^2e^{2\gamma(\Delta_1-\Delta_2)} - e^{2\gamma(\Delta_2-\Delta_1)}\right) -$$

$$- 2zy_\gamma e^{\gamma(\Delta_1-\Delta_2)}\left(1-e^{-4\gamma\Delta_1}\right)\cos 4\pi\Delta_2\Big];$$

$$y_3 = A_2\sin\varphi_2 =$$

$$= aCU\frac{(z-1)e^{-\gamma\Delta}\sin\alpha}{Zn}\Big[(z_\gamma-1)\sin 2\pi\Delta +$$

$$+\cos\alpha e^{-2\gamma\Delta_1}\left(1-ze^{2\gamma(\Delta_1-\Delta_2)}\right)\sin 2\pi(\Delta_1-\Delta_2)\Big];$$

$$y_4 = A_2\cos\varphi_2 =$$

$$= aCU\frac{(z-1)e^{-\gamma\Delta}\sin\alpha}{Zn}\Big[(1+z_\gamma)\cos 2\pi\Delta +$$

$$+\cos\alpha e^{-2\gamma\Delta_1}\left(1+ze^{2\gamma(\Delta_1-\Delta_2)}\right)\cos 2\pi(\Delta_1-\Delta_2)\Big]; \qquad (19.32)$$

$$Zn = 1 + 2z_\gamma\cos 4\pi\Delta + z_\gamma^2 + \cos^2\alpha e^{-4\gamma\Delta_1}\Big[1 + z^2e^{4\gamma(\Delta_1-\Delta_2)} +$$

$$+ 2ze^{2\gamma(\Delta_1-\Delta_2)}\cos 4\pi(\Delta_1-\Delta_2)\Big] +$$

$$+2\cos\alpha e^{-2\gamma\Delta_1}\left[\left(1+z^2e^{-4\gamma\Delta_2}\right)\cos 4\pi\Delta_1+z_\gamma\left(1+e^{4\gamma\Delta_1}\right)\cos 4\pi\Delta_2\right].$$

Now from (19.32) after some transformations we obtain the formulas for amplitudes A_1, A_2 and phases φ_1, φ_2:

$$A_1 = aCU\left\{\left[1-2z_\gamma\cos 4\pi\Delta+z_\gamma^2+\right.\right.$$

$$+2ye^{-2\gamma\Delta_1}\left((1+z^2e^{-4\gamma\Delta_2})\cos 4\pi\Delta_1-z_\gamma(1+e^{4\gamma\Delta_1})\cos 4\pi\Delta_2\right)+$$

$$\left.\left.+y^2e^{-4\gamma\Delta_1}\left(1+z^2e^{4\gamma(\Delta_1-\Delta_2)}-2ze^{2\gamma(\Delta_1-\Delta_2)}\cos 4\pi(\Delta_1-\Delta_2)\right)\right]\Big/Zn\right\}^{1/2};$$

$$\mathrm{tg}\varphi_1 = 2\left[z_\gamma\sin 4\pi\Delta-\left(e^{-2\gamma\Delta_1}+zz_\gamma e^{-2\gamma\Delta_2}\right)y\sin 4\pi\Delta_1+\right.$$

$$+z_\gamma y^2\sin 4\pi(\Delta_1-\Delta_2)\Big]\Big/\Big[1-z_\gamma^2+$$

$$+y_\gamma^2\left(z^2e^{2\gamma(\Delta_1-\Delta_2)}-e^{2\gamma(\Delta_2-\Delta_1)}\right)-$$

$$\left.-2zy_\gamma e^{\gamma(\Delta_1-\Delta_2)}\left(1-e^{-4\gamma\Delta_1}\right)\cos 4\pi\Delta_2\right]; \qquad (19.33)$$

$$A_2 = aCU\sqrt{\frac{(1-y^2)(1-z)^2e^{-2\gamma\Delta}}{Zn}};$$

$$\mathrm{tg}\varphi_2 =$$

$$=\frac{(z_\gamma-1)\sin 2\pi\Delta-ye^{-2\gamma\Delta_1}\left(1-ze^{2\gamma(\Delta_1-\Delta_2)}\right)\sin 2\pi(\Delta_1-\Delta_2)}{(1+z_\gamma)\cos 2\pi\Delta-ye^{-2\gamma\Delta_1}\left(1+ze^{2\gamma(\Delta_1-\Delta_2)}\right)\cos 2\pi(\Delta_1-\Delta_2)}. \qquad (19.34)$$

Hence, the quasisteady-state forms for currents and voltages look like the (19.18) and (19.19), where the amplitudes and phases are defined by formulas (19.33) and (19.34). To obtain the average power it is necessary to integrate the currents and voltages product by the unit time interval:

$$P_0 = \int_0^1 u(0,t)i(0,t)dt = UA_1 \int_0^1 \sin(2\pi t)\sin(2\pi t + \varphi_1)dt =$$

$$= UA_1 \frac{\cos\varphi_1}{2} = \frac{aCU^2}{2Zn}\left[1 - z_\gamma^2 + y_\gamma^2\left(z^2 e^{2\gamma(\Delta_1-\Delta_2)} - e^{2\gamma(\Delta_2-\Delta_1)}\right) -\right.$$

$$\left. -2zy_\gamma e^{\gamma(\Delta_1-\Delta_2)}\left(1 - e^{-4\gamma\Delta_1}\right)\cos 4\pi\Delta_2\right]; \qquad (19.35)$$

$$P_1 = \int_0^1 u(l,t)i(l,t)dt = R_s {A_2}^2 \int_0^1 \sin^2(2\pi t + \varphi_2)dt = \frac{R_s {A_2}^2}{2} =$$

$$= \frac{aCU^2(1-z^2)(1-y^2)e^{-2\gamma\Delta}}{2Zn}; \qquad (19.36)$$

$$z_\gamma = ze^{-2\gamma\Delta},\ y_\gamma = ye^{-\gamma\Delta},\ y_{z\gamma} = y_\gamma(1+z) = y(1+z)e^{-\gamma\Delta}.$$

The efficiency is calculated as $\eta = P_1 / P_0$ or

$$\eta = (1-z^2)(1-y^2)e^{-2\gamma\Delta} \Big/ \left[1 - z_\gamma^2 + y_\gamma^2\left(z^2 e^{2\gamma(\Delta_1-\Delta_2)} - e^{2\gamma(\Delta_2-\Delta_1)}\right) -\right.$$

$$\left. -2zy_\gamma e^{\gamma(\Delta_1-\Delta_2)}\left(1 - e^{-4\gamma\Delta_1}\right)\cos 4\pi\Delta_2\right]. \qquad (19.37)$$

In case when $\gamma = 0$ the average power takes the form

$$P_0 = P_1 = aCU^2 \frac{(1-z^2)(1-y^2)}{2Zn} = \frac{1}{2}aCU^2(1-z^2)(1-y^2) \Big/ \left\{1 + \right.$$

$$+ 2z\cos 4\pi\Delta + z^2 + y^2\left[1 + z^2 + 2z\cos 4\pi(\Delta_1 - \Delta_2)\right] -$$

$$\left. -2y\left[\left(1+z^2\right)\cos 4\pi\Delta_1 + 2z\cos 4\pi\Delta_2\right]\right\}. \qquad (19.38)$$

19.4. Quasisteady-state current and voltage forms for line with arbitrary losses

If the steady state process is considered then we can apply the equations of steady-state regime in hyperbolic functions. Let's denote as before the complex amplitudes of voltages and currents at the input-output of the electrical circuit by U_0, I_0, U_1, I_1, and at the conjunction point (where the ideal transformer is connected) by $U^+ = -kU^-$, $I^- = -kI^+$. In accordance with complex amplitude method (1.5) for the fist section of the line $0 \le x \le l_1$ we can write down the equalities

$$U^- = U_0 \mathrm{ch}(\delta l_1) - I_0 Z_0 \mathrm{sh}(\delta l_1),\ I^- = -\frac{U_0}{Z_0}\mathrm{sh}(\delta l_1) + I_0 \mathrm{ch}(\delta l_1). \quad (19.39)$$

Using the relation $U_0 = Z_{BX} I_0$ we get

$$U^- = [Z_{BX}\mathrm{ch}(\delta l_1) - Z_0 \mathrm{sh}(\delta l_1)]I_0,$$

$$I^- = [-Z_{BX}\mathrm{sh}(\delta l_1) + Z_0 \mathrm{ch}(\delta l_1)]\frac{I_0}{Z_0}. \quad (19.40)$$

For the second section of the line $l_1 \le x \le l_1 + l_2 = l$ we have

$$U^+ = U_1 \mathrm{ch}(\delta l_2) + I_1 Z_0 \mathrm{sh}(\delta l_2),\ I^+ = \frac{U_1}{Z_0}\mathrm{sh}(\delta l_2) + I_1 \mathrm{ch}(\delta l_2) \quad (19.41)$$

or according to relation $U_1 = Z_S I_1$

$$U^+ = [Z_S \mathrm{ch}(\delta l_2) + Z_0 \mathrm{sh}(\delta l_2)]I_1,$$

$$I^+ = [Z_S \mathrm{sh}(\delta l_2) + Z_0 \mathrm{ch}(\delta l_2)]\frac{I_1}{Z_0}. \quad (19.42)$$

Applying the conjunction conditions when $x = l_1$

$$U^+ = -kU^-,\ I^- = -kI^+, \quad (19.43)$$

from (19.41) and (19.43) we obtain

$$\begin{aligned}&[Z_S\,\mathrm{ch}(\delta l_2)+Z_0\,\mathrm{sh}(\delta l_2)]I_1=-k[Z_{BX}\,\mathrm{ch}(\delta l_1)-Z_0\,\mathrm{sh}(\delta l_1)]I_0,\\&-k[Z_S\,\mathrm{sh}(\delta l_2)+Z_0\,\mathrm{ch}(\delta l_2)]\frac{I_1}{Z_0}=[-Z_{BX}\,\mathrm{sh}(\delta l_1)+Z_0\,\mathrm{ch}(\delta l_1)]\frac{I_0}{Z_0}.\end{aligned}\qquad(19.44)$$

The homogeneous system of equations (19.44) possesses the solution when its determinant is equal to zero. This condition allows us to obtain the formula for input resistance Z_{BX}

$$Z_{BX}=Z_0\,\frac{Z_0\,\mathrm{sh}(\delta l_1)+Z_{BX1}\,\mathrm{ch}(\delta l_1)}{Z_0\,\mathrm{ch}(\delta l_1)+Z_{BX1}\,\mathrm{sh}(\delta l_1)},\qquad(19.45)$$

where the following notation is used

$$Z_{BX1}=\frac{Z_0}{k^2}\,\frac{Z_0\,\mathrm{sh}(\delta l_2)+Z_S\,\mathrm{ch}(\delta l_2)}{Z_0\,\mathrm{ch}(\delta l_2)+Z_S\,\mathrm{sh}(\delta l_2)}.\qquad(19.46)$$

In case of sinusoidal voltage $u(0,t)=\ =u_0\sin(\omega t)$ the active power of generator, of load and the efficiency can be calculated by the formulas

$$P_0=\frac{1}{2}\,\mathrm{Re}(U_0I_0^*)=\frac{u_0^2}{2}\,\mathrm{Re}\left(\frac{1}{Z_{BX}^*}\right)=\frac{u_0^2}{4}\left(\frac{1}{Z_{BX}^*}+\frac{1}{Z_{BX}}\right)=$$

$$=\frac{u_0^2(Z_{BX}+Z_{BX}^*)}{4|Z_{BX}|^2}=\frac{u_0^2\,\mathrm{Re}(Z_{BX})}{2|Z_{BX}|^2};\qquad(19.47)$$

$$P_1=\frac{1}{2}\,\mathrm{Re}(U_1I_1^*)=\frac{|I_1|^2\,\mathrm{Re}(Z_S)}{2}=$$

$$=\frac{u_0^2k^2\,\mathrm{Re}(Z_S)}{2|Z_{BX}|^2}\left|\frac{Z_{BX}\,\mathrm{ch}(\delta l_1)-Z_0\,\mathrm{sh}(\delta l_1)}{Z_S\,\mathrm{ch}(\delta l_2)+Z_0\,\mathrm{sh}(\delta l_2)}\right|^2;\qquad(19.48)$$

$$\eta = \frac{P_1}{P_0} = \frac{k^2 \operatorname{Re}(Z_S)}{\operatorname{Re}(Z_{BX})} \left| \frac{Z_{BX} \operatorname{ch}(\delta l_1) - Z_0 \operatorname{sh}(\delta l_1)}{Z_S \operatorname{ch}(\delta l_2) + Z_0 \operatorname{sh}(\delta l_2)} \right|^2 . \qquad (19.49)$$

20. Why transformers can not be placed close to the points $\lambda/8$, $3\lambda/8$, $5\lambda/8$

Let's formulate the problem of the transformer ratio k determination in order to reach the maximal values of transmission power and of the efficiency. We will use the exact solutions for the line with arbitrary losses. So from the formulas (19.47)–(19.49) we get

$$P_0 = \frac{u_0^2 \operatorname{Re}(Z_{BX})}{2\left|Z_{BX}\right|^2}; \qquad (20.1)$$

$$P_1 = \frac{u_0^2 k^2 \operatorname{Re}(Z_S)}{2\left|Z_{BX}\right|^2} \left| \frac{Z_{BX} \operatorname{ch}(\delta l_1) - Z_0 \operatorname{sh}(\delta l_1)}{Z_S \operatorname{ch}(\delta l_2) + Z_0 \operatorname{sh}(\delta l_2)} \right|^2 ; \qquad (20.2)$$

$$\eta = \frac{P_1}{P_0} = \frac{k^2 \operatorname{Re}(Z_S)}{\operatorname{Re}(Z_{BX})} \left| \frac{Z_{BX} \operatorname{ch}(\delta l_1) - Z_0 \operatorname{sh}(\delta l_1)}{Z_S \operatorname{ch}(\delta l_2) + Z_0 \operatorname{sh}(\delta l_2)} \right|^2 . \qquad (20.3)$$

For the input resistance Z_{BX} we introduce the notations different from the notations in previous paragraph

$$Z_{BX} = Z_0 \frac{k^2 Z_0 \operatorname{sh}(\delta l_1) + Z_{BX1} \operatorname{ch}(\delta l_1)}{k^2 Z_0 \operatorname{ch}(\delta l_1) + Z_{BX1} \operatorname{sh}(\delta l_1)}, \qquad (20.4)$$

and

$$Z_{BX1} = Z_0 \frac{Z_0 \operatorname{sh}(\delta l_2) + Z_S \operatorname{ch}(\delta l_2)}{Z_0 \operatorname{ch}(\delta l_2) + Z_S \operatorname{sh}(\delta l_2)}. \qquad (20.5)$$

Then it will be convenient to represent the formulas (20.2), (20.3) in the form explicitly containing the parameter k

$$P_1 = \frac{u_0^2 k^2 \operatorname{Re}(Z_S)\left|Z_{BX1}\right|^2}{2\left|Z_S \operatorname{ch}(\delta l_2) + Z_0 \operatorname{sh}(\delta l_2)\right|^2 \left|k^2 Z_0 \operatorname{sh}(\delta l_1) + Z_{BX1} \operatorname{ch}(\delta l_1)\right|^2}$$

or

$$P_1 = \frac{k^2 \cdot const}{\left|k^2 Z_0 \operatorname{sh}(\delta l_1) + Z_{BX1} \operatorname{ch}(\delta l_1)\right|^2}; \qquad (20.6)$$

$$\eta = \frac{k^2 \cdot const}{ak^4 + bk^2 + c}; \qquad (20.7)$$

$$a = \left|Z_0\right|^2 \operatorname{Re}\left(Z_0 \operatorname{sh}(\delta l_1)\operatorname{ch}(\delta^* l_1)\right);\ c = \left|Z_{BX1}\right|^2 \operatorname{Re}\left(Z_0 \operatorname{sh}(\delta^* l_1)\operatorname{ch}(\delta l_1)\right);$$

$$b = \operatorname{Re}\left(Z_{BX1}\right) \cdot \left|Z_0 \operatorname{ch}(\delta l_1)\right|^2 + \operatorname{Re}\left(Z_0^2 Z_{BX1}^*\right) \cdot \left|\operatorname{sh}(\delta l_1)\right|^2,$$

where the expressions independent on the parameter k are denoted by *const*.

From the formulas (20.6) and (20.7) it results that the dependence of the transmission power and of the efficiency on the parameter k is enough trivial. So, by equating to zero of the first derivative of P_1 and of η by k, we obtain the equations for determination of the optimal values of k:

$$\max_k P_1 \text{ is reached when } k_K = -\sqrt{\left|\frac{Z_{BX1} \operatorname{ch}(\delta l_1)}{Z_0 \operatorname{sh}(\delta l_1)}\right|}; \qquad (20.8)$$

$$\max_k \eta \text{ is reached when } k_\eta = -\sqrt[4]{\frac{\left|Z_{BX1}\right|^2 \operatorname{Re}\left(Z_0 \operatorname{sh}(\delta^* l_1)\operatorname{ch}(\delta l_1)\right)}{\left|Z_0\right|^2 \operatorname{Re}\left(Z_0 \operatorname{sh}(\delta l_1)\operatorname{ch}(\delta^* l_1)\right)}}. \qquad (20.9)$$

In the table 20.1 we represent the dependence of the coefficient k (from the (20.8), i.e. when the maximal values of the transmission power are reached) on the l_1 for the following parameters of the undistorting line: $R = G = 0.48$, $l = 1$. As it follows from the represented data, the transformer connection to the points $\lambda/8$, $3\lambda/8$, $5\lambda/8$ gives the maximal value of P_1

when k = -1, i.e. the transformer must act in no-operation mode (in idling). This means that the transformer connection to the indicated points is of no use.

Table 20.1. Coefficient k_K depending on l_1 for undistorting line when $R = G = 0.48$.

l_1	1/32	1/16	3/32	1/8	5/32	3/16	7/32	1/4
k_K	-2.2390	-1.5518	-1.2223	-1.0000	-0.8195	-0.6508	-0.4740	-0.3456
$P_1(k_K)/P_1(-1)$	2.4898	1.3796	1.0744	1.0000	1.0692	1.3144	1.9014	2.6232
$\eta(k_K)/\eta(-1)$	0.9553	0.9773	0.9933	1.0000	0.9897	0.9440	0.8134	0.6177

l_1	9/32	5/16	11/32	3/8	13/32	7/16	15/32	1/2
k_K	-0.4898	-0.6628	-0.8269	-1.0000	-1.2041	-1.4723	-1.8342	-2.0607
$P_1(k_K)/P_1(-1)$	1.7618	1.2564	1.0545	1.0000	1.0500	1.2066	1.4687	1.6205
$\eta(k_K)/\eta(-1)$	0.7992	0.9253	0.9826	1.0000	0.9814	0.9180	0.8023	0.7231

l_1	17/32	9/16	19/32	5/8	21/32	11/16	23/32	3/4
k_K	-1.7711	-1.4314	-1.1856	-1.1856	-0.8484	-0.7197	-0.6214	-0.5875
$P_1(k_K)/P_1(-1)$	1.4017	1.1652	1.0379	1.0000	1.0344	1.1313	1.2582	1.3105
$\eta(k_K)/\eta(-1)$	0.8112	0.9186	0.9805	1.0000	0.9808	0.9241	0.8456	0.8085

l_1	25/32	13/16	27/32	7/8	29/32	15/16	31/32
k_K	-0.6394	-0.7415	-0.8640	-1.0000	-1.1502	-1.3103	-1.4498
$P_1(k_K)/P_1(-1)$	1.2242	1.1039	1.0253	1.0000	1.0228	1.0821	1.1487
$\eta(k_K)/\eta(-1)$	0.8576	0.9322	0.9830	1.0000	0.9840	0.9412	0.8913

In the table 20.2 we represent the dependence of the coefficient k from the (20.8), i.e. when the maximal values of the transmission power are reached) on the l_1 for the following parameters of the line: R = 0.48, G = R/5, l = 1. As it follows from the represented data, there are some points in this line too where the transformer connection is of no use, because k = -1 again. However, these points are located at the left of the values $\lambda/8$, $3\lambda/8$,

$5\lambda/8$. At the same time, the transformer location at these points and in the zones at the right of them results in simultaneous increase of the transmission power and of the efficiency.

Table 20.2. Coefficient k_K depending on l_1 for line with losses $R = 0.48$, $G = R/5$

l_1	1/32	1/16	3/32	1/8	5/32	3/16	7/32	1/4
k_K	-2.2323	-1.5425	-1.212	-0.9905	-0.8108	-0.6416	-0.4545	-0.2682
$P_1(k_K)/P_1(-1)$	2.4979	1.3762	1.0705	1.0002	1.0819	1.3697	2.1749	3.9948
$\eta(k_K)/\eta(-1)$	0.9470	0.9664	0.9855	1.0006	1.0044	0.9802	0.8740	0.5715

l_1	9/32	5/16	11/32	3/8	13/32	7/16	15/32	1/2
k_K	-0.4661	-0.6565	-0.8299	-1.0118	-1.2296	-1.5351	-2.0549	-2.6436
$P_1(k_K)/P_1(-1)$	2.0022	1.2978	1.0577	1.0002	1.0700	1.2949	1.7852	2.2829
$\eta(k_K)/\eta(-1)$	0.8200	0.9294	0.9789	1.0006	0.9948	0.9449	0.8093	0.6401

l_1	17/32	9/16	19/32	5/8	21/32	11/16	23/32	3/4
k_K	-1.9848	-1.486	-1.1926	-0.9861	-0.8188	-0.6683	-0.5298	-0.4614
$P_1(k_K)/P_1(-1)$	1.6672	1.2302	1.0461	1.0003	1.0588	1.2311	1.5326	1.7277
$\eta(k_K)/\eta(-1)$	0.7868	0.9122	0.9758	1.0007	0.9890	0.9288	0.8046	0.7034

l_1	25/32	13/16	27/32	7/8	29/32	15/16	31/32
k_K	-0.5497	-0.6954	-0.8500	-1.0166	-1.2096	-1.4497	-1.7375
$P_1(k_K)/P_1(-1)$	1.4516	1.1746	1.0358	1.0004	1.0489	1.1793	1.3698
$\eta(k_K)/\eta(-1)$	0.7966	0.9096	0.9756	1.0007	0.9862	0.9260	0.8241

In the table 20.3 we represent the dependence of the coefficient k (from the (20.9), i.e. when the maximal value of the efficiency is reached) on the l_1 for the following parameters of the line: $R = 0.48$, $G = R/5$, $l = 1$.

Table 20.3. Coefficient k_η depending on l_1 for line with losses $R = 0.48$, $G = R/5$.

l_1	1/32	1/16	3/32	1/8	5/32	3/16	7/32	1/4
k_η	-0.6768	-0.7029	-0.7424	-0.7905	-0.8435	-0.8982	-0.9517	-1.0006
$\eta(k_\eta)/\eta(-1)$	1.0043	1.0073	1.0080	1.0069	1.0046	1.0022	1.0005	1.0000
$P_1(k_\eta)/P_1(-1)$	0.4785	0.5681	0.7188	0.9121	1.0789	1.1351	1.0836	0.9990

l_1	9/32	5/16	11/32	3/8	13/32	7/16	15/32	1/2
k_η	-1.0412	-1.0699	-1.0844	-1.0846	-1.0722	-1.0511	-1.0254	-0.9994
$\eta(k_\eta)/\eta(-1)$	1.0004	1.0014	1.0021	1.0023	1.0018	1.0010	1.0003	1.0000
$P_1(k_\eta)/P_1(-1)$	0.9384	0.9209	0.9441	0.9923	1.0383	1.0551	1.0360	0.9990

l_1	17/32	9/16	19/32	5/8	21/32	11/16	23/32	3/4
k_η	-0.9764	-0.9592	-0.9494	-0.9476	-0.9534	-0.9655	-0.9822	-1.0007
$\eta(k_\eta)/\eta(-1)$	1.0003	1.0008	1.0013	1.0015	1.0012	1.0007	1.0002	1.0000
$P_1(k_\eta)/P_1(-1)$	0.9681	0.9578	0.9706	0.9979	1.0241	1.0337	1.0223	0.9990

l_1	25/32	13/16	27/32	7/8	29/32	15/16	31/32
k_η	-1.0186	-1.0330	-1.0419	-1.0442	-1.0396	-1.0293	-1.0150
$\eta(k_\eta)/\eta(-1)$	1.0002	1.0006	1.0010	1.0012	1.0010	1.0005	1.0001
$P_1(k_\eta)/P_1(-1)$	0.9786	0.9716	0.9804	0.9994	1.0175	1.0242	1.0160

21. Transmission power increase by means of transformers

Let's try to determine where and with what gear ratio the transformer must be connected to the line in such a way as to increase to the maximum the transmission power.

In the previous paragraph we have obtained the formula for the transformer ratio k, which gives the maximal value of the transmission power P_1. The transmission power P_1 can be represented in the form

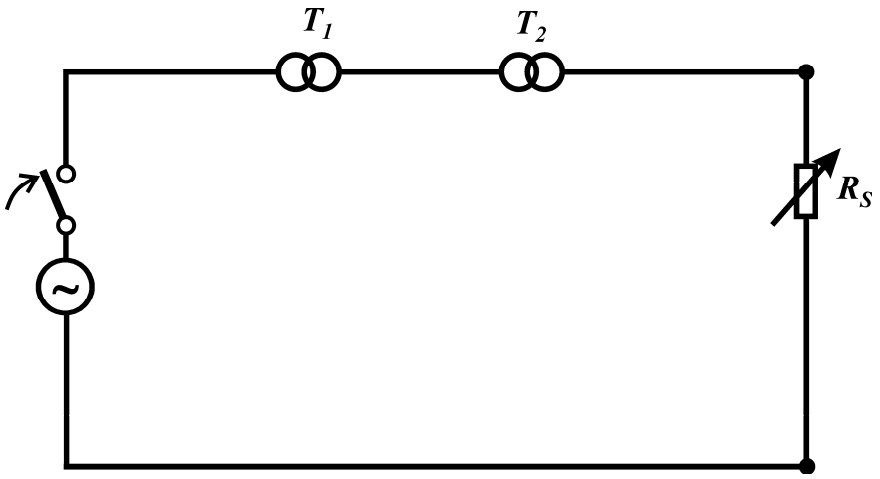

Fig. 21.1. Transformer connection to the line closed to the active resistance $R_S(t)$.

$$P_1 = \frac{u_0^2 k^2 \operatorname{Re}(Z_S)\left|Z_{BX1}\right|^2}{2\left|Z_S \operatorname{ch}(\delta l_2) + Z_0 \operatorname{sh}(\delta l_2)\right|^2 \left|k^2 Z_0 \operatorname{sh}(\delta l_1) + Z_{BX1} \operatorname{ch}(\delta l_1)\right|^2} =$$

$$= \frac{u_0^2 k^2 \operatorname{Re}(Z_S)\left|Z_0\right|^2}{2\left|Z_S \operatorname{sh}(\delta l_2) + Z_0 \operatorname{ch}(\delta l_2)\right|^2 \left|k^2 Z_0 \operatorname{sh}(\delta l_1) + Z_{BX1} \operatorname{ch}(\delta l_1)\right|^2},$$

where

$$Z_{BX} = Z_0 \frac{k^2 Z_0 \operatorname{sh}(\delta l_1) + Z_{BX1} \operatorname{ch}(\delta l_1)}{k^2 Z_0 \operatorname{ch}(\delta l_1) + Z_{BX1} \operatorname{sh}(\delta l_1)}, \qquad (21.1)$$

$$Z_{BX1} = Z_0 \frac{Z_0 \operatorname{sh}(\delta l_2) + Z_S \operatorname{ch}(\delta l_2)}{Z_0 \operatorname{ch}(\delta l_2) + Z_S \operatorname{sh}(\delta l_2)}, \; l_2 = l - l_1. \qquad (21.2)$$

From the formula (20.8) we obtain that the maximal value of P_1 is reached when the transformer ratio k gets the values

$$k = k_K(l_1) = -\sqrt{\left|\frac{Z_{BX1}\mathrm{ch}(\delta l_1)}{Z_0\mathrm{sh}(\delta l_1)}\right|}. \qquad (21.3)$$

After the substitution of the value k from (21.3) in the formula for P_1 and some simplifications we obtain the dependence of the maximal P_1 only on the l_1:

$$P_1 = 2u_0^2\,\mathrm{Re}(Z_S)\left[\left|\mathrm{sh}(2\delta l_1)\right|\cdot\left|(Z_S^2+Z_0^2)\,\mathrm{sh}(2\delta(l-l_1))+\right.\right.$$

$$\left.\left.+2Z_0Z_S\,\mathrm{ch}(2\delta(l-l_1))\right|\cdot\left|\frac{Z_0\mathrm{sh}(\delta l_1)}{|Z_0\mathrm{sh}(\delta l_1)|}+\frac{Z_{BX1}\mathrm{ch}(\delta l_1)}{|Z_{BX1}\mathrm{ch}(\delta l_1)|}\right|^2\right]^{-1}. \qquad (21.4)$$

In case of ideal line when $R = G = 0$ and $R_S = Z_B = 1$ we get

$$\delta = j\omega/a,\ \ \mathrm{ch}(\delta l_1) = \cos(\omega l_1/a),\ \ \mathrm{sh}(\delta l_1) = j\sin(\omega l_1/a),$$

$$Z_0 = Z_{BX1} = Z_S = 1.$$

Then the formulas (21.3), (21.4) can be essentially simplified and they obtain the following form

$$k = k_K(l_1) = -\sqrt{\left|\frac{\cos(\omega l_1/a)}{\sin(\omega l_1/a)}\right|} = -\sqrt{\left|\mathrm{ctg}(\omega l_1/a)\right|},$$

$$P_1(l_1) = \frac{u_0^2}{2\left|\sin(2l_1/a)\right|}.$$

As it follows from these formulas, if the frequency is equal $\omega = 2\pi$ and $a = 1$, then the transformer ratio k_K tends to zero and the power P_1 tends to infinity when the value l_1 tends to the $1/4;\ 3/4;\ 5/4\ldots$.

In case of distorting line to determine the value l_1, that gives the maximal value for P_1, we are to equate with zero the first derivative of function

P_1 by the l_1. As a result we obtain some complicated transcendental equation that can not be solved analytically. So it may be solved numerically. In the fig. 21.2 we represent the diagrams for values l_1 and k (under which the maximal value of P_1 is reached) depending on the line length l with the following parameters values: $R_S = Z_B = 1$, $R = 0.48$, $G = R/5$. The diagram for power P_1 depending on l_1, when $l = 1$ and $k = k_K(l_1)$ form (21.3) is represented in the fig. 21.2,*a*. So, we see that the maximum is reached when $l_1 = 1/4$.

Further in the fig. 21.2,*b,c* we have the coefficient k and the transformer location l_1 (under which the maximal value of P_1 is reached) depending on the line length l. One can see that for the lines with $l \geq 1/4$ the parameters k and l_1 possess the constant values independent on l. These values are $l_1 = 1/4$, $k \approx -0.268$. The transmission power in this case is approximately 4 times greater then the corresponding one in the line without transformer (see fig. 21.2,*d*).

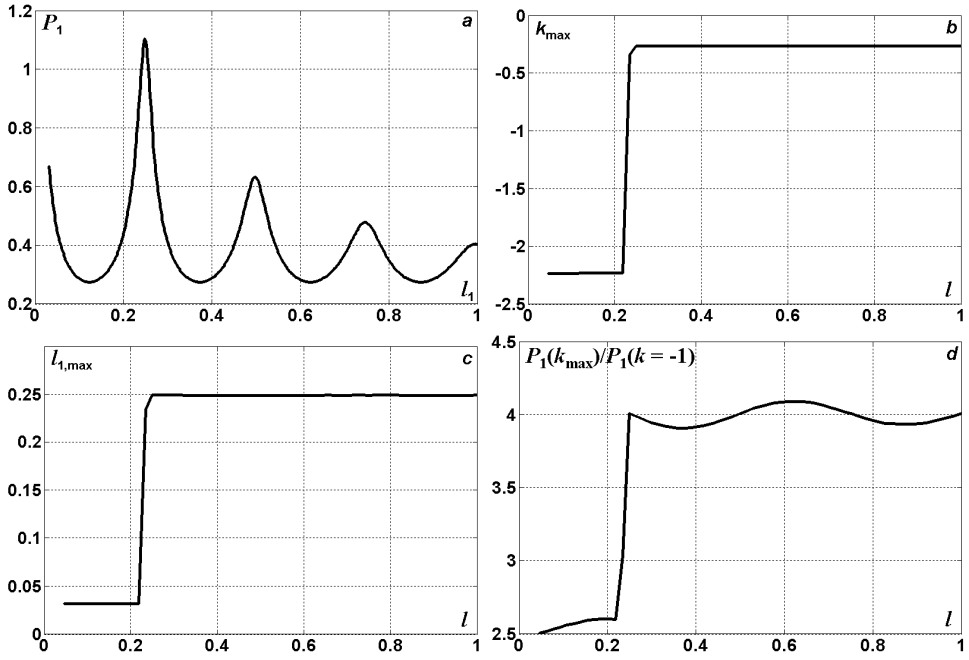

Fig. 21.2. The explanations are in the text.

In the fig. 21.3 there are represented the same diagrams as in the fig. 21.2, but for line with losses $R = 0.27$, $G = R/5$. In this case we observe the power increase in 6.8 times under the value $k \approx$ -0.2001.

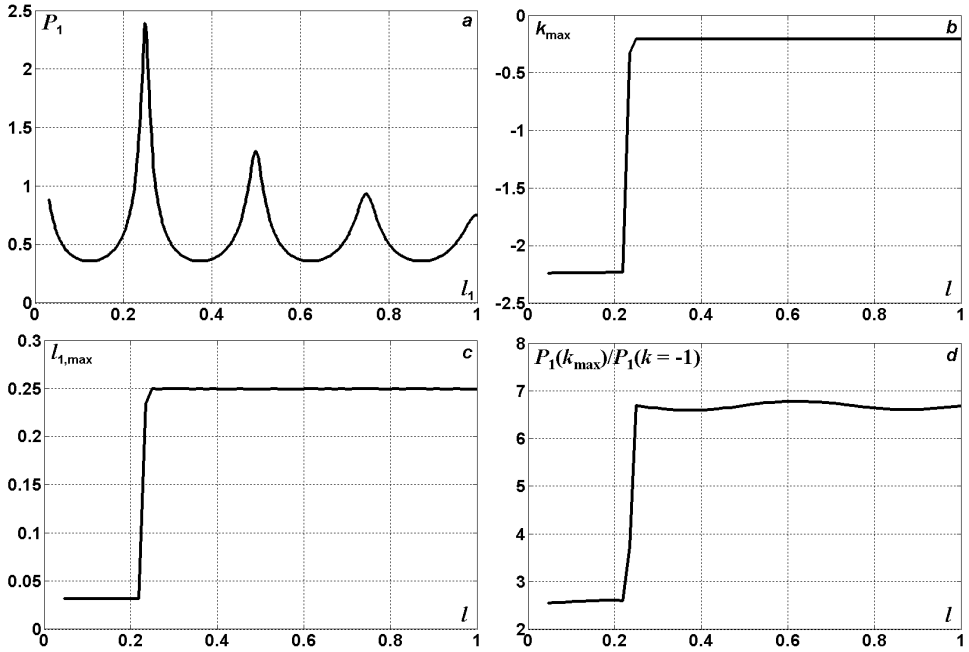

Fig. 21.3. The explanations are in the text.

Now let's consider the ideal half-wave line (l =1/2, R = G = 0), closed on the wave resistance R_S =1. If the transformer with gear ratio k_1 is connected to the middle point of the line (l_1 = 1/4), then the active transmission power will increase in $(1/k_1)^2$ times. Reasoning from this dependence, the transmission power can be increased unrestrictedly by unrestrictedly decreasing of the k_1. Let's remind that the same dependence occurs under the voltage increase at the input of the ideal homogeneous line with arbitrary length.

The dynamics of the instantaneous power values of the generator and of the load (curves 1, 2) are represented in the fig. 21.4 when k_1= –1/2; R = G = 0 (*a*); R = 0.48, G = R/5 (*b*). The transformer is connected at the time moment t = 3 and it is disconnected at t = 9. This time interval is sufficient for establishing stage attainment and for power increase in 4 times in the absence of losses. After the transformer sudden outage one can observe the power inrushes at the level of 6.2. In such a way we obtain some paradoxi-

cal result for the half-wave line. If it is required to increase the transmission power in k^2 times, then instead of the input voltage amplitude increasing in k times, it is necessary to decrease in k times the voltage in the middle of the line by means of step-down transformer connected there.

Taking into account the losses in the line (see fig. 21.4, *b*) we obtain the increase of the transmission power in nearly 3 times, but the power inrushes become twice smaller in comparison with previous variant.

Let's consider now the quarter-wave line $l = 1/4$. It is known that the transformer connection to the middle point of such line is of no sense. Then let's consider the connection of two transformers: to the point $l_1 = 1/16$ – the step-up transformer with the gear ratio $k_1 = -1.5$, and to the point $l_2 = 3/16$ – the step-down transformer with the gear ratio $k_2 = 1/k_1$. The results of calculations are represented in the fig. 21.5 for ideal line with losses. The first transformer connection results in power increase only in 1.45 times, but the second transformer connection leads to the 3.15 times increasing. The power inrushes are insignificant here and come only to 3.5. It is interesting that after the step-down transformer connection not only the transmission power increases, but also the source power factor improves (judging by negative values of the function $P_0(t)$).

The numerical information for the line with length $l = 1/8$ with connected to its middle point step-up transformer ($k_1 = -1.5$) is represented in the form of time diagrams in the fig. 21.6. The power in this case can be increased only on 30…40%. The not great generator power inrush may be observed here. The transformer connection makes the generator instantaneous power values to be negative, that serves as an indicator of the quasisteady state process initiation – the process of the electromagnetic power bilateral exchange between the receiver and the source.

It would seem that the considered problems are of only of abstract nature and the obtained results are purely of theoretical importance. However, it is not quite so. One may take note of [53], where the idea of global planetary electroenergetics system was formulated and grounded for the first time. Its practical implementation promises a great economical profit for the whole mankind. But the real implementation would require the high study of the technical realizability of the power transmission lines, the construction of the intercontinental electrical links, the elaboration of the fundamentally new approaches to electrical power transmission on great distances. The application in the engineering practice of the superconducting transmission lines also stimulates the high-performance technology and equipment elaboration, that is impossible undoubtedly without fundamental theoretical investigations in the electroenergetics.

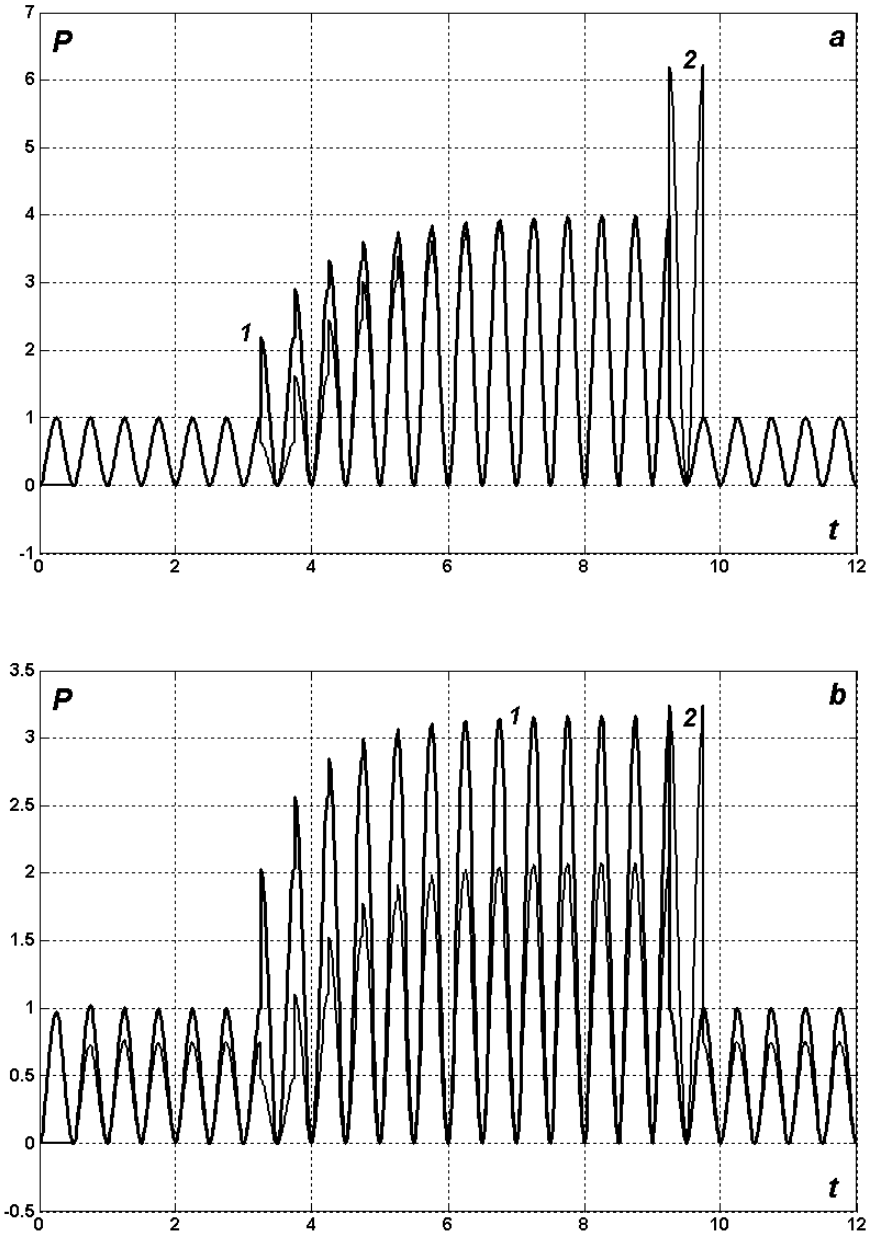

Fig. 21.4. Generator and load powers (curves 1;2) when l =1/2; l_1 = 1/4; k_1= –1/2; $R = G = 0$ (***a***); R = 0.48, $G = R/5$ (***b***).

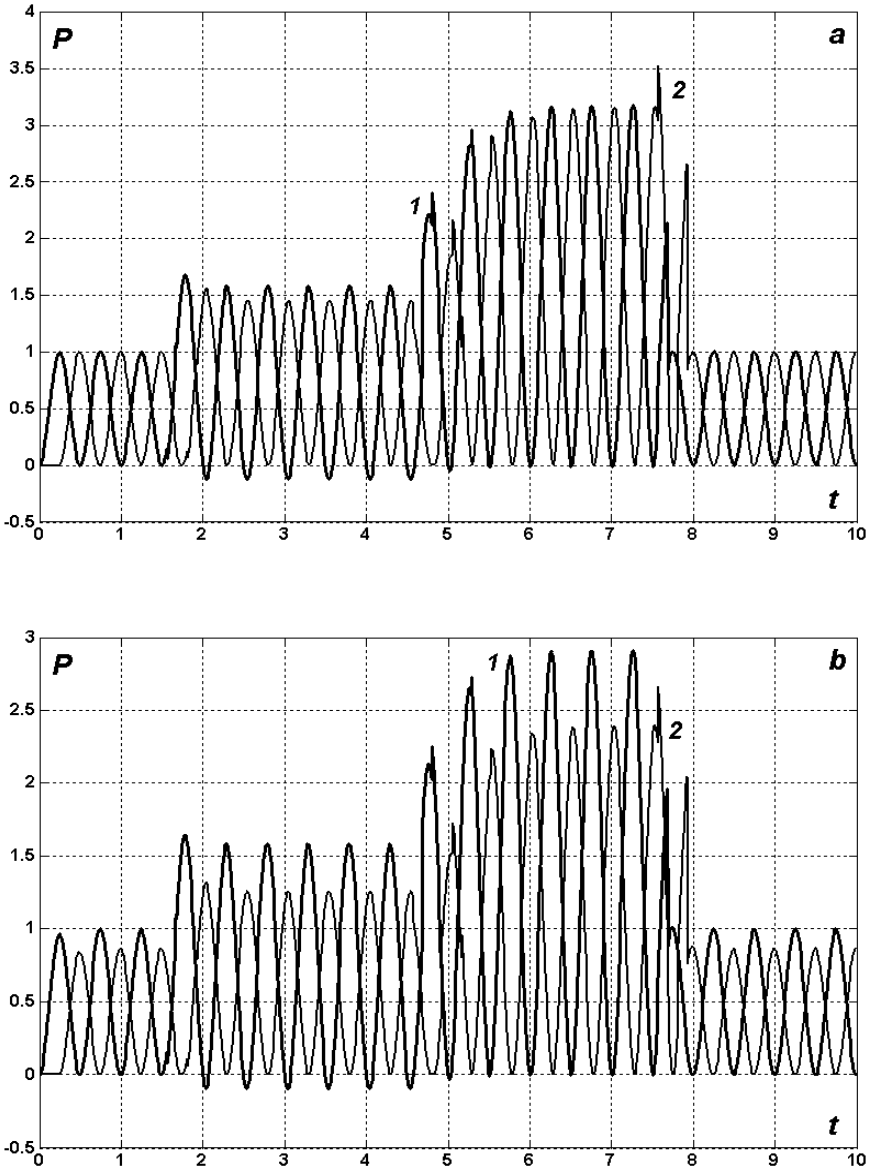

Fig. 21.5. Generator and load powers (curves 1;2) when l = 1/4; l_1 = 1/16; l_2 = 3/16; k_1 = **–** 1.5; $k_2 = 1/k_1$; $R = G = 0$ (***a***); R = 0.48, $G = R/5$ (***b***).

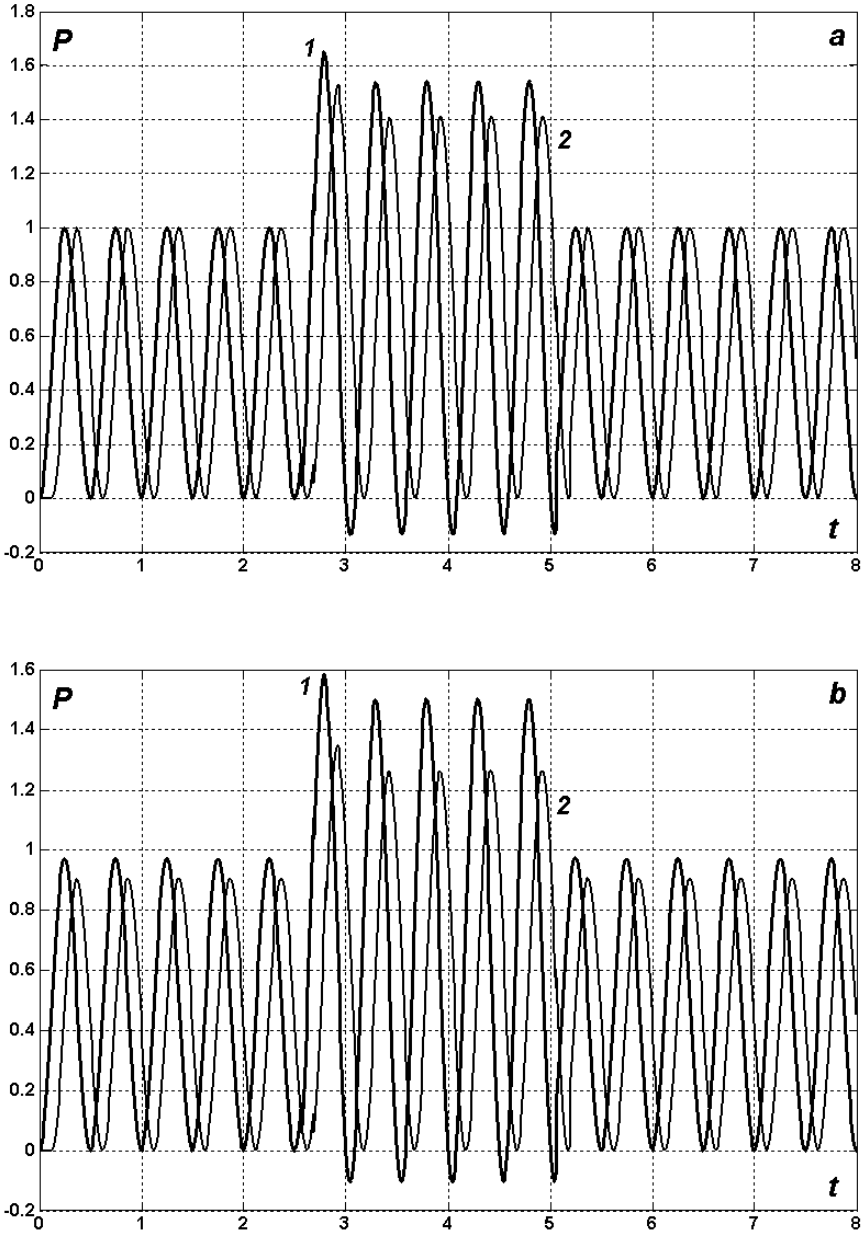

Fig. 21.6. Generator and load powers (curves 1;2) when l =1/8; l_1 = 1/16; k_1= = – 1.5; $R = G = 0$ (***a***); $R = 0.48$, $G = R/5$ (***b***).

CHAPTER IV

PIECEWISE HOMOGENEOUS AND THREE-PHASE TRANSMISSION LINES

The mathematical models that describe the processes of power transmission in nonhomogeneous and polyphase circuits are not applied practically in the modern electrotechnology and electroenergetics [14, 37, 105, 110]. Even for steady-state regimes such models are very uncommon.

In case of multiwire line, when L, C are symmetrical square matrixes of the self and mutual inductances and capacitances, the wave velocities of the potential and of the current are determined as the eigenvalues of the matrix

$$A = \begin{Vmatrix} 0 & L^{-1} \\ C^{-1} & 0 \end{Vmatrix}.$$

Here in our opinion it is to mention the following important aspect. The primary parameters used quite often in multiwire line calculations are chosen in such a way, that the electromagnetic emanation velocity occurs to be greater then the velocity of light in vacuum, that can not be accepted as correct. This is the reason why the single-velocity theory of potential and current wave propagation is applied. In this case the matrix of capacitances C and one velocity of electromagnetic wave propagation a are used as a primary initial parameters. The matrix of inductances is determined then as $L = C^{-1} / a^2$.

22. Exact solutions for composite undistorting lines by method of characteristics

Let's consider the piecewise homogeneous electrical line with *RLC*–circuit at the receiving end

$$u = R_S i + L_S \frac{di}{dt} + \frac{1}{C_S}\int_0^t i d\tau \text{ when } x = l, t > 0 . \qquad (22.1)$$

We suppose that the unknown voltages and currents are continuous at the conjunction points

$$u^- = u^+ = u ;\ i^- = i^+ = i \text{ when } x = x_n, t > 0 , \qquad (22.2)$$

and at the input of the line the voltage is given as an arbitrary function of time

$$u = u_0(t) \text{ when } x = 0, t > 0 . \qquad (22.3)$$

At first let's construct the exact solution for undistorting line that consists from two joined sections with parameters: Z_{B1}, a_1, γ_1, Z_{B2}, a_2, γ_2 (see fig. 22.1). For the sake of simplicity let's assume that $a_2 = a_1 = 1$; $l = 2x_n = 2$.

Using the relations on characteristics with negative slope $dx/dt = -a$, zero initial data in the unperturbed domains I and II and boundary conditions (22.2), we obtain the system of two equations with respect to two unknown functions

$$u - Z_{B1} i = 0; u = u_0 ,$$

from which the following solution results

$$i_3 = u_0 / Z_{B1}; u_3 = u_0 , \text{ when } x = 0, 0 < t \le 2\Delta ,$$

where $\Delta = x_n / a_1$ is the time of electromagnetic wave run along the first homogeneous section of the composite line. Evidently, that at the time interval $0 < t < 2\Delta$, $x = l$ we get the trivial solution reasoning from form the zero initial state of the uncharged line

$$u_1 = i_1 = u_2 = i_2 = 0 .$$

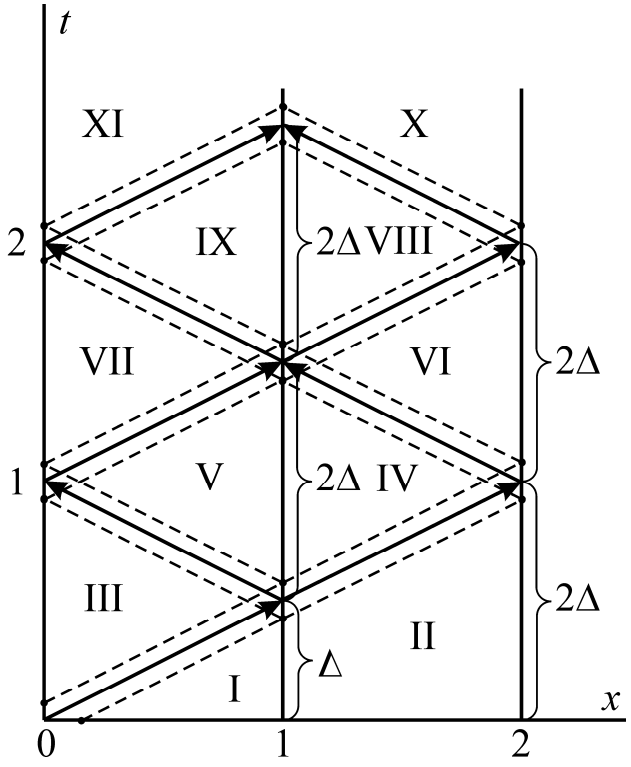

Fig. 22.1. Computational domains and wave-front configurations in piecewise homogeneous line with *RLC*–circuit at the receiving end.

Using further the relations on characteristics with positive and negative slopes and the continuity condition for solution (22.2), we obtain the following system for determination of *u* and *i* at the interior contact boundary:

$$u_4 + Z_{B1} i_4 = \left[u_3(t-\Delta) + Z_{B1} i_3(t-\Delta)\right] e^{-\gamma_1 \Delta} \equiv A_3(t);$$

$$u_4 - Z_{B2} i_4 = \left[u_2(t-\Delta) - Z_{B2} i_2(t-\Delta)\right] e^{-\gamma_2 \Delta} \equiv A_2(t) = 0$$

when $x = x_n$, $\Delta < t < 3\Delta$.

The solution of the system can be easily determined

$$i_4 = \frac{A_3(t) - A_2(t)}{Z_{B1} + Z_{B2}} = \frac{A_3(t)}{Z_{B1} + Z_{B2}};$$

$$u_4 = A_2(t) + Z_{B2} i_4 = \frac{A_3(t) Z_{B2} + A_2(t) Z_{B1}}{Z_{B1} + Z_{B2}} = Z_{B2} i_4 \,.$$

The relations on characteristics $dx/dt = a_2$ and the boundary condition at the end point of the line (22.1) form a new system of equations for voltage and current determination

$$u_6 + Z_{B2} i_6 = \left[u_4(t-\Delta) + Z_{B2} i_4(t-\Delta)\right] e^{-\gamma_2 \Delta} \equiv A_4(t)\,;$$

$$u_6' = R_S i_6' + L_S i_6'' + \frac{i_6}{C_S}$$

when $x = l,\ 2\Delta < t < 4\Delta$.

Now from the last relation we eliminate the function u_6. In this way we obtain the ordinary differential equation with constant coefficients and non-homogeneous right-hand member. The equation is with respect to i_6:

$$L_S i_6'' + (R_S + Z_{B2}) i_6' + \frac{i_6}{C_S} = A_4'(t)\,.$$

This equation must be integrated under the following initial conditions at the point $x = l,\ t = 2\Delta$:

$$i_6(2\Delta + 0) = i_6(2\Delta - 0) = A_4(2\Delta - 0)/Z_{B2} = i_0\,;$$

$$i_6'(2\Delta + 0) = \frac{1}{L_S}\left[A_4(2\Delta + 0) - (R_S + Z_{B2}) i(2\Delta) - \frac{1}{C_S}\int_0^{2\Delta} i(\tau)\,d\tau\right] =$$

$$= A_4(2\Delta + 0)/L_S = i_0^1\,.$$

To solve this Cauchy problem we apply the standard procedure in order to find unknown functions u_6 and i_6 at the time interval $2\Delta < t < 4\Delta,\ x = l$. In case when the characteristic equation

$$L_S k^2 + (R_S + Z_{B2}) k + \frac{1}{C_S} = 0$$

possesses the multiple roots

$$k_{1,2} = -\frac{R_S + Z_{B2}}{2L_S} = -k;\ \left(R_S + Z_{B2}\right)^2 = \frac{4L_S}{C_S},$$

the solution of the differential Cauchy problem ($t_0 = 2\Delta$) is the following

$$i_6(t) = \left[(i_0^1 + ki_0)(t - t_0) + i_0\right]e^{k(t_0 - t)} + \frac{1}{L_S}\int_{t_0}^{t}\int_{t_0}^{z} A_4'(\tau)e^{k(\tau - t)}d\tau dz.$$

Applying the proposed algorithm required number of times one can obtain the solution in the arbitrary domain of its existence.

Now let's cite some exact solutions in the explicit form for the following parameters values:

$$Z_{B1} = 10;\ Z_{B2} = R_S = L_S = C_S = 1;\ \ a_1 = a_2 = 1;\ \gamma_1 = \gamma_2 = \gamma > 0.$$

The direct voltage of the feeding generator: $u_0 = 1$

22.1. Current at the sending end of the line $x = 0$

$$i_1^0 = \frac{1}{10} \text{ when } x = 0,\ 0 < t \le 2\Delta$$

$$i_2^0 = i_1^0 + \frac{9}{55}e^{-2\gamma\Delta} \text{ when } x = 0,\ 2\Delta < t \le 4\Delta$$

$$i_3^0 = i_2^0 + \frac{41}{605}e^{-4\gamma\Delta} + \frac{16t_4}{121}e^{-4\gamma\Delta - t_4}$$

when $x = 0,\ 4\Delta < t \le 6\Delta;\ t_4 = t - 4\Delta$

$$i_4^0 = i_3^0 - \frac{351}{6655}e^{-6\gamma\Delta} + \frac{48t_6}{1331}e^{-6\gamma\Delta - t_6}(t_6^2 - 3t_6 + 12)$$

when $x = 0,\ 6\Delta < t \le 8\Delta;\ t_6 = t - 6\Delta$

$$i_5^0 = i_4^0 - \frac{11279}{73205}e^{-8\gamma\Delta} +$$

$$+\frac{8t_8}{219615}e^{-8\gamma\Delta-t_8}(t_8^4-810t_8^3+5270t_8^2-10950t_8+21900)$$

when $x=0,\ 8\Delta<t\le 10\Delta;\ t_8=t-8\Delta$

$$i_6^0=i_5^0-\frac{160551}{805255}e^{-10\gamma\Delta}+\frac{24t_{10}}{5636785}e^{-10\gamma\Delta-t_{10}}(27t_{10}^6-567t_{10}^5+$$

$$+6244t_{10}^4-34090t_{10}^3+116690t_{10}^2-179550t_{10}+239400)$$

when $x=0,\ 10\Delta<t\le 12\Delta;\ t_{10}=t-10\Delta$

$$i_7^0=i_6^0-\frac{1525159}{8857805}e^{-12\gamma\Delta}+\frac{2t_{12}}{186013905}e^{-12\gamma\Delta-t_{12}}(243t_{12}^8-$$

$$-8748t_{12}^7+153252t_{12}^6-1503684t_{12}^5+9087316t_{12}^4-32835040t_{12}^3+$$

$$+72933560t_{12}^2-82618200t_{12}+82618200)$$

when $x=0,\ 12\Delta<t\le 14\Delta;\ t_{12}=t-12\Delta$

$$i_8^0=i_7^0-\frac{8026191}{97435855}e^{-14\gamma\Delta}+\frac{6t_{14}}{37512804175}e^{-14\gamma\Delta-t_{14}}(243t_{14}^{10}-$$

$$-13365t_{14}^9+347820t_{14}^8-5304420t_{14}^7+51340960t_{14}^6-$$

$$-32140416t_{14}^5+1283275840t_{14}^4-3117637600t_{14}^3+$$

$$+4149714800t_{12}^2-2479554000t_{14}+1983643200)$$

when $x=0,\ 14\Delta<t\le 16\Delta;\ t_{14}=t-14\Delta$

22.2. Voltage and current at the end of the line $x=l$

$u_1^l=i_1^l=0$; when $x=0,\ 0<t\le 2\Delta$

$$u_2^l=\frac{4}{11}e^{-2\gamma\Delta}-\frac{4t_2}{11}e^{-2\gamma\Delta-t_2};\ i_2^l=\frac{4t_2}{11}e^{-2\gamma\Delta-t_2}$$

when $x=0,\ 2\Delta<t\le 4\Delta;\ t_2=t-2\Delta$

$$u_3^l = u_2^l + \frac{72}{121}e^{-4\gamma\Delta} - \frac{12t_4}{121}e^{-4\gamma\Delta - t_4}(t_4^2 - 3t_4 + 12);$$

$$i_3^l = i_2^l + \frac{12t_4}{121}e^{-4\gamma\Delta - t_4}(t_4^2 - 3t_4 + 6)$$

$$\text{when } x = 0,\ 4\Delta < t \le 6\Delta;\ t_4 = t - 4\Delta$$

$$u_4^l = u_3^l + \frac{812}{1331}e^{-6\gamma\Delta} - \frac{2t_6}{19965}e^{-6\gamma\Delta - t_6}(81t_6^4 - 810t_6^3 +$$

$$+ 5270t_6^2 - 10950t_6 + 18270);$$

$$i_4^l = i_3^l + \frac{2t_6}{19965}e^{-6\gamma\Delta - t_6}(81t_6^4 - 810t_6^3 +$$

$$+ 3650t_6^2 - 6090t_6 + 6090);$$

$$\text{when } x = 0,\ 6\Delta < t \le 8\Delta;\ t_6 = t - 6\Delta$$

$$u_5^l = u_4^l + \frac{5904}{14641}e^{-8\gamma\Delta} - \frac{6t_8}{512435}e^{-8\gamma\Delta - t_8}(27t_8^6 - 567t_8^5 +$$

$$+ 6244t_8^4 - 34090t_8^3 + 108220t_8^2 - 154140t_8 + 137760);$$

$$i_5^l = i_4^l + \frac{6t_8}{512435}e^{-8\gamma\Delta - t_8}(27t_8^6 - 567t_8^5 +$$

$$+ 5110t_8^4 - 22750t_8^3 + 51380t_8^2 - 51660t_8 + 34440);$$

$$\text{when } x = 0,\ 8\Delta < t \le 10\Delta;\ t_8 = t - 8\Delta$$

$$u_6^0 = u_5^0 - \frac{8020}{161051}e^{-10\gamma\Delta} + \frac{t_{10}}{33820710}e^{-10\gamma\Delta - t_{10}}(243t_{10}^8 - 8748t_{10}^7 +$$

$$+ 15325t_{10}^6 - 1503684t_{10}^5 + 8812888t_{10}^4 - 30090760t_{10}^3 +$$

$$+ 55078800t_{10}^2 - 45519600t_{10} + 8421000);$$

$$i_6^0 = i_5^0 + \frac{t_{10}}{33820710} e^{-10\gamma\Delta - t_{10}} (243t_{10}^8 - 8748t_{10}^7 +$$

$$+135756t_{10}^6 - 1136268t_{10}^5 + 5315632t_{10}^4 - 13489000t_{10}^3 +$$

$$+15173200t_{10}^2 - 3368400t_{10} + 1684200)$$

$$\text{when } x = 0, 10\Delta < t \le 12\Delta;\ t_{10} = t - 10\Delta$$

$$u_7^0 = u_6^0 - \frac{570024}{1771561} e^{-12\gamma\Delta} + \frac{3t_{12}}{682050985} e^{-12\gamma\Delta - t_{12}} (243t_{12}^{10} -$$

$$-13365t_{12}^9 + 347820t_{12}^8 - 5304420t_{12}^7 + 50622220t_{12}^6 -$$

$$-306310620t_{12}^5 + 1117060560t_{12}^4 - 2210161800t_{12}^3 +$$

$$+1043427000t_{12}^2 + 2300067000t_{12} - 4389184800);$$

$$i_7^0 = i_6^0 + \frac{3t_{12}}{682050985} e^{-12\gamma\Delta - t_{12}} (243t_{12}^{10} -$$

$$-13365t_{12}^9 + 321090t_{12}^8 - 4342140t_{12}^7 + 35201980t_{12}^6 -$$
$$-171092460t_{12}^5 + 449886360t_{12}^4 - 413259000t_{12}^3 +$$

$$-766689000t_{12}^2 + 1828827000t_{12} - 731530800)$$

$$\text{when } x = 0, 12\Delta < t \le 14\Delta;\ t_{12} = t - 12\Delta$$

$$u_8^0 = u_7^0 - \frac{11230852}{19487171} e^{-14\gamma\Delta} +$$

$$+\frac{t_{14}}{17555992353900} e^{-14\gamma\Delta - t_{14}} (19683t_{14}^{12} -$$

$$-1535274t_{14}^{11} + 56084886t_{14}^{10} - 1226987190t_{14}^9 + 17381642850t_{14}^8 -$$

$$-163795666320t_{14}^7+1008265343800t_{14}^6-3807228505080t_{14}^5+$$

$$+6678242811240t_{12}^4+5051548101600t_{12}^3-51547214518800t_{12}^2+$$

$$+84794542232400t_{14}-70825121967600);$$

$$i_8^0=i_7^0+\frac{t_{14}}{17555992353900}e^{-14\gamma\Delta-t_{14}}(19683t_{14}^{12}-$$

$$-1535274t_{14}^{11}+53014338t_{14}^{10}-1058107050t_{14}^9+13238867070t_{14}^8-$$

$$-105851013840t_{14}^7+518624134600t_{14}^6-1307060194440t_{14}^5-$$

$$-102960978120t_{12}^4+103573349880000t_{12}^3-28264847410800t_{12}^2+$$

$$+30353623700400t_{14}-10117874566800)$$

when $x=0, 14\Delta<t\le 16\Delta;\ t_{14}=t-14\Delta$

22.3. Voltage and current at the conjunction point $x=x_n$

$u_1^n=i_1^n=0$; when $x=x_n, 0<t\le\Delta$

$u_2^n=i_2^n=\frac{2}{11}e^{-\gamma\Delta}$ when $x=x_n, \Delta<t\le 3\Delta;\ t_1=t-\Delta$

$$u_3^n=u_2^n+\frac{58}{121}e^{-3\gamma\Delta}-\frac{80t_3}{121}e^{-3\gamma\Delta-t_3};$$

$$i_3^n=i_2^n+\frac{14}{121}e^{-3\gamma\Delta}+\frac{8t_3}{121}e^{-3\gamma\Delta-t_3}$$

when $x=x_n, 3\Delta<t\le 5\Delta;\ t_3=t-3\Delta$

$$u_4^n=u_3^n+\frac{802}{1331}e^{-5\gamma\Delta}-\frac{80t_5}{1331}e^{-5\gamma\Delta-t_5}(3t_5^2-9t_5+25);$$

$$i_4^n = i_3^n + \frac{10}{1331}e^{-5\gamma\Delta} + \frac{8t_5}{1331}e^{-5\gamma\Delta - t_5}(3t_5^2 - 9t_5 + 47)$$

when $x = x_n,\ 5\Delta < t \le 7\Delta;\ t_5 = t - 5\Delta$

$$u_5^n = u_4^n + \frac{7418}{14641}e^{-7\gamma\Delta} - \frac{8t_7}{43923}e^{-7\gamma\Delta - t_7}(81t_7^4 - 810t_7^3 +$$

$$+ 4280t_7^2 - 7980t_7 + 10020);$$

$$i_5^n = i_4^n - \frac{1514}{14641}e^{-7\gamma\Delta} + \frac{4t_7}{2196153}e^{-7\gamma\Delta - t_7}(81t_7^4 - 810t_7^3 +$$

$$+ 6260t_7^2 - 13920t_7 + 33780)$$

when $x = x_n,\ 7\Delta < t \le 9\Delta;\ t_7 = t - 7\Delta$

$$u_6^n = u_5^n + \frac{36482}{161051}e^{-9\gamma\Delta} - \frac{8t_9}{3382071}e^{-9\gamma\Delta - t_9}(243t_9^6 - 5103t_9^5 +$$

$$+ 49959t_9^4 - 244440t_9^3 + 644420t_9^2 - 772800t_9 + 468300);$$

$$i_6^n = i_5^n - \frac{28462}{161051}e^{-9\gamma\Delta} + \frac{4t_9}{16910355}e^{-9\gamma\Delta - t_9}(243t_9^6 - 5103t_9^5 +$$

$$+ 62433t_9^4 - 369180t_9^3 + 1456000t_9^2 - 2459100t_9 + 3840900)$$

when $x = x_n,\ 9\Delta < t \le 11\Delta;\ t_9 = t - 9\Delta$

$$u_7^n = u_6^n - \frac{240902}{1771561}e^{-11\gamma\Delta} - \frac{2t_{11}}{37202781}e^{-11\gamma\Delta - t_{11}}(243t_{11}^8 - 8748t_{11}^7 +$$

$$+ 142560t_{11}^6 - 1279152t_{11}^5 + 6614692t_{11}^4 - 19335400t_{11}^3 +$$

$$+ 26724320t_{11}^2 - 11516400t_{11} - 12184200);$$

$$i_7^n = i_6^n - \frac{329122}{1771561}e^{-11\gamma\Delta} + \frac{t_{11}}{186013905}e^{-11\gamma\Delta - t_{11}}(243t_{11}^8 - 8748t_{11}^7 +$$

$$+163944t_{11}^6 - 1728216t_{11}^5 + 11559940t_{11}^4 - 46334680t_{11}^3 +$$

$$+119142800t_{11}^2 - 153720000t_{11} + 177420600)$$

$$\text{when } x = x_n,\ 11\Delta < t \le 13\Delta;\ t_{11} = t - 11\Delta$$

$$u_8^n = u_7^n - \frac{8750558}{19487171}e^{-13\gamma\Delta} - \frac{2t_{13}}{22507682505}e^{-13\gamma\Delta - t_{13}}(2187t_{13}^{10} -$$

$$-120285t_{13}^9 + 2983365t_{13}^8 - 42447240t_{13}^7 + 369351180t_{13}^6 -$$

$$-1982908620t_{13}^5 + 6051656380t_{13}^4 - 8193539200t_{13}^3 -$$

$$-6777370600t_{13}^2 + 27668025000t_{13} - 32131222200);$$

$$i_8^n = i_7^n - \frac{2480294}{19487171}e^{-13\gamma\Delta} - \frac{t_{13}}{112538412525}e^{-13\gamma\Delta - t_{13}}(2187t_{13}^{10} -$$

$$-120285t_{13}^9 + 3277395t_{13}^8 - 53032320t_{13}^7 + 554786100t_{13}^6 -$$

$$-3802366260t_{13}^5 + 17047308740t_{13}^4 - 479239376000t_{13}^3 -$$

$$+81472237000t_{13}^2 - 7229999700t_{13} + 67836799800)$$

$$\text{when } x = x_n,\ 13\Delta < t \le 15\Delta;\ t_{13} = t - 13\Delta$$

The sinusoidal voltage of the feeding generator: $u_0 = \sin(\omega t),\ \omega = 2\pi$

22.4. Current at the sending end of the line $x = 0$

$$i_1^0 = \frac{1}{10}\sin(\omega t) \text{ when } x = 0,\ 0 < t \le 2\Delta$$

$$i_2^0 = i_1^0 + \frac{9}{55}\sin(\omega t_2)e^{-2\gamma\Delta} \text{ when } x = 0,\ 2\Delta < t \le 4\Delta$$

$$i_3^0 = i_2^0 + \frac{e^{-4\gamma\Delta}}{605(1+\omega^2)^2}\Big(80\omega(\omega^2-1)\cos(\omega t_4) +$$

$$+ (41\omega^4 + 242\omega^2 + 41)\sin(\omega t_4) + 80\omega(t_{\omega 4} + 1 - \omega^2)e^{-t_4}\Big)$$

$$\text{when } x = 0,\ 4\Delta < t \le 6\Delta;\ t_4 = t - 4\Delta;\ t_{\omega 4} = (1+\omega^2)t_4$$

$$i_4^0 = i_3^0 + \frac{e^{-6\gamma\Delta}}{1331(1+\omega^2)^4}\Big[576\omega(1-\omega^2)(\omega^4+1)\cos(\omega t_6) -$$

$$-\frac{3}{5}(117\omega^8 - 1932\omega^6 - 1932\omega^4 - 258\omega^2 + 117)\sin(\omega t_6) +$$

$$+ 48\omega\Big(t_{\omega 6}^3 - 6\omega^2 t_{\omega 6}^2 + 6(3\omega^4 + \omega^2 + 2)t_{\omega 6} + 12(\omega^2-1)(\omega^4+1)\Big)e^{-t_6}\Big]$$

$$\text{when } x = 0,\ 6\Delta < t \le 8\Delta;\ t_6 = t - 6\Delta;\ t_{\omega 6} = (1+\omega^2)t_6$$

$$i_5^0 = i_4^0 + \frac{e^{-8\gamma\Delta}}{14641(1+\omega^2)^6}\Big[32\omega(1-\omega^2)(365\omega^8 - 162\omega^6 + 1538\omega^4 - 162\omega^2 +$$

$$+ 365)\cos(\omega t_8) - \frac{1}{15}(33837\omega^{12} - 322578\omega^{10} + 273315\omega^8 - 1228860\omega^6 +$$

$$+ 273315\omega^4 - 322578\omega^2 + 33837)\sin(\omega t_8) + 8\omega\Big(81t_{\omega 8}^5 - 405(3\omega^2+1)t_{\omega 8}^4 +$$

$$+ 10(851\omega^4 + 568\omega^2 + 365)t_{\omega 8}^3 - 120\omega^2(223\omega^4 + 122\omega^2 + 223)t_{\omega 8}^2 +$$

$$+ 60(730\omega^8 + 285\omega^6 + 1985\omega^4 + 203\omega^2 + 365)t_{\omega 8} +$$

$$- 60(\omega^2-1)(365\omega^8 - 162\omega^6 + 1538\omega^4 - 162\omega^2 + 365)\Big)e^{-t_8}\Big]$$

$$\text{when } x = 0,\ 8\Delta < t \le 10\Delta;\ t_8 = t - 8\Delta;\ t_{\omega 8} = (1+\omega^2)t_8$$

22.5. Voltage and current at the end of the line $x = l$

$u_1^l = i_1^l = 0$; when $x = 0,\ 0 < t \le 2\Delta$

$$u_2^l = \frac{4e^{-2\gamma\Delta}}{11(1+\omega^2)^2}\Big[(1+\omega^4)\sin(\omega t_2) +$$

$$+ \omega(\omega^2 - 1)\cos(\omega t_2) + \omega(t_{\omega 2} + 1 - \omega^2)e^{-t_2}\Big];$$

$$i_2^l = \frac{4\omega e^{-2\gamma\Delta}}{11(1+\omega^2)^2}\big[2\omega\sin(\omega t_2) +$$

$$-(\omega^2 - 1)\cos(\omega t_2) + (t_{\omega 2} + 1 - \omega^2)e^{-t_2}\big]$$

when $x = 0,\ 2\Delta < t \le 4\Delta;\ t_2 = t - 2\Delta;\ t_{\omega 2} = (1+\omega^2)t_2$

$$u_3^l = u_2^l + \frac{12e^{-4\gamma\Delta}}{121(1+\omega^2)^4}\Big[6(\omega^4 + \omega^3 - \omega + 1)^2\sin(\omega t_4) +$$

$$+ 12\omega(\omega^2 - 1)(\omega^4 + 1)\cos(\omega t_4) + \omega\Big(t_{\omega 4}^3 - 6\omega^2 t_{\omega 4}^2 +$$

$$+ 6(3\omega^4 + \omega^2 + 2)t_{\omega 4} - 12(\omega^2 - 1)(\omega^4 + 1)\Big)e^{-t_4}\Big];$$

$$i_3^l = i_2^l + \frac{12e^{-4\gamma\Delta}}{121(1+\omega^2)^4}\Big[6\omega^2(3\omega^4 - 2\omega^2 + 3)\sin(\omega t_4) +$$

$$+ 12\omega(1-\omega^2)^3\cos(\omega t_4) + \omega\Big(t_{\omega 4}^3 - 6\omega^2 t_{\omega 4}^2 +$$

$$+ 6(2\omega^4 - \omega^2 + 1)t_{\omega 4} - 6(1-\omega^2)^3\Big)e^{-t_4}\Big]$$

when $x = 0,\ 4\Delta < t \le 6\Delta;\ t_4 = t - 4\Delta;\ t_{\omega 4} = (1+\omega^2)t_4$

$$u_4^l = u_3^l + \frac{2e^{-6\gamma\Delta}}{1331(1+\omega^2)^6}\Big[4(203\omega^{12} - 730\omega^{10} + 3037\omega^8 -$$

$$-2428\omega^6+3037\omega^4-730\omega^2+203)\sin(\omega t_6)+$$

$$+2\omega(\omega^2-1)(609\omega^8-808\omega^6+2350\omega^4-808\omega^2+$$

$$+609)\cos(\omega t_6)+\frac{\omega}{15}\left(81t_{\omega 6}^5-405(3\omega^2+1)t_{\omega 6}^4+\right.$$

$$+10(851\omega^4+568\omega^2+365)t_{\omega 6}^3-120\omega^2(223\omega^4+122\omega^2+223)t_{\omega 6}^2+$$

$$+30(1339\omega^8+86\omega^6+3244\omega^4-78\omega^2+609)t_{\omega 6}-$$

$$\left.-30(\omega^2-1)(609\omega^8-808\omega^6+2350\omega^4-808\omega^2+609)\right)e^{-t_6}\Big];$$

$$i_4^l=i_3^l+\frac{2e^{-6\gamma\Delta}}{1331(1+\omega^2)^6}\Big[4\omega^2(203\omega^8-486\omega^6+1214\omega^4-486\omega^2+$$

$$+203)\sin(\omega t_6)-2\omega(\omega^2-1)(203\omega^8-1136\omega^6+2506\omega^4-1136\omega^2+$$

$$+203)\cos(\omega t_6)+\frac{\omega}{15}\left(81t_{\omega 6}^5-405(3\omega^2+1)t_{\omega 6}^4+\right.$$

$$+10(689\omega^4+244\omega^2+203)t_{\omega 6}^3-240\omega^2(71\omega^4-20\omega^2+71)t_{\omega 6}^2+$$

$$+30(609\omega^8-1214\omega^6+2428\omega^4-730\omega^2+203)t_{\omega 6}-$$

$$\left.-30(\omega^2-1)(203\omega^8-1136\omega^6+2506\omega^4-1136\omega^2+203)\right)e^{-t_6}\Big]$$

when $x=0,\ 6\Delta<t\le 8\Delta;\ t_6=t-6\Delta;\ t_{\omega 6}=(1+\omega^2)t_6$

$$u_5^l=u_4^l+\frac{6e^{-8\gamma\Delta}}{14641(1+\omega^2)^8}\Big[24(41\omega^{16}-367\omega^{14}+2512\omega^{12}-$$

$$-4169\omega^{10}+6558\omega^8-4169\omega^6+2512\omega^4-367\omega^2+$$

$$+41)\sin(\omega t_8)+42\omega(\omega^2-1)(82\omega^{12}-445\omega^{10}+1378\omega^8-$$

$$-1374\omega^6+1378\omega^4-445\omega^2+82)\cos(\omega t_8)+$$

$$+\frac{\omega}{35}\left(27t_{\omega 8}^7-378(2\omega^2+1)t_{\omega 8}^6+14(689\omega^4+649\omega^2+284)t_{\omega 6}^5-\right.$$

$$-70\omega^2(933\omega^6+1097\omega^4+1015\omega^2+203)t_{\omega 8}^4+$$

$$+140(1747\omega^8+1878\omega^6+3418\omega^4+1062\omega^2+367)t_{\omega 8}^3-$$

$$-1680\omega^2(285\omega^8+85\omega^6+896\omega^4+85\omega^2+285)t_{\omega 8}^2+$$

$$+840(531\omega^{12}-841\omega^{10}+3660\omega^8-1844\omega^6+2805\omega^4-$$

$$-523\omega^2+164)t_{\omega 8}-1680(\omega^2-1)(82\omega^{12}-445\omega^{10}+$$

$$\left.+1378\omega^8-1374\omega^6+1378\omega^4-445\omega^2+82)\right)e^{-t_8}\Big];$$

$$i_5^l=i_4^l+\frac{6e^{-8\gamma\Delta}}{14641(1+\omega^2)^8}\Big[24\omega^2(205\omega^{12}-1380\omega^{10}+5627\omega^8-$$

$$-6312\omega^6+5627\omega^4-1380\omega^2+205)\sin(\omega t_8)-$$

$$-24\omega(\omega^2-1)(41\omega^{12}-490\omega^{10}+2871\omega^8-$$

$$-3564\omega^6+2871\omega^4-490\omega^2+41)\cos(\omega t_8)+$$

$$-\frac{\omega}{35}\left(27t_{\omega 8}^7-378(2\omega^2+1)t_{\omega 8}^6+14(608\omega^4+4879\omega^2+203)t_{\omega 6}^5-\right.$$

$$-140(245\omega^6+265\omega^4+305\omega^2+61)t_{\omega 8}^4+$$

$$+140(1017\omega^8+92\omega^6+1792\omega^4+248\omega^2+123)t_{\omega 8}^3-$$

$$-840\omega^2(245\omega^8-482\omega^6+1138\omega^4-482\omega^2+245)t_{\omega 8}^2+$$

$$+840(164\omega^{12}-1013\omega^{10}+3279\omega^8-3156\omega^6+2348\omega^4-$$

$$-367\omega^2+41)t_{\omega 8}-840(\omega^2-1)(41\omega^{12}-490\omega^{10}+$$

$$+2871\omega^8-3564\omega^6+2871\omega^4-490\omega^2+41)\Big)e^{-t_8}\Big]$$

when $x=0,\ 8\Delta<t\le 10\Delta;\ t_8=t-8\Delta;\ t_{\omega 8}=(1+\omega^2)t_8$

22.6. Voltage and current at the conjunction point $x=x_n$

$u_1^n=i_1^n=0$; when $x=x_n,\ 0<t\le\Delta$

$$u_2^n=i_2^n=\frac{2e^{-\gamma\Delta}}{11}\sin(\omega t_1)\ \text{ when }\ x=x_n,\ \Delta<t\le 3\Delta;\ t_1=t-\Delta$$

$$u_3^n=u_2^n+\frac{2e^{-3\gamma\Delta}}{121(1+\omega^2)^2}\Big[40\omega(\omega^2-1)\cos(\omega t_3)+$$

$$+(29\omega^4-22\omega^2+29)\sin(\omega t_3)+40\omega(t_{\omega 3}+1-\omega^2)e^{-t_3}\Big];$$

$$i_3^n=i_2^n-\frac{2e^{-3\gamma\Delta}}{121(1+\omega^2)^2}\Big[4\omega(\omega^2-1)\cos(\omega t_3)+$$

$$+(7\omega^4+22\omega^2+7)\sin(\omega t_3)-4\omega(t_{\omega 3}+1-\omega^2)e^{-t_3}\Big]$$

when $x=x_n,\ 3\Delta<t\le 5\Delta;\ t_3=t-3\Delta;\ t_{\omega 3}=(1+\omega^2)t_3$

$$u_4^n=u_3^n+\frac{2e^{-5\gamma\Delta}}{1331(1+\omega^2)^4}\Big[40\omega(\omega^2-1)\Big(25\omega^4-22\omega^2+$$

$$+25)\cos(\omega t_5)-\left(401\omega^8-1116\omega^6+2726\omega^4-\right.$$

$$\left.-1116\omega^2+401\right)\sin(\omega t_5)+40\omega\left(3t_{\omega 5}^3-18\omega^2 t_{\omega 5}^2+\right.$$

$$\left.+(43\omega^4-4\omega^2+25)t_{\omega 5}-(\omega^2-1)(25\omega^4-22\omega^2+25)\right)e^{-t_5}\Big];$$

$$i_4^n=i_3^n-\frac{2e^{-5\gamma\Delta}}{1331(1+\omega^2)^4}\Big[4\omega(\omega^2-1)\left(47\omega^4+22\omega^2+\right.$$

$$+47)\cos(\omega t_5)-\left(5\omega^8+468\omega^6+350\omega^4+\right.$$

$$\left.468\omega^2+5\right)\sin(\omega t_5)+4\omega\left(3t_{\omega 5}^3-18\omega^2 t_{\omega 5}^2+\right.$$

$$\left.+(65\omega^4+40\omega^2+47)t_{\omega 5}-(\omega^2-1)(47\omega^4+22\omega^2+47)\right)e^{-t_5}\Big]$$

when $x=x_n,\ 5\Delta<t\le 7\Delta;\ t_5=t-5\Delta;\ t_{\omega 5}=(1+\omega^2)t_5$

$$u_5^n=u_4^n+\frac{2e^{-7\gamma\Delta}}{14641(1+\omega^2)^6}\Big[80\omega(\omega^2-1)\left(167\omega^8-558\omega^6+\right.$$

$$\left.+1142\omega^4-558\omega^2+167\right)\cos(\omega t_7)+\left(3709\omega^{12}-25746\omega^{10}+\right.$$

$$+111635\omega^8-132540\omega^6+111635\omega^4-25746\omega^2+$$
$$\left.+3709\right)\sin(\omega t_7)+\frac{4\omega}{3}\left(81t_{\omega 7}^5-405(3\omega^2+1)t_{\omega 7}^4+20(376\omega^4+\right.$$

$$\left.+185\omega^2+133)t_{\omega 7}^3-60\omega^2(374\omega^4+46\omega^2+347)t_{\omega 7}^2+\right.$$

$$\left.+60(433\omega^8-408\omega^6+1292\omega^4-292\omega^2+167)t_{\omega 7}-\right.$$

$$\left.-60(\omega^2-1)(167\omega^8-558\omega^6+1142\omega^4-558\omega^2+167)\right)e^{-t_7}\Big];$$

$$i_5^n = i_4^n - \frac{2e^{-7\gamma\Delta}}{14641(1+\omega^2)^6}\Big[8\omega(\omega^2-1)\Big(563\omega^8+234\omega^6+$$

$$+1934\omega^4+234\omega^2+563\Big)\cos(\omega t_7)-\Big(757\omega^{12}-8178\omega^{10}-$$

$$-2053\omega^8-27708\omega^6-2053\omega^4-8178\omega^2+$$

$$+757\Big)\sin(\omega t_7)+\frac{2\omega}{15}\Big(81t_{\omega 7}^5-405(3\omega^2+1)t_{\omega 7}^4+20(475\omega^4+$$

$$+383\omega^2+232)t_{\omega 7}^3-60\omega^2(545\omega^4+442\omega^2+545)t_{\omega 7}^2+$$

$$+60(1027\omega^8+978\omega^6+2678\omega^4+698\omega^2+563)t_{\omega 7}-$$

$$-60(\omega^2-1)(563\omega^8+234\omega^6+1934\omega^4+234\omega^2+563)\Big)e^{-t_7}\Big]$$

when $x = x_n$, $7\Delta < t \le 9\Delta$; $t_7 = t - 7\Delta$; $t_{\omega 7} = (1+\omega^2)t_7$

23. Discrete model building and foundation for nonhomogeneous multiwire line

The equations for multiwire line with *n* wires can be represented in the form of equations (1.1):

$$L\frac{\partial i}{\partial t}+\frac{\partial u}{\partial x}+Ri=0,\ C\frac{\partial u}{\partial t}+\frac{\partial i}{\partial x}+Gu=0,\ x\in(0,l),\ t>0. \qquad (23.1)$$

Here $i(x,t)$ and $u(x,t)$ are *K*-dimensional vector-functions: $i=(i_1,...,i_K)^T$, $u=(u_1,...,u_K)^T$; L and C are symmetrical matrices $K\times K$, connected by the relation $L=C^{-1}/a^2$, where a is the speed of electromagnetic wave propagation; R and G are diagonal matrices $K\times K$ with constant values on diagonal. The boundary conditions at the input and at the output of the line are of the following form

$$u(0,t) = U_0(t),\ u(l,t) = Di(l,t),\ t > 0. \qquad (23.2)$$

It is denoted by D the matrix integro-differential operator that contains the diagonal matrices R_S, L_S and C_S

$$Di(t) = R_s i(t) + L_s \frac{di(t)}{dt} + C_S^{-1} \int_0^t i(\tau) d\tau. \qquad (23.3)$$

The finite-difference relations (7.4), (7.5) can be generalized according to the case when the linear parameters are changing along the longitudinal coordinate *x.* They also can be generalized according to the multiwire electrical circuits with point of branching, lumped elements and with other complicative factors. In case of nonhomogeneous line the partition on the elementary cells by space coordinate *x* is chosen in such a way as the condition $\tau = h_{m\text{-}1/2}/a_{m\text{-}1/2} = const$ is fulfilled necessarily for any index *m*.

We will use the grid-characteristic approach when constructing the finite-difference scheme. According to this approach we are to proceed as follows. At first on the interval $[0,l]$ we generate the uniform grid with integer and half-integer indexes:

$$x_m = mh,\ m = \overline{0,N};\ x_{m-1/2} = x_m - h/2,\ m = \overline{1,N};\ h = l/N.$$

The uniform grid is generated over the time coordinate with the step τ also with integer and half-integer indexes: $t_n = n\tau$, $t_{n+1/2} = t_n + \tau/2$, n = 0,1,2,…

Then we integrate the equations (23.1) by the cell $Q = [x_{m-1}, x_m] \times [t_n, t_{n+1}]$ of the two-dimensional grid. So we obtain the integral relations along the boundary of the cell Q

$$L \int_{x_{m-1}}^{x_m} [i(x,t_{n+1}) - i(x,t_n)]dx + \int_{t_n}^{t_{n+1}} [u(x_m,t) - u(x_{m-1},t)]dt + R \iint_Q i(x,t)dtdx = 0;$$

$$C \int_{x_{m-1}}^{x_m} [u(x,t_{n+1}) - u(x,t_n)]dx + \int_{t_n}^{t_{n+1}} [i(x_m,t) - i(x_{m-1},t)]dt + G \iint_Q u(x,t)dtdx = 0.$$

Now the one-dimensional integrals we approximate by means of quadrature midpoint rule (rectangle rule), but two-dimensional integrals – by the formula with weights α and β. As a result we obtain

$$L\frac{i_{m-1/2}^{n+1}-i_{m-1/2}^{n}}{\tau}+\frac{u_{m}^{n+1/2}-u_{m-1}^{n+1/2}}{h}+\alpha i_{m-1/2}^{n+1}+(R-\alpha)i_{m-1/2}^{n}=0;$$
$$C\frac{u_{m-1/2}^{n+1}-u_{m-1/2}^{n}}{\tau}+\frac{i_{m}^{n+1/2}-i_{m-1}^{n+1/2}}{h}+\beta u_{m-1/2}^{n+1}+(G-\beta)u_{m-1/2}^{n}=0. \quad (23.4)$$

The following notations are used here

$$i_{m\pm1/2}^{n}=i(x_m\pm h/2,t_n),\ i_{m}^{n+1/2}=i(x_m,t_n+\tau/2).$$

The values $i_m^{n+1/2}$ and $u_m^{n+1/2}$ at the half-integer time layer can be expressed from (23.4) through the variables $i_{m\pm1/2}^{n}$ and $u_{m\pm1/2}^{n}$. We'll use the relations on the characteristics with positive and negative slopes:

$$u_m^{n+1/2}+Z_B i_m^{n+1/2}=u_{m-1/2}^{n}+Z_B i_{m-1/2}^{n};\ u_m^{n+1/2}-Z_B i_m^{n+1/2}=u_{m+1/2}^{n}-Z_B i_{m+1/2}^{n}.$$

Here Z_B is the matrix of wave resistances: $Z_B=(C^{-1}L)^{1/2}=aL$.

Solving this system we obtain the following correlations

$$i_m^{n+1/2}=Z_B^{-1}\frac{u_{m-1/2}^{n}-u_{m+1/2}^{n}}{2}+\frac{i_{m-1/2}^{n}+i_{m+1/2}^{n}}{2};$$
$$u_m^{n+1/2}=\frac{u_{m-1/2}^{n}+u_{m+1/2}^{n}}{2}+Z_B\frac{i_{m-1/2}^{n}-i_{m+1/2}^{n}}{2}. \quad (23.5)$$

So, the finite-difference equations, that approximate (23.1), have the form of relations (23.4), (23.5). The boundary values $i_m^{n+1/2}$ and $u_m^{n+1/2}$ take the form

$$u_0^{n+1/2}=U_0(t_{n+1/2}),\ i_0^{n+1/2}=Z_B^{-1}\left(U_0(t_{n+1/2})-u_{1/2}^{n}\right)+i_{1/2}^{n}; \quad (23.6)$$

$$\left(D_h + Z_B\right) i_N^{n+1/2} = u_{N-1/2}^n + Z_B i_{N-1/2}^n,\ u_N^{n+1/2} = D_h i_N^{n+1/2},$$

where D_h is the finite-difference approximation for the integro-differential operator D from (23.3). The operator D_h can be represented in the following form

$$D_h i_N^{n+1/2} = R_S i_N^{n+1/2} + L_S \frac{i_N^{n+1/2} - i_N^{n-1/2}}{\tau} + C_S^{-1} \sum_{k=1}^{n} \frac{i_N^{n+1/2} + i_N^{n-1/2}}{2} \tau.$$

Then the boundary values at the right end $i_N^{n+1/2}$ and $u_N^{n+1/2}$ can be written in the explicit form

$$u_N^{n+1/2} = (B_S + Z_B)^{-1} \left[Z_B F_S + B_S \left(u_{N-1/2}^n + Z_B i_{N-1/2}^n \right) \right];$$

$$i_N^{n+1/2} = (B_S + Z_B)^{-1} \left[-F_S + \left(u_{N-1/2}^n + Z_B i_{N-1/2}^n \right) \right]; \qquad (23.7)$$

$$B_S = R_S + \frac{1}{\tau} L_S + \tau C_S^{-1};$$

$$F_S = \left(-\frac{1}{\tau} L_S + \frac{\tau}{2} C_S^{-1} \right) i_N^{n-1/2} + C_S^{-1} \sum_{k=1}^{n-1} \frac{i_N^{n+1/2} + i_N^{n-1/2}}{2} \tau.$$

The weighting coefficients α, β and the time-step τ in (23.4), (23.5) must be chosen in such a way as to ensure the minimal effect of the dispersion and dissipation phenomenon of the finite-difference scheme. In order to determine the optimal values of the parameters α, β and τ we apply the first differential approximation method for finite-difference relations. Using (23.5) we eliminate the values $i_m^{n+1/2}$, $u_m^{n+1/2}$ from the (23.4) and write out the obtained relations in the non-index form:

$$(L + \tau\alpha) i_t + u_{\dot{x}} + Ri - \frac{haL}{2} i_{\bar{x}x} = 0;$$
$$(C + \tau\beta) u_t + i_{\dot{x}} + Gu - \frac{haC}{2} u_{\bar{x}x} = 0. \qquad (23.8)$$

So the first differential approximation for this scheme has the following form

$$(L+\tau\alpha)\left(\frac{\partial i}{\partial t}+\frac{\tau}{2}\frac{\partial^2 i}{\partial t^2}\right)+\frac{\partial u}{\partial x}+Ri-\frac{haL}{2}\frac{\partial^2 i}{\partial x^2}=0;$$

$$(C+\tau\beta)\left(\frac{\partial u}{\partial t}+\frac{\tau}{2}\frac{\partial^2 u}{\partial t^2}\right)+\frac{\partial i}{\partial x}+Gu-\frac{haC}{2}\frac{\partial^2 u}{\partial x^2}=0.$$

These differential equations are approximated by finite-difference equations (23.8) with second order of accuracy by h and τ. Thus these equations can be represented in the form

$$L\frac{\partial i}{\partial t}+\frac{\partial u}{\partial x}+Ri+\tau\alpha\frac{\partial i}{\partial t}+\frac{\tau L}{2}\frac{\partial^2 i}{\partial t^2}-\frac{ahL}{2}\frac{\partial^2 i}{\partial x^2}=0;$$

$$C\frac{\partial u}{\partial t}+\frac{\partial i}{\partial x}+Gu+\tau\beta\frac{\partial u}{\partial t}+\frac{\tau C}{2}\frac{\partial^2 u}{\partial t^2}-\frac{ahC}{2}\frac{\partial^2 u}{\partial x^2}=0.$$

The original telegraph equations for the line with losses are equivalent to the following:

$$\frac{\partial^2 i}{\partial x^2}=CL\frac{\partial^2 i}{\partial t^2}+(GL+CR)\frac{\partial i}{\partial t}+GRi;$$

$$\frac{\partial^2 u}{\partial x^2}=LC\frac{\partial^2 u}{\partial t^2}+(LG+RC)\frac{\partial u}{\partial t}+RGu.$$

Taking into account above representations the first differential approximation can be transformed to the form:

$$\left(L\frac{\partial i}{\partial t}+\frac{\partial u}{\partial x}+Ri\right)+$$

$$+\tau\alpha\frac{\partial i}{\partial t}+\frac{\tau L}{2}\frac{\partial^2 i}{\partial t^2}-\frac{ahL}{2}\left[CL\frac{\partial^2 i}{\partial t^2}+(GL+CR)\frac{\partial i}{\partial t}+GR\right]=0;$$

$$\left(C\frac{\partial u}{\partial t}+\frac{\partial i}{\partial x}+Gu\right)+$$

$$+\tau\beta\frac{\partial u}{\partial t}+\frac{\tau C}{2}\frac{\partial^2 u}{\partial t^2}-\frac{ahC}{2}\left[LC\frac{\partial^2 u}{\partial t^2}+(LG+RC)\frac{\partial u}{\partial t}+RGu\right]=0.$$

This implies that the weighting coefficients α,β should be chosen in such a way as to minimize (desirable to zero) differential additions to the original equations:

$$\tau\alpha\frac{\partial i}{\partial t}+\frac{\tau L}{2}\frac{\partial^2 i}{\partial t^2}-\frac{ahL}{2}\left[CL\frac{\partial^2 i}{\partial t^2}+(GL+CR)\frac{\partial i}{\partial t}+GRi\right]\to 0;$$

$$\tau\beta\frac{\partial u}{\partial t}+\frac{\tau C}{2}\frac{\partial^2 u}{\partial t^2}-\frac{ahC}{2}\left[LC\frac{\partial^2 u}{\partial t^2}+(LG+RC)\frac{\partial u}{\partial t}+RGu\right]\to 0.$$

After collecting terms and taking into account $aL=C^{-1}/a$ and $aC=L^{-1}/a$, we obtain

$$\frac{\partial^2 i}{\partial t^2}\left(\frac{\tau L}{2}-\frac{hL}{2a}\right)+\frac{\partial i}{\partial t}\left[\tau\alpha-\frac{ahL}{2}(GL+CR)\right]-\frac{ahL}{2}GRi\to 0;$$

$$\frac{\partial^2 u}{\partial t^2}\left(\frac{\tau C}{2}-\frac{hC}{2a}\right)+\frac{\partial u}{\partial t}\left[\tau\beta-\frac{ahC}{2}(LG+RC)\right]-\frac{ahC}{2}RGu\to 0,$$

One can readily see that when $\tau=h/a$ and

$$\alpha=\frac{ahL}{2\tau}(GL+CR)=\frac{a^2L}{2}(GL+CR)=\frac{1}{2}\left(R+C^{-1}GL\right);$$

$$\beta = \frac{ahC}{2\tau}(LG + RC) = \frac{a^2 C}{2}(LG + RC) = \frac{1}{2}\left(G + L^{-1}RC\right)$$

the coefficients of time derivatives become zero, but the remaining members do not contain the derivatives and tend to zero with first order when $h \to 0$. If the matrices *R* and *G* are diagonal matrices with the same values at the diagonal, then the matrix coefficients α and β can be represented as: $\alpha = \gamma L$, $\beta = \gamma C$, $\gamma = (\gamma_G + \gamma_R)/2$, $\gamma_R = L^{-1}R$, $\gamma_G = C^{-1}G$. Hence, the proposed scheme with the weights minimizes not only the dissipation, but the difference dispersion of the numerical solution as well.

Let's prove the stability of the finite-difference scheme (23.4)-(23.7), (23.8) by initial data taking into account zero boundary conditions. In this order we write down the finite-difference scheme for new unknown functions *r* and *s*, that are known as Riemannian invariants of the system (23.1) and can be expressed through currents and voltages as follows: $r = u + Z_B i$, $s = u - Z_B i$. As the matrices L and C are related by the formula $L = C^{-1}/a^2$, Then these matrices are permutable and the matrix of wave resistances Z_B can be represented in the form $Z_B = C^{-1/2}L^{1/2} = L^{1/2}C^{-1/2}$. The system of equations (23.1) written in invariants takes the form

$$\begin{aligned} &\frac{\partial r}{\partial t} + a\frac{\partial r}{\partial x} + \frac{1}{2}(\gamma_G + \gamma_R)r + \frac{1}{2}(\gamma_G - \gamma_R)s = 0; \\ &\frac{\partial s}{\partial t} - a\frac{\partial s}{\partial x} + \frac{1}{2}(\gamma_G - \gamma_R)r + \frac{1}{2}(\gamma_G + \gamma_R)s = 0. \end{aligned} \tag{23.9}$$

The finite-difference scheme (23.8) in terms of *r* and *s* when $\alpha = L\gamma$, $\beta = C\gamma$ gets the following form

$$(E + \tau\gamma)r_t^n + ar_{\dot{x}}^n - \frac{ha}{2}r_{\bar{x}x}^n + \gamma r^n + \frac{1}{2}(\gamma_G - \gamma_R)s^n = 0;$$

$$(E + \tau\gamma)s_t^n - as_{\dot{x}}^n - \frac{ha}{2}s_{\bar{x}x}^n + \gamma s^n + \frac{1}{2}(\gamma_G - \gamma_R)r^n = 0$$

or

$$(E+\tau\gamma)r_t^n + ar_{\bar{x}}^n + \gamma r^n + \frac{1}{2}(\gamma_G - \gamma_R)s^n = 0;$$
$$(E+\tau\gamma)s_t^n - as_x^n + \gamma s^n + \frac{1}{2}(\gamma_G - \gamma_R)r^n = 0. \qquad (23.10)$$

In (23.10) r and s represent K-dimensional vector-functions: $r = (r_1,...,r_K)^T$, $s = (s_1,...,s_K)^T$. As the matrices L and C are permutable and symmetrical, then they can be reduced to the diagonal form by means of the same orthogonal matrix Q, composed from the common eigenvectors: $L = Q\Lambda_L Q^T$, $C = Q\Lambda_C Q^T$. The matrices Λ_L and Λ_C are diagonal with the elements equal to the eigenvalues of the matrices L and C correspondingly:

$$\Lambda_L = diag(\lambda_{L,1};\lambda_{L,2};...;\lambda_{L,K});\ \Lambda_C = diag(\lambda_{C,1};\lambda_{C,2};...;\lambda_{C,K}).$$

Then the matrices γ_G, γ_R and γ can also be represented in the diagonal form:

$$\gamma_G = GQ\Lambda_C^{-1}Q^T;\ \gamma_R = RQ\Lambda_L^{-1}Q^T;\ \gamma = 0.5Q(R\Lambda_L^{-1} + G\Lambda_C^{-1})Q^T.$$

Now the finite-difference scheme (23.10) with respect to unknowns $\tilde{r} = Q^T r$ and $\tilde{s} = Q^T s$ can be represented in the diagonal form

$$(E+\tau\lambda_{\gamma,k})\tilde{r}_{k,t}^n + a\tilde{r}_{k,\bar{x}}^n + \lambda_{\gamma,k}\tilde{r}_k^n + \frac{1}{2}(\lambda_{G,k} - \lambda_{R,k})\tilde{s}_k^n = 0;$$
$$(E+\tau\lambda_{\gamma,k})\tilde{s}_{k,t}^n - a\tilde{s}_{k,x}^n + \lambda_{\gamma,k}\tilde{s}_k^n + \frac{1}{2}(\lambda_{G,k} - \lambda_{R,k})\tilde{r}_k^n = 0, \qquad (23.11)$$

where $\lambda_{G,k} = G/\lambda_{C,k}$, $\lambda_{R,k} = R/\lambda_{L,k}$, $\lambda_{\gamma,k} = 0.5(\lambda_{R,k} + \lambda_{G,k})$, $k = 1,\ldots K$.

In this way this system decomposes in K systems. Each of these K systems consists of two equations for pairs of unknowns $(\tilde{r}_k, \tilde{s}_k)$, $k = 1,\ldots K$. Now for each of these systems we apply the approach of the stability proof described in the paragraph 8. This procedure results in the stability condition of the form (8.16):

$$\tau \le \frac{1}{\frac{a}{h} + 0.5 \max\limits_{k=\overline{1,K}} (\lambda_{G,k} - \lambda_{\gamma,k}; \lambda_{R,k} - \lambda_{\gamma,k})} = \frac{h}{a - 0.5h \min\limits_{k=\overline{1,K}} (\lambda_{G,k}; \lambda_{R,k})}$$

or

$$\frac{\tau a}{h} \le \frac{1}{1 - 0.5(h/a) \min\limits_{k=\overline{1,K}} (\lambda_{G,k}; \lambda_{R,k})}. \qquad (23.11)$$

24. Transient process caused by voltage source connection to two series lines in presence of capacitance or inductance at the conjunction point

Let's consider two lines with following parameters. For the first line we set the length l_1, the wave resistance Z_{B1}, the speed of the electromagnetic wave propagation a_1, for second line $-l_2$, $Z_{B2} \neq Z_{B1}$, $a_2 \neq a_1$ correspondingly. The capacity C_n or the inductance L_n is parallel-connected to the junction point (see fig. 24.1).

In is required to determine the transformation of the wave shape penetrating in the second line, the nature of current changes penetrating through these lumped elements, the resulting voltage and current distributions along the first line under the motion of the wave reflected from the junction point [15].

The transient process starts with propagation along the first line of the incident wave with rectangular front $u = U_0$ and $i = U_0 / Z_{B1}$ (see fig. 22.1). To determine the voltages and currents usually the equivalent circuit with lumped parameters is considered [15]. However this approach can not be generalized for alternating voltage lines with arbitrary losses, several generators and several loading nodes [73]. This is way the nonstationary problem has to be formulated in terms of mathematical physics setting the corresponding boundary conditions for arbitrary time moment $t > 0$ in more general integro-differential form

$$u = U_0(t) \quad \text{when} \quad x = 0;$$

$$u = R_n i + L_n \frac{di}{dt} + \frac{1}{C_n}\int_0^t i(\tau)d\tau \quad \text{when} \quad x = x_n, \tag{24.1}$$

where $u = u_1 = u_2$, $i = i_1 - i_2$.

It is evident, that for ideal capacitance modeling $0 < C_n < \infty$ it is necessary to set $R_n = L_n = 0$, but for ideal inductance modeling $0 < L_n < \infty$ it is sufficiently to set $R_n = 0$ and $C_n = \infty$.

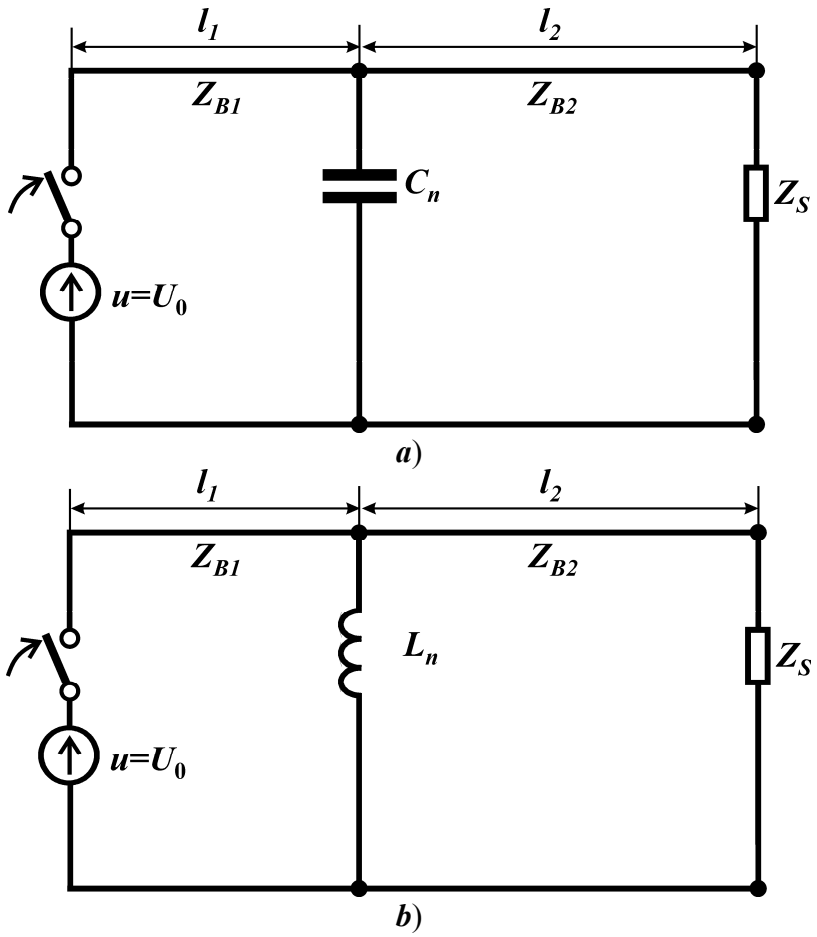

Fig. 24.1. Transverse capacitive (***a***) and inductive compensation (***b***) of cable line, conjugated with overhead transmission line.

Let's write down the relations on characteristics with positive and with negative slopes (see fig. 22.1) at the conjunction point $x = x_n$ assigning $U_0 = const$:

$$i_1 + u / Z_{B1} = 2U_0 / Z_{B1}, i_2 + u / Z_{B2} = 0 \quad \text{when} \quad x = x_n; \Delta < t < 3\Delta .$$

Hence, if we do not take into consideration the waves reflected from the ends of the line, then at the conjunction point of the overhead and cable lines we always obtain the following relation between the voltage *u* and the current step $i = i_1 - i_2$:

$$i + u \frac{Z_{B1} + Z_{B2}}{Z_{B1} Z_{B2}} = 2U_0 / Z_{B1} . \tag{24.2}$$

Taking into account the boundary condition

$$u = \frac{1}{C_n} \int_0^t i(\tau) d\tau \quad \text{when} \quad x = x_n \tag{24.3}$$

we obtain the ordinary differential equation with respect to voltage *u* as a function of time:

$$\frac{du(t)}{dt} + \frac{Z_{B1} + Z_{B2}}{Z_{B1} Z_{B2} C_n} u(t) = \frac{2U_0}{Z_{B1} C_n} .$$

To obtain the unique solution it is necessary to set the boundary condition at the point $t = \Delta$. As $i = 0$ when $0 < t < \Delta$, then the voltage determined by integral relation (24.3), is equal to zero too $u(\Delta) = 0$. The physical meaning of this condition is the follows. At the time moment when the wave entries the conjunction point, the voltage goes down to zero because the uncharged capacitance represents as it were short-circuit. Then it follows from the characteristic relations, that the input current value through the capacitance is equal to $2U_0 / Z_{B1}$. Let's write down the solution of the formulated Cauchy problem in the following form

$$u(t) = \frac{2U_0 Z_{B2}}{Z_{B1} + Z_{B2}} \left(1 - e^{-p(t-\Delta)}\right) \quad \text{when} \quad \Delta < t < 3\Delta ,$$

where $p = \dfrac{Z_{B1} + Z_{B2}}{Z_{B1} Z_{B2} C_n}$.

If instead of capacitance C_n the ideal inductance L_n is connected to at the conjunction point, then owing to boundary condition

$$u = L_n \frac{di}{dt} \quad \text{when} \quad x = x_n$$

we get again the ordinary differential equation with respect to current step *i* at the contact boundary

$$\frac{di(t)}{dt} + \frac{Z_{B1} Z_{B2}}{(Z_{B1} + Z_{B2}) L_n} i(t) = \frac{2U_0 Z_{B2}}{(Z_{B1} + Z_{B2}) L_n} .$$

Integrating this equation when $i(\Delta) = 0$, we obtain

$$i(t) = \frac{2U_0}{Z_{B1}} \left(1 - e^{-p(t-\Delta)}\right) \quad \text{when} \quad \Delta < t < 3\Delta ,$$

where $p = -\dfrac{Z_{B1} Z_{B2}}{(Z_{B1} + Z_{B2}) L_n}$.

As an example we will consider the calculations for initial data taken from [15], namely:

$$U_0 = 10 \text{ kV},\ l_1 = 60 \text{ km},\ l_2 = 100 \text{ km},\ Z_{B2} = 8 Z_{B1} = 400\ \Omega,$$
$$a_2 = 2a_1 = 300000 \text{ km/s},\ C_n = 5.62\ \mu\text{F}.$$

The purely active load with the resistance $R_S = Z_{B2} = 400\ \Omega$ is connected to the receiving end of the overhead line. In the dimensionless form we have

$$U_0 = Z_{B1} = a_2 = l_2 = 1,\ l_1 = 0.6,\ Z_{B2} = 8,\ a_1 = 0.5,\ C_n = 0.843 .$$

The voltage and current distributions along the nonhomogeneous line till the time moment when the wave reaches the end of the second line are represented in the fig. 24.2. The represented here diagrams for ideal line coincide with the same from [15] and they can be used as samples.

If we set the following losses in both lines: $R = 0.22$ Ω/km, G = = 44 μS/km, then the voltage and current amplitudes will decrease approximately by a quarter without essential changes in the form (see fig. 24.2, *b*).

As the wave motion is developed in the electrical circuit consisting from the two heterogeneous parts, the losses influence becomes essentially stronger. Let's follow the transient process evolution at the point of reactive element connection (at the conjunction point of two lines). The cable line we will reduce till 50 km in order that the time of one wave run along this line to be equal to unit (the same as in overhead line) or to 33.3 μs in the real time scale.

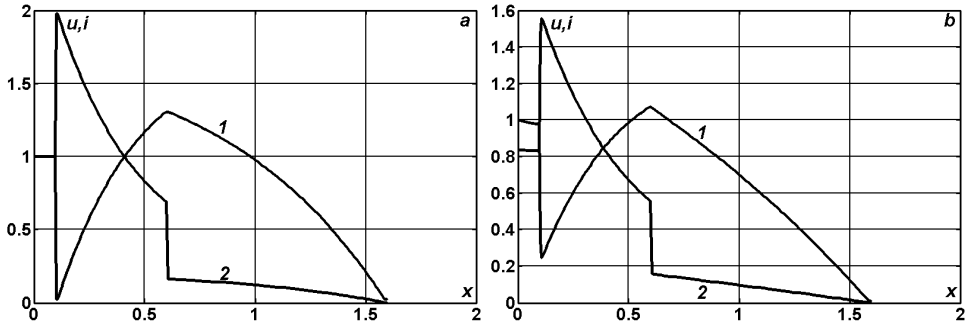

Fig. 24.2. Voltage and current distribution (curves 1, 2) along cable and overhead lines with ideal capacitance C_n = 5.62 μF at the conjunction point when $R = G = 0$ (***a***); R = 0.22 Ω/km, G = 44 μS/km (***b***).

In the fig. 24.3 we have represented the time diagrams of the voltage and current (curves 1, 2) for ideal line (*a*) and for line with losses (*b*). The curves 3 and 4 correspond to the case when the distance between the source and the receiver is such that the reflected waves have no time to reach the point of observation at the interval $0 < t < 30$.

The initial current value expressed through the capacity is equal to $2U_0 / Z_{B1}$. Then the capacitance is charging and the current through it decreases by time till zero (if there are losses in the line). In the absence of the losses the nature of voltage and current changes has explicit quasisteady-state oscillatory character. It is to mention that the voltage exhibits a tendency to stabilization. At the same time the current amplitude and its pola-

rity are changing all the time. The last means the continual energy interchange between the reactive power source and the line.

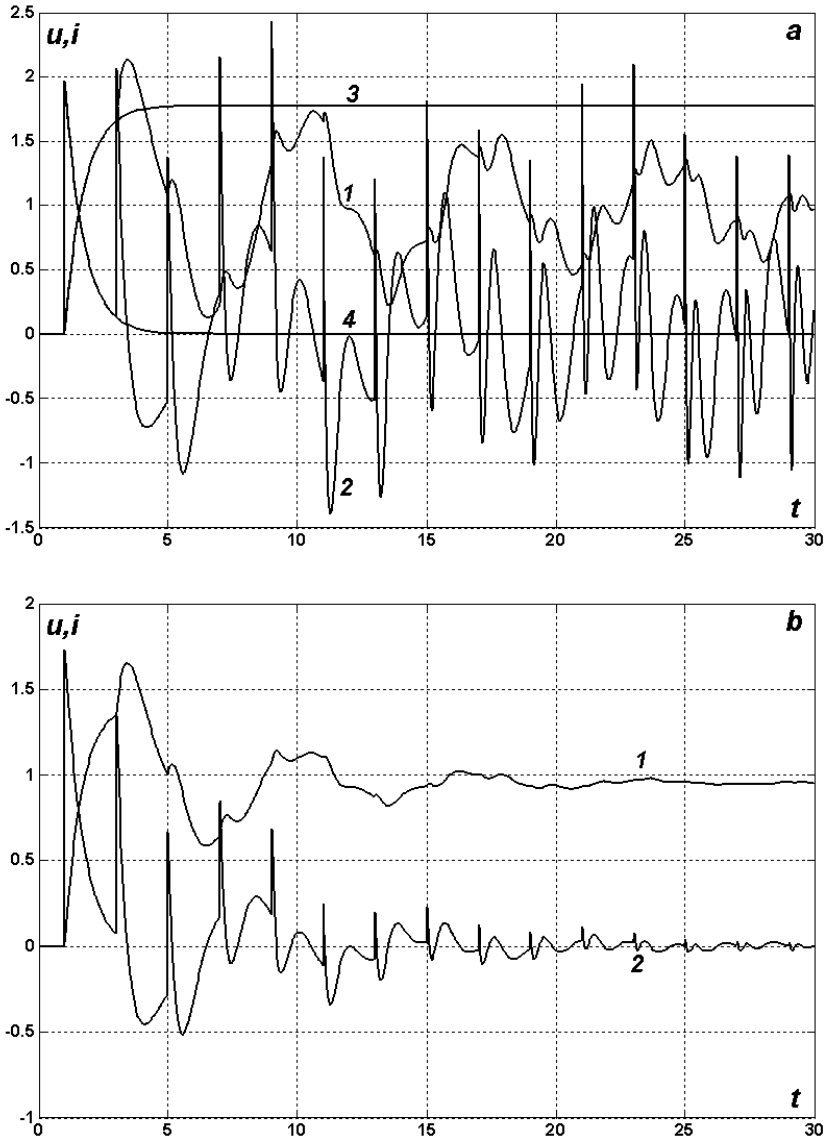

Fig. 24.3. Voltages and currents (curves 1, 2) on the ideal capacitance C_n = 5.62 μF parallel-connected to the conjunction point of cable and overhead lines when $R = G = 0$ (***a***); R = 0.22 Ω/km, G = 44 μS/km (***b***).

If now we will replace the capacitance C_n = 5.62 μF by the inductance $L_n = 0.1$ H, then we will obtain the regime closed to short-circuit. The current at the inductance unrestrictedly increases in time and the voltage tends to zero (see fig. 24.4). The voltage and current steps seriated through $\Delta t = 2$ correspond to the simultaneous arriving of the direct and reflected waves to the point $x_n = 50$ km.

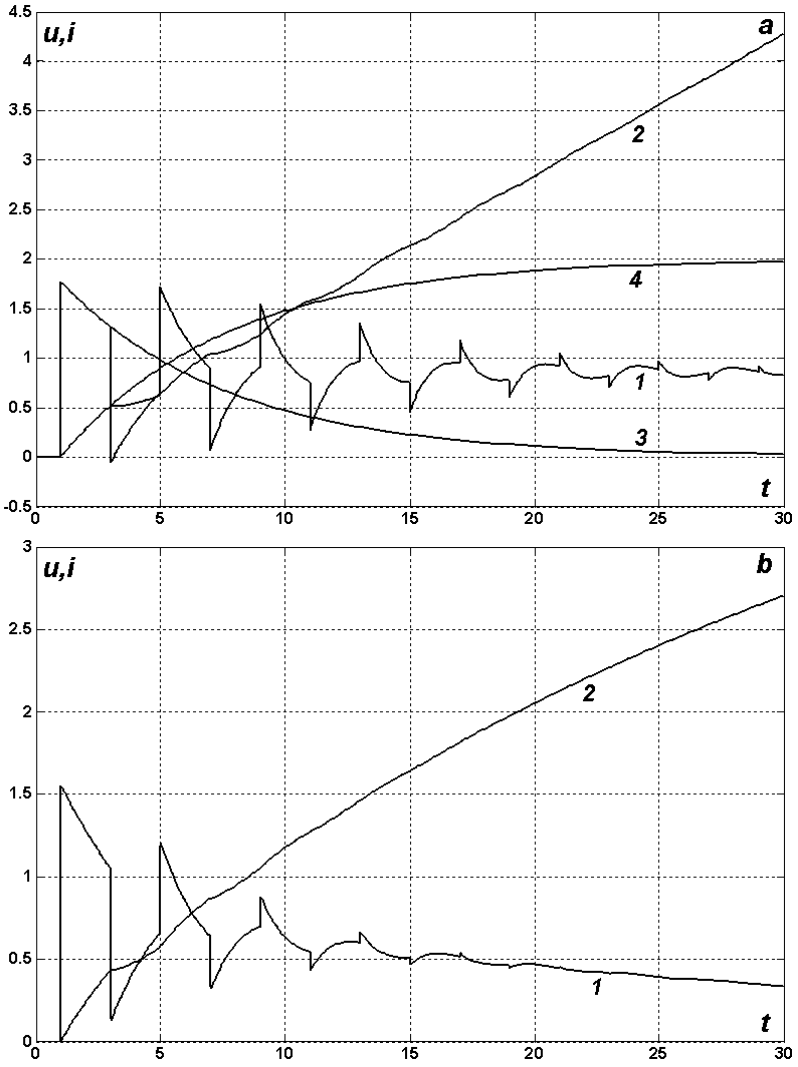

Fig. 24.4. Voltages and currents (curves 1, 2) on the ideal inductance L_n = 0.1 H parallel-connected to the conjunction point of cable and overhead lines when R = = G = 0 (***a***); R = 0.22 Ω/km, G = 44 μS/km (***b***).

Finally let's consider how the reactive power source parallel-connected to the line influences upon the load voltage losses. In the fig. 24.5 we have represented the voltages and currents at the end of the line connected by the relation $u = R_S i$ (because the load here is purely active). The comparative analysis of the represented oscillograms shows that the dozens of wave runs along the nonhomogeneous line are required to obtain the steady-state regime. The capacitance connection to the line does not affect the voltage losses (they come to 11% here), but the inductance connection results in total shunting of the power transmission from the source to the receiver.

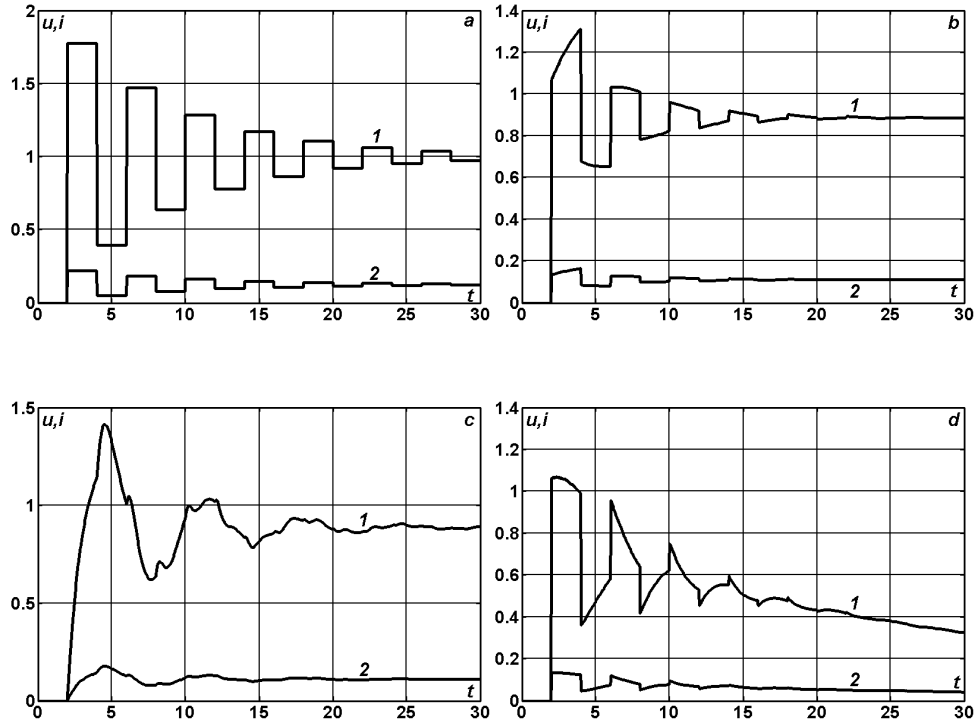

Fig. 24.5. Voltages and currents (curves 1, 2) on the load when $R = G = L_n = 0$, $C_n = \infty$ (***a***); $R = 0.22$ Ω/km, $G = 44$ μS/km (***b***); $L_n = 0$, $C_n = 5.62$ μF (***c***); $L_n = 0.1$ H, $C_n = \infty$ (***d***).

25. The replacement of power transmission line by cables. Influence of cable insertion on power flows

The interest in the development of transient and steady-state processes in the conjugated lines consisting from several heterogeneous sections is quickened permanently as a result of broad using of the traditional and superconducting cable lines in the backbone and distribution transmission lines. The cost and the cable laying are in 10…13 times greater then when overhead transmission line construction with the same parameters. But such a replacement gives several evident advantages. This is why this direction of development seems to be very promising. At the same time, the sections dedicated to nonhomogeneous alternating voltage lines are missing practically in the monographic and reference books [15, 50, 63 – 65, 79, 111, 112].

We adduce here the formulas for steady-state regimes calculations in conjugated lines of the form "overhead line – cable – overhead line" with the lumped compensative elements (represented in the form of series *RLC* – circuit) parallel-connected to the conjunction points. Then we analyze the cable insertion influence on the voltage and on the active transmission power distribution along the line. The pronounced nonlinear dependence of the electromagnetic energy propagation in conjugated line with reactive power sources is discovered. As a result of the overhead line section replacement by cable insertion (under the other equal conditions) the power flows can both increase and decrease in dozens of times.

25.1. Steady-state regime equations for piecewise homogeneous line

Let the overhead line with the length l supplies by the alternating voltage source: $u = U_0 \sin(2\pi ft)$ with the frequency f. Let's study the influence on the transmission power of the overhead line middle section replacement by the cable with the wave resistance that is in 8 or more times smaller then in the overhead line. At the conjunction points of the piecewise homogeneous line (overhead line – cable – overhead line) closed to the resistance R_S, let's place the *RLC* – circuits with complex resistances Z_n, as it is shown in the fig. 25.1.

Since the steady-state regime in sinusoidal voltage circuit is considered, then let's apply the symbolic method [59]. Here we try to evolve the general

methodology of this method as applied to the piecewise homogeneous lines [89].

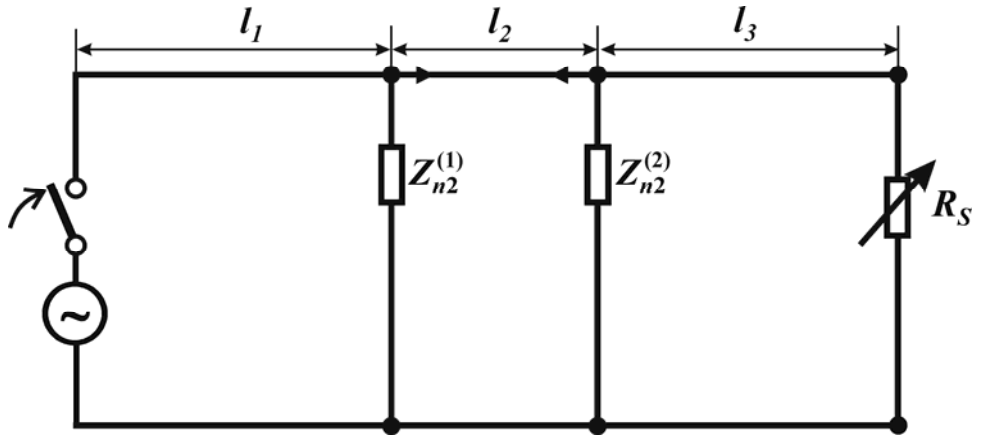

Fig 25.1. Overhead alternating voltage line with cable insertion of the length l_2.

Let's denote the complex amplitudes of the voltages and currents at the input-output of the electrical circuit by U_0, I_0, U_3, I_3, and at the points of compensative elements connection – as follows

$$U_k(x_k - 0) = U_k^{(1)},\ U_k(x_k + 0) = U_k^{(2)},\ I_k(x_k - 0) = I_k^{(1)},$$

$$I_k(x_k + 0) = I_k^{(2)},\ k = 1,2,\ U_0 = U_0^{(2)},\ I_0 = I_0^{(2)},$$

$$x_0 = 0,\ x_1 = l_1,\ x_2 = l_1 + l_2,\ x_3 = l_1 + l_2 + l_3 = l.$$

In case of homogeneous line with the parameters *L*, *C*, *R*, *G* without connected lumped elements, the problem solution at the interval $x \in [0, l]$ gets the form

$$U_0 = Z_{BX} I_0, U_3 = Z_S I_3, Z_S = R_S, \tag{25.1}$$

$$I_3 = -\frac{U_0}{Z_0}\mathrm{sh}(\delta l) + I_0 \mathrm{ch}(\delta l) = \frac{I_0}{Z_0}\left(Z_0 \mathrm{ch}(\delta l) - Z_{BX}\mathrm{sh}(\delta l)\right) =$$

$$= \frac{I_0 Z_0}{Z_S \mathrm{sh}(\delta l) + Z_0 \mathrm{ch}(\delta l)} = \frac{U_0}{Z_S \mathrm{ch}(\delta l) + Z_0 \mathrm{sh}(\delta l)}, \tag{25.2}$$

$$Z_{BX} = Z_0 \frac{Z_S \mathrm{ch}(\delta l) + Z_0 \mathrm{sh}(\delta l)}{Z_S \mathrm{sh}(\delta l) + Z_0 \mathrm{ch}(\delta l)}, \tag{25.3}$$

$$Z_0 = \sqrt{\frac{R + j\omega L}{G + j\omega C}}, \delta = \sqrt{(R + j\omega L)(G + j\omega C)}\,. \tag{25.4}$$

Here Z_{BX}, Z_0 are the input and the wave resistances if the line, δ is the propagation factor, Z_S is the load resistance, $\omega = 2\pi f$ is the angular frequency.

The solution for nonhomogeneous line with two parallel-connected lumped elements we obtain in the following manner. The conjunction conditions at the points x_k have the form

$$U_k^{(1)} - U_k^{(2)} = Z_{n1}^{(k)} I_k^{(1)}, \quad U_k^{(2)} = Z_{n2}^{(k)} \left(I_k^{(1)} - I_k^{(2)} \right), k = 1,2\,. \tag{25.5}$$

To solve the problem with such conditions we introduce the notation of input resistance $Z_{BX}^{(k)}$ for line sections $x \in [x_k, l], k = 1,2$. Then the complexes of voltages and currents at the points $x = x_k + 0$ will be connected by the relations

$$U_k^{(2)} = Z_{BX}^{(k)} I_k^{(2)}, \tag{25.6}$$

$$Z_{BX}^{(k)} = Z_0^{(k+1)} \frac{Z_n^{(k+1)} \mathrm{ch}(\delta_{k+1} l_{k+1}) + Z_0^{(k+1)} \mathrm{sh}(\delta_{k+1} l_{k+1})}{Z_n^{(k+1)} \mathrm{sh}(\delta_{k+1} l_{k+1}) + Z_0^{(k+1)} \mathrm{ch}(\delta_{k+1} l_{k+1})},$$
$$k = 1,2;\ Z_n^{(3)} = Z_S\,. \tag{25.7}$$

At the points $x = x_k - 0$ from (25.5) we have

$$U_k^{(1)} = Z_n^{(k)} I_k^{(1)}, \tag{25.8}$$

$$Z_n^{(k)} = Z_{n1}^{(k)} + \left(\frac{1}{Z_{BX}^{(k)}} + \frac{1}{Z_{n2}^{(k)}} \right)^{-1}, \quad k = 1,2. \tag{25.9}$$

The current and voltage values at the left and at the right of the points x_k and at the ends of the line are related by the following recurrence relations

$$U_k^{(2)} = \left(1 - \frac{Z_{n1}^{(k)}}{Z_n^{(k)}} \right) U_k^{(1)}, \; I_k^{(1)} = \left(1 + \frac{Z_{BX}^{(k)}}{Z_{n2}^{(k)}} \right) I_k^{(2)}, \quad k = 1,2, \tag{25.10}$$

$$I_1^{(1)} = \frac{I_0 Z_0^{(1)}}{Z_0^{(1)} \mathrm{ch}(\delta_1 l_1) + Z_n^{(1)} \mathrm{sh}(\delta_1 l_1)} = \frac{U_0}{Z_0^{(1)} \mathrm{sh}(\delta_1 l_1) + Z_n^{(1)} \mathrm{ch}(\delta_1 l_1)}, \tag{25.11}$$

$$I_3 = \frac{I_2^{(2)} Z_0^{(3)}}{Z_0^{(3)} \mathrm{ch}(\delta_3 l_3) + Z_S \mathrm{sh}(\delta_3 l_3)}. \tag{25.12}$$

Combining the formulas (25.10) – (25.12), we obtain the relation for current determination at the output of the line through the input voltage

$$I_3 = I_0 Z_0^{(1)} Z_0^{(2)} Z_0^{(3)} \left\{ \left[Z_0^{(3)} \mathrm{ch}(\delta_3 l_3) + Z_S \mathrm{sh}(\delta_3 l_3) \right] \times \right.$$

$$\left. \times \prod_{k=1}^{2} \left[\left(1 + Z_{BX}^{(k)} / Z_{n2}^{(k)} \right) \left(Z_0^{(k)} \mathrm{ch}(\delta_k l_k) + Z_n^{(k)} \mathrm{sh}(\delta_k l_k) \right) \right] \right\}^{-1}, \tag{25.13}$$

$$I_0 = \frac{U_0}{Z_{BX}}, \quad Z_{BX} = Z_0^{(1)} \frac{Z_n^{(1)} \mathrm{ch}(\delta_1 l_1) + Z_0^{(1)} \mathrm{sh}(\delta_1 l_1)}{Z_n^{(1)} \mathrm{sh}(\delta_1 l_1) + Z_0^{(1)} \mathrm{ch}(\delta_1 l_1)}. \tag{25.14}$$

The currents, voltages and active power along the line can be determined by the formulas

$$I(x) = I_k^{(2)} \mathrm{ch}\delta_{k+1}(x - x_k) - \frac{U_k^{(2)} \mathrm{sh}\delta_{k+1}(x - x_k)}{Z_0^{(k+1)}}, \tag{25.15}$$

$$U(x) = U_k^{(2)} \mathrm{ch}\delta_{k+1}(x - x_k) - I_k^{(2)} Z_0^{(k+1)} \mathrm{sh}\delta_{k+1}(x - x_k), \qquad (25.16)$$

$$x \in [x_k, x_{k+1}], k = 0,1,2 .$$

$$P(x) = \frac{1}{2} \mathrm{Re}\left(U(x) I^*(x)\right). \qquad (25.17)$$

The generator power and the load power are obtained as follows:

$$P_0 = \frac{1}{2} \mathrm{Re}\left(U_0 I_0^*\right) = \frac{U_0^2}{2} \mathrm{Re}\left(\frac{1}{Z_{BX}}\right),$$

$$P_1 = \frac{1}{2} \mathrm{Re}\left(U_3 I_3^*\right) = \frac{|I_3|^2 \mathrm{Re}(Z_H)}{2} = \frac{R_S |I_3|^2}{2}. \qquad (25.18)$$

The obtained relations (25.6) – (25.18) make it possible the comparative analysis of the cable insertion and lumped elements influence on the currents, voltages and power distribution along the line.

25.2. Comparative analysis of the numerical experiments

Let's set the initial data in the dimensionless form: $U_0 = Z_{B1} = Z_{B3} = a_1 = a_3 = 1$; $Z_{B2} = 1/8$; $a_2 = ½$; $C_{n1} = 0.05$; $R_m = 0.48$; $G_m = R_m/5$; $m = 1, 2, 3$; $l_k = l_2/l$; $l_1 = l_3 = (l - l_2)/2$. Conditionally it can be assumed that the wave resistance of the overhead line section is equal to 400 Ω, and for the cable it is in 8 times smaller, i.e. 50 Ω. The speed of electromagnetic wave propagation is 2 times smaller in the cable then in the overhead line.

In the fig. 25.2 – 25.5 we have represented the calculation results for the line without lumped reactive elements. The generated and transmission powers (curves 1, 2) depending on the load resistance $R_S = (1 + z)/(1 - z)$ are represented in the fig. 25.2. The length increase of the cable section results in some interesting particular features. For example, when $l_k = 0.2$ (see fig. 25.2, *c*) the greatest power flows may be observed (in comparison with other considered variants). Moreover, the critical resistance value (when the maximal active power is transmitted to the load) becomes four times greater then the wave resistance ($R_S = 4$). It is easy to observe that the power increase is always accompanied by the efficiency decrease. It is obvious, that

the cases when the losses under idling regime are greater then under natural power regime are unacceptable. The idling losses have to be two times smaller (as minimum), then under the natural power transmission [2, 4].

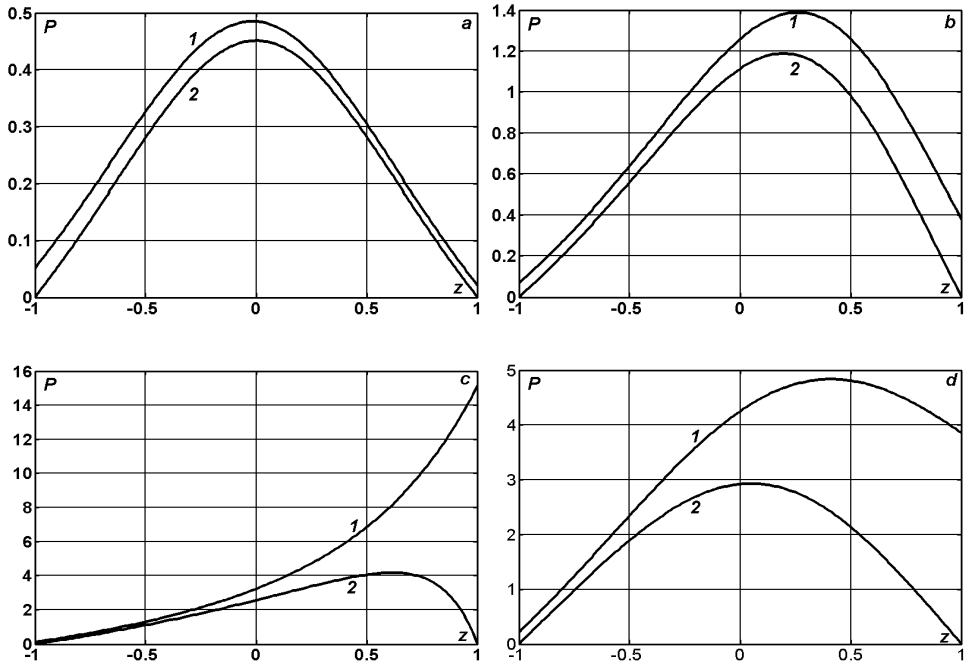

Fig 25.2. Generated and transmission power (curves 1, 2) depending on load resistance when $l = 0.125$; $l_k = 0$ (***a***); 0.1 (***b***); 0.2 (***c***); 0.3 (***d***).

In the fig 25.3– 25.4 we have represented the voltage modulus and the active power distribution along the line with length $l = 0.125$ when $l_k = 0$ (*a*); 0.1 (*b*); 0.2 (*c*); 0.3 (*d*) and $R_S = 1$ (1); 3/2 (2); 2 (3); 4 (4); 8 (5); ∞ (6). It turns out from these results that the relative length of the cable insertion may consist not more then 10% form the total length of the line. When this length reaches 20…30%, then the overvoltage ratio in the line exceeds 2 under its action on the matched load $R_S = 1$. For homogeneous line (see fig 25.3, *a*) the voltage dip is equal to 0.95 when $R_S = 1$, whereas in case of cable insertion (see fig 25.3,*b*) the voltages at the sending end and at the receiving end become nearly equal (this fact can be considered as a positive factor).

If the capacitance $C_{n1} = 0.05$ is connected to the conjunction point of the overhead and the cable lines, then the character of the voltage modulus and the active power distribution along the line changes essentially (see fig.

25.5– 25.6). For example, the reactive power source connection to the middle of the overhead line results in increase of the voltage at the load till 1.05. Also we can observe the losses increase when the generator is acting under the idling regime.

The dependence on the cable insertion length l_2 of the generated power (curve 1) and the active power (curve 2) transmitted to the load R_S = 1 is represented in the fig. 25.7 when l = 1/8 (*a*); 1/4 (*b*); 3/8 (*a*); 1/2 (*b*). If in the relative short line (l = 1/8) the presence of the cable insertion always results in transmission power increase, then in the half-wave and in the quarter-wave lines the power flows and the efficiency can descend to inadmissible down level.

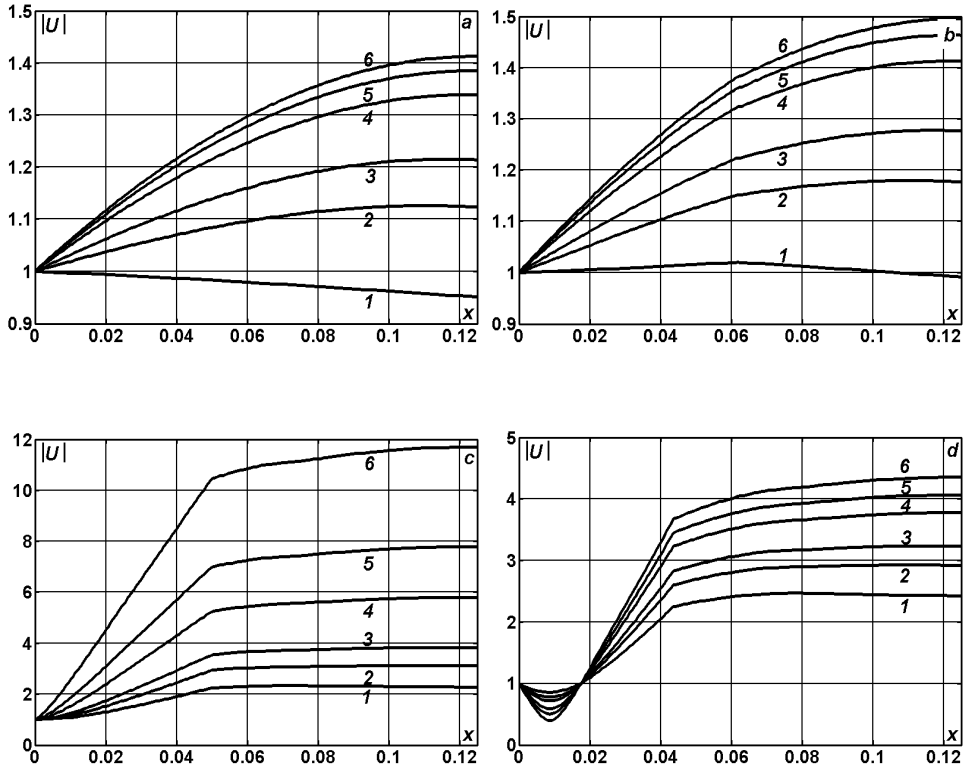

Fig 25.3. Voltage modulus distribution along the line with length l = 0.125 when l_k = 0 (***a***); 0.1 (***b***); 0.2 (***c***); 0.3 (***d***) and R_S = 1 (1); 3/2 (2); 2 (3); 4 (4); 8 (5); ∞ (6).

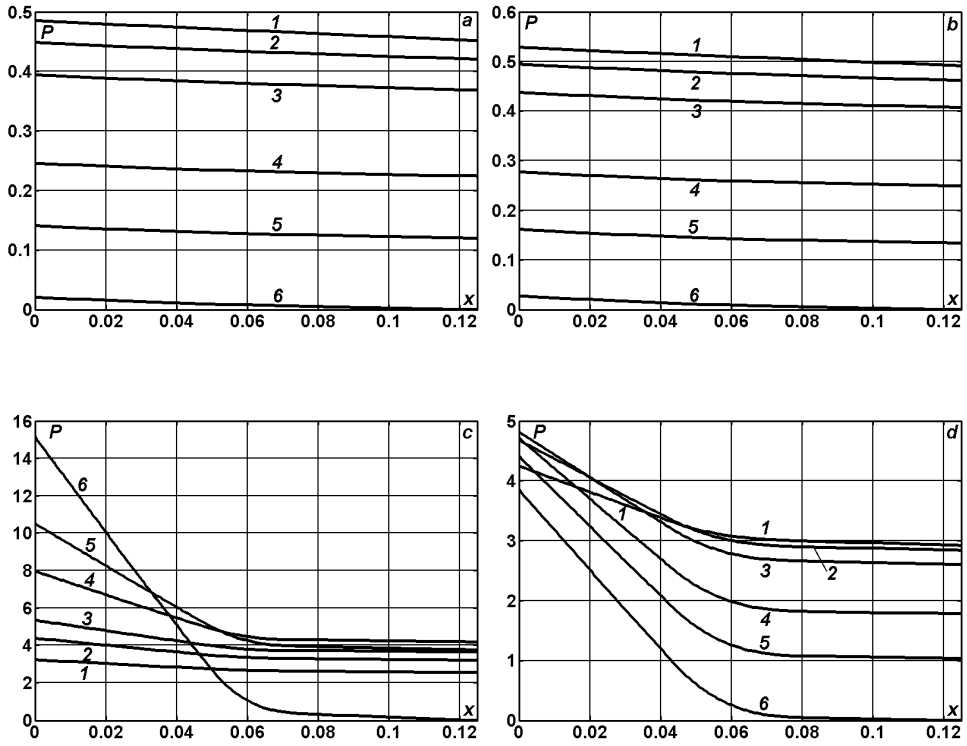

Fig 25.4. Active power distribution along the line with length $l = 0.125$ when $l_k = 0$ (***a***); 0.1 (***b***); 0.2 (***c***); 0.3 (***d***) and $R_S = 1$ (1); 3/2 (2); 2 (3); 4 (4); 8 (5); ∞ (6).

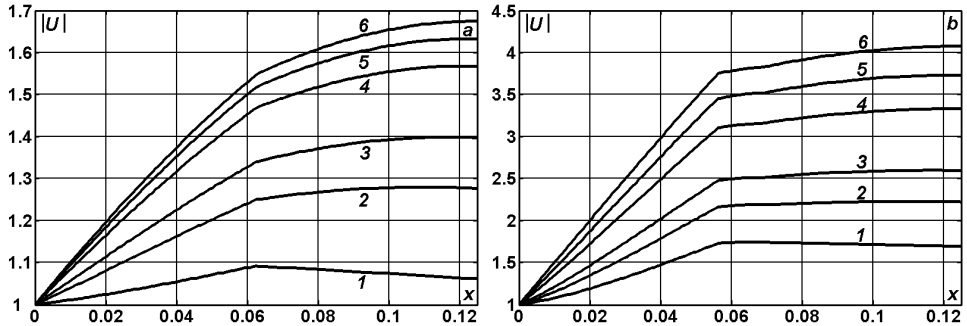

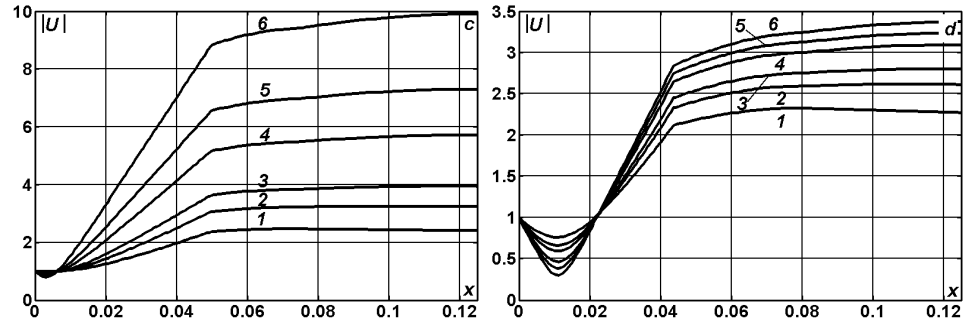

Fig 25.5. Voltage modulus distribution along the line with length $l = 0.125$ when $C_{n1} = 0.05$, $l_k = 0$ (***a***); 0.1 (***b***); 0.2 (***c***); 0.3 (***d***) and $R_S = 1$ (1); 3/2 (2); 2 (3); 4 (4); 8 (5); ∞ (6).

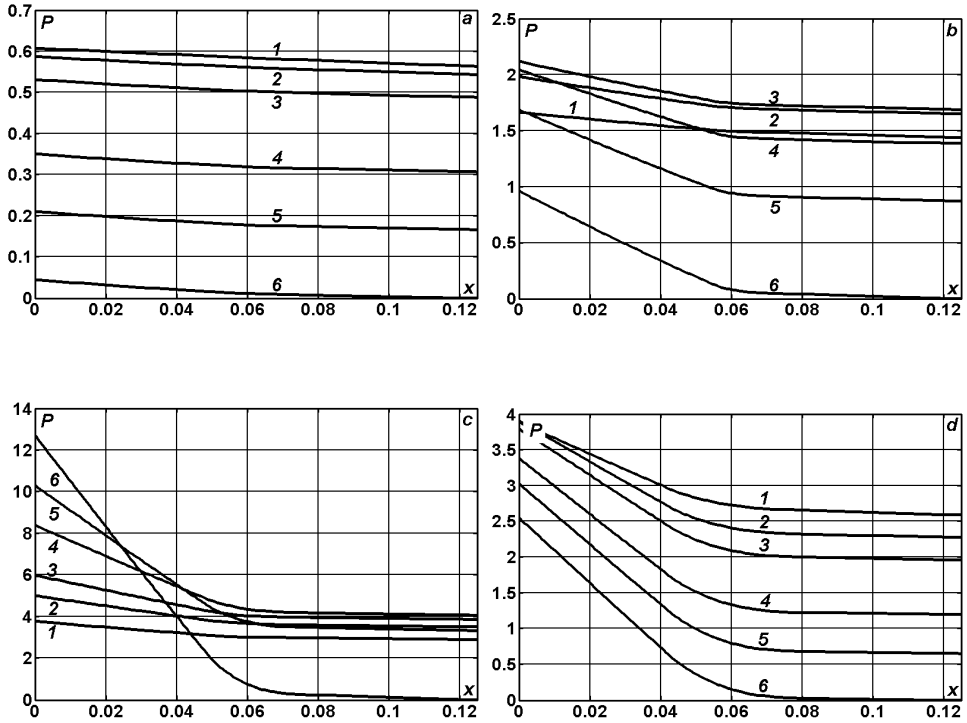

Fig 25.6. Active power distribution along the line with length $l = 0.125$ when $C_{n1} = 0.05$, $l_k = 0$ (***a***); 0.1 (***b***); 0.2 (***c***); 0.3 (***d***) and $R_S = 1$ (1); 3/2 (2); 2 (3); 4 (4); 8 (5); ∞ (6).

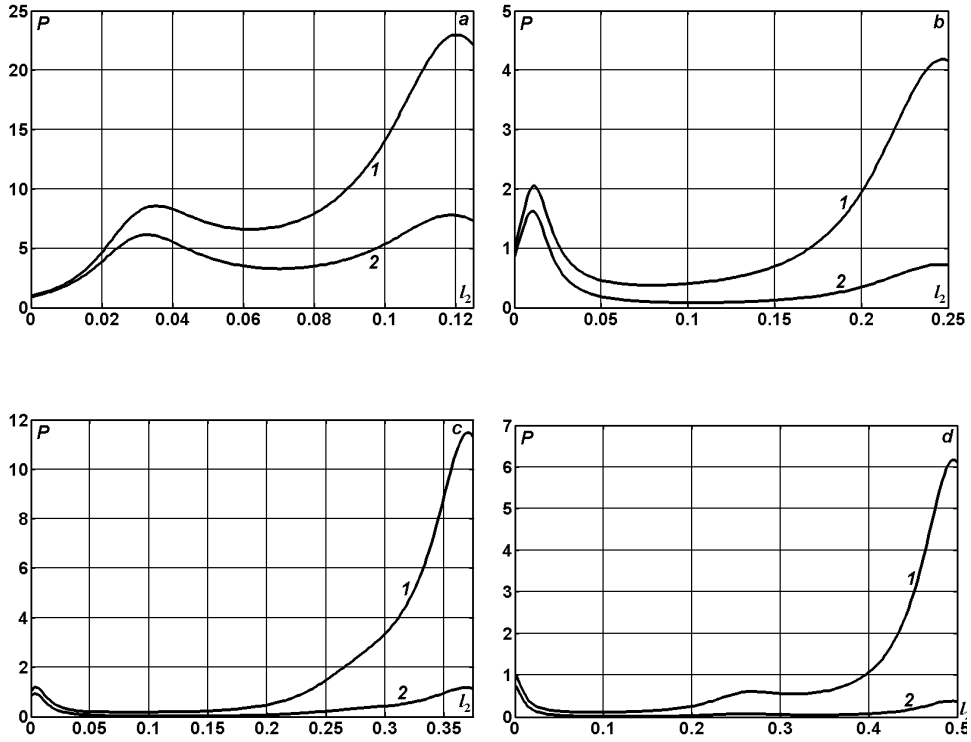

Fig. 25.7. Generated power (curve 1) and transmitted to the load R_S = 1 active power (curve 2) depending on the length of cable insertion l_2 when l = 1/8 (***a***); 1/4 (***b***); 3/8 (***a***); 1/2 (***b***).

Thus, the technique of the steady-state voltage, current and transmission power values in the overhead line concerning the cable insertion with the *RLC* – circuits parallel-connected to the conjunction points is represented. The parametrical analysis of the influence of the cable section length and of the reactive power sources on the voltage drops and on the power flows in the conjugated line has discovered several nonlinear dependences. The cable insertion in the relative short lines (l = 1/8) results not only in transmission line capacity, but also in more uniform voltage distribution along the non-homogeneous transmission line.

26. Wires interference on voltage and power distributions in three-phase transmission line

The equations for three-phase transmission line do not outwardly differ from equations for scalar case (when the single-wire representation is used)

$$L\frac{\partial i}{\partial t}+\frac{\partial u}{\partial x}+Ri=0,\ C\frac{\partial u}{\partial t}+\frac{\partial i}{\partial x}+Gu=0,\ x\in(0,l),\ t>0. \qquad (26.1)$$

Here $i(x,t)$ and $u(x,t)$ are three-dimensional vector-functions:

$$i=(i_1,i_2,i_3)^T,\ u=(u_1,u_2,u_3)^T;$$

L and C are symmetrical matrices 3×3, connected by the relation $L = C^{-1}/a^2$, where a is the speed of electromagnetic wave propagation; R and G are the diagonal matrices 3×3 with constant values at the diagonal. The boundary conditions at the input and at the output of the line have the following form

$$u(0,t)=\begin{pmatrix} u_0\sin\omega t \\ u_0\sin(\omega t-2\pi/3) \\ u_0\sin(\omega t-4\pi/3)\end{pmatrix}=U_0,$$

$$u(l,t)=Z_S i(l,t),\ Z_S=\begin{pmatrix} Z_S^{(1)} & 0 & 0 \\ 0 & Z_S^{(2)} & 0 \\ 0 & 0 & Z_S^{(3)}\end{pmatrix}. \qquad (26.2)$$

The solution of the problem in the steady-state regime can be obtained by complex amplitude method. Let's represent the functions $i(x,t)$ and $u(x,t)$ in the following form

$$u(x,t)=U(x)e^{j\omega t},\ i(x,t)=I(x)e^{j\omega t}. \qquad (26.3)$$

Then the equations (26.1) can be transformed in ordinary differential equations with respect to complex amplitudes $U(x)$, $I(x)$

$$\frac{dU}{dx}=-(R+j\omega L)I=-\widetilde{Z}I,\ \frac{dI}{dx}=-(G+j\omega C)U=-\widetilde{Y}U \qquad (26.4)$$

or

$$\frac{d^2U}{dx^2} = (R + j\omega L)(G + j\omega C)U, \quad \frac{d^2I}{dx^2} = (G + j\omega C)(R + j\omega L)I\,. \quad (26.5)$$

The solution of the problem can be represented in the form

$$U(x) = C_h(x)U_0 - S_h(x)Z_0I_0,$$

$$I(x) = Z_0^{-1}\left[-S_h(x)U_0 + C_h(x)Z_0I_0\right],\ x \in [0,l],$$

$$C_h(l) = C_h,\ S_h(l) = S_h,\ U_1 = C_hU_0 - S_hZ_0I_0,$$

$$I_1 = Z_0^{-1}\left[-S_hU_0 + C_hZ_0I_0\right],\ x = l,$$

$$U_0 = u_0\left(1, e^{-j2\pi/3}, e^{-j4\pi/3}\right)^T,\ I_0 = Z_{BX}^{-1}U_0,$$

$$U_1 = Z_SI_1, \quad Z_{BX} = \left(C_h + Z_SZ_0^{-1}S_h\right)^{-1}\left(Z_SC_h + S_hZ_0\right),$$

$$Z_0^2 = \widetilde{Y}^{-1}\widetilde{Z} = (G + j\omega C)^{-1}(R + j\omega L),$$

$$\delta^2 = \widetilde{Y}\widetilde{Z} = (G + j\omega C)(R + j\omega L)\,. \quad (26.6)$$

We have denoted here by $C_h(x)$ and $S_h(x)$ the matrix hyperbolic cosine and sine that can be determined through the eigenvalues of the matrix C in the following manner. Let the symmetric matrix C is defined by two values

$$C = \begin{pmatrix} c_1 & c_2 & c_2 \\ c_2 & c_1 & c_2 \\ c_2 & c_2 & c_1 \end{pmatrix}.$$

Then its eigenvalues take the form $\lambda_{1,2} = c_1 - c_2$, $\lambda_3 = c_1 + 2c_2$ and the matrix C can be represented by means of diagonal matrix of its eigenvalues Λ_C and of orthogonal matrix of eigenvectors Q as follows

$$C = Q\Lambda_C Q^*,\ \Lambda_C = \begin{pmatrix} \lambda_1 & 0 & 0 \\ 0 & \lambda_2 & 0 \\ 0 & 0 & \lambda_3 \end{pmatrix},\ Q = \frac{1}{\sqrt{6}} \begin{pmatrix} -\sqrt{3} & 1 & \sqrt{2} \\ \sqrt{3} & 1 & \sqrt{2} \\ 0 & -2 & \sqrt{2} \end{pmatrix}. \quad (26.7)$$

As we suppose that the matrix L can be expressed through the matrix C: $L = C^{-1}/a^2$, where a is the speed of electromagnetic wave propagation along the wires and the matrices R and G are diagonal with constant values, then the matrix of the propagation factors γ from (26.6) can be represented in the form

$$\delta = \left[(R + j\omega L)(G + j\omega C)\right]^{1/2} = Q \begin{pmatrix} \delta_1 & 0 & 0 \\ 0 & \delta_2 & 0 \\ 0 & 0 & \delta_3 \end{pmatrix} Q^*, \quad (26.8)$$

$$\delta_k = \sqrt{\left(R + \frac{j\omega}{a^2 \lambda_k}\right)(G + j\omega\lambda_k)},\ k = 1,2,3.$$

Using the representation (26.8) we can introduce the matrix exponents $E^+(x)$ and $E^-(x)$

$$E^+(x) = Q \begin{pmatrix} e^{\delta_1 x} & 0 & 0 \\ 0 & e^{\delta_2 x} & 0 \\ 0 & 0 & e^{\delta_3 x} \end{pmatrix} Q^*,\quad E^-(x) = Q \begin{pmatrix} e^{-\delta_1 x} & 0 & 0 \\ 0 & e^{-\delta_2 x} & 0 \\ 0 & 0 & e^{-\delta_3 x} \end{pmatrix} Q^*.$$

Then the matrices $C_h(x)$ and $S_h(x)$ take the following form

$$C_h(x) = 0.5\left(E^+(x) + E^-(x)\right),\quad S_h(x) = 0.5\left(E^+(x) - E^-(x)\right).$$

a) ***b***)

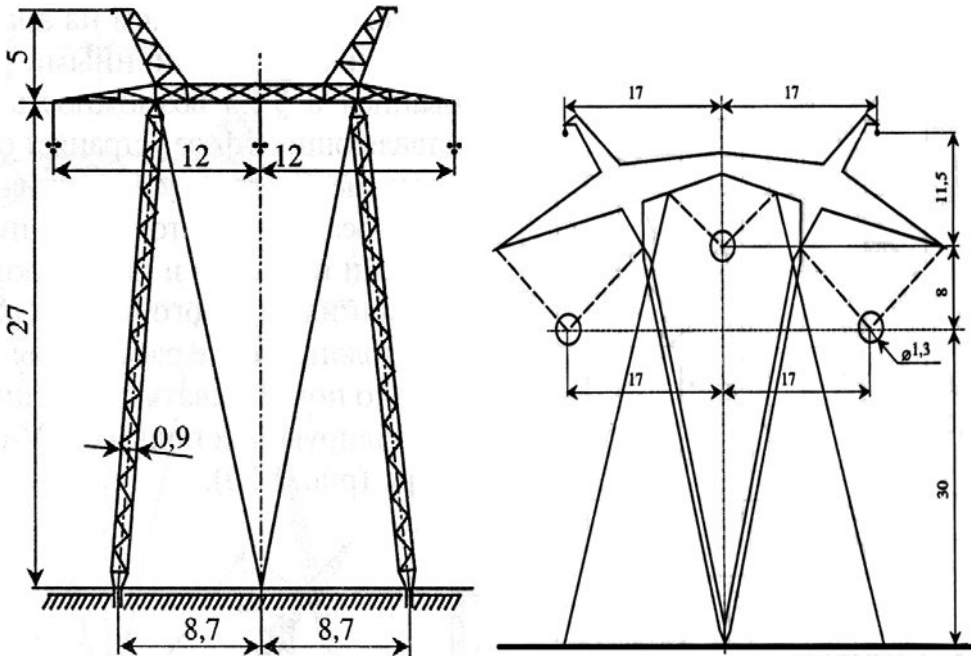

Fig. 26.1. The draft of transmission tower for 500 kV line in traditional construction (***a***) and the draft of V- transmission tower with broken line cross-arm for 1150 kV line (***b***).

In the fig. 26.2–26.7 we have represented the calculation results for the following initial data in the dimensionless form

$$U_0 = \begin{pmatrix} 1 \\ e^{-2j\pi/3} \\ e^{-4j\pi/3} \end{pmatrix},\ C_1 = \begin{pmatrix} 1 & 0 & 0 \\ 0 & 1 & 0 \\ 0 & 0 & 1 \end{pmatrix},\ C_2 = \begin{pmatrix} 1 & -0.18 & -0.04 \\ -0.18 & 1.03 & -0.18 \\ -0.04 & -0.18 & 1 \end{pmatrix},$$

$$C_3 = \begin{pmatrix} 1 & -0.18 & -0.18 \\ -0.18 & 1 & -0.18 \\ -0.18 & -0.18 & 1 \end{pmatrix},\ L = C^{-1}/a^2,\ R = 0.48,\ G = R/7\,.$$

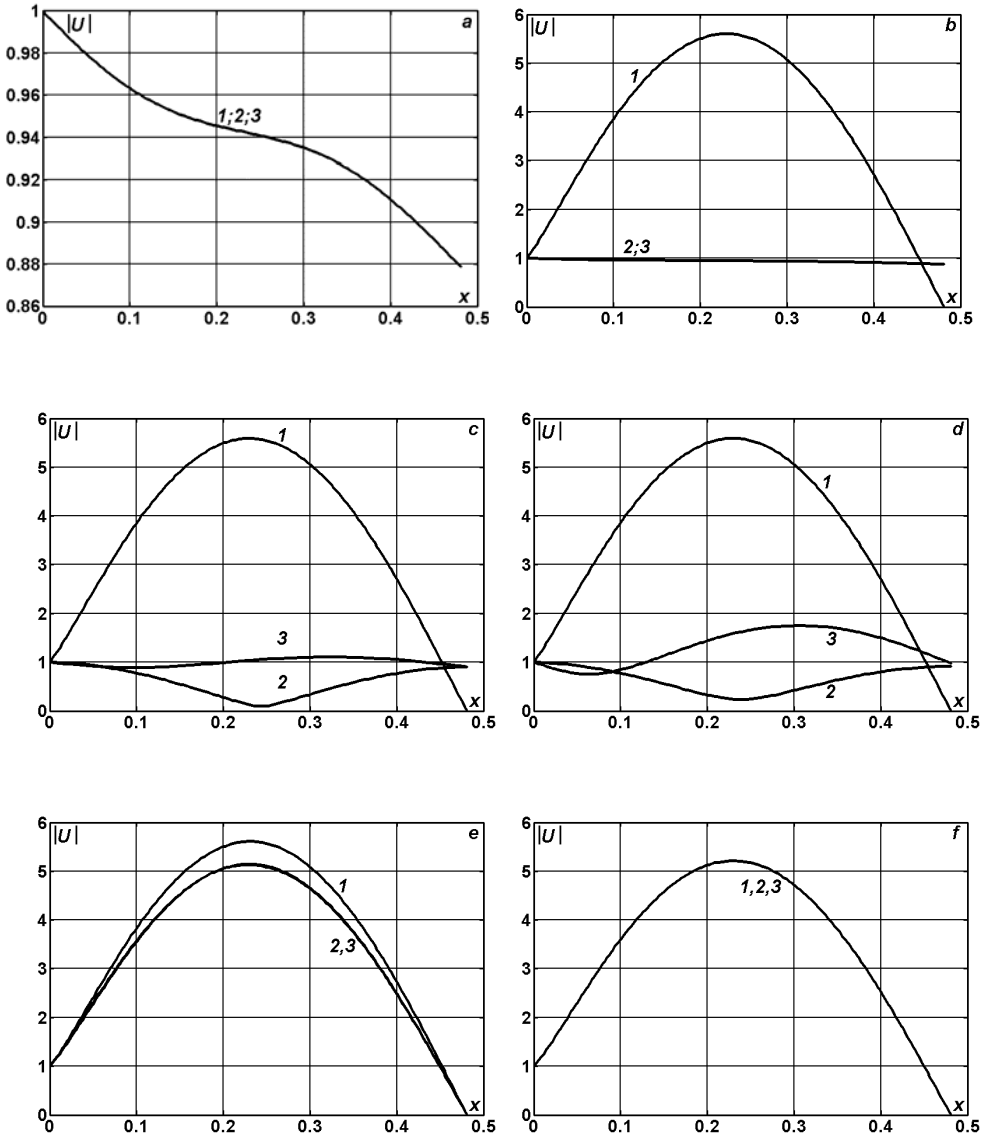

Fig 26.2. Voltage modulus distribution at the phases 1, 2, 3 (curves 1, 2, 3) along the line with length $l = 0.4805$ when $R = 0.48$ $G = R/7$ and $C = C_1$, $R_{S1} = R_{S2} = R_{S3} = 1$(***a***); $C = C_1$, $R_{S1} = 0$, $R_{S2} = R_{S3} = 1$ (***b***); $C = C_2$, $R_{S1} = 0$, $R_{S2} = R_{S3} = 1$ (***c***); $C = C_3$, $R_{S1} = 0$, $R_{S2} = R_{S3} = 1$ (***d***); $C = C_2$, $R_{S1} = R_{S2} = R_{S3} = 0$(***e***); $C = C_3$, $R_{S1} = R_{S2} = R_{S3} = 0$(***f***).

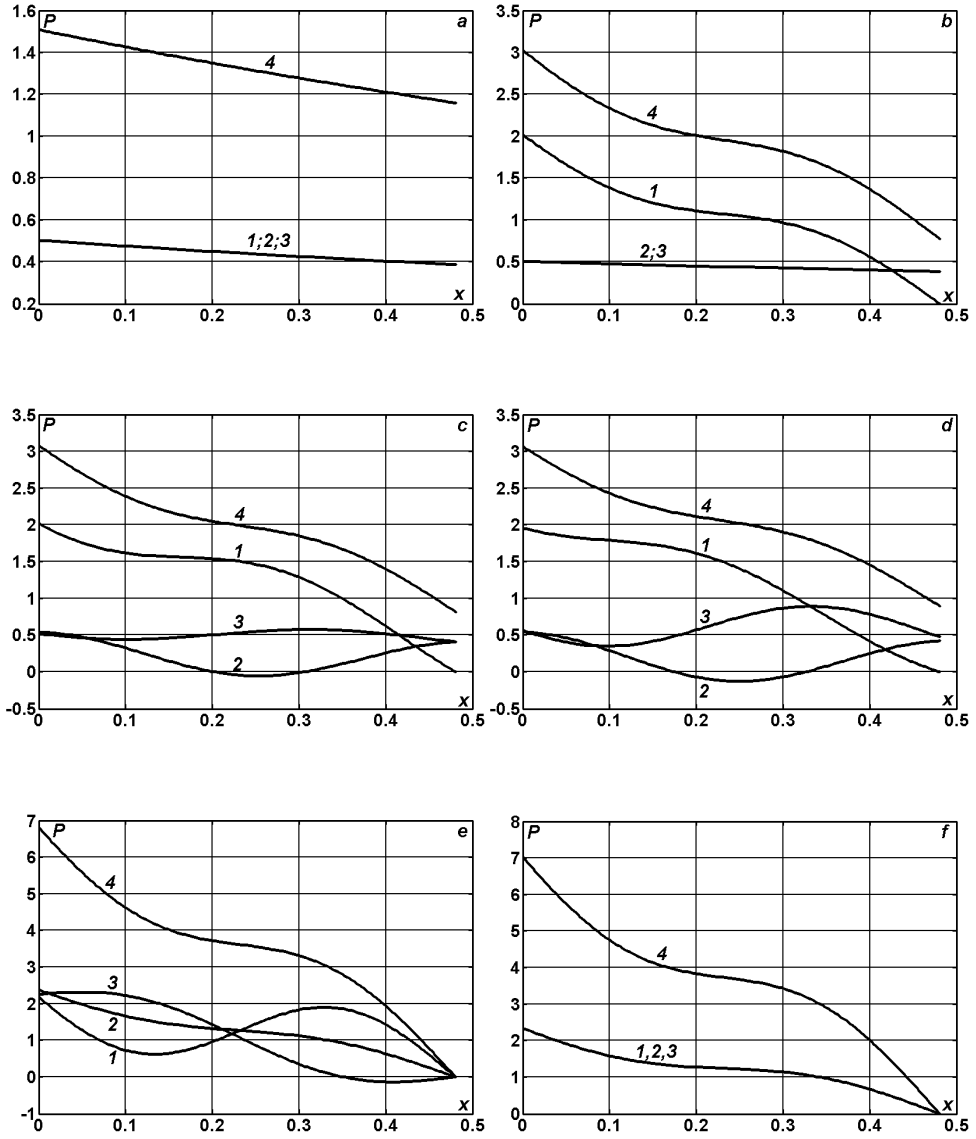

Fig 26.3. Active power distribution at the phases 1, 2, 3 (curves 1, 2, 3) and the total active power distribution (curve 4) along the line with length $l = 0.4805$ when $R = 0.48$ $G = R/7$ and $C = C_1$, $R_{S1} = R_{S2} = R_{S3} = 1$(***a***); $C = C_1$, $R_{S1} = 0$, $R_{S2} = R_{S3} = 1$ (***b***); $C = C_2$, $R_{S1} = 0$, $R_{S2} = R_{S3} = 1$ (***c***); $C = C_3$, $R_{S1} = 0$, $R_{S2} = R_{S3} = 1$ (***d***); $C = C_2$, $R_{S1} = R_{S2} = R_{S3} = 0$(***e***); $C = C_3$, $R_{S1} = R_{S2} = R_{S3} = 0$(***f***).

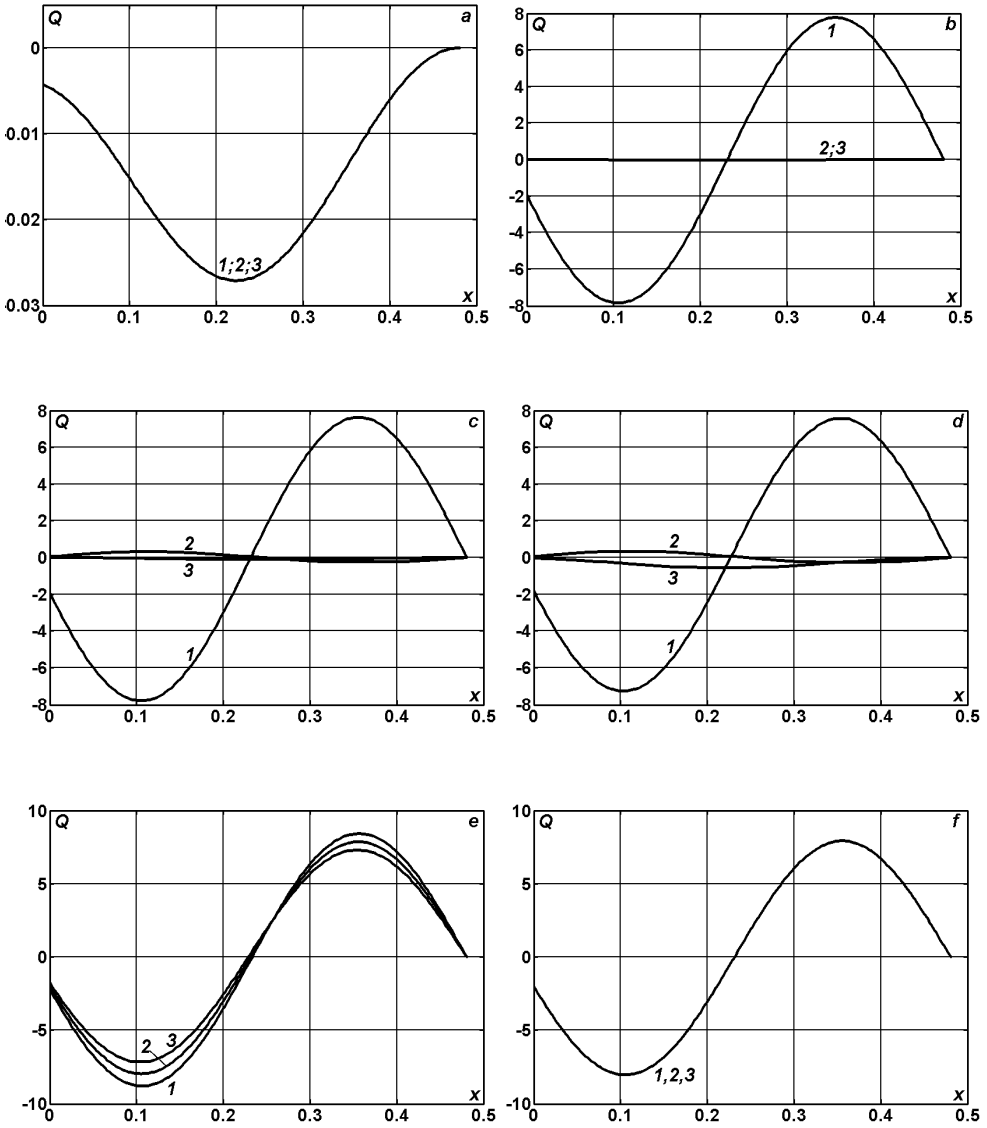

Fig 26.4. Reactive power distribution at the phases 1, 2, 3 (curves 1, 2, 3) along the line with length $l = 0.4805$ when $R = 0.48$ $G = R/7$ and $C = C_1$, $R_{S1} = R_{S2} = R_{S3} = 1$(***a***); $C = C_1$, $R_{S1} = 0$, $R_{S2} = R_{S3} = 1$ (***b***); $C = C_2$, $R_{S1} = 0$, $R_{S2} = R_{S3} = 1$ (***c***); $C = C_3$, $R_{S1} = 0$, $R_{S2} = R_{S3} = 1$ (***d***); $C = C_2$, $R_{S1} = R_{S2} = R_{S3} = 0$(***e***); $C = C_3$, $R_{S1} = R_{S2} = R_{S3} = 0$(***f***).

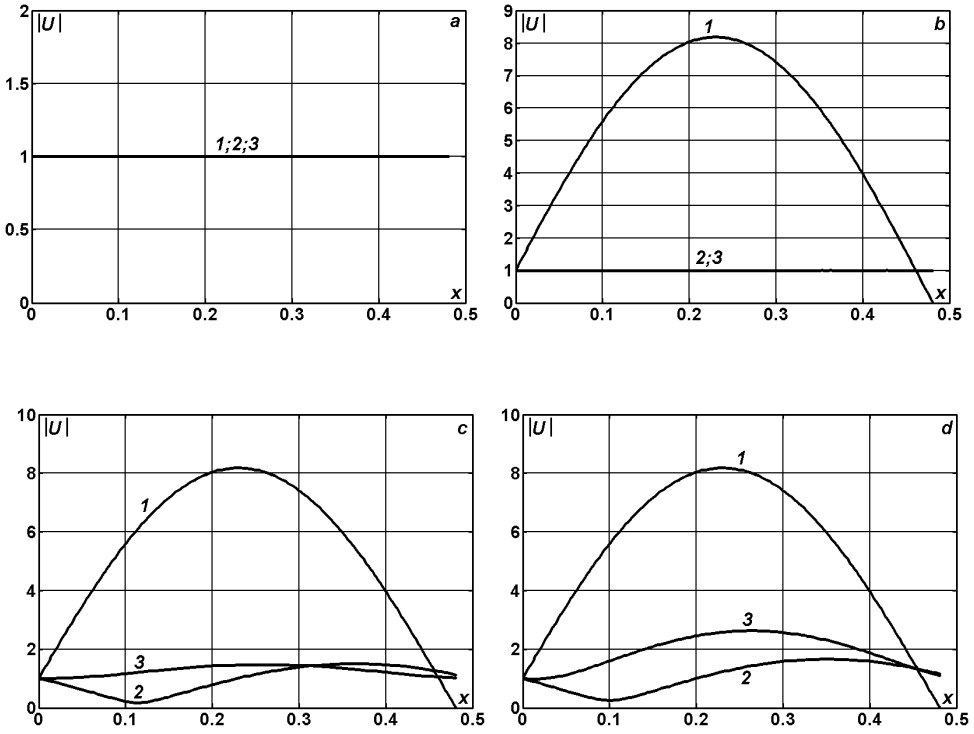

Fig 26.5. Voltage modulus distribution at the phases 1, 2, 3 (curves 1, 2, 3) along the ideal line with length $l = 0.4805$ and $C = C_1$, $R_{S1} = R_{S2} = R_{S3} = 1$(***a***); $C = C_1$, $R_{S1} = 0$, $R_{S2} = R_{S3} = 1$ (***b***); $C = C_2$, $R_{S1} = 0$, $R_{S2} = R_{S3} = 1$ (***c***); $C = C_3$, $R_{S1} = 0$, $R_{S2} = R_{S3} = 1$ (***d***).

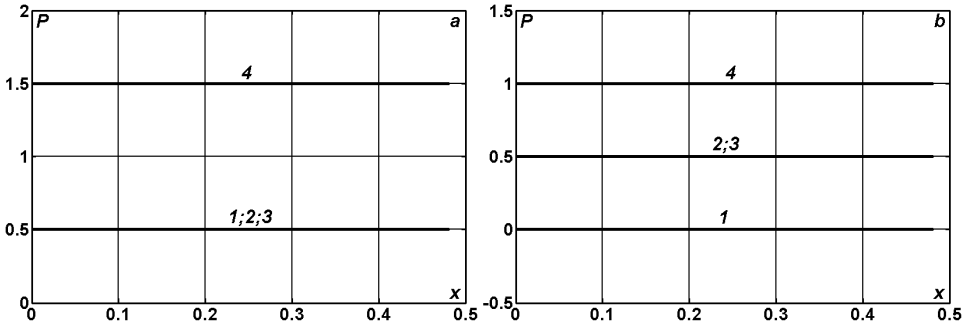

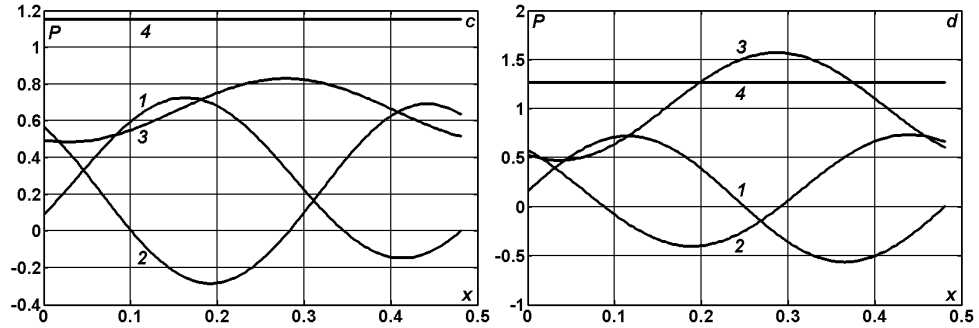

Fig 26.6. Active power distribution at the phases 1, 2, 3 (curves 1, 2, 3) and the total active power distribution (curve 4) along the ideal line with length $l = 0.4805$ and $C = C_1$, $R_{S1} = R_{S2} = R_{S3} = 1$(***a***); $C = C_1$, $R_{S1} = 0$, $R_{S2} = R_{S3} = 1$ (***b***); $C = C_2$, $R_{S1} = 0$, $R_{S2} = R_{S3} = 1$ (***c***); $C = C_3$, $R_{S1} = 0$, $R_{S2} = R_{S3} = 1$ (***d***).

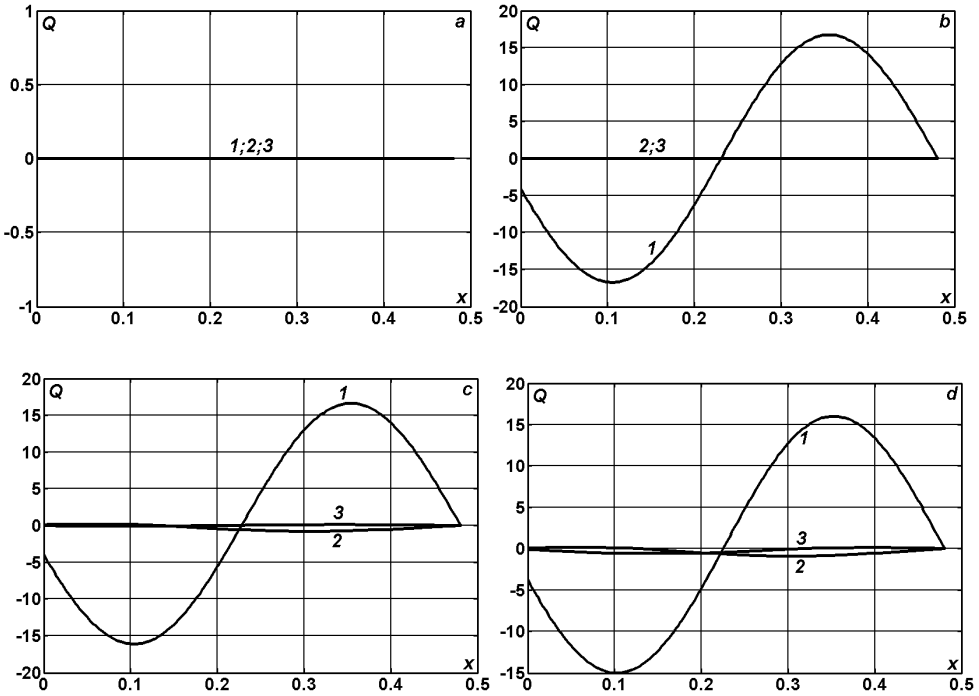

Fig 26.7. Reactive power distribution at the phases 1, 2, 3 (curves 1, 2, 3) along the ideal line with length $l = 0.4805$ and $C = C_1$, $R_{S1} = R_{S2} = R_{S3} = 1$(***a***); $C = C_1$, $R_{S1} = 0$, $R_{S2} = R_{S3} = 1$ (***b***); $C = C_2$, $R_{S1} = 0$, $R_{S2} = R_{S3} = 1$ (***c***); $C = C_3$, $R_{S1} = 0$, $R_{S2} = R_{S3} = 1$ (***d***).

In the fig. 26.8–26.10 we have represented the calculation results for the case when $U_0 = (1, 1, 1)^T$.

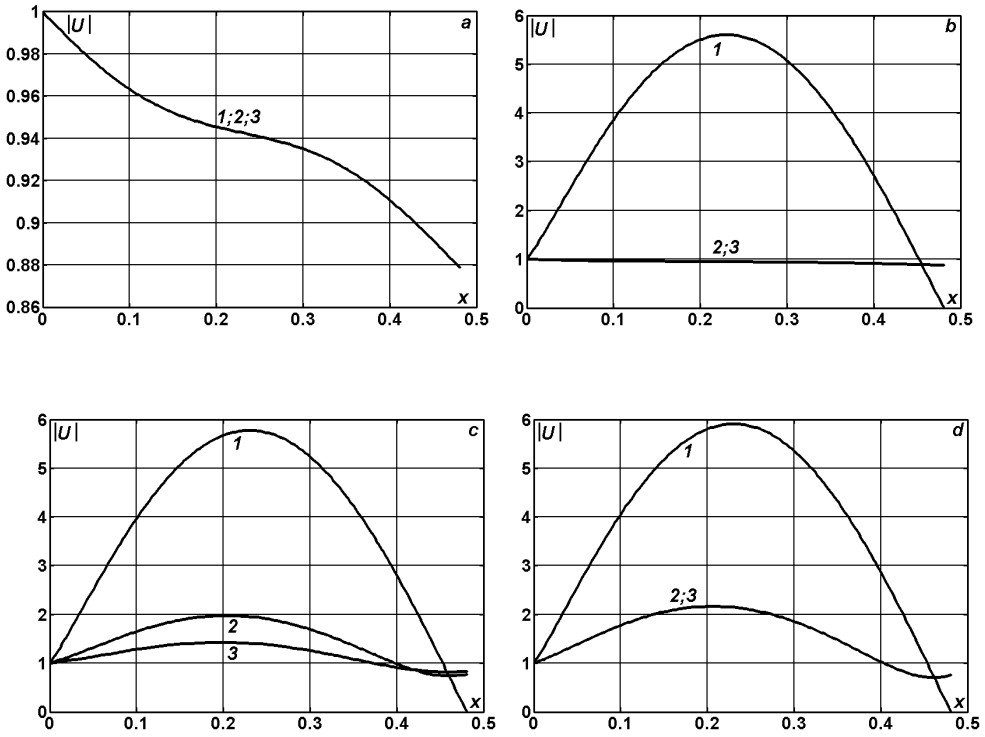

Fig 26.8. Voltage modulus distribution at the phases 1, 2, 3 (curves 1, 2, 3) along the line with length l = 0.4805 when R = 0.48 $G = R/7$ and $C = C_1$, $R_{S1} = R_{S2} = R_{S3} = 1$(***a***); $C = C_1$, $R_{S1} = 0$, $R_{S2} = R_{S3} = 1$ (***b***); $C = C_2$, $R_{S1} = 0$, $R_{S2} = R_{S3} = 1$ (***c***); $C = C_3$, $R_{S1} = 0$, $R_{S2} = R_{S3} = 1$ (***d***).

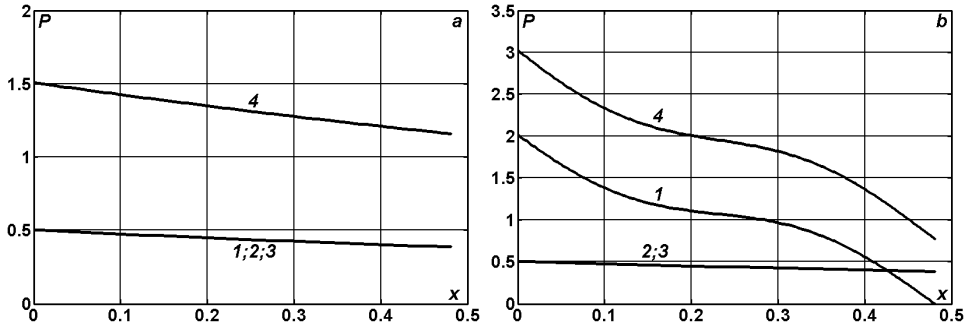

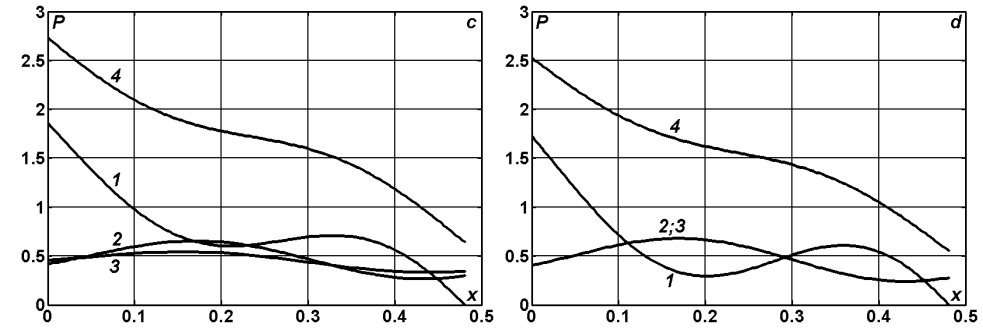

Fig 26.9. Active power distribution at the phases 1, 2, 3 (curves 1, 2, 3) and the total active power distribution (curve 4) along the line with length $l = 0.4805$ when $R = 0.48$ $G = R/7$ and $C = C_1$, $R_{S1} = R_{S2} = R_{S3} = 1$(***a***); $C = C_1$, $R_{S1} = 0$, $R_{S2} = R_{S3} = 1$ (***b***); $C = C_2$, $R_{S1} = 0$, $R_{S2} = R_{S3} = 1$ (***c***); $C = C_3$, $R_{S1} = 0$, $R_{S2} = R_{S3} = 1$ (***d***).

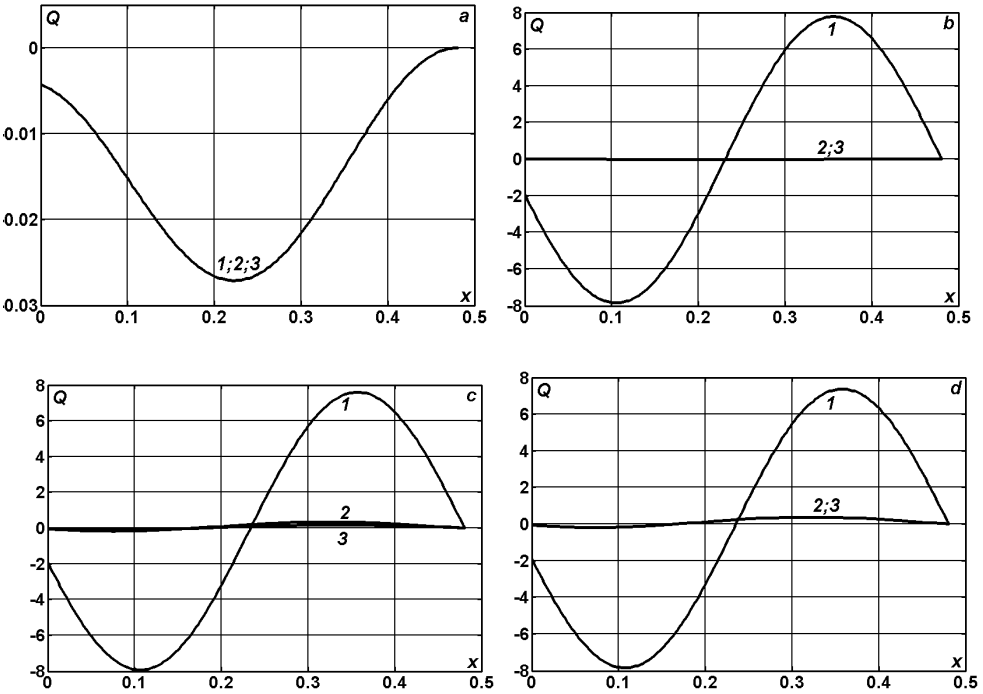

Fig 26.10. Reactive power distribution at the phases 1, 2, 3 (curves 1, 2, 3) along the line with length $l = 0.4805$ when $R = 0.48$ $G = R/7$ and $C = C_1$, $R_{S1} = R_{S2} = R_{S3} = 1$(***a***); $C = C_1$, $R_{S1} = 0$, $R_{S2} = R_{S3} = 1$ (***b***); $C = C_2$, $R_{S1} = 0$, $R_{S2} = R_{S3} = 1$ (***c***); $C = C_3$, $R_{S1} = 0$, $R_{S2} = R_{S3} = 1$ (***d***).

CHAPTER V

ELECTROSTATIC FIELDS IN MULTICONNECTED MEDIUMS: THEORY AND CALCULATIONS

The main subject of the macroscopic electrodynamics is the study of the electromagnetic fields in the substance-filled spaces. The form of the macroscopic electrodynamics equations and the meaning of the contained values depend essentially on the physical nature of the material medium as well as of the field modifications in time. In the general case the electromagnetic fields are described by total system of Maxwell equations that is usually written down in differential and integral form.

The system of equations, containing the Maxwell equations for electromagnetic field and Newton equations for particles, represents the unified system of equations describing all phenomenon conditioned by electromagnetic interaction (without taking into consideration relativistic and quantum effects). Therefore, in the strict sense, they must be solved jointly in electrodynamics problems. However, to solve the problems about electromagnetic field and substance interaction in such general formulation is extremely complicated. The complexity lies in the follows. The substance consists of immense number of particles and the motion of each separate particle can not be described. The same problem appears in classical mechanics when describing the mechanical motion of gases, fluids and solids. To avoid this difficulty the physicists has had to elaborate some special models of mechanical systems: the model of perfectly rigid body, the model of continuum medium, etc. Under the study of charged particles and electromagnetic field interaction it is necessary to introduce some models too. One of the most common models is the model of continuum medium consisting of electrical dipoles (dielectrics). This model of electrical dipole plays an important role in physics since the atoms and molecules represent the systems of charged particles whish are neutral in general, but they can possess nonzero dipole moment and so they can produce the electrical field.

The displacement current discovery gave to Maxwell an opportunity to create the unified theory of electrical and magnetic phenomenon. This theory has clarified all known at that time experimental facts and has predicted some new effects which have been confirmed afterwards. The main corol-

lary of the Maxwell theory was a conclusion about existence of electromagnetic waves propagating with light speed.

In this chapter we will consider sufficiently omnibus technique for elaboration of some numerical models for electromagnetic fields in nonhomogeneous structures. The technique is based on block discretization and finite volume method ideas. The a priori and a posteriori accuracy analysis for some real problems will be fulfilled. The considered problems are of applied importance and at the same time they can be considered as test problem for comparative analysis of the results obtained by another methods implementation.

27. Maxwell equations

The Maxwell equations form a base of the theory. These equations play the similar role in the electromagnetism doctrine as Newton's laws in mechanics or laws of thermodynamics. We cite below the total system of Maxwell equations of the classical electrodynamics in continuous medium [16, 17, 69, 103, 108].

The first pair of Maxwell equations is formed from the following equations:

$$\operatorname{rot} \vec{E} = -\frac{\partial \vec{B}}{\partial t}, \tag{27.1}$$

$$\operatorname{div} \vec{B} = 0. \tag{27.2}$$

Here vector $\vec{E}$ is the vector of electric field strength, $\vec{B}$ is the vector of magnetic field inductance.

The first equation relates the value of $\vec{E}$ with the time variation of vector $\vec{B}$, so this equation represents in essence the electromagnetic induction law. It shows that the source of the vector $\vec{E}$ rotational field is the magnetic rotational field varying in time. The second equation indicates on the absence of magnetic field sources (i.e. magnetic charges) both in vacuum and in magnetized material.

The second pair of Maxwell equations is formed from the equations:

$$\operatorname{rot} \vec{H} = \vec{j} + \frac{\partial \vec{D}}{\partial t}, \tag{27.3}$$

$$\operatorname{div}\vec{D} = \rho, \tag{27.4}$$

where $\vec{D} = \varepsilon_0\vec{E} + \vec{P}$ is the vector of dielectric strain, $\vec{H} = \frac{\vec{B}}{\mu_0} - \vec{M}$ is magnetic field strength, $\vec{M}$ is substance magnetization, $\vec{P}$ is polarization, $\vec{j}$ is the vector of current density, ρ is the charge cubic density.

The first equation establishes the relation between the conduction and displacement currents and the magnetic field generated by these currents. The second equation reveals that off-site charges serve as a sources of vector $\vec{D}$.

The cited above equations represent the differential form of Maxwell equations. It is to mention that only the main characteristics of the field (such as $\vec{E}$ and $\vec{B}$) appear in the first pair of equations. And only the auxiliary quantities $\vec{D}$ and $\vec{H}$ appear in the second pair.

We should mention also that the form of equations (27.2) and (27.4) does not depend on medium availability. At the same time the vectors $\vec{D}$ and $\vec{H}$, as well as the values ρ and $\vec{j}$, contained in equations (27.3) and (27.4), depend on substance properties and on conditions of its positioning. Any macroscopic body, considered as a continuous medium, consists of charged particles (electrons and nucleuses) possessing also magnetic moments and therefore interacting with electromagnetic field, serving at the same time as its sources. Thus, the values $\vec{D}$, $\vec{H}$, ρ and $\vec{j}$ must be determined reasoning from electrical and magnetic properties of the substance.

When deriving the formula (27.1), Maxwell had assumed the variable in time magnetic field causes the field $\vec{E}_B$ appearance in the space independent on wire contour existence in the space. The presence of the contour only allows us to detect the electrical field existence in corresponding space points by inductive current initiation in contour.

Let's consider the case of electromagnetic induction when the wire contour Γ (where the current is induced) is stationary and magnetic flow variation is caused be magnetic field changes. The inductive current appearance indicates that the magnetic field changes result in appearance in the contour of the off-site forces acting on current carriers. These off-site forces are not connected with chemical or thermal processes in the wire. They also can not represent magnetic forces because such forces do not perform the work on charges. It remains to conclude that the inductive current is caused by the

electrical field appeared in the wire. Let's denote the strength of this field by $\vec{E}_B$ (this notation is auxiliary as well as the $\vec{E}_q$). The electromotive force is equal to vector $\vec{E}_B$ circulation over given contour Γ:

$$\varepsilon_i = \int_\Gamma \vec{E}_B \, d\vec{l} \ . \tag{27.5}$$

Let's substitute the expression (27.5) for ε_i in the formula $\varepsilon_i = -\dfrac{d\Phi}{dt}$ and the expression $\int \vec{B} \, d\vec{S}$ for Φ. As a result we get the relation

$$\int_\Gamma \vec{E}_B \, d\vec{l} = -\frac{d}{dt} \int \vec{B} \, d\vec{S} \ .$$

The integral from the right-hand member is taken over arbitrary contour-supported surface. As the contour and the surface are stationary, than the differentiations by time and by surface can trade places:

$$\int_\Gamma \vec{E}_B \, d\vec{l} = -\int_S \frac{\partial \vec{B}}{\partial t} \, d\vec{S} \ . \tag{27.6}$$

Taking into consideration that vector $\vec{B}$ depends on time and on coordinates as well, than we can write down the partial time derivative under the integral sign (integral $\int \vec{B} \, d\vec{S}$ is a function of time only).

The left-hand member of the relation (27.6) we transform by means of Stokes theorem and obtain:

$$\int_S \mathrm{rot}\vec{E}_B \, d\vec{S} = -\int_S \frac{\partial \vec{B}}{\partial t} \, d\vec{S} \ .$$

As the surface of integration is chosen in arbitrary way, then the following equality should be fulfilled

$$\mathrm{rot}\vec{E}_B = -\frac{\partial \vec{B}}{\partial t} \ .$$

At every point of space the field curl $\vec{E}_B$ is equal to the time derivative of vector $\vec{B}$ with opposite sign.

The field $\vec{E}_B$, caused by magnetic field changes, differs essentially from the electrical field $\vec{E}_q$, caused by electrical charges. The electrostatic field is potential, its lines start and finish on the charges. The curl of vector $\vec{E}_q$ is equal to zero at any point:

$$\mathrm{rot}\vec{E}_q = 0.$$

According to the (27.6) the curl of vector $\vec{E}_B$ is not equal to zero. Hence, the field of $\vec{E}_B$, as well as the magnetic field, is rotational field (or curl field). Strength lines of $\vec{E}_B$ are closed.

Thus, the electrical field can be both the potential field ($\vec{E}_q$) and the curl one ($\vec{E}_B$). In general case the electrical field is composed of these two fields. If we sum up $\vec{E}_q$ and $\vec{E}_B$, then we obtain the following equation:

$$\mathrm{rot}\vec{E} = -\frac{\partial \vec{B}}{\partial t}. \qquad (27.7)$$

The existence of the interconnection between the electrical and magnetic fields is a reason why the separated considerations of electrical and magnetic fields have only relative use. Really, electrostatic field is created by system of stationary charges in some coordinate system, but these charges can move relatively another inertial reference system, so they will be mobile in the second system and, hence, will create the magnetic field. Thus, the field, that proves to be "purely" electric or "purely" magnetic relatively some coordinate system, can represent some union of electric and magnetic fields (i.e. unified electromagnetic field) relatively some other reference systems.

When deriving the formula (27.3), Maxwell had revised the equations for curl of vector $\vec{H}$ in case of stationary (not varying in time) electromagnetic field, where the curl of $\vec{H}$ at any point is equal to conduction current density:

$$\text{rot}\vec{H} = \vec{j}\,, \tag{27.8}$$

vector $\vec{j}$ here is connected with charge density at the same point by continuity equation:

$$\nabla \vec{j} = -\frac{d\rho}{dt}\,. \tag{27.9}$$

Electromagnetic field can be stationary only in condition that charge density ρ and current density $\vec{j}$ are independent on time. In this case according to (27.9) the divergence of $\vec{j}$ is equal to zero.

Thus, we can clarify if the equation (27.9) is valid in case of changing in time fields. Let's consider the magnetic field initiated by current under the charging of condenser from the direct voltage source U (fig. 27.1).

This current is not constant in time (at the time moment when the voltage at the condenser becomes equal to U, the current stops). The conduction current lines discontinue at the interval between the condense plates.

$$\int_{S_1} \text{rot}\vec{H}\, d\vec{S} = \int_{S_1} \vec{j}\, d\vec{S}\,.$$

Let's consider the circular contour Γ, covering the wire (where the current flows to condenser), and let's integrate the relation (27.8) over the surface S_1 (this surface crosses the wire and is limited by the contour):

The left-hand member of last relation we transform by means of Stokes theorem and obtain the vector $\vec{H}$ circulation on contour Γ:

$$\int_{\Gamma} \vec{H}\, d\vec{l} = \int_{S_1} \vec{j}\, d\vec{S} = I\,. \tag{27.10}$$

Here I is the current strength that charges the condenser. Now executing the same calculations for the surface S_2, we get evidently incorrect relation:

$$\int_{\Gamma} \vec{H}\, d\vec{l} = \int_{S_2} \vec{j}\, d\vec{S} = 0\,. \tag{27.11}$$

The obtained result indicates that in case of changing in time fields the equation (27.8) no longer is valid. The following conclusion arises here. In

this equation the component depending on arbitrary in time fields is missing. In case of stationary fields this component reduces to zero.

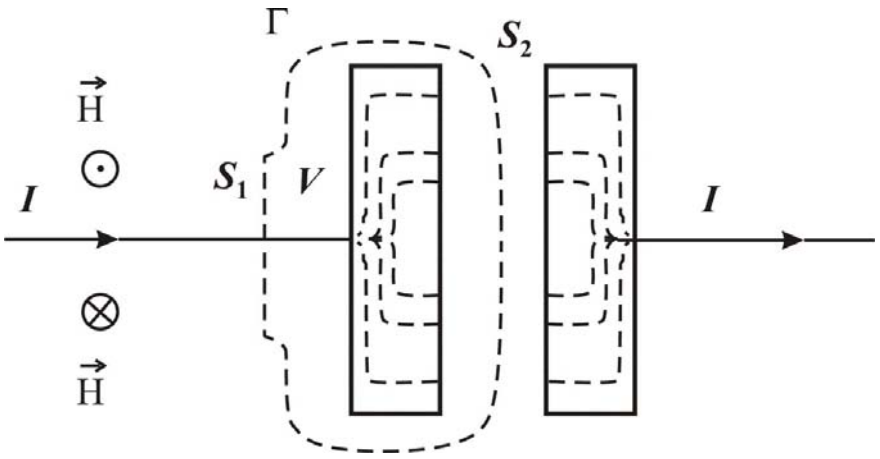

Fig. 27.1. Magnetic field initiated by current under the condenser charging from the direct voltage source.

The non validity of the equation (27.8) in case of nonstationary fields results also from the following considerations. Let's calculate the divergence from both parts of the relation (27.8):

$$\nabla\left[\mathrm{rot}\vec{H}\right] = \nabla\vec{j}.$$

The divergence of the curl must necessarily be equal to zero In this way one can get a conclusion that the divergence of vector $\vec{j}$ also must be always equal to zero. However, this conclusion contradicts with the continuity equation where $\vec{j}$ is nonzero.

To co-ordinate the equations (27.8) and (27.9), Maxwell had introduced an additional component in the right-hand member of the equation (27.8). This component may have the same dimension as current density has. Maxwell proposed to name this component as *displacement current density*. Thus by Maxwell the equation (27.8) must have the form:

$$\mathrm{rot}\vec{H} = \vec{j} + \vec{j}_{disp}\,. \qquad (27.12)$$

It is assumed that the sum of conduction current and of displacement current to be named the net current. The density of the net current is:

$$\vec{j}_{net} = \vec{j} + \vec{j}_{disp} . \tag{27.13}$$

If we assign the divergence of the displacement current equal to the divergence of conduction current with opposite sign

$$\nabla \vec{j}_{disp} = -\nabla \vec{j} , \tag{27.14}$$

then the divergence of the right-hand member of the equation (27.12), as well as the divergence of the left-hand member, always will be equal to zero.

Now let's substitute in (27.14) $\nabla \vec{j}$ according to (27.9) through $\frac{\partial \rho}{\partial t}$. We obtain the following expression for divergence of the displacement current:

$$\nabla \vec{j}_{disp} = \frac{\partial \rho}{\partial t} . \tag{27.15}$$

To get the connection between the displacement current and the values characterizing the electrical field changes in time, we use the relation:

$$\nabla \vec{D} = \rho .$$

After differentiation by time, we obtain:

$$\frac{\partial}{\partial t}\left(\nabla \vec{D}\right) = \frac{\partial \rho}{\partial t} .$$

Now let's change the order of differentiation by time and by coordinates. As a result we get the following expression for derivative of ρ by t:

$$\frac{\partial \rho}{\partial t} = \nabla\left(\frac{\partial}{\partial t}\vec{D}\right).$$

The substitution of this expression in formula (27.15) gives:

$$\nabla \vec{j}_{disp} = \nabla\left(\frac{\partial}{\partial t}\vec{D}\right).$$

In this way we obtain

$$\vec{j}_{disp} = \frac{\partial \vec{D}}{\partial t}. \tag{27.16}$$

Substituting the expression (27.16) in formula (27.13), we get the equation

$$\mathrm{rot}\vec{H} = \vec{j} + \frac{\partial \vec{D}}{\partial t}.$$

Each of the vector equations (27.1) and (27.3) is equivalent to three scalar equations which relate the vector's components from the left-hand and right-hand members of the equalities. Applying the rule of differential operators opening we can write down them as follows:

$$\frac{\partial E_z}{\partial y} - \frac{\partial E_y}{\partial z} = -\frac{\partial B_x}{\partial t};\ \frac{\partial E_x}{\partial z} - \frac{\partial E_z}{\partial x} = -\frac{\partial B_y}{\partial t};$$

$$\frac{\partial E_y}{\partial x} - \frac{\partial E_x}{\partial y} = -\frac{\partial B_z}{\partial t}; \tag{27.17}$$

$$\frac{\partial B_x}{\partial x} + \frac{\partial B_y}{\partial y} + \frac{\partial B_z}{\partial z} = 0 \tag{27.18}$$

for the first pair of equations and:

$$\frac{\partial H_z}{\partial y} - \frac{\partial H_y}{\partial z} = j_x + \frac{\partial D_x}{\partial t};\ \frac{\partial H_x}{\partial z} - \frac{\partial H_z}{\partial x} = j_y + \frac{\partial D_y}{\partial t};$$

$$\frac{\partial H_y}{\partial x} - \frac{\partial H_y}{\partial x} = j_z + \frac{\partial D_z}{\partial t}; \tag{27.19}$$

$$\frac{\partial D_x}{\partial x} + \frac{\partial D_y}{\partial y} + \frac{\partial D_z}{\partial z} = \rho \tag{27.20}$$

for the second pair.

Altogether we obtain 8 equations concerning 12 functions (these are three components of each of the vectors $\vec{E}$, $\vec{B}$, $\vec{D}$, $\vec{H}$). Since the number of equations is smaller then the number of unknown functions, then the equations (27.1) – (27.4) are not enough for fields determination by given charge and current distributions. To realize the field calculations, the Maxwell equations should be enlarged by equations relating $\vec{D}$ and $\vec{j}$ with $\vec{E}$, as well as $\vec{H}$ with $\vec{B}$. These equations have the form:

$$\vec{D} = \varepsilon\varepsilon_0 \vec{E}\ ; \tag{27.21}$$

$$\vec{B} = \mu\mu_0 \vec{H}\ ; \tag{27.22}$$

$$\vec{j} = \sigma\vec{E}\ . \tag{27.23}$$

The set of equations (27.1) – (27.23) forms the foundation of the electrodynamics of quiescent mediums.

Let's consider now the Maxwell equations in integral form.

The first pair:

$$\int_\Gamma \vec{E}\, d\vec{l} = -\frac{d}{dt}\int_S \vec{B}\, d\vec{S}\ ; \tag{27.24}$$

$$\int_S \vec{B}\, d\vec{S} = 0 \tag{27.25}$$

The second pair:

$$\int_{\Gamma} \vec{H}\, d\vec{l} = \int_{S} \vec{j}\, d\vec{S} + \frac{d}{dt}\int_{S} \vec{D}\, d\vec{S}\,; \tag{27.26}$$

$$\int_{S} \vec{D}\, d\vec{S} = \int_{V} \rho dV\,. \tag{27.27}$$

Equation (27.24) can be obtained by integrating (27.1) over arbitrary surface S with the following left-hand member transformation by means of Stokes theorem to the integral over contour Γ, bounding the surface S. The equation (27.26) can be obtained in the same manner from the relation (27.3). Equations (27.25) and (27.27) can be deduced from (27.2) and (27.4) by integrating over arbitrary volume V with the following left-hand member transformation by means of the Gauss–Ostrogradsky theorem to the integral over closed surface S bounding the volume V.

When solving the electrodynamics problems it is considered that all macroscopic bodies are bounded by surfaces. Under the transfer through these surfaces the physical properties of the macroscopic bodies are suddenly changed, therefore the electromagnetic fields generated by these bodies can be suddenly changed too. In other words, the vector functions $\vec{D}$ and $\vec{H}$ are piecewise continuous function of coordinates, i.e. they are continuous with their derivatives inside of each homogeneous domain, but can discontinue at the boundaries between two mediums. In this connection it seems to be more convenient to solve the Maxwell equations (27.1) – (27.4) in each domain bounded by some boundary surface separately and then to combine the obtained solutions by means of boundary conditions.

As to determine the boundary conditions it is convenient to use the integral form of the Maxwell equations. According to the equation (27.4) and to the Gauss–Ostrogradsky theorem we have

$$\int \operatorname{div} \vec{D}\, dV = \int D_n\, dS = \int \rho\, dV = Q\,, \tag{27.28}$$

where Q is the total charge inside the volume of integration.

Let's consider the infinitesimal volume in the form of cylinder with the height h and the base area S, placed in the mediums 1 and 2 (fig. 27.2).

The relations (27.28) in this case can be written down in the form:

$$D_{1n}S - D_{2n}S + \int_{lat} D_n\, dS = Q\,. \tag{27.29}$$

Here $\vec{n}$ is the normal to the boundary between two mediums, directed from the medium 2 to the medium 1. The sign "minus" in the second component is determined by the following: external normal $\vec{n}$ to the surface of integration in the medium 2 is directed oppositely to the normal $\vec{n}$ in the medium 1.

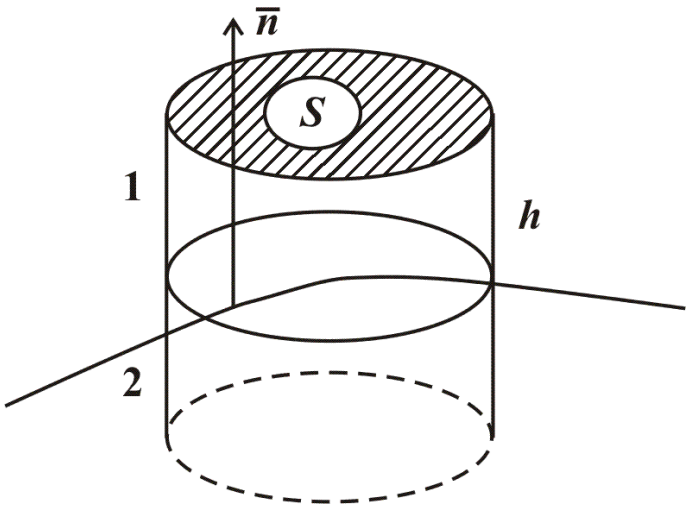

Fig. 27.2. Infinitesimal volume in the form of cylinder with the height *h* and the base area *S*, placed in the mediums 1 and 2.

Let the bases of the cylinder tend to the boundary between two mediums. As the lateral area tends to zero, then $\int\limits_{lat} D_n \, dS \to 0$, and therefore the relation (27.29) takes the form

$$D_{1n} - D_{2n} = \frac{Q}{S} = \sigma, \tag{27.30}$$

where D_{2n} and D_{1n} are the normal components of the vector $\vec{D}$ at the different sides of the boundary surface; σ is the surface density of the charges surplus with respect to the charges of the substance itself. If the boundary surface is uncharged, then in formula (27.30) it is necessary to set $\sigma = 0$. It is convenient to use the notion of surface density when surplus charges are located in a very thin stratum *d* of the substance but the field is considered

at the distance r from the surface and $r >> d$. Then from the definition of the charge cubic density $\rho = \frac{\Delta Q}{\Delta S \cdot d}$ we have:

$$\sigma = \rho d = \frac{\Delta Q}{\Delta S}.$$

Taking into account that $\vec{D} = \varepsilon_0 \vec{E} + \vec{P}$ and $\left(\vec{P} \cdot \vec{n}\right) = P_n$ is the polarized charge surface density, then the formula (27.30) can be written in the form

$$\varepsilon_0 \left(E_{1n} - E_{2n}\right) = \sigma + \sigma_{net},$$

where $\sigma_{net} = P_{2n} - P_{1n} = (\vec{P}_2 - \vec{P}_1) \cdot \vec{n}$ and σ is the surface density of the charges surplus with respect to the bound charges of the substance itself (the value σ appears in the boundary condition (27.30)).

Using the equation (27.2) and realizing the similar reasoning we obtain the boundary condition for vector $\vec{B}$:

$$B_{1n} - B_{2n} = 0 \qquad (27.31)$$

Expressions (27.30) and (27.31) represent the boundary conditions for normal components of the vectors $\vec{B}$ and $\vec{D}$. To obtain the conditions for tangential components one can apply the equations (27.1) and (27.3). Let's multiply scalarwise the equation (27.3) by positive normal $\vec{N}$ to the surface S, bounded by contour L that has a rectangular form (fig. 27.3).

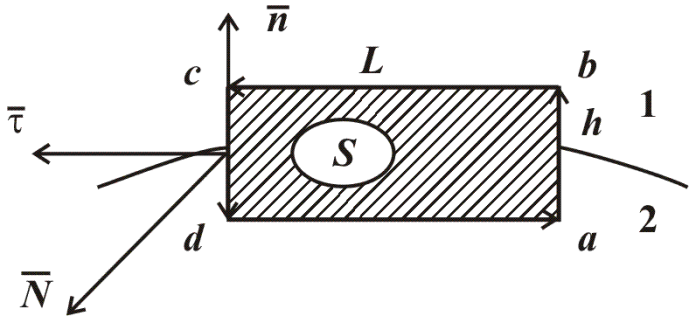

Fig. 27.3. The explanations are in the text.

Applying the Stokes theorem we obtain:

$$\int\left(\vec{N}\cdot \mathrm{rot}\,\vec{H}\right)dS=\int\limits_{L}\left(\vec{H}\cdot d\vec{l}\right)=\frac{\partial}{\partial t}\int\left(\vec{N}\cdot\vec{D}\right)dS+\int\left(\vec{N}\cdot\vec{j}\right)dS\,.$$

Let's rewrite this equation in the form:

$$\int\limits_{L}\left(\vec{H}\cdot d\vec{l}\right)=\int\limits_{a}^{b}H_n\,dh+\int\limits_{b}^{c}\left(\vec{H}_1\cdot\vec{\tau}\right)dl-\int\limits_{d}^{a}\left(\vec{H}_2\cdot\vec{\tau}\right)dl-\int\limits_{d}^{a}H_n dh=$$
$$=\frac{\partial}{\partial t}\int\left(\vec{N}\cdot\vec{D}\right)dhdl+\int\left(\vec{N}\cdot\vec{j}\right)dhdl \qquad (27.32)$$

Here $\vec{H}_1$ and $\vec{H}_2$ are the values of the vector $\vec{H}$ in the mediums 1 and 2 correspondingly, $\vec{\tau}$ is the unit vector tangent to the boundary surface, $\vec{n}$ is the normal to the boundary surface, directed from the medium 2 to the medium 1.

Let now $h\to 0$ when l is small but fixed. Then $\int H_n dh\to 0$, $\int D_n dS\to 0$ and the relation (27.32) takes the form:

$$\left(\vec{H}_1\cdot\vec{\tau}-\vec{H}_2\cdot\vec{\tau}\right)\cdot l=\left(\vec{j}\cdot\vec{N}\right)hl\,.$$

After cancellation by l we get:

$$\left(\vec{H}_1\cdot\vec{\tau}-\vec{H}_2\cdot\vec{\tau}\right)=\left(\vec{j}\cdot\vec{N}\right)h=\left(\vec{i}\cdot\vec{N}\right),$$

where $\vec{i}=\vec{j}\cdot h$. Vector $\vec{\tau}$, as it follows from the fig. 27.3, can be written in the form $\vec{\tau}=\left[\vec{N},\vec{n}\right]$. Then the previous expression takes the following form

$$\left(\vec{H}_1-\vec{H}_2\right)\cdot\left[\vec{N},\vec{n}\right]=\left[\vec{n},\left(\vec{H}_1-\vec{H}_2\right)\right]\cdot\vec{N}=\vec{i}\cdot\vec{N}.$$

Since this formula is valid for any surface orientation (and for any orientation of the vector $\vec{N}$ correspondingly), then we obtain

$$\left[\vec{n},\vec{H}_1\right]-\left[\vec{n},\vec{H}_2\right]=\vec{i}\,. \qquad (27.33)$$

In the boundary condition (27.33) the surface current density (surplus with respect to excitation currents) appears. If the currents are missing, then we should set $\vec{i}$ =0. Taking into account, that $\vec{H} = \frac{\vec{B}}{\mu_0} - \vec{M}$ and $\left[\vec{M}, \vec{n}\right]$ is the surface density of excitation current, we rewrite the formula (27.33) in the form:

$$\left[\vec{n}, \vec{B}_1\right] - \left[\vec{n}, \vec{B}_2\right] = \left(\vec{i} + \vec{i}_{exc}\right)\mu_0,$$

where $\vec{i}_{exc} = \left[\vec{M}_1, \vec{n}\right] - \left[\vec{M}_2, \vec{n}\right] = \left[\left(\vec{M}_1 - \vec{M}_2\right), \vec{n}\right]$.

Using the equation (27.1) and realizing the similar reasoning we obtain the boundary condition for vector $\vec{E}$:

$$\left[\vec{n}, \vec{E}_1\right] - \left[\vec{n}, \vec{E}_2\right] = 0 \qquad (27.34)$$

Thus, the Maxwell equations (27.1) – (27.4) must be completed by boundary conditions (27.30), (27.31), (27.33) and (27.34). These conditions determine the continuity of the vector's $\vec{E}$ tangential components (27.34) and of the vector's $\vec{B}$ normal component (27.31) when transferring the boundary between two mediums. The vector's $\vec{D}$ normal component discontinues when transferring the boundary, the vector's $\vec{H}$ tangential component discontinues also if the surface currents appear (27.33).

One more boundary condition can be obtained by means of continuity equation ($\partial\rho/\partial t + \operatorname{div}\vec{j} = 0$) and equation (27.4):

$$\frac{\partial \rho}{\partial t} + \operatorname{div}\vec{j} = \frac{\partial}{\partial t}\operatorname{div}\vec{D} + \operatorname{div}\vec{j} = \operatorname{div}\left\{\frac{\partial \vec{D}}{\partial t} + \vec{j}\right\}.$$

As the boundary condition (27.31) is a consequence of he equation (27.2), then in the analogous manner we find:

$$\frac{\partial \vec{D}_{1n}}{\partial t} + j_{1n} = \frac{\partial \vec{D}_{2n}}{\partial t} + j_{2n}. \qquad (27.35)$$

If there are no charges with time depending surface density on the boundary surface, then from (27.30) and (27.35) we obtain the continuity of current density normal components:

$$j_{1n} = j_{2n}.$$

Thus, the boundary conditions at the boundary surface between two mediums have the following form:

$$\begin{aligned} &\vec{n}\cdot\left(\vec{D}_1 - \vec{D}_2\right) = \sigma;\ \left[\vec{n},\left(\vec{E}_1 - \vec{E}_2\right)\right] = 0; \\ &\vec{n}\cdot\left(\vec{B}_1 - \vec{B}_2\right) = 0;\ \left[\vec{n},\left(\vec{H}_1 - \vec{H}_2\right)\right] = \vec{i}\ , \end{aligned} \tag{27.36}$$

where $\vec{n}$ is the normal to boundary directed from the medium 2 to the medium 1. These conditions should be fulfilled for any time moment at every point of the boundary surface.

Since the Maxwell equations (27.1) – (27.4) usually are solved in piecewise homogeneous mediums, then the boundary conditions (27.36) should be considered as an integral part of Maxwell equations.

In case of stationary electric and magnetic fields ($\partial\vec{B}/\partial t = 0$ and $\partial\vec{D}/\partial t = 0$) the system of Maxwell equations (27.1) – (27.4) decomposes in two systems:
the system of electrostatics equations:

$$\operatorname{div}\vec{D} = \rho,\ \operatorname{rot}\vec{E} = 0,\ \vec{D} = \varepsilon_0\vec{E} + \vec{P} = \varepsilon_0\varepsilon\vec{E} \tag{27.37}$$

and *the system of magnetostatics equations:*

$$\operatorname{rot}\vec{H} = \vec{j},\ \operatorname{div}\vec{B} = 0,\ \vec{B} = \mu_0\left(\vec{H} + \vec{M}\right) = \mu_0\mu\vec{H}. \tag{27.38}$$

The boundary conditions remain the same.

28. Finite volume method for electrostatic field calculation

The general problem of electric field calculation consists in determination of its strength at each point by means of given charges or potentials. In case of electrostatic field the problem is completely solved by finding the potential as a function of coordinates. If in homogeneous and isotropic medium the electric charges distribution σ is known completely, then the po-

tential distribution u can be obtained by simple integration of the charges over surface of all charged bodies. The inverse problem of finding the charge distribution in accordance with given potential distribution, can be solved by means of Laplace equation and the boundary condition $-\varepsilon\partial u/\partial n = \sigma$ at surface of the charged conducting bodies [34].

However, frequently the problem proves to be more complicated. Generally, one can consider the system of charged conducting bodies circled by dielectric that does not contain the volume charges. In this case or the potentials of all bodies u_1, u_2, …, u_k, or the total charges q_1, q_2, … q_k are given. But the charge distribution on the surface of each body is unknown and remains the subject for determination. The potential distribution in space is unknown as well. The problem became more complicated especially for heterogeneous or anisotropic medium. The solution of such boundary problems with the final analytic representation is possible only for individual particular cases [34].

In this chapter we propose the numerical model for electrostatic field calculation. To obtain this model we use the concepts of finite volume method that has been developed successfully during the last two decades and that finds more and more applications in solving the multidimensional problem of the mathematical physics [47, 90, 99, 117]. The a priori and the a posteriori analysis of the discrete solutions accuracy for bodies with complicated geometry demonstrates that such an approach offers some advantages in comparison with finite difference or with finite element methods [90]. We will try to convince the reader of the truth of this statement by considering some applied problems which are used here as a test problems.

Boundary problem definition. Let's consider the problem of determination of two-dimensional distribution of the electric field potential $u(x, y)$ in the multiply-connected domain Ω. Let the absolute permittivity $\varepsilon_a(x, y)$ possesses the piecewise constant value in this domain. The problem represents the particular case of the three-dimensional problem for cylinder with cross-section Ω, that is infinite in direction of axis z. The function $u(x, y)$ within Ω satisfies the Poisson's equation

$$\operatorname{div}(\varepsilon_a \operatorname{grad} u) = -\sigma(x, y), \tag{28.1}$$

where $\sigma(x, y)$ is the density of free charge distribution. If there are no such charges in the domain Ω, then the equation (28.1) changes into Laplace's equation $\operatorname{div}(\varepsilon_a \operatorname{grad}\varphi) = 0$, and on the boundary $\Gamma = \partial\Omega$ of the domain Ω

the values $u(x, y)$ are considered as known

$$u(x, y)\big|_{\Gamma} = \mu(x, y)\,. \tag{28.2}$$

The field strength vector $\vec{E}$ is determined through the potential u by the formula $\vec{E} = -\text{grad}\,u$, and electrical displacement vector – by $\vec{D} = \varepsilon_a \vec{E}$. At the boundaries between two heterogeneous mediums the continuity conditions $[u] = 0$ and $[(\vec{D}, \vec{n})] = 0$ are fulfilled (square brackets here denote the difference of limit values at the left and at the right of the boundary and $\vec{n}$ is the normal vector to this boundary).

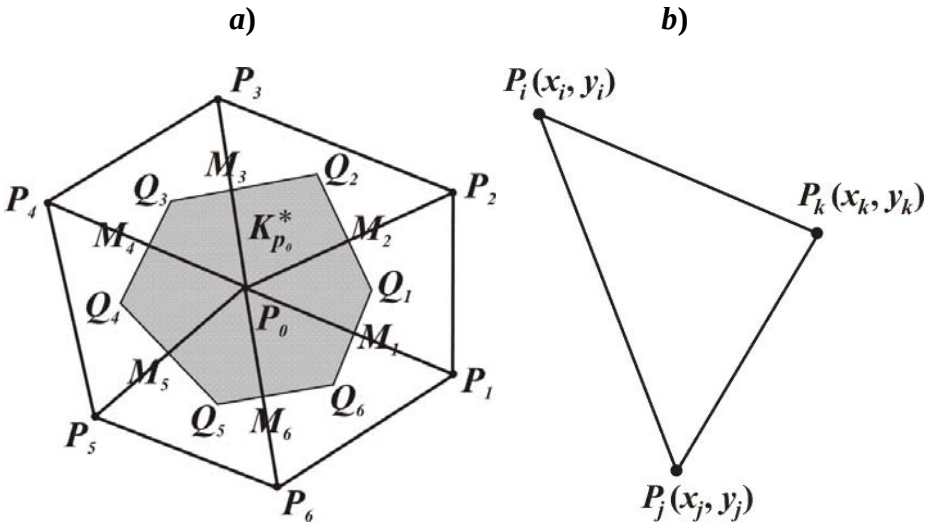

Fig. 28.1. Neighborhood of the grid point P_0 and the Voronoi cell $K^*_{P_0}$ (*a*), the triangle $\Delta P_i P_j P_k$ (*b*).

Discrete model. To solve the Dirichlet's problem let's divide the domain $\overline{\Omega} = \Omega + \Gamma$ into finite set of small triangles. Now all apexes of the triangles constitute the discrete set of grid points, that be imposed upon the continuum $\overline{\Omega}$. The grid must be constructed in such a way as the sides of the triangles to coincide with the interface between two mediums. Let denote by T_h the set of grid triangles, where h is the maximal value of the triangles lateral lengths. Let introduce also the dual grid T_h^* that consists of so-called Voronoi cells (see fig. 28.1, a). The vertexes of Voronoi cell $K^*_{P_0}$

for some grid point P_0 we denote by Q_i. These vertexes Q_i are the centers of the circles circumscribed around the triangles having the point P_0 as an apex.

As an approximate solution of the problem (28.1), (28.2) we consider the piecewise linear function $u_h(x,y)$ that must be continuous in $\overline{\Omega}$ and linear on every triangle $K \in T_h$. The function $u_h(x,y)$ on the set of triangles T_h can be defined in the following manner.

Let the triangle $K = \Delta P_i P_j P_k$ (fig. 28.1, b) be some element of the set T_h and $P(x,y)$ be an arbitrary point of this element. In this triangle for each apex we introduce the shape functions $N_i(x,y)$, $N_j(x,y)$ and $N_k(x,y)$. These functions should verify the following conditions: the functions are linear and their values at the triangle apexes are equal to 0 or 1, i.e.

$$N_i(P_i) = 1;\ N_i(P_j) = N_i(P_k) = 0;$$

$$N_j(P_j) = 1;\ N_j(P_i) = N_j(P_k) = 0;$$

$$N_k(P_k) = 1;\ N_k(P_i) = N_k(P_j) = 0.$$

The shape functions can be represented in the explicit form expressing them through the coordinates of the vertexes

$$N_i(x,y) = \frac{1}{2A}(a_i + b_i x + c_i y),$$
$$a_i = x_j y_k - x_k y_j,\ b_i = y_j - y_k,\ c_i = x_k - x_j;$$

$$N_j(x,y) = \frac{1}{2A}(a_j + b_j x + c_j y), \qquad (28.3)$$
$$a_j = x_k y_i - x_i y_k,\ b_j = y_k - y_i,\ c_j = x_i - x_k;$$

$$N_k(x,y) = \frac{1}{2A}(a_k + b_k x + c_k y),$$
$$a_k = x_i y_j - x_j y_i,\ b_k = y_i - y_j,\ c_k = x_j - x_i.$$

Here A is the area of the triangle

$$2A = \begin{vmatrix} 1 & x_i & y_i \\ 1 & x_j & y_j \\ 1 & x_k & y_k \end{vmatrix}.$$

Using the shape functions for every grid node (internal or boundary) we introduce the basis function $\varphi_i(x, y)$, $i = 1, 2, \ldots, n, n+1, \ldots, n_1$ (n and n_1 represent here the number of internal nodes and the total number of nodes correspondingly). The function $\varphi_i(x, y)$ is piecewise linear, i.e. it is continuous and linear on each triangle with unit value in the node P_i and with zero values in all other nodes. Then the approximate solution $u_h(x, y)$ can be represented as a linear combination of basis functions

$$u_h(x, y) = \sum_{i=1}^{n_1} u_i \varphi_i(x, y). \tag{28.4}$$

Owing to the piecewise linear nature of the constructed basis $\{\varphi_i\}_{i=1}^{n_1}$, the functions u_h represent the elements of Sobolev space $u_h \in W_2^1(\Omega)$. It is easy to verify that the coefficients u_i from (28.4) are equal to the unknown potential values at the node $P_i(x_i, y_i)$, i.e. $u_h(x_i, y_i) = u_i$.

It is to mention here that we apply Galerkin method to solve the problem (28.1), (28.2). This method consists in following. Let's substitute the (28.4) in the equation (28.1) and then write down the condition of orthogonality of obtained expression with respect to basis functions $\varphi_k(x, y)$ for internal nodes

$$\int_\Omega \operatorname{div}(\varepsilon_a \operatorname{grad} u_h)\varphi_k \, ds = -\int_\Omega \sigma \varphi_k \, ds, \quad k = \overline{1, n}; \tag{28.5}$$

$$\int_\Omega \operatorname{div}(\varepsilon_a \operatorname{grad} \sum_{i=1}^{n_1} u_i \varphi_i)\varphi_k \, ds = \sum_{i=1}^{n_1} \alpha_{ki} u_i = \tilde{\beta}_k; \tag{28.6}$$

$$\tilde{\beta}_k = -\int_\Omega \sigma \varphi_k \, ds; \quad \alpha_{ki} = \int_\Omega \operatorname{div}(\varepsilon_a \operatorname{grad} \varphi_i)\varphi_k \, ds = -\int_\Omega \varepsilon_a \operatorname{grad} \varphi_i \operatorname{grad} \varphi_k \, ds.$$

As the solution values are known at the boundary nodes, then the system (28.6) takes the form

$$\sum_{i=1}^{n} \alpha_{ki} u_i = \beta_k \,,\ \beta_k = \widetilde{\beta}_k - \sum_{i=n+1}^{n_1} \alpha_{ki} \mu_i \,,\ k = \overline{1,n} \,. \tag{28.7}$$

In contrast to finite element method the generalized Galerkin method is used in finite volume method. This generalized approach consists in following. There are used basis functions $\psi_k(x,y)$ of the space $W_2^0(\Omega) = L_2(\Omega)$ in the condition of orthogonality (28.5). Let's introduce new basis functions $\psi_k(x,y)$ for dual grid T_h^* by the following rule: function $\psi_k(x,y)$ possesses the constant unit values in the Voronoi cell for internal node P_k and it possesses zero values in the rest of domain. Then the condition of orthogonality (28.5) with functions $\psi_k(x,y)$ gets the form

$$\int_{\Omega} \mathrm{div}(\varepsilon_a \mathrm{grad} u_h) \psi_k \, ds = -\int_{\Omega} \sigma \psi_k \, ds, \ \ k = \overline{1,n} \,. \tag{28.8}$$

Taking into consideration that the function $\psi_k(x,y)$ is nonzero only in $K_{P_0}^*$, we obtain

$$\int_{K_{P_0}^*} \mathrm{div}(\varepsilon_a \mathrm{grad} u_h) ds = -\int_{K_{P_0}^*} \sigma \, ds \,, \tag{28.9}$$

where $K_{P_0}^*$ is Voronoi cell for node P_k.

Thus, to obtain the system of linear algebraic equations with respect to unknown values of the function u_h at the grid points by means of finite volume method we should proceed as follows. Let's consider the Poisson equation $\mathrm{div}(\varepsilon_a \mathrm{grad} u) = -\sigma(x,y,z)$ in three-dimensional space with Cartesian coordinates *Oxyz*. Let's integrate this equation over the volume of the right prism $V_{P_0}^*$ with the base coinciding with the cell $K_{P_0}^*$ and with the height equal to unit and directed on *Oz*-axis. Then we obtain

$$\int\limits_{V_{P_0}^*} \operatorname{div}(\varepsilon_a \operatorname{grad} u)\, dV = -\int\limits_{V_{P_0}^*} \sigma(x, y, z)\, dV\,. \qquad (28.10)$$

Let's mention that the volume of such prism is equal numerically to its base area $V_{P_0}^* = K_{P_0}^*$. For this prism and for function *u*, independent on coordinate *z*, the relation (28.10) coincides with (28.9). Now we apply the divergence theorem to the left-hand member of the (28.10) and obtain

$$\int\limits_{V_{P_0}^*} \operatorname{div}(\varepsilon_a \operatorname{grad} u)\, dV = \int\limits_{\partial V_{P_0}^*} \varepsilon_a \operatorname{grad} u \; d\bar{S} =$$

$$= \int\limits_{\partial V_{P_0}^*} \varepsilon_a (\operatorname{grad} u, \bar{n})\, dS = \int\limits_{\partial V_{P_0}^*} \varepsilon_a \frac{\partial u}{\partial n} dS\,, \qquad (28.11)$$

where $\partial V_{P_0}^*$ is the total surface of the prism $V_{P_0}^*$; $\bar{n}$ is the external normal to the surface $\partial V_{P_0}^*$, and $\partial u / \partial n$ is the derivative of function *u* by this normal. In this case the equation (28.10) takes the form

$$\int\limits_{\partial V_{P_0}^*} \varepsilon_a \frac{\partial u}{\partial n} dS = -\int\limits_{V_{P_0}^*} \sigma(x, y, z) dV\,. \qquad (28.12)$$

As it is supposed that the unknown functions in the problem (28.1) (28.2) are independent on coordinate *z* then the derivative $\partial u / \partial n$ is equal to zero at the prism bases. The lateral surface of the prism $V_{P_0}^*$ consists of the rectangular parts with the unit heights and with the arias numerically equal to the side lengths of the cell $K_{P_0}^*$. Therefore, the integrals from the expression (28.12) can be represented in the following form

$$\int\limits_{\partial V_{P_0}^*} \varepsilon_a \frac{\partial u}{\partial n} dS = \int\limits_{\partial K_{P_0}^*} \varepsilon_a \frac{\partial u}{\partial n} dl\,,\ \int\limits_{V_{P_0}^*} \sigma(x, y, z) dV = \int\limits_{K_{P_0}^*} \sigma(x, y) dS\,,$$

where $\partial K_{P_0}^*$ and $\bar{n}$ are the boundary and the external normal to the cell boundary $K_{P_0}^*$, $\partial u / \partial n$ is the derivative of the function *u* by this normal.

Then the expression (28.12 takes the form.

$$\int\limits_{\partial K^*_{P_0}} \varepsilon_a \frac{\partial u}{\partial n} dl = -\int\limits_{K^*_{P_0}} \sigma(x, y) dS \,. \qquad (28.13)$$

Thus, the solution of the problem (28.1), (28.2) by finite volume method reduces to the approximation of the relation (28.13) for Voronoi cells for internal nodes of the difference grid. The analogous procedure is proper to the finite difference method for grids with rectangular cells. Therefore, the finite volume method can be considered as some generalization of the finite difference method for block discretization with arbitrary shaped cells. By this reason the finite volume method keeps all advantages of the finite difference method. In comparison with finite element method the algorithm of finite-difference approximations here is not so sophisticated and we do not need to construct local and global stiffness matrices when forming the resolving system of equations of type (28.7).

Let's denote in the Voronoi cell $K^*_{P_0}$ (see fig. 28.1, a) by P_m, $m = \overline{0,6}$ the grid nodes; by Q_m, $m = \overline{1,6}$ – the vertexes $K^*_{P_0}$ for the node P_0; by M_m, $m = \overline{1,6}$ – the intersection points of the segments $\overline{P_0 P_m}$ and $\overline{Q_{m-1} Q_m}$. Then the integral from the formula (28.13) over the contour $\partial K^*_{P_0}$ (taking into account that $P_7 = P_1$, $Q_7 = Q_1$, $M_7 = M_1$) we can approximate as follows:

$$\int\limits_{\partial K^*_{P_0}} \varepsilon_a \frac{\partial u}{\partial n} dl = \sum_{i=1}^{6} \int\limits_{\overline{Q_i Q_{i+1}}} \varepsilon_a \frac{\partial u}{\partial n} dl \cong \sum_{i=1}^{6} \varepsilon_a (M_{i+1}) \frac{u(P_{i+1}) - u(P_0)}{\left|\overline{P_0 P_{i+1}}\right|} \left|\overline{Q_i Q_{i+1}}\right|,$$

where $\left|\overline{P_0 P_{i+1}}\right|$ and $\left|\overline{Q_i Q_{i+1}}\right|$ are the lengths of the segments $\overline{P_0 P_{i+1}}$ and $\overline{Q_i Q_{i+1}}$.

The integral from the right-hand member of (28.13) we approximate by formula

$$\int\limits_{K^*_{P_0}} \sigma(x, y) dS = \sigma(P_0) S_0 \,,$$

where S_0 is the area of the Voronoi cell $K^*_{P_0}$. Then the approximation of the equation (28.13) can be represented in the following form

$$\sum_{i=1}^{6} \varepsilon_a(M_{i+1}) \frac{u(P_{i+1}) - u(P_0)}{\left|\overline{P_0 P_{i+1}}\right|} \left|\overline{Q_i Q_{i+1}}\right| = -\sigma(P_0) S_0 .$$

So the final equation for the grid node P_0 takes the following form

$$\alpha_0 u(P_0) + \sum_{i=1}^{6} \alpha_i u(P_{i+1}) = -\sigma(P_0) S_0 ; \qquad (28.14)$$

$$\alpha_i = \varepsilon_a(M_{i+1}) \frac{\left|\overline{Q_i Q_{i+1}}\right|}{\left|\overline{P_0 P_{i+1}}\right|}, \; i = \overline{1,6}; \;\; \alpha_0 = -\sum_{i=1}^{6} \alpha_i$$

$$(P_1 = P_7, \; M_1 = M_7, \; Q_1 = Q_7).$$

Now we can write out the equation in the form of (28.4) for each internal grid node and we use the condition (28.2) for the boundary grid node. As a result, we obtain the system of linear algebraic equations with the symmetrical matrix. It is to mention that when solving the practically important problems the number of equations in such systems amounts to thousands or dozens of thousands. However, since each equation of the type (28.14) contains only some nonzero elements (usually there are from 3 to 9 nonzeros), then it turns out that the final matrix is sufficiently sparse matrix. For matrix inversion of similar type (banded matrix) we use usually Gauss elimination or square-root method.

The convergence of this method will be considered in the next paragraph.

The obtained solution $u_h(x, y)$ for field potential distribution in $\overline{\Omega}$ permits to construct the flux of field strength vector $\vec{E} = (E_x, E_y) = -\text{grad}\, u$. Let denote by V the flux of vector $\vec{E}$ passing through the area that is parallel to the z-axis and the condition $u(x, y) = \text{const}$ is fulfilled on the surface of this area. As it is shown in [34] the functions u and V satisfy the Cauchy-Riemann equations

$$E_x = -\frac{\partial u}{\partial x} = \frac{\partial V}{\partial y};\ \ E_y = -\frac{\partial u}{\partial y} = -\frac{\partial V}{\partial x}, \tag{28.15}$$

therefore the lines $u(x, y) = \text{const}$ and $V(x, y) = \text{const}$ generate the mutually orthogonal families. The function $V(x, y)$ can be obtained by calculation of the contour integral of function $u(x, y)$

$$V(x, y) = \int_{(x_0, y_0)}^{(x, y)} \left(\frac{\partial u}{\partial y} dx - \frac{\partial u}{\partial x} dy \right), \tag{28.16}$$

where x_0, y_0 are the coordinates of an arbitrary point from Ω and the patch of integration is situated inside of domain Ω. In case of multiply-connected domain the patch of integration also can not intersect the cuts of the domain that bring it to simply connected structure.

The capacitance C between two conducting bodies can be computed from the formula

$$C = \frac{q}{u_1 - u_2}, \tag{28.17}$$

where $(u_1 - u_2)$ is potential difference of these bodies. The charge q of the body located inside of the some three-dimensional domain V can be computed in accordance with Gauss' law of flux as a surface integral of the field strength vector $\vec{E}$ over surface $S = \partial V$

$$q = \varepsilon \int_S \vec{E} \cdot d\vec{S} = -\varepsilon \int_S \text{grad} u \cdot d\vec{S} =$$

$$= -\varepsilon \int_S (\text{grad} u \cdot \vec{n}) dS = -\varepsilon \int_S \frac{\partial u}{\partial n} dS. \tag{28.18}$$

Here by S we denoted an arbitrary surface containing the charged body, by $\vec{n}$ – the exterior normal vector to the surface S and by ε – the permittivity.

29. Convergence proof and a priori estimation of discrete solutions accuracy

Let's consider the Dirichlet's problem for elliptical equation that represents a generalization of the problem (28.1), (28.2). It is required to determine the function $u(x_1, x_2)$ that is a solution of the equation

$$Lu = -\left[\frac{\partial}{\partial x_1}\left(k_1(x_1,x_2)\frac{\partial u}{\partial x_1}\right)+\frac{\partial}{\partial x_2}\left(k_2(x_1,x_2)\frac{\partial u}{\partial x_2}\right)\right] = f(x_1,x_2), \qquad (29.1)$$

in the interior of the domain D and on the boundary $\Gamma = \partial D$ it satisfies zero boundary conditions

$$u(x,y)\big|_{\Gamma} = 0. \qquad (29.2)$$

The coefficients of the operator L satisfy the condition of strong ellipticity: $k_j^1 \ge k_j(x_1,x_2) \ge k_j^0 > 0$, $j = 1,2$. Let the right-hand member of (29.1) is quadratic integrable, i.e.. $f \in L_2(D)$. Then the solution of (29.1), (29.2) is the element of the space Q

$$u \in Q(D) = \{u \in W_2^2(D),\ u = 0 \text{ on } \Gamma\}.$$

Let's demonstrate that operator L is symmetrical and positive defined. Since $f \in L_2(D)$, then $Lu \in L_2(D)$. Let's consider the scalar product of Lu and $v \in Q(D)$ in the space L_2

$$(Lu,v) = -\int_D\left[\frac{\partial}{\partial x_1}\left(k_1(x_1,x_2)\frac{\partial u}{\partial x_1}\right)+\frac{\partial}{\partial x_2}\left(k_2(x_1,x_2)\frac{\partial u}{\partial x_2}\right)\right]v(x_1,x_2)dx_1dx_2 .$$

Applying the generalized Green's formula and taking into account the condition $u\big|_{\Gamma} = v\big|_{\Gamma} = 0$, we obtain

$$(Lu,v) = \int_D\left[k_1(x_1,x_2)\frac{\partial u}{\partial x_1}\frac{\partial v}{\partial x_1}+k_2(x_1,x_2)\frac{\partial u}{\partial x_2}\frac{\partial v}{\partial x_2}\right]dx_1dx_2 = (u,Lv), \qquad (29.3)$$

that proves the operator L symmetry.

To prove the positive definiteness of this operator we should prove at first the Friedrichs' inequality. Let's suppose that domain D is rectangular one $D = \{(x_1, x_2) : 0 \le x_k \le l_k, k = 1, 2\}$. Then the Friedrichs' inequality has the form

$$c\left(\left\|\frac{\partial u}{\partial x_1}\right\|^2 + \left\|\frac{\partial u}{\partial x_2}\right\|^2\right)^{1/2} \ge \|u\|, \; u \in W_2^1, u|_\Gamma = 0, c = \min(l_1, l_2)/2. \qquad (29.4)$$

Since the elements of the space W_2^1 may not possess the derivative in the classical meaning, we will consider the consequence $\{u_m\}$ of sufficiently smooth functions that are equal to zero on boundary Γ and converging to $u \in W_2^1$ when $m \to \infty$. As $u_m|_\Gamma = 0$, then the function $u_m(x_1, x_2)$ verifies the identity

$$u_m(x_1, x_2) = \int_0^{x_1} \frac{\partial u(\xi_1, x_2)}{\partial \xi_1} d\xi_1, \; (x_1, x_2) \in D.$$

Let's turn to modules in this equality and then apply the Cauchy-Bunyakovsky inequality. As a result we get

$$|u_m(x_1, x_2)| \le \int_0^{x_1} \left|\frac{\partial u_m(\xi_1, x_2)}{\partial \xi_1}\right| d\xi_1 = \int_0^{x_1} \left(1 \cdot \left|\frac{\partial u_m(\xi_1, x_2)}{\partial \xi_1}\right|\right) d\xi_1 \le$$

$$\le \sqrt{x_1}\left(\int_0^{x_1} \left|\frac{\partial u_m(\xi_1, x_2)}{\partial \xi_1}\right|^2 d\xi_1\right)^{1/2} \le \sqrt{x_1}\left(\int_0^{l_1} \left|\frac{\partial u_m(\xi_1, x_2)}{\partial \xi_1}\right|^2 d\xi_1\right)^{1/2}$$

or

$$|u_m(x_1, x_2)|^2 \le x_1 \int_0^{l_1} \left|\frac{\partial u_m(\xi_1, x_2)}{\partial \xi_1}\right|^2 d\xi_1 .$$

The right-hand member of the last inequality represents a product of two functions: the first one depending on x_1 only and the second one – on x_2 only. Therefore, integrating this inequality over the rectangle D, we obtain

$$\int_D |u_m|^2 dx_1 dx_2 \le \int_0^{l_1} x_1 dx_1 \cdot \int_0^{l_2}\int_0^{l_1} \left|\frac{\partial u_m(\xi_1, x_2)}{\partial \xi_1}\right|^2 d\xi_1 dx_2 =$$

$$= \frac{l_1^2}{2}\int_D \left|\frac{\partial u_m(\xi_1, x_2)}{\partial \xi_1}\right|^2 d\xi_1 dx_2 \text{ or } \|u_m\|^2 \le \frac{l_1^2}{2}\left\|\frac{\partial u_m}{\partial x_1}\right\|^2. \qquad (29.5)$$

In a similar manner the estimation by the variable x_2 can be obtained

$$\|u_m\|^2 = \int_D |u_m|^2 dx_1 dx_2 \le \frac{l_2^2}{2}\cdot\int_D \left|\frac{\partial u_m}{\partial \xi_2}\right|^2 dx_1 d\xi_2 = \frac{l_2^2}{2}\left\|\frac{\partial u_m}{\partial x_2}\right\|^2. \qquad (29.6)$$

Now let's combine (29.5) and (29.6)

$$2\|u_m\|^2 = \|u_m\|^2 + \|u_m\|^2 \le \frac{l_1^2}{2}\left\|\frac{\partial u_m}{\partial x_1}\right\|^2 + \frac{l_2^2}{2}\left\|\frac{\partial u_m}{\partial x_2}\right\|^2.$$

Now we take the square root and get the following inequality

$$\|u_m\| \le \frac{\min(l_1, l_2)}{2}\left(\left\|\frac{\partial u_m}{\partial x_1}\right\|^2 + \left\|\frac{\partial u_m}{\partial x_2}\right\|^2\right)^{1/2}. \qquad (29.7)$$

Let's remind that in W_2^1 the convergence $\partial u_m / \partial x_k \underset{m\to\infty}{\to} \partial u / \partial x_k$ and $u_m \underset{m\to\infty}{\to} u$ holds. So, considering $m \to \infty$ in the last inequality, we obtain the Friedrichs' inequality (29.4).

To prove the Friedrichs' inequality in the arbitrary domain D, one should consider the rectangle Π circumscribed around the D. The function $\widetilde{u}$ is defined in Π so as it is equal to u in the interior of D and it is equal to zero in the $\Pi \backslash D$. Applying the proved above inequality to the function $\widetilde{u}$ and

taking into account that the function $\widetilde{u}$ is equal to zero outside of D, we obtain the inequality (29.4) in the arbitrary domain D.

Now let's prove the positive definiteness of the operator L. Let's consider the inequality (29.3) when $v = u$ and use the condition of ellipticity $k_j(x_1, x_2) \geq k_j^0 > 0,\ j = 1,2$ and the Friedrichs' inequality (29.4)

$$(Lu,u) = \int_D \left(k_1 \left| \frac{\partial u}{\partial x_1} \right|^2 + k_2 \left| \frac{\partial u}{\partial x_2} \right|^2 \right) dx_1 dx_2 \geq$$

$$\geq \min(k_1^0, k_2^0) \int_D \left(\left| \frac{\partial u}{\partial x_1} \right|^2 + \left| \frac{\partial u}{\partial x_2} \right|^2 \right) dx_1 dx_2 \geq \frac{4 \min(k_1^0, k_2^0)}{[\min(l_1, l_2)]^2} \|u\|^2 = \delta \|u\|^2 .$$

Thus, we get

$$(Lu,u) \geq \delta \|u\|^2,\ \delta = \frac{4 \min(k_1^0, k_2^0)}{[\min(l_1, l_2)]^2} > 0, \qquad (29.8)$$

that proves the operator L positive definiteness. The operator L positive definiteness ensures the unique existence of the solution of (29.1), (29.2). The existence of the solution results from the condition $\delta > 0$, that ensures the existence of the inverse operator L^{-1} and, hence, of the solution $u = L^{-1} f$. To prove the uniqueness of solution it is sufficient to suppose that there exists two different solutions u_1 and u_2 and to consider their difference $u = u_1 - u_2$. Since the operator L is linear then the difference u satisfies the homogeneous equation $Lu = 0$. The last equation possesses only zero solution as the operator L is positive defined. Hence, $u_1 = u_2$.

The problem (29.1), (29.2) is solved by means of finite volume method described in details in the previous paragraph. According to this method the approximate solution is sought as an expansion by basis function $\varphi_i(x, y)$, $i = 1, 2, \ldots, n_1$ of the space $W_{2,h}^1 \subset W_2^1$

$$u_h(x, y) = \sum_{i=1}^{n_1} u_i \varphi_i(x, y) . \qquad (29.9)$$

Since the functions φ_i are continuous in D and linear in each triangle of triangulation, then the function u_h is continuous and piecewise linear too, i.e. $u_h \in W_{2,h}^1 \subset W_2^1$. In accordance with Sobolev' theory of interpolation the functions u_h approximate the solution of the problem (29.1), (29.2). Let's prove the approximation theorem in one-dimensional case [67]

Theorem. If $u(x) \in W_2^2(D)$, $D = [a, b]$ then there exists the function $u_h \in W_{2,h}^1(D)$ such as

$$\|u - u_h\|_{L_2(D)} \le c_1 h^2 \|u\|_{W_2^2(D)}, \tag{29.10}$$

$$\|u - u_h\|_{W_2^1(D)} \le c_2 h \|u\|_{W_2^2(D)}, \tag{29.11}$$

where the constants c_1, c_2 are independent on h and on $u(x)$.

Proof. Let on the grid $a = x_0 < x_1 < ... < x_{N-1} < x_N = b$, $h_i = x_i - x_{i-1}$, $h = \max\limits_i h_i$, $i = \overline{1, N}$ the following piecewise linear compact functions are defined

$$\varphi_i(x) = \begin{cases} \dfrac{x - x_{i-1}}{h_i}, x \in [x_{i-1}, x_i] \\ \dfrac{x_{i+1} - x}{h_{i+1}}, x \in [x_i, x_{i+1}] \\ 0, x \notin [x_{i-1}, x_{i+1}] \end{cases};$$

$$\varphi_0(x) = \begin{cases} \dfrac{x_1 - x}{h_1}, x \in [x_0, x_1] \\ 0, x \notin [x_0, x_1] \end{cases}; \quad \varphi_N(x) = \begin{cases} \dfrac{x_N - x}{h_N}, x \in [x_{N-1}, x_N] \\ 0, x \notin [x_{N-1}, x_N] \end{cases}.$$

The functions $\varphi_i(x)$ are linearly independent. Let's denote the linear capsule of the system $\{\varphi_i\}$ by H_N. The functions from H_N are continuous, piecewise linear functions possessing the first derivative that is additive

with any finite order. Therefore, $H_N \subset C(a,b)$, $H_N \subset W_2^1(a,b)$ and H_N can be denoted as $C_h(a,b)$ or $W_{2,h}^1(a,b)$ depending on the space where the approximation is examined by means of $\{\varphi_i\}$.

If we take the finite sum $v_N(x) = \sum_{i=0}^{N} a_i \varphi_i(x) \in H_N$, then it is easy to observe that $a_i = v_N(x_i)$. It is to mention, that the functions $\{\varphi_i\}$ represent the system of almost orthogonal functions, i.e.

$$\int_a^b \varphi_i(x)\varphi_i(x)dx = \begin{cases} = 0, |i-j| > 1 \\ \neq 0, |i-j| \le 1 \end{cases}.$$

This property results in the following: the matrix of the system of linear algebraic equations obtaining by finite volume method has a tridiagonal structure.

Since the function $u(x)$ from $W_2^1(D)$ (and especially from $W_2^2(D)$) is continuous in one-dimensional case, then $u(x)$ possesses the finite value at any grid node x_i, $i = 0, 1, \ldots, N$. Therefore we can consider the linear combination

$$u_h(x) = \sum_{i=0}^{N} u(x_i)\varphi_i(x). \qquad (29.12)$$

Let's estimate the difference $u - u_h$ in the arbitrary point $x \in (x_{i-1}, x_i)$. For that we write down the following inequalities taking into account that the function $u_h(x)$ is piecewise linear and

$du_h(x)/dx = (u(x_i) - u(x_{i-1}))/h_i$ when $x \in (x_{i-1}, x_i)$:

$$u(x) - u_h(x) = \int_{x_{i-1}}^{x} \frac{d}{d\xi}(u - u_h)d\xi = \int_{x_{i-1}}^{x} \left[\frac{du(\xi)}{d\xi} - \frac{du_h(\xi)}{d\xi} \right] d\xi =$$

$$= \int_{x_{i-1}}^{x} \left[\frac{du(\xi)}{d\xi} - \frac{u(x_i) - u(x_{i-1})}{h_i} \right] d\xi = \int_{x_{i-1}}^{x} \left[\frac{du(\xi)}{d\xi} - \frac{1}{h_i} \int_{x_{i-1}}^{x_i} \frac{du(\eta)}{d\eta} d\eta \right] d\xi =$$

$$= \frac{1}{h_i} \int_{x_{i-1}}^{x} \left[\int_{x_{i-1}}^{x_i} \left(\frac{du(\xi)}{d\xi} - \frac{du(\eta)}{d\eta} \right) d\eta \right] d\xi =$$

$$= \frac{1}{h_i} \int_{x_{i-1}}^{x} \left[\int_{x_{i-1}}^{x_i} \left(\int_{\eta}^{\xi} \frac{d^2 u(\zeta)}{d\zeta^2} d\zeta \right) d\eta \right] d\xi . \qquad (29.13)$$

Now we apply the Cauchy-Bunyakovsky inequality to the (29.13) extending at the same time the limits of integration:

$$\left| u(x) - u_h(x) \right| \le \frac{1}{h_i} \int_{x_{i-1}}^{x} \left[\int_{x_{i-1}}^{x_i} \left(\int_{\eta}^{\xi} \left| \frac{d^2 u(\zeta)}{d\zeta^2} \right| d\zeta \right) d\eta \right] d\xi =$$

$$= \frac{1}{h_i} h_i h_i \int_{x_{i-1}}^{x_i} 1 \cdot \left| \frac{d^2 u(\zeta)}{d\zeta^2} \right| d\zeta \le h_i^{3/2} \sqrt{\int_{x_{i-1}}^{x_i} \left| \frac{d^2 u}{d\zeta^2} \right|^2 d\zeta}, \; x \in (x_{i-1}, x_i) .$$

Hence,

$$\left| u(x) - u_h(x) \right|^2 \le h_i^3 \int_{x_{i-1}}^{x_i} \left| \frac{d^2 u}{d\zeta^2} \right|^2 d\zeta ,$$

$$\int_{x_{i-1}}^{x_i} \left| u(x) - u_h(x) \right|^2 dx \le h_i^4 \int_{x_{i-1}}^{x_i} \left| \frac{d^2 u}{dx^2} \right|^2 dx \le h^4 \int_{x_{i-1}}^{x_i} \left| \frac{d^2 u}{dx^2} \right|^2 dx .$$

Summing over $i = 0, 1, \ldots, N$ the last inequalities, we obtain (29.10). If now we will differentiate (29.13) and then implement the same estimations and reasoning, we will obtain (29.11).

So the theorem is proved.

30. Test problems solution and field strength calculation in irregular shaped bodies (a circle in a square)

The analytical representation for electrostatic field strength between two misaligned circular cylinders female each other is presented in [69]. It is reasonable to consider this problem as a test one, supposing the potential at the exterior boundary equal to zero and at inner boundary – equal to ten dimensionless units.

Numerical solution of the problem we begin with the block discretization of the computational domain and finite-difference grid construction. The example of such discretization for the grid with 67 grid nodes is presented in the fig. 30.1. Then, in accordance with algorithms (described for example in [82]), we create Delaunay triangulation and Voronoi diagram for the system of grid nodes. The sides of triangles are represented at fig. 30.1 by firm lines and the sides of Voronoi cells – by dashed lines. After the potential space distribution is determined, we calculate the discrete values of the flux function (field strength) by formulas (28.16).

Some numerical results are represented by diagrams on fig. 30.2. We have here the potential contl curves (continuous lines) and the contl curves for flux function (dashed lines), obtained on the essentially dense grid with 19834 grid nodes. The capacitance calculated on this grid coincides (within third significant digit) with the exact value calculated by formula [69]:

$$C = \frac{2\pi\varepsilon l}{\ln\left[\dfrac{R_2}{R_1}\cdot\dfrac{h_1+\sqrt{h_1^2-R_1^2}}{h_2+\sqrt{h_2^2-R_2^2}}\right]};\ h_1 = \left|\frac{D^2+R_1^2-R_2^2}{2D}\right|;\ h_2 = \left|\frac{D^2+R_2^2-R_1^2}{2D}\right|,$$

where R_1 is the radius of internal cylinder, R_2 is the radius of external cylinder, D is the distance between their centers, ε is the permittivity, l is the height of cylinder for which the capacity is calculated. When $R_1 = 0.3385$ m and $R_2 = 2$ m; $D = 1.1547$ m; $l = 1$ m; $\varepsilon = 8.8542$ pF/km we obtain $C =$ 41.28 pF.

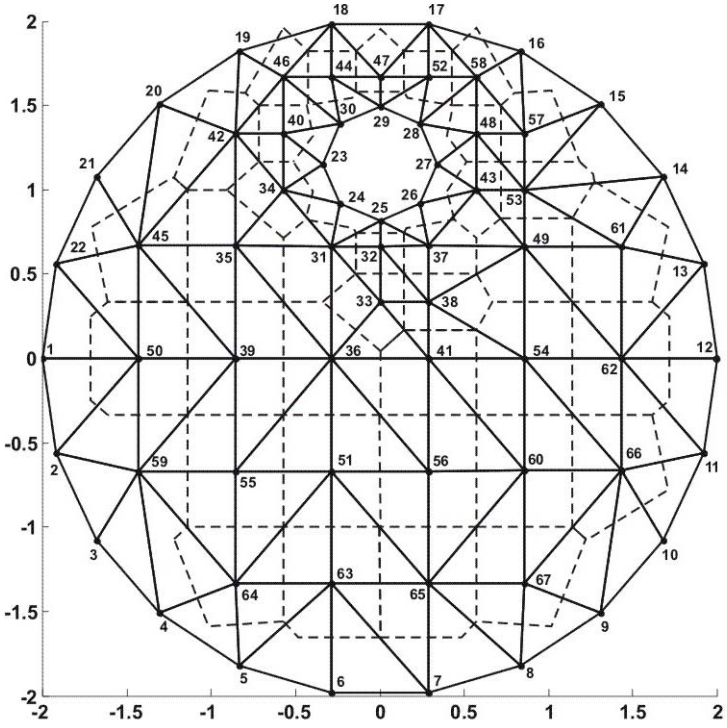

Fig. 30.1. Computational domain discretization, Delaunay triangulation and Voronoi diagram.

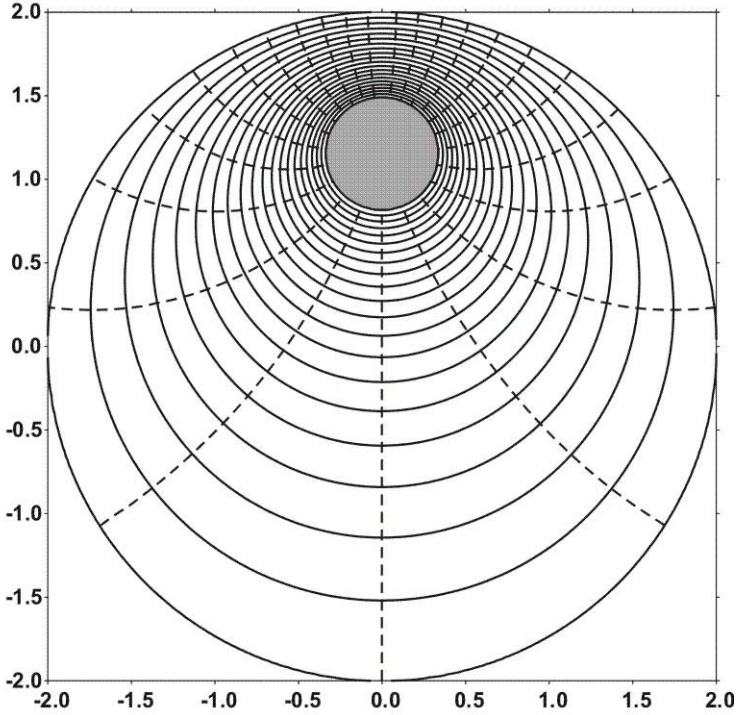

Fig. 30.2. The potential and flux function (field strength) contl curves for two misaligned cylinders.

Let's consider another test problem about the electrostatic field of the single wire with radius R located at a height of h above the earth. The exact solution of this problem is presented in [69] and the formula for capacity calculation is the following

$$C = \frac{2\pi\varepsilon l}{\ln\left[\dfrac{h+\sqrt{h^2-R^2}}{R}\right]}.$$

The computational domain (when R = 0.3385 m and h = 16.8 m) is bounded by the square 360×360 m and the potential is considered equal to zero at this square boundaries.

To optimize the number of grid nodes the non-uniform grid is used with computational cells concentration in vicinity of the wires. In the fig. 30.3 we represent the example of sufficiently coarse non-uniform grid with the grid step equal to 22.5 m near the external boundary and approximating to 7.5 m near the wire. The total number of nodes is equal to 611.

To obtain numerical results with adequate accuracy the problem was solved on an essentially dense grid. The grid step nearby external boundary is equal to 4 m and as verging towards the wires it becomes equal to 0.08 m. The numerical results obtained on the grid with 43300 nodes are represented in the fig. 30.4. The numerical capacitance value 12.10 pF differs from the exact analytical value on 2 units in the fourth significant digit.

Further we will consider some problems for a single wire with rectangular screens. The contl curves of potential and of flow function (continuous and dashed lines correspondingly) are represented in the fig. 30.5 – 30.8. The dimensionless length equal to unity corresponds to 0.1 m in real scale. The indicated capacitance values C = 28.70; 33.08; 33.80; 35.52 pF are calculated when R_1 = 0.01 m; l = 1 m and ε = 8.8542 pF/m. The number of grid nodes is chosen in such a way as their following doubling do not influence upon the third significant digit in the capacitance value C.

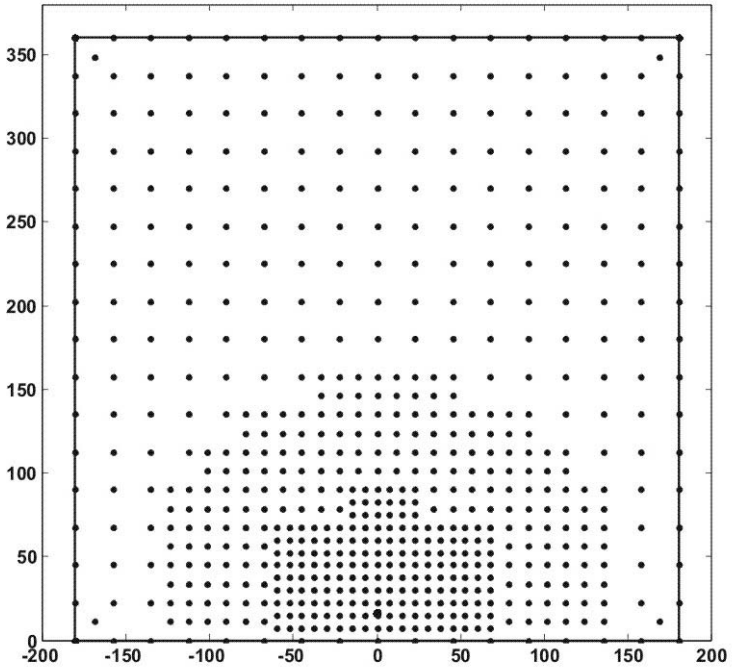

Fig. 30.3. Computational domain discretization.

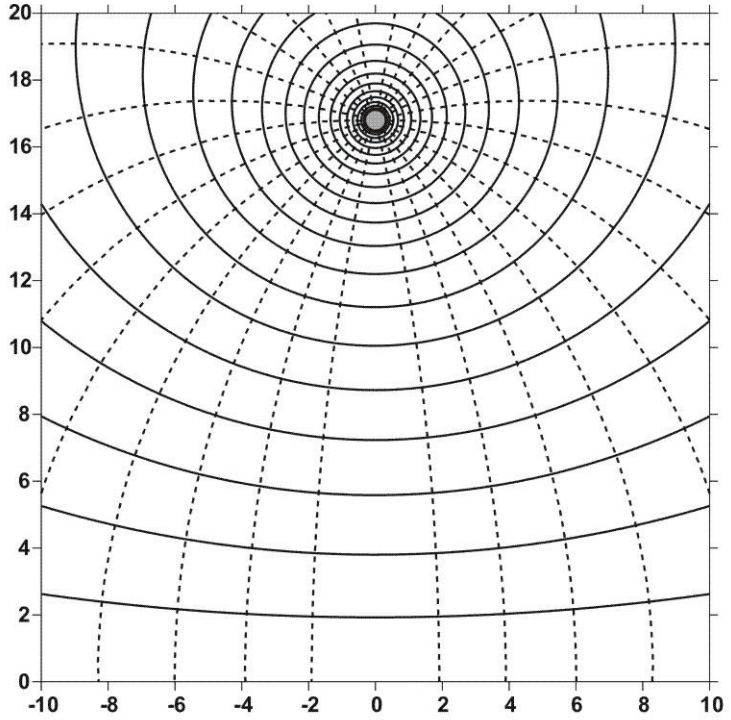

Fig. 30.4. The potential and field strength contl curves for single wire located above the earth.

As may be seen from represented results, the changes in linear dimensions and in external contour configuration (the screen with zero potential) have quite essential influence upon space strength distribution and upon electrical capacitance of doubly-connected domains. The capacitance value increases nonlinearly as the distance between the conducting bodies separated by dielectric sequentially decreases.

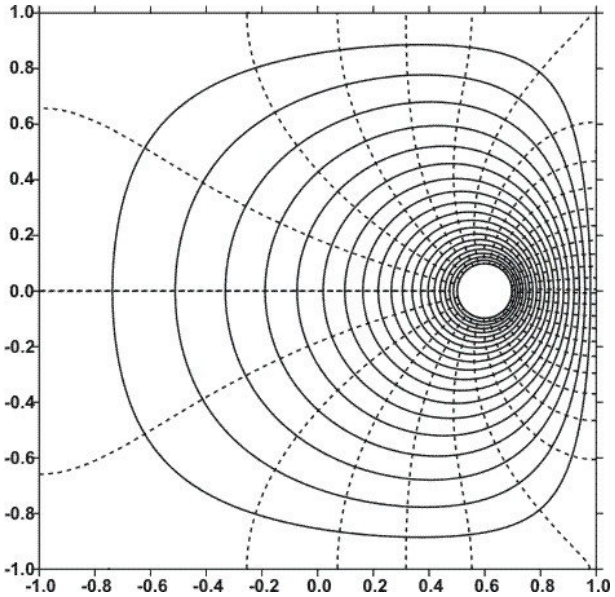

Fig. 30.5. Capacitance calculation C = 28.70 pF on the grid with 40214 nodes.

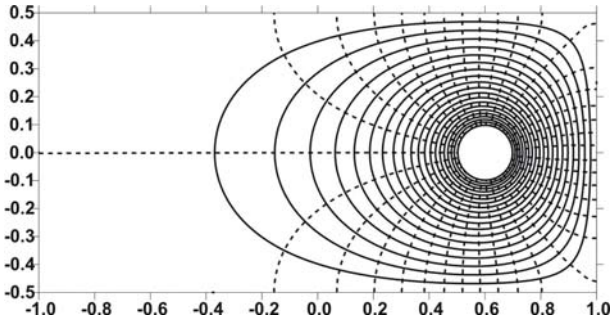

Fig. 30.6. Capacitance calculation C = 33.08 pF on the grid with 12948 nodes.

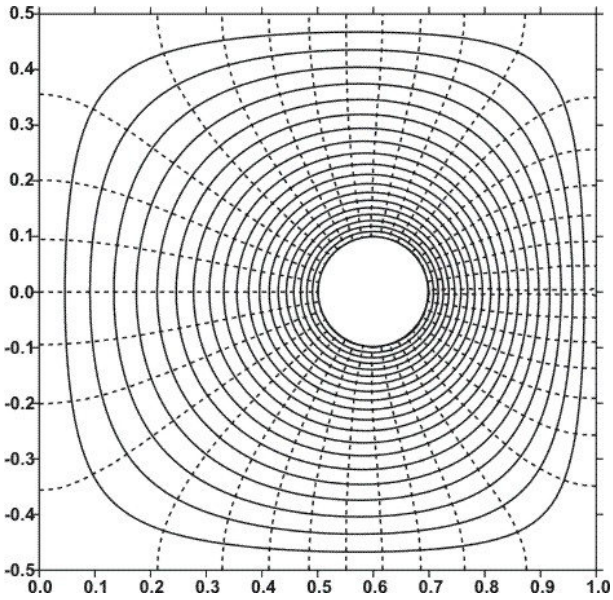

Fig. 30.7. Capacitance calculation $C = 33.80$ pF on the grid with 10014 nodes.

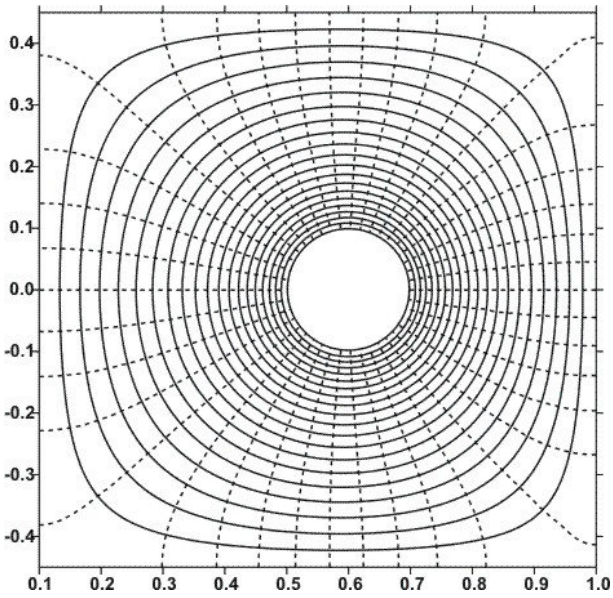

Fig. 30.8. Capacitance calculation $C = 35.52$ pF on the grid with 14253 nodes.

31. Electrostatic fields in the system: three-phase transmission line - earth

Let's consider now a problem that is important for practical implementations. It deals with the three-conductor cable with cylindrical shell used as a screen. This problem has no an analytical solution, therefore it is necessary to analyze the converging discrete solutions on the consequence of grid refinements for accuracy vindication. In the fig. 31.1 we represent the equipotential lines (continuous lines) and strength field contl curves (dashed lines) for typical cable structure. The represented numerical results are obtained on the grid with 18906 nodes. The numerical experiments have demonstrated that the doubling of the grid nodes number results in numerical solution alterations only in fourth significant digit.

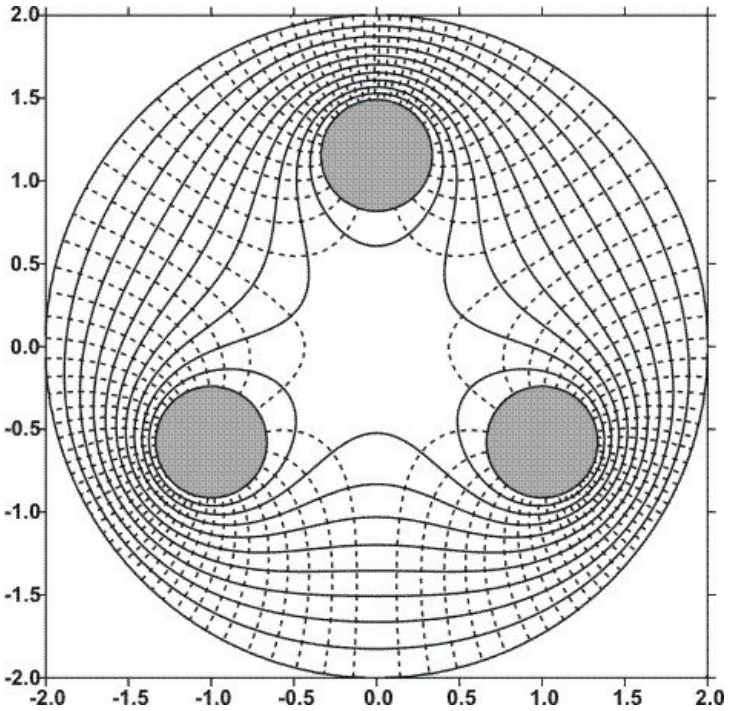

Fig. 31.1. Potential and strength field contl curves for three-conductor cable (the wire radii $R_1 = R_2 = R_3 = 0.3385$ m; the distance between their centers $D = 2$ m and the shell radius $R = 2$ m).

Using the formulas (28.17), (28.18), one can determine the matrix of self and mutual coefficients of electrostatic induction (self-capacitances and

mutual capacitances). The elements of this matrix are used as primary parameters for three-phase transmission:

$$C = \begin{pmatrix} 1.037 & -0.106 & -0.106 \\ -0.106 & 1.037 & -0.106 \\ -0.106 & -0.106 & 1.037 \end{pmatrix} \cdot 41.28 \text{ nF/km}.$$

To calculate the elements from the first row of the matrix C, we should solve the problem with nonzero potential on one of the cable conductors and with zero potential on the others and on the shell as well. When the potential field is calculated, we can determine the charge of every conductor by means of (28.18) and then the values of self and mutual capacitances by means of (28.17).

Let's consider now the problem of electrostatic field determination for the line with triangular layout of wires and with the return (neutral) wire placed in the geometrical center between them. The computational domain (in case when $R_1 = R_2 = R_3 = R_4 = 0.3385$ m, $D = 2$ m and the distance between the lower phases and the earth $H = 16.8$ m) is bounded by the square 360×360 m and the potential is considered equal to zero at this square boundaries.

To optimize the number of grid nodes the non-uniform grid is usually used with computational cells concentration in vicinity of the wires. The grid step nearby external boundary is equal to 4 m and as verging towards the wires it becomes equal to 0.08 m. The numerical results obtained on the grid with 23845 nodes are represented in the fig. 31.2.

The matrix of self and mutual capacitances for indicated conductor's configuration is as follows

$$C = \begin{pmatrix} 30.43 & -4.95 & -4.71 & -15.82 \\ -4.79 & 30.00 & -4.81 & -15.78 \\ -4.71 & -4.95 & 30.43 & -15.82 \\ -15.88 & -15.57 & -15.60 & 48.98 \end{pmatrix} \text{ nF/km}.$$

If in order to calculate the elements of this matrix we use the approximate formulas from [69], where the wire thickness is not taken into account, then we obtain the quantitative differences (disparity) in the first-second significant digit

$$C = \begin{pmatrix} 27.54 & -3.96 & -3.81 & -14.42 \\ -3.96 & 27.25 & -3.96 & -14.44 \\ -3.81 & -3.96 & 27.54 & -14.42 \\ -14.42 & -14.44 & -14.42 & 43.83 \end{pmatrix} \text{ nF/km.}$$

In the fig. 31.3 we represent the potential and strength field contl curves for three-phase line with triangular layout of wires. These results are obtained on the grid with 15106 nodes and with minimal grid step equal to 0.11 m.

The matrix of self and mutual capacitances is the following:

$$C = \begin{pmatrix} 23.72 & -8.75 & -8.89 \\ -9.12 & 22.56 & -9.01 \\ -8.89 & -8.75 & 23.72 \end{pmatrix} \text{ nF/km.}$$

When the wire thickness is not taken into account we obtain the disparity in the second-third significant digit:

$$C = \begin{pmatrix} 22.79 & -8.71 & -8.56 \\ -8.71 & 22.50 & -8.71 \\ -8.56 & -8.71 & 22.79 \end{pmatrix} \text{ nF/km.}$$

If we will layout the conductors horizontally, then we obtain the results represented in the fig. 31.4, where the distances between the wires vary from 1 m to 12 m.

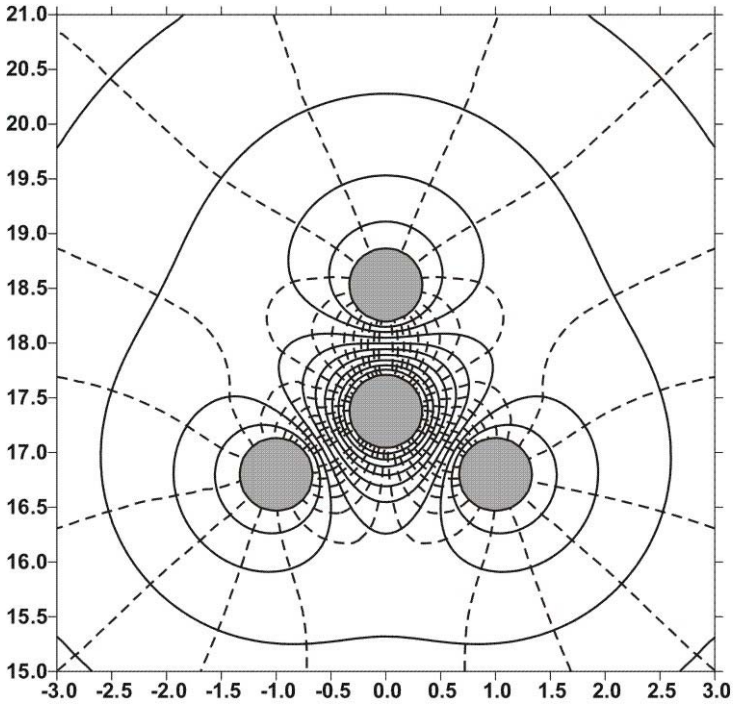

Fig. 31.2. Potential and strength field contl curves for three-phase line with zero return wire.

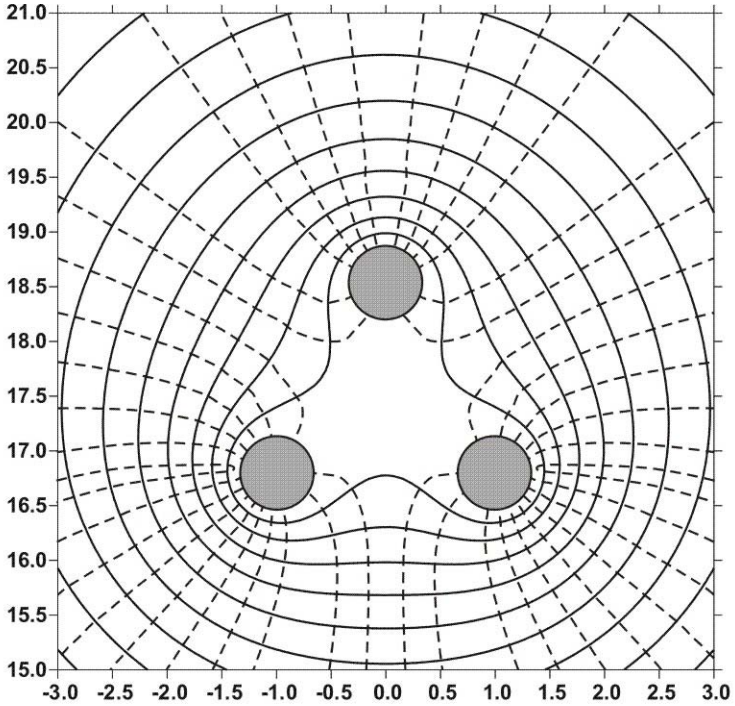

Fig. 31.3. Potential and strength field contl curves for three-phase line.

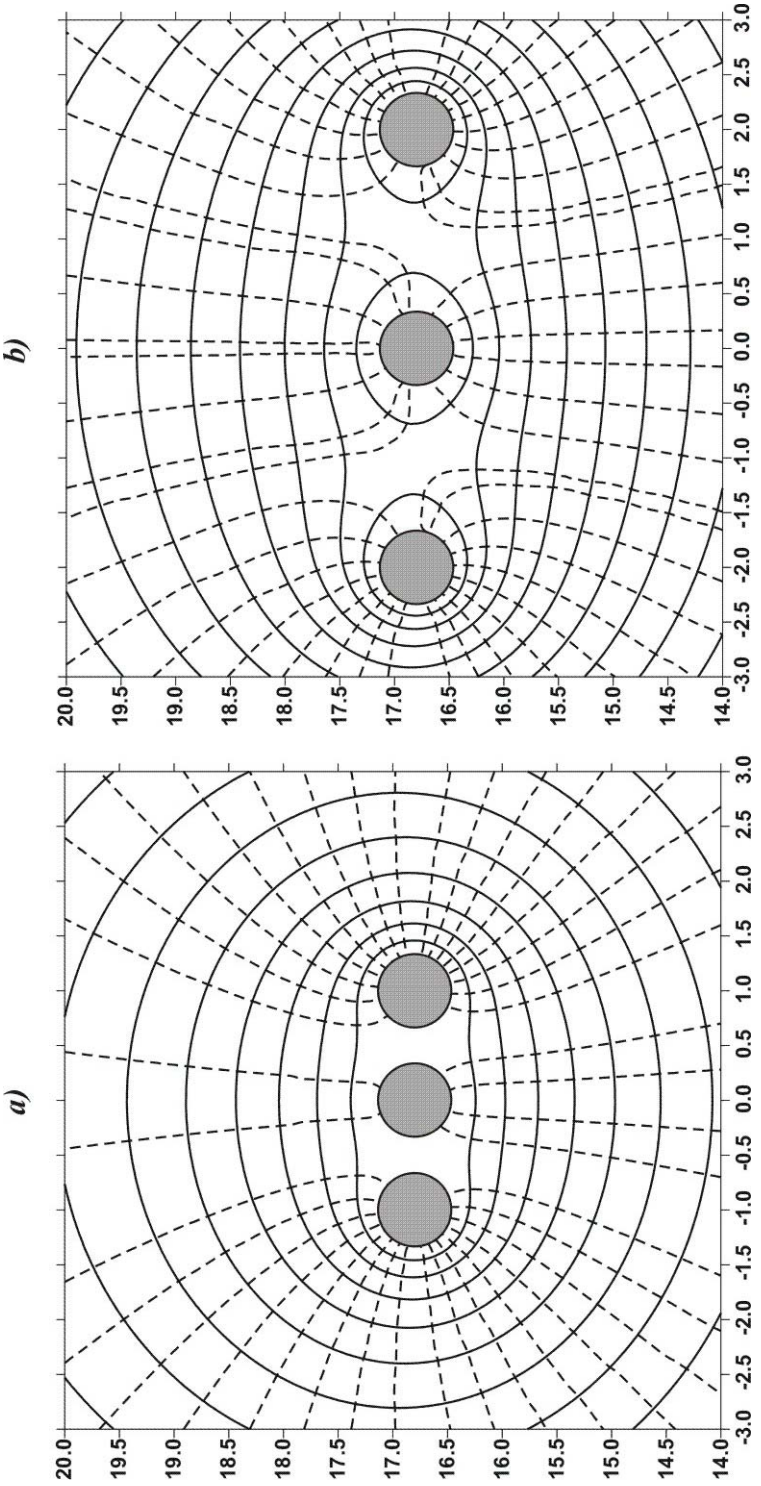
a)
b)
20.0
19.5
19.0
18.5
18.0
17.5
17.0
16.5
16.0
15.5
15.0
14.5
14.0
3.0
2.5
2.0
1.5
1.0
0.5
0.0
-0.5
-1.0
-1.5
-2.0
-2.5
-3.0

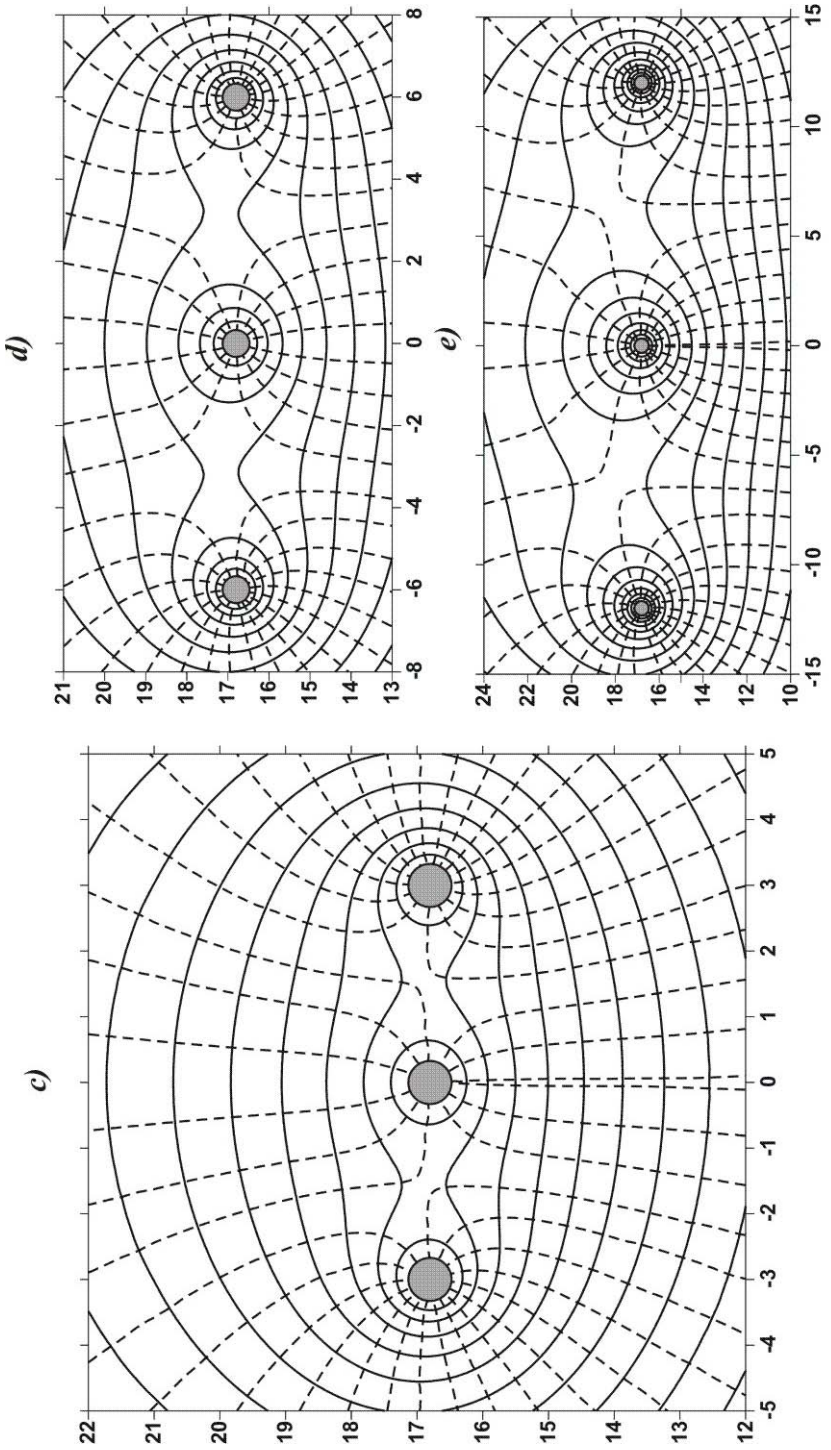

Fig. 31.4. Field contl curves when the distance between the horizontally layout wires is equal to 1 (***a***), 2 (***b***), 3 (***c***), 6 (***d***), 12 (***e***).

The capacitance matrices are cited below in the same order as in the figures (the matrix obtained by numerical solution and the matrix obtained by approximate formulas from [69]):

$$C = \begin{pmatrix} 31.98 & -22.99 & -4.04 \\ -22.99 & 50.90 & -22.99 \\ -4.04 & -22.99 & 31.98 \end{pmatrix}; \quad C = \begin{pmatrix} 29.27 & -20.78 & -2.08 \\ -20.78 & 43.87 & -20.78 \\ -2.08 & -20.78 & 29.27 \end{pmatrix} \text{ nF/km;}$$

$$C = \begin{pmatrix} 20.37 & -10.64 & -3.05 \\ -10.64 & 25.34 & -10.64 \\ -3.05 & -10.64 & 20.37 \end{pmatrix}; \quad C = \begin{pmatrix} 19.81 & -10.46 & -2.78 \\ -10.46 & 24.94 & -10.46 \\ -2.78 & -10.46 & 19.81 \end{pmatrix} \text{ nF/km;}$$

$$C = \begin{pmatrix} 17.24 & -7.76 & -2.47 \\ -7.76 & 20.38 & -7.76 \\ -2.47 & -7.76 & 17.24 \end{pmatrix}; \quad C = \begin{pmatrix} 17.07 & -7.73 & -2.39 \\ -7.73 & 20.23 & -7.73 \\ -2.39 & -7.73 & 17.07 \end{pmatrix} \text{ nF/km;}$$

$$C = \begin{pmatrix} 14.35 & -4.81 & -1.58 \\ -4.81 & 15.79 & -4.81 \\ -1.58 & -4.81 & 14.35 \end{pmatrix}; \quad C = \begin{pmatrix} 14.29 & -4.81 & -1.57 \\ -4.81 & 15.74 & -4.81 \\ -1.57 & -4.81 & 14.29 \end{pmatrix} \text{ nF/km;}$$

$$C = \begin{pmatrix} 13.02 & -2.88 & -0.84 \\ -2.88 & 13.57 & -2.88 \\ -0.84 & -2.88 & 13.02 \end{pmatrix}; \quad C = \begin{pmatrix} 12.88 & -2.85 & -0.84 \\ -2.85 & 13.45 & -2.85 \\ -0.84 & -2.85 & 12.88 \end{pmatrix} \text{ nF/km.}$$

It is to mention that, as the distance between the wires increases, the accuracy of approximate calculation of matrix elements increases right up to third significant digit.

32. Space distribution of potential in high-voltage divider

The necessity of the precise electrical capacity determination in the multiply connected piecewise-homogeneous bodies, where the potential is known at the opened contours, often appears in the engineering practice. The determination of the electrostatic fields and capacities of the high-voltage resistors (potential dividers), implemented on the base of microwire and protected by the conical or cylindrical screens (fig. 32.1), belongs to such problems with degenerated boundary conditions. Such a problem definition does not present the classical Dirichlet's problem for simply connected or multiply connected domain since the boundary conditions are specified not only at the exterior boundary, but at the two broken lines inside the domain of solution existence as well.

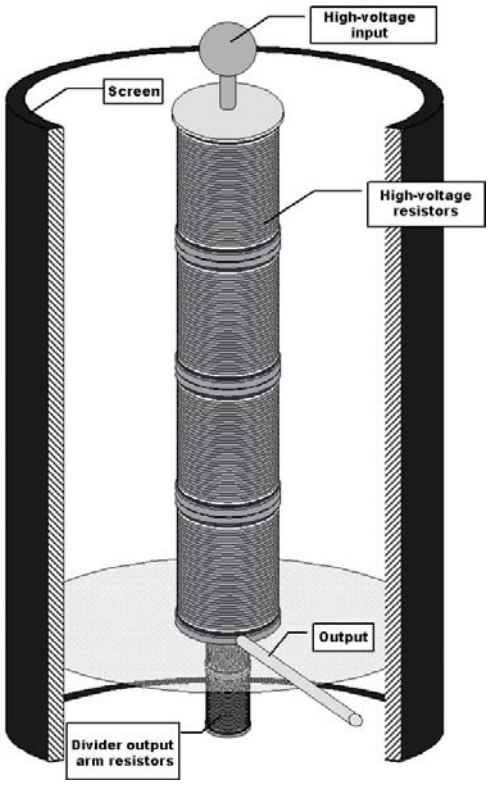

Fig. 32.1. General view of the high-voltage resistor with cylindrical screen.

As the considered problem possesses the axial symmetry property, then, to obtain the system of linear algebraic equations with respect to unknown function values u_h at the grid nodes, we will proceed as follows. Let's consider in a three-dimensional space with Cartesian coordinates *Oxyz* the Poisson's equation $\mathrm{div}(\varepsilon_a \mathrm{grad} u) = -\sigma(x, y, z)$. We direct the *Oz* axis to the resistor rotation axis and then we consider two-dimensional domain Ω in the half-plane *Oxz*. This domain is generated by intersection of the three-dimensional resistor with the positive half-plane $\{ y = 0; \quad x \geq 0; \quad z \in (-\infty, \infty) \}$. Now in Ω we introduce the system of finite-difference grid nodes, execute the triangulation and carry out the Voronoi diagram (the procedure is described in details in the paragraph 28). Then we integrate the Poisson equation over the volume of the curvilinear prism $V^*_{P_0}$ obtained by rotation of the Voronoi cell $K^*_{P_0}$ around the *Oz* axis on the angle equal to one radian. As a result we obtain

$$\int\limits_{V^*_{P_0}} \mathrm{div}(\varepsilon_a \mathrm{grad} u) dV = -\int\limits_{V^*_{P_0}} \sigma(x, y, z)\, dV \,. \tag{32.1}$$

Now let's apply the divergence theorem to the left-hand member of the (32.1)

$$\int\limits_{V^*_{P_0}} \mathrm{div}(\varepsilon_a \mathrm{grad} u) dV = \int\limits_{\partial V^*_{P_0}} \varepsilon_a \mathrm{grad} u \; d\overline{S} =$$

$$= \int\limits_{\partial V^*_{P_0}} \varepsilon_a (\mathrm{grad} u, \overline{n})\, dS = \int\limits_{\partial V^*_{P_0}} \varepsilon_a \frac{\partial u}{\partial n} dS \,, \tag{32.2}$$

where $\partial V^*_{P_0}$ is the total surface of the prism $V^*_{P_0}$; $\overline{n}$ is the external normal to the surface $\partial V^*_{P_0}$, and $\partial u / \partial n$ is the derivative of function *u* by this normal. Then the equation (32.1) can be transformed to the form

$$\int\limits_{\partial V^*_{P_0}} \varepsilon_a \frac{\partial u}{\partial n} dS = -\int\limits_{V^*_{P_0}} \sigma(x, y, z) dV \,. \tag{32.3}$$

As the unknown functions are independent on the rotation coordinate φ, then the derivative $\partial u / \partial n$ is equal to zero at the prism base. The lateral surface of the prism $V^*_{P_0}$ consists of the conical parts with the arias numerically equal to the product of the side lengths of the cell $K^*_{P_0}$ and half-sum of the distances along *Ox* axis between the corresponding cell vertexes and the rotation axis and the rotation angle $\Delta\varphi = 1$. The prism volume $V^*_{P_0}$ is equal to the product of the aria of the cell $K^*_{P_0}$ and the angle $\Delta\varphi = 1$. Therefore, the integrals from the expression (32.3) can be represented in the following form

$$\int\limits_{\partial V^*_{P_0}} \varepsilon_a \frac{\partial u}{\partial n} dS = \int\limits_{\partial K^*_{P_0}} x_Q \varepsilon_a \frac{\partial u}{\partial n} dl\,, \quad \int\limits_{V^*_{P_0}} \sigma(x,y,z) dV = \int\limits_{K^*_{P_0}} \sigma(x,z) dS\,,$$

where $\partial K^*_{P_0}$ and $\overline{n}$ are the boundary and the external normal to the boundary of the cell $K^*_{P_0}$, x_Q is the coordinate *x* of the point located at the middle of the corresponding side of the cell $K^*_{P_0}$, and $\partial u / \partial n$ is the derivative of the function *u* by the normal

Then the expression (32.3) takes the form.

$$\int\limits_{\partial K^*_{P_0}} x_Q \varepsilon_a \frac{\partial u}{\partial n} dl = -\int\limits_{K^*_{P_0}} \sigma(x,z) dS\,. \tag{32.4}$$

Approximating the equation (32.4) by the cell $K^*_{P_0}$, we obtain the equation (it is analogous with equation (28.14)) for the node P_0:

$$\alpha_0 u(P_0) + \sum_{i=1}^{6} \alpha_i u(P_{i+1}) = -\sigma(P_0) S_0\,; \tag{32.5}$$

$$\alpha_i = \varepsilon_a(M_{i+1}) \frac{\left|\overline{Q_i Q_{i+1}}\right|}{\left|\overline{P_0 P_{i+1}}\right|} \cdot \frac{r_{Q_i} + r_{Q_{i+1}}}{2},\ i = \overline{1,6};\ \ \alpha_0 = -\sum_{i=1}^{6} \alpha_i$$

$$(P_1 = P_7,\ M_1 = M_7,\ Q_1 = Q_7).$$

The equations of the type (32.5), written for every internal node, generate the system of equations with the solution that represents the potential distribution in the system resistor – dielectric (air) – screen. The conjunction conditions are fulfilled automatically in this case as well as in case of homogeneous finite difference scheme for piecewise homogeneous mediums.

The fig. 32.2 and fig. 32.3 represent the potential and field strength contl curves for typical constructions of resistive divider with screen and without it. The resistor represents the hollow glass cylinder with the height H_1 = 120 mm, the external diameter D_1 = 28 mm and the internal diameter D_2 = 18 mm. The screen is of cylindrical form with the height H = 220 mm and the diameter D = 75 mm or conical form with the height H = 220 mm; the lower diameter D_0 = 28 mm and the top diameter D_1 = 105 mm or 135 mm. The relative dielectric constant for glass is e_1 = 6, and it is e_2 = 1 for the air filling the internal and external frame hollows. The potential is given at the inner boundaries and it is linearly decreasing from 10 dimensionless units to zero.

The comparative analysis of the presented results shows that the presence of the screen with indicated dimensions approximately duplicates the electrical capacity of divider. Furthermore, the modifications of shape of the screening surface with zero potential reveal the high order effects with the object of constructive optimization reasoning from concrete technical requirements.

The fig. 32.4, 32.5 represent the potential and field strength contl curves for typical constructions of resistive voltage divider with the screens of cylindrical and conical forms under the constant potential along the winding. In this case, the field is missing inside the divider since the potential is quite closed to constant given at the contour.

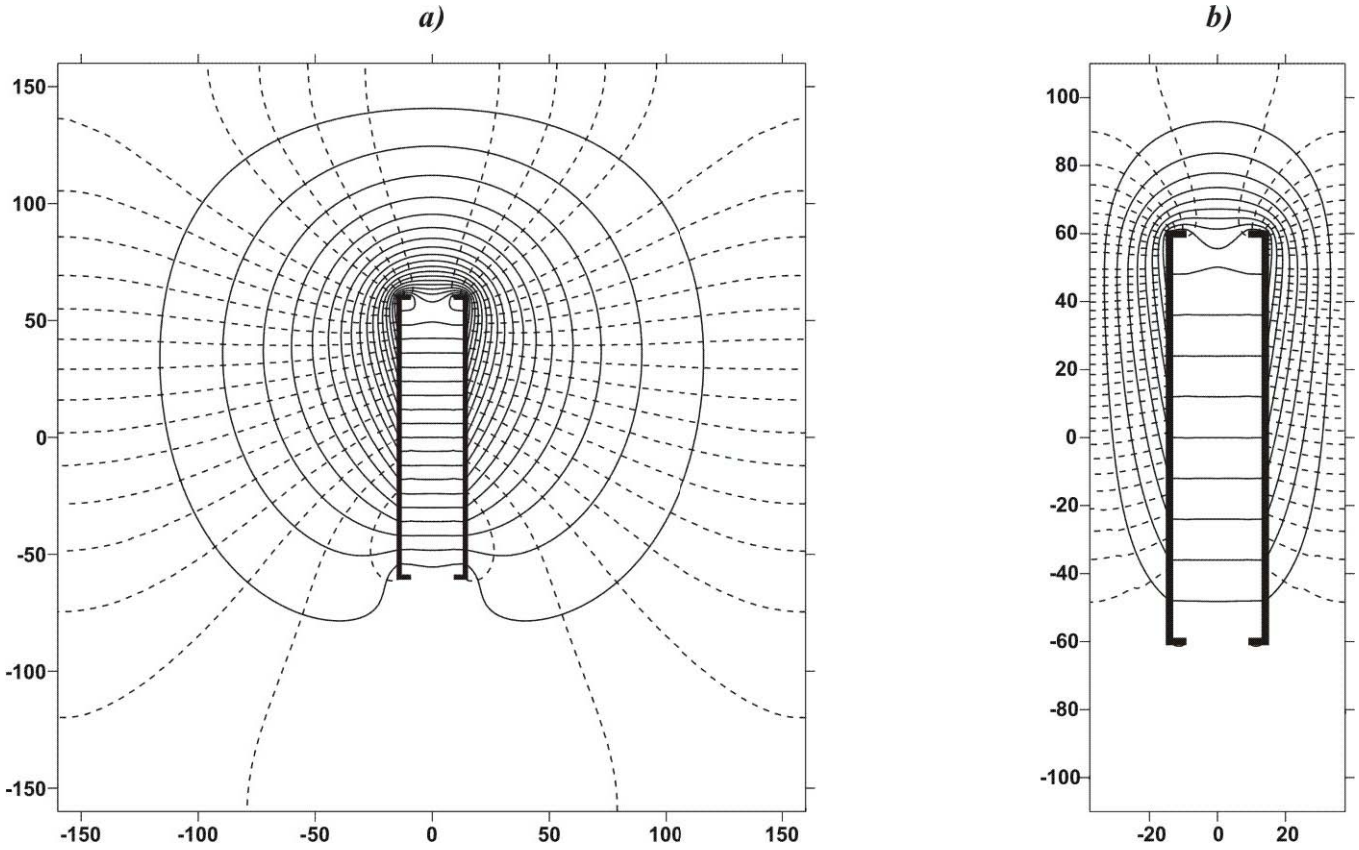

Fig. 32.2. Capacity of divider without screen $C = 22.05$ pF on the grid with 19675 nodes (***a***) and with cylindrical screen $C = 40.99$ pF on the grid with 66164 nodes (***b***).

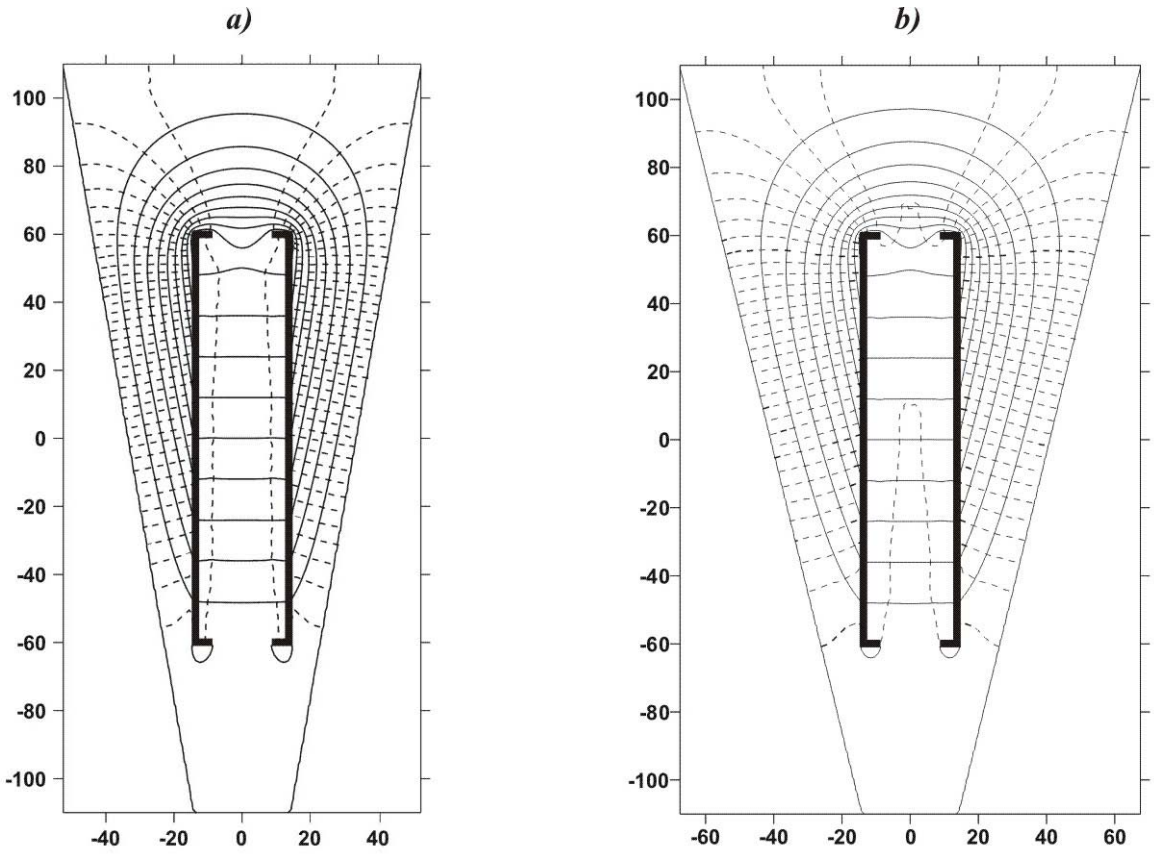

Fig. 32.3. Capacity of divider with conical screens $C = 43.08$ pF (***a***) and $C = 36.63$ pF (***b***).

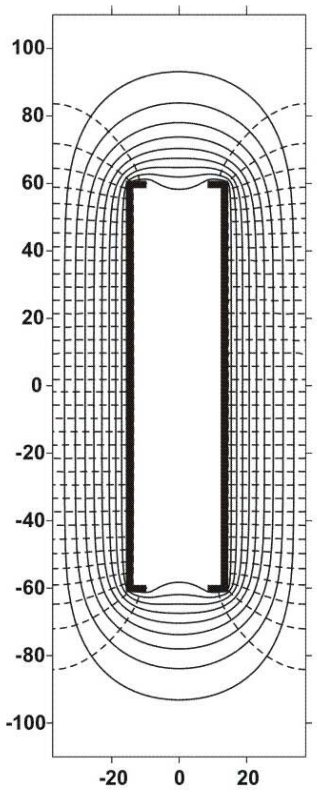

Fig. 32.4. Capacity of divider under constant potential with cylindrical screen $C = 81.89$ pF on the grid with 33963 nodes.

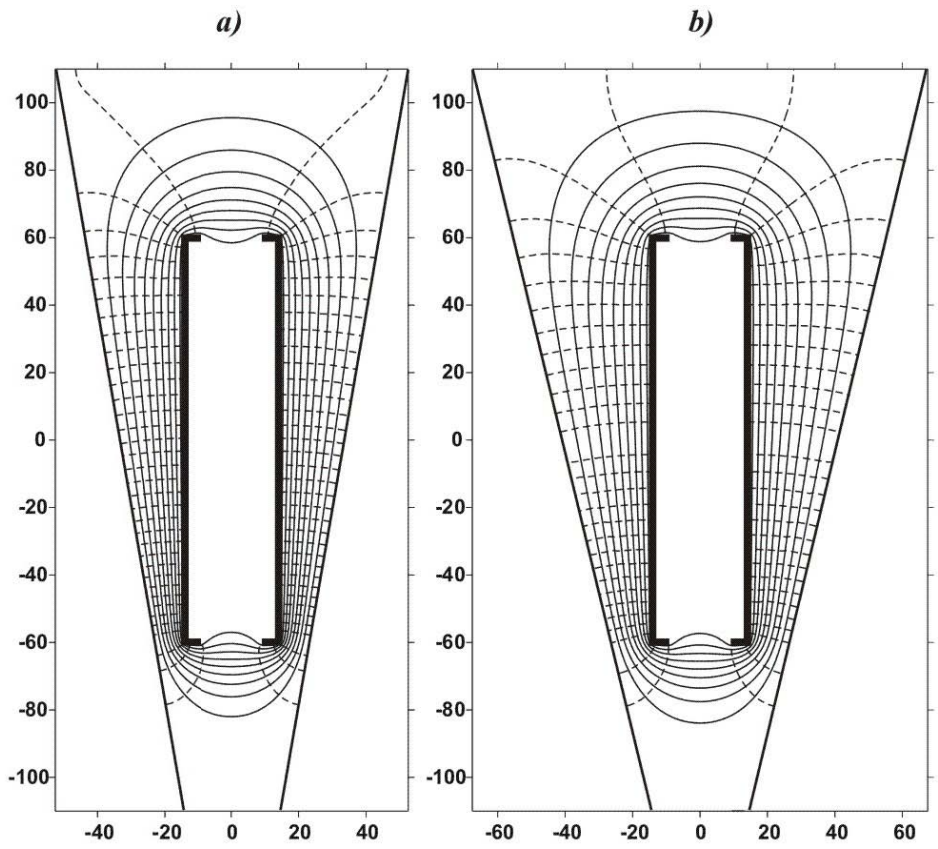

Fig. 32.5. Capacity of divider under constant potential with conical screens $C = 99.12$ pF on the grid with 59780 nodes (***a***) and $C = 82.73$ pF on the grid with 73100 nodes (***b***).

REFERENCES

1. **Агунов М.В., Агунов А.В.** Об энергетических соотношениях в электрических цепях с несинусоидальными режимами. – Электричество, 2005, № 4, с. 53 – 56.
2. **Александров Г.Н.** Передача электрической энергии переменным током. – Л.: Энергоиздат, 1990. – 190 с.
3. **Александров Г.Н.** Ограничение перенапряжений в электрических сетях. – СПб: Центр подготовки кадров энергетики. Типография «Светоч», 2003. –192 с.
4. **Алексанров Г. Н.** Передача электрической энергии. – СПб: Изд-во Политехнического университета, 2007. – 412 с.
5. **Александров Г.Н.** Быстродействующий управляемый реактор трансформаторного типа 420 кВ, 50 МВАр пущен в эксплуатацию. – Электричество, 2002, № 3, с. 64–66.
6. **Александров Г. Н.** Природа реактивной мощности линий электропередачи. – Труды СПбГТУ , 2006, № 501. Электроэнергетическое оборудование: надёжность и безопасность, с .100 –109.
7. **Александров Г.Н., Дардеер М.М.** Длинная линия электропередачи между Конго и Египтом с использованием управляемых шунтирующих реакторов. – Электричество, 2008, №3, с. 9 –14.
8. **Александров Г.Н., Ле Тхань Бак.** Уменьшение потерь мощности в дальних линиях электропередачи с управляемыми реакторами. – Электричество, 2007, № 3, с. 8-15.
9. **Александров Г.Н., Шакиров М.А.** Исследование переходных режимов работы управляемого шунтирующего компенсатора трансформаторного типа с помощью магнитоэлектрических схем замещения. – Электричество, 2005, № 6, с. 20 –32.
10. **Атабеков Г. И.** Основы теории цепей. Учебник для вузов. – М.: Энергия, 1969.
11. **Афанасьев Б.П., Гольдин О.Е., Кляцкин И.Г.** и др. Теория линейных электрических цепей. – М.: Высшая школа, 1973. – 592 с.
12. **Бадинтер Е.Я., Берман Н.Р., Драбенко И.Ф.** и др. Литой микропровод и его свойства. – Кишинев: Штиинца, 1973. – 318 с.
13. **Базуткин В.В., Дмоховская Л.Ф.** Расчеты переходных процессов и перенапряжений. – М.: Энергоатомиздат, 1983. –328 с.
14. **Беляков Ю.С.** К вопросу идентификации параметров воздушных линий электропередачи. – Электричество, 2008, №6, с. 18-23.
15. **Бессонов Л.А.** Теоретические основы электротехники. Электрические цепи /Учебник для ВТУЗов. – М.: Высшая школа, 1984. – 559 с.
16. **Бессонов Л.А.** ТОЭ. Электромагнитное поле: Учебник. – 9-е изд. – М.: Гардарики, 2001.

17. **Борисов П.А., Осипов Ю.М.** Потенциальные электрические поля. Учебное пособие по курсам ТОЭ (часть вторая) – Теория электромагнитного поля. Электромагнитные поля и волны. – СПб: ГУИТМО, 2006 – 108 с.
18. **Брянцев А.М., Долгополов А.Г., Лурье А.И.** и др. Впервые в сети 500 кВ введен в эксплуатацию новый управляемый подмагничиванием шунтирующий реактор мощностью 180 МВА. – Электричество, 2006, № 8, с. 65–68.
19. **Бушуев В.В., Путилова А.Т., Самородов Г.И.** Сверхдальние электропередачи. – Известия Академии наук РФ. Энергетика, 1994, № 2, с. 12 – 17.
20. **Веников В.А., Журавлев В.Г., Филиппова Т.А.** Оптимизация режимов электростанций и энергосистем. – М.: Энергоиздат, 1981.
21. **Веников В.А., Рыжов Ю.П.** Дальние электропередачи переменного и постоянного токов.– М.: Энергоиздат, 1985.–191 с.
22. **Вершков В.А., Нахапетян К.Т., Ольшевский О.В.** и др. Комплексные испытания полуволновой электропередачи в сети 500 кВ Европейской части СССР. – Электричество, 1968, № 8, с. 10–16.
23. **Вульф А.А.** Проблема передачи электрической энергии на сверхдальние расстояния по компенсированным линиям. – М.: Госэнергоиздат, 1941. – 100 с.
24. **Гинзбург В.Л.** Когда у России снова будет Нобелевская премия? – АиФ, № 42, (1355), 2006.
25. **Годунов С.К**. Уравнения математической физики. – М.: Наука, 1971. – 416 с.
26. **Годунов С.К., Рябенький В.С**. Разностные схемы. – М.: Наука, 1973. – 440 с.
27. **Годунов С.К., Забродин А.В., Иванов М.Я.** и др. Численное решение многомерных задач газовой динамики. – М.: Наука, 1976. – 400 с.
28. **Грамм М.И.** Вариант дедуктивной организации курса теоретической электротехники. – Электричество, 1996, № 10.
29. **Демирчян К.К.** Разложение мгновенной мощности на составляющие. – Известия Академии наук РФ. Энергетика, 1994, № 5, с. 73 – 79.
30. **Демирчян К.С.** Реактивная или обменная мощность? – Известия Академии наук СССР. Энергетика и транспорт, 1984, № 2, с. 66 – 72.
31. **Демирчян К.С.** Реактивная мощность на случай несинусоидальных функций. – Известия Академии наук РФ. Энергетика, 1992, № 1, с. 3 – 18.
32. **Демирчян К.С., Бутырин П.А.** Моделирование и машинный расчёт электрических цепей. – М.: Высшая школа, 1988.– 335 с.

33. **Демирчян К.С., Бутырин П.А.** Проблемы сохранения и развития электроэнергетической отрасли России. – Известия Академии наук РФ. Энергетика, 2008, № 1, с. 5 – 17.
34. **Демирчян К.С., Нейман Л.Р., Коровкин Н.В.** Теоретические основы электротехники. Т. 2.– СПб.: Питер, 2009. – 432 с.
35. **Джуварлы Ч.М., Дмитриев Е.В.** Математическое моделирование волновых процессов в электрических сетях. – Баку: Элм, 1975.
36. **Дикой В.П., Зильберман С.М., Кучеров Ю.Н.** и др. Организация полуволновой связи «Сибирь-Урал» на современном этапе. – Новое в российской электроэнергетике, 2002, № 12, с. 5– 15.
37. **Дмитриев Е.В., Гашимов А.М., Наир А.** и др. К вычислению расчетных параметров модели линии электропередачи с учетом коронирования проводов. – Электричество, 2007, № 12, с. 2– 14.
38. **Дмоховская Л.Ф.** Инженерные расчеты внутренних перенапряжений в электропередачах. – М.: Энергия, 1972. –288 с.
39. **Долгинов А.И.** Перенапряжения в электрических системах. –М. –Л.: ГЭИ, 1962. –511 с.
40. **Евдокунин Г.А.** Электрические системы и сети. – СПб.: Изд-во Сизова М.П., 2004.
41. **Евдокунин Г.А., Дмитриев М., Гольдштейн С.** и др. Высоковольтные ВЛ. Коммутации и воздействия на выключатели. – Новости Электротехники, 2008, № 4 (52).
42. **Ефимов Б.В.** Грозовые волны в воздушных линиях – Апатиты: изд. КНЦ РАН, 2000. –134 с.
43. **Жарков Ф.П.** Об одном способе определения реактивной мощности. – Известия Академии наук СССР. Энергетика и транспорт, 1984, № 2, с. 73 – 81.
44. **Жуков Л.А., Стратан И.П.** Установившиеся режимы сложных электрических сетей и систем: Методы расчетов. – М.: Энергия, 1979. - 416 с.
45. **Журавлев А.А., Шит М.Л., Колпакович Ю.И.** и др. Высоковольтный резистивный делитель на базе литого микропровода в стеклянной изоляции на рабочие напряжения 6-24 кВ переменного тока промышленной частоты. – Проблемы региональной энергетики, 2008, № 3 (8), с. 110-121.
46. **Зильберман С.М., Самородов Г.И.** Возможные перспективы импорта электроэнергии в Республику Молдова из Тюменского региона. – В кн.: Энергетика Молдовы – 2005. Сборник докладов. – Кишинев: Типография АНМ, 2005, с. 104 –110.
47. **Ильин В.П.** Методы конечных разностей и конечных объемов для эллиптических уравнений. – Новосибирск: Изд-во Ин-та математики, 2000. – 345 с.

48. **Каганов З.Г.** Электрические цепи с распределенными параметрами и цепные схемы. – М.: Энергоатомиздат, 1990. –248 с.
49. **Кадомская К.** Высоковольтные ВЛ. Эффективность и управляемость шунтирующих реакторов. – Новости Электротехники, 2008, № 4(52).
50. **Каменский М.К., Холодный С.Д.** Силовые кабели 1-10 кВ с пластмассовой изоляцией. Расчет активного и индуктивного сопротивлений. – Новости электротехники, 2005, № 4 (34).
51. **Караев Р.И.** Переходные процессы в линиях большой протяженности. – М.: Энергия, 1978. –191 с.
52. **Кобылин В.П., Седалищев В.А., ЛИ-ФИР-СУ Р.П.** и др. Применение регулятора-стабилизатора тиристорной системы для снижения потерь напряжения и мощности в условиях протяженных ВЛ. – Электричество, 2007, № 6, с.2–6.
53. **Ковалев Г.Ф., Лебедева П.М.** Планетарная электроэнергетическая система. – Энергия, 2006, № 9, с. 27–34.
54. **Копылов С.И.** Влияние регулируемого сверхпроводником токоограничивающего индуктивного сопротивления на устойчивость энергосистемы. – Электричество, 2007, № 6, с. 14–20.
55. **Костенко М.В., Гумерова М.И., Данилин А.Н.** и др. Волновые процессы и перенапряжения в подземных линиях. – СПб: Энергоатомиздат, 1991. – 232 с.
56. **Крогерис А.Ф., Рашевиц К.К., Трейманис Э.П.** и др. Мощность переменного тока. – Рига: Физ.-энерг.ин-т Латв. АН, 1993. – 294 с.
57. **Крон Г.** Применение тензорного анализа в электротехнике/ Пер. с англ. под ред. Э.А. Мееровича. – М.: Госэнергоиздат, 1955. –275 с.
58. **Крон Г.** Тензорный анализ сетей/ Пер. с англ. под ред. Л.Т. Кузина, П.Г. Кузнецова. – М.: Советское радио, 1978. –720 с.
59. **Круг К.А.** Основы электротехники. – Л.: ОНТИ, 1936. –888 с.
60. **Круг К.А.** Переходные процессы в линейных электрических цепях. – М.: Госэнергоиздат, 1948. –344 с.
61. **Кулигин В.А., Кулигина Г.А., Корнева М.В.** Разряд движущегося конденсатора. http:// 314159. ru/kuligin /kuligin5 .htm.
62. **Курбацкий В.Г., Томин Н.В**. Анализ потерь энергии в электрических сетях на базе современных алгоритмов искусственного интеллекта. – Электричество, 2007, № 4, с. 12 – 21.
63. **Лавров Ю.** Кабели 6–35 кВ с пластмассовой изоляцией. Особенности проектирования и эксплуатации. http:// www.news.elteh.ru/arh/2007/43/13.php
64. **Ларина Э.Т.** Силовые кабели и кабельные линии. Учебное пособие для вузов. – М.: Энергоатомиздат, 1984. – 384 с.
65. **Ларионов В.П.** и др. Техника высоких напряжений. – М.: Энергоиздат, 1982. – 296 с.

66. **Манн А.К., Спиридонов В.К.** Волновой метод определения расстояния до места повреждения кабельной линии. – В кн.: Труды ВНИИЭ. Т. 8. – М. –Л.: Госэнергоиздат, 1959, с. 28– 43.
67. **Марчук Г.И., Агошков В.И.** Введение в проекционно-сеточные методы. – М: Наука, 1981.– 416 с.
68. **Нейман Л.Р.** Теоретическая электротехника. Избранные труды. – Л.: Наука, ЛО, 1988. – 334 с.
69. **Нейман Л.Р., Калантаров П.М.** Теоретические основы электротехники. Т. 3. – М. –Л.: ГЭИ, 1954. – 416 с.
70. **Неклепаев Б.Н., Крючков И.П.** Электрическая часть станций и подстанций: Справочные материалы для курсового и дипломного проектирования. Учебное пособие для вузов. – М.: Энергоатомиздат . 1989. – 608 с.
71. **Ольшванг М.В., Остапенко Е.И., Кузнецова Г.А.** и др. Ступенчато регулируемые фазосдвигающие автотрансформаторы как средство оптимизации потокораспределения в электрических сетях // Электротехника 2010 года. – М.: ВЭИ, 1997.
72. **Ольшванг М.В**. Сферические векторные диаграммы развитых электрических сетей и их применение. Сборник научных трудов "ВЭИ 80 лет" под общей редакцией В.Д. Ковалева, Т.1. – М.: ВЭИ, 2001, с. 90–106.
73. **Пацюк В.И.** Влияние распределенных и сосредоточенных параметров на режимы линий переменного напряжения. – Проблемы региональной энергетики, 2008, № 2, (7), с. 17 – 26.
74. **Пацюк В.И.** Как настроить четвертьволновую линию на полуволновой режим работы. – Проблемы региональной энергетики, 2008, № 2, (7), с. 27 – 34.
75. **Пацюк В.И**. Несинусоидальные напряжения при синусоидальном токе на входе разомкнутой линии с потерями. – Проблемы региональной энергетики, 2008, № 3 (8), с. 47-60.
76. **Пацюк В.И.** Разряд движущегося конденсатора на длинную линию. – Проблемы региональной энергетики, 2008, № 3 (8), с. 85-100.
77. **Пацюк В.И., Римский В.К.** Волновые явления в неоднородных средах. Т.1. Теория распространения упругих и неупругих волн. – Кишинев: Издательско-полиграфический центр МолдГУ, 2005. – 254 с.
78. **Пацюк В.И., Римский В.К.** Волновые явления в неоднородных средах. Т.2. Нестационарное деформирование многосвязных тел. – Кишинев: Издательско-полиграфический центр МолдГУ, 2005. – 239 с.
79. **Платонов В.В., Быкадоров В.Ф.** Определение мест повреждения на трассе кабельной линии. – М.: Энергоатомиздат, 1993.
80. **Попков В. И**. Электропередачи сверхвысокого напряжения. – В кн.: Наука и человечество. Т. 6. – М., 1967.

81. **Поспелов Г.Е., Сыч Н.М.** Потери мощности и энергии в электрических сетях. – М.: Энергоиздат, 1981. – 216 с.
82. **Препарата Ф., Шеймос М.** Вычислительная геометрия: Введение. – М.: Мир. –1989. – 480 с.
83. **РД 153-34.3-35.125-99.** Руководство по защите электрических сетей 6–1150 кВ от грозовых и внутренних перенапряжений / Под научной редакцией Н.Н. Тиходеева. – 2-е изд. – СПб: ПЭИПК Минтопэнерго РФ, 1999. – 355 с.
84. **Римский В.К., Берзан В.П., Пацюк В.И.** и др. Как увеличить передаваемую мощность в десятки раз. – Кишинев: Типография АНМ, 2007. – 178 с.
85. **Римский В.К., Берзан В.П., Тыршу М.С.** и др. Расчет потерь и перетоков мощности в сетях постоянного и переменного тока. – Кишинев: Типография АНМ, 2007. – 60с.
86. **Римский В.К., Берзан В.П., Тыршу М.С.** Волновые явления в неоднородных линиях. Т.1. Теория распространения волн потенциала и тока. Под ред. Римского В.К. – Кишинев: Типография АНМ, 1997. – 298 с.
87. **Римский В.К., Берзан В.П., Тыршу М.С.** Волновые явления в неоднородных линиях. Т.2. Переходные процессы в линиях с сосредоточенными элементами. Под ред. Постолатия В.М. – Кишинев: Типография АНМ, 2006. – 264 с.
88. **Римский В.К., Берзан В.П., Пацюк В.И.** и др. Волновые явления в неоднородных линиях. Т.3. Передача мощности по цепям постоянного и переменного напряжения. – Кишинев: Типография АНМ, 2007. – 328 с.
89. **Римский В.К., Берзан В.П., Пацюк В.И.** и др. Волновые явления в неоднородных линиях. Т.4. Параметрические цепи. – Кишинев: Типография АНМ, 2008. – 552 с.
90. **Римский В.К., Берзан В.П., Пацюк В.И.** и др. Волновые явления в неоднородных структурах. Т.5. Теория и методы расчета электрических цепей, электромагнитных полей и защитных оболочек АЭС. – Кишинев: Типография АНМ, 2008. – 664 с.
91. **Римский В.К., Берзан В.П., Пацюк В.И.** и др. Потери активной мощности в длинных линиях при согласованных, предельных и аварийных режимах.– Проблемы региональной энергетики, 2008, № 1 (6), с. 46 – 58.
92. **Римский В.К., Берзан В.П., Пацюк В.И.** Численное моделирование переходных и установившихся процессов в электрических цепях с переменными параметрами.– Проблемы региональной энергетики, 2008, № 2 (7), с. 7 – 16.
93. **Римский В.К., Берзан В.П., Пацюк В.И.** Аварийные режимы в нагруженной полуволновой электропередаче.– Проблемы региональной энергетики, 2008, № 3 (8), с. 34-47.

94. **Рюденберг Р.** и др. Электрическая передача больших мощностей на далекие расстояния. – М.: Госэнергоиздат, 1934.
95. **Самарский А. А.** Введение в теорию разностных схем. – М.: Наука, 1971. – 554с.
96. **Самарский А.А.** Теория разностных схем. – М.: Наука, 1977. – 656 с.
97. **Самарский А.А.** Введение в численные методы. – М.: Наука, 1987.
98. **Самарский А.А., Гулин А.В.** Устойчивость разностных схем. – М.: Наука, 1973. – 416 с.
99. **Самарский А.А., Лазаров Р.Д., Макаров В.Л.** Разностные схемы для дифференциальных уравнений с обобщенными решениями. – М: Высшая школа, 1987. – 296 с.
100. **Самарский А.А., Михайлов А.П.** Математическое моделирование: идеи, методы, примеры. – М.: Наука, 1997. – 320 с.
101. **Самарский А.А., Николаев Е.С.** Методы решения сеточных уравнений. – М: Наука, 1978. – 592 с.
102. **Самарский А.А., Попов Ю.П.** Разностные схемы газовой динамики. – М.: Наука, 1975. – 352 с.
103. **Сивухин Д. В.** Общий курс физики. Электричество. – М.: Наука, 1983. – 688 с.
104. **Справочник** по проектированию линий электропередачи. Под ред. М.А. Реута и С.С. Рокотяна. – М.: Энергия , 1980. – 296 с.
105. **Солдатов В.А., Постолатий В.М.** Расчет и оптимизация параметров и режимов управляемых многопроводных линий. – Кишинев: Штиинца, 1990. – 239 с.
106. **Тамм И.Е.** Основы теории электричества. – М.: Наука, 1976. – 616 с.
107. **Тихонов А.Н., Самарский А.А.** Уравнения математической физики. – М.: Наука, 1977. – 736 с.
108. **Федорченко А. М.** Классическая электродинамика. – К.: Вища школа, 1988. – 280 с.
109. **Фельдман М.Л.** Режим передачи натуральной мощности и его энергетические показатели. – Известия Академии наук РФ. Энергетика, 1994, № 2, с. 12 – 17.
110. **Хаяси С**. Волны в линиях электропередачи. – М. –Л.: Госэнергоиздат, 1960. –343 с.
111. **Холодный С.Д., Филиппов М.М., Кричко В.А.** и др. Расчет токов в оболочках и экранах и их термической стойкости при однофазном двойном замыкании в разветвленной кабельной сети. – Электричество, 2001, № 8.
112. **Электрические** кабели, провода и шнуры. Справочник/ Н.Н. Белоусов, А.Е. Саакян, А.И. Яковлева. Под общ. ред. Н.Н. Белоусова. – М.: Энергия , 1979. – 416 с.
113. **ABB** Power Technologies. www.abb.com/FACTS/

114. **Berzan V., Rimschi V.** Procese nestaţionare în circuite electrice neomogene. Sub redacţia Postolache P. – Chişinău: Combinatul Poligrafic Chişinău, 1998. – 416 p.
115. **Berzan V., Rimschi S.** Piaţa liberalizată de energie electrică. – Chişinău: Tipografia AŞM, 2007. – 88 p.
116. **Dragan G., Golovanov N., Mazzeti C.** şi al. Tehnica tensiunilor înalte. Vol. II. – Bucureşti: Editura AGIR, 2001. –732 p.
117. **Li R., Chen Z. and Wu W.** Generalized difference methods for differential equations. Numerical analysis of finite volume methods. New York-Basel: Marcel Dekker, Inc., 2000. – 459 p.
118. **NEPLAN** by BCP Switzerland. Power Systems Engineering. www.neplan.com.
119. **Nitsch J.B., Tkachenko S.V.** Propagation of Current Waves Along Quasi-Periodic Thin-Wire Structures: Taking Radiation Losses into Account. – U.R.S.I. The Radio Science Bulletin, 2007, No 322, p. 19-40.
120. **Tirsu M.S., Berzan V.P., Rimschi V.X.** et al. Research on influence of high-voltage cable un-homogeneities on process of short waves distribution. – Electric Power Systems Research – Elsevier, 2008, Vol. 78, Issue 12, p. 2046-2052.
121. **Rimschi V.,** Nuclear Power Plant Reliability Under Emergency Conditions. – Conferinţa naţională de energie. România, Neptun. 15-18 iunie, 1992.
122. **Rimschi V. X., Patsjuk V.I.** The computation of the strength of the nuclear power plants' supporting structures. Conferinţa naţională de energie. – România, Neptun. 13-16 iunie, 1994, p. 1-6.
123. **Rimschi V. X., Patsjuk V.I.** Dinamical firmnes, safety and seismic visk of NPP. Conferinţa naţională a energiei. – România, Neptun, 2-5 septembrie, 1996.
124. **Rimschi V., Berzan V., Tîrşu M.** şi al. Soluţii precise a ecuaţiilor telegrafiştilor. – Chişinău: Tipografia AŞM, 2007. –86 p.
125. **Rimschi V.X., Berzan V.P., Patsiuc V.I.** Theory and calculation of the line circuits with distributed and lumped parameters. – Energy Technologies, 2009, Vol. 42, No 2, p. 12-22.